

Copyright is owned by the Author of the thesis. Permission is given for a copy to be downloaded by an individual for the purpose of research and private study only. The thesis may not be reproduced elsewhere without the permission of the Author.

**A High Resolution Record  
of  
Late Quaternary  
Climatic and Environmental Change  
in  
Taranaki, New Zealand**

A thesis presented in partial fulfilment of the requirements for the degree of

**Doctor of Philosophy**

**in**

**Earth Science**

at Massey University, Palmerston North New Zealand

**Robert John Tinkler**

**2013**







## Abstract

A high-resolution characterisation of climatic and environmental change in Taranaki, New Zealand over the last 80,000 years using biotic and abiotic proxies is presented. This research contributes to the small set of sediment cores that extend from the present back through the Last Glacial Maximum (LGM) in the southern North Island, and adds to the small number of near-continuous cores in New Zealand.

Fossil pollen data presented here provides a record of vegetation changes in response to climate change (temperature, wind and rainfall). In addition, the project applies a recently developed pollen temperature transfer function (Wilmshurst *et al.* 2007) to quantify, for the first time, temperature change across the entire LGM in this region, and elucidates the timing of Late Quaternary New Zealand climatic events and phases. Climate change timing and magnitude is tested against the climate event stratigraphy (CES) developed by the NZ-INTIMATE (INTEgration of Icecore, Marine and Terrestrial archives) group (Alloway *et al.* 2007), including: Last Glacial Coldest Period (LGCP); the mid-eLGM Interstadial; the Last Glacial-Interglacial Transition (LGIT); Termination I; the Antarctic Cold Reversal (ACR); the Late-Glacial Warm Period (LGWP), the Late-Glacial Reversal (LGR); and Early Holocene Warming (EHW).

During the Moerangi Interstadial between 40,000 and 30,000 cal yrs BP, both the Eltham and coastal Taranaki pollen records show that cold-climate taxa such as *Nothofagus menziesii*, *Nothofagus* subg. *Fuscospora*, *Hoheria*, *Plagianthus*, *Phyllocladus* and Poaceae dominated the pollen assemblage. In addition to being cold, low numbers of fern and tree fern spores imply that conditions were drier than present. The LGCP at Eltham (29,000 – 18,000 cal yrs BP) began around 1,200 years earlier than similar records from elsewhere in New Zealand. Transfer functions suggest that mean annual temperatures at the LGCP/ LGM at Eltham were 5.7°C cooler than present. Within the LGCP, the mid-eLGM Interstadial described in similar records from New Zealand seems to be evident in the W-MAT-derived temperature curve at Eltham, where warming of around 0.8°C occurs between 27,000 and 24,500 cal yrs BP.

The LGIT appears to have begun around 18,000 cal yrs BP and concluded around 14,600 cal yrs BP at Eltham, which agrees well with speleothem data from Northwest Nelson, but is more short-lived than at Otamangakau Bog where the LGIT is thought to have persisted for another 1,500 years. A period of sharp cooling inferred from the Eltham pollen record between 16,600 and 15,000 cal yrs BP, when mean annual temperature fell between 1°C and 4°C from the previous period, is matched in time, but not in intensity at some other western and central North Island, and some South island sites, and may be a sampling artefact. The LGWP duration at Eltham (14,600 – 13,500 cal yrs BP) broadly corresponds with NZ-INTIMATE and Northwest Nelson estimates of 14,800 – 13,500 cal yrs BP; mean annual temperatures at Eltham came within 0.6°C of modern-day mean annual temperatures at this time.

The timing of the LGR at Eltham shows good agreement with NZ-INTIMATE estimates (Alloway *et al.* 2007; Lowe *et al.* 2008), that is, from around 13,500 to 12,500 cal yrs BP. The LGR onset at Eltham preceded onset at the Auckland maars by 600 years and concluded 1,500 years earlier than at Auckland; mean annual temperature at Eltham at this time was approximately 2°C cooler than the present day MAT of 11.2°C. The EHW event commenced at Eltham around 12,500 cal yrs BP, around 1,000 years earlier than at Kaipo Bog, Otamangakau Bog; and largely synchronous with the Auckland maars and Okarito.

Pollen records from coastal Taranaki sites span  $\delta^{18}\text{O}$  Stage 5a (Otamangakau Interstadial, *c.* 80,000 yrs BP) through to  $\delta^{18}\text{O}$  Stage 2 (Last Glacial-Interglacial Transition, *c.* 18,500 cal yrs BP), and encompass the stadial complex between these two interstadials ( $\delta^{18}\text{O}$  Stage 4, *c.* 70,000 – 60,000 yrs BP). These records contribute to the small number of pollen-based paleoenvironmental and paleoclimatic narratives for New Zealand extending from the LGIT to the Otamangakau Stadial ( $\delta^{18}\text{O}$  stage 5a) time periods. A major contribution of the current

study is to reconstruct and characterise  $\delta^{18}\text{O}$  stage 5a and  $\delta^{18}\text{O}$  stage 4 temperatures based on two pollen transfer functions developed by Wilmshurst *et al.* (2007).

During  $\delta^{18}\text{O}$  Stage 5a around 80,000 cal yrs BP, conditions were warmer and wetter than the succeeding glacial.  $\delta^{18}\text{O}$  Stage 4 and the early part of  $\delta^{18}\text{O}$  Stage 3 were cool with relatively low precipitation and were likely to have been windy at coastal Taranaki sites. Although  $\delta^{18}\text{O}$  Stage 4 was cool, it was not as cold as the LGM: pollen transfer functions showed decreases in estimated mean annual temperature from  $\delta^{18}\text{O}$  stage 5a, with mean annual temperatures falling around 2°C to reach 7°C. Precipitation likely decreased during  $\delta^{18}\text{O}$  stage 4, as indicated by low levels of drought-intolerant taxa *Dacrydium cupressinum*, *Cyathea smithii*, and monolete spores, whilst low shrub diversity implies that disturbance was likely to have been low.

During early  $\delta^{18}\text{O}$  stage 3, the climate warmed and became wetter in coastal Taranaki, as indicated by increasing conifer abundance; in particular *Dacrydium cupressinum*, high abundance of *Cyathea smithii*, and a decline in cold-tolerant *Nothofagus*, *Halocarpus*, Asteraceae, and Poaceae after 60,000 yrs BP. These conditions persisted for < 5,000 years before temperatures decreased again, then between 50,000 and 40,000 yrs BP the decline in Poaceae and cold-tolerant shrubs *Phyllocladus*, *Halocarpus* and Asteraceae, as well as the sharp rise in tall tree conifers, all point to climate amelioration. Conditions were still relatively cool; although pollen transfer functions imply that that mean annual temperatures increased slightly, with mean annual temperature estimates fluctuating between 7°C and 8°C, this was approximately 3 to 4°C cooler than present.

For the first time in New Zealand, aerosolic quartz dust was extracted from organic sediments; this peat-derived data informs a paleowind narrative for Taranaki. The technique used in the current study to extract quartz from peats can be considered successful, insofar as relatively pure samples of quartz could be isolated in sufficient mass to be able to measure them, and relate the data to the age model and the coeval pollen influx.

The paleowind reconstructions from Eltham can be summarised as follows: strong winds dominated between 36,200 and 35,100 cal yrs BP, 30,746 and 32,101 cal yrs BP, 28,364 to 17,477 cal yrs BP, and 16,118 to 15,806 cal yrs BP. Intermediate winds occurred between 30,746 and 28,364 cal yrs BP, 17,477 and 16,118 cal yrs BP, and 15,619 to 14,916 cal yrs BP; winds of light intensity dominated between 34,777 and 32,101 cal yrs BP and 14,916 and 9,900 cal yrs BP. Major dust peaks at 31,358 cal yrs BP; 21,300 cal yrs BP and 15,955 cal yrs BP all correlated well with the Vostok ice core as well as marine core P69 (Stewart & Neall 1984), and Onaero and Waitui in northern Taranaki. Similarly, dust minima after about 15,000 cal yrs BP at Eltham, Vostok, marine core P69, Onaero, and Waitui suggests that the quartz dust signature at Eltham is consistent with both global and regional estimates of dust influx as the atmospheric dust load responded to changes in wind direction and strength, in particular the intensity of westerly winds, and changes to sediment source area characteristics such as vegetation cover.

Combining fossil pollen data and aerosolic quartz dust results is a new technique to investigate the relationship between wind intensity, temperature and plant assemblages. The Eltham fossil pollen and aerosolic quartz data was analysed to determine how the relative proportions of competitive, stress tolerant and ruderal taxa respond to winds of differing intensities over time, as well as quantifying the impact of wind of different intensities on plant diversity over the period 36,200 to 9,900 cal yrs BP. In essence, competitor, *C*-selected taxa increased in relative abundance, and stress-tolerant, *S*-selected and ruderal, *r*-selected taxa decreased over the last 15,000 years at Eltham, as both temperature and wind intensity ameliorated.

Wind data was examined against pollen diversity data to test the Intermediate Disturbance Hypothesis (IDH) in the vegetation of the Taranaki region. A moderate relationship between floral diversity and dust flux was found, with periods of high and low dust flux corresponding to lower diversity, and periods of intermediate dust flux corresponding to higher diversity, as predicted by the IDH.

## Acknowledgements

I am indebted to the following individuals, in particular my supervisors. Without their help and encouragement, I could not have completed this study:

- Professor Vince Neall, Institute of Agriculture & Environment (IAE), Massey University (main supervisor), for his friendly encouragement and advice; access to his encyclopaedic knowledge of Taranaki volcanism and tephrochronology, botany and the paleoenvironment; coring assistance at Irirangi; sample gathering at South Taranaki sites; and keeping me on track.
- Dr. Marcus Vandergoes, GNS Science, for his enthusiasm and advice, and coring assistance at Eltham;
- Dr. Kat Holt, IAE, Massey University for her encouragement and palynological advice.

Thank you to the following people at Massey University:

- Dr. Anke Zernack (IAE) for sharing her knowledge of coastal Taranaki sites, assistance in sample gathering in South Taranaki, and assistance in elucidating the tephrochronology for the Eltham cores;
- Associate Professor Bob Stewart (IAE) for useful discussions on quartz analysis and performing XRD analysis on the aerosolic quartz samples;
- Professor Shane Cronin (IAE) for providing access to the Eltham core, funding for x-rays, microprobing the Kawakawa sample and coring assistance;
- Dr. Clel Wallace (IAE) for useful discussions on quartz analysis;
- Associate Professor Russell Death (IAE) for helpful suggestions regarding biodiversity analysis and the Intermediate Disturbance Hypothesis;
- Ms. Amanda McDonald-Creevy (IAE) for palynological advice and assistance in the pollen laboratory;
- Mr. David Feek (IAE) for coring assistance at Irirangi and assistance in the pollen laboratory;
- Mr. Kevin Butler (School of People, Environment and Planning) for palynological advice and assistance in the pollen laboratory.

Thank you to the following people outside Massey:

- Mr & Mrs Guddopp, Eltham for allowing access to their farm for coring;
- Dr. Janet Wilmshurst, Landcare Research for running my fossil pollen data through her pollen-temperature transfer function program.

My research was supported by a Massey University Institute of Natural Resources Summer Scholarship, a Geosciences Society of New Zealand Young Researcher Travel Award, a George Mason Charitable Trust Scholarship, and financial support for  $^{14}\text{C}$  dating provided by GNS Science *Global Change with Time* program.

Thank you to my family for their support and encouragement: Sarah, Rachel, Aimee and Kate; Connor; Joan; Garry and Tina; and especially my wife Lesley. xxx

## **Table of Contents**

### **Abstract**

### **Acknowledgements**

### **Table of Contents**

### **List of Figures**

### **List of Tables**

## **1. Introduction**

- 1.1. Research Rationale and Importance of Study 1
- 1.2. Research Objectives 3
- 1.3. Research Questions 4

## **2. Taranaki Geography, Geology & Soils**

- 2.1. Introduction 5
- 2.2. North Island Tectonics and the Taranaki Volcanic Lineament 6
- 2.3. Taranaki Soils 8

## **3. Present Climate of Taranaki**

- 3.1. Introduction 8
- 3.2. Temperature 9
- 3.3. Winds
  - 3.3.1. Introduction 11
  - 3.3.2. Taranaki Winds 12
    - 3.3.2.1. Strong-Gale Force Winds, Tropical Cyclones and Tornadoes 13
- 3.4. Precipitation 14

## **4. Late Quaternary Climate Change in New Zealand 16**

## **5. Characteristics and Dynamics of Taranaki Flora, Plant Responses to Stress, Plant Strategies and Floral Biodiversity**

5.1. Vegetation History of Western North Island since 80,000 years BP	22
5.2. Modern Taranaki Vegetation	29
5.3. Plant Responses to Stress	
5.3.1. Effects of Cold Temperatures on Plants	33
5.3.2. Effects of Wind on Plants	34
5.3.3. Plant Adaptations to Resource-Rich vs. Resource-Poor Environments	36
5.3.4. Fire Regimes and Charcoal	36
5.4. Plant Strategies	
5.4.1. <i>r-K</i> Selection Theory	38
5.4.2. Grime's <i>C-S-R</i> Theory	39
5.4.3. Plant Succession Following Volcanic Disturbance	41
5.5. Floral Biodiversity	
5.5.1. Introduction	43
5.5.2. Intermediate Disturbance Hypothesis	46
5.5.3. Floral Representation in the New Zealand Pollen Rain	50
5.5.4. Pollen Transfer Functions	50

## **6. Aerosolic Dust**

6.1. Introduction	53
6.2. Aerosolic Dust and Terrestrial Biogeochemical Cycles	55
6.3. Antarctic Ice Core Studies	57
6.4. New Zealand Aerosolic Dust Studies	59
6.5. Australian Dust Sources	61
6.6. The Effects of Vegetation on Dust Entrainment	63

## **7. Methodology**

7.1. Site Descriptions and Stratigraphy	65
7.1.1. Eltham Swamp	65
7.1.2. Stent Road	76
7.1.3. Okawe Stream	78
7.1.4. Opunake Beach	83
7.1.5. Kaupokonui Beach	87

7.1.6. Lizzie Bell	89
7.2. Core Extraction	94
7.3. Palynology and Charcoal Methodology	100
7.4. Taranaki Radiocarbon Dates	
7.4.1. Eltham Radiocarbon Dates	102
7.4.2. Coastal Taranaki Radiocarbon Dates	103
7.4.3. Eltham Swamp Age Model	104
7.5. Aerosolic Quartz Methodology	114
7.6. Pollen Transfer Functions	116
7.7. Biodiversity Indices	117
<b>8. Results</b>	
8.1. Results of Pollen Analysis	
8.1.1. Eltham Swamp	120
8.1.2. Stent Road	139
8.1.3. Okawe Stream	142
8.1.4. Opunake Beach	146
8.1.5. Kaupokonui Beach	151
8.1.6. Lizzie Bell	156
8.2. Results of Quartz Analysis of Eltham Swamp	161
8.3. Results of Charcoal Analysis of Eltham Swamp	175
<b>9. Discussion</b>	
9.1. Pollen Transfer Functions	177
9.2. Climate Phases and Chronocorrelation	
9.2.1. Regional Taranaki 85,000 – 30,000 yrs BP	179
9.2.2. Eltham and NZ-INTIMATE CES	186
9.3. Aerosolic Quartz	
9.3.1. Aerosolic Quartz at Eltham	192
9.3.2. Aerosolic Dust Entrainment Distances and Wind Intensity Definitions	195
9.4. Charcoal and Fire Regimes	199
9.5. Climate Change and Biodiversity Change	201

## **10. Conclusions and Future Work**

10.1. Conclusions 209

10.2. Future Work 213

## **11. Appendices**

11.1. Taranaki Weather Stations 215

11.2. Palynological and Aerosolic Dust Sites Referred to in Text 216

11.3. Wilcoxon Signed Rank Test for Eltham Core 6 219

11.4. Aerosolic Quartz Extraction Methodology Rationale 220

## **12. References**

229

## List of Figures

1. Major Landform Regions in Taranaki
2. Tectonic and Geological setting of Taranaki Volcanoes
3. Oil Derricks at Moturoa, New Plymouth, with Ngamoti beach
4. Mount Egmont as seen from Eltham
5. New Zealand's Position in the South Pacific Ocean
6. Isotherm Map of Median Temperatures for Taranaki Region, 1971 -2000
7. Mean Monthly Temperatures for Selected Taranaki Sites.
8. Windrose, New Plymouth Aeroclub 0600-1100 hours
9. Windrose, Stratford Demonstration Farm
10. Windrose, Normanby EDR
11. Isohyet Map, January–December 2011
12. Mean Annual Rainfall vs Altitude for Selected Taranaki Sites
13. Eltham Swamp Pollen Diagrams *c.* 3,000 – 14,000 ys BP
14. Seed size (cm), production (seeds m<sup>-2</sup>) and periodicity (1961-1967) for five New Zealand podocarps
15. The Frequency of *C*-, *S*- and *R*-strategies along the *r*-*K* Continuum
16. Intermediate Disturbance Hypothesis Parabola
17. Relationship between Disturbance and Diversity for Japanese Forests
18. Species Richness of Tree Communities in French Guiana as a Function of Pioneer Stems
19. Antarctica Ice Core Drilling Sites
20. Lake Eyre and Murray Darling Dust Sources
21. Australian Dust Sources and Trajectories Across the Tasman Sea
22. Quartz Distribution in Ocean Sediments around Australia, and South-eastern Dust Path
23. Satellite photograph of Eltham Area
24. Eltham Swamp Lithology Core A
25. Eltham Swamp Lithology Key
26. Taranaki Study Sites
27. Stent Road Site
28. Okawe Stream Site and Lithology
29. Opunake Beach South Site and Lithology
30. Kaupokonui Beach Site and Lithology
31. Lizzie Bell Site and Lithology
32. Coastal Taranaki Sites Lithology Key
33. Taranaki Pollen Site Tephra and Debris Avalanche Correlations
34. Coring Rig at Eltham
35. Livingstone Coring Apparatus at Eltham
36. Eltham Swamp Lithology Core B, and Core A and B Correlation
37. Age-Depth Models for Eltham Swamp
38. Rarefaction Curve for Eltham Swamp
39. Eltham Swamp Pollen Diagram 40,000 – 9,750 cal yrs BP
40. Samples Containing Low Pollen Counts, 21,000 – 18,000 cal yrs BP

41. Eltham Swamp Pollen Diagram 19,400 – 9,750 cal yrs BP
42. Stent Road Pollen Diagram 24,730 – 18,540 cal yrs BP
43. Okawe Stream Pollen Diagram 33,730 – 24,770 cal yrs BP
44. Opunake Beach Pollen Diagram 33,800 – 25,565 cal yrs BP
45. Kaupokonui Beach Pollen Diagram 55,000 - 33,900 cal yrs BP
46. Lizzie Bell Pollen Diagram 80,000 – 55,000 cal yrs BP
47. Aeolian Mass Accumulation Rate for Marine Core E26.1
48. Weight of Quartz per cm<sup>3</sup> of Sediment by Size Class, Eltham Swamp
49. Eltham Quartz Dust Concentration and Eltham and Vostok Dust Influx
50. Dust Accumulation Rates and Fossil Pollen Curves for Marine Core P69
51. Eltham Quartz Grain Distribution for Individual Samples
52. Eltham Quartz Grain Distribution Combined Samples and Cumulative Distribution
53. Modern Australian Dust Samples
54. Quartz Dust Grain Size Distribution and Influx at Waitui and Onaero
55. Vostok Dust Concentration and Influx
56. Dust Particle Size Distribution from Marine Cores E39.75 and E26.1
57. Eltham LPG Ratio, Charcoal Concentrations, Temperature Reconstruction & Correlation to NZ Climate Events
58. Eltham LPG Ratio, Shannon Index, Temperature Reconstruction and Correlation to NZ Climate Events
59. Windroses, Normanby and Waitara
60. Taxa Richness vs Wind Disturbance, Eltham Swamp
61. Taxa Richness vs Mean Annual Temperature, Eltham Swamp
62. Eltham Quartz Concentration by Size Class, Proportion of C-, S- or R- taxa
63. Eltham Quartz Concentration by Size Class and Influx, Proportion of C-, S- or R- taxa; Diversity Indices
64. Eltham Quartz Concentration by Size Class and Influx, Proportion of C-, S- or R- taxa; Charcoal Concentration
65. XRD Plots for Selected Eltham Quartz Dust Samples

## List of Tables

1. Relationship between 2007 NZ-INTIMATE CES and 2013 NZ-INTIMATE CES
2. Modern Limits of New Zealand Flora as a Function of Altitude, Latitude and Temperature
3. Typical Differences between *r*-selected and *K*-selected Plants
4. Basis for the Evolution of C-S-R Strategies in Vascular Plants
5. Red Queen and Court Jester Models at Different Geographic and Temporal Scales
6. Classification of Eolian Materials by Size
7. Mineral Composition, New Zealand Dust Storms
8. Taranaki Radiocarbon Dates
9. Age Ranges for Eltham Swamp and Coastal Taranaki Sites
10. Correlation between Mean Annual Temperature and Pollen Types for Taranaki Sites
11. Comparison Between Inferred Climate at Taranaki and Other New Zealand Sites 85,000- 30,000 cal yr BP
12. Comparison Between Inferred Climate Events at Eltham and NZ-INTIMATE Defined Climate Events
13. Maximum Quartz Grain Entrainment Distances for Selected Wind Velocities, Turbulence and Grain Sizes
14. Correlations for Quartz Dust, Charcoal, MAT, C-, S-, and R-selected Taxa for Eltham Swamp

15. Wilcoxon Signed Rank Test for Eltham Core 6
16. Percentage Recovery of Quartz and Albite after  $\text{H}_2\text{SiF}_6$  Treatment at Various Temperatures
17. Percentage Recovery of Untreated and Pre-treated Quartz after ten washing-centrifugation-decantation cycles
18. Times to Separate Different Grain Size Fractions by Sedimentation and Centrifugation

# 1. Introduction

## 1.1 Research Rationale and Importance of Study

Climate change is potentially the most significant and contentious issue of our time (Ban 2009; Anderson 2009). While some debate still exists around the role of anthropogenic activities in changing our current climate, there is no doubt that the Earth's climate has changed in the past in response to natural influences and that it will continue to do so in the future, whether influenced by humans or not (Petit *et al.* 1999). Understanding the timing and magnitude of past climatic fluctuations is critical to understanding and preparing for future climatic fluctuations (Tausch *et al.* 1993; von Storch *et al.* 2004; Moberg *et al.* 2005). High resolution multiproxy palaeoenvironmental and palaeoclimatic records from sediment archives have been identified as one of the most accurate ways of investigating past climate change (Woodward & Shulmeister 2006; Alloway *et al.* 2007).

Milankovitch theory proposes that the forces driving global paleoclimate change, in particular glaciation patterns, are temporal cycles of changes in the Earth's orbit around the sun. These orbital perturbations are: (i) eccentricity of the earth's orbit, with periodicities of 400 kyr, 125 kyr, 105 kyr and 95 kyr (often listed as one 100 kyr cycle); (ii) orbital inclination, with a periodicity of 100 kyr; (iii) obliquity of the Earth's axis, with a periodicity of 41 kyr; and (iv) precession of the equinoxes, with a period of 22,000 years (Imbrie & Imbrie 1979; Muller & MacDonald 2001). The combination of the 41,000 year obliquity cycle and the 22,000 year precession cycles, plus the smaller eccentricity cycle, affects the relative seasonality of summer and winter, and is likely to control the growth and retreat of ice sheets.

In addition to these > 10,000-year-scale, Milankovitch climate oscillations, millennial-scale climate cycles also occur; ice-core records from Greenland have distinguished as many as 25 discrete stadial-interstadial climate changes known as Dansgaard-Oeschger cycles between 110,000 and 14,000 years before present (Dansgaard *et al.* 1993; Björck *et al.* 1998). These cycles of warming and cooling were also detected in the EPICA ice cores (Petit *et al.* 1999; Watanabe *et al.* 2003; Delmonte *et al.* 2004, 2007) but the Antarctic oscillations are slightly asynchronous with, and less pronounced than, the Greenland oscillations (EPICA 2006; Newnham *et al.* 2011).

Determining how these climatic episodes relate to each other, their spatial and temporal extents, and regional differences in timing of onset, are necessary to understand mechanisms of climate change (Barrell *et al.* 2013). Testing the interhemispheric climate linkages requires robust, high resolution paleoclimate climate records that are chronologically well constrained. Such endeavours have been the focus of the Australasian-INTIMATE (INTegration of Icecore, Marine and TERrestrial archives) group and its subsidiary, NZ-INTIMATE, established in 2003 to undertake robust paleoclimate reconstructions (Alloway *et al.* 2007).

New Zealand is internationally recognised as a critical location for investigating the timing and magnitude of Quaternary climate fluctuations in the Southern Hemisphere (Newnham *et al.* 1999). It is geographically important with respect to paleoclimate reconstruction because it is a sensitive monitor of climate change, due to its (i) remote, oceanic and southern location spanning 17 degrees of the mid-latitudes; as a consequence New Zealand's climate responds quickly to changes in the ocean-atmospheric circulation system without the effects of continentality confounding climate signals; (ii) mountain ranges that face prevailing westerly winds, and are high enough to maintain glaciers and produce strongly differentiated regional climates that amplify climate signals; (iii) geologically young and dynamic landscape with a very short prehistory and therefore a relatively intact, unmodified forest cover compared to many other countries until around 700 years ago; and (iv) relative abundance of potential biotic paleoclimate proxies compared to other areas in Australasia by way of numerous peat swamps (McGlone 1988; Newnham *et al.* 1999).

The nature and extent of the interhemispheric climate linkages remains uncertain; evidence of an earlier LGM cooling in New Zealand compared to other regions of the world prompted Newnham *et al.* (2007) to introduce the term 'extended LGM (eLGM)' for the New Zealand climate event stratigraphy; furthermore, the Australasian INTIMATE group was hesitant about using Antarctic ice cores to establish a regional event

stratigraphy because of a disconnect between Antarctic and Australasia due to strong, Southern Hemisphere westerly winds and the Antarctic Circumpolar Current (Barrell *et al.* 2013). As a result of this conflicting evidence, the nature and extent of the interhemispheric climate linkages remains uncertain; as a consequence there is a need to increase reliability and robustness of proxy climate reconstructions in Southern Hemisphere mid-latitudes.

Although there are a considerable number of published palaeoenvironmental records from New Zealand, there is still a paucity of high resolution<sup>1</sup> multiproxy records that span long continuous periods of time (Vandergoes *et al.* 2005; Alloway *et al.* 2007). While there are a number of high resolution palynological studies from New Zealand, they typically cover periods of only a few hundred (e.g. Horrocks & Ogden 1998b) to a few thousand years (e.g. Horrocks & Ogden 1998a; Newnham & Lowe 2000); furthermore, they generally do not involve multiple proxies.

The NZ-INTIMATE subgroup prepared a provisional Climate Event Stratigraphy (CES) covering the last 30,000 years (Alloway *et al.* 2007). It is apparent that there are differences in the occurrence, timing and magnitude of these NZ-INTIMATE defined climate phases from region to region, no doubt due in part to latitudinal and altitudinal differences, differences in microclimate between sites, differences in analytical resolution and chronological control, and geographic lags and leads in climate change (Barrell *et al.* 2013). Furthermore, a single, composite CES can obscure some detail at the regional level, and regional events, especially those of short (less than say, one or two centuries) that do not conform to common climate patterns may be rejected as anomalous or unreliable (Blaauw 2012; Barrell *et al.* 2013).

A potential weakness of the CES is that due to the limited number of high resolution, continuous records available in New Zealand generally, only five of the continuous records used in the CES extend past the Last Glacial-Interglacial Transition (LGIT) and Last Glacial Maximum (LGM); therefore some uncertainty and disagreement remains regarding timing, duration and magnitude of important climate events, in particular (i) the timing of the Late Glacial Coldest Period (LGCP) onset; (ii) timing and duration of the LGCP warming complex; (iii) timing and duration of the Late Glacial Reversal (LGR); (iv) timing of Termination I; and (v) timing of the Early Holocene Warming (EHW) period.

A consequence of these weaknesses is that the CES requires thorough testing (Barrell *et al.* 2013). The current study contributes toward addressing these limitations by providing a chronologically well-constrained fossil pollen and aerosolic quartz narrative from Eltham Swamp, complemented with fossil pollen data from three coastal Taranaki sites covering the last 30,000 years. Barrell *et al.* (2013) highlighted the value of using a single, pollen-based proxy in constructing a climate stratotype for the New Zealand region, noting that a fossil pollen assemblage is both a simple measure of vegetation change, and is readily related to climate change. Furthermore, pollen is preserved in a range of environments, and there are now many published pollen records available to populate climate models. Barrell *et al.* (2013) selected records that likely represented regional-scale climate events, had good chronological controls, were of sufficiently high resolution, and could be temporally linked to other records by way of tephra deposits. The Eltham Swamp component of the current study covers *c.* 40,000 – 10,000 cal yrs BP, and therefore meets at least in part the criteria described by Barrell *et al.* (2013); furthermore, the primary core (Core A) was sampled for aerosolic quartz in addition to fossil pollen to provide a second paleoclimate proxy and insight into paleowind intensity during this time frame.

The resultant data provides a record of vegetation changes in response to climate change and allows quantitative paleotemperature reconstruction and qualitative estimates of paleowind intensity. Since the primary Eltham

---

<sup>1</sup> Although there is no generally accepted definition of ‘high resolution,’ other research in New Zealand described as ‘high resolution’ had reported resolutions ranging from *c.* 24 years, (Newnham & Lowe 2000) to *c.* 137 years, per sample (Horrocks & Ogden 1998b). Resolution for the most intensively analysed part of the Eltham core to date is around 40 years per sample.

Swamp core (Core A) spans around 10,000 to 40,000 cal yrs BP it covers significant climatic events that are well documented in ocean cores, ice cores and terrestrial records from both the Northern and Southern Hemispheres. The age of Core A makes it significant in that relatively few sediment cores have been extracted from this time range in the south-west of the North Island, and very few cores that span  $\geq 30,000$  years have been extracted in New Zealand.

The paleovegetation assemblage derived from fossil pollen data from Eltham Swamp was used as the basis to calculate biodiversity indices and to make inferences about changes in plant survival and reproductive strategies. Apart from their usefulness in helping to characterise changes in vegetation patterns through time, changes in biodiversity indices and plant strategy ratios can help make sense of the impacts of climatic and environmental disturbance drivers. For example, the Intermediate Disturbance Hypothesis (section 5.5.2) holds that biodiversity is highest under intermediate disturbance regimes, thus when aerosolic quartz data is combined with fossil pollen data, it is possible to determine changes in plant diversity in response to paleowinds of differing intensity.

Lignite deposits at five coastal Taranaki sites (Stent Road, Okawe Stream, Opunake Beach, Kaipokonui Beach and Lizzie Bell) were also sampled for fossil pollen in order to extend the paleovegetation and paleotemperature record back to around 80,000 years BP. The Eltham swamp and coastal Taranaki fossil pollen narratives augment pollen data from other cores in the Taranaki region (Bussell 1988; Alloway *et al.* 1992; Pillans *et al.* 1993; McGlone & Neall 1994); and in particular adds to the small set of cores that extend from the present back to the Last Glacial Maximum for New Zealand (e.g. McLea 1990; Newnham 1992; Lees *et al.* 1998; Newnham *et al.* 2007, 2008). The current study supplements an even smaller set of widely separated cores that encompass the Otamangakau Interstadial ( $\delta^{18}\text{O}$  stage 5a) to the Moerangi Interstadial ( $\delta^{18}\text{O}$  stage 3) period (e.g. McGlone *et al.* 1984; McGlone 1985; Shulmeister *et al.* 2001; Newnham *et al.* 2004) and provides the first quantitative temperature estimates for this time zone based on fossil pollen assemblages.

## 1.2 Research Objectives

This project aims to produce a high resolution, pollen-based palaeoenvironmental record from Eltham Swamp, eastern Taranaki, complemented with aerosolic quartz data from Eltham, and pollen data from lignites at coastal South Taranaki sites. This will ultimately further our understanding of vegetation and climate change in the New Zealand region over the last 80,000 years; in addition, a specific component of this project will involve testing the regional application of the NZ-INTIMATE climate event stratigraphy (CES) for Taranaki, informed in part by applying quantitative temperature estimates from pollen transfer functions. The rationale behind collecting aerosolic quartz data is that increased aerosolic quartz dust accumulation reflects a strengthening in wind intensity in response to steepening temperature gradients, and a more extensive terrestrial coastal plain to the west of the current New Zealand shoreline during lowered sea-levels during cold climate periods. This project is intended to:

- (i) produce a qualitative vegetation and quantitative paleotemperature reconstruction of regional Taranaki vegetation during the  $\delta^{18}\text{O}$  stage 5a (80,000 yrs BP) to the  $\delta^{18}\text{O}$  stage 3 (30,000 yrs BP) period using biotic proxies; specifically, through the production of a detailed palynological profile, for coastal Taranaki sites;
- (ii) produce a high-resolution, well-dated characterisation of environmental change and quantitative paleotemperature reconstruction for Eltham Swamp, New Zealand spanning 10,000 – 40,000 yrs bp using biotic proxies; specifically, through the production of a detailed palynological profile;
- (iii) derive a quantitative temperature reconstruction for the 40,000 to 10,000 year time period, to determine the magnitude of climate cooling over this time period, and investigate the timing of late

Quaternary New Zealand and Southern Hemisphere climatic events as identified by the NZ-INTIMATE community (Alloway *et al.* 2007; Lowe *et al.* 2008; Barrell *et al.* 2013) and to compare these temperature estimates to published estimates for other regions of New Zealand. Primary periods of interest include: Last Glacial Coldest Period (LGCP); Last Glacial Maximum (LGM); the Last Glacial-Interglacial Transition (LGIT); the Late-Glacial Warm Period (LGWP), the Late-Glacial Reversal (LGR); and Early Holocene Warming (EHW);

- (iv) produce a qualitative wind intensity determination using aerosolic quartz dust derived from peats at Eltham Swamp for the period 10,000 – 40,000 years before present, comparing results to other published results; and
- (v) use palynodiversity indices to assist in identifying and elucidating paleoclimate disturbances, and to test the responses of taxa richness to disturbance.

### 1.3 Research Questions

Specific research questions are:

- (i) What is the vegetation history from Eltham Swamp and the coastal Taranaki sites? How do they compare to other western North Island, and wider New Zealand, vegetation histories with respect to LGM cooling, LGIT and LGR climate change and EHW warming?
- (ii) How extreme was cooling during  $\delta^{18}\text{O}$  stage 4 compared to the LGM? Is there regional consistency between North Island and West Coast South Island records?
- (iii) What was the nature of the climate during  $\delta^{18}\text{O}$  stage 3?
- (iv) Does the Eltham pollen record distinguish millennial-scale climate events occurring over the last 30,000 years identified by NZ INTIMATE? If so, what is the inferred magnitude and timing of those events? How does the magnitude and timing of these climate events compare to events identified in the North Island, New Zealand?
- (v) Can aerosolic quartz be extracted from peat in sufficient quantities to elucidate past wind patterns?
- (vi) Were intense winds more prevalent during the LGM, as suggested by previous research?
- (vii) What is the impact of wind intensity and direction on vegetation patterns?
- (viii) Can biodiversity indices assist in paleoenvironmental and paleoclimate reconstruction or interpretation?

## 2. Taranaki Geography, Geology and Soils

### 2.1. Introduction

The Taranaki peninsula and the adjacent inland region can generally be divided into six major landform regions (Figure 1): (i) a volcanic landscape and ring plain located in the west of the region at the apex of the peninsula, surrounding Mount Taranaki /Mount Egmont (hereinafter referred to as Mount Egmont) and including both the Pouakai and Kaitake Ranges; (ii) mainly steepeland country occurring as a narrow strip to the east of the ring plain with a more or less N-S orientation, extending northeast of Inglewood in the north, to northeast of Hawera in the south; (iii) inland hill country to the east of the frontal hill country, occupying much of the ‘base’ of the peninsula and extending from the north-east coast towards the south-east coast, excluding a 10-15km wide coastal corridor extending from Hawera to the Waitotara River catchment (Taranaki Regional Council 2003).

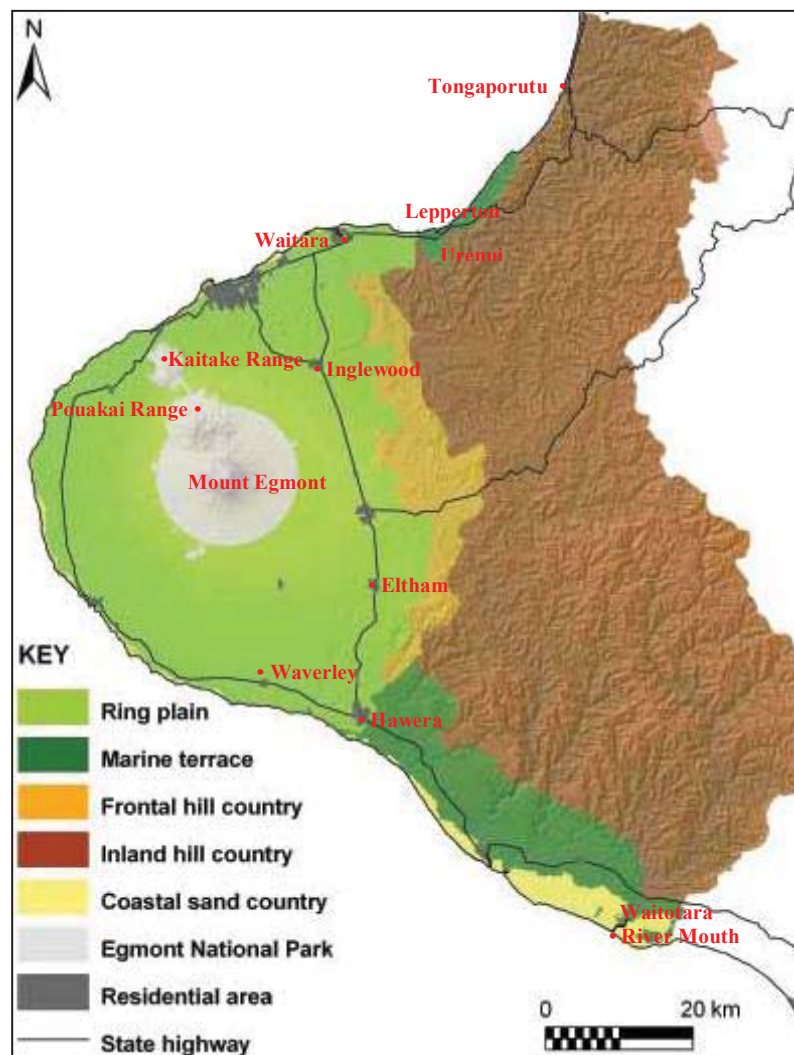


**Figure 1. Major Landform Regions in Taranaki.** *Source:* Taranaki Regional Council (2009)

This corridor encompasses three other general landform types: (iv) a 10km strip of inland terraces that run more or less parallel with the southeastern coast of the peninsula; and (v) a narrower strip of coastal terraces (also found in a smaller area in the north between Urenui and Tongaporutu). Together, these marine terraces reach up to 20km inland between Waitara and Lepperton on the northern part of the peninsula, and south of Hawera. (vi) coastal sand areas border much of the predominantly cliff coastline around the Taranaki peninsula as narrow, < 1km wide dunefields, which broaden south of Hawera, reaching around 7 km inland near Waverley.

Overall, just over 2% of the Taranaki region is comprised of coastal sand country (Taranaki Regional Council 2003).

## 2.2. North Island Tectonics and the Taranaki Volcanic Lineament

An active lithospheric plate boundary formed by the Pacific Plate plunging underneath the Australian Plate, extends 2,800 km south from the Tongan Island Arc, through the Kermadec Arc to the Hikurangi Trough lying to the east of the North Island (Figure 2). The Taupo Volcanic Zone is the southern-most expression of the Tonga-Kermadec portion of the subduction system, extending around 300 km from the Bay of Plenty in a SSW direction, whereas the Taranaki volcanic succession lies 140 km to the west of the TVC and is the western-most expression of subduction-related volcanism in New Zealand. The Benioff-Wadati zone, an area of seismic activity delineating the upper surface of the subducting slab lies around 180 km beneath Mount Egmont (Price *et al.* 1999).

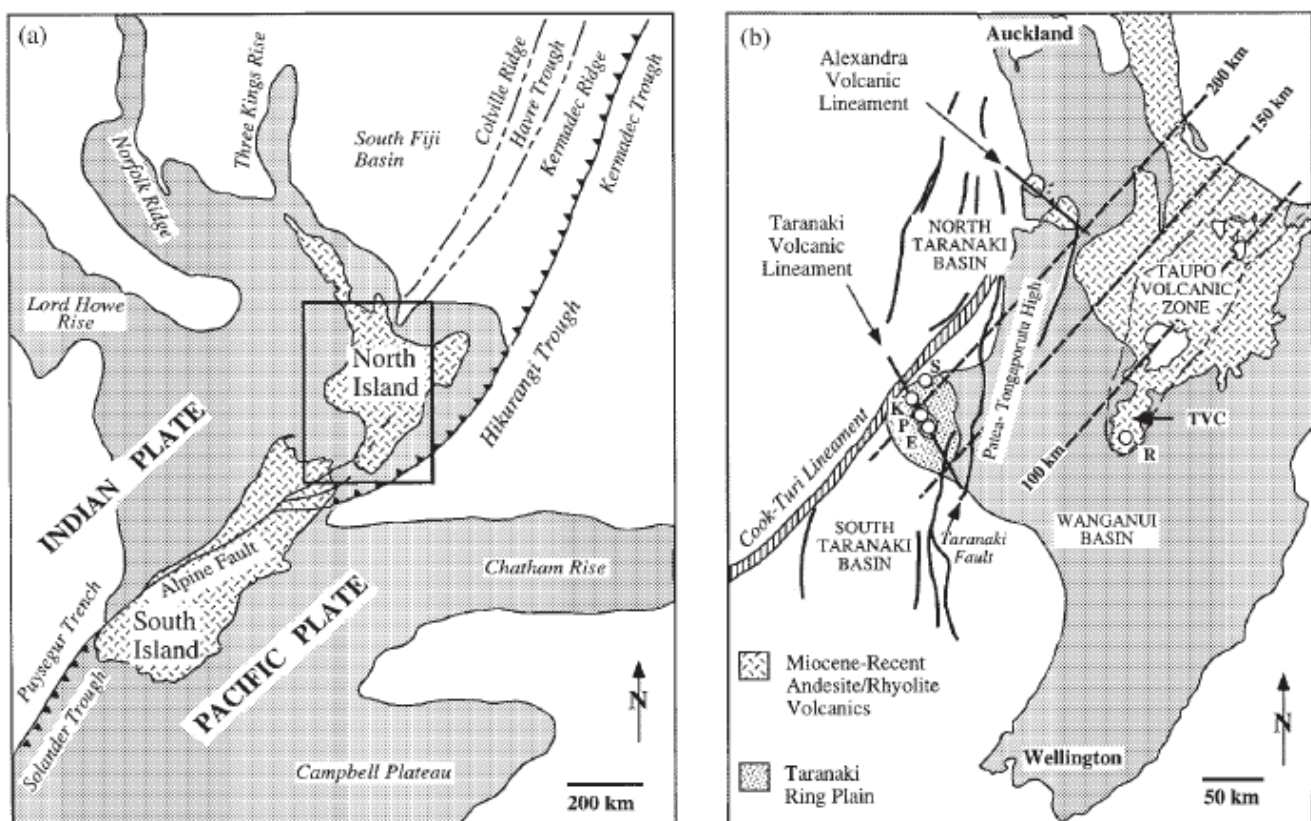


**Figure 2. Tectonic and Geological Setting of Taranaki Volcanoes.** (a) Regional tectonic setting, showing the active subduction zones (Hikurangi, Kermadec and Solander Troughs), and the submarine continental crust in grey. (b) North Island geological setting. The 100, 150 and 200 km isobaths show the depth to the Wadati-Benioff zone; the Taranaki Volcanic lineament is comprised of, from North to South: Sugar Loaf Islands –Paritutu (S), Kaitake Volcano (K), Pouakai Volcano (P) and Mt Egmont (E). *Source:* Price *et al.* (1999)

The alignment of four Quaternary andesitic cones in a northwest to southeast direction represents the migration of volcanism to the southeast over time: (i) Paritutu Volcano is the oldest centre in the lineament, dated at around 1.7 million years old (Neall 1979). The remains of this centre are the Sugar Loaf Island cumuldomes off the coast of New Plymouth, and the volcanic spine Paritutu rock (Figure 3). These remnant edifices are composed of plagioclase-phyric, strongly porphyritic andesites (Grant-Taylor 1964, Price *et al.* 1999); (ii) farther inland and to the south of Paritutu lies Kaitake Volcano; this stratovolcano was active 575,000 years BP, and is comprised of hornblende andesite and some diorite (Price *et al.* 1999). (iii) To the southeast of Kaitake lies Pouakai Volcano (1,399m), active between 675,000 and 270,000 yrs BP (Neall 1979) and comprised of hornblende andesites; and (iv) Mount Egmont (2,518m) lying southeast of Pouakai Volcano is New Zealand’s largest andesitic stratovolcano with a base 25 km in circumference (Alloway *et al.* 1995), and is

the youngest volcano in the Taranaki Volcanic Succession (Figure 4). Mount Egmont began its volcanic activity between 130,000 (Zernack 2008) and 200,000 years BP (Neall 1975; Zernack *et al.* 2009; Turner *et al.* 2011) and the composition of its lavas varies between vesicular red and black scoria to non-vesicular or holocrystalline, porphyritic lavas, with a geochemistry dominated by a high-K basaltic andesite. Egmont tephra are markedly more potassic than andesites and dacites from nearby volcanoes such as Ruapehu (Price *et al.* 1999).



**Figure 3. Oil Derricks at Moturoa, New Plymouth, with Ngamoti beach on the right.** Taken by an unknown photographer *c.* 1910. Paritutu is on the left, with the Sugar Loaf Islands on the right. *Source:* Alexander Turnbull Library, Wellington, New Zealand, Ref: 1/1-007630-G. <http://beta.natlib.govt.nz/records/22738542> downloaded 13.08.12



**Figure 4. Mount Egmont as seen from Eltham 05. 12. 2011**

Mount Egmont has erupted andesitic tephra at least 16 times since 28,000 yrs BP (Alloway *et al.* 1995); some of the resultant tephras are used as age controls in the pollen chronology as described in section 7.4. In addition, Zernack *et al.* (2011) utilised exposed debris avalanches and lahar deposits on the coast to show that Mount Egmont has undergone at least 14 cone-building and collapse cycles; these volcanoclastic lithofacies have also been used to provide chronological constraints for >20,000 year old fossil pollen age models.

### 2.3. Taranaki Soils

The major volcanic ash soils on the Egmont ring plain are Andisols, derived from Late Quaternary Egmont fine-grained andesitic tephra showers and lapilli that have periodically accumulated and subsequently weathered. These Andisols are manifest as classic Allophanic Soils (Hewitt 1992), characterised by a high allophane content, high porosity and permeability, and friable consistency (Stewart *et al.* 1977), low plasticity and stickiness (Neall 1977) and low bulk densities (Franks *et al.* 1991). The allophane clays are informally referred to as amorphous but in fact are poorly crystalline and have a strong affinity for organic matter (Neall 1977).

One notable characteristic of some Taranaki soils is the formation of iron pans on sites that are or were at one time poorly drained; high rainfall on Mount Egmont mobilises large quantities of iron from the andesites. Iron accumulates at the interface between the original deposit and subsequent tephra deposits; if rapid tephra deposition occurs a free-draining soil with a friable B-horizon is formed, whereas slow tephra deposition may result in the formation of a continuous iron pan. This iron pan impedes drainage and a perched water table and gley soils form (Neall 1977); iron pans can be seen at Okaweu Stream (Figure 28) and a thinner iron pan at Stent Road (Figure 27). Further tephra emplacement elevates the developing soil mass above the water table, so that it becomes friable and free draining.

Coastal Egmont loams occur in South Taranaki with either (i) black topsoils formed under *Phormium tenax* and *Pteridium esculentum* scrub proximal to the coast, or (ii) brown topsoils, formed under podocarp-hardwood forest inland from the coast.

Peat deposits occur in areas where tephra deposits are of insufficient thickness to overwhelm the peats and transform them into Andisols (Alloway *et al.* 1992). Lahars and landslides may block drainage outlets allowing water bodies to grow in size, and a peat-forming, wetland to persist, enhancing peat accumulation. Subsequent burial by lahar, landslide or airfall deposits preserves the peats, as has occurred at Eltham. Therefore, the Eltham series that is mapped in the Eltham and Ngaere Swamps is classified as an Organic Soil (Hewitt 1992), derived from parent material of woody peat with interbedded tephra (Franks *et al.* 1991). This soil series is described as a poorly drained peat interbedded with thin, andesitic tephra layers, irregular pumiceous and lithic lapilli, and partly decomposed wood and twig fragments and fibres (Franks *et al.* 1991).

## 3. Present Climate of Taranaki

### 3.1. Introduction

Since “The climate of an area may be considered as the integrated effect of various weather situations that affect it,” (Thompson 1981), this section briefly describes Taranaki weather in order to establish the basic atmospheric processes that drive climate, and to assist interpretation of paleovegetation and paleoclimate proxy data. In general, since the Taranaki region is located on the western side of the North Island and is bordered by ocean to the north, west and south, it is subject to weather systems moving from the north and west whilst simultaneously exposed to a temperate, oceanic climate. As a result, a subtropical belt of travelling anticyclones to the north of New Zealand and westerly airflows to the south (Figure 5) expose the Taranaki region to northwesterly winds so that disturbed, windy and mild weather systems from the Tasman Sea predominate much of the time.

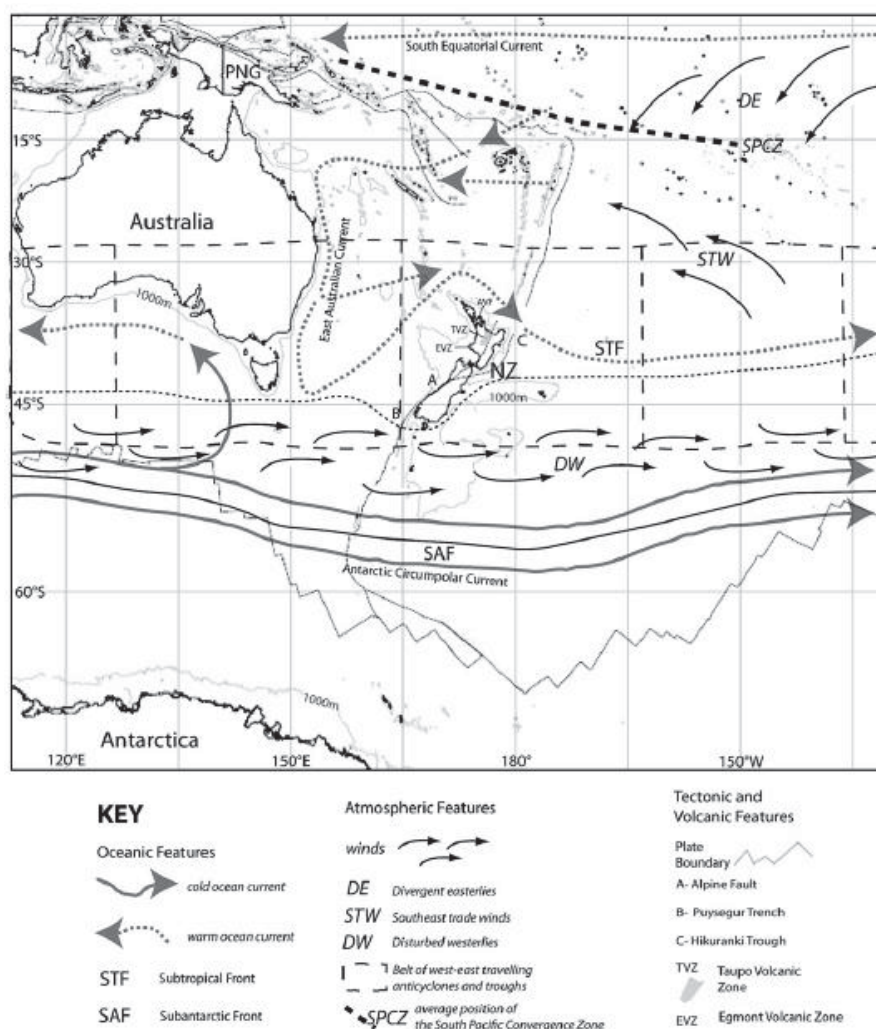


Figure 5. New Zealand's Position in the South Pacific Ocean, and Major Ocean Currents and Winds. Source: Lorrey *et al.* 2012

### 3.2. Temperature

Mean annual terrestrial temperatures in Taranaki range between 11°C and 14°C at low altitudes. Summer daytime maximum air temperatures are mild, typically ranging from 19°C to 24°C; similarly, winters are relatively mild with maximum air temperatures ranging from 10°C to 14°C, and frosts largely restricted to inland areas in the absence of wind in winter.

The 13°C isotherm for median annual temperature generally follows the 100m contour. Median temperatures in the eastern stepland range from 10 - 12°C. The isotherms are compressed over Mount Egmont and the Pouakai Range in response to rapidly steepening terrain, and the warmest part of the region lies between Cape Egmont and Motonui on the north-west coast, where median temperatures are 14 - 15°C (Figure 6).

In general, temperatures decrease with altitude and with distance from the sea (Figure 7). For example, the mean annual temperatures at Stratford Mountain House (altitude 846m) and North Egmont (altitude 955m) are approximately the same as the mean July temperature at the lowland, coastal station at Manaia demonstration farm (altitude 98m). This pattern is to be expected from simple lapse rate calculations; for example, using an environmental lapse rate of 0.65°C/100m the predicted temperature difference between Stratford Mountain House (Appendix 11.1) and Manaia is 4.79°C in July, which compares with an observed difference of 4.75°C. Similarly, the predicted mean temperature difference between Cape Egmont and North Egmont is 6.06°C in July, which

compares with an observed difference of  $5.75^{\circ}\text{C}^2$ .

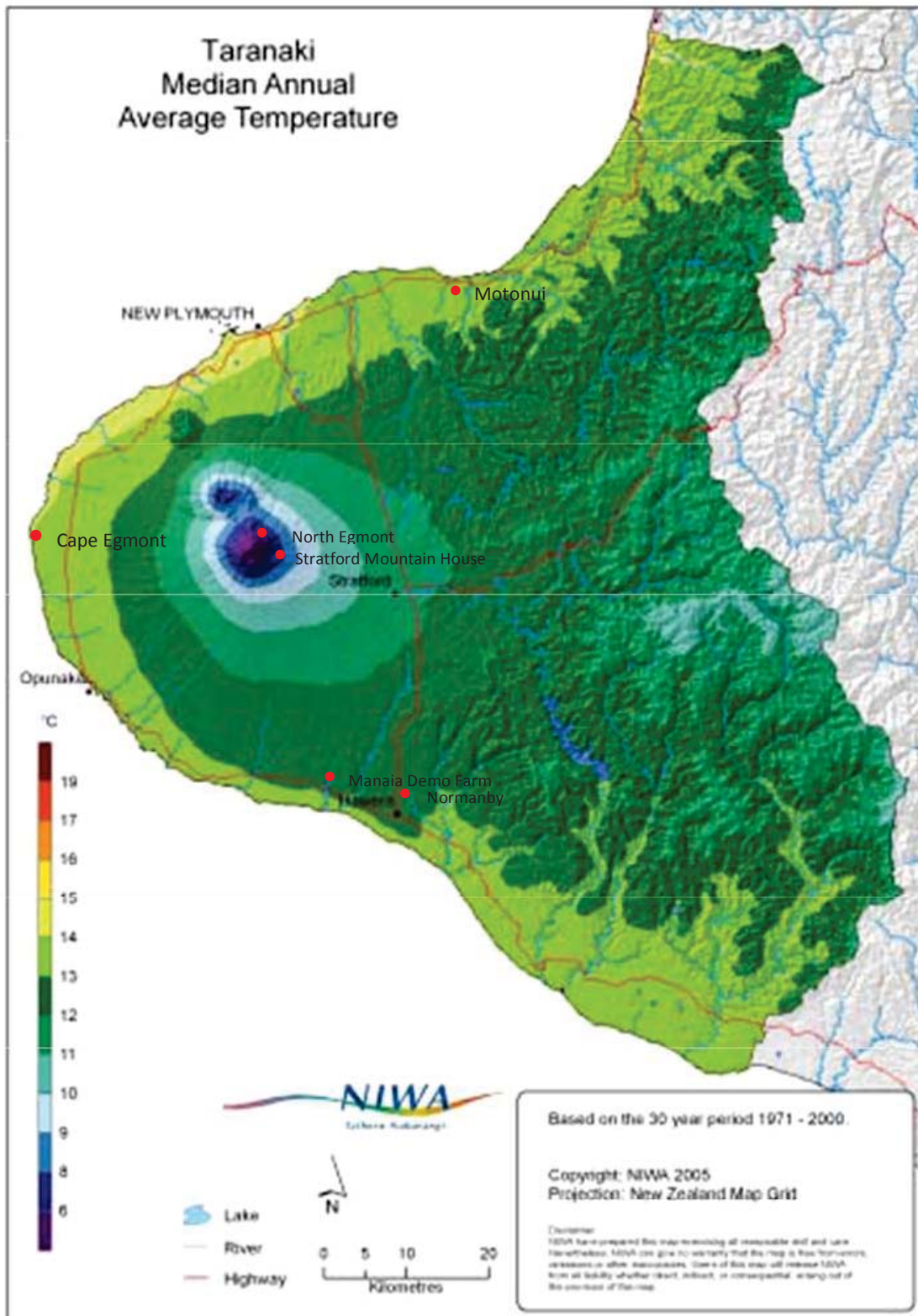


Figure 6. Isotherm Map of Median Temperatures for Taranaki Region, 1971 -2000. Source: Baldi & Salinger (2008)

<sup>2</sup> Stratford Mountain House altitude - Manaia altitude =  $0.846 \text{ km} - 0.098 \text{ km} = 0.748 \text{ km}$ ;  $0.748 \times 6.4^{\circ}\text{C} = 4.787^{\circ}\text{C}$ ; North Egmont altitude - Cape Egmont altitude =  $0.955 \text{ km} - 0.008 \text{ km} = 0.947 \text{ km}$ ;  $0.947 \text{ km} \times 6.4 = 6.061^{\circ}\text{C}$ .

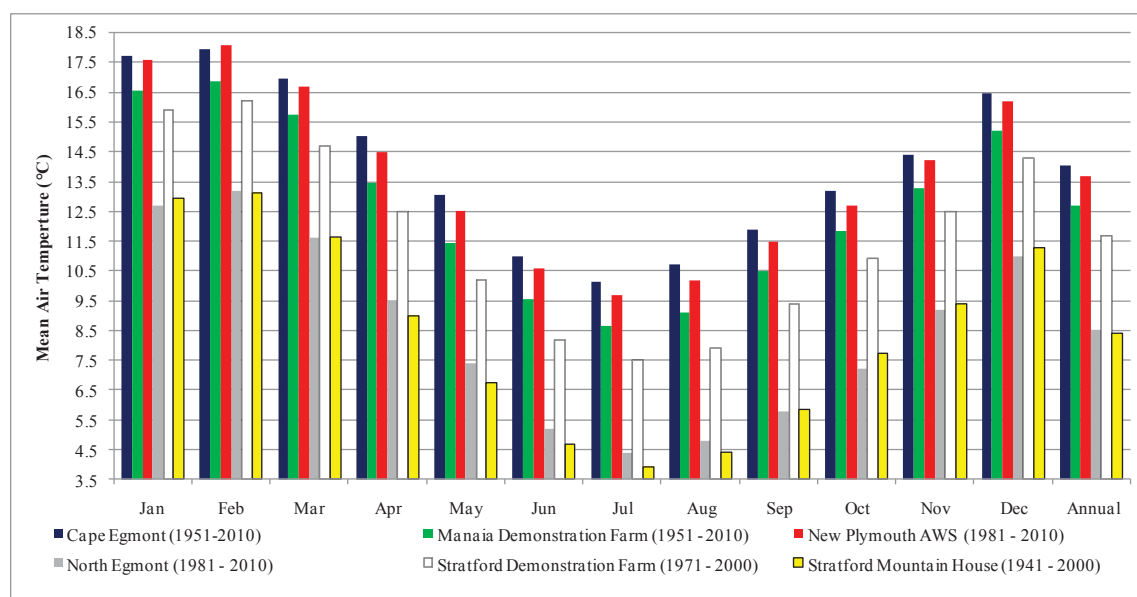


Figure 7. Mean Monthly Temperatures for Selected Taranaki Sites.

### 3.3. Winds

#### 3.3.1. Introduction

Modern-day New Zealand lies within an atmospheric belt of east-moving anticyclones, troughs, depressions and fronts that lie between 30°S and 50°S and also within the oceanic and east-moving, subtropical front. These belts are bounded to the south by the Antarctic Circumpolar Current (ACC) and to the north by the southern boundary of the South-easterly Trade Winds (STW) (Sturman & Tapper 2006; Lorrey *et al.* 2012). As a consequence of these atmospheric and oceanic currents, the New Zealand landmass is influenced by both subtropical and sub-Antarctic climates in the context of a maritime setting.

Subtropical and sub-Antarctic climates have climatic teleconnections to regional-scale climatic cycles that operate at different time scales (Lorrey *et al.* 2012): (i) The Southern Annular Mode (SAM) is a meridional shift of the tropospheric jet from its mean climatological position coinciding with the seasons (Kidston *et al.* 2009) so that during summer (positive SAM) more easterly winds occur across the country, but in winter (negative SAM) winds from the NE are more common over the North Island. When SAM is positive rainfall is lower in all districts apart from Northland and east coast North Island, where orographic subsidence is reduced and showers are more likely.

(ii) The El Niño-Southern Oscillation (ENSO) cycle occurs irregularly over periods of three to seven years, and lasts about 12 months, alternating with La Niña events. During El Niño phases, ‘zonal’ circulation is more frequent and more intense; the easterly trade wind to the north of New Zealand weakens, whilst the south-westerly flow strengthens, so that precipitation is higher in the southwest and drier conditions prevail in the north and east of the country (Kidson 2000), due to the foehn effect. In contrast, La Niña events are characterised by ‘meridional’ circulation: north easterly winds strengthen, with northern and eastern districts experiencing higher rainfalls, and drier conditions are more common in the south and west as a consequence of westerly ‘blocking’ by large, stationary anticyclones situated in the Tasman Sea (Sturman & Tapper 2006).

(iii) The Interdecadal Pacific Oscillation (IPO) causes abrupt shifts in Pacific circulation patterns that persist for decades. The positive phase of the IPO produces more westerly winds over the country; in the negative phase more easterlies and north easterlies occur over northern New Zealand, with increased tropical disturbances (Thompson 1981); in addition, the IPO modulates ENSO-related climate variability (Salinger *et al.* 2001) such that during positive phases of the IPO (when sea surface temperatures in the tropical Pacific Ocean are raised)

the effects of ENSO and Australasian climate are weakened. Conversely, during negative IPO phases, the relationship between ENSO and annual rainfall and temperatures are enhanced (Sturman & Tapper 2006).

### 3.3.2. Taranaki Winds

Both high altitude and surface winds are strongly influenced by local topographic features, including Mount Egmont, the central high country and the alignment of the coast (Thompson, 1981). Strong or very strong, predominantly westerly winds are a feature of sites > 1000m, with airflow over Mt Egmont often influencing winds on the lowlands. The most common wind at New Plymouth Airport in addition to the westerly is the southeasterly, occurring around one quarter of the time (Figure 8). The latter winds occur because Mount Egmont deflects southerly airflows to the south-east.

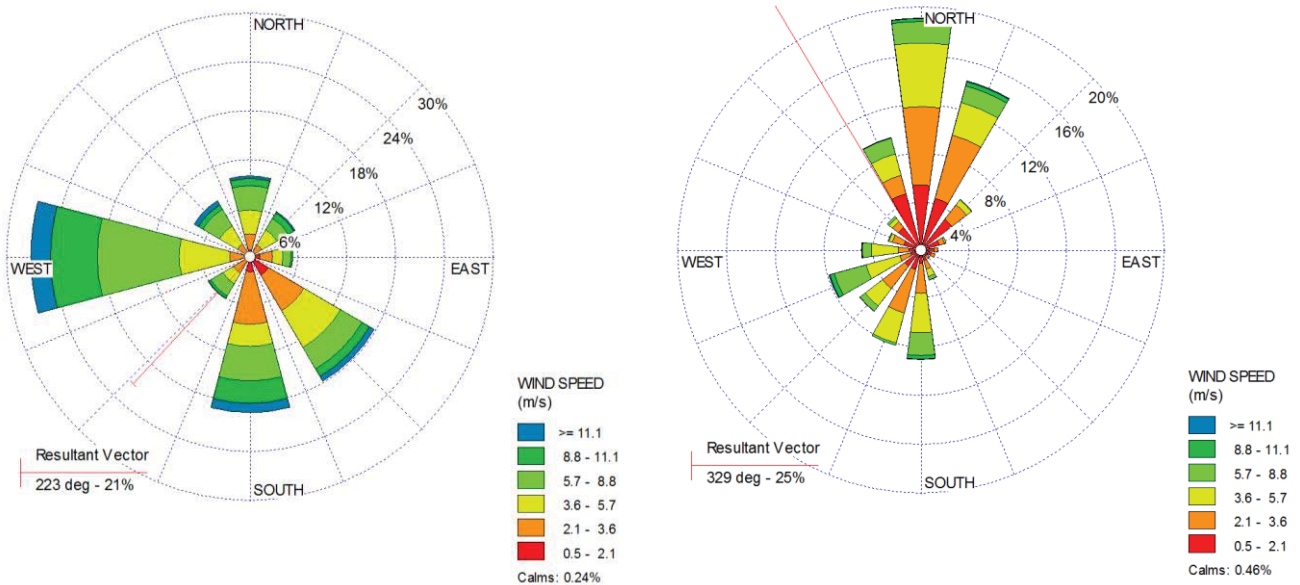


Figure 8 Windrose New Plymouth Aero<sup>3</sup> 0600-1100 hrs      Figure 9. Stratford Demonstration Farm (17.09.02–19.02.11)

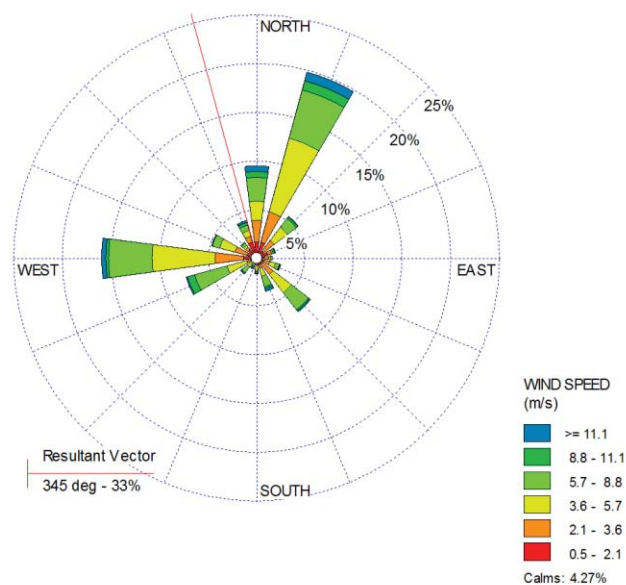


Figure 10. Normanby (20.05.96–08.03.04)

<sup>3</sup> New Plymouth Aerodrome station readings are from 20.05.2005 to 31.03.2012.

At Stratford Demonstration Farm, c. 10 km north of Eltham, meridional winds dominate from the north and the south. According to Thompson (1981) at the Egmont East weather station, westerly and north-westerly winds are deflected around the northern side of Mt Egmont and are therefore manifested as northerlies, whereas surface south-easterlies from South Taranaki are manifested as southerlies. Stratford Demonstration Farm has few easterlies, with most winds from the northerly and southerly quarters. Westerly winds are deflected by Mount Egmont to the south, forming a north westerly wind at Stratford. At Normanby the westerlies are no longer deflected by Mount Egmont, so westerly and north-easterly winds predominate.

Orographic lifting of airmasses on the windward side of Mount Egmont lead to cooling and expansion at the dry adiabatic lapse rate,  $\Gamma$  ( $0.98^{\circ}\text{C}/100\text{m}$ ) until the airmass reaches its condensation level, and clouds form, precipitating rain on the windward side. As the airmass descends on the leeward side it is compressed and warms at the saturated adiabatic lapse rate  $\Gamma_s$  ( $0.7^{\circ}\text{C}/100\text{m}$ ), giving rise to a foehn wind on the leeward side that is warmer, drier and therefore has a higher lifting condensation level, than the airmass on the windward side of the mountain.

In addition to blocking and deflecting airflow, mountains like Mount Egmont cause disturbances including production of eddies, lee waves, foehn effects and lee troughs, and modify synoptic features through lee cyclogenesis, increased rainfall and effects on fronts (Sturman & Tapper 2006).

### 3.3.2.1. Strong - Gale Force Winds, Tropical Cyclones and Tornadoes

Strong and gale force winds are relatively common over the Taranaki region, occurring most frequently from either the south or northwest. Wind gusts  $> 62$  km/h occur on average around 80 days per year at lower elevations, and 120 days per year at more exposed sites or higher altitudes. Wind gusts exceeding 94 km/h happen about five days per year at lowland sites, and 20 days per year at higher altitudes.

Most ex-tropical cyclones affecting the Taranaki region have their origins within convective areas over the warm tropical waters (SSTs  $> 27^{\circ}\text{C}$ ) of the Coral Sea around Vanuatu. Once ex-tropical cyclones enter the north Tasman Sea they usually track east to southeast between Australia and New Zealand (Baldi & Salinger (2008). One or more ex-tropical cyclones occurred in Taranaki in 22 of the 37 years (59%) between 1968 and 2005. Most ex-tropical cyclones occur during February and March since SSTs are highest in these months. Tropical cyclones affecting Taranaki are 25% more likely to occur during La Niña or neutral conditions, when they form further south in the Pacific (near Vanuatu) than during El Niño conditions (near the Solomon Islands) and enter the Tasman Sea (Baldi & Salinger 2008).

When the centre of a tropical cyclone lies to the north of the Taranaki region, high winds result from the southeast, whereas if the centre of the cyclone lies to the west, northerly gales occur. Strong to gale force north or northwest winds over the Taranaki region result from northerly airflows ahead of fronts, depressions or cyclones. For example, northerly gusts of 133 km/h recorded at Egmont East during Cyclone Alison in March 1975 downed lines of *Beilschmiedia tawa* in northwest Egmont National Park (Burgess *et al.* 2006).

South or southeast winds can be particularly strong with deep depressions or strong cyclones, as the windflow is either channelled by Cook Strait up from the south, or are downslope leeward winds from the central North Island high country. Northwest or westerly winds that result from westerly airstreams, when high pressure systems move to the north of the country, and migratory depressions lie to the south of New Zealand. In contrast, southerly or southeast winds arise when a depression occurs to the east or southeast of the North Island and anticyclones lie south or southeast of the country. Strong southeast winds are manifested as downslope leeward winds from the central North Island high country, or as very strong south or southeast winds channelled by Cook Strait from the south associated with deep depressions or strong cyclones (Baldi & Salinger 2008). For example, in March 1988 a large pressure gradient over the North Island formed between southward-

tracking Cyclone Bola, and an area of elevated air pressure over the South Island. This pressure gradient produced southeast gale force winds in excess of 118 km/h at the Maui gas platform (Burgess *et al.* 2006).

Strong winds and tornadoes occur over Taranaki in response to large scale weather patterns affecting New Zealand: strong northerly to westerly airflows migrating from the Tasman Sea bring intense fronts, troughs, deep depressions or cyclones; whilst south-easterly airflows over the region are associated with down-slope leeward winds from the central North Island. Although the highest gusts at New Plymouth came from the southeast where the 50 year return period was in excess of 145 kph, gusts just below 110 kph are more common from the west, with return periods up to five years (Baldi & Salinger 2008).

Tornadoes often have their genesis in well-developed thunderstorm cells on cold fronts where an advancing mass of cold air overtakes and displaces pre-existing warmer humid air; others originate at sea as strong waterspouts which migrate across the coast, to form a tornado as the twisting funnel moves from land to sea (Baldi & Salinger 2008). Burgess *et al.* (2007) and Salinger *et al.* (2007) found that 61 tornadoes and waterspouts occurred within the Taranaki region between 1951 and 2007, suggesting that on average about one tornado will occur somewhere in the Taranaki region each year, with severe tornadoes occurring about one year in four. Most Taranaki tornadoes had estimated maximum wind speeds in the 116 – 180 kph range, with ten percent or more attaining wind speeds > 180 kph. Track or damage widths ranged from 15 to 500 m (average 100 m) with track lengths ranging from 1.5 to 16 km (average 5 km).

Weather conditions indicating the presence of a trough of low pressure and associated frontal activity over or west of Taranaki typically precede tornadoes. These conditions include cumulonimbus cloud and/or associated thunderstorms, moderate to heavy intensity rainfall or hail, low air pressure at sea level, and N to W winds.

### 3.4. Precipitation

Much of Taranaki receives an annual rainfall > 1800mm although rainfall totals vary across the region with topography and elevation (Thompson 1981), with coastal areas receiving 1400 - 1600 mm per annum, in contrast to the upper slopes of Mount Egmont receiving > 5000 mm per annum. The Taranaki region's heaviest rainfall arises when warm moist northerly airflow moves from the tropics onto the district, as occurs when fronts lying near Taranaki to the north or south become slow moving, or when depressions move across the region from the west.

Mount Egmont intercepts moist air moving to the south, then orographic lifting forces the moisture to precipitate out to the north. As a consequence a rain shadow is produced so that lowland areas to the southeast of Mount Egmont receive less rainfall than areas to the north and east of the mountain. The rainshadow is shown in Figure 11 between the 2000mm isohyet that encompasses Eltham and the 1500mm isohyet that encompasses weather stations at Omoana, Taumatatahi and Nukuhau to the southeast. Rawhitiroa road, where the Eltham core came from, translates as 'sun shining for a long time,' a reference to the higher number of sunshine hours that occur in the rain shadow.

Figure 12 shows the relationship between altitude and rainfall for selected sites in Taranaki; there is a strong correlation between altitude and rainfall ( $r = 0.97$ ), in other words 94% of the variance in annual rainfall is explained by elevation. In contrast, the correlation between latitude and rainfall is weak ( $r = 0.25$ ).

Droughts (higher than normal potential evapotranspiration deficit, PED) are infrequent in the Taranaki region, with dry conditions most often occurring during episodes of easterly flow with increased frequencies of anticyclones occurring east of the South Island (Baldi & Salinger 2008). These episodes of easterly airflow and increased numbers of anticyclones to the east of the South Island account for 29% of the total variability in PED over the North Island (Salinger *et al.* 2006). Conversely, wetter seasons typically occur when more troughs than usual cross the region.

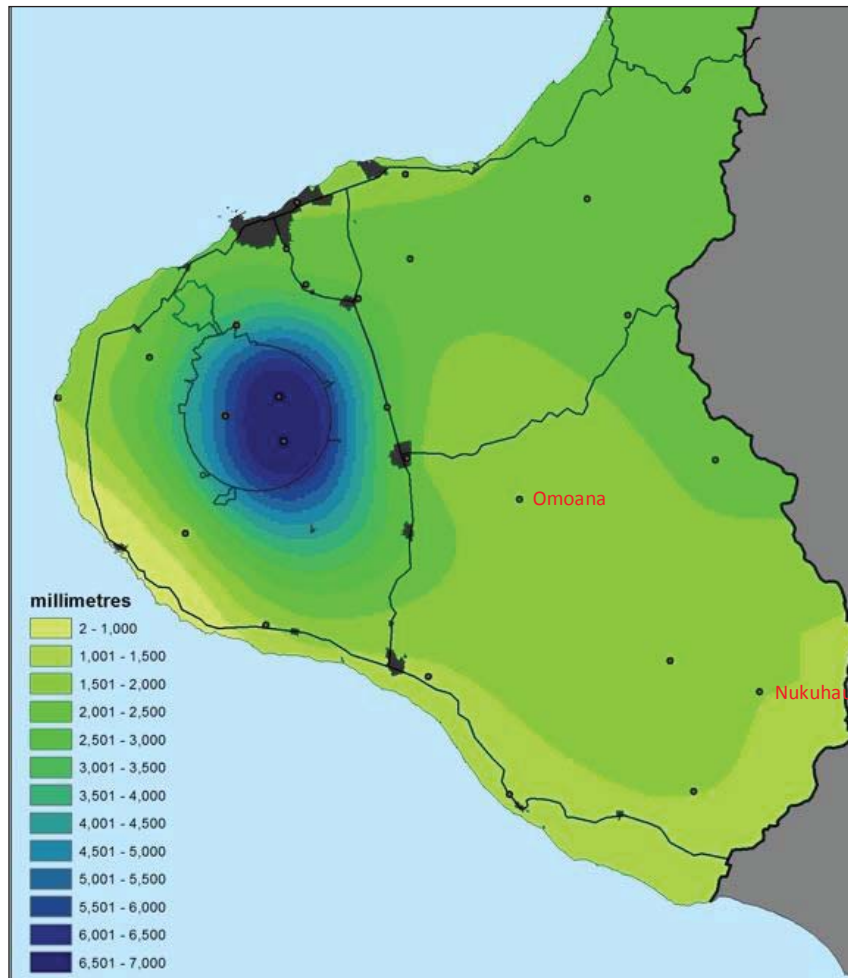


Figure 11. Isohyet Map, January–December 2011 Source: Taranaki Regional Council 2012

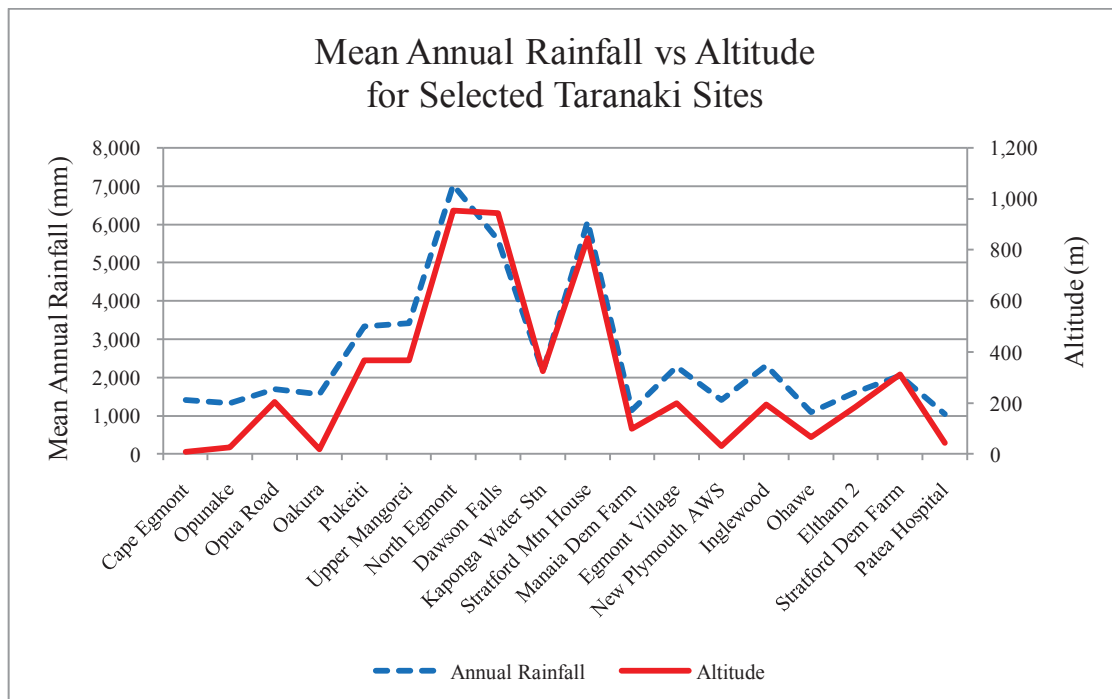


Figure 12. Mean Annual Rainfall vs Altitude for Selected Taranaki Sites. Altitude of sites increases left to right.

The long term annual average (1972-73 to 2001-02) PED for Taranaki shows quite small moisture deficits except for a narrow coastal strip, between Okahu River in the north and Kaipokonui stream in the south. Baldi & Salinger (2008) note the northern part of the Taranaki region experiences some moisture deficit, but the southern coast is drier, with annual moisture deficits ranging from 25 to 75mm immediately east of Mount Egmont to as much as 200mm along parts of the southern coast.

During El Niño years, stronger and more frequent west to southwest winds occur in Taranaki; this causes relatively cool conditions with lower average land and sea surface temperatures, and as a consequence there is lower rainfall overall. Although precipitation is reduced, occasional heavy showers may occur due to a higher incidence of cool blustery southwest winds. Conversely, during La Niña events, westerlies weaken in summer, and northerly winds become more common in winter, such that rainfall increases during winter and spring. Heavy rainfall events in Taranaki increase in frequency during La Niña years, often in response to subtropical lows coming from the north Tasman (Baldi & Salinger 2008).

#### 4. Late Quaternary Climate Change in New Zealand

The purpose of this section is to briefly review late Quaternary climate change in New Zealand in the context of the New Zealand INTIMATE (Integration of Ice, Marine and Terrestrial Records) climate event stratigraphy (CES) framework (Alloway *et al.* 2007; Lowe *et al.* 2008; Barrell *et al.* 2013). This provides a temporal framework at a continental scale to aid in interpreting the findings from the current study for the period 30,000 - 9,750 cal yrs BP, and also provides the opportunity for regional comparisons to elucidate climate patterns in the past. At the time of writing, the generally accepted chronology of Late Quaternary climate change events is based on NZ-INTIMATE group determinations given in Barrell *et al.* (2013), however much of the current study uses an earlier NZ-INTIMATE schema, as given in Alloway *et al.* (2007). The relationship between Alloway *et al.* (2007) and Barrell *et al.* (2013) is shown in Table 1.

**Late Glacial Coldest Period (LGCP) 28,800 ± 400 - 18,000 cal yrs BP.** The NZ-INTIMATE group (Barrell *et al.* 2013) determined that the LGCP occurred 29,000 to 18,000 cal yrs BP, comprised of four overlapping divisions:

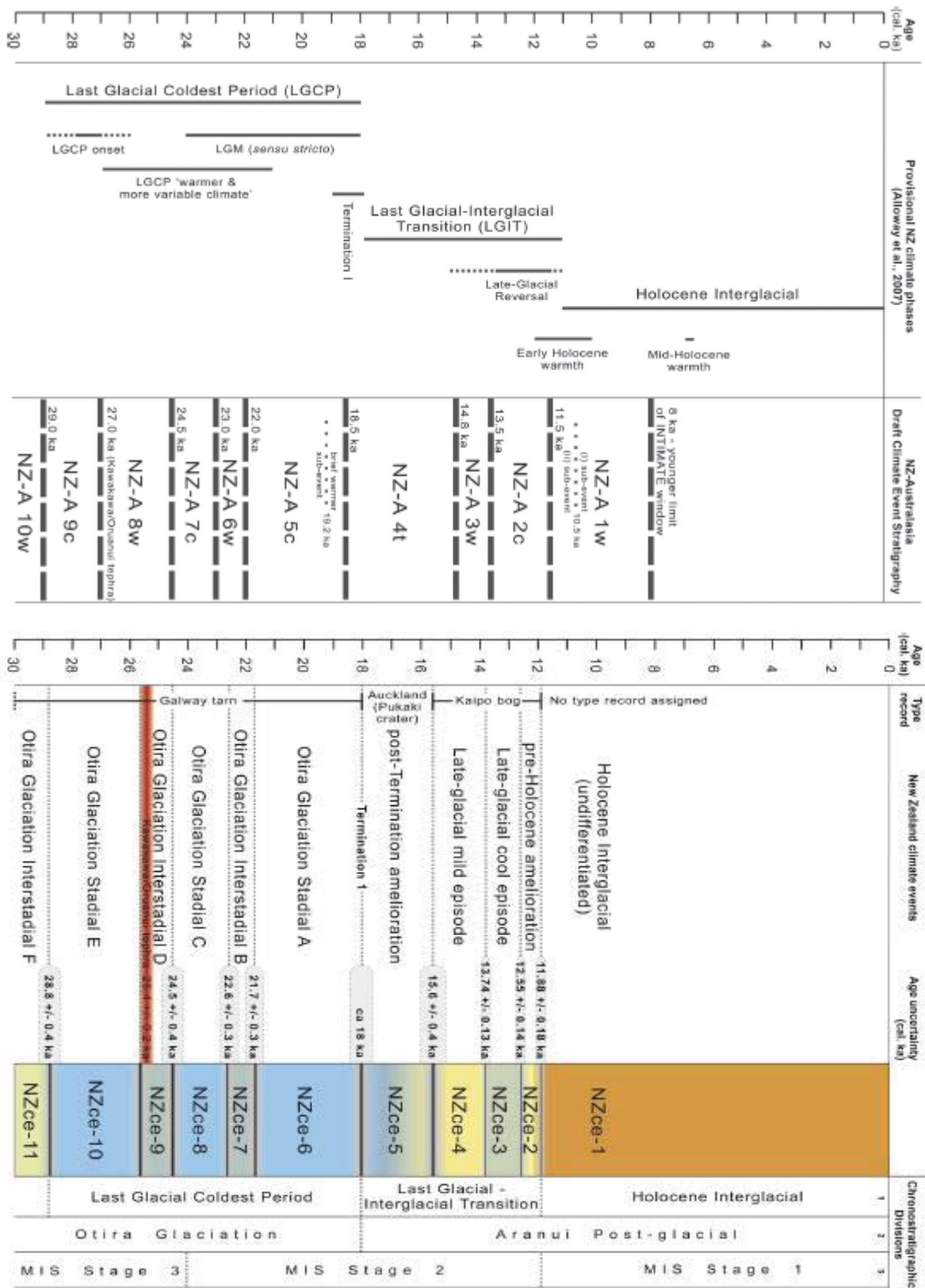
(1) **LGCP onset c. 29,000 – 26,000 cal yrs BP.** This part of the LGCP climate phase was marked by a decrease in mean annual temperatures throughout New Zealand, as indicated by a increase in the relative proportion of pollen from cold tolerant herbaceous taxa and a corresponding decrease in pollen from cold-intolerant taxa from sites including Onepoto<sup>4</sup> and Lake Pupuke craters and Pukaki (Alloway *et al.* 2007) in Auckland, and Okarito, on the West Coast, South Island (Vandergoes *et al.* 2005; Newnham *et al.* 2007).

The onset of the New Zealand LGCP as defined by NZ-INTIMATE is later than several other New Zealand estimates, for example glacial advance associated with cooling commenced earlier at Taramakau Glacier, north Westland between 34,000 and 28,000 cal yrs BP (Suggate & Almond 2005; Sutherland *et al.* 2007), and later than other Southern Hemisphere estimates, for example between 32,000 and 35,000 years BP in Chile (Denton *et al.* 1999; Fairbanks *et al.* 2006) and between 39,000 and 46,000 years BP in Tasmania (Barrows *et al.* 2002). This event was re-named the **Otira Glaciation Stadial E** (NZce-10) by the NZ-INTIMATE group (Barrell *et al.* 2013) and the age range redefined as 28,800 ± 400 – 25,358 ± 162 cal yrs BP.

(2) **Mid-Late Glacial Coldest Period warmer and more variable interval (27,000 – 21,000 cal yrs BP).** A milder period with cooler intervals punctuating the LGCP is weakly signalled at the Auckland crater lakes between 26,700 and 21,000 cal yrs BP (Alloway *et al.* 2007) based on increases in the log ratio of lowland podocarp: grass pollen (LPG ratio) at Pukaki (Sandiford *et al.* 2001, 2003) and total organic carbon content in

---

<sup>4</sup> Locations of palynological and aerosolic dust sites referred to in this section are shown in Appendix 11.2.



2007

Table 1. Relationship between 2007 NZ-INTIMATE CES and 2013 NZ-INTIMATE CES Source: Alloway et al. (2007); Barrell et al. (2013).

Onepoto lake sediments (Hägg & Augustinus 2003) as the floral assemblage and biomass production responded to climate amelioration.

$\delta^{18}\text{O}$  records from Nettlebed and Exhaleair caves, north-west South Island speleothems (Hellstrom *et al.* 1998) indicate that the general cooling associated with the LGCP was interspersed with a six thousand-year period of fluctuating, generally milder temperatures; fossil pollen records from Okarito (Newnham *et al.* 2007) indicate this period was itself interspersed with a *c.* two thousand-year interval of intense cooling between 25,000 and 23,000 years BP.

The period 27,000-21,000 cal yrs BP described by the NZ-INTIMATE group in Alloway *et al.* (2007) was refined and divided by the NZ-INTIMATE group in Barrell *et al.* (2013) into three stadials and two interstadials, as follows:

- (i) the latter half of the cold, **Otira Glaciation Stadial E** (NZce-10);
- (ii) the cool, **Otira Glaciation Interstadial D** (NZce-9), spanning  $25,358 \pm 162$  to  $24,480 \pm 360$  cal yrs BP;
- (iii) the cold **Otira Glaciation Stadial C** (NZce-8), with the age range given as  $24,480 \pm 360$  -  $22,640 \pm 290$  cal yrs BP;
- (iv) the cool, **Otira Glaciation Interstadial B** (NZce-7) spanning  $22,640 \pm 290$  -  $21,690 \pm 340$  cal yrs BP; and
- (v) the early part of the cold, **Otira Glaciation Stadial A** (NZce-6), with an age range of  $21,690 \pm 340$  *c.* 18,000 cal yrs BP.

(3) **Last Glacial Maximum (LGM) sensu stricto** (*c.* 24,000 - 18,000 cal yrs BP). The LGM *sensu stricto* was a global phenomenon marking the most recent period of persistent glaciation that surpassed the poles and extended into the mid latitudes, and was associated with cooler climates in the low latitudes *c.* 21,000 – 18,000 years BP (CLIMAP 1981), or “...the most recent interval when global ice sheets reached their maximum integrated volume during the last glaciation,” (Mix *et al.* 2001, p.633). This period of time encompasses a global sea level lowstand of 135 m below present levels at 19,000 years BP (Yokoyama *et al.* 2000; Mix *et al.* 2001), indicating that mean planetary temperatures were at or near their minimum. A strong signal of cold conditions at this time was provided by  $\delta^{18}\text{O}$  –derived sea surface temperatures (SSTs) from core SO136-G3, extracted off the West Coast, South Island; LGM SSTs were up to 5.5°C cooler than present (Barrows *et al.* 2007).

However, the onset of these lower temperatures commenced around 3,000 years earlier in New Zealand than the CLIMAP-defined ‘global’ LGM therefore local climate event intervals have been proposed (Newnham *et al.* 2012) including the LGCP described above (Alloway *et al.* 2007), and extended LGM (Newnham *et al.* 2007) (*c.* 29,000 – 19,000 years BP):

(4) **Extended LGM (eLGM)** (*c.* 29,000 – 19,000 yrs BP). Newnham *et al.* (2007) argued that an eLGM might be a more appropriate chronozone for the New Zealand paleoclimate record than a 18,000-24,000 years BP LGM chronozone, on the basis of glacial moraine data from Lake Mapourika, north Westland (Suggate & Almond 2005; Sutherland *et al.* 2007), cold climate taxa in the fossil pollen records from the Kohuora and Pukaki craters and Mount Richmond, Auckland (Newnham *et al.* 2007; Lancashire *et al.* 2002; Sandiford *et al.* 2003), paleoecological records from Okarito (Vandergoes *et al.* 2005; Newnham *et al.* 2007), and aerosolic quartz dust deposits from Taranaki (Alloway *et al.* 1992a).

Newnham *et al.* (2007) suggested that the eLGM was comprised of two cold phases, between 29,000 and 26,000 cal yrs BP and 24,500 and 19,000 cal yrs BP, interspersed with a period marked with a sharp decline in the fossil Poaceae pollen at Kohuora and Pukaki craters and Mount Richmond from 26,000 to 24,000 cal yrs BP referred to as the mid-eLGM Interstadial.

The cooler, North island intervals were from 28,000 – 27,000 cal yrs BP and 21,000-19,000 cal yrs BP; in contrast, the mild period at Okarito began around 300 years earlier than at Auckland (Vandergoes *et al.* 2005) and was comprised of three, rather than two cooler periods, just prior to the Kawakawa / Oruanui tephra deposit of  $25,360 \pm 160$  cal yrs BP (Vandergoes *et al.* 2013), as well as periods coeval with the Auckland craters, that is between 28,000-27,000 cal yrs BP and 21,000-19,000 cal yrs BP. The NZ-INTIMATE group (Barrell *et al.* 2013) appear to have abandoned this chronozone, so it is not used further in the current study.

**Termination I (c. 19,000 - 18,000 yrs BP).** The end of the LGM / LGCP cold climate phase and the start of climate amelioration were marked by an abrupt and marked change (Lowe *et al.* 2008) known as Termination I, that occurred between c. 19,000 and 18,000 years BP. The Rerewhakaaitu tephra was erupted from the Okataina Volcanic Centre and deposited between  $17,900 \pm 200$  cal yrs BP (Newnham *et al.* 2003) and  $17,625 \pm 425$  cal yrs BP (Alloway *et al.* 2007); this is a widely-used reference marker for this transition between cold climates and warming conditions. This demarcation was marked by the expansion of podocarp forest at the expense of beech forest and shrubland-grassland mosaics at Pukaki and Onepoto craters in Auckland, accumulation of peat at Kaipo wetlands in eastern North Island (Hajdas *et al.* 2006) and the replacement of herbs with shrubs at Okarito (Vandergoes *et al.* 2005).

Between  $19,310 \pm 200$  cal yrs BP and  $17,900 \pm 200$  cal yrs BP (coinciding with deposit of the Rerewhakaaitu Tephra), increased fluvial activity following the LGM is likely to have created aerosolic dust by cold climate processes such as freezing, thawing and glacial grinding, and fluvial processes themselves such as abrasion and comminution. Maximum quartz accumulation occurred at marine core P69 off the east coast of the North Island as aerosolic dust was deflated from the resultant aggradational surfaces (Stewart & Neall 1984; Figure 50) and braided river-flood plains (Eden & Hammond 2003).

Such a pattern is likely to have occurred on the North Island west coast as well, although the source area for Eltham would by necessity be smaller than that for core P69. The timing of changes in dust deposits coincident with Rerewhakaaitu tephra is significant. Around 17,900 cal yrs BP multiple and widespread examples of climate amelioration occurred, including (i) changes in the pollen spectrum from subalpine plants to tall podocarps at Lake Rotomanuka and Lake Okoroire in the Waikato (Newnham *et al.* 2003); (ii) glacial retreat in western South Island; and (iii) paleolimnological changes took place at Lake Maratoto, Waikato, including increased precipitation (Green & Lowe 1985).

**Last Glacial-Interglacial Transition (LGIT) (c. 18,200 -14,800 cal yrs BP).** Around 18,000 cal yrs BP the climate began to ameliorate, as indicated by an increase in warm-climate pollen taxa in cores from Waikato lakes (Newnham *et al.* 1989), an increase in stream incision and erosion of fluvial terraces as sediment supplies declined, implying increased rainfall in the eastern North Island (Lowe *et al.* 2008), and a rise in sea-levels to around 75 m below current levels (Carter *et al.* 2000).

Barrell *et al.* (2013) re-defined the younger age limit for the LGIT as c.  $11,880 \pm 180$  cal yrs BP; this chronozone was divided into:

(i) **LGIT - Post Termination Amelioration** (NZce-5) c. 18,000 –  $15,640 \pm 410$  cal yrs BP;

(ii) **LGIT – Late Glacial Mild Episode** (NZce-4)  $15,640 \pm 410$  –  $13,740 \pm 130$  cal yrs BP. This equates approximately to the previous NZ-INTIMATE chronozone **Late-Glacial Warm Period (LGWP) (c. 14,800 – 13,500 cal yrs BP)** (Alloway *et al.* 2007). Sometime between 13,700 and 13,500 cal yrs BP sea-levels reached 56 m below current levels; this level may have persisted for around 1,000 years (Carter *et al.* 2000; Carter & Manighetti 2005).

(iii) **LGIT - Late Glacial Cool Episode** (NZce-3)  $13,740 \pm 130$  -  $12,550 \pm 140$  cal yrs BP. This equates approximately to the previous NZ-INTIMATE chronozone **Late-Glacial Reversal (LGR) (c. 13,500 – 11,600 cal yrs BP)**. Williams *et al.* (2005) used  $\delta^{18}\text{O}$  records from speleothems from northwest South Island to show

that a reversal in the general warming trend occurred between 13,500 and 11,600 yrs BP; at the same time, weak signals for the LGR cooling event are indicated by the lowland podocarp: grass pollen ratio reversing the earlier trend at Otamangakau and Pukaki (McGlone & Topping 1977; Alloway *et al.* 2007), and reversals in total organic carbon content at Onepoto (Alloway *et al.* 2007). Franz Josef Glacier re-advanced at this time (Denton & Hendy 1994, Turney *et al.* 2007); Anderson & Mackintosh (2006) ran mass balance model simulations on data from Franz Josef to show that LGR conditions were more likely driven by a decline in temperature rather than a decline in precipitation.

Limited, but persistent cooling was inferred from the pollen record from the Kaipo wetland, where cooling lasted 1,000 years, from sometime between 13,820 and 13,590 cal yrs BP to between 12,780 and 12,390 cal yrs BP (Hajdas *et al.* 2006; Alloway *et al.* 2007). Newnham & Lowe (2000) found “unequivocal evidence” for a 1,000-year cooling event at Kaipo Bog at this time, with a decline in thermophilous taxa such as *Prumnopitys taxifolia*, *Nothofagus* subg. *Fuscospora* and *Halocarpus*, and an increase in cold-tolerant taxa such as *Phyllocladus* and *Poaceae*. Weak signals for cooling are also evident from Okarito (Vandergoes *et al.* 2005), indicated by the decline in warm-loving forest taxa in favour of cold-adapted shrubs.

The general global warming that characterised the latter part of the Late Glacial was interrupted in the Northern Hemisphere by a stadial known as the Younger Dryas or Greenland Stadial 1 (Björck *et al.* 1998). Despite good evidence for the ubiquity of this stadial in the Northern Hemisphere, the existence of a coeval event in the Southern Hemisphere is highly contentious; however, determining whether a Younger Dryas – synchronous event occurred in the Southern Hemisphere is critical to understanding global paleoclimate change and modern climate modelling. Although researchers found indications of glacial advances and by inference a cooling interval coeval with the Younger Dryas stadial in Ecuador and Tierra del Fuego, Argentina (Clapperton 1993; Heuser & Rabassa 1987), other researchers found evidence for rapid glacial retreat in Tierra del Fuego and on the western flank of the Cordillera Real in Bolivia at this time (Rodbell & Seltzer 2000; Abbott *et al.* 1997).

The nature and extent of the interhemispheric climate linkages remains uncertain; evidence from New Zealand is conflicting, for example Denton & Hendy (1994) and Ivy-Ochs *et al.* (1999) concluded that glacier advance at Franz Josef Glacier was coeval with the Younger Dryas (YD) stadial (*c.* 12,900 – 11,600 cal yrs BP), suggesting that interhemispheric climate events were synchronous, whereas Blunier *et al.* (1997) found evidence that the Antarctic Cold Reversal (ACR) preceded the YD by at least 1,800 years, suggesting that interhemispheric climate events were asynchronous.

Subsequent re-assessment of the moraine data places doubt upon the conclusions of Denton & Hendy (1994) and Ivy-Ochs *et al.* (1999); Barrows *et al.* (2007) suggested that the glacier advance at Franz Josef was not a YD event, but coincided with a period of warmer oceans around New Zealand. Barrows *et al.* (2007) used  $^{10}\text{Be}$  and  $^{36}\text{Cl}$  cosmogenic exposure dating to give a mean deposit age for the Waiho Loop moraine of  $10,480 \pm 240$  cal yrs BP, showing that it was deposited well after the YD chronozone. Similarly, Kaplan *et al.* (2010) also found evidence of warming at this time, based on cosmogenic dating of glacial equilibrium line altitudes at Irishman Stream, on the eastern side of the Southern Alps.

The Australasian situation is also equivocal; no evidence of glacial re-advance for the Younger Dryas was found in either the Snowy Mountains or the Tasmanian highlands, the only areas of LGM glaciation in Australia (Barrows *et al.* 2002), and Singer *et al.* (1998) found no evidence for a cooling event at any time around the time of the Younger Dryas in pollen cores from NW Nelson.

**LGIT- Pre-Holocene Amelioration** (NZce-2)  $12,550 \pm 140 - 11,880 \pm 180$  cal yrs BP, and **Holocene Interglacial** (NZce-1),  $11,880 \pm 180$  cal yrs BP to present. This latter chronozone correlates to Alloway *et al.* (2007) **Early Holocene Warming (EHW)** (*c.* **11,600 – 10,600 cal yrs BP**).  $\delta^{18}\text{O}$  data from Northwest South Island indicate a warm peak occurred 11,100 yrs BP, with temperatures remaining largely unchanged for the next 4,500 years (Williams *et al.* 2005a). Coeval warming at the Auckland maar lakes occurred between 11,000

and 10,000 cal yrs BP, as evidenced by the rise in total organic carbon curves at Onepoto, and an increase in the LPG ratio at Pukaki (Alloway *et al.* 2007).

Pollen evidence shows that the Otamangakau wetland lowland podocarp forest had replaced montane forest by around 11,000 cal yrs BP (McGlone *et al.* 2005), and Newnham & Lowe 2000) note that the forests around the Kaipo wetland expanded and were comprised of full interglacial taxa sometime between 11,400 and 11,000 cal yrs BP. Early Holocene warming occurred at Okarito between 12,000 and 11,000 cal yrs BP, as indicated by a strong rise in the warmth-loving taxon *Dacrydium cupressinum* (Vandergoes *et al.* 2005). Further evidence of warm conditions at this time were provided by  $\delta^{18}\text{O}$  –derived SSTs from core SO136-G3, that indicated that temperatures *c.* 11,000 cal yrs BP were up to 1.5°C warmer than present (Barrows *et al.* 2007).

## 5. Characteristics and Dynamics of Taranaki Flora, Plant Responses to Stress, Plant Strategies and Floral Biodiversity

The purpose of this chapter is to summarise (i) the principal changes in the Quaternary vegetation history of Taranaki; (ii) plant responses to stress, and resultant (iii) plant strategies, and (iv) succession; in order to elucidate the nature of, and mechanisms that influence the way in which plants respond to climate and environmental change. (v) Measures of floral diversity are described, using the fossil pollen assemblage as a proxy for paleodiversity, and linking diversity to (vi) the Intermediate Disturbance Hypothesis (IDH). (vii) Floral representation in the pollen rain is briefly described to place the palynological analysis presented in the current study in a botanical context.

### 5.1. Vegetation History of Western North Island since 80,000 yrs BP

The purpose of this section is to briefly review and summarise the vegetation history of the Taranaki region to help place the Eltham and coastal Taranaki pollen records in context. A substantial body of paleoclimate- and paleovegetation-reconstruction literature covering the period since the Last Glacial Maximum exists for Taranaki and the wider central-western North Island (McGlone & Topping 1977; Lees 1986; McGlone & Neall 1994; Newnham *et al.* 1999); in contrast, literature covering pre-LGM times is more sparse (Grant-Taylor 1978; McGlone *et al.* 1984; McGlone 1985; Bussell 1993). In both cases, much of this research is based upon analysis of the fossil pollen record. Sites referred to in the following discussion are shown in Appendix 11.2.

**90,000 – 80,000 years BP.** Sometime after  $95,000 \pm 20,000$  years BP *Prumnopitys taxifolia* and *Dacrycarpus dacrydioides* in particular, declined as a percentage of the pollen sum at Inaha Terrace, Hawera (McGlone *et al.* 1984), although *Prumnopitys taxifolia* remained at levels of between 5 and 15% of the pollen sum. The conifers were largely replaced by *Leptospermum / Kunzea* and *Coprosma* as the predominant woody taxon; at the same time, the sedge taxon Cyperaceae increased to levels of around 40% of the pollen sum for a period.

By the end of the period  $95,000 \pm 20,000$  years BP Poaceae, Asteraceae, *Coprosma* and *Dracophyllum* pollen all showed strong increases, with more modest increases in *Dacrydium cupressinum* and pollen from *Libocedrus* and *Nothofagus* subg. *Fuscospora* montane taxa. Although *Prumnopitys taxifolia* decreased as a proportion of the pollen sum, it remained the most common large-tree taxon at around 5-10% of the pollen sum.

A similar pollen signature occurred in the core from Ararata Road (Bussell 1993) where *Prumnopitys taxifolia* was present in higher concentrations than *Dacrydium cupressinum* between 95,000 and 80,000 years BP. At this time the Ararata Road fossil pollen assemblage was also marked by lower levels of *Metrosideros* and the tree ferns *Cyathea smithii* and *C. dealbata* than had occurred in previous, presumably wetter, times; and an increase in both *Nothofagus* subg. *Fuscospora*, and *Nothofagus menziesii*.

In essence, *Prumnopitys taxifolia* and *Dacrycarpus dacrydioides* tended to dominate Taranaki lowland forests 95,000 years ago, whereas prior to clearance by European settlers, modern Taranaki forests were dominated by *Dacrydium cupressinum*. Given the similarities between the pollen assemblage from this time at Inaha Terrace and contemporary pollen rain found in the drier, eastern parts of New Zealand, McGlone *et al.* (1984) suggested that mean annual rainfall 95,000 years BP was likely to have been much less than the 1,200 mm per year currently experienced, and may have been as low as 600 to 800mm per year and may have also been drought-prone.

In addition to reduced precipitation, temperatures may have also been cooler, as evidenced by the increase in beeches at Ararata Road (Bussell 1993). An alternative explanation for the dominance of *Prumnopitys taxifolia* and *Dacrycarpus dacrydioides* over *Dacrydium cupressinum* proposed by McGlone *et al.* (1984) is that *Prumnopitys taxifolia* and *Dacrycarpus dacrydioides* appear to out-compete *Dacrydium cupressinum* on fresh alluvial soils or recent volcanic ash deposits.

**80,000– 70,000 years BP.** The Manaia Lignite from Taranaki (McGlone *et al.* 1984) indicates warmer conditions than the preceding cool climate episode due to the dominance of *Prumnopitys ferruginea* and *Dacrycarpus dacrydioides*. However the absence of other interglacial taxa suggests conditions were still cooler than present. Rainfall in lowland Taranaki was likely to have been lower given the absence of *Dacrydium cupressinum* in the Manaia Lignite; this contrasts with the pollen assemblage at Lake Omapere in Northland showing podocarp/kauri/beechness forest dominated in the period from 80,000 to 74,000 years BP, suggesting a mild climate (Newnham *et al.* 2004). Milne (1973) named loess deposited in the Rangitikei-Manawatu district during this cool,  $\delta^{18}\text{O}$  Stage 4 stadial as Porewa loess, hence this period is known as the Porewan substage. The Waimahoe lignites at Waikanae (Mildenhall 1973; McGlone 1985), Otamangakau lignite at Tongariro, and the pollen assemblage from Lake Poukawa to the east where low levels of *Dacrydium cupressinum* and high levels of *Cyathea* persisted prior to 59,000 years BP suggest that precipitation was at least as high as it is today (McGlone 1985; Shulmeister *et al.* 2001).

**55,000 – 25,000 years BP.** Milne (1973) and Cowie & Milne (1973) named loess deposited in the Rangitikei-Manawatu district during this cold,  $\delta^{18}\text{O}$  Stage 3 stadial as Rata loess, hence this cool and windy period is known as the Ratan substage. Grant-Taylor (1978) suggested the period 37,000 – 31,800 years BP was very cold relative to present, noting that grasses were dominant in polleniferous sediments extracted from within a sequence of Opunake lahars at Hawera dated from 34,200  $\pm$  1,500 to 31,800  $\pm$  1,400 years BP; and McGlone *et al.* (1984) described a pollen record preserved within the Inaha Terrace near the mouth of Inaha Stream from 33,300  $\pm$  1,100 years BP. At the start of this period the landscape around Hawera was essentially a shrubland-grassland, as suggested by low levels of tree pollen but high levels of Poaceae (21%) and Asteraceae (60%) pollen; by the middle of McGlone *et al.*'s (1984) 33,300 years BP pollen zone at Inaha Terrace, Asteraceae had fallen to <30% of the sum, and the shrubs *Halocarpus bidwillii* and *Coprosma* spp increased to around 50% and 10% of the sum, respectively.

Although pollen from *Nothofagus* subg. *Fuscospora*, *N. menziesii*, *Libocedrus* and *Prumnopitys taxifolia* were relatively common in the latest part (top) of the pollen record, tall tree taxa only contributed around 10% to the sum, with *Coprosma* spp, Asteraceae and Poaceae pollen making up around 40% of the pollen spectrum.

Milne (1973) and Cowie & Milne (1973) named loess deposited in the Rangitikei-Manawatu district during this cold,  $\delta^{18}\text{O}$  Stage 2 stadial as Ohakea loess, hence this windy period is known as the Ohakean substage.

**The Last Glacial Maximum *sensu stricto* 24,000 - 18,000 cal years BP.** Vegetation during the LGM in coastal Taranaki and the Taranaki lowlands was dominated by grasslands, woody shrub species that typically occur in modern subalpine environments such as *Phyllocladus alpinus* and *Halocarpus* spp (McGlone 1985), and patches of *Nothofagus menziesii* forest in eastern Taranaki (Blaschke 1988, cited in Crozier & Pillans 1991).

At first glance, this apparent lowering of the treeline relative to present implies a cooling of around 8°C. McGlone (1985) suggests that trees in upland areas of both islands would have been eliminated in response to cooling to this extent. However, palynological and macrofossil evidence indicate this did not occur; therefore one must infer that environmental influences other than mean air temperature were largely responsible for the treeline depression.

**Late Glacial Interglacial Transition 18,000 - 11,600 cal years BP.** After 18,000 years BP the North Island became reforested over the next 5,000 years; revegetation initially occurred in the Waikato lowlands between 15,000 and 14,000 years BP (Newnham *et al.* 1999), in most other North Island areas except Wellington by 12,000 years BP, and the Wellington area by 10,000 years BP (Lewis & Mildenhall 1985).

Around 17,150 cal years BP western Taranaki was a grassland-shrubland community, since the herbaceous taxa Poaceae (80%) and Apiaceae (4-5%) comprised most of the pollen sum for a core from Eltham swamp, with *Phyllocladus* and *Nothofagus* subg. *Fuscospora* the only other taxa to attain any significance in the pollen sum,

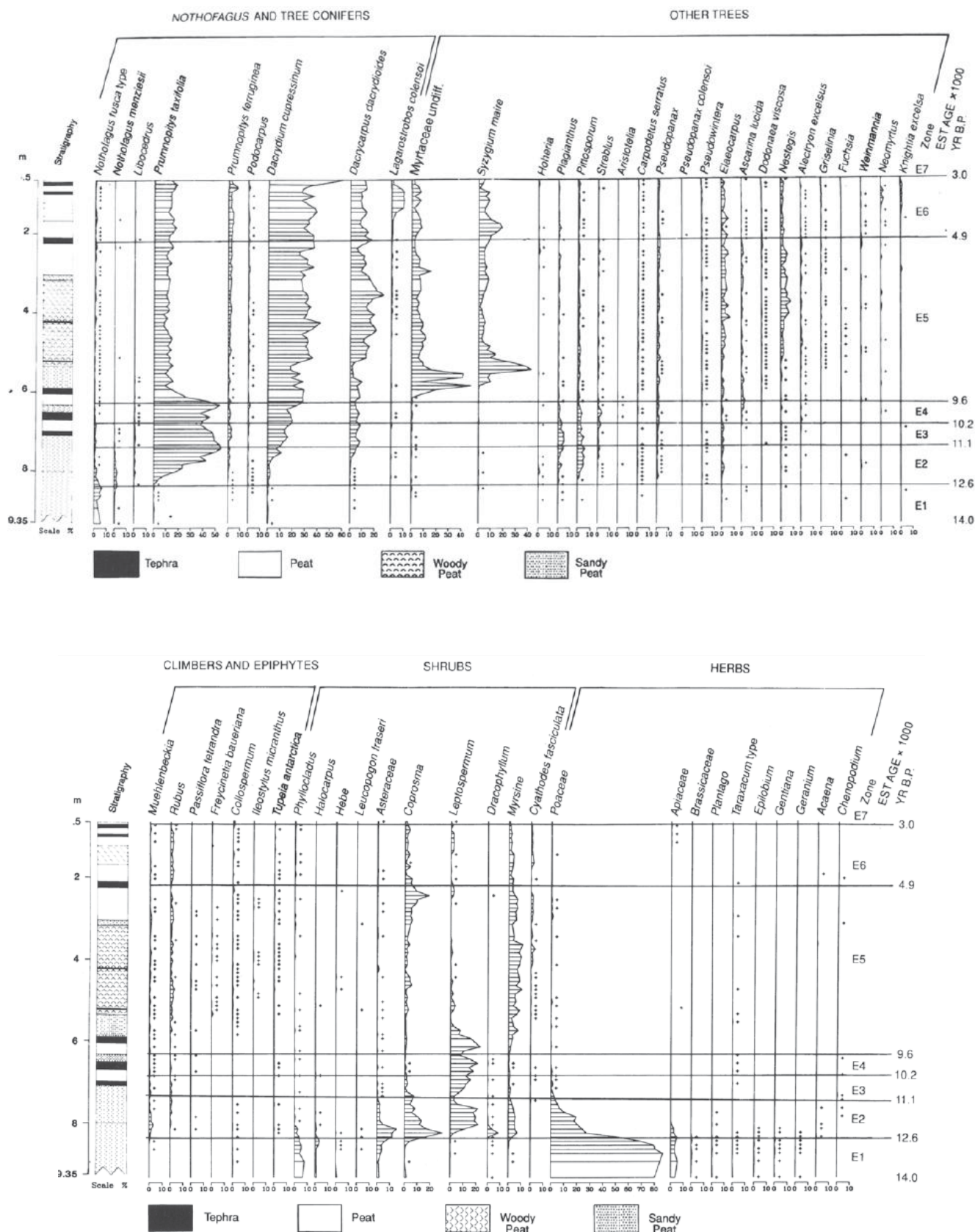
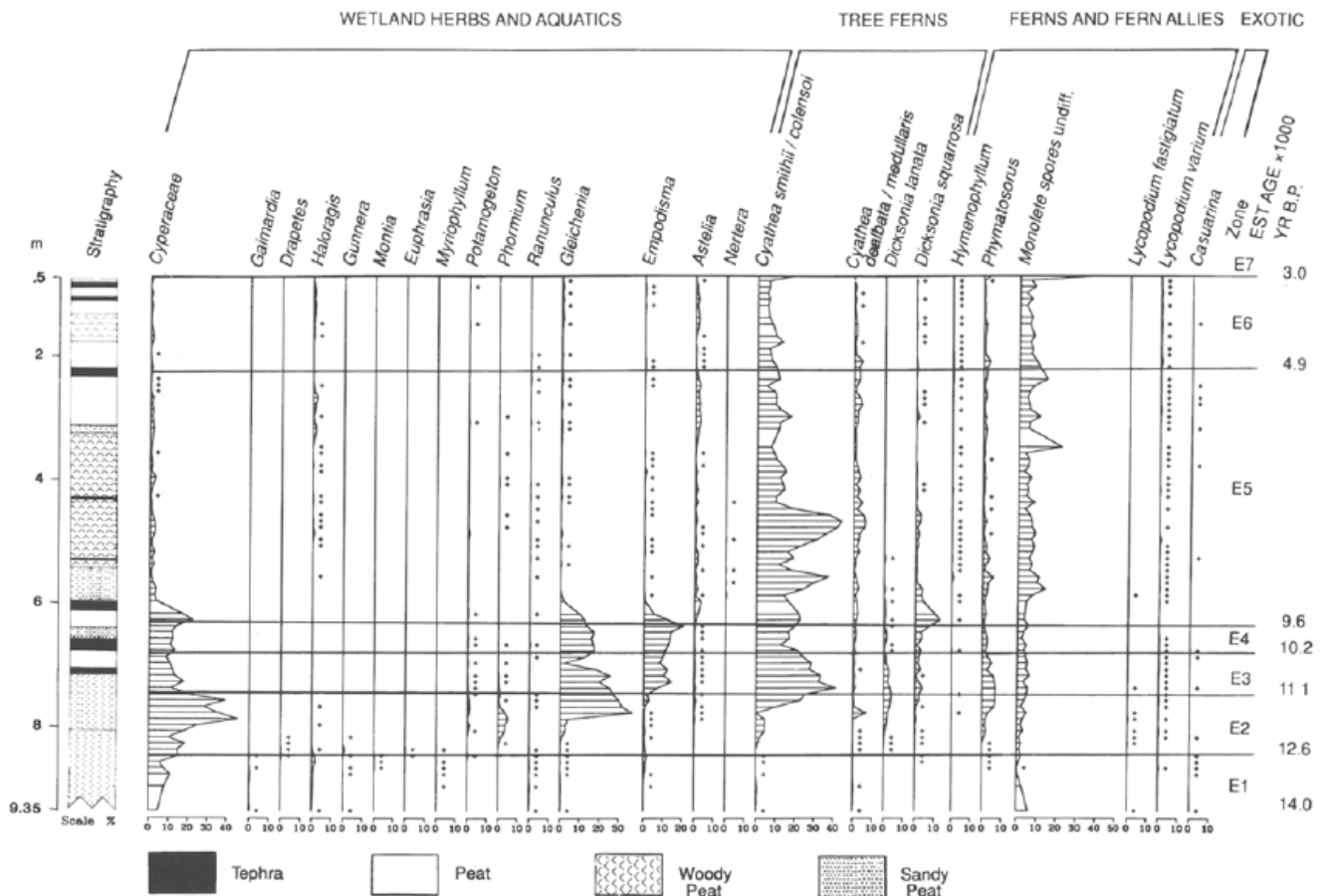


Figure 13. Eltham Swamp Pollen Diagrams, c. 3,000 – 14,000 yrs BP. Source: McGlone & Neall (1994). Dates are uncalibrated; the estimated age of 14,000 yrs BP at 9.35m  $\approx$  17,080  $\pm$  160 cal yrs BP.



**Figure 13 (continued). Eltham Swamp Pollen Diagrams, c. 3,000 – 14,000 yrs BP.** Source: McGlone & Neall (1994). Dates are uncalibrated; the estimated age of 14,000 yrs BP at 9.35m  $\approx$  17,080  $\pm$  160 cal yrs BP.

each contributing around 5% (McGlone & Neall 1994) (Figure 13). Note that McGlone & Neall's (1994) study only extends back to an estimated 17,000 cal yrs BP, hence the need for the current study, which spans approximately 10,000 to 40,000 cal yrs BP.

Approximately 16,450 cal years BP western Taranaki was a grassland-shrubland community dominated by grasses (Poaceae spp) and a diverse assemblage of shrub taxa, including *Leptospermum* -type, *Halocarpus bidwillii*, *Myrsine*, and *Coprosma* spp, indicated by a core from Durham Road near Inglewood (Alloway *et al.* 1992). Tree taxa made up around one third of the pollen sum, represented by *Nothofagus menziesii* (around 7-8% of the pollen sum), and *Nothofagus* subg. *Fuscospora* species (around 2-3% of the pollen sum). The tall podocarps *Prumnopitys taxifolia*, *Podocarpus totara* and *Libocedrus* each contributed around 7-8% of the pollen sum, and *Prumnopitys ferruginea* and *Dacrydium cupressinum* contributing around 2-3% each.

By around 15,550 cal years BP the grassland-shrubland communities at Durham Road (Alloway *et al.* 1992) had largely been replaced by tall tree taxa, with *Prumnopitys taxifolia* increasing to 40% of the pollen sum, small increases in *Prumnopitys ferruginea* and *Dacrydium cupressinum*, and the first appearance of *Dacrycarpus dacrydioides*. *Myrsine*, *Coprosma* spp and Poaceae all declined as a percentage of the pollen sum, with *Halocarpus bidwillii*, *Phyllocladus* and Asteraceae becoming virtually absent.

At 14,800 cal yrs BP grass pollen from the Eltham core had decreased to around two-thirds of the pollen sum and shrubby plants including *Coprosma* (15%), Asteraceae (10%), and *Halocarpus* (5%) became more important components of the forest assemblage (McGlone & Neall 1994).

**14,700 – 13,165 cal years BP.** In north-western Taranaki, tree taxa continued to increase as a proportion of the pollen sum, at the expense of shrubs and herbs. At Durham Road, *Prumnopitys taxifolia*, *Prumnopitys ferruginea*, *Dacrycarpus dacrydioides* and *Dacrydium cupressinum* all increased, with *Dacrydium cupressinum* replacing *Prumnopitys taxifolia* as the predominant tree (Alloway *et al.* 1992). *Monoao colensoi* and *Meterosideros* first appear in the Durham Road pollen record at around 14,700 BP; at the same time, *Nothofagus* subg. *Fuscospora* and *Nothofagus menziesii* virtually disappeared. Poaceae species and the shrubs *Myrsine* and *Coprosma* spp all declined as a percentage of the pollen sum, with *Halocarpus bidwillii*, *Phyllocladus* and Asteraceae becoming virtually absent.

Western Taranaki shows a similar trend; by around 14,700 cal years BP at Warea River *Prumnopitys taxifolia* made up 30% of the pollen sum (McGlone & Neall 1994); by 12,950 cal years BP the core from Eltham swamp (McGlone & Neall 1994) showed that *Prumnopitys taxifolia* made up 50% of the pollen sum, with *Dacrydium cupressinum* and *Dacrycarpus dacrydioides* each contributing around 10%, and *Plagianthus* and *Pittosporum* making up around 5% of the pollen sum. This expansion of conifer-broadleaved forest came at the expense of grass pollen which decreased to around 5% of the pollen sum.

At Warea River at 13,165 cal years BP *Dacrydium cupressinum* and *Prumnopitys taxifolia* made up 60% and 15% of the pollen sum respectively; minor components of the pollen sum included *Dacrycarpus dacrydioides*, *Podocarpus totara*, *Prumnopitys ferruginea* and *Libocedrus* (all <5%). The small trees *Pittosporum* and *Pseudopanax* also contributed <5% to the pollen sum, and the tree ferns <5% *Cyathea smithii* / *Cyathea colensoi* were plentiful (McGlone & Neall 1994).

In contrast to the disappearance of the lower montane taxa *Libocedrus* and *Nothofagus menziesii* at Durham Road, McGlone & Neall (1994) interpreted low, but persistent counts (each around 1% of the sum) at Eltham as indicative of presence either on Mount Egmont, or remnant pockets near the coring site. Presumably either local presence or dispersal from Mount Egmont were also responsible for low levels of *Libocedrus* pollen found at Warea River at around 13,165 cal years BP (McGlone & Neall 1994).

**12,450 – 11,600 years BP.** By around 12,450 cal years BP, small volumes of *Ascarina lucida* pollen (<1% of the pollen sum) appear in the Durham Road record (Alloway *et al.* 1992), suggesting a warmer, wetter climate than present (McGlone & Moar 1977). Shrub and herb species in South Taranaki also decreased at this time, with only *Myrsine* and *Coprosma* spp registering more than 1% of the pollen sum at Eltham.

By 11,600 cal years BP tall tree taxa at Durham Road comprised > 95% of the pollen sum, with *Dacrydium cupressinum* becoming the predominant species, and *Libocedrus* disappearing from the pollen sum (Alloway *et al.* 1992). Shrub and herb taxa all but disappeared from the pollen record, with only *Coprosma* spp registering more than 1% of the pollen sum.

**Early Holocene 11,775 – 5,750 cal years BP.** Between 11,775 and *c.* 10,950 cal years BP the vegetation assemblage at Eltham had fewer lowland-lower montane elements and became more lowland broadleaf-podocarp forest in nature. The pollen sum was still dominated by *Prumnopitys taxifolia* (making up over 50% of the pollen sum), however, *Dacrydium cupressinum* in particular (30% of the pollen sum), and *Podocarpus totara*, and *Prumnopitys ferruginea* became increasingly important components of the pollen assemblage (McGlone & Neall 1994).

Shrub species associated with warmer and wetter climates than present such as *Ascarina lucida* appeared at low levels in the pollen assemblage at Eltham, and *Alectryon excelsus* was consistently present at trace levels. Conversely, lower montane taxa decreased below levels seen in the previous thousand years or so: *Nothofagus menziesii* was no longer detectable in the pollen assemblage, and *Nothofagus* subg. *Fuscospora* and *Libocedrus* began to occur only in trace amounts.

Between *c.* 10,950 and *c.* 5,750 cal years BP *Prumnopitys taxifolia* levels at Eltham decreased to a relatively constant level, comprising 10-20% of the pollen sum. *Prumnopitys taxifolia* was replaced by *Dacrydium cupressinum* as the dominant species, which increased towards 40% of the pollen sum. *Dacrycarpus dacrydioides* also increased over this time, comprising 10-20% of the pollen sum.

The period *c.* 10,950 to *c.* 5,750 cal years BP at Eltham was notable for dramatic increases in Myrtaceae (most likely *Metrosideros* spp) and *Syzygium maire* above trace levels for the first time: Myrtaceae made up 40% of the pollen sum for a time, before decreasing to a relatively constant level of around 15% of the pollen sum for the next 4,500 years or so. The sudden increase of Myrtaceae was closely followed by an increase in *Syzygium maire* which also made up around 40% of the pollen spectrum before decreasing to a relatively constant level at around 10% of the sum.

At Warea River (McGlone & Neall 1994) around 7,990 cal years BP *Dacrydium cupressinum* and *Ascarina lucida* dominated the pollen assemblage, at 45% and 35% of the pollen sum respectively, and spores of the treefern *Cyathea smithii/ colensoi* were also very abundant. Although *Prumnopitys taxifolia* was the third-most common taxon at 10% of the pollen sum, it was at the lowest level observed for the whole core. A similar picture emerged at Waiweranui Stream (McGlone & Neall 1994): by around 7,805 cal years BP *Dacrydium cupressinum* and *Ascarina lucida* also dominated the pollen assemblage, at 55% and as high as 40% of the pollen sum respectively; in contrast, *Metrosideros* and *Pseudopanax* were more important elements of the pollen assemblage at Waiweranui Stream than at Warea River, whereas abundance of *Cyathea smithii/ colensoi* was much lower than at Warea River.

The pollen assemblage from a site at Waverley Beach (Bussell 1988b) around 7,830 cal years BP was dominated by *Prumnopitys taxifolia* (*c.* 20% of the pollen sum); this climbed to 30% by about 6,800 years BP, whilst *Dacrydium cupressinum* increased from 15 to 20%, and *P. totara* rapidly increased from 5% to 30% by about 7,680 cal years BP. Around 15% of the pollen sum was comprised of each of *Ascarina lucida* and *Dodonea viscosa* at 7,830 cal years BP, decreasing to 5% by around 7,660 cal years BP.

Bussell (1988b) suggested that despite the lack of fossil pollen evidence, *Beilschmiedia tawa* was likely common, if not a dominant species in forest along the Waverley coast 7,830 cal years BP, presumably based on its modern distribution relative to other canopy taxa, as well as modern pollen rain data. Common podocarps including *D. cupressinum*, *P. taxifolia*, and *Podocarpus totara* were likely emergents above the *B. tawa* canopy, whereas *Prumnopitys ferruginea* and *Dacrycarpus dacrydioides* were scarce. The Waverley Beach site was likely to have lacked abundant water, as evidenced by a general lack of swamp and aquatic taxa (Bussell 1988b), although the presence of *Ascarina* and tree ferns suggests that the site was not drought-prone, but was free from frosts, and lacked a dense canopy cover.

After *c.* 7,660 cal years BP moisture-loving *D. cupressinum* dominated the pollen assemblage at Waverley Beach, at around 40% of the pollen sum, at the expense of *P. totara* and *P. taxifolia* which decreased to around 10% and 15% of the pollen sum, respectively, by 7,470 cal years BP. This vegetation change implies the establishment of swamp conditions; this hypothesis is supported by the presence of the green freshwater algae *Pediastrum* and an increase in tree fern abundance. Although *Dodonea viscosa* increased to around 15% of the pollen sum over this period, *Ascarina lucida* decreased to around 5% of the sum by 7,470 cal years BP (Bussell 1988b); the *Ascarina* decline, together with an increase in *Metrosideros*, implies drier, and possibly frostier, conditions than had existed previously.

After *c.* 6,550 cal years BP *Dacrydium cupressinum* and *Prumnopitys taxifolia* were still the predominant taxa at Waverley Beach (around 30% and 20% of the pollen sum respectively) with *Metrosideros* making up around 10% of the assemblage (Bussell 1988b). *Podocarpus totara* decreased to around 5% of the pollen sum, and *Ascarina lucida* and *Dodonea viscosa* made up around 4% and 2% of the assemblage, respectively.

**5,750 to 800 cal years BP.** McGlone & Neall's (1994) core from Eltham Swamp indicates *Dacrydium cupressinum* was the dominant species, comprising > 40% of the pollen sum, achieving close to 60% of the pollen sum by 3,000 cal years BP. *Prumnopitys taxifolia* and *Dacrycarpus dacrydioides* levels remained relatively constant, each comprising 10-20% of the pollen sum, with Myrtaceae and *Syzygium maire* also remaining significant components of the pollen spectrum, contributing 10-15% of the total.

The most significant changes between 5,750 and 3,000 cal years BP at Eltham Swamp were increases in *Manoao colensoi* to around 15% of the pollen sum; and either a decline to less than 1% of the pollen sum, or complete absence in the pollen record of *Ascarina lucida*. At the same time, *Dodonaea viscosa* was present in trace amounts only some of the time in the period 4,900 to 3,000 years BP, whereas it had been consistently present at trace levels in the period 9,600 and 4,900 years BP.

The weakening of the pollen signal for *Ascarina lucida* and *Dodonaea viscosa* at Eltham Swamp suggest that climate after 5,750 cal yrs BP became more seasonal with harsher frosts and a drier climate, since both taxa are known to be drought and cold sensitive. These declines in the *Ascarina* signature at Eltham match those at Tongariro, the Ruahines and Lake Poukawa (McGlone & Moar 1977) and declines in both the *Ascarina* and *Dodonaea* pollen record match those at Motukarara and Waipara in Canterbury (Moar & Mildenhall 1988).

A core extracted from Potaema Bog (McGlone *et al.* 1988) six kilometres south-west of Egmont crater showed that between 3,785 and 500 cal years BP, tree conifers increased from 10% to 30% of the pollen sum, and woody taxa increased from 20% to around 55% of the sum. Offsetting these increases were decreases in mire plants (45% to 5%), herbs (10% to around 2%), and ferns (5% to around 2%), whilst tree ferns remained in relatively constant abundance at around 10% of the pollen sum throughout the three thousand-year sequence.

In general, all tall tree taxa throughout the sequence showed an upward trend in pollen frequency: the dominant taxon *Dacrydium cupressinum* increased from around 20% to 35% of the pollen sum; *Prumnopitys taxifolia* increased from 10% to 15%, *Metrosideros* 5% to 15%, *Prumnopitys ferruginea* 2% to 15%, and *Libocedrus* 2% to 5% of the pollen sum. Interestingly, *Nothofagus* pollen was found in significant concentrations (up to 5% of the sum) throughout the core, and traces of *Agathis australis* pollen in the lower parts of the core, although neither taxon are found, or were likely to be found, in the Potaema Bog area.

Bussell (1988b) described a core from Lake Waiau Swamp near Waverley, noting that at around 3,000 cal yrs BP *Dacrydium cupressinum*, *Prumnopitys taxifolia* and *Knightia excelsa* were the predominant taxa, making up around 35%, 32% and 25% of the pollen sum respectively; *Metrosideros* varied between 2% and 10% of the pollen sum. Copious spores from the tree ferns *Cyathea dealbata* and *Cyathea smithii* were present at this time; in contrast, swamp and aquatic taxa including Cyperaceae and *Typha orientalis* (raupo) were relatively scarce.

**800 to 100 cal years BP.** By around 800 cal years BP *Dacrydium cupressinum* remained the predominant taxon in Lake Waiau Swamp, but *Prumnopitys taxifolia* and *Knightia excelsa* both decreased, to around 10% and 5% of the pollen sum, respectively; at the same time, *Metrosideros* began to increase to around 15% of the pollen sum. Although *Cyathea dealbata* abundance declined, *Cyathea smithii* spore frequency remained similar over the previous period. The swamp taxa Cyperaceae and *Typha orientalis* increased in abundance at this time.

Bussell (1988b) suggested that forest in the Lake Waiau Swamp area prior to deforestation was most likely dominated by *Beilschmiedia tawa* despite the lack of fossil pollen evidence; *Dacrydium cupressinum*, *Prumnopitys taxifolia*, *Prumnopitys ferruginea*, *Metrosideros*, *Podocarpus totara* and *Dacrycarpus dacrydioides* were likely to have been emergents above the *Beilschmiedia tawa* canopy. Bussell (1988b) further suggested that *Knightia excelsa* distribution throughout the Lake Waiau Swamp core is different to present day distribution on undisturbed sites, noting that *Knightia excelsa* is a common pioneering species on ridges following fires; this suggestion is supported by the apparent correlation between *Knightia excelsa* and charcoal levels that occurred between 3,000 and 100 cal years BP.

The reduction in large tree pollen between 800 and 140 years BP from Lake Waiau Swamp clearly demonstrates deforestation following both pre- and post-European firing. Increases in *Leptospermum* -type pollen indicate early succession on burnt areas, with high levels of *Pteridium esculentum* reflecting Maori agricultural practices of burning to encourage growth of bracken fern for food. After 100 years BP increases in Poaceae, *Taraxacum*-type, Asteraceae and Apiaceae pollens reflect the European development of grass pasture and associated weeds; at this time, too, the exotic *Pinus radiata* pollen first occurs in the pollen spectrum.

Bussell (1988b) compared pollen surface samples with current flora in Lake Waiau Swamp and found that physiognomically important elements such as *Cordyline australis*, *Coprosma robusta*, *Coprosma tenuicaulis*, *Melicytus ramiflorus*, *Solanum* spp, *Geniostoma rupestre* var *ligustrifolium*, *Phormium tenax* and exotic taxa such as *Ulex europaeus* (gorse) were either severely under-represented in, or absent from, the pollen spectra; in contrast, *Pteridium esculentum* is greatly over-represented.

## 5.2. Modern Taranaki Vegetation

**Coastal and Semi-Coastal Forest** The lower flanks and surrounding ring plain of Mt Egmont (Figure 1) were swathed in dense podocarp-hardwood forest when Europeans settled Taranaki. Nicholls (1956) noted that milling of native trees was never undertaken on a large scale in Taranaki, due to the relatively small volume of scattered, harvestable trees, so much of the clearing and burning that occurred post-European settlement was to provide land for agriculture. Following clearing and burning, forest generally only occurs as remnants in scenic nature reserves, and in the 33,500 hectare Egmont National Park that was established in 1900.

The lower, north-western slopes of the Kaitake Range known as the 'Patuha Open Lands' have been heavily modified by human activity, including some logging before 1926, establishment of *Pinus radiata* plantations between 1927 and 1935, then clearfelling until 1971 (Clarkson 1985). Following logging, *Rubus fruticosus* (blackberry) and *Ulex europaeus* became widespread; in addition, introduced cattle (*Bos primigenius*), possums (*Trichosurus vulpecula*) and goats (*Capra hircus*) have modified the vegetation in the area. Despite extensive anthropogenic modification, Druce's (1986) vegetation survey from sea level to the summit of Mt Egmont and both the Pouakai Range and Kaitake Range demonstrated that the area has a diverse assemblage of higher plants. Druce found a total of 667 species of indigenous higher plants, including nine species of gymnosperms, four species of monocot trees and shrubs, 118 species of dicotyledonous trees and shrubs, 23 species of lianes, 118 species of tree ferns, ferns and fern allies, and 43 species of orchid.

**Lowland Podocarp-Hardwood Forest** According to McGlone *et al.* (1988) lowland forest occurs around most of Mount Egmont and the Pouakai Range at altitudes lower than 760m, and all of the Kaitake Range. For areas unaffected by the Burrell eruptions that occurred 350 years BP, the predominant vegetation assemblage at the base of Mount Egmont is *Dacrydium cupressinum* - *Metrosideros robusta* / *Weinmannia racemosa* forest (Druce 1964). Lowland areas to the ESE affected by the Burrell eruptions are clad in *Dacrydium cupressinum*-*Metrosideros robusta* / *Melicytus ramiflorus* - *Weinmannia racemosa* forest; and poorly drained lowland soils on the eastern flank of Mount Egmont are dominated by *Dacrydium cupressinum*-*Dacrydium cupressinum* / *Weinmannia racemosa* forest.

Clarkson (1985) found that in general, *Dysoxylum spectabile* (kohekohe) and *Knightia excelsa* (rewarewa) were the predominant canopy species up to 240m on the Kaitake Range peaks, with *D. spectabile* also an important understory species. Canopy and subcanopy species of lesser importance included *Corynocarpus laevigatus* (karaka), *Cyathea medullaris* (mamaku), *Macropiper excelsum* (kawakawa), and *Cyathea dealbata* (silver fern).

*Dysoxylum spectabile* appears to be an important component of early secondary succession on the Kaitake Range peaks since it was found in thickets of the subcanopy species *Pseudopanax crassifolius* (lancewood). *D. spectabile* was most prominent on coast-facing slopes, and *Knightia excelsa* was especially dominant on drier, coast-facing ridges or previously disturbed sites. *Microlaena avenacea* (bush rice grass) and *Uncinia* spp

(hooked sedges) were the major ground cover taxa at all altitudes examined by Clarkson (1985), with *Blechnum discolor* (crown fern) also prominent below 440m.

Between 240m and 300m *Beilschmiedia tawa* (tawa) and *Knightia excelsa* were the dominant trees, with *Hedycarya arborea* (pigeonwood) and *Laurelia novae-zelandiae* (pukatea) the major subcanopy taxa in the Kaitake Range peaks. *Beilschmiedia tawa* was dominant over all aspect types, but was particularly common, and achieved maximum altitude on the coastward sides of ridges with medium slope where temperatures were cooler, precipitation was highest and soils were shallow and leached (Clarkson 1985). In contrast, *Beilschmiedia tawa* was poorly represented in sites that had previously been logged.

In addition to *Beilschmiedia tawa*, *Laurelia novae-zelandiae* was most commonly associated with *Rhopalostylis sapida* (nikau) and the tree fern *Dicksonia squarrosa* (wheki), most common on gentle slopes on the coastward side of the Kaitake Range, reaching its maximum altitude in the bottom of valleys. The foremost shrub layer species at this altitude was the liane *Freycinetia baueriana* subsp. *banksii* (kiekie). From 300m to 370m *Laurelia novae-zelandiae* replaced *Beilschmiedia tawa* and *Knightia excelsa* as the dominant canopy species, with *Hedycarya arborea*, *L. novae-zelandiae*, and *Freycinetia* remaining the predominant subcanopy and shrub layer taxa, respectively.

Mount Egmont National Park is somewhat unusual in that it lacks any beech trees; this is likely to be a legacy of volcanic disturbance, the geographical isolation of Mount Egmont from other mountains and the limited dispersal capacity of *Nothofagus* species. With respect to alpine vegetation, Mount Egmont is effectively an island in a sea of lowland vegetation: even during the LGM, the climate was not cold enough to depress the treeline of alpine species low enough to form migration corridors between Mount Egmont and nearby ranges to the east where *Nothofagus* is found<sup>5</sup>, therefore it became biogeographically isolated.

**Lower Montane Vegetation** On the Kaitake Range peaks *Elaeocarpus dentatus* (hinau), followed by *Weinmannia racemosa* (kamahi), are the major canopy species between 370m and 490m. Whereas *Elaeocarpus dentatus* was dominant on ridge slopes and crests, reaching maximum altitude on the coastward side of the ranges, slope aspect was not an important factor when *Weinmannia racemosa* was dominant.

*Hedycarya arborea* and *Laurelia novae-zelandiae* were still important subcanopy species on the Kaitake Range, although the latter was replaced by *Meliccytus ramiflorus* (mahoe) and *Cyathea smithii* (soft tree fern or katote) as the second-most important subcanopy dominant between 440m and 490m. *Cyathea smithii* was the major shrub layer species at this altitude, followed by kiekie. As mentioned above, *Microlaena avenacea* and *Uncinia* spp were the predominant ground cover taxa, with *Blechnum fluviatile* (kiwikiwi) replacing *Blechnum discolor* at altitudes > 440m.

*Weinmannia racemosa* was the major canopy species at altitudes between 490 and 659m on the Kaitake Ranges, with *Cyathea smithii* both the predominant subcanopy and shrub layer taxon. Clarkson (1985) noted that *Weinmannia racemosa* at these altitudes on the Kaitake Range peaks typically has a low stature, has a small diameter trunk and is multi-leadered. Species associated with *Weinmannia racemosa* include *Myrsine salicina* (toro), *Pseudowintera axillaris* (horopito), epiphytic *Coprosma grandiflora* (kanono), *Dacrydium cupressinum* and *Prumnopitys ferruginea*.

Lower montane, *Weinmannia racemosa* - dominated canopy on Mount Egmont is relatively smooth and even in height, with few emergents. The predominance of *Weinmannia* in the canopy gives rise to a distinctive dull, greyish green colour (Druce 1964).

---

<sup>5</sup> Ravine (1996) described beech species in the Matemateonga Ecological District: *Nothofagus fusca* and *N. menziesii* occur in the Retaruke area, around 90km NE of Eltham (Appendix 11.2); *N. solandri* var *solandri* and *N. truncata* in the Whangamomona- Tangarakau area 50 km to the NE; *N. solandri* var *solandri* 40km SE at the Moumahaki Lake catchment, and 45km SE in the Waverly- Waitotara area.

**Upper Montane Vegetation** From around 750 to 1,200m, vegetation on Mt Egmont is predominantly a relatively open, *Weinmannia racemosa* - dominated forest interspersed with *Podocarpus cunninghamii* var. *hallii* (mountain totara) (Gould 2008). Both of these species are often wind-stunted and covered in mosses, lichens and *Hymenophyllum* spp (filmy ferns) giving rise to the colloquial term 'goblin forest' (Gould 2008), and *Cordyline indivisa* (mountain cabbage tree) is found in areas of disturbance such as alongside tracks or clearings.

In general, the highest part of the upper montane forest zone is dominated by *Libocedrus bidwillii* - *Podocarpus cunninghamii* var. *hallii*, broadleaved shrubs and *Griselinia*, however McGlone *et al.* (1988) note there is significant variation in the relative proportions of these taxa in the NE, E and SE slopes as a consequence of differential effects of recent eruptions. In contrast, young *Metrosideros robusta* – *Weinmannia*, *Weinmannia* – *Myrsine*, and *Kunzea ericoides* forests are established on recent block and ash flows on the NW slopes. Furthermore, the treeline is depressed to 790m in the NW, compared with 1,050m in other quarters.

Druce (1964) noted that in contrast to the lower montane canopy, the upper montane canopy on Mt Egmont is irregular and uneven due to the reduction in even-height *Weinmannia racemosa* with altitude, and the presence of emergent *Podocarpus cunninghamii* var. *hallii* and *Libocedrus bidwillii*.

Druce (1964) examined *Libocedrus bidwillii* trees on the eastern side of Mount Egmont at an altitude of 990m. These *Libocedrus* were alive at the time of the Burrell eruptions, and they survived the deposits of cold pumice that destroyed many of the other species present. Because they lacked neighbouring competing plants, they were able to send out lateral branches, giving rise to a distinctively squat, short-boled physiology when compared with modern, long-boled *Libocedrus bidwillii*. Dendrochronological analysis on these short-boled *Libocedrus* trees was used to date the Burrell eruption to 1655 AD (Druce 1964).

Several species found on rocky outcrops of the Kaitake Range peaks are also found in subalpine scrub on the adjacent Pouakai range and Mount Egmont. Clarkson (1985) suggested that *Pseudopanax colensoi* (mountain five finger), *Melicytus lanceolatus* (narrow-leaved mahoe), *Cassinia vauvilliersii* (mountain cottonwood), *Coprosma* spp, and *Senecio elaeagnifolius* on the Kaitake Range peaks all appear to be seral species, and are unlikely to persist if succession to a *Weinmannia racemosa*-dominant forest can occur, for example if browsing ungulates are removed. In contrast, *Helichrysum* spp and *Olearia arborescens* (common tree daisy) are thought to be climax species restricted to rocky outcrops on the peaks.

**Subalpine Vegetation** The subalpine scrub and shrubland area on Mt Egmont lies between 1,000 and 1,500m (Gould 2008). The canopy here is mostly comprised of tightly packed, even-surfaced *Brachyglottis rotundifolia* (leatherwood) around 2m in height (Druce 1964), in the company of *Pseudopanax colensoi* (mountain fivefinger), *Pseudopanax simplex* (haumakaroa), and *Coprosma pseudocuneata*.

Disturbance by landslips allows early colonisation by *Dracophyllum longifolium* (inaka); this is followed by succession of *Brachyglottis rotundifolia* var. (*B. elaeagnifolia*) (muttonbird scrub) (McGlone *et al.* 1988; Gould 2008) and *Pseudopanax* species. Since the subalpine zone is an area of transition between tree-dominated montane forest and herb and grass-dominated alpine tussock lands, stunted and wind sculpted trees including kaikawaka, *Podocarpus hallii* (mountain totara) and broadleaved taxa are scattered throughout the zone, but become increasingly rare with altitude.

With increasing altitude, the *Brachyglottis rotundifolia*-dominant canopy is replaced by *Cassinia vauvilliersii* (mountain cottonwood), *Coriaria pteridoides* (tutu), *Hebe odora*, *Myrsine divaricata* (weeping mapou, or weeping matipo) and *Dracophyllum longifolium* (McGlone *et al.* 1988; Gould 2008); by 1,500m *Hebe stricta* var. *egmontia* (koromiko) is the only shrub remaining (Druce 1964). Eventually these shrub species are replaced entirely by tussock and herb species, with *Chionocloa rubra* (red tussock) dominating above 1,250m on Mount Egmont and on poorly drained soils on the highest peaks of the Pouakai Range (McGlone *et al.* 1988).

The deforested Kaitake Range peaks now support grassland-scrub communities; secondary succession by tall trees such as *Weinmannia racemosa* is hindered by browsing by goats. Grass and herb species found on the peaks include *Anthoxanthum odoratum* (sweet vernal), *Microlaena avenacea*, *Rytidosperma gracile*, *Gnaphalium gymnocephalum* (creeping cudweed) and *Lagenifera pumila*; on the margins of the grass swards *Sticherus cunninghamii* (umbrella fern), *Rubus cissoides* (bush lawyer), *Blechnum* spp and *Metrosideros perforata* (climbing rata) occur (Clarkson 1985).

Steep faces and sides of cliffs in the Kaitake Range support *Phormium cookianum* subsp *hookeri* (mountain flax), *Lycopodium scariosum* (creeping club moss) and *Coprosma robusta* (karamu). Clarkson (1985) noted that several orchid species, including *Dendrobium cunninghamii*, *Earina mucronata* (peka-a-waka or hanging tree orchid), *E. autumnalis* (raupeka or Easter orchid) and *Bulbophyllum pygmaeum* (bulb-leaf orchid), and dense mats of *Metrosideros diffusa* (climbing rata), *M. fulgens* (scarlet rata) and *M. perforata* (white climbing rata) were sometimes found amongst exposed rocks.

**Alpine Vegetation** At altitudes above 1,500m on Mount Egmont *Chionocloa rubra* (red tussock) is replaced by moss-herbfields, in particular the moss *Racomitrium*. Moss-herbfields become intermittent above 1,650m, and are largely restricted to stable hollows and crevices. By 1,750m plant cover is very scarce (McGlone *et al.* 1988), although Druce (1964) noted that at altitudes >1,650m there are over 30 species of flowering plants found on debris slopes and lava flows. Floral biodiversity rapidly decreases with altitude: by 2,300m there are around 10 species; by 2,360m five flowering species occur, and at 2,440m only a single flowering plant species is found – an unnamed *Colobanthus* species. Plant life in the area between 2,440m and the crater is restricted to mosses and lichens (Druce 1964). Given that these environments tend towards low disturbance but high stress, and high disturbance and high stress respectively, under Kuatsky's (1988) model *Colobanthus* and mosses/lichens are classified as 'stunted' and 'biomass storing,' respectively.

**Aquatic Vegetation** McGlone & Neall (1994) note that wetland taxa in Taranaki are distinctive due to "...the absence of *Empodisma* and the highly localised occurrence of *Gleichenia dicarpa* in Taranaki, and the general low abundance of many oligotrophic or raised bog species," (p267). These characteristics may be a consequence of the dominance of swamp forest on poorly drained sites due to the climate throughout the Holocene, augmented with frequent addition of nutrients by way of tephra deposits.

The predominant taxa in ombrotrophic, raised bogs in New Zealand are herbaceous plants from the monocotyledonous angiosperm family Restionaceae (restiads), in particular the New Zealand lesser wire rush *Empodisma minus*, the primary peat forming taxon, and the New Zealand greater wire rush, *Sporodanthus ferrugineus* (Campbell 1964). The dominance of restiads in New Zealand raised bogs distinguishes them from Northern Hemisphere raised bogs where *Sphagnum* spp are the primary peat-developing taxa (Thompson *et al.* 1999; Clarkson *et al.* 2004), although the two bogs are ecologically equivalent (Kuder *et al.* 1998).

Succession from minerotrophic to ombrotrophic mire or mesotrophic to oligotrophic conditions (section 6.2) is determined by two main variables, water supply and mineral supply (Clarkson *et al.* 2004). Shearer (1997) described the successional sequence of Whangamarino (Clarkson & Stanaway 1994) and the remnant Moanatuatua (Cranwell 1953) raised bogs in Waikato, and Kopouatai bog (Newnham *et al.* 1995) on the Hauraki Plains as:

- (i) *Leptospermum* / *Kunzea scoparium* canopy with dense *Baumea teretifolia*, *B. rubiginosa* and *B. tenax* understory. Occasional *Coprosma tenicaulis* and *Gleichenia dicarpa* present. At this time, the bog was mesotrophic.
- (ii) Dense canopy of *Baumea* and *L. scoparium*; understory of *Empodisma minus*, *Schoenus brevifolius*, *Tetraria capillaris* and *Gleichenia*. The bog was still mesotrophic at this stage.

- (iii) Dense canopy of *Empodisma minus* with some *Baumea* spp, protruded by occasional *L. scoparium*. The bog was intermediate between mesotrophic and oligotrophic at this time.
- (iv) Dense sub-canopy of *Empodisma minus* overtopped by *Sporadanthus ferrugineus*; occasional *L. scoparium*. By this stage the bog was oligotrophic.

### 5.3. Plant Responses to Stress

#### 5.3.1. Effects of Cold Temperatures on Plants

Many New Zealand trees demonstrate clear spatial preferences (altitude and latitude), as demonstrated by Sakai & Wardle (1978). These researchers partially replicated an experiment by Cockayne (1897) when they collected twigs of 42 native woody plants and tested them for freezing resistance by subjecting them to progressively colder temperatures and assessing frost injury. The measurements obtained coincided remarkably well with the geographical and ecological distribution of the taxa. Table 2 shows plant distribution by latitude and altitude of some major New Zealand trees; the numbers given refer to the maximum freezing resistance of buds after four hours exposure at that temperature.

The general correlation between minimum experimental freezing temperature and observed spatial preference is modified by factors other than temperature that vary with altitude (as well as latitude and aspect) such as insolation, precipitation, wind regimes and soils, and proximity to the moderating influence of the ocean. The strength of the correlation between a given taxon's latitudinal and altitudinal preferences may be ascertained by using data from modern pollen rain studies and plotting them on response surfaces (Bartlein *et al.* 1986; Huntley 1990c; 1994). However until recently the relatively small number of modern pollen rain (compared to fossil pollen) studies conducted in New Zealand and a paucity of quantitative accounts of species-climate relationships precluded this (Leathwick & Mitchell 1992).

Freezing temperature information assists in making inferences about past climates; for example, if abundant fossil pollen from the upper montane taxon *Libocedrus bidwillii* (maximum freezing resistance, FR = -13.0°C) that is generally restricted to altitudes above 850m (Haase 1986; Druitt *et al.* 1990) was found in a site at sea level, and there was an absence of lowland forest taxon pollen such as *Dacrydium cupressinum* (FR = -8.0°C), cooler temperatures than present are indicated; more specifically, assuming an environmental lapse rate of 0.65°C/100m, a *Libocedrus bidwillii* depression of 750m suggests that mean annual temperatures were 5.5°C cooler than present.

Under freezing conditions, ice crystals form in a plant's extracellular spaces so that water flows out under osmosis to condense on the ice body, desiccating the cell. In frost hardy plants the water returns to the cell when the ice melts, and they continue to metabolise, whereas damage to cell membranes and other organelles may have occurred in frost-intolerant plants such that the water cannot return to the cells and metabolism is retarded or stops altogether (Salisbury & Ross 1992). Both cold and dehydration cause stress on plants; whereas freezing merely removes water from the protoplasts without removing it from the tissues, desiccation causes more damage since water that is evapotranspired through the leaves cannot be replaced because conducting channels in the roots and stems are frozen and the tree dehydrates and dies.

**Table 2. Modern Limits of New Zealand Flora as a Function of Altitude, Latitude and Temperature (bud freezing temperatures, °C).**

Lat. North of	Altitude			
	Lowland	Lower Montane	Upper Montane	Subalpine
39°S	<i>Avicennia resinifera</i> >-3 <i>Metrosideros excelsa</i> -3 <i>Beilschmiedia tarairi</i> -4 <i>Planchonella novozelandea</i> -8	<i>Agathis australis</i> -7		
41°20S	<i>Libocedrus plumosa</i> -7	<i>Knightia excelsa</i> -8 <i>Phyllocladus trichomanoides</i> -10		
43°30S	<i>Elaeocarpus dentatus</i> -5	<i>Quintinia acutifolia</i> -8		
46°30S (Foveaux Strait)	<i>Ascarina lucida</i> -3 <i>Hedycarya arborea</i> -3	<i>Podocarpus totara</i> -8.2 <i>Pittosporum eugenoides</i> -7 <i>Nothofagus menziesii</i> -12.4 <i>Coprosma lucida</i> -8	<i>Nothofagus fusca</i> -10.4	<i>Nothofagus solandri</i> -10 <i>Lagarostrobos colensoi</i> -13 <i>Phyllocladus alpinus</i> -20
47°20 (Stewart Is)	<i>Dacrycarpus dacrydioides</i> -7	<i>Prumnopitys ferruginea</i> -7 <i>Prumnopitys taxifolia</i> -11.1 <i>Dacrydium cupressinum</i> -8	<i>Plagianthus betulinus</i> -5 <i>Weinmannia racemosa</i> -8 <i>Podocarpus hallii</i> -13	<i>Leptospermum / Kunzea scoparium</i> -7 <i>Halocarpus bidwillii</i> -25
51°S (Auckland Is)			<i>Metrosideros umbellata</i> -8	<i>Dracophyllum longifolium</i> -10

Source: Sakai & Wardle (1978); Allan (1982); Bannister & Lord (2006).

### 5.3.2. Effects of Wind on Plants

The purpose of this section is to briefly describe the impacts of wind of different intensities on individual plant function, growth strategies and senescence, and on forest assemblage. The different plant and plant assemblage responses to winds of different intensities results in changes in plant distribution over time; these changes should be reflected in fluctuations in individual taxa, taxa groups (for example, *Nothofagus* and tree conifers vs. shrubs, or podocarps vs. herbs), and changes in the relative abundance of C, S and R-strategists in the fossil pollen record (discussed in section 5.4). Furthermore, winds of different intensity over time may be a major diversity driver (Hiura 1995; Flenley & Butler 2001; Molino & Sabatier 2001), which can be tested against the Intermediate Disturbance Hypothesis (5.6.2). de Langre (2008) notes that the effects of wind on plants occurs at various spatial and temporal scales, with spatial scales ranging from  $10^{-6}$  m (pollen) to  $10^3$  m (plant populations) across nine orders of magnitude, and from  $10^{-2}$  seconds (photosynthetic reactions) to  $10^{15}$  seconds (evolutionary time scales) or 17 orders of magnitude.

Direct impacts of wind on plants include increases to transpiration and desiccation, greater exposure to freezing temperatures as the boundary layer around leaves is removed, resulting in reduced photosynthesis under moderate winds, and frost damage under strong winds. Wadsworth (1959) grew *Brassica napus* (rape) in wind tunnels to determine that light winds ( $\approx 0.0005$ -  $0.9 \text{ ms}^{-1}$ ) normally increase the photosynthetic rate because they reduce the thickness of the boundary layer, facilitating diffusion of  $\text{CO}_2$  into the leaf wall. In contrast, stronger

winds (between 2.2 and 27 ms<sup>-1</sup>) reduce the rate of photosynthesis (i) directly, by cooling leaves and reducing metabolic rates (van Gardingen & Grace 1991; Smith *et al.* 1995) and causing leaf curl, therefore reducing the leaf surface area and therefore the effective photosynthesising area; and (ii) indirectly, by causing the stomata to close up to reduce water loss, but also retarding the entry of CO<sub>2</sub> into the leaf wall (Smith & Ennos 2003, Telewski 2012).

Indirect effects of wind on photosynthesis include modifying light shedding by leaf flutter in the canopy, so that light can penetrate into the lower canopy. Leaf flutter influences the number and duration of sunflecks that diffuse light into the understory, allowing carbon assimilation in the lower leaves. Understory leaves are more efficient at utilising rapidly fluctuating light than 'sun leaves' at the top of the canopy that are disadvantaged by changes to the ambient light conditions such as diurnal fluctuations, cloud cover, and canopy and leaf movement in windy conditions; therefore photosynthesis can continue under a range of light environments (Roden 2003).

Mechanical damage such as uprooting, stripping leaves and breaking branches can kill the plant outright; less severe damage has an indirect effect on photosynthesis by reducing the area of photosynthetic tissue. Mechanical abrasion of leaves and stems by wind-borne sand, dust, snow and ice crystals leads to polishing of cuticle waxes and damage to epidermal cells, although mild polishing leads to increases in transpiration for some taxa such as *Trifolium* (clover) and *Malus* (apple). Van Gardingen & Grace (1991) suggest that abrasion may disturb the turgor balance between guard cells and epidermal cells, upsetting the normal functioning of stomata so that they remain open at night or are further ajar than normal during the daytime, leading to excess transpiration and water loss. Mechanical abrasion also occurs in large-leaved shrubs exposed to strong winds as a result of repeated collisions among leaves and between leaves and twigs; as a result photosynthetic tissue and therefore photosynthesis declines.

Plants exposed to winds generally develop smaller leaves, with higher proportions of mechanical tissues and corresponding decrease in photosynthesising tissues (Smith & Ennos 2003). Smaller leaves have thinner boundary layers that are highly conductive, and therefore temperatures of small leaves are closer to the ambient air temperature than for large leaves (Van Gardingen & Grace 1991). Since airflow thins the boundary layer and increases its conductance (forced convection), small leaves undergo less dramatic temperature change in response to wind than large leaves, and are better adapted to cold temperatures.

New Zealand has a relatively large number of divaricating plants – some shrubs and young heteroblastic trees characterised by small leaves and divergent branch angles that create an intricate three-dimensional, springy twiggy lattice with most leaves occurring on the inside of the structure. This form is considered an adaption to windy, arid and cold climates (Cockayne 1912; McGlone & Webb 1981), with its small leaves and a flexible, twiggy outside that forms a windbreak (i) reducing transpiration losses from interior leaves; (ii) reducing mechanical damage from leaves striking each other; (iii) acting as a frost screen, so that interior leaves are not frozen; and (iv) possibly providing a heat trap on cold but clear days, raising the rate of photosynthesis.

These mechanisms enable the divaricating shrubs *Myrsine divaricata* and *Coprosma parviflora* to survive in frost hollows (Wardle 1980); this may be relevant to the Eltham Swamp pollen assemblage, since the Eltham site may have been a frost hollow in the past, given its altitude is 10m lower than the adjacent Ngaere Swamp.

Plants with a divaricating habit are most frequently found in disturbed areas such as forest margins and successional habitats such as river terraces (Wardle 1977; McGlone & Webb 1981) suggesting that divaricates may be implicated in the Intermediate Disturbance Hypothesis (section 5.5.2), that is, since they are *r*-selected pioneers, their numbers should increase following periods of disturbance such as strong winds (section 5.4). An alternative interpretation regarding the high proportion of divaricating plants is adaptation to browsing by *Dinornis* (moa) (Greenwood & Atkinson 1977). New Zealand is unique in that ratites were present in the absence of browsing mammals, and were sufficiently abundant to exert browsing stress on the vegetation.

Unfortunately, it is difficult to demonstrate causal relationship between *Dinornis* browsing and divarication, given the mobility of moa and the lack of divaricating species in the fossil pollen record.

### 5.3.3. Plant Adaptations to Resource-Rich vs. Resource-Poor Environments

The structure and diversity of New Zealand's forests are primarily driven by two major factors: (i) underlying environmental variations, which influence general patterns of taxa composition and diversity in canopy trees, for example angiosperms dominate fertile, well-drained soils, whereas conifers are more common on infertile, poorly drained soils (Urlich *et al.* 2005); and (ii) disturbance, which creates new opportunities for reforestation, with the nature and frequency of disturbance impacting upon each taxon differently. As a consequence of differences in individual taxon responses to resource levels, changes in resources over time should also contribute to changes in the relative proportion of *C*, *S* and *R*-strategists (section 5.4) in the fossil pollen narrative.

In general, resource-rich environments are occupied by plant species that have a high capacity to acquire all resources from the environment and utilise them in photosynthesis, whereas resource-poor environments are occupied by species with a lower capacity for photosynthesis and a lower capacity to acquire all major resources (Schulze & Chapin 1987). Because of the relative difference in growth rates, species adapted to resource-rich environments are referred to as fast-growing species, and species adapted to resource-poor environments are referred to as slow-growing species.

### 5.3.4. Fire Regimes and Charcoal

The purpose of this section is to describe the relationship between fire and charcoal production and dispersal, and the use of charcoal fragments preserved within sediment cores in paleoenvironmental reconstruction. Palynologists traditionally regard peaks in charcoal influx as evidence of changes in past fire regimes (including fire frequency and intensity), "...or, more conservatively, the relative importance of fire at different times and places," (Clark 1988, p. 67). Specifically, large charcoal fragments (> 50 µm) are assumed to remain close to the source of the fire, whereas smaller fragments (< 20 µm) are more widely dispersed, so may be from either local or long distance sources.

Three main assumptions regarding charcoal dispersal underpin the ability of microscopic charcoal fragments within sediments to provide local or regional fire histories: (i) most charcoal fragments fall out of the atmosphere close to their source, so that peaks in charcoal influx within a sediment column indicate local fires, where 'local' ranges from tens or hundreds of metres, to tens of kilometers from the source fire (Higuera *et al.* 2007; Butler 2008) and/or size of the fire and burn intensity, such that fine charcoal is lifted by thermal buoyancy higher into the atmosphere (Clark 1988; Butler 2008). (ii) Secondary charcoal deposition by way of inwash or re-deposition does not obfuscate primary deposition from airfall (Higuera *et al.* 2007); since charcoal is chemically inert and very resistant to decay (Cope & Chaloner 1980), admixing of primary and secondary deposits can be problematic. (iii) Sediment sampling provides sufficient temporal resolution to distinguish fire occurrence; for example Clark (1988) recommended sampling intervals that were  $< \frac{1}{5} \times$  the fire return-period of interest.

However, the charcoal: fire regime relationship is likely to be complex. Butler (2008) noted that charcoal particles were present in almost all samples from a core from Lake Kai Iwi in Northland, noting that this would imply a near-continuous,  $44,700 \pm 1150$  cal yr BP pattern of fire. He considered this was highly improbable, given that extant *Agathis australis* forests are not adapted to tolerate frequent, large fires, compared with say sclerophyllous, fire-adapted forests in Australia.

Many Australian taxa are adapted to, and rely upon fire to complete their life cycles; for example Eucalypts (family Myrtaceae) possess fire-promoting traits, including production of copious litter, volatile leaf oils and

flammable bark, and fire-tolerant organs such as lignotubers and epicormic shoots that enables them to recover quickly from fire and out-compete rainforest taxa that do not have these adaptations. Further, the presence of flammable taxa that occur in modern-day *Agathis australis* forests such as *Phyllocladus*, *Halocarpus* and *Dracophyllum* should provide plenty of fuel, leading to large scale damage and increases in seral taxa between fires; however examination of the pollen diagram for Kai Iwi shows that this did not occur. *S*-selected taxa such as *Coriaria* and *Myrsine*, and *R*-selected taxa such as Poaceae remain at fairly constant levels throughout the 44,700 cal yr BP pollen sequence; *Agathis australis* increased to > 40% of the pollen sum some time before 10,980 cal yrs BP, around the same time that > 50 µm charcoal fragments were first observed in the core; this is the opposite of what is expected if the traditional, large fragments = local fire relationship holds.

Pyne (1991) noted the relationship between N and NW winds and the approximate four-year return period of droughts in south-east Australia; along with the characteristics of fire-promoting Eucalypts described above, these factors lead to frequent, large-scale fires in the south-eastern 'fire flume' part of Australia. These fires were likely ignited by lightning and by Aboriginals engaged in 'firestick farming'; Pyne (1991) estimated that historically, 20% and 12% of fires in SE and SW Australia, respectively, were ignited by lightning; with as much as 97% of the land area burnt in 1974-1975 (15% of all Australia) attributable to lightning-ignited fires.

In contrast to more northern fires on the Australian continent, the incidence of lightning ignition in Tasmania was likely to be negligible (< 0.09% of the total land area burned), with firestick farming being the main ignition source over the last 20,000 years. This may be significant with respect to the New Zealand situation: since New Zealand is biogeographically similar to Tasmania, yet has a much shorter prehistory, neither lightning nor humans were likely to have been a significant ignition source for New Zealand fires. Only around 1% of forest fires in New Zealand between 1987 and 2002 were caused by lightning (Butler 2008), and the area burnt was very small (< 35 hectares in total); this low frequency and impact may reflect the fact that most lightning strikes in New Zealand are accompanied with heavy rainfall, and also the majority of lightning strikes occur on the West Coast, South Island where high annual rainfall largely suppresses forest fires. Other potential ignition sources include meteorite strike, spontaneous combustion, sparking from falling rocks (Cope & Chaloner 1980) and in New Zealand in particular, hot magma or ash proximal to volcanic eruptions, and also lightning discharges caused by the friction between ash clouds and steam clouds (Wilmshurst & McGlone 1996).

Small (5-20 µm) charcoal fragments may be entrained and carried aloft by thermally buoyant plumes driven by the fire below, and dispersed thousands of kilometres, and there is almost invariably a skip distance separating the charcoal source and sink areas (Clark 1988). In addition, large charcoal fragments are derived from primary sedimentation, and are therefore most abundant proximal to the fire (Patterson *et al.* 1987; Asselin & Payette 2005) because they are transported a shorter distance, and also because secondary sedimentation will lead to corrosion of fragments. Quantitative measurement of charcoal is difficult for similar reasons, since fragments may be crushed and fractured during (pollen) sample preparation. In contrast, areas that have not been burnt typically have predominantly small (< 20 µm) fragments present, or no charcoal at all (Patterson *et al.* 1987).

## 5.4. Plant Strategies

The purpose of this section is to briefly describe the concept of plant strategies, where a plant strategy is defined as "...a grouping of similar or analogous genetic characteristics recurring widely among species or populations, which leads to similarity in ecology," (Grime 1988a). Plant strategies are a useful conceptual framework to describe New Zealand taxa with respect to successions, understanding plant distribution, making sense of plant life histories and tying plant ecosystem studies to other biological disciplines such as population genetics. As a consequence, the concept of plant strategies goes some way toward explaining why discrete taxa and taxa groups respond the way they do to stressors, and therefore what the fossil pollen assemblage means in terms of plant community responses to changes in stressor intensity over time. Two simple plant strategies are described, *r-K* selection theory, and Grime's *C-S-R* theory.

### 5.4.1. *r-K* Selection Theory

*K*-selection predominates in stable environments where the population is close to the carrying capacity, and the ability to compete with other individuals for scarce resources is important (McArthur & Wilson 1967). As a consequence, *K*-selected organisms include those whose life expectancy is long and who devote only a small proportion of energy and other captured resources to reproduction (Table 3). In contrast, in environments with no crowding, genotypes that harvest the most resources will produce the most offspring and be most fit, therefore evolution favours productivity; this is *r*-selection. In other words, *r*-selection is predominant in unstable or unpredictable environments where the ability to reproduce quickly is more important than having adaptations that enable the individual to compete with others. Therefore, *r*-selected organisms have a short life expectancy and devote a large proportion of energy and other captured resources to reproduction. In practice, most organisms fall between the two extremes, so *r-K* selection can be seen as a continuum.

**Table 3. Typical Differences between *r*-Selected and *K*-Selected Plants**

	<i>r</i> -Selected Plants	<i>K</i> -selected Plants
<i>(i) Morphology</i>		
Stature	Small plants	Large plants
Size of offspring	Small offspring	Large offspring
Harvest index	High HI	Low HI
<i>(ii) Life History</i>		
Longevity	Short-lived	Long-lived
Mortality	Often catastrophic, non-directed, density-independent	More directed, density-dependent
Maturation rate	Fast maturation; early reproduction	Slow maturation; delayed reproduction
Population size	Variable in time, usually below <i>K</i> ; ecological vacuums; re-colonisation each year	Fairly constant in time; usually at or near <i>K</i> ; saturated communities; no re-colonisation necessary
Reproduction rate	High reproduction rate	Low reproduction rate
Intra- and interspecific competition	Variable, often lax	Usually keen
Dispersal	Medium range	Short range
Energy efficiency	Waste energy	Energy efficient

Most ecologists now, however, consider that *r-K* selection theory is too simplistic (Whittaker & Goodman 1979; Silvertown 1982; Kautsky 1988) criticising the *r-K* model on the basis that (i) there may be three selection forces, rather than two as in the *r-K* model, involving (a) survival in a predominantly unfavourable environment, where carrying capacity *K* is near its minimum with occasional episodes of considerably increased carrying capacity (adversity selection); (b) utilisation of an unpredictable and intermittently favourable environment, where *K* fluctuates around an intermediate modal value (exploitation selection); and (c) competition in a favourable and fully occupied environment (carrying capacity *K* is near its maximum) (saturation selection). (ii) Assumptions regarding the inverse relationship between *r*- and *K*-characteristics: since a species could not excel at everything at once, it was assumed that development of *r*-characteristics occur at the expense of *K*-characteristics, and vice-versa. However, Whittaker & Goodman (1979) note that the necessary trade-off failed when comparing pairs of traits if both traits are subject to optimisation rather than maximisation when considered independently.

On balance, the major strength of *r-K* theory is its versatility as a comparative tool: it enables us to compare phenotypes and strategies both between and among different plant species and vegetation assemblages, and serves as a basis for more sophisticated models, such as Grime's (1977) *C-S-R* model, discussed below.

*r-K* selection is a useful way to describe New Zealand taxa with respect to successions. According to Ogden (1985), pioneer species including *Leptospermum scoparium* and *Aristotelia serrata* can be described as *r*-type species, whereas climax species such as *Prumnopitys ferruginea* and *Bielschmedia tawa* are *K*-selected species.

*r*-*K* selection may also be used to contrast related taxa, for example *L. scoparium* is more *r*-adapted than *Kunzea ericoides* since it has a shorter life cycle, shorter stature, greater ecological amplitude, is less shade tolerant and may produce more seeds. Similarly, climax species can be ranked in terms of their relative *K*-selection on the basis of seed size and production (Figure 14).

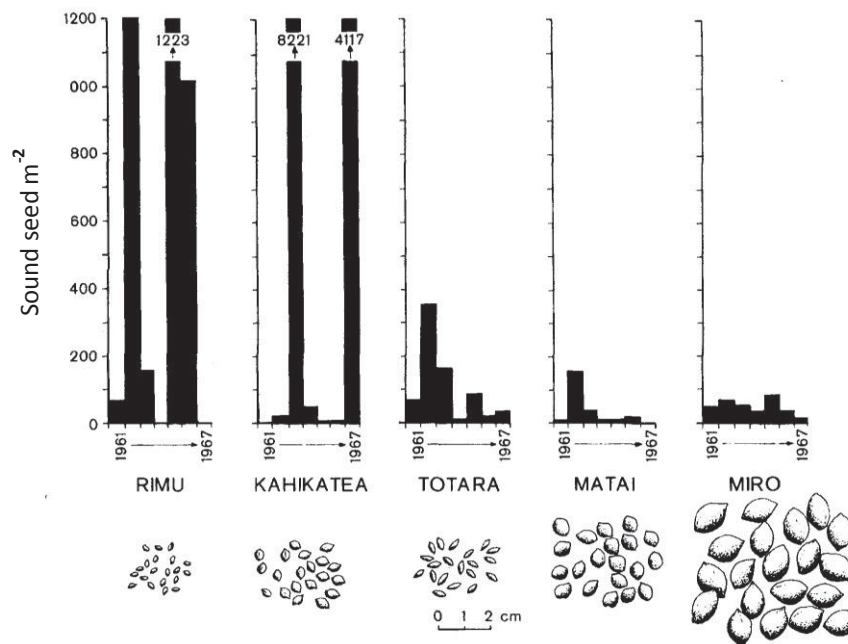


**Figure 14.** Seed size (cm), production (seeds  $m^{-2}$ ) and periodicity (1961-1967) for five New Zealand podocarps. Source: Ogden (1985)

Thus *K*-selection for *Prumnopitys ferruginea* (miro) > *Prumnopitys taxifolia* (matai) > *Podocarpus totara* (totara) > *Dacrydium cupressinum* (rimu). Note the increase in seed size from left to right in Figure 14; taxa to the left of Figure 14 have greater, but more erratic seed production than taxa to the right, with some mast years, another *r*-adaptation.

#### 5.4.2. Grime's C-S-R Theory

Grime (1977) suggested that external factors that limit plant growth in an environment may be classified as either (i) *stress* - conditions that restrict biomass production – including nutrient, water and light deficiencies and suboptimal temperatures; and (ii) *disturbance* – the partial or total destruction of plant biomass – due to damage by herbivores, pathogens, anthropogenic activities such as pruning or mowing, and damage from wind, desiccation, frosts and fire.

When the four combinations of external factors were compared (Table 4), Grime (1977) noted that only three of them were viable as plant habitats, since in highly disturbed habitats subjected to severe stress vegetation was unable to recover or re-establish. This observation formed the basis of Grime's *C-S-R* theory: three primary strategies – *C* (competitors), *S* (stress tolerators) and *R* (ruderals – early colonisers) are selected for under extreme competitive, stressful or disturbed conditions respectively.

Table 4. Basis for the Evolution of C-S-R Strategies in Vascular Plants		
	Stress Intensity	
Disturbance Intensity	Low	High
Low	Competitive Strategy	Stress-tolerant Strategy
High	Ruderal Strategy	No Viable Strategy

Grime's (1977) *C-S-R* theory can be reduced to two fundamental hypotheses: (i) the significance and intensity of competition in vegetation is inversely related to the significance and intensity of stress and disturbance; and (ii) the different equilibria that become established among stress, disturbance and competition in vegetation are associated with the evolution of distinct and predictable strategies.

The *C-S-R* model describes and explains recurring sets of plant characteristics that over significant periods of time and under specific conditions seem to have a selective advantage in vegetation assemblages (Grime 1988b). A competitive strategy occurs in plants found in habitats that have infrequent disturbance and high resource supply. The competitive strategy includes traits that enhance and trap resources and maximise production of dry matter such as a dense canopy, large stature, high root surface, and high morphological plasticity. Under a competitive strategy a drift towards monoculture is predicted since weaker competitors are confined to depleted areas of the environment (Grime 1988b).

Stress-tolerant strategies are adopted by plants whose habitats have both low frequencies of disturbance and low resource levels. Under these conditions, occupation by slow-growing and long-lived evergreens is expected, since these taxa have efficient retention and protection of their nutrient capital. Stress-tolerant species traits include slow growth rates, long-lived organs and luxury uptake and nutrient storage under resource-rich conditions. Plants living in conditions of high disturbance and high resource supply utilise a ruderal strategy; these plants are also known as ephemerals.

The relationship between *C-S-R* theory and *r-K* theory from which it is derived, is shown in Figure 15. Grime (1977) noted that *R*- and *S*-strategies correspond most closely to the extremes of *r*- and *K*-selection, with *C*-strategy occupying an intermediate position. The most significant difference between the two models is that stress tolerance in the *C-S-R* model is a distinct strategy selected in unproductive environments or under conditions of extreme resource deficits caused by the vegetation itself.

In summary, the *C-S-R* model provides a concise framework for describing the major variables in the functional characteristics of organisms and enables analysis of the structure and dynamics of communities. The value of the *C-S-R* model in the current study is that it provides a classification schema to assist in identifying vegetation assemblage changes in response to environmental and climatic changes over time, that supplements the broad vegetation categories frequently used in presenting fossil pollen data such as *Nothofagus* – conifer –other trees-shrubs-herbs categorisation.

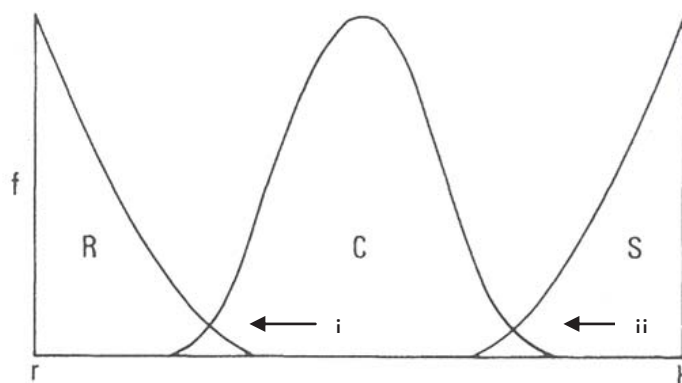


**Figure 15. The Frequency of Competitor, Stress tolerant and Ruderal (*C-S-R*) Strategies along the *r-K* Continuum.** There are two critical points along the *r-K* continuum; at (i) the intensity of disturbance becomes insufficient to prevent exclusion of ruderals by competitors; and (ii) the level of supply of resources is depleted below the level required to sustain the high rates of reinvestment of captured resources characteristic of competitors, and selection begins to favour the more conservative physiologies of stress tolerators (Grime 1979). *Source:* Grime (1977).

### 5.4.3. Plant Succession following Volcanic Disturbance

Lees & Neall (1993) extracted fossil pollen cores from multiple sites within Egmont National Park. The oldest core, from Stratford Mountain Road clearly demonstrated the destruction of *Brachyglottis elaeagnifolia* (leatherwood) scrub by a pyroclastic flow that occurred around  $1,940 \pm 75$  cal yrs BP; this species did not return to its status as the predominant shrub taxon until just before the Newall eruption, 450 years BP. Severe damage to canopy species such as *Dacrydium cupressinum* allowed rapidly colonising, *R*-selected taxa such as *Coriaria* to take advantage of increased understory light intensity and dominate the pollen assemblage, followed by *Dracophyllum*, *Myrsine* and *Coprosma*.

McGlone *et al.* (1988) analysed pollen from Potaema Bog, on the eastern flank of Mount Egmont, and Ahukawakawa Swamp between the northern flank of Mount Egmont and the southern flank of the Pouakai Range that had been emplaced around the times of the Newall and Burrell (350 yrs BP) eruptions. Prior to the Newall eruption, the forest assemblage surrounding Potaema Bog had been relatively stable for three thousand years, with *Dacrydium cupressinum* and *Metrosideros* representing the dominant tall tree taxa, with an understory dominated by *Elaeocarpus*, *Nestegis*, and the tree fern *Cyathea smithii*.

Following the Newall eruption, large areas of upper montane vegetation on Mount Egmont were damaged or destroyed by a *nueé ardente*, with a sudden decline in the relative abundance of all podocarp pollen, as well as *Libocedrus* and *Nothofagus* subg. *Fuscospora* pollen. Damage at Potaema Bog was more limited (McGlone *et al.* 1988; Lees & Neall 1993) since much of the hot density flow was directed to the north-west of Mount Egmont, and cooler gases and tephra were deposited to the east.

Subsequent secondary succession involved a sharp, but short-lived rise in the mycorrhizal initiating taxon *Leptospermum* / *Kunzea* followed by nitrogen-fixing *Coriaria arborea* (McGlone *et al.* 1988; Lees & Neall 1993). This rise in *Leptospermum* / *Kunzea* and *Coriaria* is an example of the tolerance model: both taxa were able to tolerate high light levels, since there were no other plants to provide shade; and low levels of soil nutrients, since the lack of vegetation precluded the accumulation of bulk organic matter in the soil substrate.

The length of time that a primary tephra fall impacts upon vegetation can often be relatively short; Newnham & Lowe (2000) found *c.* 22 cm of Waiohau tephra (deposited  $13,460 \pm 100$  cal yrs BP) at Kaipō Bog resulted in a short-lived ( $\approx 50$  years) decline in trees, followed by a spike in the lowland podocarp: grass ratio, prompting Alloway *et al.* (2007) to conclude that the tephra fall may have been beneficial to plant communities that were adapted to the prevalent climate. The improvement of substrate nitrogen levels and a reduction in light levels at the soil surface at Potaema Bog is an autogenic change bringing about facilitation and relay floristics<sup>6</sup>: the next step in the successional sequence was establishment of a *Weinmannia*-dominated forest, with *Elaeocarpus* present in greater relative abundance than it had been previously (McGlone *et al.* 1988).

The replacement of *Coriaria* is an example of inhibition by *Weinmannia*, which grows to a greater height than, and overtops, *Coriaria*. Clarkson (1990) suggests that a tolerance model is also applicable at this step, since young *Weinmannia* can tolerate shading by a *Coriaria* canopy. This observation supports Finegan's (1984) assertion that facilitation, tolerance, inhibition and allogenic mechanisms of succession are interdependent and may occur simultaneously with respect to an individual plant.

In contrast to the dramatic reduction in the tree ferns *Cyathea dealbata*-type and *Cyathea smithii*-type in the understory, *Aristotelia*, *Pseudopanax* and *Coprosma* all rose in relative abundance, with *Pteridium* and *Blechnum capense* becoming major ground cover taxa at Potaema Bog. In this case, the role of succession or

---

<sup>6</sup> The facilitation and relay floristics model (Clements 1928) holds that succession occurs when pioneers modify their environment making it more amenable for a later species to invade (facilitation); the sequence of change continues until a climax vegetation assemblage was achieved (relay) for a given climate regime. Thus facilitation and relay floristics is synonymous with autogenic change (Clarkson 1990).

the successional mechanism involved is not clear. Since by definition successional models are applicable only where climate remains effectively unchanged, if these vegetation changes were a response to climate change such as reduced rainfall, then invoking succession to explain the *Leptospermum* → *Coriaria* → *Weinmannia* sequence is invalid.

At Ahukawakawa Swamp, succession following the Newall eruption saw a more modest increase in the rise of *Coriaria* than occurred at Potaema Bog, and no discernible change in *Leptospermum*. Although there was a marked decline in the relative abundance of the tall tree taxon *Libocedrus*, the abundance of neither the podocarps nor the beeches appeared to be unduly affected by ash fall (McGlone *et al.* 1988).

Succession at Potaema Bog 150 years after the Burrell eruption was characterised by the overwhelming dominance of *Coriaria*, comprising 90% of the pollen sum; this indicates damage following the Burrell eruption was more severe at Potaema than after the Newall eruption (McGlone *et al.* 1988). In contrast to succession after the Newall eruption, *Leptospermum* was neither a significant pioneering species following the Burrell eruption, nor was it present in high numbers for another 200 years. The composition of the tall tree taxa changed following the Burrell eruption, with *Metrosideros*, comprising 55% of the pollen sum, being the clear dominant for a few decades after the eruption before it was overtaken by *Dacrydium cupressinum*, and equalled by *Prumnopitys ferruginea* and *Prumnopitys taxifolia* by 100 years BP (that is, 1850 AD).

The brief period of dominance by *Metrosideros* at Potaema Bog may be the result of coppicing from damaged trunks and/or colonisation on bare surfaces (McGlone *et al.* 1988), suggesting that *Metrosideros* is *r*-selected on the *r*-*K* selection continuum (discussed above) relative to the podocarps that replaced it, since *Metrosideros* is less shade tolerant (that is, tolerance model is applicable) and may produce more seeds than the podocarps; *Metrosideros* may have in turn provided conditions suitable for podocarps, such as providing shade (facilitation and relay floristics). The decline in the low-fertility-tolerant *Leptospermum* abundance following the Burrell eruption may be due to an inability to compete with the obligate moderate-fertility taxa *Blechnum capense* –type ferns, *Phormium tenax* and sedges that colonised and formed a dense cover (McGlone *et al.* 1988).

This is an example of the inhibition model, and also highlights the difference between plant species adapted to resource-rich environments, which generally have higher relative growth rates than species adapted to low resource environments under conditions of high resource supply (luxury uptake). The inhibition model holds that once early colonising taxa occupy a site and utilise resources, they inhibit invasion by other taxa, and/or suppress the growth of taxa that were already resident. Taxa that were already present are only able to increase in number when the dominant taxa are damaged or destroyed, releasing their resources (Clarkson 1990); in other words, succession occurs when short-lived plants are replaced by longer-lived plants.

The minimum tephra thickness required to cause discernible damage (for example, defoliation, death etc) to the forest assemblage is difficult to determine, since it largely depends upon the taxa in question, and their respective plant morphologies and plant strategies they employ. Efford *et al.* (2012) compared the treeline taxa composition on Mt Egmont with Burrell Lapilli (*c.* 350 years BP) isopachs, noting that although *Weinmannia* was abundant outside the lapilli deposit, it was absent within the deposit. *Libocedrus* appeared to be more resistant to the affects of the lapilli airfall than *Weinmannia*, since it was only absent in the thickest, 25-40 cm isopach. In contrast, in areas of moderate lapilli deposits (5-25 cm), *Libocedrus* and *Podocarpus* were able to establish, although *Griselinia* and *Podocarpus* are the most successful treeline taxa. A 25 cm-thick deposit of Burrell Lapilli being was sufficient to exclude *Libocedrus* on Mt Egmont (Efford *et al.* 2012); whilst a 30 cm-thick deposit of Newall Lapilli affected drainage at Potaema Bog so that the size of the bog increased, allowing Cyperaceae to temporarily thrive, followed by colonisation by *Leptospermum*, *Phormium*, *Astelia* and Poaceae (Lees & Neall 1993).

In contrast to Ahukawakawa Swamp (McGlone *et al.* 1988), Potaema Bog (McGlone *et al.* 1988; Lees & Neall 1993) or Mt Egmont (Efford *et al.* 2012) the Eltham pollen record shows little or no successional patterns following volcanic ash fall. Although this could be a consequence of sampling at intervals too coarse to amplify

the pollen signature for successional taxa, this seems unlikely given that average sampling resolution was around one sample for every 61 years, and large parts of the core (in particular, LGIT to EHW time period) were sampled contiguously; on balance it seems more likely that even the thickest ash deposits during the period under consideration had little or no effect on the vegetation assemblage.

This lack of response to ash fall is seen most clearly in the peat deposit at Opunake Beach (Figure 44); a 12 cm layer of unidentified coarse andesitic tephra had no discernible effect on the composition of the pollen assemblage, with the relative abundance of *Nothofagus* and tree conifer, other tree and shrubs pollen largely unchanged; a 10% increase in Poaceae pollen is countered by a 10% decrease in *Leptospermum*-type pollen, both *r*-selected (*sensu* McArthur & Wilson 1967) or *R*-selected (*sensu* Grime 1977) taxa that might be expected to increase in response to disturbance. In contrast, volcanic disturbances in the form of very large debris-avalanche deposits at the coastal Taranaki sites obliterated the vegetation. The resultant succession was manifest in the lignites overlying debris-avalanche deposits by the preponderance of *r*-selected successional grasses and shrubs in the pollen assemblage.

## 5.5. Floral Biodiversity

### 5.5.1 Introduction

Palynological data can assist understanding contemporary diversity by (i) providing base line data under natural conditions; (ii) elucidating slow environmental processes such as podzolisation or long term succession; (iii) highlighting historical vegetation and climate that are not observable today (Odgaard 1999), and (iv) suggest how environmental changes might occur in the future (Weng *et al.* 2006). In the present study, however, changes in the fossil pollen assemblage are used to make inferences about paleoenvironmental and paleoclimate variables. Biodiversity patterns can highlight paleovegetation changes that might otherwise remain undetected, and allow vegetation change to be quantified over time.

The inferred vegetation change in turn may flag a perturbation in the paleoclimate or paleoenvironment, and one can draw some conclusions about the likely parameters of the palaeoclimatic variables. For example, Flenley (2003) used a simple measure of number of fossil pollen taxa or ‘palyno-richness’ to demonstrate that latitude explained 83% of the variance in diversity from published Holocene mid-latitude lowland sites and tropical lower montane sites. A similar approach is used in this study to highlight temperature and wind intensity changes, and to a lesser extent changes in precipitation and fire regimes.

Community biodiversity is often assumed to be the result of processes at a local scale including taxon adaptation, interactions between species such as competition or predation, and random events; however processes at regional scales such as climate and climate stability, disturbance, energy availability, primary production and the heterogeneity of habitats are also important (Birks & Line 1992; Weng *et al.* 2006).

An alternative, non-mutually exclusive view of community biodiversity is the Red Queen-Court Jester dichotomy used to describe speciation rates. Van Valen (1973) saw evolution as driven by Darwinian, biotic processes such as competition and predation, whereby a species must continually adapt to maintain its fitness and competitive advantage over other species that it is co-evolving with, over short (Milankovitch-scale, or shorter) time spans, based primarily on intrinsic factors such as morphology, tolerance to stress, or colonising ability: this is the Red Queen hypothesis. In contrast, the Court Jester hypothesis<sup>7</sup> (Barnosky 2001) holds that abiotic and unpredictable extrinsic changes are the primary instigators of major changes in organisms and ecosystems, including changes in diversity; typically these abiotic changes occur over time periods > 1My.

---

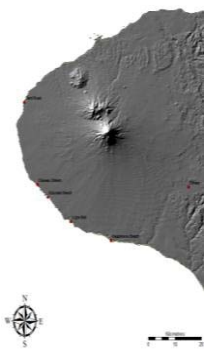
<sup>7</sup> The Red Queen label comes from Lewis Carroll’s *Through the Looking Glass*, where the Red Queen tells Alice “...it takes all the running you can do, to keep in the same place. If you want to get somewhere else, you must run twice as fast as that!” The ‘Court Jester’ refers to “...the capricious behaviour of the licensed fool of Medieval times,” (Benton 2009).

Bringing both the local-regional and Red Queen-Court Jester paradigms together gives Table 5; the Court Jester (abiotic) model of diversity is driven at least in part by climate fluctuations at both the local and regional scales, and the Red Queen (biotic) model is driven in part by primary production at the regional level. Since (biotic) primary production is also a function of abiotic variables such as insolation and other climate variables, it is clear that on balance, climate is a major, if not *the* major, determinant of floral biodiversity.

The statistical relationship between taxonomic richness and latitudinal gradients in general has been long recognised (von Humboldt 1808, Wallace 1878, cited in Erwin 2009) and between climate and taxonomic richness in plant communities in particular (Currie & Paquin 1987; O'Brien 1993). This relationship may be a consequence of differences in the energy flux at different latitudes, expressed as differences in evapotranspiration and transpiration (Benton 2009) and temperature (Erwin 2009); surprisingly, there is little correlation between photosynthetically active radiation and diversity (Hawkins *et al.* 2003). The Energy-richness hypothesis holds that diversity is a function of the number of individuals in an area, whose numbers are limited by net primary productivity (NPP), which is in turn influenced by climate. If the proportion of NPP sequestered by a broad taxonomic group (for example, higher plants) varies little with NPP, there will be more taxa in the broad taxonomic group in areas of high primary productivity, and diversity will increase (Currie *et al.* 2004). Thus, we might expect that diversity of the pollen assemblage at Eltham would increase with climate amelioration, *ceteris paribus*.

Benton (2009) suggested that there are two broad approaches for studying species diversity over time; (i) the taxic approach, which simply involves counting taxa over time, and (ii) phylogenetic techniques that involve the use of cladograms, that attempt to define taxonomic groups on the basis that all members of a given taxon are derived from a common ancestor. The current study uses Benton's (2009) taxic approach to investigate biodiversity changes within a single habitat (alpha diversity), as opposed to between-habitat diversity (beta diversity). Descriptions of the individual diversity indices are given in methods section 7.7.

**Table 5. Red Queen and Court Jester Models at Different Geographic and Temporal Scales**

					
		<b>Local</b>	<b>Regional</b>		
<b>Temporal Scale</b>	Genus Life Span (3-6 My)		<ul style="list-style-type: none"> <li>• Disturbance                             <ul style="list-style-type: none"> <li>○ Landslide</li> <li>○ Debris avalanche</li> <li>○ Flood</li> <li>○ Fire</li> <li>○ Isostatic sea level change</li> <li>○ Eruption</li> </ul> </li> <li>• Microscale and mesoscale weather patterns</li> </ul>	<ul style="list-style-type: none"> <li>• Climate stability</li> <li>• Energy availability</li> <li>• Habitat Heterogeneity</li> <li>• Eustatic sea level change</li> <li>• Synoptic scale and macroscale weather patterns</li> <li>• Dust/nutrient inputs</li> </ul>	
	Species Life Span (1-2 My)				<b>Court Jester</b>
	Milankovitch Scale (100 ky)		<ul style="list-style-type: none"> <li>• Taxon adaptation</li> <li>• Competition</li> <li>• Predation</li> <li>• Colonising ability</li> <li>• Ecological specialisation</li> <li>• <i>r</i>-selected vs. <i>K</i>-selected strategies</li> </ul>	<ul style="list-style-type: none"> <li>• Primary production</li> </ul>	
Millennial–Sub-Millennial Scale	<b>Red Queen</b>				
		Locality	Species Range	Biotic Region / Climate Zone	Continent
<b>Geographical Scale</b>					

Source: based on Benton (2009)

### 5.5.2. Intermediate Disturbance Hypothesis (IDH)

In addition to biodiversity information being useful in its own right, diversity data can be combined with disturbance data to test the Intermediate Disturbance Hypothesis (IDH) for a given disturbance regime. This section describes the IDH –the hypothesis that species richness was influenced by disturbance -with special reference to the New Zealand flora. Disturbance in this context is any event that alters niche opportunities accessible to taxa in an ecosystem (Connell & Slayter 1977; Shea *et al.* 2004) such as fire, flood, drought, storms, and volcanic eruptions. Species richness is predicted to be lowest when disturbance is either frequent or rare, and predicted to be highest somewhere between these extremes. The current study tests the IDH by comparing floral diversity data to aerosolic quartz dust (that, is, paleowind) data from Eltham and to a lesser extent freezing temperatures (section 5.3.1). In addition, other types of disturbance that might be expected to occur in Taranaki over the time period under consideration are discussed elsewhere, including cyclones, extreme winds and tornadoes (section 3.3) drought (section 3.4), volcanic disturbance (section 5.4.3) and fire (section 5.3.4).

Low species richness during times of stability is interpreted to be the product of the fact that as vegetation approaches its ‘climax’ carrying capacity, it will typically be dominated by a small number of good competitor (*K*-selected) taxa. In contrast, low species richness during times of frequent or intense disturbance occurs when species are continually driven to extinction, so only a few specialised colonising (*r*-selected) taxa persist, and low species richness also occurs (Townsend *et al.* 1997); in other words, disturbance causes a reversion of the community to an earlier successional state so that species that had been expelled by superior competitors can re-establish themselves (Sheil & Burslem 2003). The highest species richness occurs somewhere between the two extremes, such that *K*-selected and *r*-selected taxa co-exist.

In the absence of disturbance, diversity is a function of the range of available resources and the degree to which taxa are specialised to exploit the resources, and the concept of competitive exclusion applies (Catford *et al.* 2012): in a stable, closed ecosystem, superior competitors reduce interspecies competition as a result of being specialised and competitively superior to other taxa at exploiting a particular resource (Sousa 1979) forcing inferior competitors to extinction, and diversity declines (Sheil & Burslem 2003; Shea *et al.* 2004). When demonstrated graphically, IDH predicts a hump-shaped parabola (Molino & Sabatier 2001; Sheil & Burslem 2003; Svensson *et al.* 2007; Biswas & Mallik 2010; Catford *et al.* 2012) (Figures 16-18).

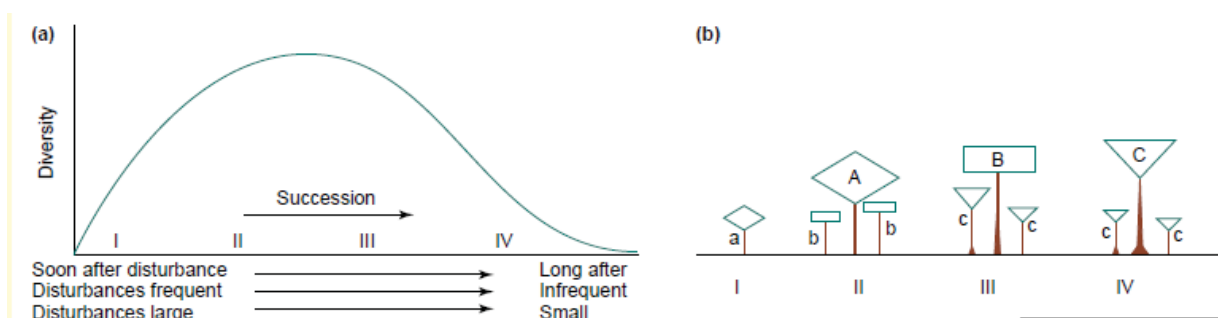


**Figure 16. Intermediate Disturbance Hypothesis Parabola.** (a) Diagram shows how time after disturbance, frequency and size of disturbance drive changes in diversity. (b) Theoretical successional sequence, showing low diversity at Stages I and IV, and higher diversity at Stages II and III, with a, b and c representing understory taxa, and A, B and C representing canopy taxa. *Source:* Sheil & Burslem (2003)

Hiura (1995) investigated the location, size and timing of gap formation in beech (*Fagus crenata*) forests in Japan to determine if the Intermediate Disturbance Hypothesis was applicable at local scales. Neither the mean gap size nor latitude showed a correlation with species diversity (expressed by Shannon’s indices, Figure 17; also section 7.7); however there was a positive correlation between both storm frequency and temperature and species diversity. The author concluded that the hypothesis was partially supported: although there is an

apparent relationship between the disturbance interval and diversity (Figure 17), with the characteristic ‘hump-shaped’ graph predicted by the Intermediate Disturbance Hypothesis, mean annual temperature was a better predictor of forest diversity.

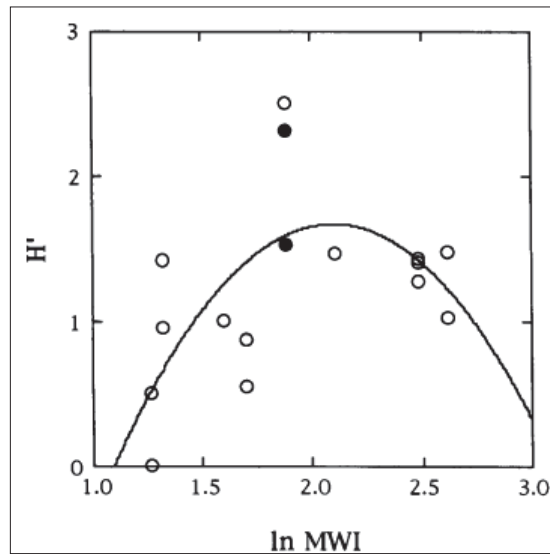


**Figure 17. Relationship between Disturbance Interval and Species Diversity for 23 Japanese Forests.**  $H'$  = Shannon's Index,  $\ln MWI$  = logarithm of mean windstorm interval. Solid circles represent data from stands which have different flora from the other stands (open circles). Source: Hiura (1995)

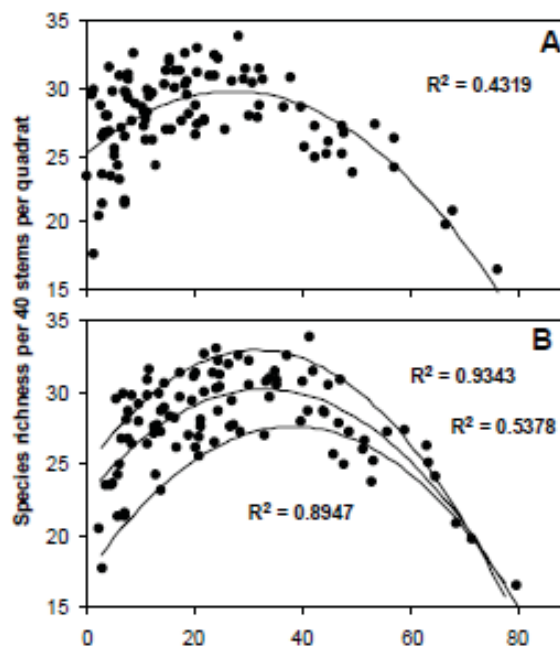


**Figure 18. Species Richness of Tree Communities in Paracou, French Guiana as a Function of the Percentage of Pioneer Stems (A) or Heliophilic Stems (B)** Source: Molino & Sabatier (2001)

Jane (1986) found that in inland Canterbury: (i) under low disturbance, *Nothofagus solandri* var *cliffortioides* stands proceeded until maturity; natural mortality reduced the density of the stand, producing gaps available for stand replacement by light-demanding *Nothofagus solandri* var *cliffortioides* juveniles to the exclusion of shade tolerant species. In *Libocedrus bidwillii* / *Podocarpus hallii* forests, low disturbance lead to shade tolerant *Podocarpus hallii* and *Griselinia littoralis* preventing the establishment of mountain beech. In either case, diversity remains fairly constant. (ii) Under high disturbance conditions such as large scale wind throw, rapid regeneration at frequent intervals (100-150 years) of *N. solandri* var *cliffortioides* excludes *Podocarpus hallii* and *Griselinia littoralis*; this massed regeneration may be a mechanism to ensure the monoculture persists (Jane

1986), and diversity remains largely unchanged. (iii) Under intermediate disturbance, massed regeneration and mono-specific associations are less likely to occur; succession progresses by invasion of the extant forest such as *Weinmannia racemosa* forest by a later successional type such as *Podocarpus totara* / *Beilschmeidia tawa* or *Weinmannia racemosa* / *Beilschmeidia tawa* to pure *Beilschmeidia tawa*, and overall taxa richness increases.

Urlich *et al.* (2005) investigated whether canopy tree regeneration following disturbance varied with soil drainage at Mt Harata in Buller. They found that following severe disturbance (earthquakes), both conifers (*Dacrydium cupressinum* and *Dacrycarpus dacrydioides*) and angiosperms (*Nothofagus* subg. *Fuscospora*, *Nothofagus menziesii* and *Weinmannia racemosa*) colonised poor soils, but only the angiosperms colonised well drained soils. Following intermediate (storm) damage, faster growing *Nothofagus* subg. *Fuscospora* occupied elevated microsites, precluding *D. cupressinum* and thus reducing diversity. This suggests that diversity in New Zealand is only partially determined by disturbance frequency and intensity, and/or other factors enhance or dampen the effects of disturbance. For example, earthquake damage was probably greater for conifers because of their preference for poor soils which are more prone to liquefaction and therefore tree toppling.

Earthquakes that occurred along the Alpine Fault over the last 650 years caused forest destruction over 80% of the study area by initiating landslides, tree toppling and river aggradation (Wells *et al.* 1999; Wells *et al.* 2001; Cullen *et al.* 2003). These researchers found evidence that massive aggradation, erosion and sedimentation events had instigated the formation of cohorts of early colonising conifers (*Prumnopitys taxifolia*, *Prumnopitys ferruginea*, *Podocarpus hallii*, *Dacrydium cupressinum* and *Dacrycarpus dacrydioides*): younger age classes had established in erosion channels among older cohorts; and large root plates of older trees exposed by erosion, and trunks of partially buried older trees were occupied by younger trees. Wells *et al.* (2001) suggested that the dominance of the older tree cohort, and fewer younger to intermediate aged trees, reflected the length of time since the last major earthquake along the Alpine Fault.

Smith *et al.* (1995) note that co-occurring species in stressful environments should exhibit similar adaptations to the hostile abiotic conditions, therefore functional diversity should be low in stressful environments. Based on their study at Old Man Range in Central Otago, the authors found an increase in functional diversity with increasing snow depth (since deeper snow insulated plants from freezing conditions); therefore we might predict that the numbers of adaptations to stressors like wind to decrease with stressor intensity (for example, divarication as an adaptation to wind) at Eltham. Smith *et al.* (1995) suggested that in alpine zones, only increasing diversity as stress declined from high to medium would occur, and their results did not support the increase in diversity as stress increased from low to medium as predicted by IDH.

Some support for Intermediate Disturbance Hypothesis is provided by the regeneration behaviour of New Zealand podocarps on nutrient rich soils: although New Zealand podocarps endure in deep shade, their height is suppressed by shading and they do not grow past the seedling stage, therefore the prospect for regeneration is limited to areas of disturbance (Coomes & Bellingham 2011). Large-scale disturbances appear to be critical in initiating regeneration of *S*-adapted taxa (Wells *et al.* 1999); as a consequence *Dacrycarpus dacrydioides*, *Podocarpus hallii*, *Dacrydium cupressinum* and *Prumnopitys ferruginea* rely upon catastrophic disturbance such as debris avalanches and floods to open up gaps for regeneration (Smale 1984; Bellingham & Richardson 2006) on nutrient rich soils. On the other hand, Wilson *et al.* (1996) found no evidence of a relationship between site stress and species richness in podocarp/broadleaf forests and beech forests at 90 coastal Otago sites, concluding that the hump-backed relationship may not apply to woody taxa.

The longevity of podocarps enables them to survive between infrequent catastrophic events (Coomes & Bellingham 2011); a consequence of podocarp regeneration in this fashion is a reduction in overall diversity, since the podocarps dominate the forest assemblage. Intermediate disturbance is insufficient for podocarp regeneration; Coomes *et al.* (2005) showed that isolated fallen trunks are seldom colonised by conifers; rather, fast-growing, small-seeded angiosperms and ferns quickly establish in these niches, and diversity is higher than under severe or mild disturbance.

Although the IDH is intuitively appealing, it needs to be tested due to questions regarding its validity on empirical grounds – a diversity maximum at intermediate disturbance levels appears to occur in < 20% of published studies (Mackey & Currie 2001; Hughes *et al.* 2007) and also on theoretical grounds, with a lack of consensus on the nature of the relationship between disturbance and diversity (Death & Barquín 2012). Potential flaws in the assumptions underpinning IDH include: (i) although disturbance reduces the density of *C*-selected taxa, allowing *S*- and *R*-selected taxa to increase in number, disturbance also reduces the strength of competition required to exclude the poorer competitors (Fox 2013); (ii) rather than intermediate disturbance retarding competitive exclusion by reducing the density of all taxa to low levels and allowing all taxa to increase, it is the difference in average growth rates between *C*-selected and *S*- and *R*-selected taxa that determines the rate of competitive exclusion (Fox 2013); (iii) changes to the relative timescale of disturbance is not a prerequisite to alter long-term competitive outcomes and therefore diversity (Fox 2013); and (iv) the relationship between disturbance intensity and diversity is not unidirectional. Disturbance intensity can be both a cause and effect of local diversity such that the extent of biomass loss from a community may be dependent upon the diversity of the community prior to disturbance (Hughes *et al.* 2007).

The intended application of the IDH was high-diversity ecosystems whose extant taxa can be comprehensively enumerated, whereas the current study analyses fossil pollen records whose accuracy in recording past plant diversity is limited by differences in taxa pollen production, preservation and dispersal, and by the low levels of resolution that can be achieved for some taxa (for example, to Family level). Nevertheless, various researchers have examined changes in biodiversity and tested the IDH using fossil pollen data: Flenley & Butler (2001) found evidence of near-continuous, likely anthropogenic, fire disturbance in the Sumatran Rift Valley over the last 7,000 years, however their qualitative analysis found that the effects of fire disturbance on biodiversity were negligible. In contrast, Colombaroli *et al.* (2013) found that palynological richness (using rarefaction analysis) was greatest under intermediate levels of burning disturbance during Mesolithic-Neolithic (8,400-7,000 cal yr BP) times in the Valais, Switzerland.

Despite the potential weaknesses outlined above, IDH has value in that it reinforces the concept that plant communities seldom reach equilibrium, and it continues to provide a conceptual framework for ecological hypotheses that relate disturbance and diversity (Collins & Glenn 1997). Moreover, IDH is contentious because it is seldom tested directly, but is inferred after disturbance events to quantify differences between communities where the definitions of disturbance vary between communities (Collins & Glenn 1997); if these assertions are correct, the argument opposing IDH on the grounds of a lack of predicted, modal diversity-intermediate disturbance relationships raised by Mackey & Currie (2001) and Hughes *et al.* (2007) is weakened.

Interestingly, Mackey & Currie's (2001) analysis of published IDH studies suggested that disturbance appears to be more important in determining temporal patterns of diversity than spatial patterns of diversity: temporal gradients of disturbance explained 64.5% of variation in diversity (Shannon's Index and Simpson's Index) and 61.1% of variation in species richness, compared with 52.3% of diversity and 41.8% of species richness for spatial gradients of disturbance. Furthermore, Collins (1992) and Collins *et al.* (1995) examined the effects of fire frequency on prairie vegetation in Kansas, the United States to show that although plant diversity did not reach a maximum at intermediate frequency of fire, diversity did reach a peak after intermediate intervals since disturbance (Figure 16). Together, these studies imply that IDH is an appropriate model for examining within patch, alpha diversity at least, and therefore is an appropriate model for examining biodiversity change in response to disturbance at Eltham Swamp.

### 5.5.3. Floral Representation in the New Zealand Pollen Rain

Although there are fewer wind pollinated (anemophilous) taxa than insect pollinated (entomophilous) taxa in New Zealand, the dominant canopy taxa (podocarps, *Laurelia* and *Nothofagus*) are anemophilous, as are a few shrub and small tree taxa including *Ascarina*, *Coprosma* and *Dodonaea*. Wind pollination is uncommon amongst herbs, with the exception of the genera *Gunnera* and *Acaena*, and also members of the Cyperaceae, Poaceae and Restionaceae families (McGlone 1988).

The anemophily-entomophily dichotomy is significant with respect to how well the pollen rain represents the extant vegetation. Since the major wind-pollinated taxa typically dominate canopies, they tend to be well-represented or over-represented in the pollen rain. Conversely, although some insect and bird-pollinated canopy taxa (e.g. *Metrosideros*, *Quintinia*, *Elaeocarpus* and *Weinmannia*) produce high volumes of pollen, the pollen is not dispersed far from the source plant and therefore may be under-represented in the regional pollen rain (Pocknall 1978; McGlone 1988). An extreme example of under-representation in the pollen rain is *Beilschmiedia tawa*, a species that is likely to be both wind and insect-pollinated (Smale 2008). Despite being a common North Island canopy tree, it is seldom registered in fossil pollen histories (MacPhail 1980; MacPhail & McQueen 1983; Lees & Neall 1993).

The low volumes of pollen from entomophilous taxa observed in modern pollen rain may be due in part to the dense structure of podocarp-broadleaf forest that retard the movement of entomophilous pollen into anoxic environments suitable for preservation. Since fossil pollen sites tend to be bogs, or were bogs in the past, the fossil pollen record may be biased towards very local taxa that are more tolerant of water-logged environments such as *Leptospermum*-type taxon, and especially species tolerant of high water tables such as *Dacrycarpus dacrydioides* and *Syzygium maire* whose pollen is dispersed only short distances (McGlone 1988).

Although many key indicator taxa (e.g. *Nothofagus menziesii*, *Dacrydium cupressinum*, *Prumnopitys taxifolia*, *Prumnopitys ferruginea*, *Ascarina lucida*) have distinctive pollen morphologies, some plants produce pollen that is not distinguishable from other taxa within the same genus, family or taxa group, but are nevertheless ecologically distinct (McGlone 1988). For example, genera such as *Coprosma* and *Myrsine* are represented by a range of plant types, including lowland canopy tree, subcanopy tree and short, divaricating lower alpine shrub species.

Similarly, although *Phyllocladus alpinus* is a subalpine, medium-sized tree found throughout New Zealand with a freezing temperature of  $-20^{\circ}\text{C}$ , and *Phyllocladus trichomanoides* is a lower montane, small tree found only in the North Island and north-west Nelson with a freezing temperature of  $-10^{\circ}\text{C}$  (Sakai & Wardle 1978; Allan 1982), the pollen of the two species cannot be distinguished from each other. Since assigning *Phyllocladus* pollen data to the wrong species could result in erroneous conclusions to be drawn regarding paleotemperatures, pollen analysts typically augment *Phyllocladus*-genera pollen counts with habitat information and pollen data from other taxa to determine the likely species.

### 5.5.4. Pollen Transfer Functions

Wilmshurst *et al.* (2007) produced a model of the pollen rain-climate relationship by performing Principal Components Analysis on published data from 135 pre-history (nominally  $>750$  cal yrs BP) mainland bogs and lakes to construct training datasets to drive pollen transfer functions. Principal Components Analysis (PCA) are used to find the variables (components) that account for as much of the variance in multidimensional data as possible, so that a complex dataset is reduced to only a few, important principle elements (Haslett 2002). Pollen transfer functions are algorithms derived from PCA that relate species abundance to environmental variables such as temperature, precipitation and insolation by way of a training dataset that relates modern plant taxa to the environmental principal components. These models may be applied to the fossil record to estimate past environmental conditions.

The Partial Least Squares (PLS) method models the relationship of each taxon to climate using regression analysis, thus assumes that data behave in a linear fashion. This yields a climate function which is used to transform the entire fossil pollen assemblage into a quantitative estimate of the past climate variable of interest (Birks *et al.* 2010). Thus the PLS method can extrapolate an estimate for the climate variable when there are no appropriate modern analogues, but consequently suffers from the inclusion of taxa that have wide environmental tolerances and therefore has a loss in predictive power. The Weighted Modern Analogue Technique (WMAT) uses chi-squared distance of dissimilarity measures to establish which of the modern analogue assemblages are closest to the fossil pollen assemblages, then takes the weighted average of the 10 closest modern analogues for each fossil pollen signature to quantify past climate variables.

Each model's performance was assessed by comparing outputs with (i) bootstrapped  $r^2$  (the strength of the correlation between observed and calculated mean annual temperature); (ii) root mean square error (RMSE, an estimate of training set accuracy) and (iii) root mean square error of prediction (RMSEP, an estimate of training set precision) values (Wilmshurst *et al.* 2007). The datasets were cleaned by removing samples whose residuals (observed values minus predicted values) were greater than the standard deviation in the training data set, and applying the principle of parsimony to utilise the smallest number of useful samples in the training dataset<sup>8</sup>.

On the basis of these statistical tests, Wilmshurst *et al.* (2007) determined that the WMAT model and the PLS model with two components (PLS-C2) performed best. The PLS-C2 model, with estimated errors of 1.50°C had slightly higher precision than WMAT (estimated errors of 1.51°C), but the correlation between observed and estimated mean annual temperature was stronger for the WMAT model ( $r^2 = 0.82$ ) than PLS-C2 ( $r^2 = 0.77$ ); at the same time, WMAT had a lower maximum bias of 2.02°C compared with 2.44°C for PLS-C2. As a consequence, WMAT is statistically more robust than PLS-C2, and is the preferred model when possible.

Wilmshurst *et al.* (2007) applied both WMAT and PLS-C2 transfer functions to McGlone & Neall's (1994) Eltham pollen dataset, and found that the modelled temperatures for 750 cal yr BP were within  $\pm 1.5^\circ\text{C}$  of modern MAT (11.2°C), which is within the prediction error for both models (Wilmshurst *et al.* 2007). Accordingly, we can have some confidence in the modelled temperatures when the climate is equitable. However, under cold conditions, both models are adversely affected by a relatively small number of modern pollen sites from alpine or treeless environments in the training dataset and therefore tend to underestimate low MATs (Wilmshurst *et al.* 2007; Newnham *et al.* 2012). Although WMAT is more accurate than PLS when there are modern analogues available, it suffers when there are not; conversely, the PLS method is able to impute a value using modern samples that are not necessarily the best analogues, with resultant estimates that are better than WMAT estimates. Furthermore, Telford *et al.* (2004) note that because WMAT is prone to autocorrelation, such that neighbouring sites resemble each other more than randomly selected sites, samples lack independence and incorrect inferences can be drawn regarding the pollen-environmental variable relationship.

Attempts to quantify the relationship between pollen and climate variables have been confounded by large scale, anthropogenic vegetation destruction (Newnham *et al.* 2012). For example, Norton *et al.* (1986) used principal components analysis to analyse 161 sites and group them into clusters with similar pollen assemblages, then applied multiple regression analysis to derive transfer functions that determined the relationship between the pollen assemblage and three environmental variables - mean summer temperature, annual temperature range and mean annual precipitation. The resultant transfer functions were somewhat disappointing from a paleoclimate-reconstruction perspective, in that the correlations between pollen frequency and temperature were weak, with pollen frequency accounting for only 26% of the variance in mean summer temperature, and 37% of annual temperature.

---

<sup>8</sup> A useful component was one that gave a reduction in prediction error of  $\geq 5\%$  of the mean square error (MSE). For the Taranaki temperature reconstructions in this report, the following sites were excluded: eastern North Island ( $n = 3$ ), Canterbury ( $n = 2$ ), southern North Island ( $n = 1$ ) and Otago ( $n = 1$ ).

Norton *et al.*'s (1986) model suffered from (i) a bias towards wetter, western pollen sites, in particular sites from northwest South Island, to the detriment of eastern and in particular East Coast North Island sites, since the former sites were more likely to have at least some native forest cover with which to derive a modern pollen rain – modern forest cover relationship. However, neither past nor extant vegetation cover in the western sites is likely to be representative of forests in the eastern part of the country. (ii) Norton *et al.* (1986) either used published modern pollen rain data, or collected pollen from moss polster or lichen tuft surface samples, which yielded pollen signatures that were distorted by anthropogenic disturbance of the parent taxa. The authors concluded that despite the significant relationships between pollen rain and major climatic variables, their regression equations were not sufficiently robust to be used to reconstruct climate histories from fossil pollen.

The pollen data base assembled by Wilmshurst *et al.* (2007) had a better spatial coverage than that of Norton *et al.* (1986); in particular, many more eastern sites in both islands, and more North Island sites were included. Overall, the database covered wide latitudinal, altitudinal, mean annual temperature and precipitation ranges (34° to 37° S; 0 - 1,540 m; 3.2° to 16.1°C, and 476 to 8,149 mm yr<sup>-1</sup> respectively), with the western North Island –Taranaki region well covered.

However potential weaknesses that remain in the dataset include: (i) sites from a variety of sources (bogs, swamps and lakes) were utilised rather than small lakes only; sole use of the latter would reduce the bias toward coring-site pollen in the pollen assemblage that is inherent in bog and swamp cores;

(ii) the resolution of pollen typically achieved and reported in the literature is a potential weakness in the dataset; 55% of pollen types recorded in the training dataset are comprised of one or more species within a genus (for example *Coprosma*, *Pittosporum*, *Metrosideros*, *Libocedrus*, and *Phyllocladus*), and 5% of pollen types comprised of one (for example, Poaceae) or more (for example, monolete fern spores) family groups. However, the taxon within each genera or group may have very different environmental distributions, for example *Phyllocladus trichomanoides* is a lower-montane taxon with a freezing temperature of -10°C, but the palynologically indistinguishable *Phyllocladus alpinus* is a subalpine plant with a freezing temperature of -20°C (Table 2). As a consequence of these temperature disparities, the training dataset may be compromised in its ability to provide appropriate temperature reconstructions.

(iii) A major assumption of this approach is that the climate at 750 cal yrs BP was similar to the modern day climate, however  $\delta^{18}\text{O}$  evidence from *Porites* corals at Palmyra Island (approximately halfway between Hawaii and American Samoa) indicates that around this time the tropical Pacific experienced cool and dry conditions whilst the rest of the planet experienced the Medieval Warm Period (MWP, *c.* 1,050–750 cal yrs BP); conversely, the central Pacific was relatively warm, wet and stormy whilst the northern hemisphere cooled during the Little Ice Age (LIA), around 600-150 cal yrs BP (Cobb *et al.* 2003; Mayewski *et al.* 2004; Allen 2006). Consequently, this assumption may or may not hold, in particular given that supposed 750 year-old polleniferous sediment for a given site may be contaminated by cooler or warmer taxa coeval with the MWP or LIA, respectively.

## 6. Aerosolic Dust

### 6.1. Introduction

Examination of ice core records show that the atmosphere was much dustier during glacial times than it is today (Delmonte *et al.* 2007). This increased dust load was due to numerous factors including (i) changes to source areas, including the addition of arid and semi-arid land more prone to wind erosion, and marine regressions resulting in the exposure of large areas of the current continental shelf; (ii) higher wind speeds and altered transport routes, due to equator-ward displacement of baroclinic zones leading to higher baroclinicity, and shorter transit times across the baroclinic zone; and (iii) changes in the atmospheric hydrological cycle such as reduced rainfall (Anderson & Ditlevsen 1995).

Wind-blown sediments deflated from land areas and dispersed by the atmosphere are critically important to both the climate system (Harrison *et al.* 2001; Zhang & Carmichael 1999; Delmonte *et al.* 2007) and biogeochemical cycles (Swap *et al.* 1992; Falkowski *et al.* 1998; Martínez-García *et al.* 2011). Dust fluxes influence climate by way of radiative forcing and cloud nucleation, and are themselves influenced by source areas and sinks, wind patterns and precipitation regimes. Aerosolic dusts strongly influence productivity of terrestrial and marine ecosystems by way of nutrient supply (Swap *et al.* 1992; Mahowald & Luo 2003) and therefore impact upon paleoenvironment and paleoclimate due to the influence on the global carbon cycle.

Since changes in the atmospheric dust loading is likely to have a large influence on future climate change scenarios (Kohfeld & Harrison 2001; Tegen *et al.* 2002), it follows that testing atmospheric general circulation models (AGCMs) against paleodust and paleowind data will be critically important.

Mineral aerosols are the primary proxy for studying paleowind (Shulmeister *et al.* 2004). Although dust deposits have most often been examined in loess deposits (Alloway *et al.* 1992, Figure 54), marine cores (Stewart & Neall 1984, Figure 50) or ice cores (Petit *et al.* 1999; Watanabe *et al.* 2003; Delmonte *et al.* 2007), dust deposits in peats provide an as yet under-utilised resource for developing high resolution reconstruction (Weiss *et al.* 2002; Le Roux *et al.* 2008). Aerosolic dust grain size is an indicator of wind velocity, in particular modal grain size which indicates average wind patterns rather than extreme events (Hess & McTainsh 1999; Shulmeister *et al.* 2004); dust accumulation rates provide information about source area, such as availability and erodibility of windblown material, regional hydrology, precipitation regimes, and the nature of the wind blowing over the source (Marx *et al.* 2009).

The New Zealand terrestrial landmass created large volumes of mineral dust during cold climate periods due to accelerated erosion as a consequence of high rates of orogeny, glaciation and volcanic activity, combined with reduced forest cover and intensified westerly winds (Eden & Hammond 2003). As a result, > 10% of New Zealand's land surface carries loess > 1m thick, and soils with a loess component cover as much as 60% of the surface (Bruce *et al.* 1973; McCraw 1975).

Aerosolic dust of New Zealand origin is mostly quartzo-feldspathic in mineralogy, derived from Mesozoic turbidite sequences in the main axial ranges and uplifted Neogene marine sequences (greywackes, argillites and schists) with a 20-60  $\mu\text{m}$  mode (Eden & Hammond 2003). Allochthonous quartz-rich dusts can be isolated from local mafic and andesitic dusts, providing information about the nature of aeolian or fluvial transport characteristics. In other words, since quartz is not derived from andesitic material, one can be certain that quartz dust found in regions such as Eltham is derived from elsewhere and must be aerosolic in nature. Furthermore, because quartz is chemically stable and resistant to mechanical damage (Haldorsen 1981; Sharp & Gomez 1985; Pye 1987) it is ubiquitous in terrestrial and marine sediments (Dauphin 1980), and is therefore the best mineral to analyse when quantifying aerosolic dust flux.

Eolian (wind-blown) materials can be described by their (i) transportation pathway in the atmosphere; (ii) persistence in the atmosphere; (iii) their particle size (Syers *et al.* 1969b); (iv) oxygen isotope

characteristics; and (v) geochemistry and provenance (Marx *et al.* 2009). Marx *et al.* (2009) suggest that wind-blown dust is  $< 50 \mu\text{m}$  but generally  $< 30 \mu\text{m}$ ; most authors agree that aerosolic dust is a fine-grained aeolian component either suspended in air, or a deposit of such particles (Pye 1987), there is less agreement on what particle size distinguishes aerosolic dust from other aeolian components.

In general, most atmospheric dust is smaller than  $100 \mu\text{m}$ ; grains  $20\text{-}100 \mu\text{m}$  settle out of the atmosphere quite quickly when strong winds dissipate, whereas grains transported very long distances are generally  $< 10 \mu\text{m}$  and frequently much less than  $2 \mu\text{m}$  in diameter. Aerosolic dust is  $1\text{-}20 \mu\text{m}$  in diameter, whilst a ‘typical’ loess ranges from  $4$  to  $63 \mu\text{m}$  in diameter, with a mode between  $20$  and  $40 \mu\text{m}$  (Pye 1987); grains  $> 63 \mu\text{m}$  in diameter have a local provenance and therefore reflect local climate, with grains  $< 5 \mu\text{m}$  diameter having a global source and therefore reveal global climate patterns (Table 6). Syers *et al.* (1969b) used dust grains  $1\text{-}10 \mu\text{m}$  as tracers of aerosolic dust; Stewart & Neall (1984, Figure 50) selected dust grains  $2\text{-}5 \mu\text{m}$  in diameter to represent aerosolic dust, with the  $20\text{-}63 \mu\text{m}$  fraction representing loess.

**Table 6. Classification of Eolian Materials by Size**

Type of Eolian Material	Particle Size ( $\mu\text{m}$ )	Transport Pathway	Range (km)	Atmospheric Persistence	Author			
Dune sand	400-200	at or near ground level	$10^{-3}$ to $10^0$	highly transient phase	Syers <i>et al.</i> (1969)			
Loess	50-10	lower troposphere	$10^{-1}$ to $10^2$	transient phase	Syers <i>et al.</i> (1969)			
	50-10				Mokma <i>et al.</i> 1972			
	63-4				Pye (1987)			
Aerosolic dust 20 - 1 $\mu\text{m}$		middle and upper troposphere	$10^4$ to $10^6$	residence time depends on frequency of precipitation – thought to be days or weeks	Syers <i>et al.</i> (1969)			
	<i>Diameter of aerosolic dust tracers (<math>\mu\text{m}</math>)</i>							
	10 -1				Syers <i>et al.</i> (1969)			
	10-2				Rex <i>et al.</i> (1969)			
	5-2				Mokma <i>et al.</i> (1972)			
5-2	Stewart & Neall (1984)							
Stratospheric dust	$< 1$	stratosphere	$10^9$	residence time is years	Syers <i>et al.</i> (1969)			
Extraterrestrial dust	10-0.01	interplanetary space	$10^{12}$	unknown	Syers <i>et al.</i> (1969)			

Other components in wind-blown materials include exotic biological matter such as Australian-sourced *Casuarina* pollen, sponge spicules and diatoms (McTainsh 1989). In contrast to minerogenic sediment-based proxies for wind strength, microfossil paleowind proxies are typically driven by responses to the secondary effects of wind flows such as influence on temperature or rainfall and their subsequent impact on biological growth, as opposed to the direct impact of wind flow itself. For example, stronger winds enhance oceanic upwelling so that the nutrient flux increases and diatom blooms occur (Shulmeister *et al.* 2004<sup>9</sup>; Rojas *et al.* 2009; Moreno *et al.* 2010).

The volume of dust in the atmosphere is controlled by climatic factors (temperature, precipitation regimes and wind patterns), but the dust load also affects climate by chemical and physical means, so feedbacks between dust and climate occur (Arimoto 2001). Therefore, the focus of this part of the study is the analysis of the

<sup>9</sup> Although the authors caution that it is difficult to attribute such changes entirely to wind strength because blooms may be generated by factors other than upwelling.

quartz component of mineral dust and loess from Eltham Swamp, in order to characterise climate patterns since 40,000 cal yrs BP, and to derive a narrative of vegetation responses to, and influence on, the local wind regime.

## 6.2. Aerosolic Dust and Terrestrial Biogeochemical Cycles

The purpose of this section is to note the importance of wind-borne nutrient supply in the context of the trophic status of regional soils and in particular the nature of ombrotrophic and minerogenic peats, since this (i) influences regional soil fertility; (ii) influences the composition of local (bog) plant communities; and (iii) influences the taphonomy of fossil pollen assemblages found in a peat bog such as Eltham. Most importantly, (iv) the trophic status of the bog may influence how well aerosolic dust grains are preserved.

Since rock-derived elements such as calcium, magnesium, potassium and phosphorus are not replaced over sub-geological time scales, autochthonous, biologically available minerals in soils become depleted over millennial timescales (Chadwick *et al.* 1999). In contrast, allochthonous elements from atmospheric dust may be renewed continuously, therefore young ecosystems have low concentrations of atmospherically derived nutrients, and old ecosystems have low concentrations of nutrients derived from local substrates.

Chadwick *et al.* (1999) evaluated the mineral nutrient limitations to forest growth and net primary production at three sites in Hawaii. These researchers used strontium isotopes to determine that 90% of calcium and magnesium in soils younger than 2,100 years was derived from local rock, whereas for soils older than 150,000 years the atmosphere accounted for > 80% of these elements. Because soils accumulate immobile trace elements such as neodymium, hafnium and thorium, differences in the isotope ratios between Asian dust and Hawaiian basalts were used to determine that although autochthonous phosphorus persists in ecosystems for as long as a million years - much longer than either calcium and magnesium – much of the indigenous phosphorus had been depleted from the oldest soils studied, and was mostly of Asian, and therefore aerosolic dust, origin.

Syers *et al.* (1969) used oxygen isotope analysis to describe the provenance and distribution of aerosolic dusts originating from Africa and transported by trade winds across the Atlantic Ocean to the Caribbean islands and North Carolina in the United States; and dust from Asia carried in the troposphere by the westerly jet streams across the Pacific Ocean to the Hawaiian Islands and pelagic sediments in the east-central Pacific (Syers *et al.* 1969; Rex *et al.* 1969).

A good example of the importance of nutrient supply via aerosolic dust is an ombrogenous bog. Shearer (1997) distinguished between bogs as peat-forming wetland systems that are typically raised above the level of surrounding dryland; and fens, which also accumulate peat, are not raised above the surface of the surrounding land). Ombrogenous bogs are true peat-forming bogs that receive all their water from precipitation, and all their nutrients by way of wet or dry deposition of aerosolic dust from allochthonous sources except at the margins; this is in contrast to minerogenic bogs that typically lie adjacent to, and are fed by, freshwater streams and rivers, and are primarily influenced by mineral-fluid interactions in surface waters and ground waters (Shotyk *et al.* 2001).

As a result, ombrogenous bogs are oligotrophic (mineral poor), whereas minerogenic bogs, or the minerogenic margins of raised bogs, are either eutrophic or mesotrophic, that is, high or intermediate in mineral status (Shearer 1997). Marshes (wetlands with large mineral substrates) and mires (peat-forming wetlands) often intergrade (McGlone 2009), for example ombrogenous bogs sitting above the water table can be inundated by flooding or changes to the local hydrology, temporarily grading into a topogenous mire, or more permanently into a soligenous minerogenic mire, in either case leading to upward diffusion of minerals (Weiss *et al.* 2002).

Cores from ombrogenous bogs and ice cores are the only archives that document solely aerosolic deposition (Shotyk *et al.* 2001; Weiss *et al.* 2002), but bog cores have the advantage that they are much more widespread than ice cores. Only a small number of studies into the dissolution of silicate minerals in peat bogs have occurred because of the difficulty in conducting quantitative analyses on samples that are predominantly peat,

with only a few percent mineral mass (Steinmann & Shotyk 1997a), and there is disagreement among the few quantitative studies that have been reported in the literature.

Although peat bog waters can be very acidic<sup>10</sup>, fine mineral particles including quartz grains tend not to undergo further weathering because (i) the solubility of amorphous SiO<sub>2</sub> in equilibrium with quartz is at its lowest in acidic solution (Stumm & Morgan 1996)<sup>11</sup>; (ii) protective organic coatings are deposited on the grain surfaces (Steinmann & Shotyk 1997a); and (iii) mineral dust particles introduced to the bog may already be the product of strong weathering in the source area (Weiss *et al.* 2002). Thus ferromagnesian silicate minerals were better preserved in tephras deposited in the Waikato lakes Ngaroto, Ngaroroiti, and Rotopiko than in adjacent terrestrial sub-aerial deposits (Lowe 1988).

Conversely, Hodder *et al.* (1991) described an almost total loss of ferromagnesian minerals such as biotites in Kaharoa tephras emplaced around 770 yrs BP at the oligotrophic Kopouatai Bog, near Hamilton. Bioturbation in the acrotelm (the top layer of the peat bog consisting of the living parts of mosses and dead and partly decomposed plant material, and the zone where living activities such as rooting occur) at Kopouahi Bog extending to four metres in depth (based on the presence of oligochaete worms and rhizomes of tall sedges of the genus *Baumea* and *Schoenus*), provided a possible explanation for the mineral depletion. However, Hodder *et al.* (1991) suggested the most likely cause of the loss of biotite was rapid chemical dissolution under conditions of low pH and low silica concentrations, based on surface etching on mineral grains observed under SEM microscopic examination, and high levels of dissolved silica and metal cations (Mg<sup>2+</sup>, Ca<sup>2+</sup>, Fe<sup>2+</sup> and Fe<sup>3+</sup>).

There are two major methods available to determine the transition from ombrotrophic peat to minerogenic peat; biological methods, and chemical methods. Biological methods involve distinguishing taxa that are predominantly peat bog-forming such as *Empodisma minus* and *Sporodanthus traversii* from taxa that are predominantly minerogenic fen peat-forming such as *Baumea* and *Leptospermum* –type taxa (Hodder *et al.* 1991; Shearer 1997)<sup>12</sup>.

Chemical methods include determining Ca<sup>2+</sup>:Mg<sup>2+</sup> ratios; the rationale behind this approach is that peat bog plants have higher calcium concentrations than minerotrophic fen plants, because rainwater in coastal areas has a Ca<sup>2+</sup>:Mg<sup>2+</sup> ratio similar to that of seawater (1:5), whereas the Ca<sup>2+</sup>:Mg<sup>2+</sup> ratio in the Earth's crust is closer to 1:1. Because Ca<sup>2+</sup>-rich feldspars are less resistant to chemical weathering than Mg<sup>2+</sup>-rich minerals such as pyroxene, amphibole and biotite, calcium is released preferentially over magnesium, and river waters reflect this disparity with global average Ca<sup>2+</sup>:Mg<sup>2+</sup> ratios of 2.2 : 1.

As a result, ombrotrophic bog peats have Ca<sup>2+</sup>:Mg<sup>2+</sup> ratios ≤ rainwater, compared with minerogenic peats that must have had an additional, non-atmospheric Ca<sup>2+</sup> source, and have Ca<sup>2+</sup>:Mg<sup>2+</sup> ratios ≥ rainwater (Weiss *et al.* 1997). Calcium concentrations in the interstitial water of 2-3mg L<sup>-1</sup> indicate mesotrophic status, and values lower than this point towards ombrotrophic status (Glaser *et al.* 1981; Glaser 1983). However since the abundance of calcium is affected by the supply of calcium at the time the plants were living, and also additions and removals during peat diagenesis, the ratio of calcium to magnesium in the exchangeable cation fraction of peats is a more reliable measure than calcium concentrations alone (Shotyk 1996).

---

<sup>10</sup> Weiss *et al.* (2002) suggested that a constant mean pH of 3.2 in the bogs at Palangka Raya indicated that any dissolution of minerals was insufficient to neutralise the acidity caused by decomposing vegetation and other organic matter.

<sup>11</sup> Thus, Bennett *et al.* (1991) found no recognisable weathering of quartz in acidic peat bogs with pH < 5, whereas Bennett & Siegel (1987) suggest that organic acids in the pH range 6-8 found in minerogenic mires may dissolve quartz.

<sup>12</sup> Shotyk (1996) cautions against relying on biological markers to distinguish between swamp types because a number of plant taxa have a wide range of chemical tolerances, and because the composition of these biological remains may have altered post-deposition.

Weiss *et al.* (2002) distinguished between ombrotrophic and minerotrophic parts of cores studied from bogs at Palangka Raya in southeast Borneo by comparing  $\text{Ca}^{2+} : \text{Mg}^{2+}$  ratios from peat to local rainwater values, reasoning that peats with  $\text{Ca}^{2+} : \text{Mg}^{2+}$  ratios  $\leq$  rainwater were ombrotrophic, whereas peats with  $\text{Ca}^{2+} : \text{Mg}^{2+}$  ratios  $\geq$  rainwater must have had non-atmospheric  $\text{Ca}^{2+}$  input and were minerotrophic.

Results suggested that most of the core was strongly ombrotrophic, with only minor influx of Mn, Sr and Ca from minerotrophic sources. Further, analysis of Al : Ti and Fe : Ti ratios indicated that dust provenance changed over time, with local dust sources most important between 9,500 and 7,800  $^{14}\text{C}$  yrs BP, and longer distance transport (most likely from China) most important between 22,120 and 9,500  $^{14}\text{C}$  yrs BP and from 7,800  $^{14}\text{C}$  yrs BP to present. Enhanced dust accumulation and/or reduced peat accumulation occurred between 10,830 and 9,470  $^{14}\text{C}$  yrs BP; Weiss *et al.* (2002) interpreted this as a Younger Dryas-type event with more intense winds; the Holocene, in contrast was a period of reduced dust flux at Palangka Raya.

Dickinson *et al.* (2002) applied  $\text{Ca}^{2+} : \text{Mg}^{2+}$  ratio analysis and pH measurements to determine wetland trophic status at Dome Mire and Roaring Lion Mire, part of the Nokomai Mire complex in Southland; determining that Dome Mire was mesotrophic and Roaring Lion Mire was intermediate between mesotrophic and slightly ombrotrophic.

The implication of these findings, together with the observation that marshes and bogs intergrade, with ombrotrophic bogs occasionally overlying minerotrophic bogs (Shotyk 1996; McGlone 2009), is that ideally, we would determine the depth at which peats change from ombrotrophic to minerogenic to correctly interpret quartz flux data: changes in the apparent quartz dust flux could be a function of differential preservation as much as it is a function of dust entrainment. In addition, quantifying the extent of intergrading between ombrotrophic bog and minerogenic fen would provide a more detailed paleoenvironmental history of Eltham Swamp.

The length of time that elapsed between core extraction and pollen extraction (six years) precluded the use of chemical methods such as those used by Shotyk (1996) who used high performance liquid chromatography to measure  $\text{Mg}^{2+}$  and  $\text{Ca}^{2+}$  in pore water in Swiss peat bogs. However, analysis of the fossil pollen narrative from Eltham shows consistently high levels of *Empodisma minus* throughout the core; the relative percentages are higher than *Leptospermum* –type taxon at all times, apart from around 12,750 to 13,500 cal yrs BP when *Leptospermum* –type taxon relative percentages are  $\geq$  *Empodisma*. Notwithstanding the fact that frequencies for these taxa may reflect very localised abundance, we can have some confidence that Eltham was largely ombrotrophic throughout most of the period under investigation, and that changes in the quartz flux are unlikely to be the result of post-depositional corrosion. Since ombrotrophic bogs are also preferred to minerogenic bogs for fossil pollen analysis (de Vleeschouwer *et al.* 2011) the likely ombrotrophic nature of Eltham Swamp is fortuitous for paleoenvironment and paleoclimate reconstruction.

### 6.3. Antarctic Ice Core Studies

This section briefly summarises studies of Antarctic ice cores to assist in placing the Eltham dust narrative and other New Zealand dust studies (section 6.4) in a wider, Southern Hemisphere context. The Eltham dust record is compared to Vostok dust volumes and dust flux (Petit *et al.* 1999) in the results section (section 8).

Despite the Antarctic dust flux being very low, with estimates ranging from 15 to 50  $\text{ng g}^{-1}$  during interglacials, compared with 800 to 1,000 – 2,000  $\text{ng g}^{-1}$  during glacial periods (Gabielli *et al.* 2010; Petit *et al.* 1999), ice core dust records are particularly useful paleoclimate indicators since (i) the long distance transport required to deposit dust implies that dust particles recorded in ice cores are both exclusively allochthonous and aerosolic in provenance, originating from a limited number of possible Southern Hemisphere sources (Delmonte *et al.* 2004; Gabielli *et al.* 2010); and (ii) the long, Milankovitch-scale temporal sequences covered by the cores means that

they may encompass several glacial-interglacial cycles (Petit *et al.* 1999; Watanabe *et al.* 2003; Delmonte *et al.* 2007).

Aerosolic dust records from the 420,000 year old Vostok ice core showed that dust fallout in eastern Antarctica was up to 40 times higher during glacial periods than interglacials, suggesting that continental landmasses (dust sources) were more arid, and dust mobilisation and transport were enhanced during cold climates, confirming patterns seen in studies elsewhere (Petit *et al.* 1999). The presence of larger dust particles from LGM times in particular indicated more intense wind regimes, coupled with lower atmospheric water vapour levels and reduced hydrological fluxes contributed to reduced wet deposition over the mid-latitudes and increased dry deposition rates over eastern Antarctica.

Petit *et al.* (1999) found that the correlation between dust deposition rates and temperature was weak; this is somewhat surprising given that cooler temperatures during glacial times affected the climate of South America, the likely dust source for eastern Antarctica: the extension of sea ice into the South Atlantic likely pushed the polar front northward, and the belt of westerlies northward over the Andes.

Intensified westerlies over the Andes would result in a cooler and drier climate with increased fluvial and glacial erosion and increased dust entrainment. At the same time, dust transport to the pole would be enhanced by steeper meridional temperature gradients due to the northward expansion of sea ice; the net result would be increased dust deposition in eastern Antarctica.

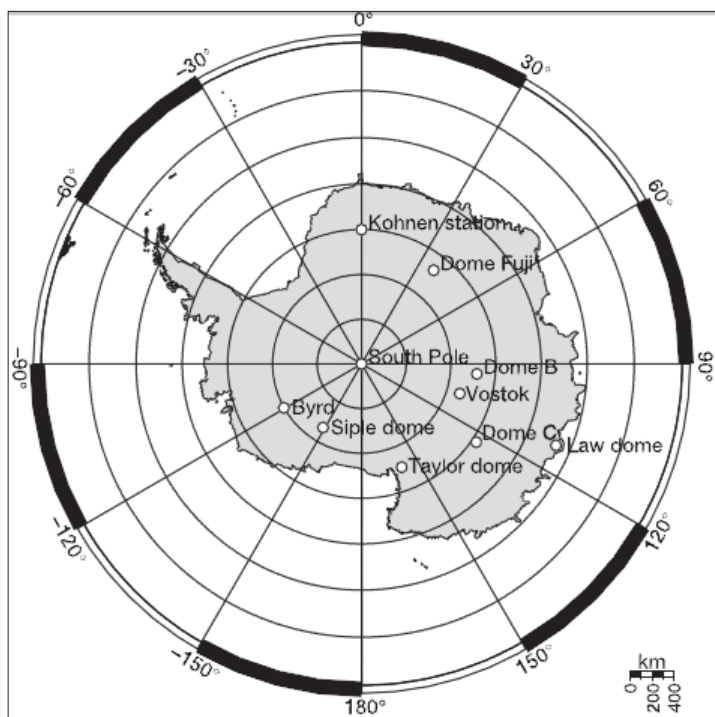


**Figure 19. Antarctica Ice Core Drilling Sites.** Includes Vostok (Petit *et al.* 1999), Dome B (Delmonte *et al.* 2004, 2007), EPICA Dome C (Gabrielli *et al.* 2010), and Dome Fuji (Watanabe *et al.* 2003). Source: Watanabe *et al.* (2003)

The EPICA Dome C core (Figure 19) extends back to 740,000 years BP and therefore covers the last eight glacial cycles. Delmonte *et al.* (2004) used  $^{87}\text{Sr}/^{86}\text{Sr}$  and  $^{143}\text{Nd}/^{144}\text{Nd}$  isotopic analysis to investigate potential source areas (PSAs) for Dome C dust. These researchers determined that the main source of Antarctic dust was southern South America, specifically Patagonia; in contrast, New Zealand was unlikely to be a source, based on the absence of tephra from the Taupo Volcanic Zone. Gabrielli *et al.* (2010) offered an alternative view, using rare earth elements (REE) concentrations<sup>13</sup> to determine that in addition to Patagonian aerosols there were distinctive New Zealand, Australian and South African dust signatures in Dome C ice, as well as autochthonous dust.

The dust profile at Dome C has similar patterns of dust concentration to both the Vostok and Dome Fuji cores, with a very low dust flux during the interglacials ( $0.4 - 0.6 \text{ mg m}^{-2} \text{ yr}^{-1}$ ), and fluxes up to 50 times higher during the glacials (Delmonte *et al.* 2007). Revel-Rolland *et al.* (2006) used Sr and Nd isotopes to show that the dust contribution from Australia may have been dominant to Antarctica during interglacial periods (Holocene and Marine Isotopic Stage 5.5). They suggested that the greater contribution of Australian dust inferred for interglacial ice compared with glacial ice was related to weakening of the South American sources during interglacial time relative to Australian sources.

<sup>13</sup> REEs are useful geochemical tracers because they are not strongly fractionated by weathering and diagenetic processes. As their atomic mass increases and their atomic radius decreases, they keep the same electronic configuration and their chemical properties are largely unchanged, enabling REEs to behave like isotopes; (ii) REEs are lithophilic refractory elements that are transported in the particulate phase due to their low solubility (Gabrielli *et al.* 2010).

The high LGM dust levels at Dome B (850 ppb) and Dome C (730 ppb) declined rapidly after 18,000 years BP to reach typical Holocene levels (18 ppb) by 14,500 years BP; this period of low dust levels was interrupted by a doubling of mean Holocene dust levels (25-46 ppb) until 12,200 years BP coeval with the Antarctic Cold Reversal<sup>14</sup>. Between 12,100 and 11,300 years BP dust levels fell to a pre-Holocene dust minimum (7-9 ppb), before typical Holocene levels (18 ppb) were achieved once again (Delmonte *et al.* 2004), highlighting the fact that the volume of dust entrained in the atmosphere can change very quickly, over the space of mere decades (Jouzel *et al.* 2003; Arimoto 2001).

#### 6.4. New Zealand Aerosolic Dust Studies

The earliest documented studies of dust in New Zealand were provided by Marshall (1903) and Marshall & Kidson (1929) who reported strong westerly gales and associated dust storms over New Zealand in November 1902, and a heavier storm in October 1928 estimated to have deposited between 200,000 and one million tonnes of dust on New Zealand (Marx & McGowan 2005), respectively. In both cases, the dust was inferred to be of Australian origin (Gregory 1930; Windom 1969): the predominantly quartz or augite grains deposited at many sites across New Zealand were coloured red with oxide and sesqui-oxide coatings<sup>15</sup>; most grains were < 30 µm in diameter (Marshall 1903), with few > 40 µm (Marshall & Kidson 1929). Windom (1969) noted that many dust samples demonstrated a bimodal grain size distribution with modes at < 2 µm and 30-40 µm; the clay size fraction was attributed to an Australian origin, with the coarser fraction possibly having a more cosmopolitan origin.

	2 November 1902 (Otakaia)	6 October 1928 (Queenstown)
SiO <sub>2</sub>	53.68	57.20
Al <sub>2</sub> O <sub>3</sub>	18.44	18.00
Fe <sub>2</sub> O <sub>3</sub>	6.54	4.24
CaO	0.95	2.16
MgO	1.52	0.98
K <sub>2</sub> O	2.58	2.64
Na <sub>2</sub> O	1.67	1.59
H <sub>2</sub> O	14.60	12.62

Source: Marshall & Kidson (1929); Gregory (1930); Windom (1969)

McTainsh (1989) notes that whilst in the 20<sup>th</sup> century there have been at least seven documented wind storms depositing Australian dust in New Zealand, it is likely that many other less intense, undocumented events have occurred in recent times, given that haze from dust storms occurs over Brisbane at least three times per year.

Mokma *et al.* (1972, 1973) reported the presence of aeolian quartz (including aerosolic dust) in two basaltic soils from Northland. Quartz particle size distribution (20-5 µm, and 5-2 µm) in the surface horizons of both soils was higher than in deeper soil horizons, indicating loess and aerosolic dust origins, respectively. Further, δ<sup>18</sup>O values suggested that the quartz was derived from somewhere other than the parent basalts or central North Island rhyolitic tephra.

The presence of aeolian quartz in Northland basaltic soils prompted Stewart *et al.* (1984) to further investigate the provenance of the quartz. These researchers found three distinct populations of quartz particles in six Northland soils based on δ<sup>18</sup>O values, grain size distribution, and grain morphology as determined by scanning electron microscope inspection: (i) a non-aeolian, high temperature, quartz sand in the > 250 µm size fraction, derived from central North Island rhyolitic tephra, including Kaharoa Ash; (ii) predominantly locally derived,

<sup>14</sup> The same ACR dust concentration was seen in the Komosmolskaia ice core.

<sup>15</sup> These are the result of aerobic weathering in sub-tropical environments (Shulmeister *et al.* (2004).

loess-sized (63-20)  $\mu\text{m}$  material, transported by wind; and (iii) aerosolic dust (5-2  $\mu\text{m}$ ) acquired from globally circulating tropospheric dusts (Stewart *et al.* 1984).

Stewart & Neall (1984, Figure 50) examined aerosolic quartz and biogenic sediments from the marine core P69 extracted off the east of the North Island. Both sediment types accumulated more rapidly during glacial times, with a mean sedimentation rate of  $594 \text{ mm kyr}^{-1}$ , with an abrupt decline occurring at the time the Rerewhakaaitu tephra was deposited,  $17,900 \pm 200 \text{ cal years BP}$  to  $150 \text{ mm kyr}^{-1}$ . Specifically, quartz grains in the 2-5  $\mu\text{m}$  range (aerosolic dust) had a peak sedimentation rate between 16,200 and 17,900 cal yrs BP, whereas quartz in the 20-63  $\mu\text{m}$  range (loess) had two peaks, between 16,200 and 17,900 cal yrs BP, and between 17,900 and the time of the Okareka eruption, 21,900 cal yr BP.

The authors attributed this change to a shift in the meridional (northerly and southerly) wind system: increased fluvial activity following the LGM lead to increased erosion of material from the New Zealand high country to form lowland aggradational surfaces, and this material was entrained by intense westerly winds and deposited to the east of the country. By the time the Rerewhakaaitu Tephra was erupted from the Okataina Volcanic Centre, the westerly wind system retreated to the south in response to weakening circumpolar wind systems. Not only was the aerosolic dust source depleted at this time relative to the LGM, but the capacity of the wind to entrain aerosolic material was much reduced.

Alloway *et al.* (1992) used quartz grain-size characteristics to demonstrate likely provenance and wind patterns at Waitui and Onaero in northern Taranaki since oxygen isotope sub-stage 5e (125,000 years BP). Major peaks in aerosolic quartz (both loess and aerosolic dust) particles co-incident with oxygen isotope stages 2 and 4 suggest that the North Island was in the grip of full glacial climates at those times. Dust accumulation was higher since (i) the current continental shelf to the west of the North Island was more exposed, because sea levels were as much as 120m lower due to cooler temperatures; at the same time (ii) the south-westerly winds over New Zealand were likely to have been stronger in response to steeper temperature gradients that resulted from a northward extension of the Antarctic sea-ice boundary.

Alloway *et al.* (1992a) note that the quartz accumulation rate was higher during oxygen isotope stage 2 than  $\delta^{18}\text{O}$  stage 4; this implies that temperature was cooler and winds were stronger between 11,000 and 24,000 years BP than between 60,000 and 71,000 years BP. Based on levels of locally eroded and re-deposited andesitic detritus, Alloway *et al.* (1992a) surmised that conditions during mid-oxygen isotope stages 3 and both the sub-stages of  $\delta^{18}\text{O}$  stage 5 were cool but less severe than both  $\delta^{18}\text{O}$  stages 2 and 4.

Marx *et al.* (2009) examined Holocene dust deposits (including quartz dust) in peats from Upper Ruined Hut Bog in central Otago, noting that dust deposits at this site can only be derived from aeolian sources; that is, there was no opportunity for colluvial or fluvial deposits to occur. The provenance of the dust was determined by comparing trace element composition to that of potential source rocks in New Zealand and Australia.

The strength of the match between Upper Ruined Hut Bog and the potential source was determined by summing the differences between 20 trace elements from each site, with the lowest sum of differences deemed the best match and therefore the most likely source. Mineral dust content was both higher (20-45% by weight) at 10,000 years BP and larger grain size (mode of 30  $\mu\text{m}$ ) than at 900 years BP (8-10% dust content, 10-13  $\mu\text{m}$  mode). Furthermore, the deduced source changed over time, with dust deposited between 7,500 and 2,500 years BP derived from south-east Australia<sup>16</sup>, and after 2,500 years BP the source area broadened and moved north to eastern and central Australian areas<sup>17</sup> (Marx *et al.* 2009).

---

<sup>16</sup> Murray River, Darling-Riverina Plain, upper Darling River and Flinders.

<sup>17</sup> Mulga Lands, Lake Eyre Basin, southern Flinders, Darling Basin and Darling-Riverina.



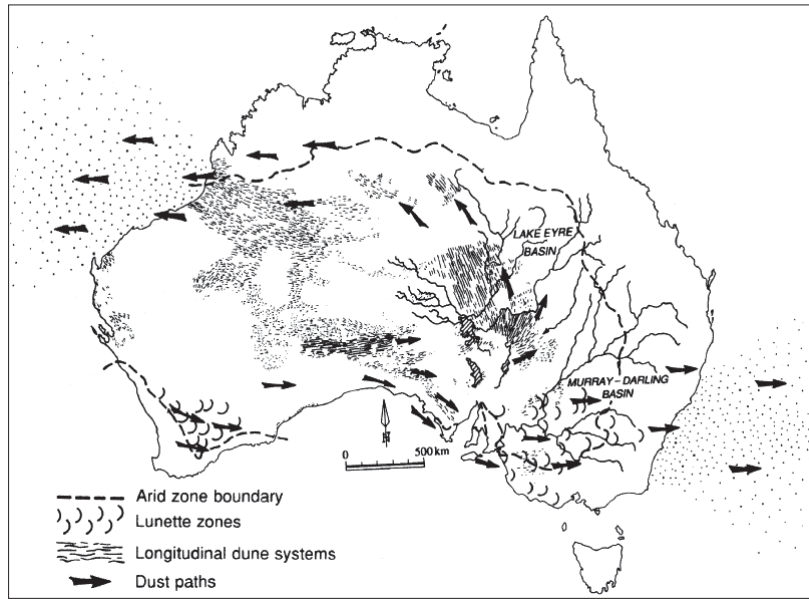


**Figure 21. Australian Dust Sources and Trajectories across the Tasman Sea.**

Source: Hesse & McTainsh (2003)

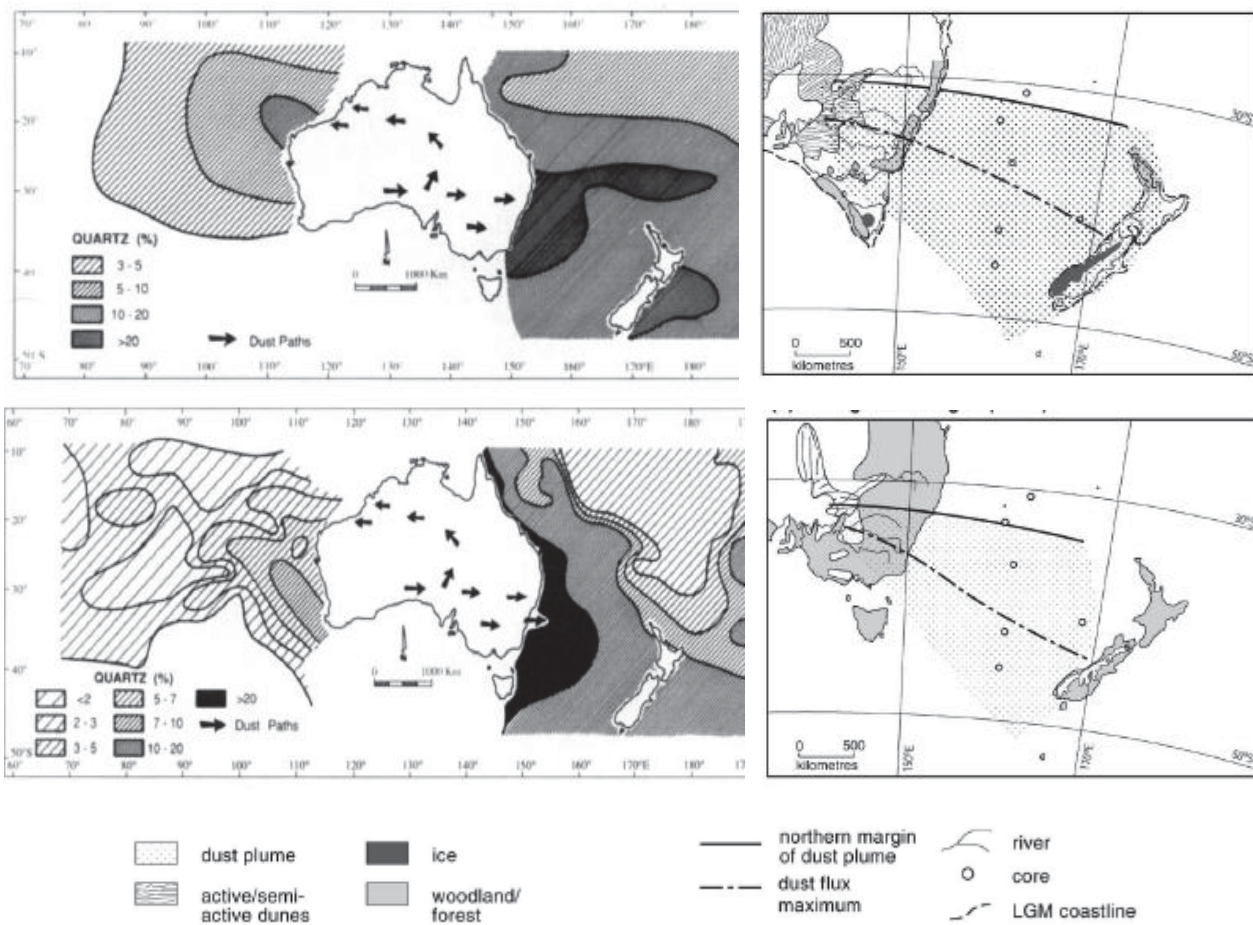


**Figure 22. Quartz Distribution in Ocean Sediments around Australia, and South-eastern Dust Path.** Left, top: LGM oceanic quartz distribution; Bottom, left: Holocene oceanic quartz distribution. Top, right: LGM south-eastern dust path; Bottom, right: Holocene south-eastern dust path. Source: McTainsh (1989); Hesse & McTainsh (2003).

Westerly fronts in Australia produce haboob-like walls of dust that are transported eastward to New Zealand if the dust ascends high enough; in addition, nor-westerly winds in the Broken Hill region may entrain dust southwards to meet the westerly dust plume. Sediment supply likely increased between 35,000 and 25,000 years BP when there was a transition from humid to arid conditions, rainfall seasonality became more marked, and increased dust entrainment began around 25,000 years BP (McTainsh 1989).

Based on (i) quartz sediment distribution patterns off the Australian coast, and (ii) the increase of coarse silt relative to fine silt and clay grains deposited in the Tasman Sea, Thiede (1979) suggested that a narrow zone of high aerosolic dust input of Australian provenance extended around 20° in longitude farther to the east, and lay much further to the north, than it does today. Whereas Thiede's (1979) data show dust mineralogy and indirectly, grain size, it is not a map of dust flux, nor did his record from core Z2108 show an LGM increase in dust. In contrast, Hesse & McTainsh (1989) suggested that although wind speeds during the LGM were no greater than Holocene wind speeds; rather, a larger dust source area and higher dry deposition rate (that is, lower dust sequestration by rain) was responsible for increased dust deposits. A tongue of maximum quartz dust concentration at 30°S extending eastward to around 175°W during the late Pleistocene; by the early Holocene this tongue had extended south to about 35°S and retracted westward to 165°E (Figure 22).

The right-hand side of Figure 22 shows the more intense dust plume extending both further east and south during the LGM than during the Holocene. Cores extracted from the Tasman Sea demonstrate a steady decline in quartz grain modal size with distance from source; a modal size of 26 µm in the central Tasman represents gravity (dry) fallout; whereas a modal size of 20 µm in the eastern Tasman is due to raindrop sequestering rather than falling out under gravity. Based on this grain size distribution, Hesse & McTainsh (2003) inferred that the LGM was drier than the Holocene.

The dust provenance study conducted by Marx *et al.* (2009) described above is interpreted as evidence of changes to source area characteristics over the Holocene, rather than changes in dust transport trajectories. The authors concluded that for the period 7,800 to 4,800 years BP the Intertropical Convergence Zone pushed the subtropical high pressure belt to the south, blocking sub-Antarctic cyclones and cold fronts, both reducing precipitation over South Australia and the Murray River area and therefore reducing dust supply, and decreasing westerly wind circulation over Australia. The net result was a decrease in dust entrainment and transport to New Zealand.

## 6.6. The Effects of Vegetation on Aerosolic Dust Entrainment

The purpose of this section is to describe how changes in dust source emissivity may be modified by vegetation cover, demonstrating that the wind: vegetation relationship is bidirectional – not only can wind modify the vegetation assemblage and relative cover, but the amount and type of vegetation cover can modify wind velocity at ground level, and therefore the volume and size of dust entrained.

Changes in emissivity may arise due to changes in aridity, with very dry areas becoming rapidly deflated by strong winds since they are not replenished by fluvial activity, or a strong reduction in aridity so that revegetation can occur, reducing the shear stress at ground level. The presence and density of plant cover strongly influences the volume of dust emitted from the land surface. The fast growth of annual grasses and herbs in semiarid areas following rain restrains dust emission for periods of days to weeks (Tegen *et al.* 2002), and even when they are not in leaf, desert scrub suppresses dust emission (Wolfe & Nickling 1996; Wyatt & Nickling 1997).

Wolfe & Nickling (1997) investigated the impact of vegetation on the ability of wind to entrain mineral particles in a range of vegetation types and over a range of wind velocities. The proportion of wind that is exerted on the ground and on vegetation is determined by shear stress partitioning, described by the following equations:

$$F_0 = F_V + F_S \quad (1)$$

where  $F_O$  is total wind force exerted on a rough surface,  $F_V$  is wind force applied to vegetation and  $F_S$  is wind force applied to the bare surface. The division of wind force is described by the term total shear stress,  $\tau_o$ :

$$\tau_o = \frac{F_O}{A_O} = \frac{F_V}{A_O} + \tau_s \left( \frac{A_S}{A_O} \right) \quad (2)$$

where  $A_O$  is the surface area of the vegetated surface,  $A_S$  is the area of the unvegetated surface and  $\tau_s$  is the surface shear stress. Equation (2) can be rewritten to give the shear stress ratio, which describes the fraction of total momentum flux that is exerted on the ground using either (i) the threshold shear velocity ratio or the onset of dust particle movement in an unvegetated ( $u_{*ts}$ ) versus vegetated ( $u_{*tv}$ )<sup>19</sup> environment:

$$1 - \left( \frac{F_V}{A_O \tau_o} \right) = R_t^2 \left( \frac{A_S}{A_O} \right) \quad (3)$$

where  $R_t$  is the threshold shear velocity ratio  $u_{*ts} / u_{*tv}$ ; or (ii) the shear velocity ratio (that is, ignoring the threshold) for shear velocities of dust in an unvegetated ( $u_{*s}$ ) versus vegetated ( $u_{*v}$ ) environment, where  $R$  is the threshold shear velocity ratio  $u_{*s} / u_{*v}$ :

$$1 - \left( \frac{F_V}{A_O \tau_o} \right) = R^2 \left( \frac{A_S}{A_O} \right) \quad (4)$$

Wolfe & Nickling (1996) applied these models to empirical data and found that even very sparse vegetation cover dramatically reduced wind erosion: as little as 0.04% velvet mesquite (*Prosopis juliflora* var. *velutina*) cover on abandoned farmland in the Sonoran Desert, Arizona, absorbed 19% of the total momentum flux of wind; this increased to 88% of the total momentum flux of wind absorbed by only 10.3% creosote bush (*Larrea tridentata*) cover.

Wyatt & Nickling (1996) showed that porous obstacles such as shrubs are more effective at preventing dust entrainment than solid obstacles because they have greater drag coefficients. The dimensionless drag coefficient  $C_s$  represents the efficiency of a given surface at extracting momentum from wind; in other words, it describes the degree to which the force of the wind  $u_z$  is reduced by surface drag:

$$C_s(z) = \frac{\tau}{\rho u_z^2} = \frac{u_*^2}{u_z^2} \quad (5)$$

where  $\rho$  is the density of air,  $\tau$  is the shear stress at the surface,  $u_z$  is the wind speed at height  $z$ ,  $u_*$  is the shear velocity. The corresponding drag coefficient for a solid object,  $C_R$ , is

$$C_R = \frac{F}{\rho A_t u_z^2} \quad (6)$$

where  $A_t$  is the cross sectional area of the object, and  $F$  is total wind force.

Wyatt & Nickling (1996) determined  $u_*$  and aerodynamic roughness length  $z_o$  at sites sparsely vegetated with creosote (*Larrea tridentata*) and white bursage (*Ambrosia dumosa*) near Las Vegas, Nevada. The researchers found that drag coefficients for these shrubs were higher than coefficients for solid objects at all wind velocities; the mean drag coefficient for creosote shrubs was 0.485 compared with only 0.3 for a solid sphere and 0.19 for a solid cylinder; in essence, porous, flexible trees have higher momentum and extraction potential than rigid shapes, because they can bend and sway; in other words, vegetation is more efficient at dissipating wind energy since it exerts more drag than solid objects (that is,  $C_s > C_R$ ) due to its porous and flexible nature.

---

<sup>19</sup> Wolfe & Nickling (1996) note the threshold shear velocity of bare soil is determined by variables including texture, crustal thickness and moisture, such that a sparsely vegetated but crusted surface may have a much higher shear velocity than a sparsely vegetated, uncrusted or disturbed surface.

## 7. Methodology

### 7.1. Site Descriptions and Stratigraphy

This purpose of this section is to briefly describe the six sites used in this study and their geospatial relationships with each other, and their stratigraphic context.

#### 7.1.1. Eltham Swamp

Eltham Swamp is a relict peat swamp around 6 km in length lying to the east and almost immediately adjacent to the small South Taranaki township of Eltham (population 2,100) at the junction of the west Taranaki lowlands and east Taranaki uplands (McGlone & Neall 1994). A second relict peat swamp, Ngaere Swamp, lies 15m higher than, and to the north of Eltham Swamp, separated by a low ridge traversed by Rawhitiroa Road. Both swamps formed after lahar and debris avalanches that occurred between 50,000 and 23,000 years ago<sup>20</sup>, blocked the western exits of the respective valleys so that drainage impedance and peat accumulation occurred (McGlone & Neall 1994). The approximate position of the lahar and debris deposits responsible for water entrapment and swamp creation are shown (Figure 23); prior to 50,000 years ago, both valleys most likely drained into the forerunner of the Waingongoro River to the west. Note that neither Eltham Swamp nor Ngaere Swamp are approved Geographic Board names.

Today, both swamps are well drained farmland utilised for dairy farming. Drainage and decay have caused the peats to shrink and consolidate so that the surface is significantly lower than what it was prior to agricultural activity. McGlone & Neall (1994) found evidence of peat layers around 3 m higher than present at the edge of the basin, 600 m NW of their drilling site (Figure 23).

The locations of Eltham Swamp, Ngaere Swamp and Lake Rotokare relative to Eltham township are shown in Figure 23; the drilling site for the 'new' Eltham core is situated at the farm of Mr Gudopp, 458A Rawhitiroa Road, 39° 26' 17.73" S, 174° 20' 07.60" E.



**Figure 23. Satellite photograph of Eltham Area.** The yellow star is the site of the present study; the red asterisk is the site of McGlone & Neall's (1994) study; the red line is the approximate eastern extent of the debris avalanche.

<sup>20</sup> Presumably closer to 50,000 than 23,000 years ago, given we now have calibrated <sup>14</sup>C dates making Eltham Swamp older than 36,000 years.

Eltham Core A consists of *c.* 1,800 cm of peat sediments interspersed with around 130 tephra layers that range from 0.1 to 18 cm in thickness, as well as loams up to 70 cm thick, tephric loess layers up to 19 cm thick, sandy layers up to 96 cm thick, and a few very thin silt units. The lithology of Core A is given in Figure 24, starting at 600 cm, the top-most section of core that was studied in the current study. As noted above, an earlier study by McGlone & Neall (1994) at Eltham covered the period of *c.* 3,000 to 14,000 yrs BP, so the period before *c.* 9,863 cal yrs BP was not examined in the current study to minimise duplication.

A limitation of the stratigraphic diagrams is that only one type of sediment is recorded for each unit; that is, units are described in the diagram as 'peat' or 'loam', but are in fact some intermediate sediment, such as 'peaty loam' or 'loamy peat' with considerable intergrading occurring. This is a particular problem with respect to the coastal sites, where units described as 'paleosols' are invariably highly polleniferous, peat or lignite rich sediments.

All tephra identifications were made by Professor Vince Neall and Dr. Anke Zernack, on the basis of stratigraphic position, Munsell colour, sorting characteristics, grain size, likely isopach thicknesses at Eltham (based on Alloway *et al.* 1995) and the  $\delta^{14}\text{C}$  dates given in Table 8. Professor Shane Cronin and Dr. Kat Holt identified the Kawakawa / Oruanui Ash based on microprobing and stratigraphic position.

The uppermost 400 cm of the core under consideration (that is, Core A (4) and Core A (5), 600 cm – 1,000 cm, is comprised predominantly of very dark-brown to black peat, interspersed with *c.* 50, relatively thin tephra layers. Peat layers in the upper-most part of Core A (4) were frequently fibrous, with twiggy fragments and occasional seeds identifiable in the organic matrix. Peats lower in the core were darker, more amorphous and compact, with no macrofossils identifiable by the naked eye, however sedge fragments were retrieved for  $\delta^{14}\text{C}$  dating as deep as 1,084 cm and identified under a low-powered, stereo microscope (Table 8). After about 1,050 cm depth, peats give way to tephric loess layers and polleniferous peaty loams. Nineteen samples were extracted from Core A for  $\delta^{14}\text{C}$  dating (Table 8), twelve of these were submitted as part of the current study, and seven were submitted by Michael Turner as part of his study on the eruption history of Mount Egmont (Turner 2008).

Tephtras in Core A (4), 600 -800 cm (Figure 24 a), were identified by Professor Neall as five members of the Kaponga series (A-E), a closely spaced set of orange coloured, coarse ash and lapilli units; and the finely vesicular, closely spaced lapilli beds known as Konini A and Konini B; a 15 cm isopach of Konini Tephtras runs in a broad lobe eastward from Mount Egmont through Eltham (Alloway *et al.* 1995). The sedimentation rate for the well dated, bottom half of Core A (4) - from the Kaponga E tephra at 684 cm to the  $\delta^{14}\text{C}$  dated, horizontally bedded wooded twigs at 774 cm (Table 8) was  $0.036 \text{ cm}^{-1}\text{yr}^{-1}$ . A new tephra age provided by  $\delta^{14}\text{C}$  dating of adjacent organic sediments is given for Kaponga A,  $\leq 10,910 \pm 110$  cal yrs BP.

Tephtras in Core A (5), 800 -1,000 cm (Figure 24 b) were identified by Professor Neall as two units of the four Mahoe Tephtras, pumiceous lapilli that are found in 5 cm thick isopachs 4-5 km NW of Eltham (Alloway *et al.* 1995); and a thin layer of yellowish-red to reddish-yellow pumiceous lapilli known as Kaihouri H, the youngest member of the Kaihouri Tephtras (Alloway *et al.* 1995). New tephra ages provided by  $\delta^{14}\text{C}$  dates from this study are given for Mahoe A,  $\leq 13,520 \pm 80$  cal yrs BP; and Kaihouri H,  $15,570 \pm 490$  cal yrs BP; Mahoe B tephra is estimated to have been erupted between  $12,470 \pm 80$  and  $12,660 \pm 60$  cal yrs BP. The sedimentation rate from 819 cm to 983 cm in Core A (5) was  $0.045 \text{ cm}^{-1}\text{yr}^{-1}$ .

Core A (6), 1,000 -1,200 cm (Figure 24 c), is comprised of *c.* 54 cm of peat interspersed with pumiceous ash, lying above a layer of tephric loess 18cm thick. Immediately beneath the tephric loess is a layer of re-worked Kawakawa / Oruanui Ash; that in turn lies above a thin peat layer containing sedge fragments dated at  $18,180 \pm 210$  cal yrs BP and  $20,180 \pm 140$  cal yrs BP. One-half metre of pumiceous ash and pumiceous lapilli layers fall between the thin peat layer and a second layer of tephric loess 18 cm thick, that in turn lies above a dispersed layer of Kawakawa / Oruanui Ash. The Kawakawa / Oruanui Ash was positively identified by Professor Cronin and Dr. Holt by microprobe analysis, as well as the re-deposited layer of Kawakawa / Oruanui Ash higher in the

core. This key marker tephra was difficult to discern by eye, and initially it was thought that it may have been lost during core extraction, hence the decision to extract the second core from Eltham to try and locate it.

Professor Neall identified two members of the 15-member Poto Tephra formation lie immediately below the Kawakawa / Oruanui Ash (Poto E and Poto C); these ash layers are described as well-sorted, normal-graded, and grey to dark grey coarse ash and lapilli tephra (Alloway *et al.* 1995). A bulk peat sample extracted from peaty loam at 1,177 cm (Turner 2008) was dated by liquid scintillation  $\beta$ -counting, giving  $29,210 \pm 270$  cal yrs BP.

Clearly, the sedimentation rate for Core A (6) was very low: the sedimentation rate from 1,084 cm to 1,177 cm is  $0.010 \text{ cm}^{-1}\text{yr}^{-1}$ , compared with the sedimentation rate for Core A (5) which at  $0.045 \text{ cm}^{-1}\text{yr}^{-1}$  was more than four times faster. This very slow sedimentation rate is most likely due to cold, dry and windy LGM conditions such that primary production was much lower, and biomass (peat) accumulation was very low. Such conditions mean that pollen production was suppressed (there are generally less plants to produce pollen), and pollen preservation was also reduced, due to lack of suitable, anaerobic environments; this is seen in the Eltham pollen diagram (Figure 39).

Core A (7) 1,200 -1,400 cm (Figure 24 d) is characterised by two sandy units, extending from 1,200 to 1,229 cm and 1,304 to 1,400 cm, separated by eight peaty loam layers, that are themselves separated by thin, unidentified pumiceous ash and pumiceous lapilli units. A bulk peat sample extracted from the uppermost peaty loam unit yielded a radiocarbon date of  $26,630 \pm 270$  cal yrs BP. The sedimentation rate for Core A (7) was much more rapid than for Core (A) 6; influx from 1,239 cm to 1,444 cm near the top of Core A (8)<sup>21</sup> is  $0.050 \text{ cm}^{-1}\text{yr}^{-1}$ , similar to the sedimentation rate for Core A (5).

Core A (8) 1,400 -1,600 cm (Figure 24 e) is comprised mainly of polleniferous peaty loams, interspersed with 13 layers of unidentified pumiceous ash (with a thickest layer of 18cm), lithic-rich ash and pumiceous lapilli. The sedimentation rate for Core A (8) is *c.*  $0.057 \text{ cm}^{-1}\text{yr}^{-1}$ ; this is the most rapid sedimentation rate for the entire core.

Core A (9) 1,600 -1,800 cm (Figure 24 f) is also comprised mainly of ashy loams, interspersed with a single, 5 cm layer of unidentified pumiceous lapilli. Due to a paucity of organic material, no  $\delta^{14}\text{C}$  dating was conducted, and no sedimentation rate data is available. Other than determining that there was little or no pollen present in this core, no palynological analysis was conducted, nor was any aerosolic quartz analysis conducted on Core A (9).

---

<sup>21</sup> That is, the next radiocarbon date with which to calculate the sedimentation rate.

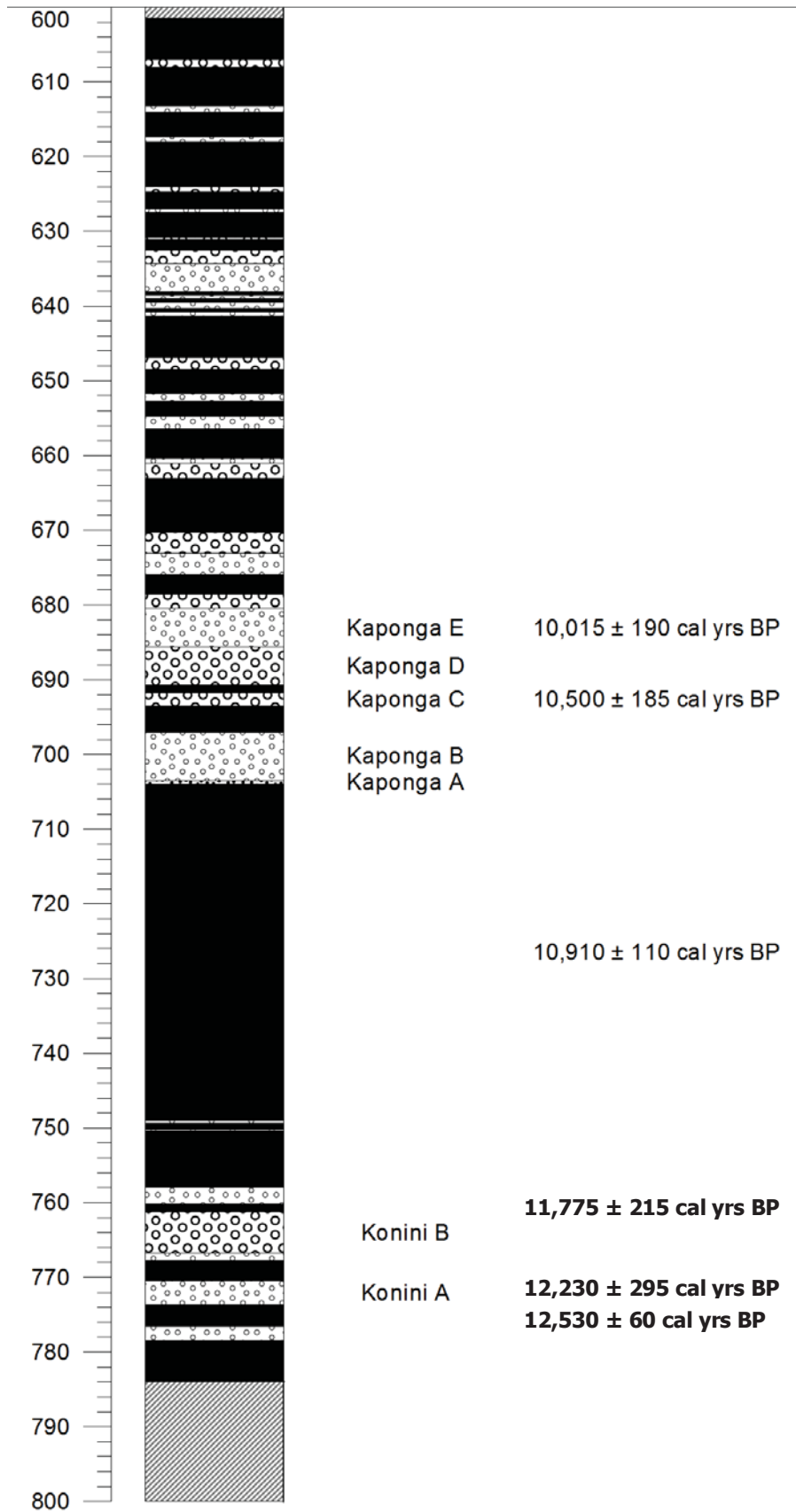


Figure 24(a). Eltham Swamp Lithology Core A (4) (6-8m)

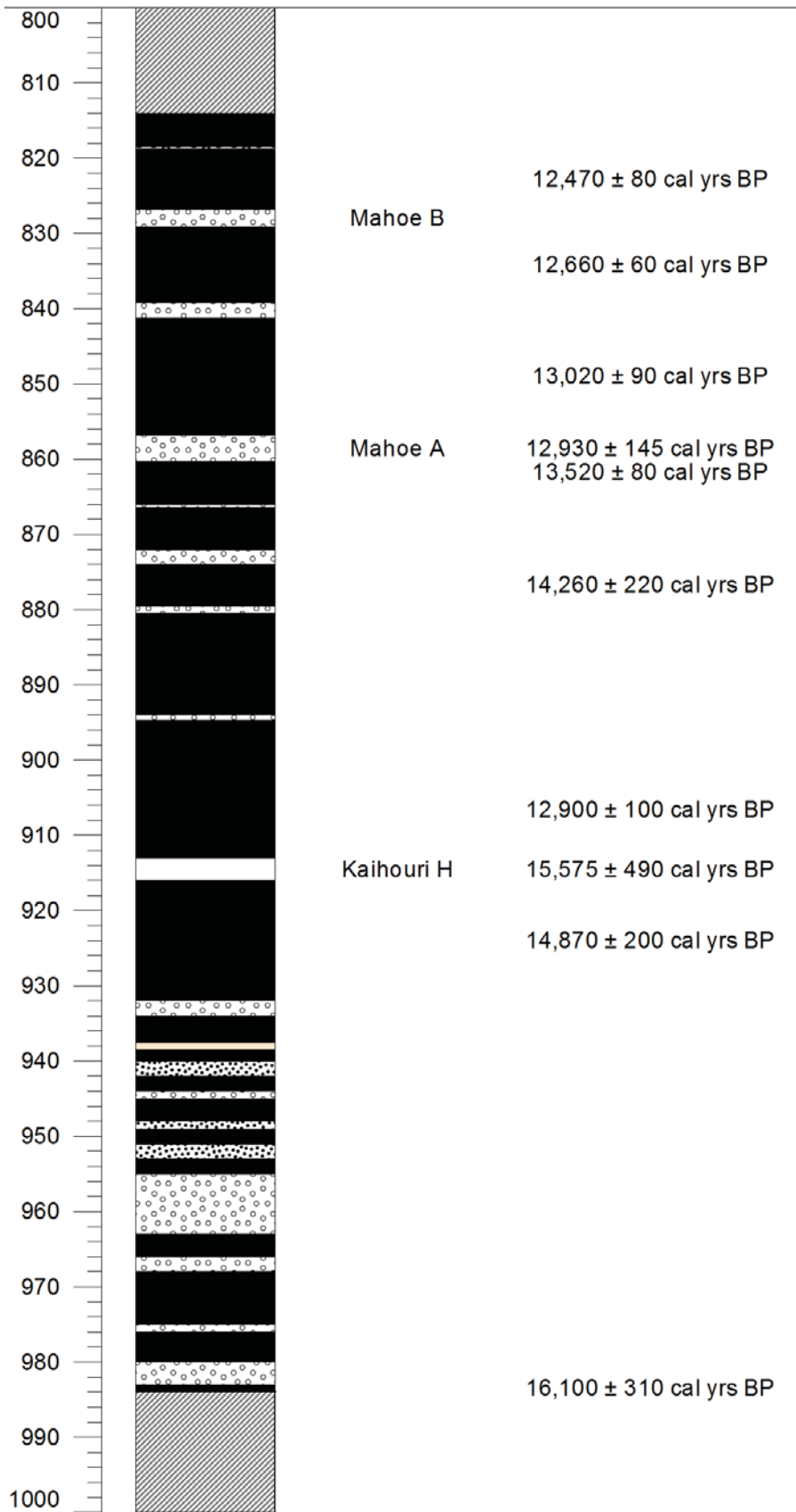


Figure 24(b). Eltham Swamp Lithology Core A (5) (8-10m)

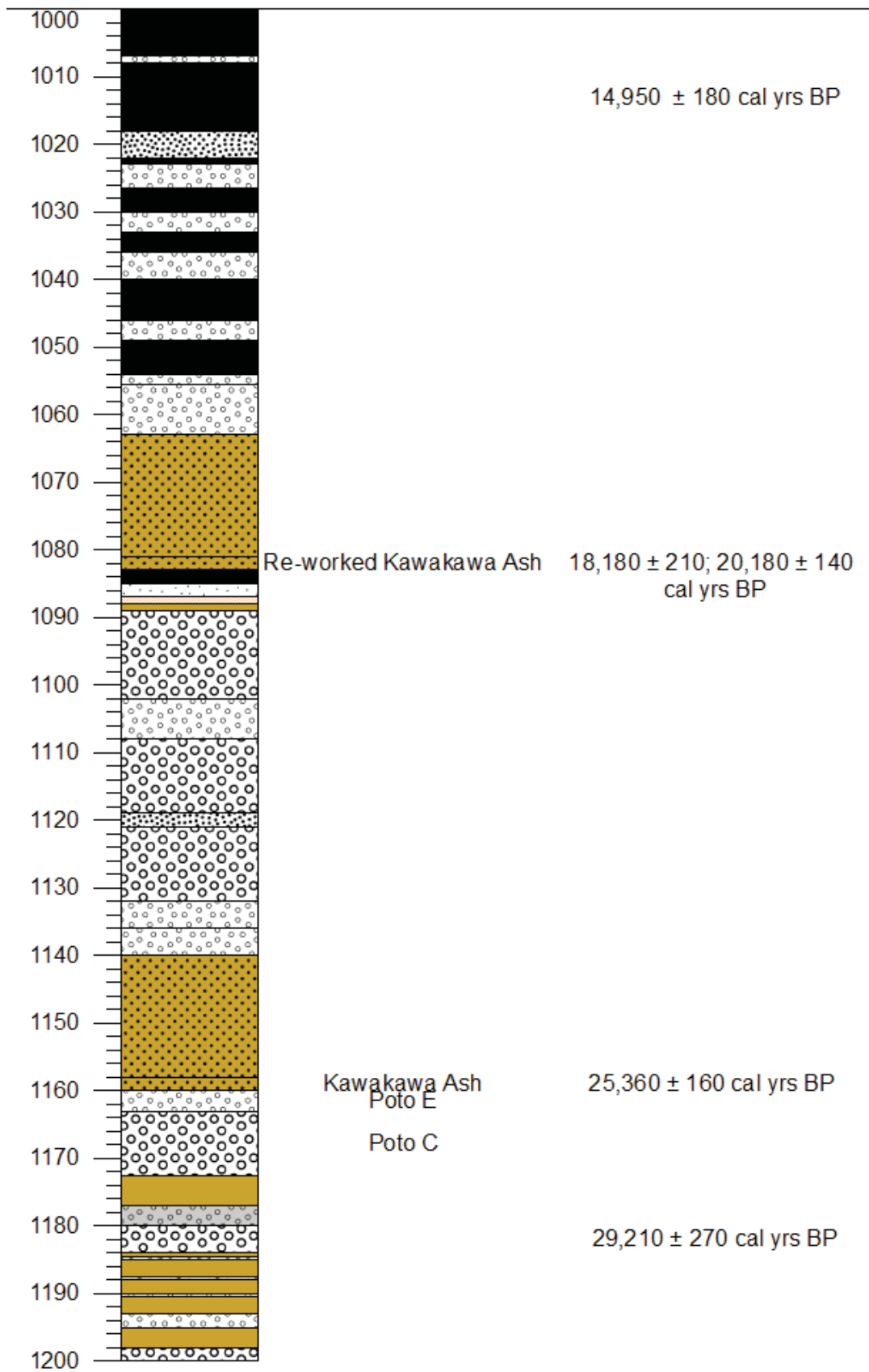


Figure 24(c). Eltham Swamp Lithology Core A (6) (10-12m)

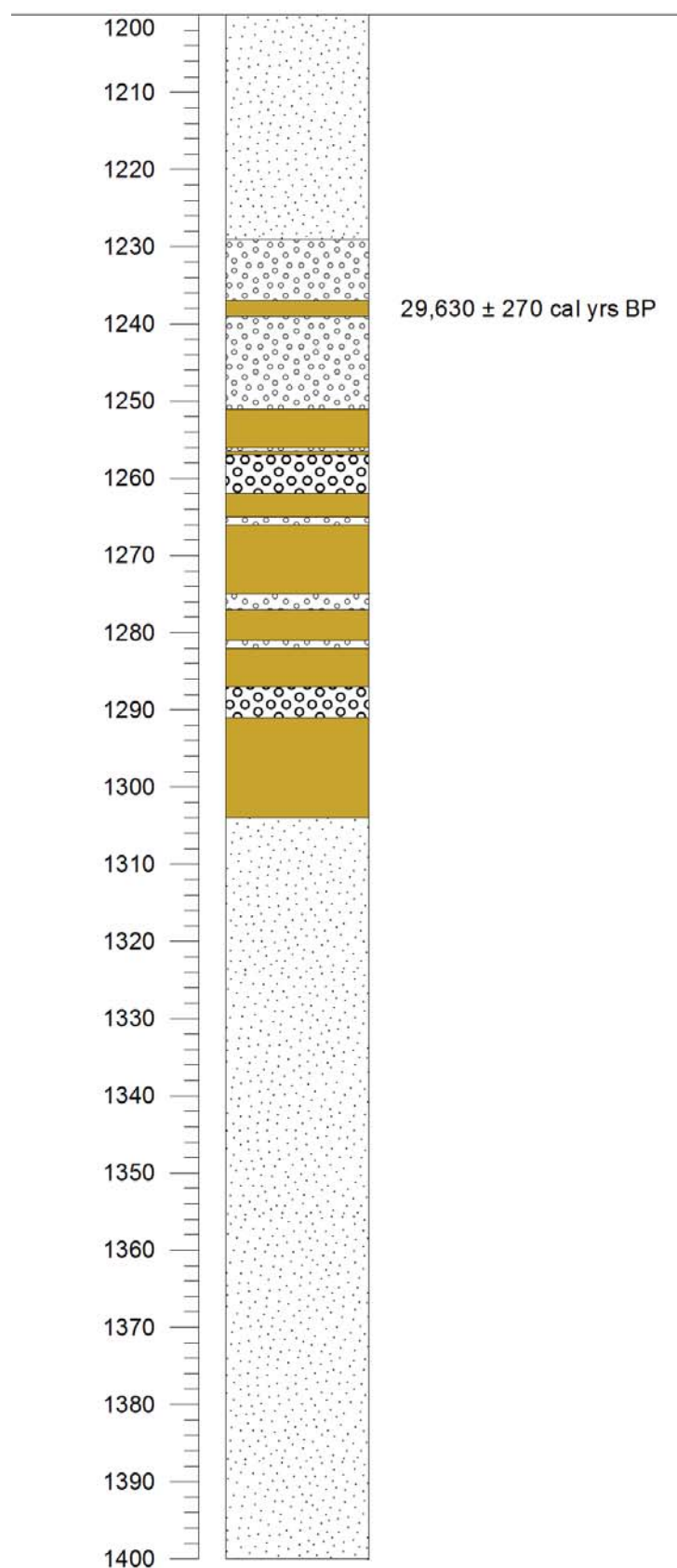


Figure 24(d). Eltham Swamp Lithology Core A (7) (12-14m)



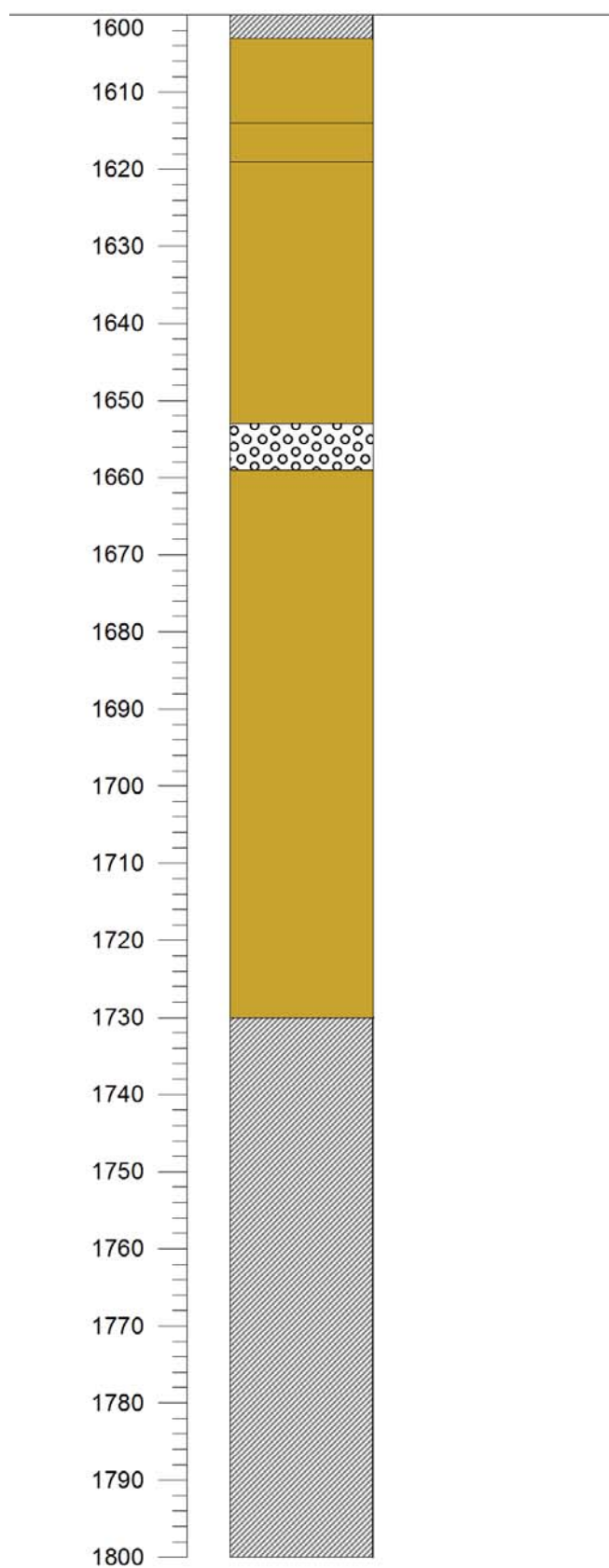


Figure 24(f). Eltham Swamp Lithology Core A (9) (16-18m)

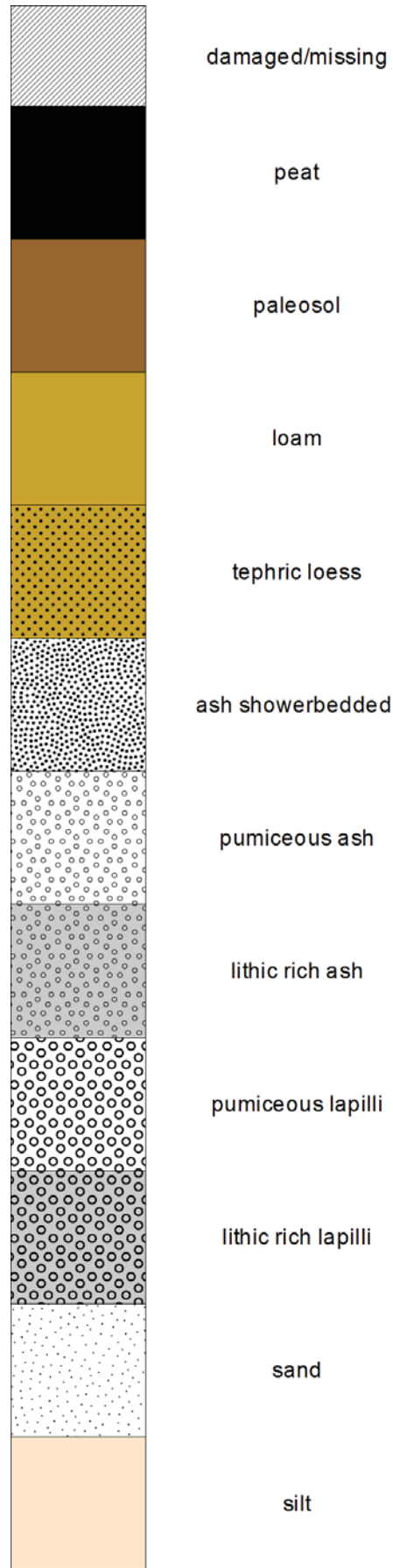


Figure 25. Eltham Swamp Lithology Key

## Coastal Taranaki Sites

The following section gives information about the five coastal Taranaki site locations and their stratigraphic context. All sediment identifications and lithology diagrams (as well as several of the site photographs) for Okaweu Stream, Opunake Beach, Kaipokonui Beach and Lizzie Bell were kindly provided by Dr. Anke Zernack (Zernack 2008; Zernack *et al.* 2011; Anke Zernack *pers comm.* 2012).

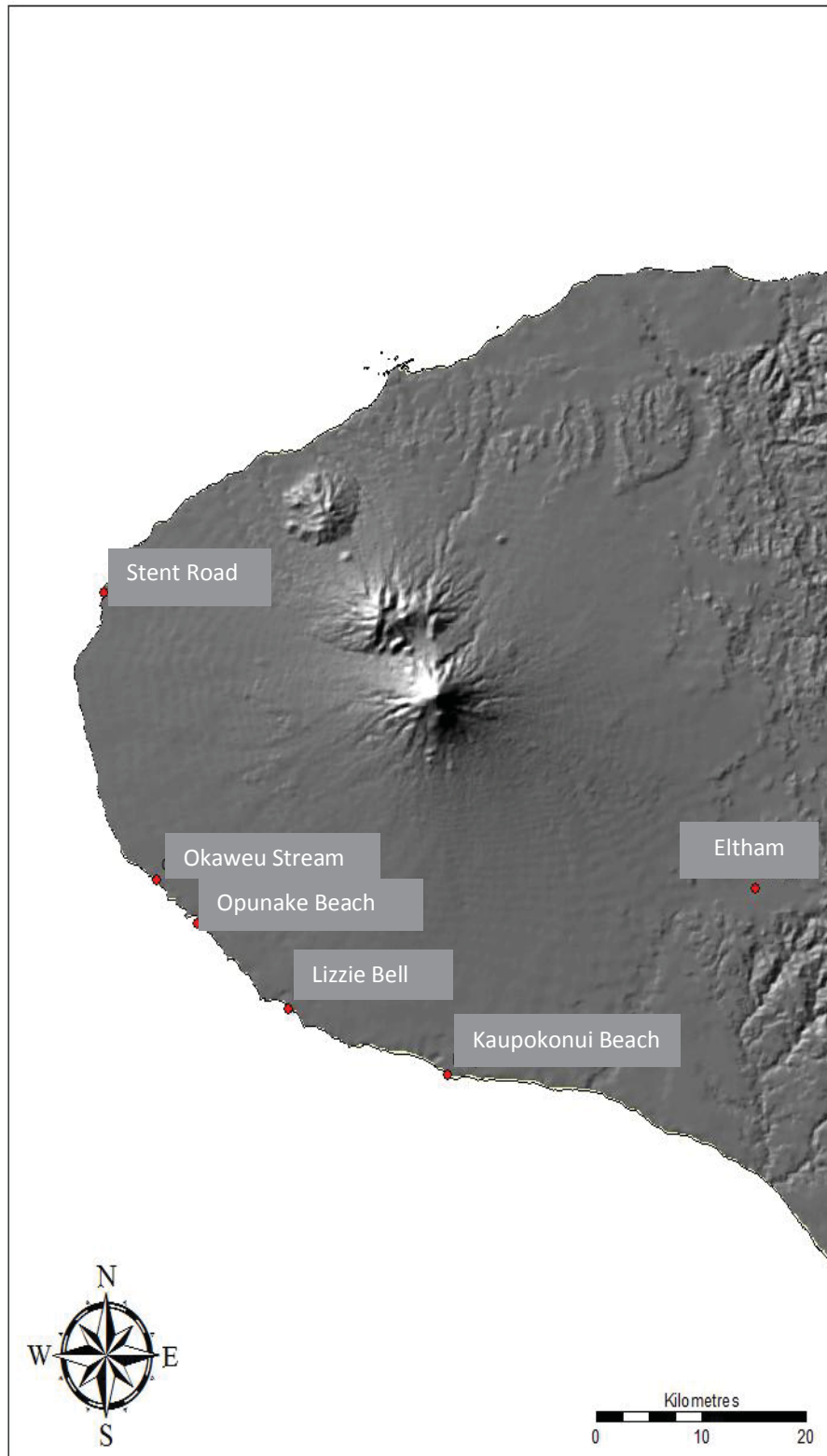


Figure 26. Taranaki Study Sites

### 7.1.2. Stent Road

The Stent Road site (39° 13' 18.14" S, 173° 46' 39.79" E) lies around 6 km north of Cape Egmont, along the coast between the intersection of Stent Road and Coast Road, and the car park at the north end of Coast Road (Figure 26). A 34 cm -thick lignite sequence lies at the base of a low,  $\leq 4$  m coastal cliff (Figure 27).

Deposits from the Pungarehu debris avalanche<sup>22</sup> event lie at the base of the sequence; this debris avalanche was thought to have occurred sometime after  $30,770 \pm 745$  cal yrs BP (Ui *et al.* 1986). However, wood found within the marginal facies of the Pungarehu Formation dated at  $24,510 \pm 585$  cal yrs BP (Neall 1979) and a peat deposit directly beneath the Pungarehu debris-avalanche deposit dated at  $24,730 \pm 220$  cal yrs BP (Zernack 2008) are likely to be the best estimates for the maximum age of the deposit. The dated peat closely overlies the Kawakawa / Oruanui ash with a recently revised age of  $25,360 \pm 160$  cal yrs BP (Vandergoes *et al.* 2013), supporting Zernack's (2008) maximum date; furthermore, since the Pungarehu debris-avalanche deposit it is found underlying the Stent Road lignites in the current study, it can be assumed to have a minimum age of (that is, it is older than)  $21,440 \pm 110$  cal yrs BP (this study).

The Pungarehu debris-avalanche deposit covered between 200 and 250 km<sup>2</sup> with a mean thickness of 30m, and extends from Stony River (Neall 1979), *c.* 6 km north of Stent Road, to just north of Okahu Stream in the south (Neall 1979), *c.* 10 km south of Stent Road.

An earlier study by McGlone & Neall (unpublished; cited in Pillans *et al.* 1993) yielded a date of  $21,910 \pm 480$  cal yrs BP for the 'peat beneath the lahar' at this site; this compares with ages of  $18,540 \pm 120$  cal yrs BP for organic silts at the top of the lignite sequence, and  $21,440 \pm 110$  cal yrs BP for organic silts at 18-20 cm depth in the current study, and Zernack's (2008) age of  $24,730 \pm 220$  for peats at the base of the lignite sequence.

Owing to time constraints in the field, a full stratigraphic description for the Stent Road site sequence was not prepared, however the lahar overlying the peat deposits is most likely the 13,000 to 22,500 yrs BP Warea Formation (Neall 1979). This formation does not represent a single event, but rather a time series of events, and therefore is recognised as a chrono-stratigraphic unit (Stewart *et al.* 2006). The deposit is described as a laharic conglomerate breccia and sandstone, whose type locality is comprised of a coarse sandy matrix that contains poorly sorted, dense, sub-angular, black andesitic clasts ranging from 1 cm to 10 cm in diameter. A unique characteristic of the Warea Formation is its strong lithification and plentiful radial fractured, breadcrusted volcanic bombs as large as 30 cm in diameter (Stewart *et al.* 2006).

---

<sup>22</sup> Lahar is defined as "a rapidly flowing mixture of rock debris and water (other than normal streamflow) from a volcano," (Smith & Fritz 1989); hyperconcentrated stream flow deposits are "mainly sandy, well-bedded and clast-supported diamictons, where a diamicton is a nonlithified, conglomeratic, or brecciated volcanoclastic deposit, which is poorly sorted and includes coarser particles dispersed through a sandy or muddy matrix," (Lecointre *et al.* 1998). Debris-avalanche deposits "result from major sectoral collapse of the flanks of a volcano," (Lecointre *et al.* 1998).



**Figure 27(a).** Stent Road Site.

*Photo: Anke Zernack*



**Figure 27(b).** Stent Road Site. The lignite layer was partially buried by cobbles and pebbles from the current beach.

### 7.1.3. Okawe Stream

Two sites were sampled at Okawe Stream; site 1 lies just to the north of Okawe Stream mouth (Figure 28 a), (39° 25' 56.21" S, 173° 49' 19.48 " E) and site 2 is < 100m south, in the cliff formed by fluvial incision and wave action on the southern bank of the stream, around 2.5km north of Opunake.

The stratigraphy of the sites is as follows. A deposit from the Te Namu debris avalanche (Zernack 2008; Zernack *et al.* 2011) lies at the base of the 10.5m-high cliff. This debris avalanche is exposed to the east of Okawe Stream and extends nearly 9 km south along the coast, and was emplaced *c.* 33,710 ± 540 cal yrs BP.

The Te Namu debris avalanche is at least 5 m thick and is comprised of pebble- to boulder-sized clasts, rip-up clasts in excess of 1.5 m in diameter, and thixotropic allophane clays and peats (possibly Hihiwera Peats, described in section 7.1.4). Zernack *et al.* (2011) note that the debris avalanche is topped by a distinctive soil sequence, comprised of dark paleosols, and separated by coarse andesitic ash and pale pink silt layers.

The third paleosol<sup>23</sup> layer, estimated to be 29,000 cal yrs in age (Zernack 2008), had rivulets of fresh water running over it, and roots of modern vegetation intruding into the deposit (Figure 28 b). Since this section may have been contaminated by modern pollen and translocated fossil pollen, the analogous lignite deposit from site 2 was used for pollen analysis for this layer only, hence pollen zones OK 1, OK 2 and OK 4 in Figure 43 are derived from site 1, and pollen zone OK 3 is derived from site 2. Figure 43 does not record the depth of the samples, but merely records the sample number, as well as calibrated  $\delta^{14}\text{C}$  age. The analogous layer at site 2 was drier, was not overgrown with modern vegetation, and the lignite layer was thicker than at site 1, therefore it was assumed that contamination would be minimised compared with site 1. Figure 28 (e) shows the stratigraphic correlation between the two sites.

Hyperconcentrated-flow deposits lie above these paleosols / silt layers; in turn, the hyperconcentrated-flow deposits are topped with a thin organic soil layer, a thin layer of the distinctive Kawakawa/ Oruanui Ash, deposited 25,360 ± 160 cal yrs BP (Vandergoes *et al.* 2013) and two lignite layers.

A Pungarehu debris avalanche deposit is next in the sequence; this deposit is between 0.8 and 2 m thick at Opunake to the south of Okawe Stream, and is comprised of cobble- to boulder-sized clasts, shattered clasts and megaclasts. The shattered clasts are thought to be the result of blocks being split apart by collisions with the ground surface and with other blocks during transport, resulting in aggregations of large blocks forming hummocky hills in the central part of the debris avalanche, whilst the smaller clasts flow further from their source (Ui *et al.* 1986). Based on a peat sample dated at 24,801 ± 268 cal yrs BP taken from directly below the debris avalanche, the debris avalanche is estimated to be 24,000 yrs old (Zernack *et al.* 2011). A paleosol layer separates the Pungarehu debris avalanche from the Opua debris avalanche; this younger debris avalanche has an estimated age of 7,500 years (Neall 1979), and has an estimated minimum volume of between 1.98 and 2.38 km<sup>3</sup> (Procter 2009).

---

<sup>23</sup> See section 7.1.4 for discussion regarding nomenclature of paleosols, lignites, etc.



Figure 28(a). Okawe Stream Site 1. Arrows indicate lignite layers.

*Photo: Anke Zernack*



Figure 28(b) Okawe Stream Site 1. Note iron staining of the lignite layers.

Figure 28(c). Okawe Stream, Site 1 Lithology. Source: Zernack( 2008), Zernack *et al.* (2011)

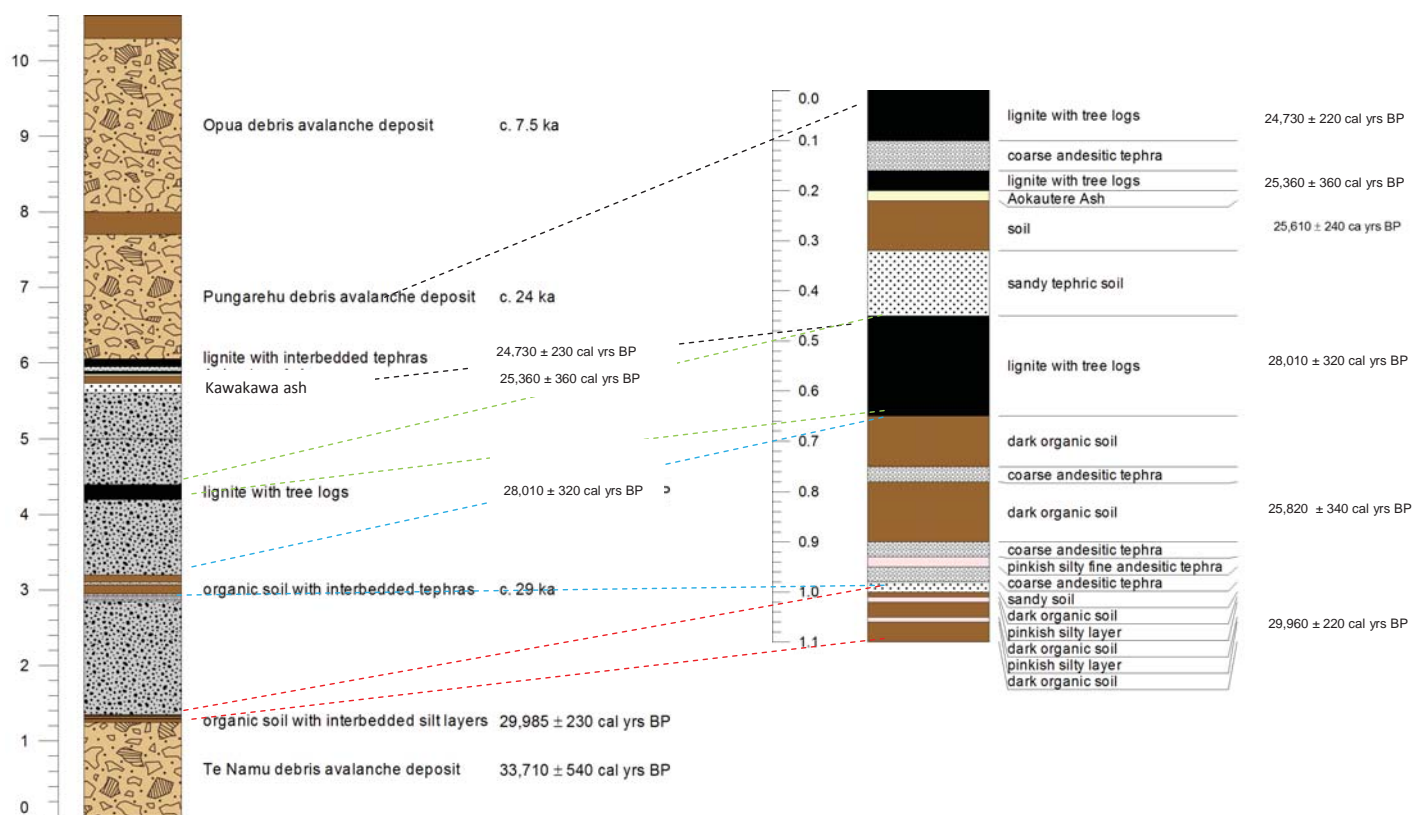
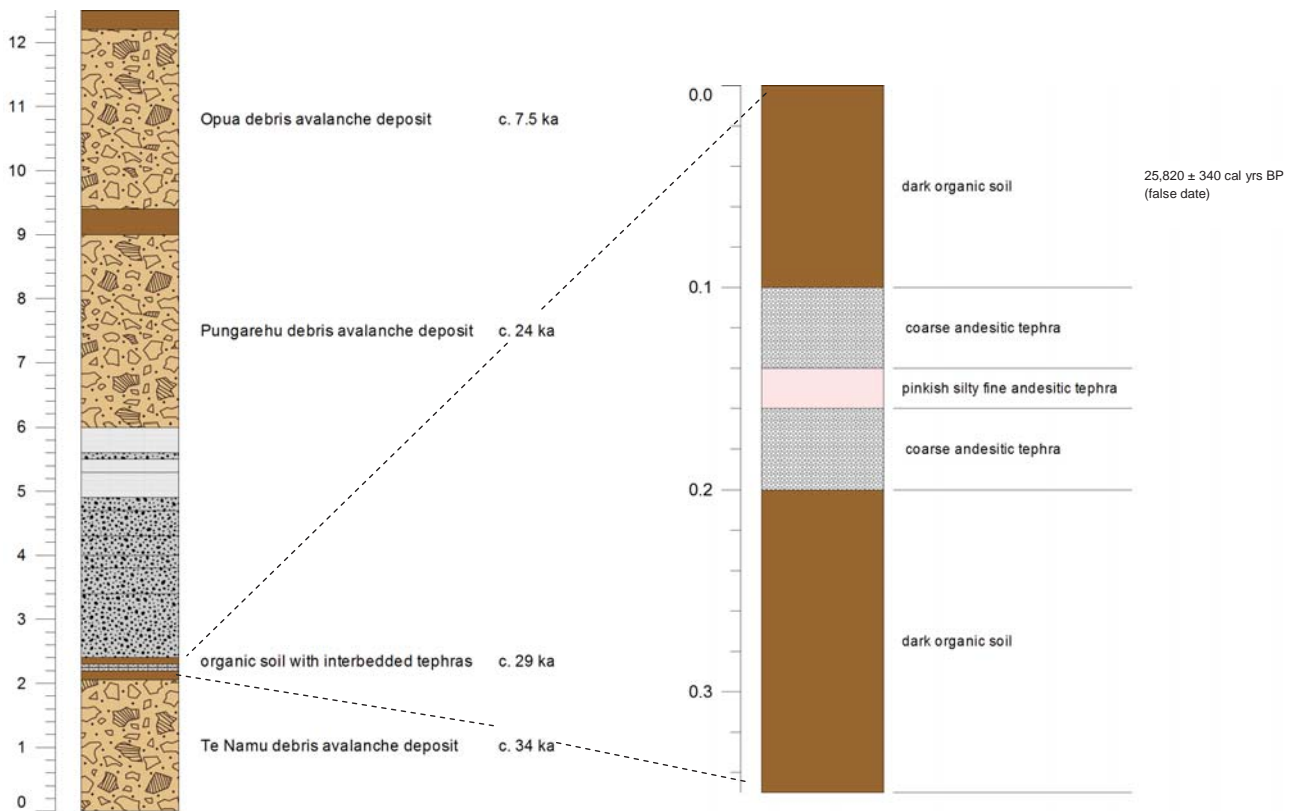


Figure 28(d). Okawe Stream, Site 2 Lithology. Source: Zernack (2008), Zernack *et al.* (2011)





Okawe Stream, Site 1.

Photo: Anke Zernack



Okawe Stream, Site 2.

Photo: Anke Zernack

**Figure 28(e). Okawe Stream Correlation Between Sites 1 and 2.** Note the thin layer of the Kawakawa / Oruanui Tephra (bounded by the red broken lines) that is more distinct at Site 2 than at Site 1.

#### 7.1.4. Opunake Beach South

The Opunake Beach South (Figure 29) site (39° 27' 48.32" S, 173° 51' 26.24" E) is around 1.5 km south of Opunake township. A 1.4 m lignite layer interspersed with paleosols and thin andesitic tephra layers lies at the base of a 14m-high cliff; pieces of well-preserved wood protruding from the lignite were dated by Zernack (2008) at 33,435 ± 460 cal yrs BP, and organic silts recovered from the base of the lignite were dated at 33,800 ± 425 cal yrs BP in this study (Table 8).

The base of the 14m-high cliff at Opunake Beach South is comprised of coarse, channel-fill debris-flow deposits; this is followed by a 1.4 m lignite layer interspersed with paleosols and thin andesitic tephra layers. Zernack *et al.* (2011) note that “Two thick peat / organic paleosols sequences are relatively widespread in [south-western Taranaki] ... the younger peat sequence is thickest in the Opunake area ... and is here named Hihiwera Peat.” (p. 1941). An AMS-derived  $\delta^{14}\text{C}$  date of 33,760 ± 440 cal yrs BP was derived for this peat in the current study (Table 8); this compares with dates ranging from 38,679 ± 1,097 to 34,227 ± 283 cal yrs BP (for the top of the peat layer) in Zernack *et al.* (2011) and 39,735 ± 1,143 cal yrs BP in Grant-Taylor (1964).

Pollen preservation was very good at all the coastal sites in the current study, as indicated by high absolute pollen counts and low incidence of pollen grain corrosion. This suggests that the polleniferous matrices were in fact peats, lignites or at least, peaty loams or peaty paleosols; and/or burial by debris avalanches can have the same effect as tephra in sealing off paleosols from the environment so that they are almost as efficient as peats in preserving pollen grains.

The Hihiwera Peat is overlain by a 2.4 m thick layer of coarse, channel-fill debris-flow deposits; these deposits in turn were overlain by 3.8 m of hyperconcentrated-flow deposits; next in the sequence came Pungarehu and Opua debris-avalanche deposits, as described in section 7.1.3. The correlations between these two debris-avalanche deposits at Okaweu Stream and Opunake Beach are shown in Figure 33.

Note that Zernack *et al.* (2011) tend to use terms like ‘peat,’ ‘paleosols,’ and ‘organic soils’ somewhat interchangeably, belying their emphasis on volcanology and tephrochronology, rather than an emphasis on palynology and taphonomy. The nature of these different organic sediments with respect to pollen preservation may be significant, since conventional wisdom holds that pollen normally preserves better in anaerobic (reducing), acidic, and sedentary environments such as peat deposits, than in aerobic (oxidising), alkaline, and energetic conditions such as soils (Tinkler 2005).

However, Banks *et al.* (2003a) compared pollen preservation between peat deposits and paleosols at three sites around National Park, finding that there was little difference in the rate of pollen preservation between the sites, inferred from a comparison of absolute fossil pollen counts vs. *Lycopodium* marker counts. Further, Banks *et al.* (2003b) found that tephra layers could preserve pollen spores within paleosols, noting that a primary deposit of Taupo Ignimbrite not only prevented pollen grains from percolating downwards and contaminating lower sediment levels, but could also preserve the pollen grains, presumably by providing a low energy, anoxic environment. This phenomena was also observed in paleosols underlying the Kawakawa / Oruanui tephra at sites around Lake Taupo (McGlone & Topping 1983), and also in exposed roadside cuttings and drains around Taranaki (Lees 1987). On balance, since Zernack’s *et al.* (2012) ‘organic soils’ and ‘paleosols’ were observed to be well preserved, highly polleniferous compacted lignites in the field and in the laboratory, and given the findings of Banks *et al.* (2003a, 2003b), concerns regarding the taphonomy of these deposits can be disregarded.



**Figure 29(a).** Opunake Beach South Site. Arrows indicate lignite layers.

*Photo: Anke Zernack*



**Figure 29(b).** Opunake Beach South Site. Arrows indicate lignite layers.

*Photo: Anke Zernack*

Figure 29(c). Opunake Beach Lithology | Source: Zernack (2008), Zernack *et al.* (2011)

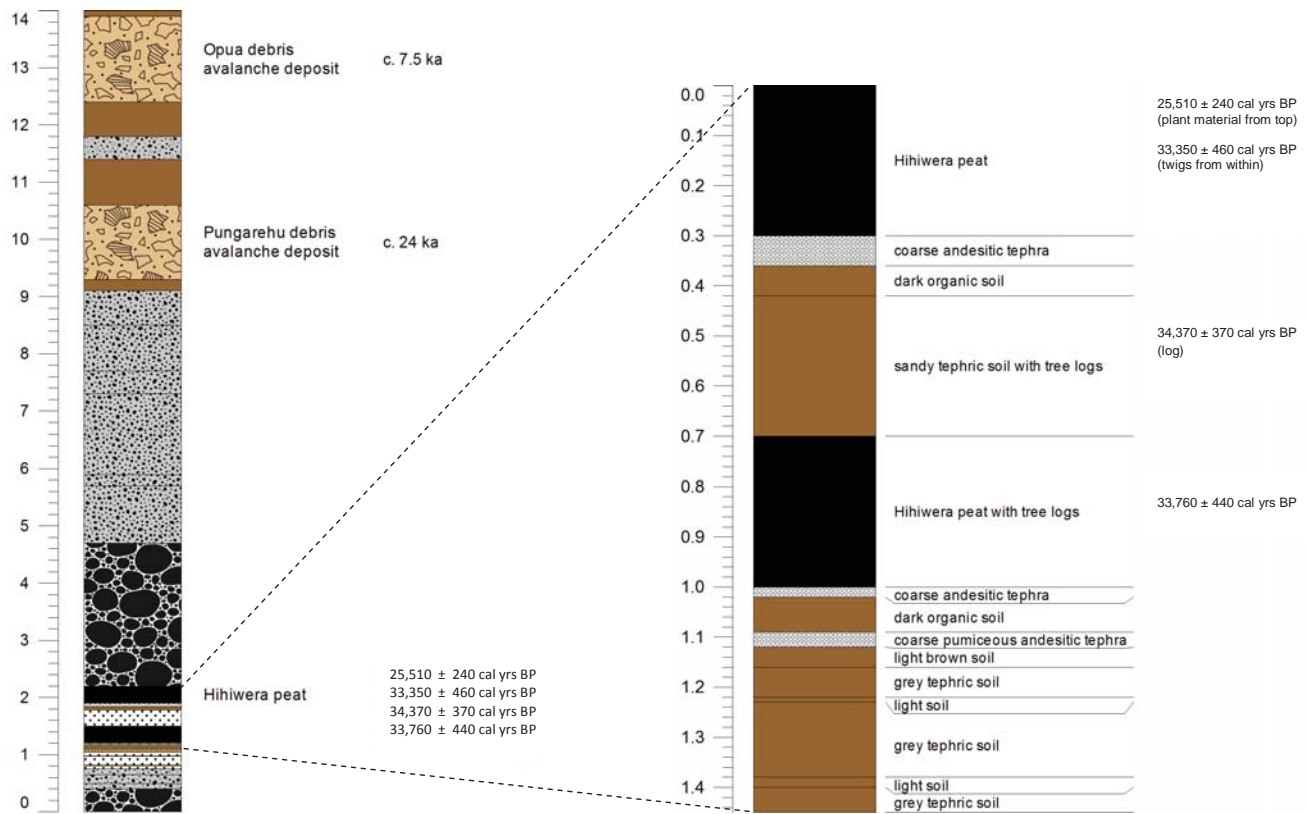




**Figure 30(a).** Kaupokonui Beach Site. Arrow indicates lignite layers



**Figure 30(b).** Kaupokonui Beach site. Tape measure indicates position of the 1.3m lignite layer

### 7.1.5. Kaupokonui Beach

The Kaupokonui Beach site (39° 34' 30.22" S, 174° 04' 19.03" E) is in a 24m-high cliff section, 4km SW of Manaia (Figure 30).

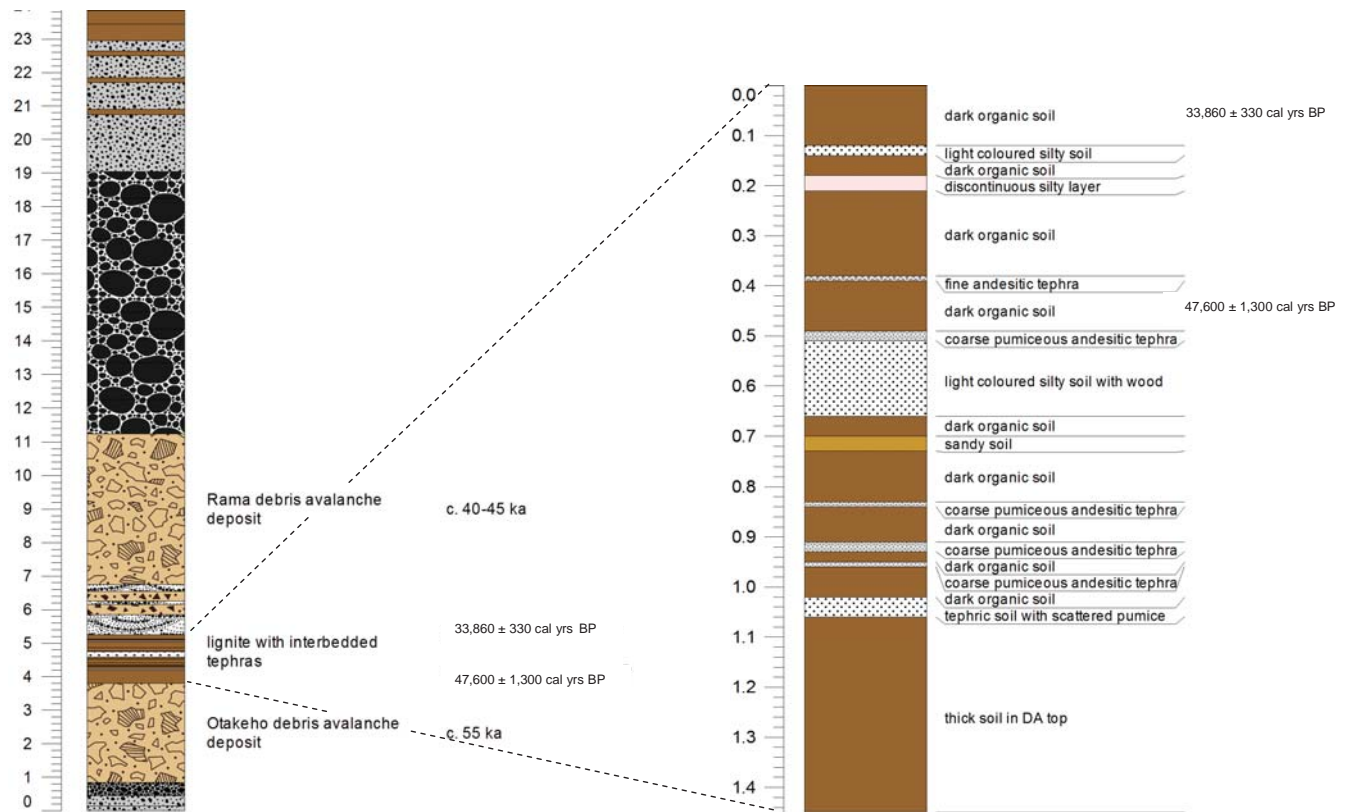
The Otakeho debris avalanche lies at the base of the cliff; this debris avalanche is 2.5 m thick at its type location, Otakeho Stream, 1 km north of Kaupokonui Stream site. The deposit is massive, containing pebble – to cobble-sized clasts, small rip-up clasts and a coarse clay-rich matrix that comprises more than 85% of the debris avalanche deposit (Zernack *et al.* 2011).

A 1.3m thick sequence of thin paleosol - lignite deposits interbedded with thin silty soil layers follows; wood extracted from the debris avalanche was dated to > 55,000 years old (that is, background levels) by liquid scintillation  $\beta$ -counting, hence the estimated age of the lignite bed is 45-55,000 years old (Zernack 2008); similarly, a date of  $47,600 \pm 1,300$  cal yrs BP (also close to background levels) was obtained in the current study.

Coarse, hyperconcentrated-flow deposits up to 60 cm thick separate the Otakeho debris avalanche from the Rama debris-avalanche deposit. This younger debris avalanche is around 5.5 m thick at its type section, and is comprised of pebble- to cobble-sized clasts as well as rip-up clasts (Figure 30); in addition, the Rama debris-avalanche deposit contains large (up to 5.5 m) brecciated megaclasts (Zernack *et al.* 2011). McGlone *et al.* (1984) suggested a minimum age of  $38,679 \pm 1,097$  cal yrs BP for the Rama debris-avalanche deposit.

A layer of coarse channel fill debris-flow deposits *c.* 6.5 m thick overlays the Rama debris-avalanche deposit; this in turn is overlain by a 4 m thick layer of hyperconcentrated-flow deposits interspersed with thin paleosol/lignite lenses.

Figure 30(c). Kaupokonui Beach Lithology Source: Zernack (2008), Zernack *et al.* (2011)



### 7.1.6. Lizzie Bell

The Lizzie Bell site (not an official Geographic Board name<sup>24</sup>) (39° 31' 34.89" S, 173° 56' 06.76 " E) is located at the foot of a 17m-high wave-cut cliff on a small headland around 1km south of the walking track off Puketapu Road, Pihama (7 km southeast of Opunake) (Figure 31a).

A hyperconcentrated-flow deposit at the base of the section is overlain by a 6 m layer of well-sorted, cross-stratified dune sands known as the Punehu Sands (Zernack *et al.* 2011). These sands are likely to have blown inland from the Hauriri shoreline when the sea-level was around 20 m lower, and further offshore, than present, forming the Hauriri marine terrace *c.* 80,000 yrs BP (Pillans 1983), leading Zernack *et al.* (2011) to surmise that the depositional age of these sands is 60,000 to 80,000 years BP.

Overlying the Punehu Sands are three thin, lignite-organic soil sections, covering  $\delta^{18}\text{O}$  stages 3, 4 and 5a. These organic sections are interspersed with thin pumiceous and andesitic tephra layers, as shown in Figure 31 (c). The younger organic sequences are estimated by Zernack (2008) to be around 55,000 years old.

Otakeho debris-avalanche deposits (characterised in section 7.1.5) *c.* 1 m thick overly the lignite - organic soil sections; the correlation between this debris-avalanche deposit at Kaupokonui Beach and the Lizzie Bell site are shown in Figure 33. The Otakeho debris-avalanche deposit is followed by a layer of coarse channel fill debris-flow deposits *c.* 3m thick. Finally a layer of hyperconcentrated-flow deposits interspersed with thin layers of paleosols occurs at the top of the sequence.

---

<sup>24</sup> The barque *Lizzie Bell* was wrecked on the nearby Waimate Reef on July 24, 1901; the Lizzie Bell cemetery is on Puketapu Road.



Figure 31(a). Lizzie Bell Site. Arrow indicates sampling site.



Figure 31 (b). Lizzie Bell Site. .

Figure 31 (c). Lizzie Bell Lithology Source: Zernack (2008), Zernack *et al.* (2011)

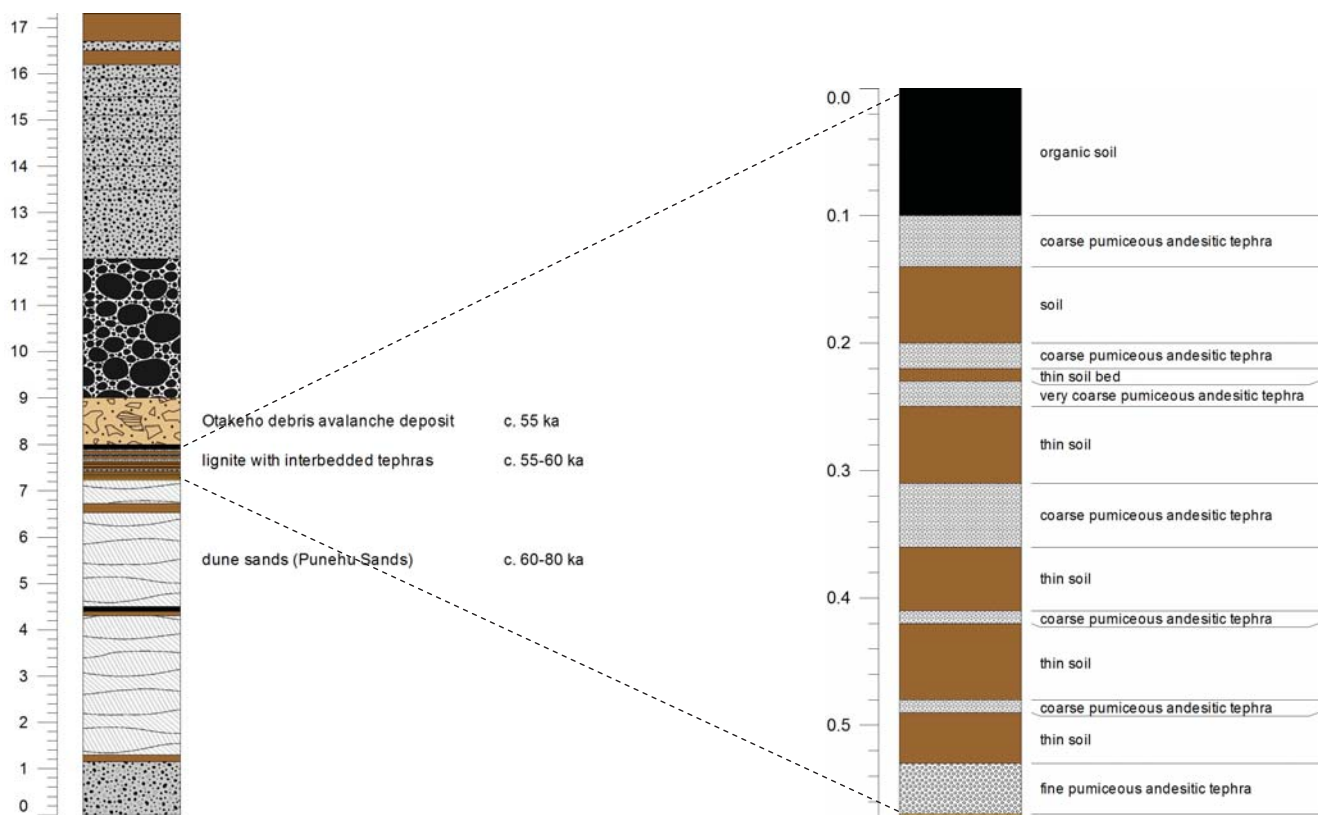


Figure 32. Coastal Taranaki Sites Lithology Key

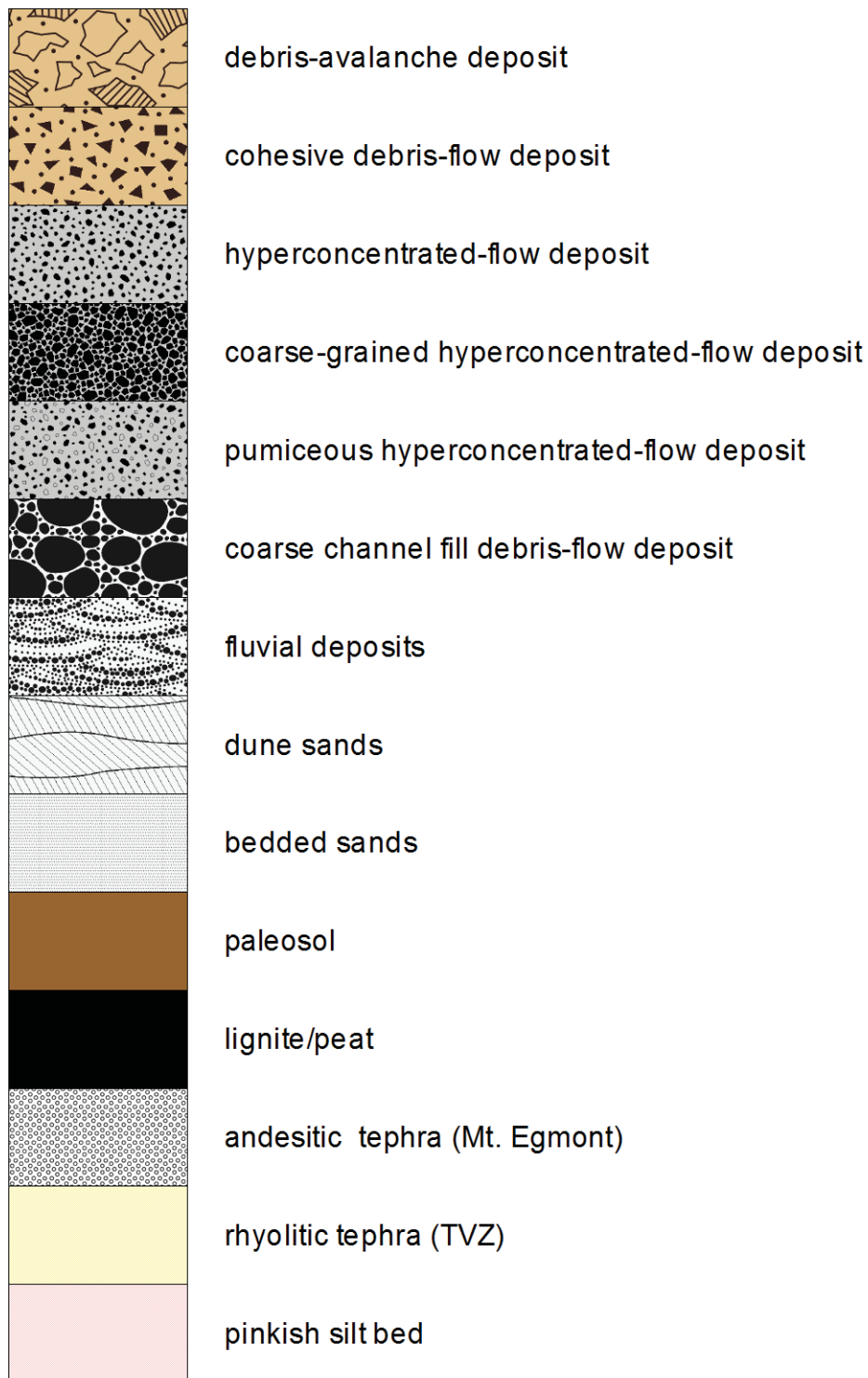
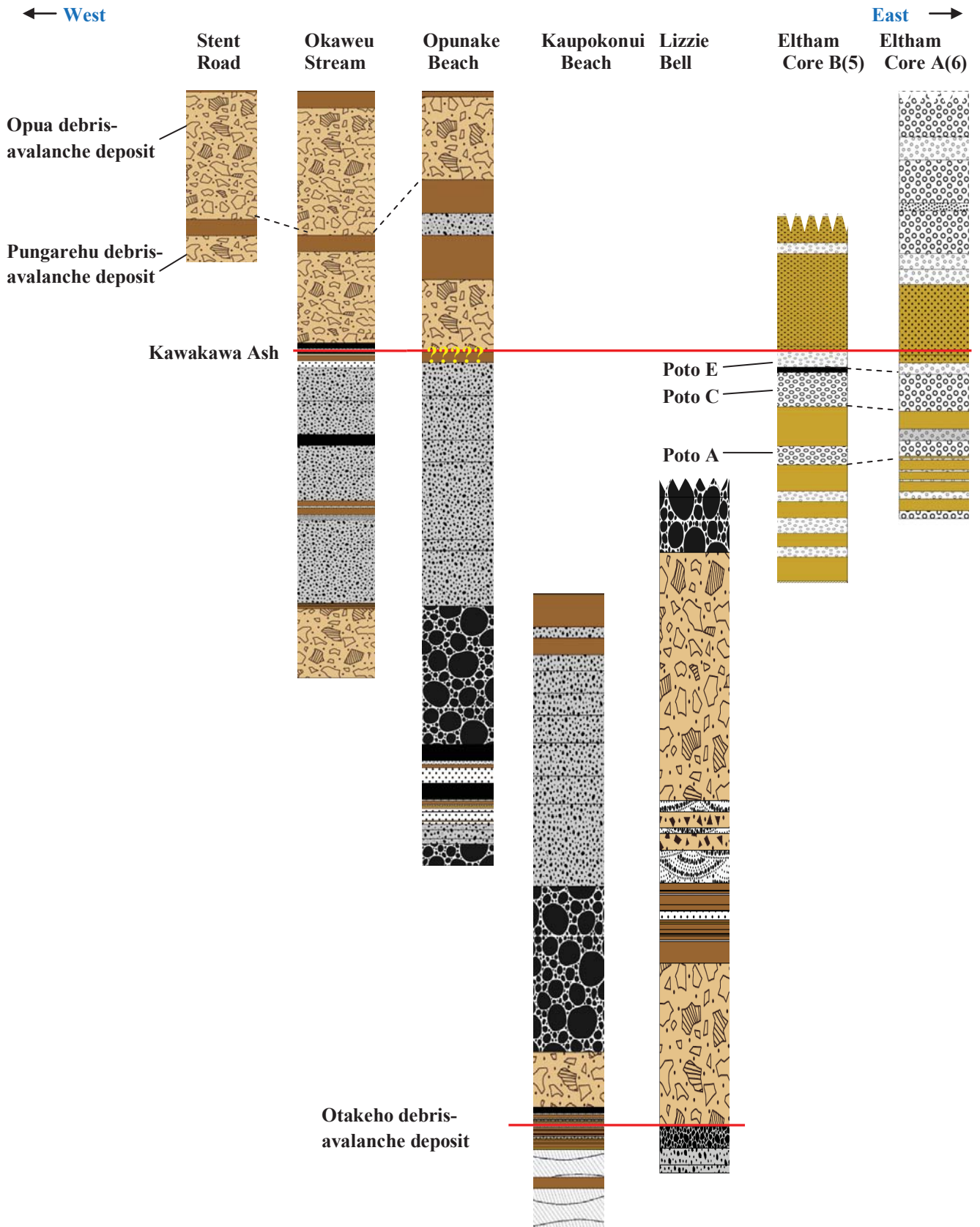


Figure 33. Taranaki Pollen Site Tephra and Debris-Avalanche Deposit Correlations.



## 7.2. Core Extraction

Eltham Core A was extracted from Eltham Swamp in 2008 using a commercial (PRO-DRILL Ltd) hydraulic drilling rig mounted on the back of a tractor (Figure 34a). The core was high-pressure water extruded into 2 m lengths of 100 mm PVC pressure pipe. The core tubes were labelled then cut in half longitudinally using a skill saw, wrapped in plastic, and refrigerated at 4°C to prevent desiccation and contamination. One half of each 2 m length of core was used for tephrochronological analysis by Volcanic Risk Solutions group, and the other half was put aside for pollen work.

There were questions as to whether the coring process may have resulted in the loss of some material due to the use of pressurised water to extrude the core from the casing (Figure 34b), highlighted by the apparent lack of a macroscopic Kawakawa tephra, therefore Eltham Swamp was re-cored in 2011 (Figure 35) to elucidate the stratigraphy of Eltham Core A; this second core is referred to as Eltham Core B.



Figure 34(a). Coring rig at Eltham, 2008.

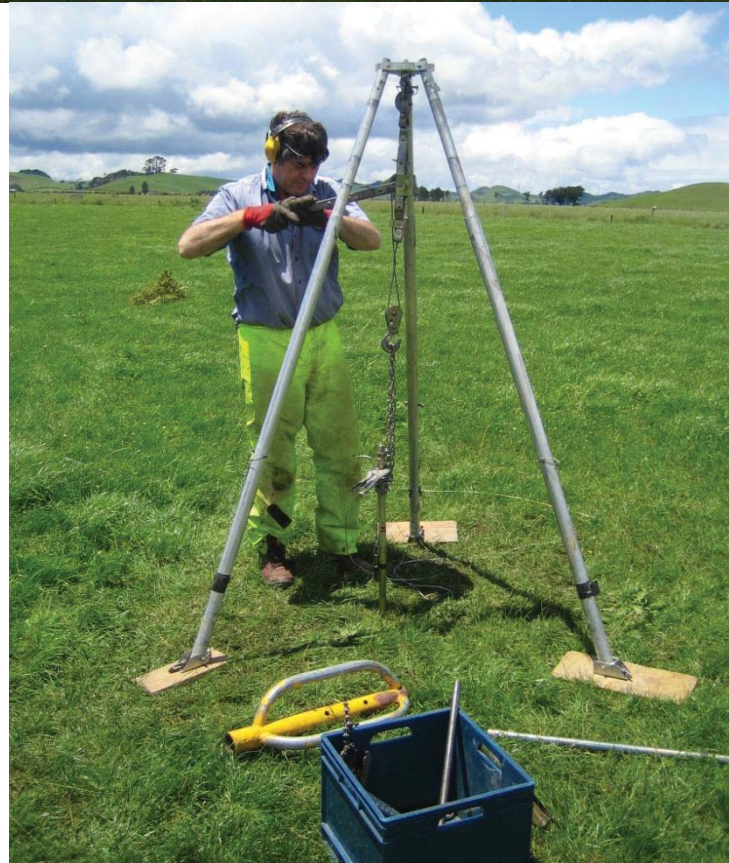
*Photo: Shane Cronin*



Figure 34(b). Water extrusion of core from bore casing, 2008.

*Photo: Shane Cronin*

Figure 35 shows the coring apparatus used to acquire Eltham Core B at Eltham; it was determined that Core B was located < 100 m of Core A, based on GPS data, and likely < 50m based on reference to landmarks in photos of Core A (e.g fences and water troughs) and the farmer's best estimate. The coring setup for Core B consisted of a Livingston piston corer driven into the ground using a post driver, with a ratchet lever hoist anchored to a tripod to assist in retrieval. It was possible to retrieve sediments from 13 m depth using this apparatus. The cores were wrapped in plastic, x-rayed and refrigerated at 4°C to prevent desiccation and contamination.



**Figure 35. Livingston Coring Apparatus at Eltham, 2011.** *Photo: Marcus Vandergoes (bottom)*

Figure 36 (a). Eltham Swamp Lithology Core B (4) (8-9m)

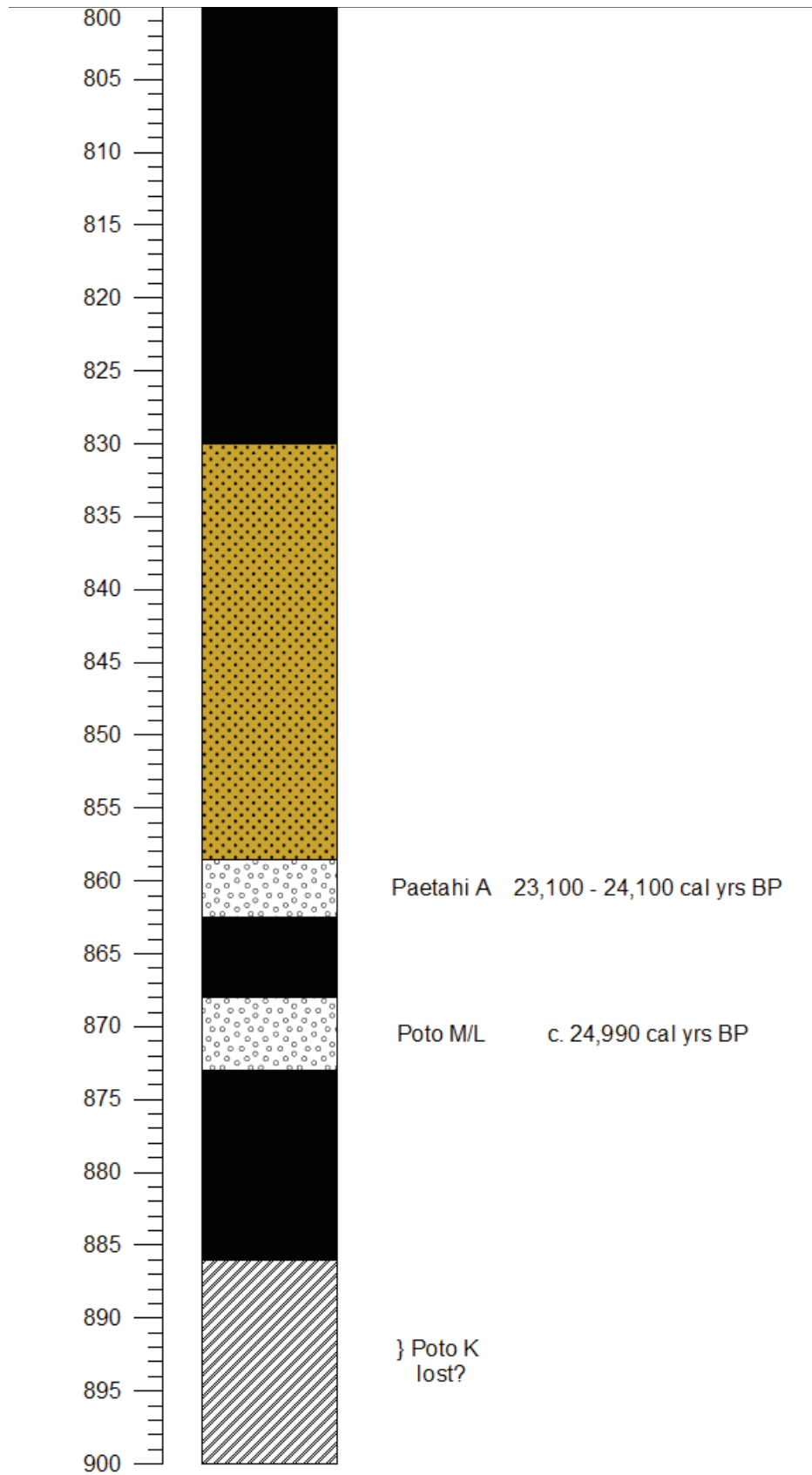


Figure 36(b). Eltham Swamp Lithology Core B (5) (9-10m)

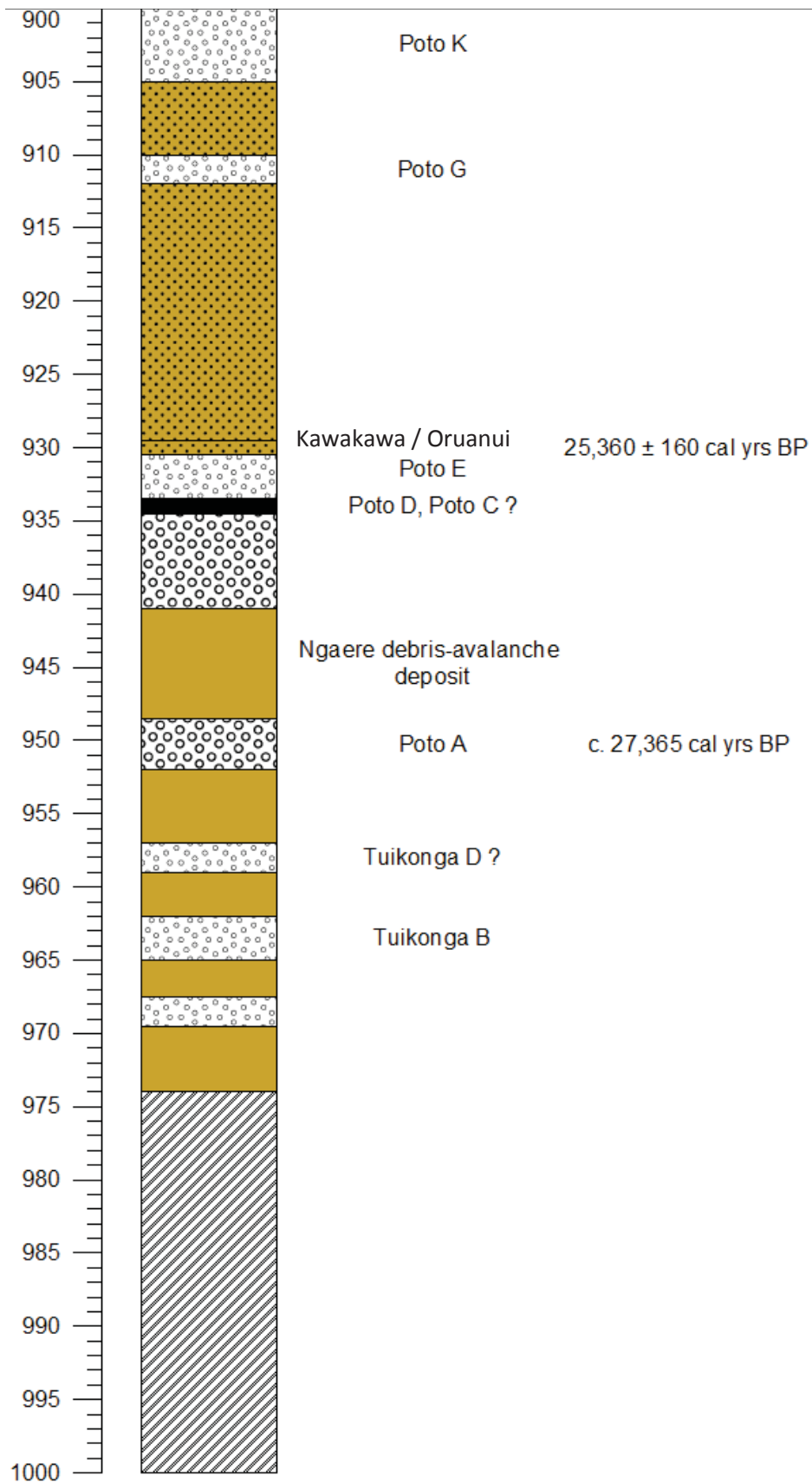


Figure 36 (c). Eltham Swamp Lithology Core B (6) (10-11m)

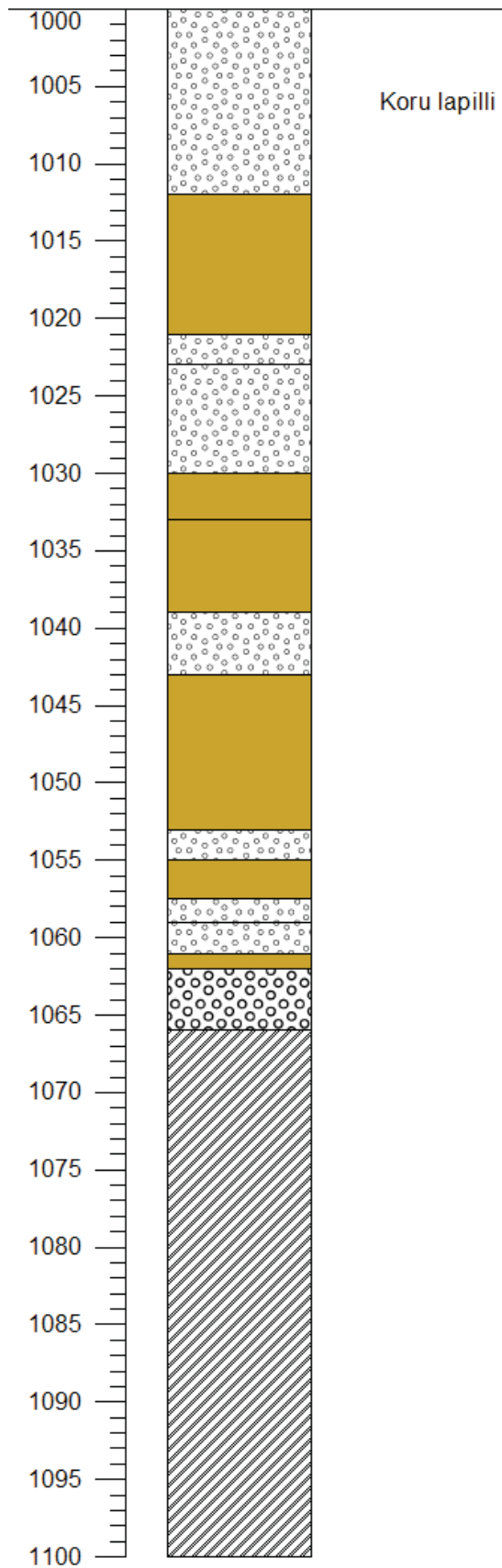
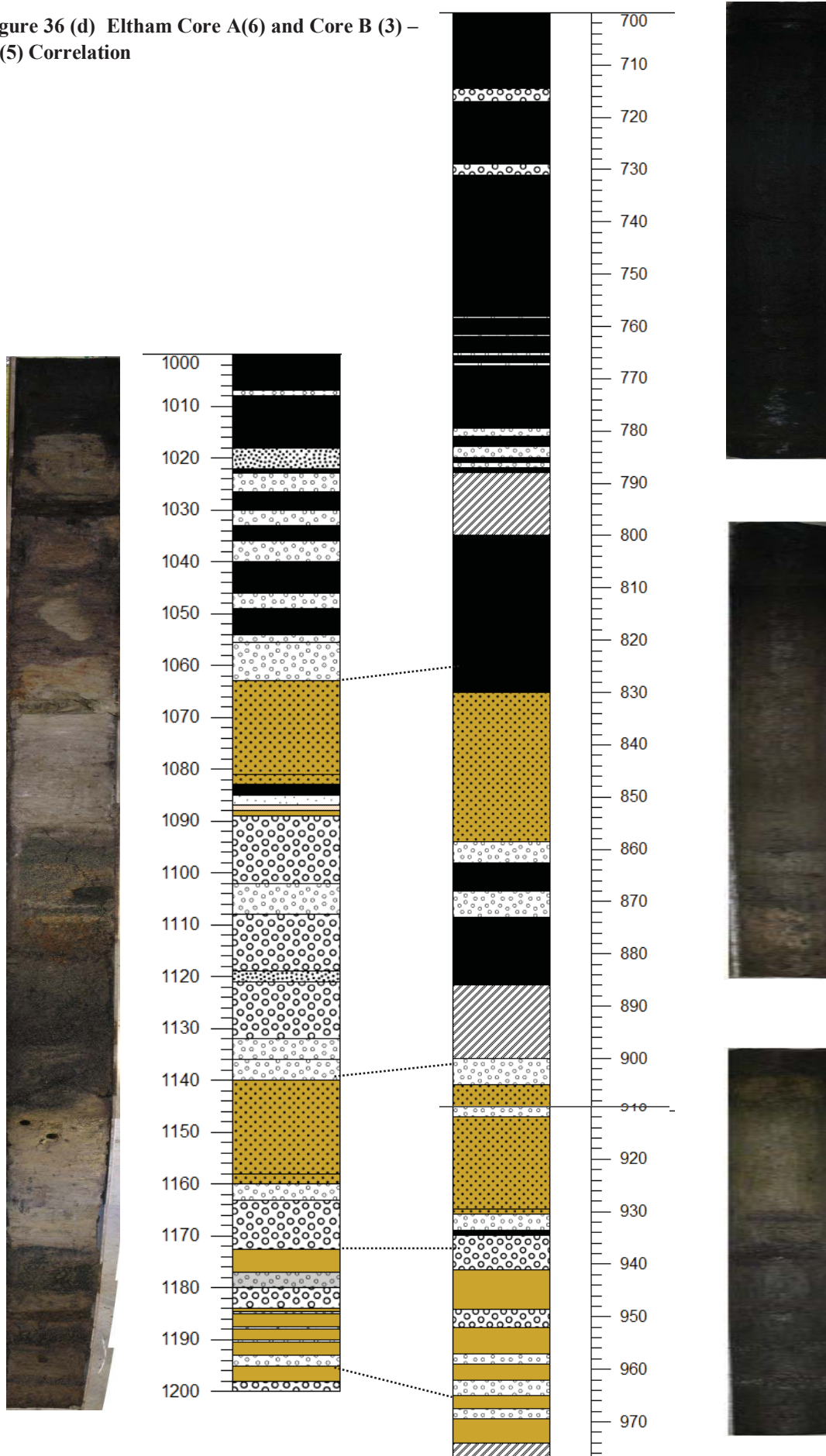


Figure 36 (d) Eltham Core A(6) and Core B (3) – B (5) Correlation



Core A(6)

Core B (3), (4) and (5)

### 7.3. Palynology and Charcoal Methodology

Eltham Core A was prepared for sampling by scraping off the surface layer with a scalpel, taking care to scrape at right angles to the core to minimise contamination. The scalpel was constantly rinsed in deionised water / Pyroneg<sup>®</sup> solution to further reduce the likelihood of cross-contamination. Once the core was cleaned a steel tape measure was laid along the core segment, and the core lithology was recorded.

The sampling strategy adopted was 10 mm contiguous sampling in peat; sediments that were clearly not peats such as tephric loess and loams were sampled at approximately 5cm intervals. Each sample was extracted from the core by plunging a sterile, 5 ml Terumo brand<sup>®</sup> hypodermic syringe with the threaded end (Luer lock) removed (10 mm diameter) into the sediment, and extracting approximately 1 cc of sediment. A fresh syringe was used for each sample to prevent pollen cross-contamination. Approximately 1 cc of sediment was extruded from each syringe into a 15 ml test tube, the sample was weighed to 0.01 g accuracy and the weight recorded.

Since “ ‘Standard’ palynological processing methods can be very variable, with researchers using different sample sizes, different concentrations and volumes of acids, different sieve materials and sizes, and different sequences of sample treatment,” (Lignum *et al.* 2008) the processing steps are described in greater detail than is the norm.

‘Standard’ palynological procedures outlined in Fægri & Iverson (1964) and Fægri *et al.* (2000) were used to extract pollen from the sediment samples, as follows:

- (i) *Lycopodium* spiking - two Stockmarr *Lycopodium* marker tablets (Stockmar 1971) were added to the sample to allow pollen quantification;
- (ii) Carbonate removal – (a) 10% HCl was added to the sample to remove CaCO<sub>3</sub>; (b) the samples were washed in distilled water, centrifuged (3,000 rpm for three minutes), and decanted.
- (iii) Humic acid removal, and disaggregation and deflocculation of sediments - (a) a 50:50 mixture of 10% KOH and 0.1mol NaP<sub>2</sub>O<sub>7</sub> was added to the samples; (b) samples were heated to 100°C in a water bath for two minutes; (c) samples were washed in distilled water and centrifuged.
- (iv) Coarse sieving – (a) samples were filtered using a coarse (1mm) terylene gauze to remove large detritus; (b) the gauze was rinsed with distilled water, and the filtrate was centrifuged and decanted.
- (v) Silicate removal – (a) 40% HF was added to samples to dissolve SiO<sub>2</sub>; (b) samples were heated to 100°C in a hot block for three minutes; (c) samples were washed in 5% HCl to stop the reaction and centrifuged; (d) samples were washed in distilled water, centrifuged and decanted.
- (vi) Cellulose removal - acetolysis – (a) samples were washed in dilute acetic acid, centrifuged and decanted; (b) the residue was washed in glacial acetic acid, centrifuged and decanted; (c) the residue was washed in a 9:2 mixture of acetic anhydride and concentrated H<sub>2</sub>SO<sub>4</sub>; (d) samples were heated to 100°C in water bath for three minutes; (e) the samples were washed in glacial acetic acid to stop the reaction, centrifuged and decanted; (f) the residue was washed in dilute acetic acid, centrifuged and decanted; (g) the residue was washed in distilled water, centrifuged and decanted.
- (vii) Fine sieving – (a) the samples were filtered using a fine (6µm) nylon gauze to remove fine detritus; (b) the filtrate was rinsed off the gauze with distilled water and retained; (c) the samples were then centrifuged and decanted.

- (viii) Alcohol dehydration – preservation and pre-mounting treatment - (a) the samples were washed in 95% ethanol, centrifuged and decanted; (b) the residue was washed in 100% ethanol, centrifuged and decanted; (c) the residue was washed in a 50:50 mixture of 100% ethanol and tertiary butyl alcohol, centrifuged and decanted; (d) the residue was washed in pure tertiary butyl alcohol, centrifuged and decanted; (e) a 50:50 mixture of pure tertiary butyl alcohol and 2000 cs silicone oil (dimethylpolysiloxane) was added to samples; (f) the samples were centrifuged (but not decanted); (g) samples were placed in an oven at 50°C overnight to allow the alcohol to evaporate. Alcohol dehydration removes water from the sample to prevent the growth of microorganisms, and because water is immiscible with silicone oil, it must be removed to avoid sample clumping.
- (ix) Mounting – (a) a drop of each sample was placed on a clean microscope slide using a fresh capillary tube for each sample and a 22 mm × 22 mm cover slip placed on top; (b) hot wax was placed on the edge of the cover slip and allowed to move by capillary action around the circumference of the cover slip to seal the slide; (c) two glass slides were prepared for each sample and the slides were cleaned of excess wax and labelled.

Pollen slides were read at 400 × magnification under brightfield conditions using an Olympus binocular microscope equipped with a mechanical stage. Major pollen taxa were identified using identification keys, photographs and descriptions found in the literature.<sup>25</sup> Grains that remained cryptic were compared to the pollen reference collection at Massey University's pollen laboratory to assist identification.

Raw data was loaded into the TILIA program (Grimm 2007) to create relative and absolute pollen diagrams. Pollen percentages are based on a pollen sum of all dryland plants, excluding aquatic plants, ferns and fern allies. A minimum of 200 pollen grains of dryland plants was used for all pollen percentage calculations. Taxa within each of the dryland taxa groups in the pollen diagrams are ordered lowest to highest correlation of pollen concentration to mean annual temperature (Wilmshurst *et al.* 2007); in other words, cold tolerance declines from left to right within each group.

The need to manually estimate biostratigraphic zones was largely avoided by utilising CONISS (**CON**strained cluster analysis by the method of **I**cremental **S**um of **S**quares), a program that operates within TILIA. CONISS performs a stratigraphically constrained cluster analysis to create a dendrogram that shows the hierarchical relationships between clusters of adjacent, like-samples; these were used to derive the biostratigraphic zones in the pollen diagrams.

Charcoal particles > 6µm and < 1mm were enumerated during pollen counting, with three sizes differentiated: < 20 µm, 20-50 µm and > 50 µm. Sizes were either measured by vernier scales on a Zeiss microscope in the Massey University palynology laboratory, or estimated by comparison to pollen grains with well-documented sizes: grains smaller than *Nothofagus* subg. *Fuscaspora* were assessed as < 20 µm, since these grains are 23-27 µm in the equatorial plane (Moar 1993); grains that were ≥ *Nothofagus* subg. *Fuscaspora* but smaller than *Nothofagus menziesii* (46-60 µm in the equatorial plane, Moar 1993) were deemed to be 20-50 µm in size; and grains ≥ *Nothofagus menziesii* were designated as > 50 µm in size. Concentrations were calculated in the same way as for calculating pollen concentration (Stockmarr 1971; Tinner *et al.* 2006) and expressed as grains g<sup>-1</sup>: charcoal grains counted × (*Lycopodium* grains added ÷ *Lycopodium* grains counted) × (1 ÷ sample weight).

---

<sup>25</sup> Moar (1993), dicotyledons; Cranwell (1952) monocotyledons; Large & Braggins (1991) fern and fern ally spores; Pocknall (1981a) conifers; Pocknall (1981b) *Phyllocladus*; Argue (1986) *Glossostigma*; MacPhail (1980) *Beilschmiedia tawa*; and Quinn *et al.* (2005) *Cyathodes*.

## 7.4. Taranaki Radiocarbon Dates

### 7.4.1 Eltham Radiocarbon Dates

Nineteen  $^{14}\text{C}$  dates were collected for Core A; six of these were collected by Turner (2008) from the half of the core used by the Volcanic Risk Solution group for tephrochronological work, and thirteen dates were collected from the other half of the core saved for pollen work as part of the current study. Turner's (2008) dates were all derived from bulk peat samples and most were determined using liquid scintillation Beta counting at the Waikato Radiocarbon Dating Laboratory (Table 8). In contrast, the new dates determined for this study are derived from a range of organic material, including bulk peat samples, organic silts, woody twigs, sedge fragments and seeds; most of these dates were determined by accelerator mass spectrometry (AMS) at Rafter Radiocarbon Laboratory.

All dates were adjusted for the -44-year Southern Hemisphere reservoir offset (Hogg *et al.* 2009), calibrated to calendar years using the OxCal v 4.1 calibration program and IntCal09 calibration curve; mean calibrated ages and their associated ages are shown in Table 8. It is evident that some of the dates are in the wrong stratigraphic order:

- At first glance, either NZA37491 (12,470  $\pm$  80 cal yr BP; 819 cm) is too young, or the sample above it, NZA37215 (12,530  $\pm$  60 cal yr BP; 774 cm) is too old.
- NZA37492 (12,900  $\pm$  100 cal yr BP; 904 cm) appears to be too young, or samples higher in the column (NZA37216 at 843 cm, and Wk22243 at 877cm) are too old;
- either NZA37495 (14,950  $\pm$  180 cal yr BP; 1,011 cm) is too young, or NZA 37514 (16,100  $\pm$  310 cal yr BP; 983 cm) is too old;
- Wk25349 (22,570  $\pm$  270 cal yr BP; 1,170 cm) appears to be too young relative to the Kawakawa / Oruanui tephra that lies above.

Ages that appear to be too old may be due to fractionation effects: extant plant  $^{14}\text{C}$  content can sometimes be 5% below atmospheric levels due to preferential assimilation of  $^{12}\text{C}$  (Lageard 1997). Different organisms will contain different  $^{14}\text{C} : ^{12}\text{C}$  ratios because of differences in their metabolism and chemical structure, due to  $^{14}\text{C}$  and  $^{13}\text{C}$  having a greater mass than  $^{12}\text{C}$ . This phenomenon is known as fractionation.

The magnitude of fractionation that occurs in plants is due in part to the particular photosynthetic pathway utilised (Edwards & Walker 1983; Bradley 1999). The highest  $^{13}\text{C}$  depletion occurs in plants that utilise the Calvin photosynthetic cycle; these so-called  $\text{C}_3$  plants include large trees and peat forming taxa such as *Sphagnum*. The lowest  $^{13}\text{C}$  depletion occurs in taxa utilising the Hatch-Slack (HS) photosynthetic cycle ( $\text{C}_4$  plants) that include cereal grains and related grasses and sedges. Succulent plants fix carbon in their tissues by either the Calvin or Hatch-Slack cycle utilising crassulacean-acid metabolism. Uncorrected dates for sediments composed of HS plants would appear younger (to the order of 200 - 300 years) than Calvin cycle plants that are stratigraphically equivalent.

Since New Zealand peats are mostly composed of both  $\text{C}_3$  and  $\text{C}_4$  taxa such as *Sphagnum cristatum* (Lintott & Burrows 1973; McGlone & Wilmshurst 1999), *Empodisma minus*, *Gleichenia dicarpia*, the sedges *Cladium* spp and *Schoenus brevifolius* (Newnham 1992), all of which are either semi-aquatic or mire-dwelling taxa, and woody roots and fragments of *Leptospermum scoparium* and *Kunzea ericoides* (Newnham 1992), there may be fractionation effects occurring to differing degrees, depending on whether bulk peat or macrofossil samples were used. In addition, erosional activity may allow old leaf litter or charcoal (or old carbonaceous rock, but this is unlikely to be a problem at Eltham) to be deposited directly in the sedimentary column leading to

anomalously old dates (McGlone & Wilmshurst 1999); accordingly radiocarbon dates may be supplemented with tephra dates (Newnham *et al* 1998).

The apparent over-estimate of the age of NZA37215 may be due to fractionation effects, since the difference in age between this sample and the next sample (NZA37491) falls within the estimated potential discrepancy of 200-300 years provided by Edwards & Walker (1983) and Bradley (1999), although some doubt remains since both samples are twiggy materials that would presumably have similar photosynthetic pathways and therefore similar  $^{14}\text{C}:$  $^{12}\text{C}$  ratios. Alternatively the discrepancy could be due to younging (discussed below) of sample NZA37491; however this seems less likely given that the reported age places it in the right chronological and stratigraphical order relative to the samples below it, and also the Konini tephra above it. Note that at  $2\sigma$ , NZA37491 could be as old as 12,630 cal yrs, and NZA37215 could be as young as 12,410 cal yrs, placing the samples in the correct stratigraphic order, implying that 12 cm of peat accumulated in 220 years at this time.

Ages that appear to be too young can occur due to contamination following significant down-washing of organic material, translocation by earthworms or other soil fauna, or aeolian or fluvial reworking. Since the  $^{14}\text{C}$  content of fossil samples is very low, introduction of additional 'young' carbon into a sample (e.g by modern rootlets extending into a peat sample) may lead to an underestimation of the age of the sample. 'Younging' can arise when weakly organic sediments are infiltrated by humic-rich groundwater; for example McGlone & Basher (1995) found silty loams at Winterton Bog, Inland Kaikoura Range gave younger apparent ages than peats overlying them, possibly due to infiltration of waters saturated in young organic colloids.

Sample NZA 37514 ( $16,100 \pm 310$  cal yr BP; 983 cm), an organic silt sample, is unlikely to be over-estimated due to fractionation alone, since the potential discrepancy caused by fractionation is insufficient to explain the difference in ages (*c.* 1,100 years) between it and sample NZA37495 ( $14,950 \pm 180$  cal yr BP; 1,011 cm), a bulk peat sample. A more likely explanation is that the reported age for sample NZA37495 is too young, due to downward translocation of younger carbonaceous material (for example, by invertebrates or tree roots), or contamination during core extraction. The anomalously low date for NZA37492 ( $12,900 \pm 100$  cal yr BP; 904 cm) appears to be due to translocation to a lower depth (possibly during coring), since samples higher in the column (NZA37217 at 862 cm, and Wk22243 at 877cm) are in the order of 620 to 1,360 years older than NZA37492. As a consequence, neither NZA37495 nor NZA37492 are used to prepare the age model.

The date for NZA37253 ( $18,180 \pm 210$  cal yr BP; 1,084 cm) is at odds with NZA38107 and NZA38109 (actually two subsamples from the same sample) from the same depth that have calibrated dates of 20,180 yrs BP and 20,220 yrs BP respectively. All three samples are sedge fragments and would therefore be expected to yield very similar ages since the photosynthetic pathways and carbon assimilation processes would be the same for plant material in each sample, however the Rafter laboratory reported removing modern fibres from the NZA37253 sample during pre-treatment, suggesting they were carried down by the coring barrel from the surface. If any modern fibres remained in the sample, this would lead to anomalously young dates. In contrast, no modern contaminants were noted in either NZA38107 or NZA38109, and the close match in  $^{14}\text{C}$  dates demonstrates that the radiocarbon dating process is at least internally consistent. Consequently, NZA37253 is not used in the age model.

Positive identification of the Kawakawa tephra ( $25,360 \pm 360$  cal yrs BP (Vandergoes *et al.* 2012); section 7.4.3) at 1,159 cm demonstrates that the position of Wk25349 ( $22,570 \pm 270$  cal yr BP) at 1,170 cm is stratigraphically inconsistent, and is likely due to downward translocation of younger material. As a consequence, Wk25349 was not used in the age modelling.

#### **7.4.2. Coastal Taranaki Radiocarbon Dates**

Due to the small number of radiocarbon dates available for the coastal Taranaki sites, no age model was prepared; furthermore, three of the coastal Taranaki radiocarbon dates are also in the wrong stratigraphic order: (i) at Opunake Beach, sample NZA51184 at 98-100 cm has an age of  $33,760 \pm 440$  cal years BP; this age range

overlaps the radiocarbon age range of the sample above at 34-36 cm, NZA51105 ( $34,370 \pm 370$  cal yrs BP). It is highly unlikely that the true ages of sediments at these depths are the same, since they are separated by 60 cm of fairly compact lignite; it is more likely that some younger material was translocated downwards. Fine, modern rootlets were removed from both samples by GNS, followed by an acid-alkali-acid pre-treatment to remove cellulose; therefore both samples may have been contaminated by residual, younger material. Furthermore, NZA51105 yielded more than twice the mass of carbon (0.68 mg) than NZA51184 (0.3 mg), so it is reasonable to assume that the anomalous NZA51184 was more susceptible to sample error than NZA51105.

(ii) at Okawe Stream, sample NZA22187 ( $25,820 \pm 340$  cal yrs BP) underlies NZA22350 ( $28,010 \pm 320$  cal yrs BP); further, NZA22187 lies around 20cm below the Kawakawa / Oruanui Ash ( $25,360 \pm 160$  cal yrs BP (Vandergoes *et al.* 2013), followed by layers of organic and sandy tephric soil. This suggests the sample was contaminated by younger material such as roots or branches from fallen logs protruding deeper into the sequence.

(ii) A similar situation exists for Stent Road sample NZA51106 ( $19,140 \pm 140$  cal yrs BP), which has an apparent age as much as 2,780 years younger than NZA51083 ( $21,440 \pm 110$  cal yrs BP) at the  $2\sigma$  level despite being stratigraphically older. In addition to the possibility of contamination by younger rootlets, NZA51083 yielded nearly four times as much carbon (1.9 mg) than NZA51106 (0.48 mg), suggesting that the radiocarbon date for NZA51083 was more reliable than that for NZA51106. Table 9 shows the radiocarbon age ranges and overlaps for Eltham Swamp and coastal Taranaki sites.

### 7.4.3. Eltham Swamp Age Model

The acceptable calibrated ages described in section 7.4.1 were loaded into TILIA (Grimm 2011) and a cubic B-spline curve was generated (Figure 37a) to produce the chronology in both the Eltham pollen diagram and the Eltham quartz dust graphs.

The rationale for using a cubic  $\beta$ -spline over other types of smoothing splines available in TILIA (linear interpolation, polynomial functions and LOWESS smoothing) was that when the principle of parsimony is applied to age-depth curves, the best models are those that minimise the curvature (Walanus 2008), however because the number of degrees of freedom and the polynomial order selected strongly impacts upon the age-depth curve (Telford *et al.* 2004), some curves gave ages that did not increase monotonically with depth, and were therefore unacceptable. In contrast, cubic smoothing splines can overcome the problem of extreme outliers that beset traditional splines, because the latter treat observations as deterministic or without error (Weber *et al.* 2012).

Telford *et al.* (2004) applied various age-depth models against simulated radiocarbon dates based on varved sediment sequences to determine which the best models were, when they were populated with both small (six) and large (48) numbers of dates. The researchers assessed model accuracy by determining the root mean square error of prediction (RMSEP) between radiocarbon dates and the varve timescale; they found an inverse relationship between the numbers of dates and the RMSEP. Cubic smooth spline curves with a large number of dates had the lowest RMSEP, whereas polynomial curves had the highest RMSEP; in contrast, none of the models populated with only a few dates provided a satisfactory fit to actual ages.

Since smoothing splines populated with dates whose number is high relative to their uncertainty ignore noise and yield a better fit than linear and spline interpolation (approximately 24 dates in Telford *et al.*'s. 2004 study), and given its ability to resist imputing reversals in the age-depth relationship, a cubic-B spline model was selected to determine the age-depth relationship for Eltham. In addition, the work by Telford *et al.* (2004) implied that it was not worth deriving age models for the coastal Taranaki sites, given the small number of  $^{14}\text{C}$  dates available for each site.

The set of radiocarbon dates for the organic sediments collected in the present study were complemented with well-dated tephrochronology dates (Konini A and B tephra and Kawakawa / Oruanui ash; the tephra were identified using grain size characteristics, mineralogy descriptions and isopach data given in the literature (Alloway *et al.* 1995; Donoghue *et al.* 1995; Zernack 2008; Zernack *et al.* 2011).

The Kawakawa / Oruanui tephra in Core A was difficult to discern since it was dispersed amongst tephric loess, so a second Eltham core was extracted in 2011. Since the Kawakawa Tephra also proved elusive in the second core, Zernack *et al.* (2012) (i) established the stratigraphic relationship between the Poto series of tephra deposits and the Kawakawa tephra at a roadside cutting from Cardiff (approximately 12 km NW of Eltham); (ii) used the Cardiff stratigraphy and mineralogy to locate the Kawakawa tephra in section 5 of Core B (Core B (5)), which was used in turn to (iii) locate the very thin, dispersed, Kawakawa tephra in the section 6 of Core A (Core A (6)). The identity of Kawakawa tephra was subsequently confirmed by Electron Microprobe analysis by Professor Shane Cronin in April 2013.

From *c.* 40,000 to 30,000 cal yr BP the sedimentation rate at Eltham Swamp was *c.* 0.029 cm yr<sup>-1</sup> (Figure 37a). The sedimentation rate slowed dramatically between 30,000 and 20,750 cal yrs BP, with the sediment accumulation falling to one-fifth of the previous rate, at 0.0055 cm yr<sup>-1</sup>. After *c.* 20,750 cal yrs BP a hiatus in sedimentation lasting 1,200 years occurs, when the sediment influx rate falls to near zero and the age-depth curve is near vertical, indicating the very cold conditions that persisted near the end of the LGM. After the hiatus, the peat sedimentation rate increases again, to 0.039 cm yr<sup>-1</sup>; the age depth curve is trending upwards, indicating that peat accumulation rate was increasing in the youngest part of the core.

A weakness of TILIA age models is that they are given without any indication of chronological uncertainties, such as a 95% confidence interval of the calibrated <sup>14</sup>C curve, and resolution and accuracy of age-depth curves may be compromised by individually calibrated <sup>14</sup>C dates (Telford *et al.* 2004; Blaauw 2010; Macken *et al.* 2013). When all 22 <sup>14</sup>C dates available for Eltham Swamp were plotted against depth, it is apparent that sedimentation rate is not uniform, so the age-depth relationship cannot necessarily be modelled by a simple mathematical function such as a cubic  $\beta$ -spline. Furthermore, Blaauw (2010) notes that since <sup>14</sup>C dates have highly asymmetric calibration distributions, reducing them to single points for plotting splines is problematic.

Bayesian models offer a more flexible approach, incorporating uncertainty in calibrated ages and allowing for different sedimentation rates, including the hiatus seen at Eltham. Bayesian models integrate *priors*, or information already known about the core such as stratigraphic information including depth and order of samples, and metadata derived from the information itself called *likelihoods* such as <sup>14</sup>C data that form probability distribution functions (PDFs) to produce probabilistic modelled outputs called *posteriors*, as well as quantifying the uncertainty in the age-depth model.

A distribution of probable age-depth relationships is produced by repeated sampling and iteration procedures using Markov Chain Monte Carlo (MCMC) sampling; the highest probability density (HPD) range is calculated for the MCMC iterations; this represents the shortest temporal interval that encompasses 95% of the samples (Parnell *et al.* 2011); the HPD can then be plotted in an age-depth curve (Bronk Ramsey 2008). Bayesian statistics are particularly powerful when used to simultaneously calibrate multiple <sup>14</sup>C determinations, so that joint probabilistic modelled outputs (posteriors) are consistent with all available priors (Parnell *et al.* 2011). For example, when multiple <sup>14</sup>C dates that relate to the same event occur, OxCal analyses the dates simultaneously to determine if the dates are consistent with each other and whether any of the dates are outliers.

The Bayesian models presented in the current study were produced by the software package OxCal ver. 4.2.3 (Bronk Ramsey 2008, 2009, 2013). The IntCal09 (Reimer *et al.* 2009) calibration curve was used to calibrate <sup>14</sup>C dates, after subtracting 44 ± 17 yrs for the Southern Hemisphere offset correction (Lowe *et al.* 2013). *Boundaries* were applied to the top and bottom of the <sup>14</sup>C date sequence, set at 675 and 1,220 cm to

**Table 8. Taranaki Radiocarbon Dates**

Reference	Material	$\delta^{13}\text{C}$	Uncal. $^{14}\text{C}$ date	+/-	Uncal. $^{14}\text{C}$ date, 44 yr SH offset	Method	actual depth (cm)	depth after tephra removed (cm)	Calib. $^{14}\text{C}$ date $\mu$	$\sigma$	2 $\sigma$ low	2 $\sigma$ high	Source <sup>26</sup>
<b>Eltham Swamp</b>													
<b>Wk-24442</b>	Bulk peat	-27.1	9,598	30	9,554	$\beta$	712	686.7	10,910	110	10,720	11,090	MT
	Konini B Tephra						761	732.9	11,775	215			
	Konini A Tephra						773	738.3	12,230	295			
<b>NZA37215</b>	Horizontally bedded twigs	-24.8	10,625	40	10,581	AMS	774	739.7	12,530	60	12,420	12,640	RT
<b>NZA37491</b>	Woody twigs and seeds	-28.1	10,547	40	10,503	AMS	819	754	12,470	80	12,220	12,610	RT
<b>NZA37241</b>	Woody twigs	-21.9	10,797	50	10,753	AMS	838	773	12,660	60	12,560	12,770	RT
<b>NZA37216</b>	Twigs; sedge fragments	-25.1	11,193	45	11,149	AMS	843	778	13,020	90	12,830	13,200	RT
<b>NZA37217</b>	Organic Silt / woody macros	-25.1	11,710	45	11,666	AMS	862	795.9	13,520	80	13,360	13,690	RT
<b>Wk-24443</b>	Bulk peat	-26.7	12,333	48	12,289	$\beta$	877	808.5	14,260	220	13,950	14,860	MT
<b>NZA37492</b>	Woody twigs ( <i>not used in model</i> )	-26.3	11,069	40	11,025	AMS	904	835.6	12,900	100	12,710	13,090	RT
<b>NZA38108</b>	Woody twigs	-25.6	12,653	50	12,609	AMS	919	847.5	14,870	200	14,270	15,210	RT
<b>NZA37514</b>	Organic Silt	-30.2	13,254	40	13,210	AMS	983	910.5	16,100	310	15,470	16,650	RT
<b>NZA37495</b>	Bulk peat ( <i>not used in model</i> )	-27.4	12,693	45	12,649	AMS	1,011	917.3	14,950	180	14,590	15,230	RT
<b>NZA37253</b>	Sedge fragments ( <i>not used in model</i> )	-29.3	14,908	65	14,864	AMS	1,084	987.2	18,180	210	17,810	18,520	RT
<b>NZA38107</b>	Sedge fragments	-29.7	17,037	70	16,993	AMS	1,084	987.2	20,180	140	19,880	20,400	RT
<b>NZA38109</b>	Sedge fragments	-29.7	17,078	75	17,034	AMS	1,084	987.2	20,220	140	19,910	20,450	MT
	Kawakawa / Oruanui Tephra						1,159	1,011.2	25,360	360			MV
<b>Wk-25349</b>	Bulk peat ( <i>not used in model</i> )		18,919	140	18,875	$\beta$	1,170	1,012.2	22,570	270	22,170	23,260	MT
<b>Wk-24444</b>	Bulk peat	-19.3	24,481	176	24,437	$\beta$	1,177	1,019.7	29,210	270	28,570	29,600	MT
<b>Wk-24445</b>	Bulk peat	-21.0	24,765	181	24,721	$\beta$	1,239	1,037.2	29,630	270	29,210	30,210	MT
<b>NZA37519</b>	Organic Silt	-22.6	29,050	240	29,006	AMS	1,444	1,124.7	33,710	420	33,000	34,520	RT
<b>Wk-24446</b>	Bulk peat	-19.8	31,842	450	31,798	$\beta$	1,587	1,212.7	36,220	600	35,090	37,350	MT

<sup>26</sup> Source: RT = current study; MT = Turner (2008); AZ = Zernack (2008) and Zernack *et al* (2009, 2011), MV = Vandergoes *et al.* (2012).

A High Resolution Record of Late Quaternary Climatic and Environmental Change in Taranaki, New Zealand

Reference	Material	$\delta^{13}\text{C}$	Uncal. $^{14}\text{C}$ date	+/-	Uncal. $^{14}\text{C}$ date, 44 yr SH offset	Method	actual depth (cm)	depth after tephra removed (cm)	Calib. $^{14}\text{C}$ date $\mu$	$\sigma$	2 $\sigma$ low	2 $\sigma$ high	Source
<b>Kaupokonui Beach</b>													
NZA51081	Plant material	-27.0	29,192	135	29,148	$\beta$	0-2	-	33,860	330	33,300	34,500	RT
NZA51104	Plant material	-29.2	44,330	1,757	44,286	$\beta$	48-50	-	47,600	1,300	45,450	$\approx \infty$ <sup>27</sup>	RT
<b>Opunake Beach</b>													
NZA51183	Plant material	-23.1	21,393	119	21,349	AMS	0	-	25,510	240	25,070	25,950	RT
Wk-19143	Twigs	-24.1	28,824	237	28,780	$\beta$	20-24	-	33,350	460	32,570	34,470	AZ
NZA51105	Plant material	-26.6	29,788	296	29,744	$\beta$	36-38	-	34,370	370	33,570	34,980	RT
NZA51184	Organic silt	-28.8	29,106	285	29,062	AMS	98-100	-	33,760	440	32,990	34,560	RT
<b>Okaweu Stream</b>													
NZA22349	Peat	-23.3	20,776	170	20,732	AMS	6	-	24,730	220	24,280	25,160	AZ
NZA51226	Fine twigs / roots	-23.4	16,470	71	16,426	AMS	7	-	19,620	130	19,370	20,060	RT
NZA51103	Organic silt	-29.1	21,247	117	21,203	$\beta$	24	-	25,340	220	24,950	25,800	RT
NZA22350	Peat	-24.2	23,230	232	23,186	AMS	56	-	28,010	320	27,020	28,590	AZ
NZA22187	Organic soil	-30.2	21,629	194	21,585	AMS	84	-	25,820	340	25,100	26,620	AZ
Wk16401	Organic soil	-29.2	25,198	167	25,154	$\beta$	108	-	29,960	220	29,540	30,350	AZ
NZA22895	Tree log	-23.4	29,074	399	29,030	AMS	-	-	33,670	550	32,590	34,660	AZ
<b>Stent Road</b>													
NZA51085	Organic silt	-29.1	15,322	40	15,278	$\beta$	0-2	-	18,540	120	18,180	18,700	RT
NZA51083	Organic silt	-28.6	18,035	50	17,991	$\beta$	18-20	-	21,440	110	21,210	21,660	RT
NZA51106	Plant material	-30.2	16,001	67	15,957	$\beta$	32-34	-	19,140	140	18,880	19,400	RT
NZA22349	Peat		20,776	170	20,732	AMS	>32-34	-	24,730	220	24,280	25,160	AZ

<sup>27</sup> The level of  $^{14}\text{C}$  in this sample is close to background levels, so the radiocarbon date should be used with caution.

A High Resolution Record of Late Quaternary Climatic and Environmental Change in Taranaki, New Zealand

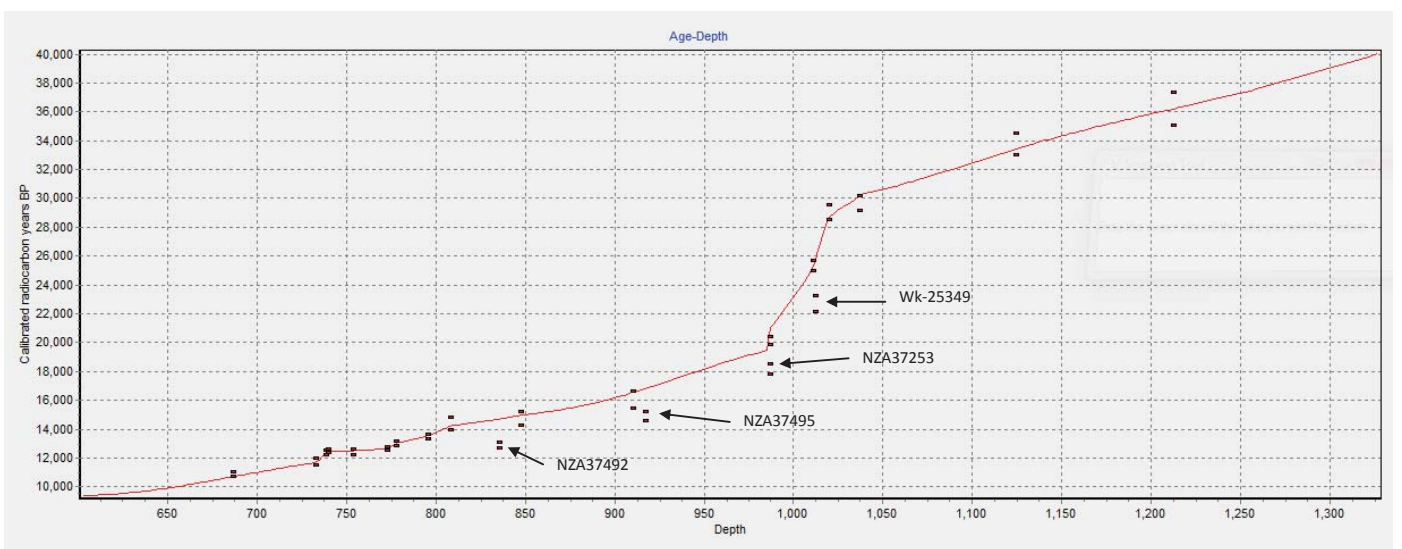
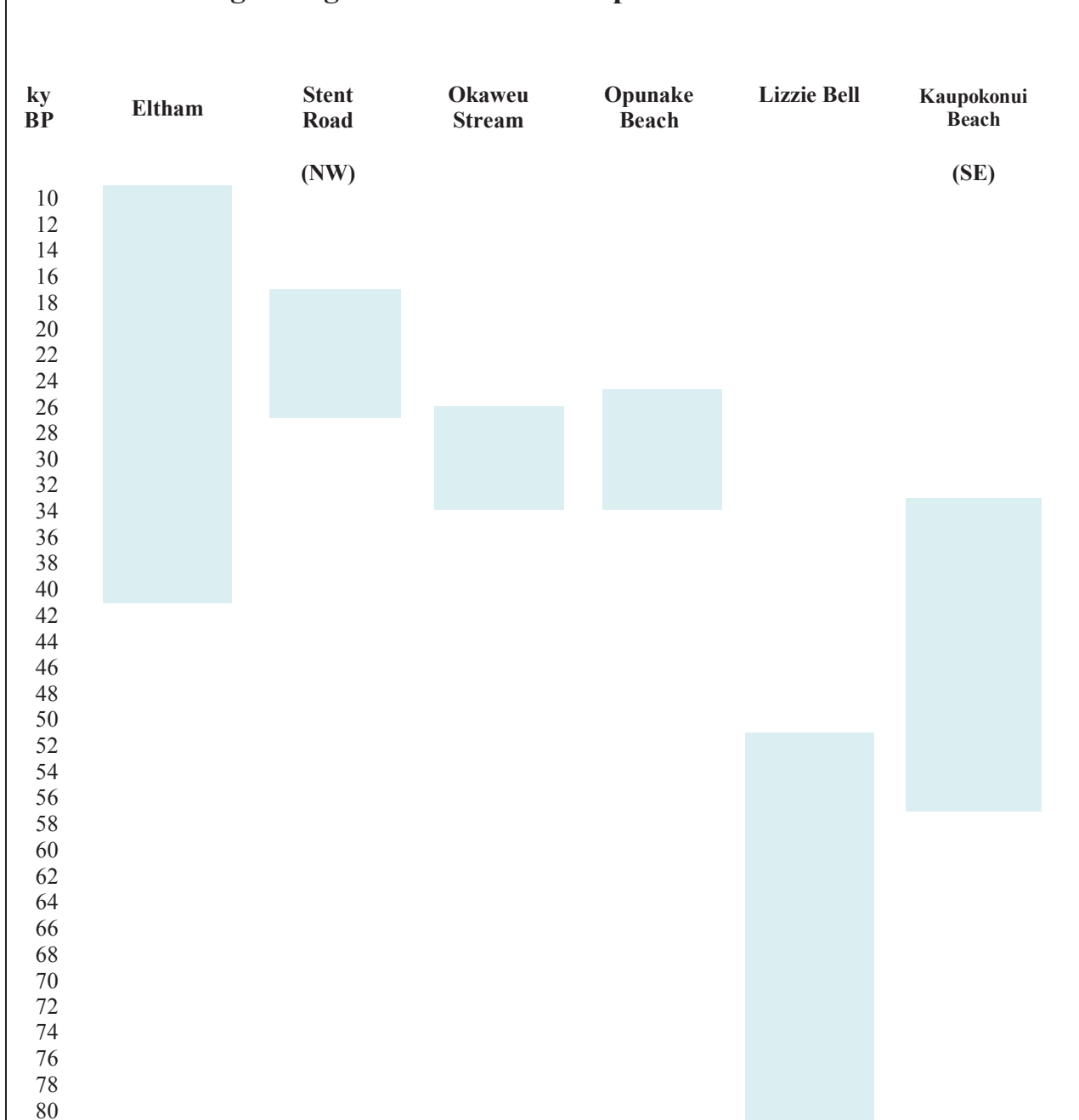


Figure 37 (a). Age-Depth Curve for Eltham Swamp (Cubic B-spline). Radiocarbon dates not used in cubic  $\beta$  spline curve generation are labelled.

**Table 9. Age Ranges for Eltham Swamp and Coastal Taranaki Sites**



conservatively encompass the youngest and oldest  $^{14}\text{C}$  ages. All dates were loaded as *R\_Dates*, apart from the three tephra dates which were loaded as *C\_Dates* which are previously calibrated, normally distributed dates.

Although some radiocarbon dates can be intuitively identified in age-depth modelling as obvious outliers and manually removed, Bayesian methods can be utilised to objectively assess suitability of dates for age-depth modelling (Bronk Ramsey 2009). OxCal can assign a prior probability for a sample being an outlier, and down-weight the sample in age-depth modelling if necessary (Bronk Ramsey 2008).

OxCal provides several outlier models that differ on the basis of what type of error is assumed to have occurred: (i) the radiocarbon measurement of a given sample might be in error (*s*-type error); (ii) the radiocarbon ratio of a given sample may differ from the carbon reservoir (*r*-type); (iii) the set of radiocarbon measurements might be systematically biased, due to all measurements being biased, or the reservoir effect in (ii) applying to the whole set of measurements (*d*-type); or (iv) the given sample may not relate to the time period being dated (*t*-type).

Bronk Ramsey (2009) suggested that only one model be used, and that outlier modelling be kept as simple as possible. In situations where there may be some possible contamination due to translocation or bioturbation ( $t$ ), or addition of radiocarbon from other reservoirs ( $r$  or  $d$ ) where the appropriate offsets needed to inform the outlier model are not known, he recommended using the general model that gives a conservative output because it draws from a long-tailed distribution so will not be too affected by an occasional, extreme outlier, yielding wide confidence intervals.

The outlier analysis function *Outlier\_Model 'General'* (Bronk Ramsey 2009) was run with an equal outlier probability of 5% applied to all samples, since all samples yielded  $> 100 \mu\text{g}$  extracted carbon, and therefore an increased prior outlier probability of say, 10%, was not required for samples  $< 100 \mu\text{g}$  extracted carbon. The rationale for different priors in this scenario is that samples with very low levels of extracted carbon are more likely to be anomalous due to low mass of carbon available for  $\beta$ -counting or AMS analysis (Macken *et al.* 2013). The *Outlier\_Model 'General'* accounts for  $t$ -type errors, allowing the modelled dates to have a student  $t$ -distribution with 5 degrees of freedom, with a scale of between  $10^0$  and  $10^4$  years (Bronk Ramsey 2009).

It was found that samples NZA 37492, NZA 37495, NZA 37253 and Wk-25379 were such extreme outliers that including them prevented OxCal from running, therefore these four samples were excluded to allow OxCal to execute; the same four samples also had to be excluded from TILIA to allow cubic  $\beta$ -spline curve-generation (Figure 37a). Removing these four samples from the dataset<sup>28</sup> and re-running OxCal showed that NZA 38107 was also an outlier, with a posterior outlier probability of 100%. In addition, OxCal calculates an overall agreement index ( $A_{\text{model}}$ ); if this index  $> 60\%$  it indicates that there is probably no issue with the model as a whole, and no samples need to be rejected (Bronk Ramsey 2009). The calculated  $A_{\text{model}}$  rose to  $> 95\%$  when all five outliers were excluded from the model.

Bronk Ramsey (2008) recommended consideration of depositional processes to help determine the most appropriate choice of priors for Bayesian age models, including (i) mechanisms underlying sedimentation: this would include a range of factors such as climatic conditions (temperature and precipitation characteristics, and wind characteristics at both source and sink), vegetation cover, hydrological characteristics of the wider catchment area and hydrosere stages at Eltham Swamp, and local sediment characteristics such as secondary tephra deposits, and aerosolic dust and their transport (Macken *et al.* 2013); (ii) random events, such as lahars and debris-avalanche deposits and ash showers; and (iii) abrupt changes in deposition mode. At Eltham, climatic events such as LGM cooling and aridity, as well as random events such as ash showers affected the sediment deposition rate, although the impacts of tephra showers has been minimised by excluding the thicker ash layers from the pollen calculations.

The only assumption (prior) applied to the OxCal *Sequence* model is that the Law of Superposition holds; that is, deposition is monotonic, so that differences in dates between the dated depths may only have positive values (Parnell *et al.* 2011), but the deposition rate is extremely random. Macken *et al.* (2013) suggested that *Sequence* depositional models in OxCal are particularly useful when analysing data from complex deposits as they are based on fewer assumptions regarding sedimentation rates and processes than other models, and when there are relatively few  $^{14}\text{C}$  dates available relative to the time-span under consideration. However, *Sequence* is the most conservative of the OxCal models, giving wide confidence intervals (Bronk Ramsey 2008).

In contrast to the *Sequence* model, other OxCal deposition models make additional prior assumptions about deposition rates: the *U\_Sequence* model assumes that deposition rate is unknown, but is completely constant, and the *V\_Sequence* model assumes that the accumulation rate is known approximately, with normally distributed uncertainty. Bronk Ramsey (2008) notes that since no model will capture all of the details of real world processes, it is desirable to use simple models to clarify what assumptions were made. However, he suggests that *P\_Sequence* models are the best choice because no deposition is truly uniform (therefore not

<sup>28</sup> Numerous other researchers report manually excluding some samples in order for OxCal to run, including Parnell *et al.* (2011); Thorndycraft *et al.* (2011); and Lowe *et al.* (2013).

favouring selection of *U\_Sequence* or *V\_Sequence* models) nor is deposition completely uninformative, so that a *Sequence* model sacrifices precision for accuracy, and is not recommended either. Eltham has relatively many  $^{14}\text{C}$  dates, therefore more precise alternatives to a *Sequence* model can be constructed; however, a *Sequence* model is provided for completeness (Figure 37b), as well as a *U\_Sequence* model (Figure 37c).

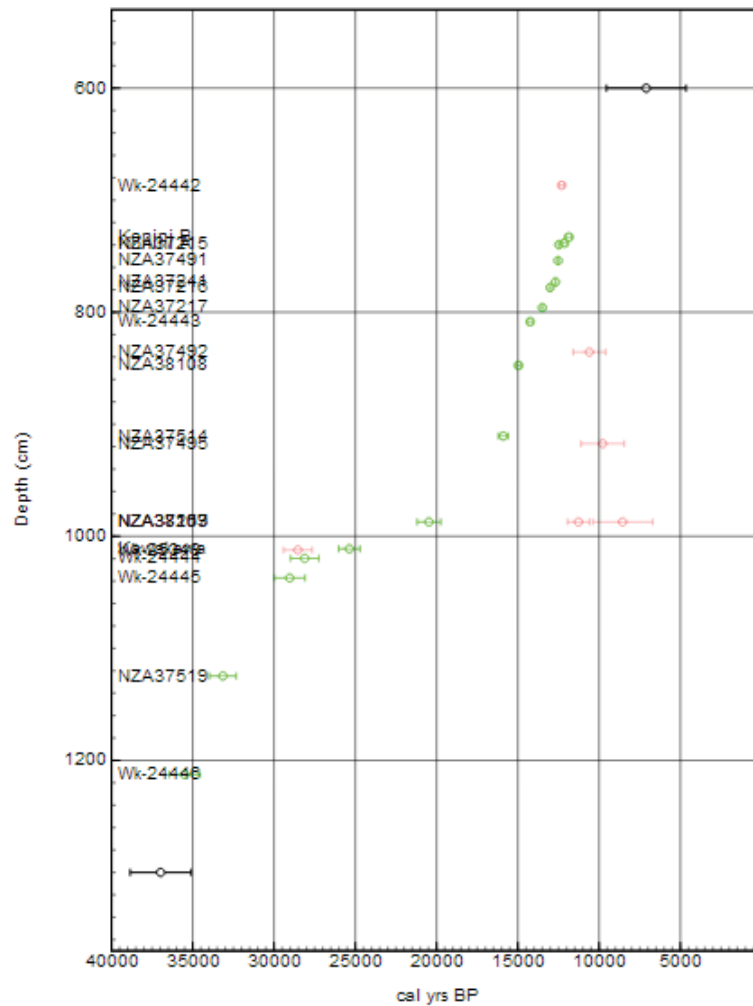


**Figure 37(b).** Posterior Age-Depth Model for Eltham Swamp using the *Sequence* function in OxCal v4.2.3. The green data points show the mean and  $1\sigma$  calibrated ages for each sample; the red data points are outliers as indicated by the *Outlier\_General* mode (NZA 37492, NZA 37495, NZA 37253, Wk-25379 and NZA 38107).

The *P\_Sequence* model allows for fluctuations in sedimentation rate; this is assumed to be governed by the Poisson process with a given step size, represented by the model parameter  $k$ , which determines the number of accumulation events per unit of depth, and is monotonic. Step sizes are governed by sediment grain size, expressed in the same units as depth, for example  $k = 0.1$ , as used for modelling the Eltham curve, equates to a sediment size of 1 mm, so is appropriate for modelling a very fine-grained sediment (peat) that can vary strongly and abruptly at any time (Goslar *et al.* 2009), and  $k = 1$  equates to a sediment size of 1 cm, which is more appropriate for much coarser sediments (Bronk Ramsey 2008), and has a more uniform accumulation rate.

By setting  $k$  at a very low value, the sedimentation rate can vary strongly at any time; in contrast, a high value for  $k$  implies a uniform rate of deposition (and is therefore similar to the OxCal *U\_Sequence*). High  $k$  values yield relatively straight age-depth curves with sharp changes reflecting abrupt changes in sedimentation rate and little ‘bowing’ of uncertainty between dated depths (Parnell *et al.* 2011), and narrow confidence intervals. In contrast, very low  $k$  values that assume slow changes in peat deposition rates yield very wiggly age-depth curves with wide confidence intervals, with a high degree of ‘bowing’ of uncertainty between dated depths; this may be more desirable in modelling cores that have very variable sediment accumulation rates (Goslar *et al.* 2009; Parnell *et al.* 2011).

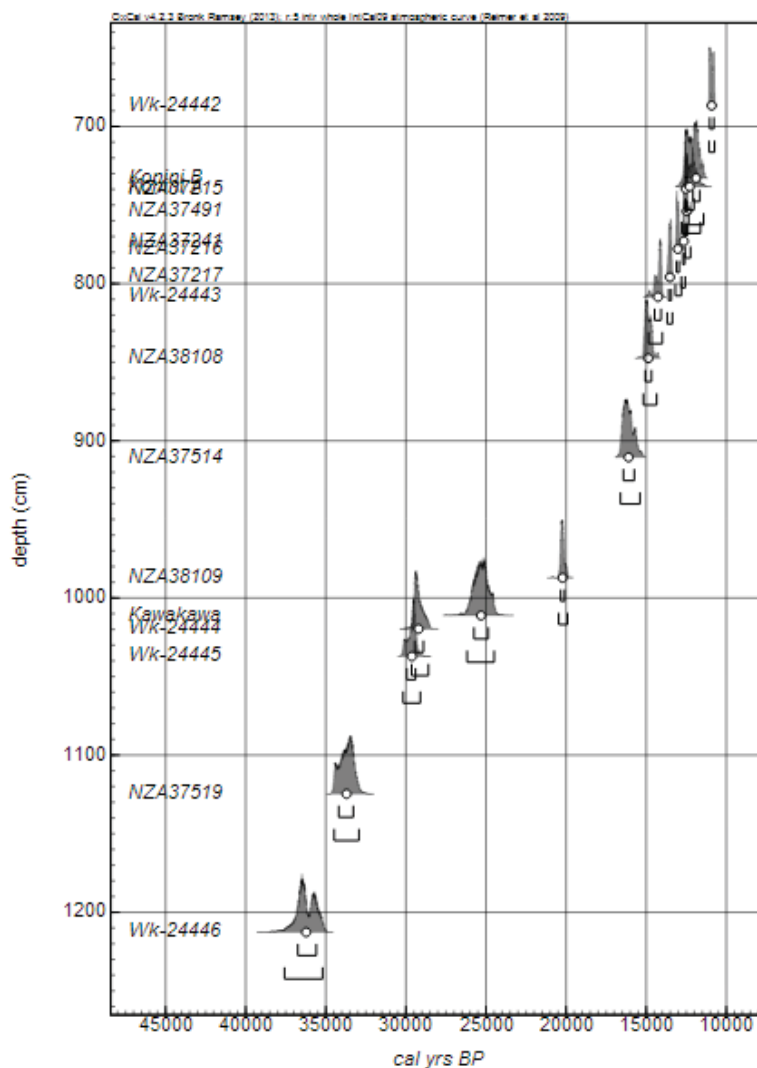


**Figure 37(c). Posterior Age-Depth Model for Eltham Swamp using the *U\_Sequence* function in OxCal.** The dark grey curves are the marginal posterior distributions that take into account the depth model. The brackets encompass the  $2\sigma$  (wide) and  $1\sigma$  (narrow) calibrated ages, with the open circles showing the mean calibrated age.

As a consequence of the foregoing discussion, a *P\_Sequence* model was selected for modelling the Eltham Swamp age-depth relationship, using the *Outlier\_General* subroutine, parameter  $k = 0.1$ , and running 500,000 MCMC iterations (Figure 37d). The light grey curves are distributions for the single calibrated dates (likelihoods); the dark grey curves are the marginal posterior distributions that take into account the depth model. The depth model curves are envelopes for the 95.4% (wider, pale blue band) and 68.2% (narrow, dark blue band) HPD ranges.

The *P\_Sequence* age-depth curve shows a reasonably constant sedimentation rate before 29,500 cal yrs BP ( $0.029 \text{ cm yr}^{-1}$ ) which very closely matches the sedimentation rate shown in the cubic  $\beta$ -spline curve produced by TILIA for the period *c.* 40,000 to 30,000 cal yrs BP. This is followed by a hiatus of very low, LGM sediment accumulation ( $0.0036 \text{ cm yr}^{-1}$ ), lasting until *c.* 20,500 cal yrs BP. This rate is of the same magnitude as that shown in the cubic  $\beta$ -spline curve for the period *c.* 30,000 to 20,750 cal yrs BP, although slower than the cubic  $\beta$ -spline rate of  $0.0055 \text{ cm yr}^{-1}$  (a difference of *c.* 19 cm kyr<sup>-1</sup>). The *c.* 1,200 year period of near-zero influx seen in the cubic  $\beta$ -spline between 20,750 and 19,500 is not evident; this is because OxCal has treated sample NZA 38170 as an outlier and ignored it during curve generation, whereas TILIA has tried to accommodate this date. This has the effect of reducing and smoothing the average influx rate over the entire hiatus period in the *P\_Sequence* compared with the cubic  $\beta$ -spline curve. The accumulation rate accelerated again, post-LGM to  $0.032 \text{ cm yr}^{-1}$ ; this compares favourably with the cubic  $\beta$ -spline curve produced by TILIA

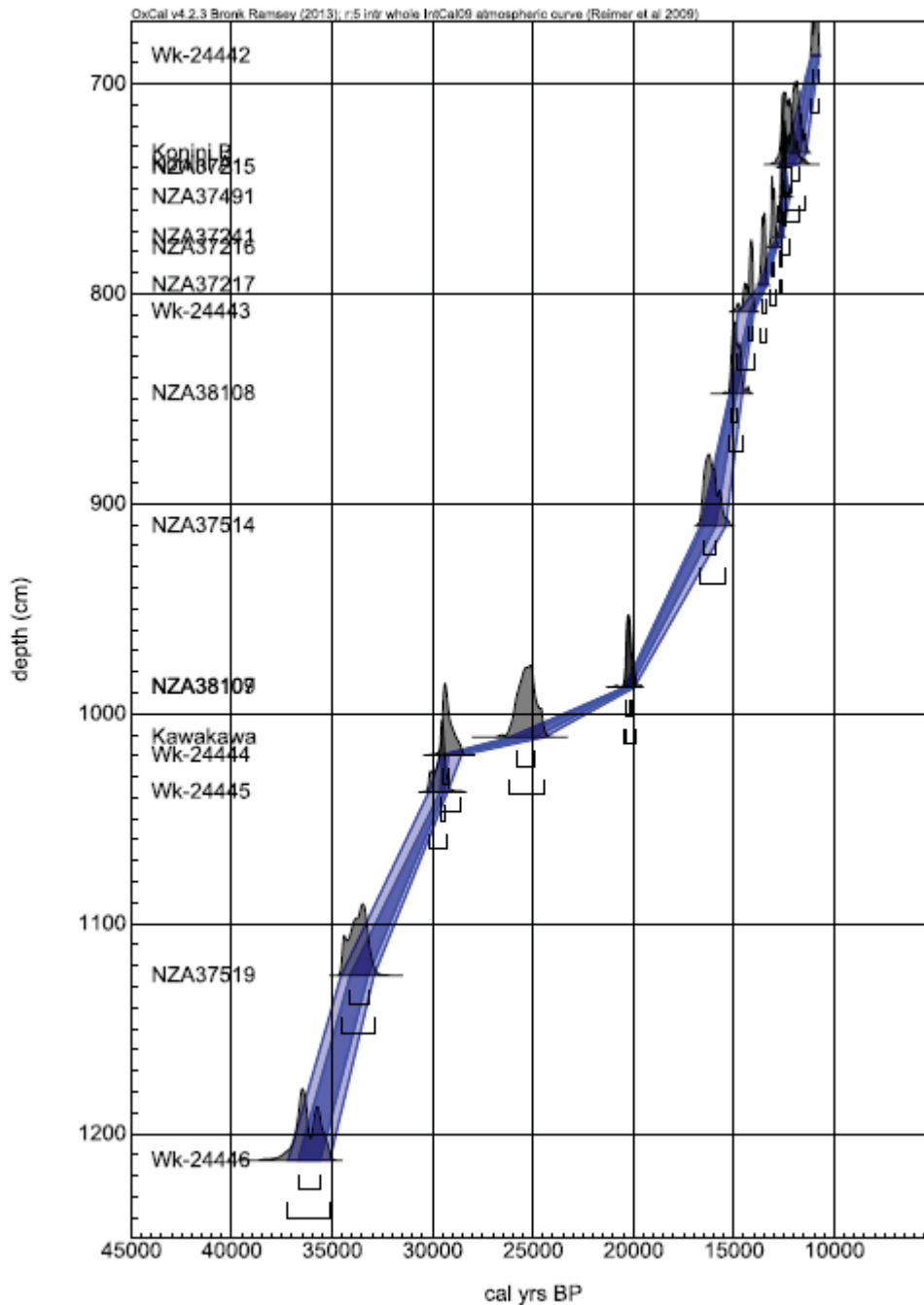


**Figure 37(d). Posterior Age-Depth Model for Eltham Swamp using the *P\_Sequence* function in OxCal.** The light grey curves are distributions for the single calibrated dates (likelihoods); the dark grey curves are the marginal posterior distributions that take into account the depth model. The depth model curves are envelopes for the 95.4% (wider, pale blue band) and 68.2% (narrow, dark blue band) HPD ranges.

( $0.039 \text{ cm yr}^{-1}$ ) for the period *c.* 20,750 to 10,000 cal yrs BP. Overall, the OxCal-generated *P\_Sequence* model largely supports the general trends, magnitude and timing of the age-depth relationship provided by the TILIA-generated cubic  $\beta$ -spline curve, and shows that the samples manually excluded from the model as outliers in TILIA were also rejected by OxCal (because it was unable to run). Bronk Ramsey (2008) recommended intuitively identifying outliers and physically eliminating them from models, “If this is possible, then it is probably the best approach since it is then entirely clear what data are being used to support the analysis,” (p. 3). Nevertheless, running the *Outlier\_General* model was useful since it identified a further sample (NZA 38170) that required removal from the model. Although NZA 38170 might have also been rejected from the cubic  $\beta$ -spline, leading to a smoother hiatus with a more uniform influx rate, the general patterns of very low sediment influx for this period would remain the same for the *P\_Sequence*, original cubic  $\beta$ -spline and any modified cubic  $\beta$ -spline model that excluded NZA 38170.

## 7.5. Aerosolic Quartz Methodology

Aerosolic quartz is not typically extracted from peat deposits, therefore additional details on the rationale behind the aerosolic quartz methodology used in the current study are described in Appendix 11.4. The method used to isolate quartz from peat samples was as follows:

- (i) a sample of approximately 17.75 cc (that is, one half of a 1cm slice across half a cylinder of 4.75 cm radius) was extracted from Core A, and the depth recorded;
- (ii) the sample was dried overnight in an oven at 50°C and the dry weight recorded;
- (iii) the sample was placed in a beaker of deionised water and allowed to sit overnight to rehydrate;
- (iv) the sample was placed in a beaker with a drop of household shampoo (active ingredient: sodium laureth sulphate), followed by agitation in an ultrasonic bath for one hour to break up / deflocculate the sample;
- (v) the sample was oxidised in 35% H<sub>2</sub>O<sub>2</sub> for as long as necessary (typically for 72 hours) to remove organic matter;
- (vi) the sample was rinsed in deionised water, centrifuged at 5,000 rpm for 5 minutes and decanted;
- (vii) the sample was dried overnight in an oven at 50°C and the weight recorded
- (viii) the sample was dry sieved through 2 mm sieves;
- (ix) the < 2 mm fraction was treated with 50:50 mixture of 0.2 M ammonium oxalate and 0.2 M oxalic acid to dissolve short-range order clays, in particular allophane, ferrihydrite materials and imogolite, and remaining organic material (Alloway *et al.* 1992b), then rinsed in deionised water, centrifuged and decanted in 50ml polypropylene falcon tubes;
- (x) the < 2 mm fraction was given citrate-bicarbonate-dithionate (CBD) treatment, where iron oxides were present (Aguilera & Jackson 1953):
  - i. sample was split to give 5-6 g sediment per falcon tube;
  - ii. 40 ml C<sub>6</sub>H<sub>5</sub>Na<sub>3</sub>O<sub>4</sub>·H<sub>2</sub>O (sodium citrate) (0.3M) and 5 ml NaHCO<sub>3</sub> (1M) were added to each tube;
  - iii. tubes were placed in a water bath, stirred and heated to 75°C (80° C absolute maximum) and 1g Na<sub>2</sub>S<sub>2</sub>O<sub>4</sub> (sodium dithionite) added.
  - iv. tubes were stirred and a further 1g sodium dithionite added after 5 minutes;
  - v. steps (ii) to (iv) were repeated, stirring intermittently;
  - vi. 10 ml saturated NaCl plus up to 10ml acetone were added to each tube where required for flocculation.
  - vii. each tube washed with 2M NaCl, then centrifuged and decanted;
  - viii. samples washed in distilled water.

In addition to removing amorphous iron, CBD treatment also removes manganese oxides when present (Schramm & Leinen 1987).

- (xi) samples were dry sieved to derive < 63  $\mu\text{m}$  and 63-2000  $\mu\text{m}$  fractions and the weights recorded;
- (xii) the < 63 $\mu\text{m}$  fraction was treated with 6N HCl for six hours to dissolve any calcite, dolomite (Syers *et al.* 1969) carbonates, hydrous iron oxides (Jackson *et al.* 1971) present, and then washed with distilled water and decanted three times;
- (xiii) the sample was dried overnight in an oven at 50°C;
- (xiv) the neutralised, < 63 $\mu\text{m}$  fraction was treated with 1M hydrofluorosilicic acid (hexafluorosilicic acid,  $\text{H}_2\text{SiF}_6$ ) for three days to dissolve mica, feldspars (Rex *et al.* 1969; Chapman *et al.* 1969) amorphous silica (Sridhar *et al.* 1975), and plagioclases.
  - i. the solution was stirred at least once every 24 hours to break up the sludge layer and to ensure that mineral grains were adequately exposed to the  $\text{H}_2\text{SiF}_6$ ;
  - ii. after 72 hours the solution was rinsed three times in deionised water, centrifuged and decanted (that is, reactants were not neutralised with HCl as would occur when using HF to dissolve silicates in pollen extraction);
  - iii. the solution was neutralised with 1 M  $\text{H}_3\text{BO}_3$  (boric acid) then rinsed three times in deionised water, centrifuged and decanted;

No additional tests were performed to determine if quartz was being dissolved; the assumption is that quartz recovery rates were very high (> 97%) as achieved by Chapman (1969) at temperatures  $\leq 18^\circ\text{C}$ , described in appendix 11.4.

- (xv) the < 63 $\mu\text{m}$  quartz sample was dried by rinsing through a Microscience MS 5AF filter paper or Whatman #41 filter paper with acetone to remove water, dried under an infrared lamp, and the weight recorded;
- (xvi) the < 63 $\mu\text{m}$  subsamples were examined by powder X-ray diffraction (XRD) to determine mineral content (Alloway *et al.* 1992), that is, to determine the purity of the quartz (described in Appendix 11.4). Where feldspars remained, steps (xiv) and (xv) were repeated (repeated XRD testing demonstrated that a minimum of six days of exposure to  $\text{H}_2\text{SiF}_6$  was required);
- (xvii) the < 63 $\mu\text{m}$  subsamples were analysed by Horiba Partica LA-950 particle size analyser to quantify grain-size distribution, and the results tabulated in GRADISTAT (Blott & Pye 2001).

## 7.6. Pollen Transfer Functions

Two of the pollen transfer functions developed by Wilmshurst *et al.* (2007) (section 5.5.4) are used in the current study to derive mean annual temperatures for Eltham: (a) partial least squares regression (PLS), and (b) the weighted modern analogue technique (W-MAT) where the ten closest modern analogues of the fossil pollen assemblage are identified, and the mean of the modern annual temperature for the ten analogues is weighted by relative abundance.

The Eltham taxa used in the transfer function models are shown, along with the correlation coefficients between mean annual temperature and pollen frequencies (Wilmshurst *et al.* 2007) (Table 10). The correlation coefficients are also shown at the foot of individual taxon graphs within the pollen diagrams to highlight the temperature preferences within each broad vegetation type. In addition, bud freezing temperatures for selected taxa are shown (from Table 2).

Table 10. Correlation between Mean Annual Temperature and Pollen Types for Taranaki Sites, and Selected Bud Freezing Temperatures					
Pollen Taxa	MAT correlation	Freezing Temp (°C)	Pollen Taxa	MAT correlation	Freezing Temp (°C)
<i>Phyllocladus trichomanoides</i>	<b>0.64</b>	-10.0	<i>Pseudowintera</i>	-0.02	
<i>Cyathea dealbata</i>	<b>0.63</b>		<i>Weinmannia</i>	-0.04	-8.0
<i>Metrosideros undiff.</i>	<b>0.57</b>	-8.0	<i>Coprosma</i>	-0.07	-8.0
<i>Dacrydium cupressinum</i>	<b>0.51</b>	-8.0	<i>Prumnopitys ferruginea</i>	-0.09	-7.0
<i>Libocedrus plumosa</i>	<b>0.49</b>	-7.0	<i>Libocedrus bidwillii</i>	-0.09	
<i>Nestegis</i>	<b>0.46</b>		<i>Plagianthus</i>	-0.09	-5.0
<i>Ascarina lucida</i>	<b>0.43</b>	-3.0	<i>Hoheria</i>	-0.12	
<i>Griselinia</i>	<b>0.42</b>		<i>Hebe</i>	<b>-0.15</b>	
<i>Knightia excelsa</i>	<b>0.39</b>	-8.0	<i>Dracophyllum</i>	<b>-0.24</b>	-10.0
<i>Freycinetia</i>	<b>0.33</b>		<i>Nothofagus subg. Fuscospora</i>	<b>-0.38</b>	-10.0
<i>Dacrycarpus dacrydioides</i>	<b>0.31</b>	-7.0	Asteraceae	<b>-0.39</b>	
<i>Syzygium maire</i>	<b>0.29</b>		Poaceae	<b>-0.49</b>	
<i>Dodonaea viscosa</i>	<b>0.28</b>		<i>Nothofagus menziesii</i>	<b>-0.51</b>	-12.1
<i>Elaeocarpus</i>	<b>0.22</b>	-5.0	<i>Halocarpus</i>	<b>-0.59</b>	-25.0
<i>Collospermum</i>	<b>0.21</b>		<i>Phyllocladus alpinus</i>	<b>-0.65</b>	-20.0
<i>Cyathea smithii</i>	<b>0.21</b>				
<i>Pittosporum</i>	0.20	-7.0			
Monolete spores	0.17				
<i>Quintinia</i>	0.15	-8.0			
<i>Hedycarya arborea</i>	0.14	-3.0			
<i>Dactylanthus taylorii</i>	0.14				
<i>Pseudopanax</i>	0.13				
<i>Dicksonia squarrosa</i>	0.12				
<i>Podocarpus totara</i>	0.09	-7.0			
<i>Leucopogon fasciculatus</i>	0.08				
<i>Fuchsia</i>	0.07				
<i>Prumnopitys taxifolia</i>	0.06	-11.1			
<i>Myrsine</i>	0.04				
<i>Dicksonia fibrosa</i>	0.03				
<i>Hymenophyllum</i>	0.02				

Source: Wilmshurst *et al.* (2007); Sakai & Wardle (1978). This list is a subset of Wilmshurst *et al.* (2007) list, that is, only includes those taxon or taxa groups enumerated at Eltham or the coastal Taranaki sites. The MAT correlations shown in bold are statistically significant at the 99.9% probability level, and are the ‘critical taxa’ referred to in Newnham *et al.* (2012).

## 7.7. Biodiversity Indices

The purpose of this section is to briefly describe how the diversity indices used in this study are calculated, as well as some consideration of the relative strengths and weaknesses of the various indices.

(i) **Species richness** is the most basic measure of biodiversity; it is simply a count of the number of species. Species richness can be generalised higher taxonomic levels (Hammer & Harper 2006); in this study, ‘palynorichness’ (Flenley 2003) or the number of taxa are given. A well-established weakness of species richness as a measure of diversity is that richness does not take into account relative abundance and therefore is susceptible to the size of the sample: the more individuals counted, the greater the number of taxa likely to be enumerated (Peet 1974; Tipper 1979; Brewer & Williamson 1994). Techniques that account for different sample sizes are:

(ii) **Rarefaction Curves** are used for both standardising sample sizes, and as an index in their own right. Rarefaction curves show the expected number of taxa as a function of  $n$ , under assumptions of homogeneity and randomness (Brewer & Williamson 1994). When the rarefaction curve flattens out at larger values of  $n$ , this indicates that the original sample captured most of the taxa. Heck *et al.* (1975) and Tipper (1979) calculated  $E(S_n)$  or expected number of species using:

$$E(S_n) = \sum_{i=1}^s \left[ 1 - \frac{\binom{N-N_i}{n}}{\binom{N}{n}} \right] \quad (7)$$

where  $N_i$  is the number of individuals in species  $i$  of the un-rarefied sample.

In other words, during the initial part of the pollen count, taxa richness rapidly increases but the rate of taxa richness slows and reaches an asymptote where additional counting uncovers no new taxon. This ‘moment of saturation’ (Weng *et al.* 2006) varies amongst ecosystems, with the asymptote occurring at a low pollen count in a low diversity, temperate ecosystem such as a beech forest, compared with a higher pollen count in a high diversity ecosystem such as a tropical rainforest. Figure 38 shows the rarefaction curve for Eltham Swamp dryland pollen taxa (red) with 95% confidence intervals (blue). Note that the curve begins to flatten off at  $n = 200$ , with a taxa count of around 20. This compares with the goal of a minimum dryland pollen count of 200, excluding ferns, so we can be 95% confident that on average, pollen counts of 200 capture most dryland taxa present (mean dryland pollen count at Eltham = 223.3).

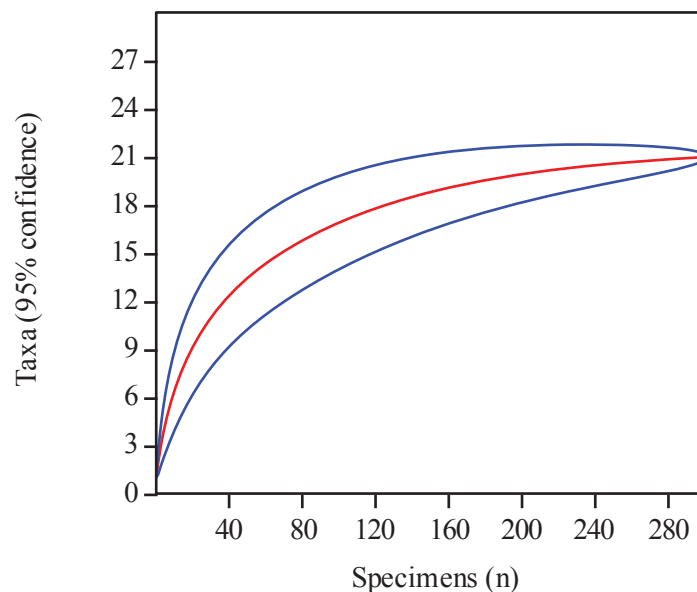


**Figure 38. Rarefaction Curve (red) with 95% Confidence Intervals (blue) for Eltham Swamp**

Rarefaction analysis of fossil pollen has been used to determine Holocene floral diversity in Crose Mere, central England and the Isle of Skye in western Scotland; Late Glacial diversity in Abernathy Forest, eastern Scotland (Birks & Line 1992); Late Holocene vegetation in Finland (Grönlund & Asikainen 1992); and southern Sweden (Lindbladh & Bradshaw 1995). A search of the literature did not reveal any similar study in New Zealand.

**(iii) Menhinick's richness ( $M_R$ ) index**

Menhinick (1964) compared several diversity indices for species of insects against two criteria: (i) the indices must be applicable for a given 'universe' (population) regardless of sample size; and (ii) the indices must differentiate between populations that had different numbers of species for a given number of individuals. Menhinick examined species/log individuals, species  $-1/\text{natural log of individuals}$ , log species/log individuals, and species/ square root of individuals; only the latter index met both of the criteria, therefore he proposed that species richness (sample size,  $S$ ) increases with  $n$ , but does so non-linearly, at the square root of  $n$ :

$$MR = S/\sqrt{n} \quad (8)$$

Menhinick's index has been used by various researchers (Kumar *et al.* 2006; Deb & Sundriyal 2011; Dobhal *et al.* 2011; Caçador *et al.* 2013) to measure vegetation richness of extant, northern hemisphere forests.

**(iv) Margalev's richness ( $M_R$ ) index:**

$$MR = (S - 1)/\ln n \quad (9)$$

Hammer & Harper (2006) point out that whether the number of taxa in a sample increases more like the square root of the sample size as in Menhinick's index) or the logarithm of the sample size (as in Margalev's index) depends upon relative taxa abundances, so neither solution is always applicable.

**(viii) Berger-Parker ( $D_{BP}$ ) index** (Berger & Parker 1970) is a measure of how common the most abundant taxon is:

$$D_{BP} = \frac{N_{MAX}}{N} \quad (10)$$

Where  $N$  = total number of individuals in a sample, and  $N_{MAX}$  is the total number of individuals in the most common taxon. As a consequence, if one taxon dominates a community, it is not very diverse as measured by the Berger-Parker index. Since more diverse communities have a lower Berger-Parker index, a complement form is often used, that is

$$D_{BPC} = 1 - D_{BP} \quad (11)$$

Therefore, values of  $D_{BPC}$  range from 0 (low diversity) to 1 (high diversity). The non-complement form is given in the present study, that is, equation (10) rather than equation (11).

**(ix) Simpson diversity ( $D_S$ ) index** (Simpson 1949) calculates the probability of any two individuals selected at random from a population belonging to the same taxon:

$$D_S = \sum_{i=1}^S P_i^2 \quad (12)$$

where  $P_i^2$  is the proportion of individuals in the  $i$ th species. Since  $D_S$  and diversity are inversely related, a complement index called the Gini-Simpson index is often used (and is used in the current study), that is

$$D_{GS} = 1 - D_S \quad (13)$$

Like the Berger-Parker index, both the Simpson and Gini-Simpson index are biased towards the most abundant species, so therefore are of limited use when the population has many rare species, although  $D_S$  and  $D_{GS}$  are

more accurate than  $D_{BP}$  because they utilise a broader array of taxa, whereas  $D_{BP}$  only uses data for the most prominent taxon.

A second broad group of diversity indices are known as information statistic indices. These indices are based on the concept that diversity can be estimated in a similar manner to calculating uncertainty in a code; as a consequence rare species are weighted more in information statistic indices than they are in dominance indices (Stirling & Wilsey 2001):

(x) *Shannon index* ( $H_S$ )

$$H_S = - \sum_{i=1}^S P_i \ln P_i \quad (14)$$

where  $P_i$  is the proportion of individuals in the  $i$ th species, and  $\ln$  is the natural logarithm. A strength of  $H_S$  is that even the rarest taxon contributes to the index. It is essentially a measure of the information required to define an assemblage (Berger & Parker 1970). The Shannon index is a measure of the number of common taxa, whereas the Simpson index is a measure of the *very* common taxa (Brewer & Williamson 1994). Values for natural communities typically range between 1.5 (low diversity) and 3.5 (high diversity).

Since diversity indices combine two concepts – taxa richness and abundance evenness – and since the emphasis on either component varies from one index to the next, finding a balance is problematic. In addition, applying these indices to fossil pollen data is complicated by problems inherent in palynology in general, such as differential pollen production, dispersal and preservation. As a consequence, Weng *et al.* (2006) suggest the simplest measure, Species Richness, may provide the most meaningful pollen diversity information. The same palynological limitations prompted Birks & Line (1992) to recommend avoiding the use of diversity indices such as Shannon’s or Simpson’s indices in favour of rarefaction analysis.

In contrast, Buckland *et al.* (2005) note that although no single index is able to encompass all the dimensions of diversity change, both Simpson’s and Shannon indices perform well against five out of the six criteria they suggest are appropriate to measure diversity indices against<sup>29</sup>. Neither index satisfied criterion 2; this is unfortunate given the pollen diagram for Eltham (Figure 39) shows that pollen influx is not constant over time, but increases towards the top of the core. Buckland *et al.* (2005) suggested applying a modified version of the Shannon index that satisfied all six criteria; in particular the estimator decreased if absolute abundance of all taxa declined at the same rate. However, the modified Shannon index had no theoretical foundation and was purely a pragmatic solution to satisfy all six criteria (Buckland *et al.* 2005) and has not been rigorously tested (Buckland *et al.* 2011). Given the foregoing discussion, it seemed most prudent to provide a selection of diversity measures for Eltham.

A weakness of applying biodiversity indices to palynological data is that the indices were generally designed to describe populations where identification to species level is possible, however in palynology ‘taxa’ may relate to different taxonomic levels, that is, species (*Dacrycarpus dacrydioides*), genus (*Libocedrus*, *Pittosporum*), Family (Asteraceae) or groupings based on pollen morphology (*Nothofagus* subg. *Fuscospora*, *Leptospermum*-type). Furthermore, there may be an indeterminable number of species within a higher taxonomic level, for example Asteraceae or *Coprosma*. This makes it difficult to make definitive inferences about diversity change, however the alternative would be to only enumerate those taxa identifiable to species level, and this could also limit the usefulness of this type of analysis and also result in misleading inferences.

---

<sup>29</sup> Non-statistical criteria are (i) for a system that has a constant number of species, overall abundance and species evenness, but with varying abundance of individual species, the index should show no trend; (ii) if overall abundance is decreasing, but the number of species and species evenness are constant, the index should decrease; (iii) if species evenness is decreasing, but the number of species and overall abundance are constant, the index should decrease; and (iv) if the number of species is decreasing, but overall abundance and species evenness are constant, the index should decrease. Statistical criteria are (v) the index should have an estimator whose expected value is not a function of sample size; and (vi) the estimator of the index should have good and measurable precision (Buckland *et al.* 2005).

## 8. Results

### 8.1. Pollen Analysis

The results of the pollen analysis for the six sites (Eltham Swamp, Stent Road, Okawe Stream, Opunake Beach, Kaupokonui Beach and Lizzie Bell) are presented below including results of pollen-based quantitative temperature reconstructions (section 8.1). For Eltham Swamp I also provide results and interpretation of quartz and charcoal analysis (section 8.2 and 8.3) respectively.

#### 8.1.1. Eltham Swamp

The fossil pollen assemblage from Eltham Swamp is shown in Figure 39 and expanded for the Late Glacial in Figure 41. Both figures include all major pollen types identified. The core chronology and depths are summarised alongside the diagram and radiocarbon dates are presented in Table 8. Diversity indices, charcoal results and temperature reconstructions are also shown next to the pollen diagram. The pollen results are described and interpreted for each pollen zone as identified using cluster analysis, along with their associated quantitative temperature reconstructions. The Eltham pollen diagrams are given with the tephra layers excluded from the analysis so that the pollen curves are plotted against age, not depth; conversely, the core stratigraphy given in Figure 24 includes tephra so is plotted against depth.

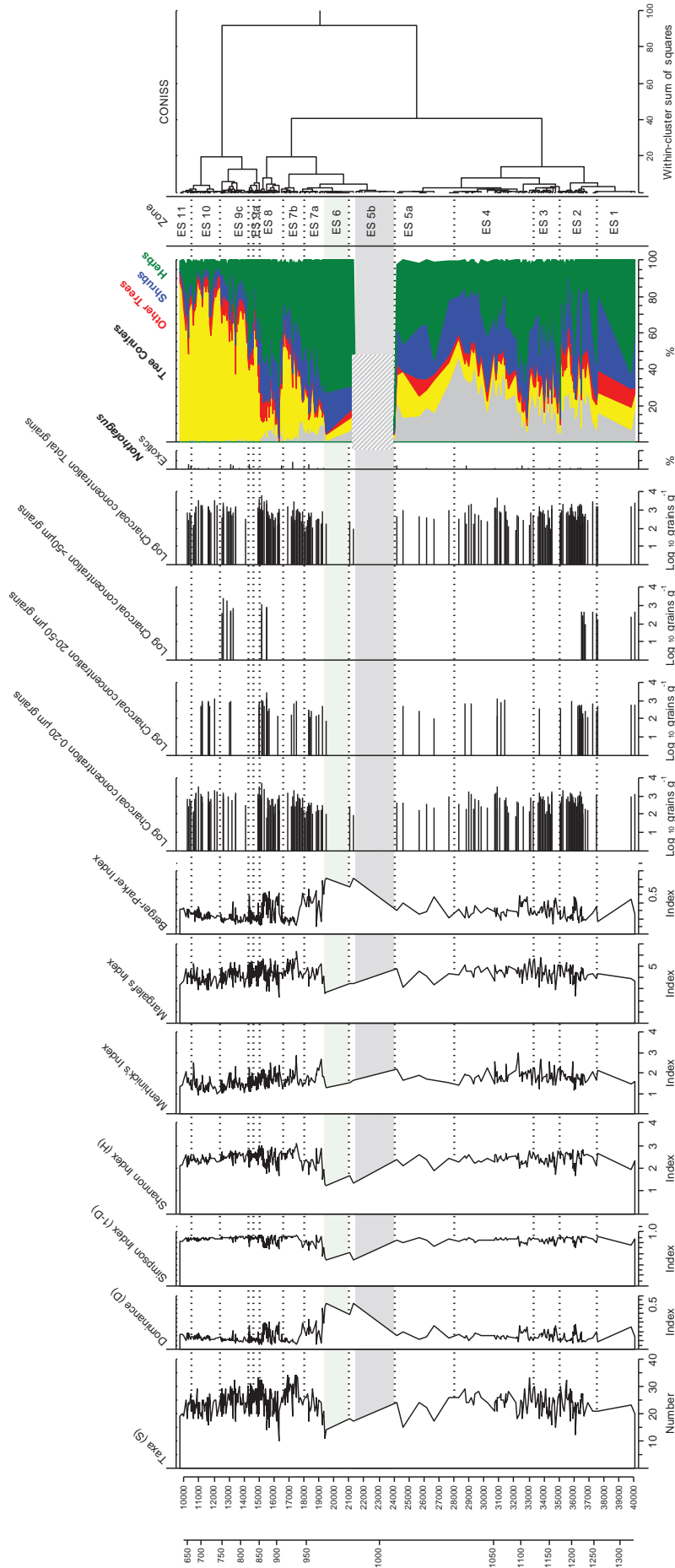
#### **Zone ES 1. 40,000 – 37,500 cal yrs BP ( $\delta^{18}\text{O}$ stage 3; Moerangi Interstadial)**

- *Nothofagus* and Tree Conifer relative abundance varied between 20 and 40% of the pollen sum across this zone; the dominant taxon, *Nothofagus menziesii*, varied between 10 and 35%, and *Nothofagus* subg. *Fuscospora* made up between 5 and 10 % of the sum. Conifer percentages were low; *Podocarpus totara*, *Dacrydium cupressinum*, *Prumnopitys taxifolia*, *Prumnopitys ferruginea* and *Libocedrus* made up < 5% of the pollen sum, and *Dacrycarpus dacrydioides* was virtually absent from the pollen record for this zone.
- Other trees made up around 10% of the pollen sum at the start of the zone; only cold-tolerant *Hoheria* and *Plagianthus* occurred at frequencies >5%.
- Shrubs increased from around 10% of the pollen sum at 40,000 cal BP, to around 35% at the top of the zone. *Coprosma* was the major genus, comprising 20-25% of the pollen sum across the zone, whilst *Phyllocladus* Asteraceae, *Dracophyllum* and *Myrsine* made up around 5% each of the sum. *Halocarpus*, *Hebe*, and *Leptospermum*-type taxon were also present, but in much lower numbers.
- Herbs fluctuated between 20% and 60% of the pollen sum, comprised almost entirely of Poaceae.
- Tree Ferns were present in low numbers in zone ES1, and of the Ferns and Fern Allies taxa, only undifferentiated monolete fern spores, *Cyathea smithii* and *Phymatosorus* occurred in significant numbers, each approached 5% of the pollen sum.

#### **Interpretation**

Results from pollen zone ES 1 must be interpreted with caution; since the top of Core A (9) was comprised of sandy loams that do not favour pollen preservation, only ten samples covering the uppermost 50 cm of core were extracted. Of these ten samples, only five yielded pollen, and this was in very low concentrations, ranging from 3,600 to 5,000 grains  $\text{g}^{-1}$ , compared with pollen zone ES 2 which had an average pollen concentration of 18,000 grains  $\text{g}^{-1}$ . In addition, the pollen influx rate was very low, at <100 grains  $\text{g}^{-1} \text{yr}^{-1}$  compared with > 650 grains  $\text{g}^{-1} \text{yr}^{-1}$  for pollen zone ES 2; overall, this suggests that pollen production was low (due to reduced vegetation cover) and/or pollen preservation conditions were poor.





Red vertical line in transfer function = modern MAT (11.2°C); grey band indicates area of low pollen counts; blue band indicates area of low pollen counts where no pollen was encountered.

The dominance of *Nothofagus menziesii* relative to other tall tree taxa in this zone indicates a cooler climate than present, since it does not typically occur below 600m today (Wardle 1967). *Nothofagus menziesii* tends to be under-represented in the pollen rain (McKellar 1973; MacPhail & McQueen 1983) so its true abundance may have been even greater. Assuming an environmental lapse rate of 0.65°C/100m applied 40,000 years ago, a *Nothofagus menziesii* depression of 356m<sup>30</sup> suggests that mean annual temperatures were at least 2.3°C cooler than present. Although the pollen assemblage at lower altitudes is unknown, it is unlikely that Eltham was the lower altitudinal limit for *Nothofagus menziesii*. Since the sea level 40,000 cal yrs BP is estimated to have been 120-130m lower than today (Yokoyama *et al.* 2000; Mix *et al.* 2001) and the coast was pushed tens of kilometres to the west, a cool, more continental-type climate would have extended seaward for some distance, providing a niche for *Nothofagus menziesii* and other cold-adapted taxa. Temperatures are thought to have been as much as 5°C cooler at this time (Shulmeister *et al.* 2003)

*Nothofagus menziesii* has a maximum frost resistance (FR) of -12.4°C (Bannister & Lord 2006, section 5.3.1) therefore it was able to out-compete the second-most dominant tall tree taxon, *Nothofagus fusca* (FR = -10.4°C) and the conifers that are present in much lower frequencies - *Podocarpus totara* (FR = -8.2°C) and *Dacrydium cupressinum* (FR = -8°C). The high levels of *Coprosma* indicate that the tall forest cover was patchy and discontinuous, whilst low levels of tree ferns and *Dacrydium cupressinum* suggest conditions were relatively dry and possibly windy. Although the abundance of Herb pollen was high, it is not at maximum levels relative to the rest of Core A. Assuming that the peak of herb pollen indicates peak cooling, this suggests that although temperatures were much cooler than today, cooling was not at its maximum; the W-MAT transfer function gives an estimated mean annual temperature of between 6.5°C and 7.5°C at this time.

The high relative abundance of cold-tolerant taxa (*Nothofagus menziesii*, *Nothofagus* subg. *Fuscospora*, Asteraceae, *Coprosma* and *Myrsine*), and low frequency of thermophilous conifers and tree ferns were mirrored at Inaha in southern Taranaki (McGlone *et al.* 1984), and at Lake Poukawa in Hawke's Bay (Shulmeister *et al.* 2001), implying that lower temperatures were not confined to Eltham at this time.

### **Zone ES 2. 37,500 - 35,000 cal yrs BP ( $\delta^{18}\text{O}$ stage 3; Moerangi Interstadial)**

- The relative abundance of the *Nothofagus* and Tree Conifer group fluctuated between 40% and 50% of the pollen sum across the zone; the fluctuation was mainly driven by a reduction in abundance of *Nothofagus menziesii* from 35% to 20%. Slight increases in the relative abundance of *Prumnopitys taxifolia* and *Podocarpus totara* (but from a low base), the appearance of *Libocedrus* and relatively stable levels of the remaining conifers were insufficient to offset the decline in *Nothofagus menziesii*.
- The Other Trees Group was more diverse in Zone ES 2 than in ES 1; the absence of the weakly cold tolerant taxon *Pseudowintera* was offset by the appearance of *Pittosporum*, *Elaeocarpus*, *Griselinia*, and *Macropiper excelsum*.
- Shrubs made up 40% of the pollen sum with *Coprosma* making up 20-35% of the sum; *Phyllocladus* and *Dracophyllum* decreased in relative abundance.
- Herbs remained at a similar level across most of zone ES 2 but decreased dramatically to around 10% of the pollen sum by the end of the zone, again, comprised almost entirely of Poaceae.
- Tree Ferns, Ferns and Fern Allies decreased across the zone, with monoete spores *Phymatosorus* and *Cyathea smithii* all decreasing to < 5% of the pollen sum.

---

<sup>30</sup> Since Eltham Swamp lies at around 244m above sea level today (c. 364m asl 40,000 years ago), 600 – 244 = 356m.

### **Interpretation**

The reduction in *Nothofagus menziesii* and Poaceae pollen and a slight increase in warmth-loving shrubs, combined with a decline in spore relative abundance in the Tree Ferns and Ferns and Fern Allies groups, indicate that the period 37,500 - 35,500 cal yrs BP was slightly warmer and drier than the previous period. Pollen transfer data (W-MAT) suggests temperatures increased between 0.5 and 1.5°C from the previous zone to around 8°C; in comparison the modern-day mean annual temperature is 11.2°C.

### **Zone ES 3. 35,000 – 33,250 cal yrs BP ( $\delta^{18}\text{O}$ stage 3; Moerangi Interstadial)**

- The *Nothofagus* and Tree Conifer group displayed a downward trend across zone ES 3, decreasing from 40% to 10% of the pollen sum, driven by a major decrease in both *Nothofagus menziesii* and in particular *Nothofagus* subg. *Fuscospora*, partially offset by small increases in *Podocarpus* and *Dacrydium cupressinum*.
- Herbs increased dramatically, to 55% of the pollen sum. *Chenopodium*, *Epilobium* and *Taraxacum*-type taxon appeared for the first time in the pollen assemblage.
- Other Trees fell sharply, making up <5% of the pollen sum. A decline in *Hoheria* and *Plagianthus* was partially offset by an increase in *Macropiper excelsum*.
- The Shrubs group makes up 25% to 35% of the pollen sum; the decline in *Coprosma* was partially offset by increases in *Phyllocladus*, Asteraceae and *Leptospermum* –type taxon.
- Tree Ferns, Ferns and Fern Allies increased slightly across the zone, driven by the increase in monoete spores and the appearance of *Hymenophyllum*.

### **Interpretation**

The decrease in relative frequency for the *Nothofagus* and Tree Conifers group and the increase in Poaceae pollen suggest zone ES 3 was cooler than the previous period; these changes in taxa abundance drive the slight decline in inferred temperature from both PLS-C2 and WMAT transfer functions (c. 1°C each). Since abundance for both the Tree Ferns and Ferns and Fern Allies groups remained largely unchanged from the previous period, fairly dry conditions are likely to have persisted.

### **Zone ES 4. 33,250 – 28,000 cal yrs BP ( $\delta^{18}\text{O}$ stage 3; Moerangi Interstadial)**

- The *Nothofagus* and Tree Conifer group rose sharply to 45% of the pollen sum, driven by *Nothofagus* subg. *Fuscospora* grains and *Nothofagus menziesii* in particular. The proportion of conifers in the pollen sum remained fairly constant across the zone, with the exception of *Podocarpus*, which increased to around 10% of the pollen sum.
- The Other Trees group decreased to very low levels; the most abundant taxa on this group, *Hoheria* and *Plagianthus*, made up less than 2.2% of the pollen sum each.
- Shrub taxa decreased as a proportion of relative pollen abundance, making up around 20% of the pollen sum; an increase in *Coprosma* and *Phyllocladus* was offset by a decline in Asteraceae and *Leptospermum*.
- Herb taxa decreased across zone ES 4 to make up 20% of the pollen sum. Although much of the decline was due to a decrease in Poaceae, *Chenopodium*, *Epilobium* and *Taraxacum*-type taxon also decreased in abundance.

- Tree Ferns, Ferns and Fern Allies decreased across the zone: the increase in *Cyathea dealbata* was offset by the decrease in monolete spores to around 5% of the pollen sum.

### **Interpretation**

Zone ES 4 was a period of cooling, given the upward trend in the *Nothofagus* taxa, and maintenance of grasses at relatively high levels. Cooling was likely to be moderate, given that *Dacrydium cupressinum* declined only slightly, or remained at similar levels to the previous zone, and highly cold-tolerant taxa like *Phyllocladus* or *Halocarpus* did not increase dramatically in relative abundance. Pollen transfer data suggests a fall of perhaps 0.5°C, although caution should be used since small changes of this magnitude fall within the error bounds of the transfer function. As in zone ES 3, Tree Ferns and Ferns and Fern Allies relative abundance is depressed, suggesting that rainfall was also depressed and dry conditions relative to the Late Holocene persisted.

The apparent discrepancy between purported cooler temperatures, but an increase (although slight) in the relative abundance of *Podocarpus* pollen compared to either of the more cold tolerant *Nothofagus* taxa (*Nothofagus fusca* FR = -10.4°C, *Nothofagus menziesii* FR = -12.4°C), could be due to resolution of *Podocarpus* to only the genera level: this may mask the contribution of *Podocarpus* ecotypes such as *Podocarpus nivalis* and *Podocarpus hallii* that have an even lower freezing resistance than *Nothofagus* (FR -22°C and -13°C respectively; Sakai & Wardle 1978). Cranwell & von Post (1936) noted the pollen of *Podocarpus hallii* is difficult to distinguish from *Podocarpus totara* (FR = -8.2°C) due to their very similar morphology and is often not recognised<sup>31</sup>.

Pocknall (1981) found that contrary to studies by Cranwell (1940) and Couper (1953), *Podocarpus totara*, *Podocarpus nivalis* and *Podocarpus hallii* could not be distinguished by total grain length, corpus width or shape or saccus length, and saccus ornamentation was the only definite distinction. This implies that grains for these taxa need to be well preserved in order to differentiate between them; however pollen and spore preservation was generally poor at Eltham (McGlone & Neall 1994) with many grains corroded and damaged. Alternatively, since the absolute abundance of tall tree pollen grains is low, the apparent (and slight) dominance of *Podocarpus* over the other conifers may be a consequence of a relatively small sample size, and the apparent difference is not significant. On balance, it would seem most likely that at least some of the grains recorded under *Podocarpus totara* – type are either *Podocarpus nivalis*, or more likely *Podocarpus hallii* since this species is a significant component of the montane forest above 800m on the flanks of Mount Egmont today (McGlone 1982; Druce 1986); in any event, the sharp rise in Poaceae alone lends some confidence to the cooling interpretation.

### **Zone ES 5a. 28,000 – 24,000 cal yrs BP ( $\delta^{18}\text{O}$ stage 3 - 2, Last Glacial Cold Period)**

- Zone ES 5 was characterised by a sharp fall in *Nothofagus* and Tree Conifers; an increase in the relative abundance of *Prumnopitys ferruginea*, *Prumnopitys taxifolia* and *Dacrydium cupressinum* was insufficient to offset the sharp fall in both beech taxa, and to a lesser extent, the absence of *Libocedrus*.
- The Other Trees group remained largely unchanged from zone ES 4; the decline in *Hoheria* and *Plagianthus* was countered by a rise in *Macropiper excelsum*.
- Shrubs remained constant as a proportion of the pollen rain; the rise in *Phyllocladus* and Asteraceae was offset by a decline in *Coprosma* from 25 % to 15 % of the pollen sum, and a fall in *Myrsine* from around 5% of the sum to < 1%.

---

<sup>31</sup> Furthermore, Pocknall (1981) notes that *Podocarpus hallii* may be delicate and poorly preserved, since grains being prepared for scanning electron microscopy often collapse. This suggests that *Podocarpus hallii* is both under-represented in the pollen assemblage and under-reported in the literature.

- Herb pollen abundance increased to around 70% of the pollen sum (although this is based on only two observations). The decrease in *Chenopodium*, *Epilobium* and *Taraxacum*-type taxon was not sufficient to offset the increase in Poaceae.

### **Interpretation**

Much of Zone ES 5a is likely to have been cooler than previously, despite the decline in relative abundance of *Nothofagus* subg. *Fuscospora* and *Nothofagus menziesii* taxa, and the increase in *Dacrydium cupressinum* relative to *Prumnopitys taxifolia*. At the start of the zone, the relative abundances of both *Nothofagus* taxa, in particular *Nothofagus menziesii*, are close to the highest at any period in the core. At the top of the zone, however, this situation is reversed; the decline in relative abundance of both *Nothofagus* taxa, and strong increase in Poaceae imply cooling. Although *Dacrydium cupressinum* increases relative to *Prumnopitys taxifolia*, which typically implies warmer conditions, the relative abundances of both taxa were lower than in the Holocene, and lower than extant cold-climate taxa such as *Nothofagus menziesii* and Poaceae, therefore this zone is likely to have been cooler than the previous zone. Pollen transfer data supports this inference, with mean annual temperatures decreasing around 0.5°C cooler than the previous pollen zone, falling to around 6°C.

Rainfall throughout zone ES 5a is likely to have been slightly higher than zone ES 4, that is, low, but presumably droughts were less frequent than in zone ES 4 given the relatively higher abundance of drought-intolerant taxa such as *Dacrydium cupressinum* and presence of *Cyathea dealbata*. This conclusion is based on a small number of observations, and *Cyathea* tends to be over-represented in the pollen rain (Bussell 1988), so caution is required when making inferences about tree fern abundance in this zone.

A similar pattern of increases in the relative abundance of thermophilous conifers, at the expense of cold-tolerant *Nothofagus* subg. *Fuscospora* and *Nothofagus menziesii* occurred at Pukaki crater in Auckland (Sandiford *et al.* 2003), although conditions at Pukaki may have been more arid than at Eltham given the low abundance of tree fern spores.

### **Zone ES 5b. 24,000 – 21,000 cal yrs BP ( $\delta^{18}\text{O}$ stage 2, Last Glacial Maximum)**

- The period 24,000 to 21,000 cal yrs BP was associated with very slow accumulation of tephric loess, in the order of 5cm per thousand years at Eltham (see stratigraphic log for Core A (6), Figure 26 c). In addition, the Eltham site may have been dryland for at least the early part of the time interval, lacking a standing water body in both the immediate vicinity, and the wider area encompassed by the valley.
- As a consequence, very low quantities of pollen were recovered from this subzone, with < 30 total dryland taxa pollen grains enumerated for each sample, even after counting up to four pollen slides per sample. Because the pollen counts were so low, the pollen assemblage is not considered to be a reliable representation of the extant vegetation, so temperature estimates from pollen transfer data are not considered reliable either, and not considered for this zone.
- It must be emphasised that this data is indicative only. As discussed in section 9.5, the rarefaction curve shows that samples of around 200 dryland pollen grains are needed to be 95% confident that all pollen taxa in the sample are enumerated. Figure 38 shows that for counts of < 30 taxa at Eltham, the rarefaction is very steep, so that one can have little confidence that all taxa are enumerated, let alone that the relative proportions of taxa are an accurate representation of the pollen population.
- These severe limitations notwithstanding, pollen zone ES 5b is highlighted in Figure 39 as a zone of low pollen counts; in addition, Figure 40 gives individual pie graphs for the samples from this zone. Figure 40 shows that the oldest two samples which are derived from the middle of the tephric loess layer above the Kawakawa/ Oruanui tephra, are dominated by herb taxa (mostly Poaceae) which make

up between half and three-quarters of the pollen assemblage. *Nothofagus* and podocarps (*Dacrydium cupressinum* and *Podocarpus*) are also present.



Figure 40. Samples Containing Low Pollen Counts 24,000 – 21,000 cal yrs BP

- By the top of the tephric loess layer *Nothofagus menziesii* and shrub taxa (Asteraceae and *Coprosma*) dominated, with smaller quantities of Poaceae present. Podocarps and Other Trees were absent from this part of the core.
- Between 21,860 and 21,432 cal yrs BP *Nothofagus* was absent whilst podocarps become the dominant taxa type, in particular *Podocarpus totara* and *Dacrydium cupressinum*. By 21,432 cal yrs BP Poaceae dominated the pollen assemblage.
- Between 23,998 and 22,016 cal yrs BP there were no wetland herb or aquatic plant pollen grains in the record; in contrast, between 21,860 and 21,432 cal yrs BP very low numbers of Cyperaceae, *Astelia*, *Empodisma* and *Haloragis* grains appeared in the record. *Cyathea dealbata* and *Phymatosorus* increased in abundance between 23,998 and 21,432 cal yrs BP.

### **Interpretation**

As a consequence of very cold temperatures and generally dry conditions during this period there was a decline in primary plant production so that peat accumulation largely ceased, and ombrogenous bog-forming conditions (section 6.2) were retarded, particularly in the earlier part of this time interval when both aquatic plants and drought-intolerant tree ferns are either absent or present in very low numbers.

As a result of this hiatus, pollen preservation conditions were not favourable: site conditions at this time were likely highly energetic due to high winds so that pollen grains were subject to increased mechanical abrasion and oxidising due to the absence of permanently wet, anoxic swamp conditions. Pollen influx was as low as *c.* 125 grains g<sup>-1</sup> yr<sup>-1</sup>, an order of magnitude lower than zone ES 7a where influx rates were *c.* 3,200 g<sup>-1</sup> yr<sup>-1</sup>.

The very low number of pollen grains counted in this subzone suggests that one cannot make a definitive statement about the distribution of extant vegetation or climate change for the zone, other than to conclude that the taxa described, including some warm-loving taxa such as *Dacrydium cupressinum* were present for at least part of the period 24,000 to 21,000 cal yrs BP, but overall conditions were cold and dry, and clearly windy given the accumulation of tephric loess (section 8.2).

### **Zone ES 6. 21,000 – 19,400 cal yrs BP ( $\delta^{18}\text{O}$ stage 2, Last Glacial Maximum)**

- No pollen was recovered from this zone; as with zone ES 5b, this was likely due to reduced vegetation cover and therefore reduced pollen influx, as well as conditions that were unfavourable for pollen preservation including low peat production in a high-energy, oxidising environment.

### **Interpretation**

The period 21,000 – 19,400 cal yrs BP was also a hiatus, associated with slow accumulation of sediments, primarily tephric loess at Eltham, and given the complete absence of pollen, was likely to have been even colder and/or drier and/or windier than pollen zone 5b. Since pollen zone ES 6 may represent the coldest part of the Last Glacial Maximum, it is unfortunate that there was no pollen present in order to make either a qualitative statement regarding environmental conditions, or to quantify mean annual temperatures using the pollen transfer functions. However, conditions at Stent Road were more amenable for pollen preservation at this time, so some record of environmental and climatic conditions is available from the wider Taranaki fossil pollen record (section 8.1.2).

### Eltham Swamp 19,400 – 9,750 cal yrs BP

Figure 41 covers the topmost part of Core A (19,400 to 9,750 cal yrs BP), and provides a subset of Figure 39 which covers the entire core. Splitting Figure 39 in this way allows closer examination of pollen zone ES 9 in particular, which is split into three subzones in Figure 41.

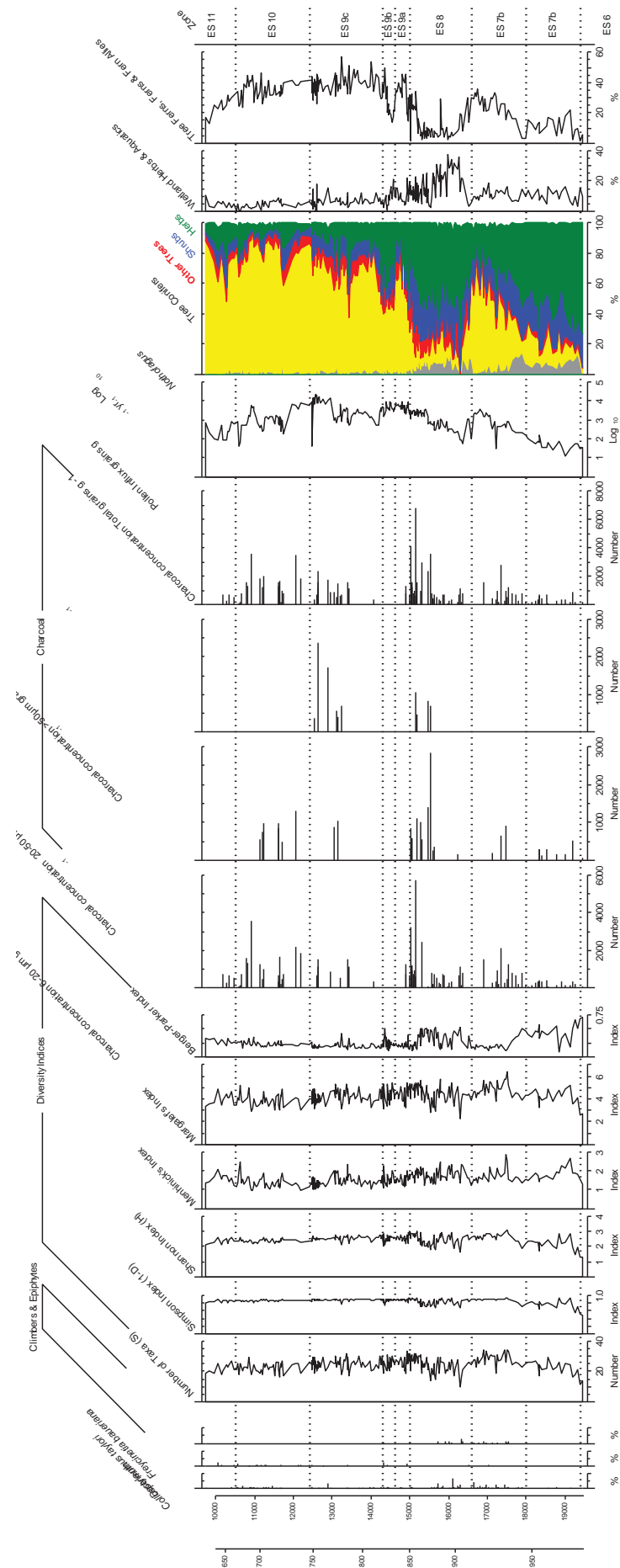
#### Subzone ES 7a. 19,400 – 18,000 cal yrs BP ( $\delta^{18}\text{O}$ stage 2, Last Glacial-Interglacial Transition- Late Glacial Warming)

- The sediments in zone ES 7 were clearly polleniferous once again, with pollen influx increasing from around 125 grains  $\text{g}^{-1} \text{yr}^{-1}$  to 3,200  $\text{g}^{-1} \text{yr}^{-1}$  across the zone.
- Herb taxa made up around 65% of the pollen sum for zone ES 7a, comprised predominantly of Poaceae, with smaller amounts of Apiaceae and *Chenopodium*.
- *Nothofagus* and Tree Conifer pollen started to increase up the zone, comprising around 25% of the pollen sum, with *Nothofagus menziesii* and *Podocarpus* the major tall tree taxa. *Nothofagus* subg. *Fuscospora*, *Prumnopitys taxifolia* and *Dacrydium cupressinum* were all present at low levels (c. 5%). *Prumnopitys ferruginea* (10%), and *Dacrycarpus dacrydioides* are virtually absent; *Libocedrus* is consistently present, at low levels (<5%).
- The Other Tree taxa group made up < 5% of the pollen sum across the subzone; cold-tolerant taxa *Plagianthus*, *Pseudowintera* and *Nestegis* were present at low levels; cold-intolerant *Ascarina lucida* is absent.
- Shrubs peaked at around 25% of the pollen sum at the top of the subzone, dominated by cold-tolerant taxa *Phyllocladus* and Asteraceae, and the more warmth-adapted *Coprosma*.
- Tree ferns and ferns were present in low numbers; *Cyathea smithii* and monolete fern spores each made up around 5% of the pollen sum.

#### Subzone ES 7b 18,000- 16,600 -cal yrs BP ( $\delta^{18}\text{O}$ stage 2, Last Glacial-Interglacial Transition- Late Glacial Warming)

- *Nothofagus* and Tree Conifer pollen abundance strongly increased from Zone ES 5, from around 25% to 60% of the pollen sum. Although both *Nothofagus menziesii* and *Nothofagus* subg. *Fuscospora* taxa decreased to c. 10% and c. 5% of the pollen sum respectively over zone ES 5 levels, this is more than compensated for by strong rises in *Dacrydium cupressinum* (>20% of the pollen sum), *Podocarpus totara* (20%), *Prumnopitys taxifolia* (15%), *Prumnopitys ferruginea* (10%), and *Dacrycarpus dacrydioides* and *Libocedrus* (5% of the pollen sum each) by the top of zone ES 7.
- Shrubs decreased to 10% of the pollen sum at the top of the zone; the biggest declines were in *Phyllocladus* and Asteraceae, whereas *Coprosma* remained at a constant abundance.
- The Other Tree taxa group also rose in relative pollen abundance, rising to > 10% across the subzone; both cold-tolerant taxa (*Plagianthus*, *Pseudowintera* and *Fuchsia*) and warm-loving taxa (*Elaeocarpus*, *Griselinia*, *Pseudopanax*, *Ascarina lucida* and *Nestegis*) increased. *Ascarina* was consistently present across this zone, albeit at low levels.
- Herb taxa showed a strong decline from pollen zone ES 7a, falling to around 20% of the pollen sum by the end of the subzone;
- Tree Fern relative abundance showed a strong increase in subzone ES 7b, with *Cyathea smithii*, *Cyathea dealbata*, and monolete fern spores each achieving 10-15% of the pollen sum.





### **Interpretation**

The reappearance of pollen in significant numbers in pollen zone ES 7 indicated warmer, wetter and likely less windy conditions than those that persisted previously; these conditions favoured an increase in plant biomass and allowed for improved pollen preservation. W-MAT pollen transfer data suggests that mean annual temperatures were around 1°C warmer than pollen zone ES 5a, fluctuating between 7.25°C and 7.5°C throughout pollen zone ES 7a, climbing to 9.25°C by the top of pollen zone ES 7b. The increased dominance of *Dacrydium cupressinum* in particular is indicative of wetter, maritime climates than existed previously, although both temperature and annual precipitation were likely to have been less than at present, since *Libocedrus bidwillii*<sup>32</sup> is not common on consistently wet soils, and is now generally found higher than 875m on Mt Egmont and > 600m in the central North Island (McGlone & Neall 1994). Furthermore, *Libocedrus* has the capacity to colonise open sites after wind-throw and slipping (McGlone *et al.* 1988).

The ratio of *Prumnopitys taxifolia* and *Dacrydium cupressinum* frequencies is enlightening. *Prumnopitys taxifolia* is the least competitive of the podocarps in the presence of mesophytic broadleaved vegetation, with a slower growth rate than *Dacrydium cupressinum* on all but the most fertile sites, such as fresh alluvial soils (McGlone & Neall 1994). Therefore when climatic conditions were drier and more drought and frost prone, faster growing, more competitive but less stress-tolerant *Dacrydium cupressinum* with a frost resistance (FR) of -8°C was disadvantaged compared to *Prumnopitys taxifolia* (FR = -11.1°C) (Sakai & Wardle 1978; Bannister & Lord 2006).

The appearance of *Dacrycarpus dacrydioides* is notable; this taxon favours fertile soils but lower altitudinal limits (FR = -7°C) and a preference for wet climates and sites, therefore it had a more restricted distribution than *Dacrydium cupressinum* in the Late Glacial (McGlone & Neall 1994). On balance, the rise in both *Dacrydium cupressinum* and *Libocedrus bidwillii* suggests that both precipitation and temperatures at Eltham were lower than at present, but higher than in the previous zone and that disturbance due to windier conditions was higher.

Despite the apparent windiness relative to present, increased abundance of the lianes *Freycinetia* and *Metrosideros*, and greater relative abundance of epiphytic plants such as *Collospermum* and *Phymatosorus* are indicative of a well established, species-rich lowland forest (Lees *et al.* 1998). The appearance of *Ascarina* also heralds warmer temperatures; *Ascarina* prefers cool annual temperatures (*c.* 10°C), low incidence of frost (FR = -3°C; Sakai & Wardle 1978) and drought, but thrives over a wide range of temperatures. Interestingly, *Ascarina* is very rare in Taranaki today, with only six individual plants found in the Pouakai Range adjacent to Mt Egmont (McGlone & Neall 1994), suggesting that the climate regime 19,400 – 16,600 cal yrs BP may have been less seasonal than today, that is, summers may have been cooler, and winters warmer than currently experienced.

Climatic conditions at Eltham were similar to those at Pukaki crater in Auckland: thermophilous *Dacrydium cupressinum*, *Podocarpus taxifolia* and Malvaceae all began to increase after emplacement of the Rerewhakaaitu Tephra, as did drought-intolerant *Cyathea smithii*, *Phymatosorus* and monolete ferns; similarly, there was a concomitant decline in cold tolerant beeches and shrub taxa (Sandiford *et al.* 2003).

### **Zone ES 8. 16,600 – 15,000 cal yrs BP ( $\delta^{18}\text{O}$ stage 2, Last Glacial-Interglacial Transition)**

- *Nothofagus* and Tree Conifer pollen displayed a sharp decline in relative abundance over the previous zone, falling to 20% of the pollen sum. *Nothofagus menziesii*, *Nothofagus* subg. *Fuscospora*, both *Prumnopitys* species, *Podocarpus* and *Dacrycarpus dacrydioides* decreased across the zone;

---

<sup>32</sup> It is very difficult to distinguish between *Libocedrus plumosa*, a lowland northern species, and *L. bidwillii*, a southern montane species, therefore caution is needed when interpreting *Libocedrus* in the fossil pollen rain.

*Libocedrus* comprises >5% of the sum at the start of the zone but was absent in the top half of the zone, and *Dacrydium cupressinum* fell to < 5% of the sum after high levels in ES 7.

- The relative abundance of Other Trees increased slightly on the previous zone, driven by a strong rise in *Pseudowintera* and more modest rises in cold-tolerant *Plagianthus* and *Aristotelia*, *Pittosporum* and *Elaeocarpus*. The only warm-loving taxon to increase in abundance was *Nestegis* at the start of the zone; *Dodonea viscosa* is consistently present, at low levels.
- Shrub taxa showed a strong increase in relative abundance in this zone, averaging around 30% of the pollen sum. The increase was due mainly to a strong rise in cold-loving *Phyllocladus* and Asteraceae to around 10% of the pollen sum each. *Dracophyllum* also increased, particularly in the upper half of zone ES 8, and *Hebe* appears for the first time. Cold-intolerant *Myrsine* increased at the top of the zone, but its relative abundance (c. 5% of the pollen sum) was much less than abundances of the cold-loving taxa.
- Herb taxa accounted for 15% of the pollen sum at the bottom of zone ES 8, rising to 55% by the middle of the zone. The strong increase over the previous zone was due mostly to Poaceae and to a lesser extent Apiaceae, with other herb taxa remaining at similar proportions as before.
- The Tree Ferns and Ferns and Fern Allies groups showed a sharp decline in relative abundance in this zone; spores for *Cyathea smithii*, *Cyathea dealbata*, and monoletes all falling to < 5% of the pollen sum, before recovering slightly at the top of the zone.
- Wetland taxa, including Cyperaceae, *Empodisma*, *Phormium tenax*, *Gunnera* and *Myriophyllum* all increased sharply at the start of zone ES 8 before falling to levels similar to those in zone ES 7.

### **Interpretation**

A sharp rise in grass pollen, along with the early dominance of *Nothofagus menziesii* and *Libocedrus bidwillii* and decline in warm-climate, tall-tree taxa relative to other tall tree taxa, indicates a return to much cooler temperatures. *Libocedrus* is now common only > 875m on Mt Egmont and > 600m in the central North Island (McGlone & Neall 1994). Drier conditions are also indicated by *Libocedrus* distribution; *Libocedrus* is not common on consistently wet soils, but has the capacity to colonise open sites after windthrow and slipping. Furthermore, McGlone *et al.* (1988) found that *Dracophyllum* at Ahukawakawa Swamp favours drier areas, and *Dodonea viscosa* is commonly found at warm, sunny coastal sites that are well drained and often dry. Finally, *Dodonea* doesn't usually occupy the same sites as *Ascarina*; this may be due in part to its greater frost resistance (-8.1°C; Sakai & Wardle 1978) than *Ascarina*.

Collectively, these changes in taxa relative abundance suggest that conditions were much cooler than previously, at least for the bottom of the zone, with some climate amelioration toward the top of the zone, with precipitation less than at present in the Eltham area. The W-MAT estimated temperature fell around 1.25°C from the previous zone, fluctuating between 7.5°C and 8°C across the zone. The PLS-C2 transfer function suggests that temperatures fell to below 6°C at the coldest part of zone ES 8, in contrast to zone ES 7b where mean annual temperatures were between 7 and 10°C for much of the zone.

McGlone *et al.* (1988) distinguished between alluvial inwash phases, which lead to more shrubs, especially *Hebe*, and monolete ferns, and less *Cyperaceae*; in contrast to peat sedimentation phases which lead to increase in *Cyperaceae*, herbs and aquatic plants, and Poaceae. The rise in *Pseudopanax*, *Elaeocarpus* and *Myrsine* and the first appearance of *Hebe*, which is common in fresh alluvium deposits (McGlone *et al.* 1988) may have been in response to increased alluvium inwash, but driven by windier conditions rather than increased rainfall. Windier conditions might also account in part for the strong presence of scrub taxa *Coprosma* and *Myrsine*, and occasional appearance of *Cyathodes fasciculata*, which suggest that the forest canopy was discontinuous.

The low relative abundance of *Leptospermum* -type taxon at this time (or any other time) at Eltham is slightly puzzling. *Leptospermum scoparium* and *Kunzea* are characteristic of the early stages of succession in a wide range of environments (Grant 1967) so might be expected to demonstrate periodic spikes in the pollen record following numerous tephra falls seen throughout Core A as described for other sites (McGlone *et al.* 1988; Lees & Neall 1993)<sup>33</sup>. Rapid replacement of *Leptospermum* by either nitrogen-fixing taxa such as *Coriaria*, or more C-selected taxa is an example of Clements' (1928) facilitation and relay floristics succession (section 5.4.3).

#### **Subzone ES 9a. 15,000 – 14,600 cal yrs BP ( $\delta^{18}\text{O}$ stage 1, Late Glacial Warm Period)**

- Subzone ES 9a represents a transition from grassland –shrubland to a conifer-broadleaved forest. *Nothofagus* and Tree Conifer pollen increased sharply in relative abundance compared to the previous zone, increasing to > 65% of the pollen sum. All conifers, with the exception of *Libocedrus*, displayed a strong increase in relative abundance. *Podocarpus* was the major taxon in the pollen assemblage, making up 30% of the pollen sum, followed by *Dacrydium cupressinum* (15-20%) *Prumnopitys taxifolia* (10-20%), *Prumnopitys ferruginea* (10%) and *Dacrycarpus dacrydioides* (5 - 10%). In contrast, *Nothofagus menziesii* and *Nothofagus* subg. *Fuscospora* decline, to around 3% and around 1% of the pollen sum, respectively; thus the forest assemblage was now lowland in character.
- Other Tree taxa relative abundance decreased to around 10% of the dryland pollen sum by the top of the subzone. *Pseudowintera*, *Aristotelia*, *Elaeocarpus* and *Nestegis* all decreased in relative abundance.
- The relative abundance of Shrub taxa comprised around 10% of the pollen sum across the zone, caused by a decline in cold-tolerant *Phyllocladus* and especially Asteraceae, which decreased from 10% of the pollen sum to 1%; these declines in cold-tolerant taxa are offset to some extent by declines in warm-loving *Coprosma* and *Myrsine*.
- The sharp decrease in Herb pollen relative abundance to around 10% of the pollen sum was driven mainly by a decrease in Poaceae; in addition, Apiaceae pollen is absent from the zone.
- All Tree Fern, Ferns and Fern Allies taxa showed an upward trend in subzone ES 9a, with *Cyathea dealbata* and *Cyathea smithii* spores increasing in relative abundance to 20% of the pollen sum.
- *Astelia*, Cyperaceae, *Empodisma*, *Phormium* and *Myriophyllum* relative abundance in zone ES 9 fell from the previous zone, whereas *Gleichenia* increased sharply.

#### **Interpretation**

Forest dominated by *Prumnopitys taxifolia* with a *Plagianthus* and *Pittosporum* understory is similar to extant forests in the eastern and southern North Island and the South Island (McGlone & Neall 1994). Given that the abundance of *Prumnopitys taxifolia* pollen was relatively high in the pollen rain in subzone ES 9a, but subordinate to *Podocarpus* and *Dacrydium cupressinum*, temperatures were probably slightly lower at Eltham than they are today (since the pollen assemblage resembled that from forests from cooler areas to the south), the climate was much warmer than at the start of Core A, but the transition to a full Holocene climate had yet to occur. This is reinforced by the WMAT –derived mean annual temperature for the subzone, which increased 2°C from zone ES 8 to around 10°C, but was still *c.* 1.2°C cooler than the present-day MAT.

---

<sup>33</sup> In addition to achieving permanent dominance on sites unfavourable to climax forest (sites too wet, dry, cold, windy, infertile or unstable) *Leptospermum* is a seral plant – an early pioneer in succession to forest (Stephens *et al.* 2005). It is a hardy plant, tolerant of high water tables or even submergence (Cook *et al.* 1980), grazing and fire, and produces copious amounts of seed capable of germinating over a wide range of temperatures (Grant 1967). *Leptospermum* exploits soil via its mycorrhizal associations and enhances beech recruitment, since beeches also rely on mycorrhizal associations for the efficient uptake of phosphates and other nutrients (Baylis 1980; Stephens *et al.* 2005).

The small increase in *Leptospermum* relative abundance at this time may be related to mire succession rather than dryland succession in response to disturbance; examination of Core A shows there was no evidence of major volcanic disturbance for this time period (the stratigraphic log shows that only Mahoe B and another pumiceous ash, both  $\leq 2$ cm thick were deposited at this time), nor was there any significant aerosolic quartz accumulation. Higher rainfall may have driven Eltham Swamp's transition from a wooded fen to a wooded bog at this time (McGlone 2009), as signalled by changes to Aquatic and Wetland taxa composition: a reduction in relative abundance of Cyperaceae, *Empodisma*, *Phormium*, and *Myriophyllum* occurred as the mire became less oligotrophic in nature. However, it is difficult to reconcile McGlone's (2009) seral interpretation with evidence of low aerosolic dust inputs, given that an oligotrophic bog by definition relies upon aeolian mineral inputs.

The Eltham pollen record generally shows little or no successional patterns following volcanic ash fall. Although this could be a consequence of sampling at intervals that are too coarse to amplify the pollen signature for successional taxa, this seems unlikely given that the average resolution for much of Core A is around one sample every 75 years, and some sections of the core are sampled contiguously (particularly the LGIT to EHW periods). It seems more likely that only the thickest ash sequences in Core A had any discernible impact on the vegetation assemblage, in common with findings at Kaipō Bog (Newnham & Lowe 2000) and Ahukawakawa Swamp and Potaema Bog (McGlone 1988), with some deposits benefitting primary production (Alloway *et al.* 2007; Clarkson 1990), as discussed in section 5.4.3.

The sharp rise in thermophilous, drought-intolerant *Dacrydium cupressinum* and tree ferns, and concomitant decline in cold-tolerant (*Nothofagus menziesii*, *Nothofagus* subg. *Fuscospora*, Poaceae, *Phyllocladus* and *Halocarpus*) after 15,000 cal yrs BP also occurred at Durham Road on the north-east flank of Mount Egmont (Turney *et al.* 2003). Of particular note at Durham Road was the reversal in the *Prumnopitys taxifolia*: *Dacrydium cupressinum* relationship that mirrors the situation at Eltham, indicating pronounced warming and a reduction in the frequency of droughts.

#### **Subzone ES 9b. 14,600 – 14,300 cal yrs BP ( $\delta^{18}\text{O}$ stage 1, Late Glacial Warm Period)**

- *Nothofagus* and Tree Conifer pollen fell in relative abundance to  $< 45\%$  of the pollen sum: *Nothofagus menziesii* and *Nothofagus* subg. *Fuscospora* remained at low levels ( $< 5\%$  and *c.* 1% respectively); however, *Prumnopitys taxifolia* and *Prumnopitys ferruginea* both increase throughout the subzone, with *Prumnopitys taxifolia* reaching 35% by the top of the subzone. The other conifers all trended downwards, with *Dacrydium cupressinum* decreasing from around 15% to average *c.* 10% for the subzone.
- Other Tree taxa relative abundance remained at similar relative abundance to the previous zone, although *Pseudowintera* increased and *Dodonea viscosa* disappeared from the record.
- Shrub taxa remained at similar relative abundance to the previous zone; *Halocarpus* and *Dracophyllum* reappeared, and *Coprosma* increased in abundance.
- Herb pollen relative abundance increased sharply, with Poaceae comprising 20-35% of the pollen sum.
- All Tree Fern, Ferns and Fern Allies taxa showed an upward trend in subzone ES 9a, increasing in relative abundance to *c.* 50% of the pollen sum.
- Wetland Herbs and Aquatic pollen fell to  $< 10\%$  of the pollen sum; the relative abundance for this group remains around this level for the remainder of Core A.

#### **Interpretation**

Pollen subzone ES 9b represents a decrease in mean annual temperature over the previous subzone, but the cooling is less marked than the temperature decline between zone ES 8 and subzone ES 9a: the pollen transfer

functions imply a MAT of  $< 9^{\circ}\text{C}$  prevailed, a cooling of around  $1^{\circ}\text{C}$  over subzone ES 9a. In addition to being slightly cooler, conditions at this time are likely to have been much wetter than previously, given the large increase in tree fern and fern spores, high abundance of *Prumnopitys taxifolia* and *Prumnopitys ferruginea* and the persistence (albeit at lower relative abundances) of drought-intolerant conifers such as *Dacrydium cupressinum*.

#### **Subzone ES 9c. 14,300 – 12,400 cal yrs BP ( $\delta^{18}\text{O}$ stage 1, Late Glacial Warm Period-LGR?)**

- The *Nothofagus* and Tree Conifer group increased in relative pollen abundance over the previous zone, to reach around 70% of the pollen sum by the top of the zone.
- *Prumnopitys taxifolia* and *Podocarpus totara* each fluctuated between 15% and 25% of the pollen sum; *Dacrydium cupressinum* increased from around 10% to  $> 20\%$  of the pollen sum. Whilst *Prumnopitys ferruginea* and *Dacrydium dacrydioides* decreased slightly at the top of the subzone, *Nothofagus menziesii* and *Nothofagus* subg. *Fuscospora* increased in abundance at the top of the subzone, albeit to low levels.
- Other Tree taxa increased in abundance in subzone ES 9c to around 10% of the pollen sum, mainly driven by an increase abundance of warmth-loving taxa *Griselinia*, *Nestegis* and undifferentiated *Metrosideros*.
- The relative abundance of Shrub taxa averaged around 10% of the pollen sum in this zone; cold-tolerant taxa including *Phyllocladus* decreased in relative abundance, offset by increases in the warm-loving taxon *Myrsine*, before recovering slightly at the top of the zone.
- Herb taxa show a downward trend across the subzone; Poaceae remained the dominant herb taxon but decreased to  $< 20\%$  of the pollen sum.
- Tree ferns, Ferns and Fern Allies increase to  $> 40\%$  of the pollen sum, driven by a rise in monolet spores and the warmth-loving *Cyathea dealbata*.

#### **Interpretation**

Pollen subzone ES 9c marked the start of a long-term trend of relatively constant warming that persisted right through to the Holocene. Temperatures were cooler than present: both the PLS-C2 and WMAT pollen transfer functions indicate that mean annual temperatures were  $> 9.5^{\circ}\text{C}$ , around  $1.7^{\circ}\text{C}$  cooler than present-day MAT, hence Holocene temperatures had not yet occurred. Conditions were likely very wet; the relative abundance of Tree Ferns and Fern spores were the highest level at any time in the core. However, against this general trend of climate amelioration, the upper part of the subzone (and extending into the bottom of pollen zone ES 10) showed some evidence of a period of slight cooling, with a decrease in warm-loving *Dacrydium dacrydioides* and also *Prumnopitys ferruginea* relative to an increase in cold-tolerant *Nothofagus* and *Phyllocladus*. The pollen transfer functions suggest a *c.*  $1.25^{\circ}\text{C}$  decrease in mean annual temperature at Eltham at this time. It should be emphasised that this apparent cooling is very subtle, and within the error bounds of the pollen transfer function model, therefore caution is needed. As a consequence, the apparent cooling may or may not signal the Late Glacial Reversal that occurred in other areas at this time.

#### **Zone ES 10. 12,400 – 10,500 cal yrs BP ( $\delta^{18}\text{O}$ stage 1, LGR? – Early Holocene Warming)**

- The *Nothofagus* and Tree Conifer group continued its upward trend in relative pollen abundance over the previous zone, achieving around 90% of the pollen sum by the top of the zone, the highest level achieved.

- *Dacrydium cupressinum* and *Prumnopitys taxifolia* each increased in relative abundance across the zone, with *Dacrydium cupressinum* increasing from around 30% to > 45% of the pollen sum, and *Prumnopitys taxifolia* comprising between 20% and 25% of the pollen sum for the zone. *Prumnopitys ferruginea* reaches around 20% relative abundance, and *Dacrycarpus dacrydioides* around 8%, by the end of zone ES 10. *Podocarpus totara* fluctuated between 10% and 30% of the pollen sum throughout zone ES 10.
- *Nothofagus* subg. *Fuscospora* and *Nothofagus menziesii* were consistently present, but remained at low levels of relative abundance (1-2%), whilst *Libocedrus* was virtually absent.
- The cold-tolerant Other Tree taxa declined in abundance in zone ES 10: *Plagianthus* decreased to around 2% of the pollen sum, whilst *Pseudowintera*, *Fuchsia* and *Aristotelia* disappeared from the assemblage. In contrast, the abundance of warmth-loving taxon *Ascarina lucida* increased over zone ES 9. Other taxa to decline in zone ES 10 include *Pittosporum* and *Elaeocarpus*.
- The relative abundance of Shrub taxa averaged around 10% of the pollen sum in this zone; all taxa decreased in relative abundance, with the decline in *Coprosma* and *Phyllocladus* being the most dramatic, each falling from around 8% to 2% of the sum.
- Herb taxa show a steady decline from the previous zone, falling to 10% of the pollen sum, the lowest level for the entire core. Poaceae remains the dominant herb taxon.
- The warmth-loving *Cyathea dealbata* decreased from 25% at the start of the zone to 10% of the pollen sum at the end, whereas *Cyathea smithii* spores increased to around 20% of the pollen sum by the end of the zone. The more cold-tolerant *Dicksonia fibrosa* decreased from around 5% to 1% by the end of the zone; in contrast, *Dicksonia squarrosa* increased from around 2% to 12% of the pollen sum.

### **Interpretation**

The period 12,400 – 10,500 cal yrs BP was one of steady warming, as evidenced by the marked decline in the cold climate taxa *Nothofagus menziesii*, *Nothofagus* subg. *Fuscospora* and herb taxa, and only sporadic appearance of *Libocedrus*. The continued rise in relative abundance of the conifers, in particular *Dacrydium cupressinum* and a peak in *Ascarina lucida* abundance give further weight to this interpretation. W-MAT pollen transfer function results suggest mean annual temperatures fluctuated between 9.5°C and the modern mean annual temperature of 11.2°C, although the modern mean annual temperature was seldom exceeded.

Zone ES 10 was also likely wetter, as suggested by the rise in *Dacrydium cupressinum* and *Dacrycarpus dacrydioides*. Higher rainfall continued to drive Eltham Swamp's transition from a wooded fen to a wooded bog at this time as Cyperaceae, *Myriophyllum* and *Gleichenia* continued to decline in relative abundance.

The relationship between *Prumnopitys taxifolia* and *Dacrydium cupressinum* discussed in pollen zone ES 7 is now reversed. Wetter and less drought and frost prone climatic conditions allowed the faster growing, more competitive but less stress tolerant *Dacrydium cupressinum* to out-compete *Prumnopitys taxifolia*, and *Dacrydium cupressinum* became dominant relative to *Prumnopitys taxifolia*. Combined with evidence of sharp declines in *Phyllocladus* and Poaceae, the *Prumnopitys taxifolia* - *Dacrydium cupressinum* relationship leads us to conclude that this period was warmer than the preceding period; further, pollen zone ES 10 was likely to have been considerably wetter than pollen zone ES 8 given the large increase in relative abundance of Tree Ferns (that do not tolerate dry conditions) and Ferns & Fern Allies.

At Durham Road, near Inglewood, *Dacrydium cupressinum* continued to increase in abundance, whilst *Prumnopitys taxifolia* declined; the latter remained the second most abundant taxon for much of the period, until it was supplanted by *Ascarina lucida* as the second-most important taxon after about 12,000 cal yrs BP, and made up around 15% of the pollen sum by 10,950 cal yrs BP (Alloway *et al.* 1992; Turney *et al.* 2003).

The pollen assemblage at Durham Road lacked many of the cold-tolerant taxa that were present earlier, such as *Nothofagus menziesii*, *Nothofagus* subg. *Fuscospora*, Poaceae, *Phyllocladus* and *Halocarpus*. The much lower levels of *Ascarina* at Eltham may indicate that the Eltham coring site was a frost hollow, or was impacted by cold air drainage from the higher ground at the adjacent Ngaere Swamp.

#### **Zone ES 11. 10,500 – 9,750 cal yrs BP ( $\delta^{18}\text{O}$ stage 1, Early Holocene Warming)**

- The *Nothofagus* and Tree Conifer group remains at 85-90% of the pollen sum, but the mix of taxa within the group changes. *Nothofagus* subg. *Fuscospora*, *Nothofagus menziesii* and *Libocedrus* are no longer consistently present, and continue their downward trend to very low levels of relative abundance (1-2%).
- After an initial decline, *Prumnopitys ferruginea*, *Prumnopitys taxifolia* and *Podocarpus totara* increase to reach 10, 20 and 12% of the pollen sum at the top of zone ES 11, respectively. *Dacrydium cupressinum* remains the dominant taxon in zone ES 11, reaching 45% of the pollen sum.
- The Other Tree taxa group continues to show a decline in taxa at the cold-end of the temperature tolerance spectrum, with *Hoheria*, *Plagianthus*, *Weinmannia*, *Pseudowintera*, *Fuchsia* and *Aristotelia* either absent or present only at very low levels. In contrast, *Ascarina* and *Nestegis* are consistently present in zone ES 11.
- Cold-tolerant shrubs are at very low levels (*Phyllocladus*, Asteraceae, and *Dracophyllum*) or absent (*Halocarpus*, *Hebe*) from zone ES 11. The warmth-loving taxon *Myrsine* is only sporadically present, at low levels.
- Herb taxa continue their downward trend in zone ES 11 with Poaceae making up only 5% of the pollen sum by the top of the zone.
- Tree Fern, Fern and Fern Allies abundance decreases in this zone; relative abundance for the most abundant taxon for this group, *Cyathea smithii* comprises <10% of the pollen sum by the end of the zone. Both *Dicksonia fibrosa* and *Dicksonia squarrosa* are close to 0% of the pollen sum by the end of the zone, the lowest level seen throughout the entire core for these taxa.

#### ***Interpretation***

The initial, short decline in relative abundance of conifer pollen may indicate a brief period of cooling before the climate recovered. For zone ES 11 overall, climatic conditions 10,500 – 9,700 cal yrs BP still favour the dominance of *Dacrydium cupressinum* over *Prumnopitys taxifolia*, indicating that conditions were at least as equable as they were in zone ES 10, and likely warmer, given a slight decline in *Ascarina* pollen from this zone, since *Ascarina* prefers cool annual temperatures (*c.* 10°C), and low incidence of both frost (FR = -3°C) and drought, but thrives over a wide range of temperatures (Sakai & Wardle 1978). On balance there are clear signals of Holocene warming, although the pollen transfer data suggests mean annual temperatures were much the same as in the previous zone.

Annual rainfall was likely to have been lower, and/or droughts more common, than ES 10, given the low abundance of Tree Fern and Fern & Fern Allies taxa; at the same time, the low relative abundance of taxa suited to disturbance such as *Libocedrus*, *Coprosma* and *Leptospermum*, suggests that conditions may have been relatively settled during this period.

### 8.1.2. Stent Road

The results of pollen analysis from Stent Road are shown in Figure 42, including all pollen types identified. Three radiocarbon dates and depths are given alongside the diagram, and temperature reconstructions are also shown next to the pollen diagram. The pollen results are described and interpreted for each pollen zone as identified using cluster analysis, along with their associated quantitative temperature reconstructions.

#### **Zone SR 1 >24,730 ± 220 cal yrs BP ( $\delta^{18}\text{O}$ stage 3 Late Glacial Cold Period)**

- The *Nothofagus* & Tree Conifers group is very small, with *Nothofagus menziesii* and *Nothofagus* subg. *Fuscospora* each making up around 1-2% of the pollen sum.
- The Other Trees group is also very small, with *Pseudopanax*, *Griselinia*, *Ascarina lucida*, *Nestegis* and *Metrosideros* all comprising around 1% of the sum throughout the zone.
- Shrubs are the biggest group in SR 1, with *Myrsine* the predominant taxon at >25% of the pollen sum. *Dracophyllum* (15%) and Asteraceae (>10%) are also large components of the pollen sum.
- Herbs comprise 30-35% of the pollen sum, dominated by Poaceae;
- Wetland Herbs & Aquatics are at low levels, with only *Gleichenia* spores present in any number.
- Tree Ferns, Ferns & Fern Allies are also at low levels.

#### ***Interpretation***

The high relative abundance of cold-tolerant shrub taxa, high levels of grass pollen and absence of warmth-loving conifers suggests that temperatures were cool at the beginning of the lignite sequence at Stent Road. The much higher abundance of shrubs relative to the *Nothofagus* and Tree Conifers group and the Other Trees group suggest that the vegetation was recovering from a period of very high disturbance; in addition, the low level of tree fern and fern spores suggests that precipitation was low. The W-MAT pollen transfer function shows that mean annual temperatures were approximately 8°C prior to 24,730 cal yrs BP, whilst the PLS-C2 estimate is around 1°C cooler, at 7°C.

The abundance of ruderal shrub taxa likely represents primary succession following massive disturbance due to the Pungarehu debris avalanche event that was thought to have occurred sometime between 24,730 ± 220 cal yrs BP (Zernack 2008) and 21,440 ± 110 cal yrs BP (current study; refer to section 7.1.2). As discussed in section 7.1.2, the Pungarehu debris-avalanche deposit covered a large area, c. 200 - 250 km<sup>2</sup> with a mean thickness of 30 m (Neall 1979) hence could have potentially inundated and destroyed a large area of extant vegetation, followed by an equally extensive surface available for primary succession to occur.



**Zone SR 2. c. 21,440 ± 110 cal yrs BP ( $\delta^{18}\text{O}$  stage 2 Last Glacial Maximum)**

- The *Nothofagus* & Tree Conifers group remains at low levels; the only notable change is an increase in relative abundance of *Nothofagus menziesii* to > 5% of the pollen sum.
- The Shrubs group increases in abundance in SR 2; Asteraceae doubles in relative frequency to 30% of the pollen sum, whilst *Myrsine* drops to about 10% of the sum. *Halocarpus* appears for the first time.
- Herbs decline in importance as a result of a drop in Poaceae to 20% of the pollen sum;
- Tree Ferns, Ferns & Fern Allies remain at low levels; *Cyathea dealbata* increases in abundance.

**Interpretation**

The slight increase in *Nothofagus menziesii* and moderately cold tolerant shrub taxa Asteraceae and *Dracophyllum*, tempered by an increase in the relatively thermophilic *Myrsine*, indicates that the climate remained cool. Precipitation may have increased slightly given the small increase in tree fern and fern spores, including *Gleichenia*. Disturbance likely remained high during this time.

**Zone SR 3 < 21,440 ± 110 > 18,540 ± 120 cal yrs BP ( $\delta^{18}\text{O}$  stage 2, Last Glacial Maximum)**

- The *Nothofagus* & Tree Conifers group remain at low levels; a short-lived and small increase in *Dacrydium cupressinum* occurs at the start of the zone.
- Shrubs are still the biggest group in SR 3; decreases in Asteraceae and *Dracophyllum* to 20% and 10% of the sum respectively are offset by increases in cold-tolerant *Halocarpus* and *Phyllocladus* to 20% and 18% of the pollen sum respectively.
- Poaceae falls slightly to 15% of the pollen sum.
- Wetland Herbs & Aquatics remain at similar levels, with *Gleichenia* increasing slightly in abundance.

**Interpretation**

The sharp rise in *Phyllocladus* and *Halocarpus*, continuing relatively high levels of Poaceae and decline in *Myrsine* indicates that temperatures were as cool as, if not colder than, previously. The decline in tree ferns and fern spores (from already low levels) suggests that conditions remained dry, and this zone most likely represents the height of the LGM. The W-MAT pollen transfer function data implies that mean annual temperatures remained fairly constant, with temperatures of c. 8°C persisting between 24,730 and 18,540 cal yrs BP, however this likely demonstrates the weakness of the W-MAT technique when there is a lack of modern analogue taxa in the fossil pollen assemblage, and the PLS-C2 may provide a better estimate for this time period at Stent Road.

The PLS-C2 pollen transfer function suggests that mean annual temperatures were as low as 4.5°C. Pollen zones SR 3 to SR 5 compensate for the LGM data gap in the Eltham Swamp record to some extent, bearing in mind the Stent Road site is a coastal site and Eltham Swamp is farther inland, and assuming that the Stent Road PLS-C2 temperature estimate is reliable.

**Zone SR 4 < 21,440 ± 110 > 18,540 ± 120 cal yrs BP  $\delta^{18}\text{O}$  stage 2, Last Glacial-Interglacial Transition)**

- The *Nothofagus* & Tree Conifers group remain at similar levels to zone SR 3;
- Within the Shrubs group *Halocarpus* increases to 35% of the pollen sum; this is offset by a decline in *Phyllocladus* to 8% of the sum.
- Poaceae remains at similar levels to zone SR 3;
- Wetland Herbs & Aquatics increase in equivalent relative abundance, driven by a rise in *Gleichenia*.

**Interpretation**

Conditions remained much as they were in zone SR 3; the continuing increase in *Gleichenia* suggests that the bog conditions were becoming more oligotrophic (mineral poor). The PLS-C2 pollen transfer function indicates that mean annual temperature in pollen zone ES 4 reached c. 4°C, the coldest point in the sequence.

**Zone SR 5 c. 18,540 ± 120 cal yrs BP ( $\delta^{18}\text{O}$  stage 2, Last Glacial-Interglacial Transition)**

- The *Nothofagus* & Tree Conifers group remain at very low abundance;
- Within the Shrubs group *Halocarpus* increases to 45% of the pollen sum; this is offset by the continuing decline in *Phyllocladus* and Asteraceae to < 5% and 15% of the pollen sum, respectively.
- Poaceae decreases to only 10% of the pollen sum, the lowest level throughout the core;
- Wetland Herbs & Aquatics increase in equivalent relative abundance, driven by a rise in *Gleichenia* to its highest relative abundance in the core.

**Interpretation**

The strong decline in *Phyllocladus*, Asteraceae and Poaceae outweigh the increase in *Halocarpus*, suggesting that temperatures were warmer and conditions were more disturbed at the top of the lignite sequence. The PLS-C2 pollen transfer function suggests that mean annual temperature increased by 2°C from the coldest part of pollen zone SR 4 to reach 6°C at the top of the sequence. The persistence of low levels of tree fern and fern spores indicates that dry conditions continued. Disturbance in pollen zone SR 5 likely reflects inundation by the unidentified lahar described in section 7.1.2, especially given that the lignite sequence –lahar boundary is very sharp and abrupt (Figure 27 b), and given that conditions for plant growth had been improving during the LGIT.

### 8.1.3. Okawe Stream

Figure 43 provides the results of all pollen types identified for Okawe Stream. This diagram is a composite of the two Okawe Stream sites, as described in section 7.1.3. Six radiocarbon dates and approximate depths are given alongside the diagram, and pollen results are described and interpreted for each pollen zone as identified using CONISS cluster analysis.

**Zone OK 1. c. 37,000 - 33,670 ± 550 cal yrs BP ( $\delta^{18}\text{O}$  stage 3, Moerangi Interstadial)**

- *Nothofagus* & Tree Conifers comprise 5-20% of the pollen sum across zone OK 1, with all taxa <5%, except for *Dacrycarpus dacrydioides* which is absent from this zone.

- Other Trees are also at low levels, comprising 10-15% of the pollen sum. *Pittosporum*, *Griselinia* and *Metrosideros* are the only taxa present in any number, but all amount to less than 2% of the pollen sum.
- Shrubs are by far the largest group in zone OK 1; cold-tolerant taxa Asteraceae and *Halocarpus* make up around 10% of the pollen sum each, with *Coprosma* and *Leptospermum*-type taxa reaching 10-15% of the pollen assemblage by the top of the zone.
- Herbs make up around 25% of the pollen sum; this group is dominated by Poaceae, with only traces of *Chenopodium* present.
- Wetland Herbs & Aquatics are dominated by *Gleichenia* and *Empodisma*, together making up around 45% of the equivalent relative abundance sum.
- Tree Ferns, Ferns & Fern Allies display low abundance throughout the core.

### **Interpretation**

The climate at Okawe Stream at this time was cool and dry, as indicated by low abundance of warmth-loving, drought intolerant conifers such as *Dacrydium cupressinum* and the tree fern *Cyathea smithii*, and high abundance of cold-tolerant taxa Asteraceae and Poaceae, and to a lesser extent *Halocarpus* and *Dracophyllum*. The high abundance of shrubs, in particular *Leptospermum* -type taxon, and the presence of *Libocedrus* are a successional response to high volcanic disturbance in the form of the Te Namu debris avalanche, as well as a hyperconcentrated-flow deposit at this time.

Both of the pollen transfer functions imply that mean annual temperatures throughout the sequence were very stable, with W-MAT around 7.5°C for the entire sequence, and PLS-C2 around 7°C until the end of pollen zone OK 3. This apparent stability is driven by consistently low abundance or absence of critical taxa (shown in Table 2 and discussed in section 9.1) that are positively correlated to mean annual temperature (that is, warmth-loving taxa) such as *Dacrydium cupressinum*, *Dacrycarpus dacrydioides* or *Metrosideros*, and consistently moderate-high levels of critical taxa negatively correlated to mean annual temperature (cold-tolerant taxa) such as Poaceae, *Halocarpus*, Asteraceae and *Dracophyllum*.

### **Zone OK 2. 33,670 ± 550 – c. 31,000 cal yrs BP (δ<sup>18</sup>O stage 3, Moerangi Interstadial)**

- *Nothofagus* & Tree Conifers remain at low levels; *Nothofagus menziesii* reaches 7% of the pollen sum by the top of the zone, but all other taxa are less than 1% of the sum.
- Other Trees remain at low levels;
- Shrubs make up around 60% of the pollen sum in zone OK 2; Asteraceae and *Coprosma* fluctuate between 10% and 20% of the pollen sum each.
- Herbs fluctuate between 20 and 35% of the pollen sum;
- Wetland Herbs & Aquatics decline in equivalent abundance, driven by falls in *Gleichenia* and *Empodisma*.



### **Interpretation**

The near exclusion of all tall tree taxa, with only low levels of *Nothofagus menziesii* and *Nothofagus* subg. *Fuscospora* remaining, and the rise in Asteraceae and Poaceae, all suggest cooling between 34,000 and 31,000 yrs BP occurred at Okaweū. The high abundance of *Leptospermum* suggests that disturbance remained high. Conditions were likely to have been as dry as they were previously, given the persistence of low values of tree ferns and ferns.

### **Zone OK 3. c. 31,000 – c. 27,000 cal yrs BP ( $\delta^{18}\text{O}$ stage 3, Moerangi Interstadial)**

- Shrubs continue to dominate the pollen assemblage; *Dracophyllum* increases dramatically, rising from 5% to 35% of the pollen sum in zone OK 3. Asteraceae fluctuates between 10% and 15% of the pollen sum, whilst *Coprosma* fluctuates between 20 and 25% of the sum. *Leptospermum* declines abruptly, from as high as 25% of the sum, to negligible levels.
- Poaceae declines to around 20% of the pollen sum.
- Wetland Herbs & Aquatics are at low equivalent abundance, except for *Gunnera* which spikes abruptly mid-zone.

### **Interpretation**

Temperatures are likely to have remained low or slightly improved around 30,000 cal yrs BP, given that cold-tolerant *Dracophyllum* and *Coprosma* strongly increased their relative abundance, whilst taxa that are even more cold tolerant such as *Halocarpus*, Asteraceae and Poaceae either remained unchanged or declined in abundance. Although the environment was likely to have been as arid as it was previously since tree ferns and fern abundance remains low, the abundance of *Leptospermum*-type taxa decreases sharply, suggesting that disturbance is much reduced.

### **Zone OK 4. c. 27,000 - 24,730 $\pm$ 220 cal yrs BP ( $\delta^{18}\text{O}$ stages 3 - 2, Late Glacial Coldest Period Onset)**

- *Nothofagus* & Tree Conifers remain at low levels, as does the Other Trees group throughout much of the zone; *Podocarpus* increases to 12% of the sum at the very top of the core.
- Shrubs increase to around 75% of the pollen sum in zone OK 5; *Halocarpus* declines briefly before increasing to > 50% of the pollen sum whereas Asteraceae, *Dracophyllum* and *Coprosma* decrease to 5%, 8% and 4% of the pollen sum respectively after reaching as high as 20% of the sum.
- Poaceae initially increases, then declines to around 8% of the pollen sum.
- Wetland Herbs & Aquatics remain at low levels, although *Drosera* increases slightly over the previous zone.

### **Interpretation**

The temperature at Okaweū Stream was largely unchanged around 25,000 yrs BP from the previous zone, given the large increase in cold-tolerant *Halocarpus* was offset by a decrease of the same order by Poaceae, and smaller decreases in Asteraceae and *Dracophyllum*. This change in relative abundance between *Halocarpus* and Poaceae in particular drives a 1°C decrease in mean annual temperature for much of pollen zone OK 4 from the previous zone, to 6°C. Precipitation is likely to have remained low, as suggested by the absence of tree fern and fern spores and drought intolerant *Dacrydium cupressinum*, and disturbance over the zone as a whole was likely to have been high given the increase in *Halocarpus*, despite paucity of early succession taxa such as ruderal herbs and *Leptospermum*. The very top of the lignite sequence at 24,730  $\pm$  220 cal yrs BP is sandwiched

between a thin layer of Kawakawa / Oruanui Ash and the Pungarehu debris-avalanche deposit; the Kawakawa / Oruanui Ash may be responsible for the brief hiatus in *Dracophyllum* expansion, sharp fluctuations in the *Halocarpus* curve, and the peak in abundance of pioneering taxa such as Poaceae.

Conditions at Okaweu Stream contrast sharply with those at Eltham Swamp (ES 5) and at Pukaki crater (Sandiford *et al.* 2003), where *Nothofagus* subg. *Fuscospora* and *Nothofagus menziesii* declined in abundance whilst thermophilous conifers increased in relative abundance, suggesting conditions were less equable at Okaweu than more easterly and northerly sites, whilst inferred low rainfall at Okaweu Stream is likely to have been similar to zone ES 5 at Eltham.

#### 8.1.4. Opunake Beach

The pollen diagram from Opunake Beach is provided as Figure 44, including all pollen types identified. Four radiocarbon dates and depths are given alongside the diagram, and temperature reconstructions are also shown next to the pollen diagram. Pollen results are described and interpreted for each pollen zone as identified using cluster analysis, along with their associated quantitative temperature reconstructions.

##### Zone OBS 1. >34,370 ±370 cal yrs BP ( $\delta^{18}\text{O}$ stage 3, Moerangi Interstadial)

- The *Nothofagus* & Tree Conifers group comprises 80% of the pollen sum. The predominant taxa are *Prumnopitys taxifolia* and *Prumnopitys ferruginea*, which make up 35% and 25% of the pollen sum respectively. *Podocarpus*, *Dacrycarpus dacrydioides* and *Dacrydium cupressinum* increase in abundance towards the top of the zone, making up 5-10% of the sum. *Nothofagus menziesii* and *Nothofagus* subg. *Fuscospora* are consistently present throughout the entire core, but at low levels.
- The Other Trees group is very small, with *Macropiper excelsum* occurring at low frequencies (<2%).
- The Shrubs group declines from 70% of the pollen sum to 15% in OBS 1; the most important taxa in this group are *Coprosma*, which declined from a high of >20% of the pollen sum to <10%, *Halocarpus* (30% to 2%), Asteraceae (30% to 2%), and *Myrsine* (18% to 2%). *Phyllocladus* is present at low levels throughout the core.
- Herbs, dominated by Poaceae, decrease from 20% of the pollen sum to zero at the top of the zone OBS 1.
- Wetland Herbs & Aquatics are dominated by *Gleichenia* at the start of the zone and *Empodisma* at the top.
- Tree Ferns, Ferns & Fern Allies are dominated by *Cyathea smithii*, which decreases towards the top of zone OBS 1.



### **Interpretation**

The upward trend in relative abundance of *Prumnopitys ferruginea*, *Prumnopitys taxifolia* and *Myrsine*, along with the decline in cold-tolerant *Halocarpus*, Asteraceae and Poaceae is a strong signal of warming in the oldest lignite zone at Opunake Beach. The PLS-C2 pollen transfer function is likely to provide a better temperature reconstruction for the oldest part of the core, given the lack of critical taxa at this time. Estimated temperature at the start of the lignite sequence is *c.* 6°C, which increases to 8°C at the top of pollen zone OBS 1. A decrease in tree fern and fern spores shows that the initially wet conditions became drier by the top of the zone.

This pollen assemblage and time period is approximately coeval with the assemblage at the top of the Manaia Lignite at Inaha (McGlone *et al.* 1984) which was dominated by *Nothofagus* subg. *Fuscospora*, *Nothofagus menziesii*, *Prumnopitys ferruginea*, and *Dacrydium cupressinum*. McGlone (1985) noted that the pollen assemblage at the top of the Inaha sequence is a shrubland period dated to 38,320 ± 1,310 cal yrs BP which may equate to the (cool) Moerangi Interstadial.

### **Zone OBS 2. >34,370 ± 370 cal yrs BP ( $\delta^{18}\text{O}$ stage 3, Moerangi Interstadial)**

- The *Nothofagus* & Tree Conifers group decreases to 50% of the pollen sum across the zone. A sharp rise in *Podocarpus* and *Dacrydium cupressinum* to 10-15% of the sum is not enough to offset declines in *Prumnopitys taxifolia* (to 12% of the sum), *Prumnopitys ferruginea* (to 10% of the sum) and *Dacrydium dacrydioides* (<5%). *Libocedrus* makes a brief appearance at low levels at the start of zone OBS 2.
- Overall abundance of taxa in the Other Trees group remains low.
- The Shrubs group fluctuates between 30 and 40% of the pollen sum in OBS 2. *Coprosma* consistently comprises more than 8% of the pollen sum. *Dracophyllum*, *Hebe*, and *Phyllocladus* have modest increases across the zone.
- Herbs recover to 20% of the pollen sum.
- Wetland Herbs & Aquatics decline in equivalent abundance, driven by sharp declines in *Gleichenia* and *Empodisma*.
- Tree Ferns, Ferns & Fern Allies increase in equivalent abundance, driven by a strong rise in the abundance of *Cyathea smithii* spores.

### **Interpretation**

A strong rise in *Dacrydium cupressinum*, along with a decline in *Prumnopitys ferruginea* and *Prumnopitys taxifolia* indicates warming; further, the increase in *Dacrydium cupressinum* relative to *Prumnopitys taxifolia* suggests that conditions were wetter, and droughts and frosts were less frequent than before. This conclusion is supported by an increase in *Cyathea smithii*, which is both warmth-loving and drought intolerant. Conditions may have been unsettled, given the slight increase in shrub taxa *Halocarpus*, Asteraceae and *Dracophyllum*, and Poaceae. Both temperature transfer functions show considerable variation throughout zone OBS 2, ranging between 8.5°C and 7°C for modern analogue technique, and 8.2°C to 6.2°C for the partial least squares method.

**Zone OBS 3. >34,370 ± 370 cal yrs BP ( $\delta^{18}\text{O}$  stage 3, Moerangi Interstadial)**

- The *Nothofagus* & Tree Conifers group increases to 60% of the pollen sum across the zone. A sharp rise in *Prumnopitys taxifolia* and *Prumnopitys ferruginea* to 30% and 20% of the sum, respectively, offsets a small decline in *Dacrydium cupressinum*. *Libocedrus* is mostly absent from zone OBS 3.
- *Pseudopanax* and *Pittosporum* show small increases in relative abundance, but overall abundance of taxa in the Other Trees group remains low, and only comprises around 5% of the pollen sum.
- The Shrubs group fluctuates between 30% and 40% of the pollen sum in OBS 3; *Coprosma*, and *Leptospermum*-type taxa show small decreases.
- Herbs remain at around 20% of the pollen sum.
- Wetland Herbs & Aquatics continue to decline in equivalent abundance, again driven by a decrease in both *Gleichenia* and *Empodisma*.
- Tree Ferns, Ferns & Fern Allies continue to increase in equivalent abundance, still determined by a rise in the abundance of *Cyathea smithii* spores.

**Interpretation**

The rise in *Prumnopitys ferruginea* and *Prumnopitys taxifolia* and simultaneous decline in *Podocarpus*, *Dacrycarpus dacrydioides* and *Dacrydium cupressinum* indicates cooling; the transfer functions suggests that temperatures decreased to between 6.5°C (PLS-C2) to 7.5°C (W-MAT) where they remained across the pollen zone. This cooling is accompanied by increases in cold-tolerant shrub taxa *Halocarpus* and Asteraceae and a decline in *Coprosma*. In contrast, warmth-loving *Cyathea smithii* increases; this may indicate that previously, precipitation was more of a limiting factor to *Cyathea* expansion than was temperature, since one would expect this tree fern to decrease in abundance as temperature decreases.

**Zone OBS 4. >34,370 ± 370 cal yrs BP ( $\delta^{18}\text{O}$  stage 3, Moerangi Interstadial)**

- The *Nothofagus* & Tree Conifers group undergoes a sharp decrease to 25% of the pollen sum. All of the conifers decrease in abundance, and now comprise < 10% of the pollen sum each. *Dacrycarpus dacrydioides* declines to very low levels, and *Libocedrus* is still mostly absent from the zone.
- The overall abundance of taxa in the Other Trees group remains low; *Metrosideros* shows a small increase;
- The Shrubs group increases markedly to 65% of the pollen sum in OBS 4, driven by a sharp rise in the abundance of *Leptospermum* and smaller rises in Asteraceae, *Coprosma* and *Myrsine*.
- Herbs remain at around 20% of the pollen sum;
- Wetland Herbs & Aquatics return to similar levels as at the start of zone OBS 3, driven by a recovery in equivalent abundance of both *Gleichenia* and *Empodisma*.
- Tree Ferns, Ferns & Fern Allies decline in equivalent abundance, driven by a halving in relative abundance of *Cyathea smithii*.

### **Interpretation**

Although all conifers decrease in abundance, the fall in *Prumnopitys ferruginea* and *P. taxifolia* is more marked than the decline in *Dacrydium cupressinum*; in addition, the fall in Poaceae, and slight increase in *Coprosma* and *Metrosideros*, all indicate slight warming, although conditions were likely still cool, and droughts were infrequent, as suggested by maintenance of warmth-loving *Cyathea smithii* at high levels. Both pollen transfer functions show very slight (< 0.5°C) warming at this time. The upper boundary for pollen zone OBS 4 was marked by a shower of coarse andesitic tephra (Figure 29).

#### **Zone OBS 5. c. 33,350 ± 460 cal yrs BP ( $\delta^{18}\text{O}$ stage 3, Moerangi Interstadial)**

- The *Nothofagus* & Tree Conifers group continue to decline, making up only 15% of the pollen sum by the top of zone OBS 5. The slight increase in *Nothofagus menziesii* and *Nothofagus* subg. *Fuscospora* is not sufficient to offset the decrease in conifer abundance.
- The Shrubs group remains the dominant group in the pollen assemblage; *Coprosma* and *Leptospermum*-type taxa are the dominant taxa.
- Herbs increase to around 30% of the pollen sum.
- Wetland Herbs & Aquatics return to similar levels as at the start of zone OBS 3, driven by a recovery in equivalent abundance of both *Gleichenia* and *Empodisma*.
- Tree Ferns, Ferns & Fern Allies decline in equivalent abundance, driven by continuing reduction in equivalent relative abundance of *Cyathea smithii*.

### **Interpretation**

The decrease in *Prumnopitys ferruginea* and *Prumnopitys taxifolia* and persistent low levels of *Nothofagus*, along with a slight increase in *Dacrydium cupressinum* and *Coprosma*, indicates slight warming over the previous zone, although again, the climate was likely to have remained cool, and disturbance was high. The rise in tree fern and fern spores points to a wetter climate. Both pollen transfer functions show a gradual upward trend in temperature, reaching 8°C sometime before 25,510 cal yr BP.

The pollen assemblage at Opunake Beach at this time was similar to that at Okaweu Stream (OK 3) and also at Otamangakau canal, Tongariro, and Inaha in south-west Taranaki (McGlone 1985), that is, a shrubland-grassland adapted to cool, disturbed conditions.

#### **Zone OBS 6. c. 25,510 ± 240 cal yrs BP ( $\delta^{18}\text{O}$ stage 3, Late Glacial Coldest Period onset)**

- The *Nothofagus* & Tree Conifers group relative abundance declines to its lowest level, making up only 5% of the pollen sum by the top of zone OBS 6. *Prumnopitys ferruginea*, *Dacrycarpus dacrydioides* and *Libocedrus* are absent from the pollen record in OBS 6.
- The Shrubs group increases to 65% - 80% of the pollen sum. *Asteraceae*, *Coprosma*, *Dracophyllum* and *Myrsine* all increase, to 30, 20, 10 and 8% of the pollen assemblage.
- Herbs remain between 30% and 40% of the pollen sum.
- Wetland Herbs & Aquatics increase in equivalent relative abundance, driven by increases in *Gleichenia* and the appearance of *Gunnera*, *Haloragis* and *Myriophyllum*.

- Tree Ferns, Ferns & Fern Allies decline in equivalent abundance, driven by continuing reduction in equivalent relative abundance of *Cyathea smithii* and also monolete spores. A strong increase in the club moss *Lycopodium varium* occurs in OBS 6.

### **Interpretation**

At first glance, the virtual disappearance of the *Nothofagus* and Tree Conifers and the Other Trees groups, rise in Asteraceae, *Dracophyllum*, *Coprosma*, *Myrsine* and Poaceae, and a decrease in *Cyathea smithii* together indicate cooling, increased aridity, and greater disturbance than previously. However, a cooling inference is supported by neither the PLS-C2 derived temperatures, which remain largely unchanged from the previous pollen zone, nor the W-MAT temperature curve, which increases slightly over OBS 5. Although it was almost certainly windier at this time (section 8.2), the paucity of *C*-selected taxa, in particular the conifers *Dacrydium cupressinum*, *Dacrycarpus dacrydioides*, *Podocarpus* and both *Prumnopitys* species, and abundance of ruderal shrub taxa at the top of the lignite sequence likely reflects severe disturbance that occurred prior to the Pungarehu debris-avalanche deposit that occurred around 24,771 cal yrs BP (Zernack 2008), as described in the Stent Road discussion, above.

## **8.1.5. Kaupokonui Beach**

The pollen assemblage from Kaupokonui Beach is shown in Figure 45, including all pollen types identified. Three radiocarbon dates and depths are given alongside the diagram, and temperature reconstructions are also shown next to the pollen diagram. The pollen results are described and interpreted for each pollen zone as identified using cluster analysis, along with their associated quantitative temperature reconstructions.

### **Zone KB 1. c. 55,000 cal yrs BP ( $\delta^{18}\text{O}$ stage 4, 'Stadial Complex')**

- The *Nothofagus* & Tree Conifers group are a very low proportion of the pollen sum, with only *Nothofagus menziesii* exceeding 5% of the sum, at the top of the zone;
- The Other Trees group is virtually absent;
- Shrubs make up around 50% of taxa in the zone, with the dominant taxon Asteraceae declining from around 50% of the pollen sum at the base of the zone to 20% at the top. *Halocarpus* increases from approximately 2% of the pollen sum at the start of zone KB 1 to 10% of the sum, whilst *Coprosma* appears mid-zone and reaches 15% of the sum at the top. *Myrsine* also increases at the top of the zone, reaching 20% of the sum.
- The Herb group is dominated by Poaceae, which decreases from 40% of the pollen sum at the start of the zone, to 15% at the top;
- Wetland Herbs & Aquatics, and Tree Ferns, Ferns & Fern Allies groups are both at very low levels.

### **Interpretation**

The pollen assemblage at the start of the sequence reflects primary succession that followed inundation by the Otakeho debris avalanche (section 7.1.5): *r*-selected shrub and herb taxa greatly outnumber tree taxa. The persistence of this floral assemblage for the next 7,400 years, long after succession to a climax forest assemblage might have otherwise occurred, implies that conditions at Kaupokonui at this time were cool, as indicated by cold-tolerant *Nothofagus menziesii* outnumbering other tall tree taxa, and in particular high abundance of cold-tolerant shrubs Asteraceae and *Halocarpus*.



The pollen transfer functions indicate that mean annual temperatures were somewhere between 6°C (PLS-C2 estimate) and 7°C (W-MAT estimate). The Kaupokonui site was also likely to have been quite dry, given the paucity of pteridophyte spores. The low number of aquatic and wetland spores is a consequence of the age of the sample, that is, the peat bog that gave rise to the lignites is in its early stages of development.

**Zone KB 2. < 55,000 > 47,600 ± 1,300 cal yrs BP ( $\delta^{18}\text{O}$  stage 3, 'Stadial Complex')**

- The *Nothofagus* & Tree Conifers group remains at very low levels, with *Nothofagus menziesii* decreasing to 1% of the sum.
- The Other Trees group remains at very low levels.
- Shrubs are still the most significant group; *Coprosma* increases to 50% of the sum, whilst *Dracophyllum* and *Hebe* appear for the first time. Asteraceae continues its decline, to 5% of the pollen sum; *Myrsine* also decreases, to <5% of the sum.
- Poaceae increases slightly in relative abundance, from 17% to 25% of the pollen sum.
- Wetland Herbs & Aquatics begin to appear in significant numbers, with Cyperaceae reaching as high as 10% of the equivalent pollen sum, and *Empodisma*, *Phormium* and *Gleichenia* fluctuating around 5% of the equivalent pollen sum.
- The Tree Ferns, Ferns & Fern Allies group remains at low levels.

***Interpretation***

The climate is likely to have warmed slightly, given a decline in cold tolerant shrubs, and a rise in *Myrsine* which is more competitive in a warmer climate. The small rise in ferns indicates a slightly wetter environment than before, whilst the increase in wetland taxa may represent expansion in the wetland area.

The pollen assemblage and inferred climate at Kaupokonui zone KB 2 correlates to Lizzie Bell's zone LB 6, and coeval sites at Lake Poukawa and Lake Omapere where by 55,000 yrs BP temperatures had ameliorated and droughts were very infrequent. At both Lake Poukawa and Lake Omapere (Shulmeister *et al.* 2001; Newnham *et al.* 2004) mixed podocarp-beech forests developed, with thermophilous conifers dominating the pollen assemblages, *Cyathea* spore abundance was high, and Poaceae abundance was low. Overall, a warmer, wetter climate persisted at all three sites than before. Both pollen transfer functions support this to a limited extent; the W-MAT mean annual temperature estimate increased between 0.5 and 1°C to 8°C over pollen zone KB 1, and the PLS-C2 estimate increased around 1°C to 7°C by the top of the pollen zone; in both cases, the inferred temperature increase lies within the error bounds of the estimates, so should be used cautiously.

**Zone KB 3. 47,600 ± 1,300 cal yrs BP ( $\delta^{18}\text{O}$  stage 3, 'Stadial Complex')**

- The *Nothofagus* & Tree Conifers and the Other Trees groups remain at very low levels;
- Shrubs are still the most significant group; although still dominated by *Coprosma*, this taxon declines to 25% of the sum. The relative proportion of all the other taxa in the shrubs group remains remarkably constant, apart from *Dracophyllum*, which disappears from the zone, and *Leptospermum*, which appears for the first time.
- Poaceae continues to increase, rising to 35% of the pollen sum;

- Wetland Herbs & Aquatics remain at similar levels to the previous zone;
- Tree Ferns, Ferns & Fern Allies increase sharply due to an abrupt rise in *Phymatosorus*.

### **Interpretation**

The climate continued to warm, evidenced by further decline in cold-tolerant *Halocarpus* and Asteraceae shrubs and to a lesser extent, declines in *Nothofagus menziesii* and *Nothofagus* subg. *Fuscospora*; conversely, warmth-loving *Coprosma* declined at this time; the pollen transfer function estimates indicate that mean annual temperatures were between 7°C (PLS-C2), and 8°C (W-MAT). The sharp rise in *Phymatosorus* suggests that the environment was wetter than before.

### **Zone KB 4. < 47,600 ± 1,300 cal yrs BP ( $\delta^{18}\text{O}$ stage 3, Moerangi Interstadial)**

- The *Nothofagus* & Tree Conifers group undergoes a sharp rise, making up 55% of the pollen sum by the top of the zone. The most dramatic increase occurs in *Prumnopitys taxifolia*, which increases to 35% of the sum. *Dacrydium cupressinum*, *Dacrycarpus dacrydioides* and *Prumnopitys ferruginea* all comprise >5% of the pollen sum.
- Shrubs decrease sharply in abundance, driven almost entirely by a fall in *Coprosma* from 30% to 5% of the sum.
- Poaceae declines to 15% of the pollen sum;
- Wetland Herbs & Aquatics remain at similar levels to the previous zone;
- Tree Ferns, Ferns & Fern Allies decrease; the sharp fall in *Phymatosorus* is partially offset by an increase in *Cyathea smithii*.

### **Interpretation**

The sharp rise in tall tree conifers and the decline in cold-tolerant shrubs *Phyllocladus*, *Halocarpus* and Asteraceae, and Poaceae all point to climate amelioration, although it was still relatively cool given the abundance of *Prumnopitys taxifolia* is several times greater than the more competitive, warmth-loving *Dacrydium cupressinum* (that is, up to 40% of the pollen sum, vs. 5%). The pollen transfer functions imply that that mean annual temperatures increased slightly, with both PLS-C2 and W-MAT estimates fluctuating between 7°C and 8°C across the pollen zone. Further, the increase in abundance of drought-intolerant tall tree taxa and tree ferns indicate that the climate was almost certainly wetter than previously.

### **Zone KB 5. < 47,600 ± 1,300 > 33,860 ± 330 cal yrs BP ( $\delta^{18}\text{O}$ stage 3, Moerangi Interstadial)**

The *Nothofagus* & Tree Conifers group continues to increase in abundance throughout the oldest part of this zone. All taxa in this group increase, with *Prumnopitys taxifolia* still the most important species, followed by *Prumnopitys ferruginea*.

- Other Trees increase, driven by *Pittosporum* and *Pseudopanax*.
- Shrubs decline slightly across the zone; the large fall in *Coprosma* is partially offset by rises in *Halocarpus* and Asteraceae, and the reappearance of *Dracophyllum*.
- Wetland Herbs & Aquatics remain at similar levels to the previous zone;

- Tree Ferns, Ferns & Fern Allies decrease; the sharp fall in *Phymatosorus* is partially offset by an increase in *Cyathea smithii*.

### **Interpretation**

The stronger rate of increase in abundance of *Prumnopitys ferruginea* relative to *Prumnopitys taxifolia*, and a slight increase in the abundance of *Nothofagus menziesii* and *Nothofagus* subg. *Fuscospora*, the appearance of *Libocedrus* (at trace levels), and an increase in cold tolerant shrubs and Poaceae all indicate a reversal in the climate amelioration that characterised the previous zone. Both pollen transfer function estimates imply a slight cooling of between 0.5°C and 1°C, with a mean annual temperature of 7°C at the top of the pollen zone. Despite being cooler, precipitation remained high as indicated by consistently high tree fern abundance.

### **Zone KB 6. 33,860 ± 330 cal yrs BP ( $\delta^{18}\text{O}$ stage 3, Moerangi Interstadial)**

- The *Nothofagus* & Tree Conifers group declines to around 10% of the pollen sum; the decline is almost entirely driven by a fall in both *Prumnopitys* species.
- Shrubs increase sharply in abundance, driven by increases in Asteraceae from 2% to 15% of the sum; *Halocarpus*, rising from 5% to 35%, and the reappearance of *Dracophyllum*, making up 52% of the sum.
- Poaceae declines to 15% of the pollen sum;
- Wetland Herbs & Aquatics remain at similar levels to the previous zone, with an increase in *Gleichenia* at the top of the core;
- Tree Ferns, Ferns & Fern Allies also remain at similar levels to the previous zone.

### **Interpretation**

At first glance, the climate appears to have been more variable at Kaupokonui at this time than it had been previously, given the partial least squares –derived mean annual temperature varied between 6°C and 8.5°C. Relative abundance of the more thermophilic conifers *Dacrydium cupressinum* and *Dacrycarpus dacrydioides* remain fairly constant, whilst the cold tolerant taxa such as *Nothofagus* subg. *Fuscospora* decline in abundance, indicating that mean annual temperatures were similar, if not warmer than before.

The spike in cold-tolerant *Halocarpus* is more likely driven by disturbance than temperature decrease, given that more warmth-loving shrub taxa such as *Coprosma*, and to a lesser extent *Myrsine*, also increased, and cold-tolerant Poaceae declined in relative abundance. In addition, the pollen transfer functions imply that the warmest temperatures of the lignite sequence prevailed, with mean annual temperatures somewhere between  $\geq 7^\circ\text{C}$  (PLS-C2) and  $\geq 8^\circ\text{C}$  (W-MAT). The disturbance in pollen zone KB 6 is most likely attributable to an hydrological event such as flooding or a changing river channel that transported the fluvial sediment deposits to the site. Inundation by the Rama debris-avalanche deposit, as described in section 7.1.5, has terminated the organic sequence in this part of the core; around 16 m of volcanic material accumulated at Kaupokonui Beach until organic matter was encountered again.

### 8.1.6. Lizzie Bell

The fossil pollen assemblage identified for Lizzie Bell for the period *c.* 80,000 cal yrs BP - *c.* 55,000 cal yrs BP is shown in Figure 46, including all pollen types identified. Three estimated dates from Zernack (2008) and depths are given alongside the diagram, and temperature reconstructions are also shown next to the pollen diagram. The pollen results are described and interpreted for each pollen zone as identified using cluster analysis, along with their associated quantitative temperature reconstructions.

#### Zone LB 1. *c.* 80,000 cal yrs BP ( $\delta^{18}\text{O}$ stage 5a, Otamangakau Interstadial)

- *Nothofagus* & Tree Conifers comprise 80% of the pollen sum at the start of zone LB 1, falling to 45% at the top of the zone. *Dacrydium cupressinum* and *Prumnopitys taxifolia* initially make up 30% of the pollen sum, with *Prumnopitys taxifolia* falling to 7% of the sum by the top of the zone. *Prumnopitys ferruginea* makes up around 5% of the sum, whilst *Podocarpus* and *Dacrycarpus dacrydioides* contribute < 5% to the sum.
- Other Trees are at low levels at LB 1 except for *Syzygium maire*, *Metrosideros* and *Macropiper excelsum* which each make up around  $\geq$  5% of the pollen sum.
- Shrubs make up around 10% of the pollen sum each, with *Halocarpus*, *Coprosma* and *Leptospermum* the dominant taxa.
- Herbs are dominated by Poaceae, with small amounts of *Chenopodium*; this group increases from 10% to 20% of the pollen sum by the top of the zone.
- Wetland Herbs & Aquatics are at low levels, with *Gleichenia* the main taxon.
- Tree Ferns, Ferns & Fern Allies are dominated by *Cyathea smithii*, which decreases from 60% of the equivalent sum to 20% by the top of zone LB 1.

#### Interpretation

High abundance of warmth-loving taxa *Dacrydium cupressinum*, *Prumnopitys taxifolia* and *Cyathea smithii*, and low levels of cold-tolerant shrub taxa and Poaceae show that temperatures at the Lizzie Bell site 80,000 years BP were relatively equable; pollen transfer function estimates indicate that mean annual temperatures were somewhere between 9°C (W-MAT estimate) and 10°C (PLS-C2 estimate) at the top of pollen zone LB 1. High levels of *Cyathea smithii* and monolete spores indicate that moist conditions prevailed at this time, although a decline in these two taxa at the top of the zone suggests that conditions became drier.

Conditions at Lizzie Bell were similar to those at Lake Omapere in Northland (Newnham *et al.* 2004) at this time. A mixed podocarp-beech-*Agathis australis* forest predominated, indicating mild-warm conditions, since it was a mixture of very thermophilous taxa: *Agathis australis* pollen has a strong positive correlation with mean annual temperature ( $r = 0.59$ ; Wilmschurst *et al.* 2007); *Phyllocladus trichomanoides* ( $r = 0.64$ ) and *Ascarina lucida* ( $r = 0.43$ ), and cold-tolerant taxa such as *Nothofagus* subg. *Fuscospora* ( $r = 0.26$ ).

A similar scenario existed at Otamangakau canal: high relative frequencies of *Podocarpus* and *Dacrydium cupressinum* and lower values of *Nothofagus* subg. *Fuscospora* and Poaceae pollen (McGlone 1985) also indicate warm temperatures. Fossil pollen from Manaia (McGlone *et al.* 1984) indicates warmer conditions than the preceding cool climate episode due to the dominance of *Prumnopitys ferruginea* and *Dacrycarpus dacrydioides*; although conditions were still cooler than present, as indicated by the scarcity of other interglacial



taxa. Further, the absence of *Dacrydium cupressinum* in the Manaia Lignite suggests that rainfall in lowland Taranaki was likely to have been lower than present.

### **Zone LB 2. c. 60,000 cal yrs BP ( $\delta^{18}\text{O}$ stage 4, 'Stadial Complex')**

- *Nothofagus* & Tree Conifers decline to 5% of the pollen sum, driven primarily by large decreases in *Dacrydium cupressinum* and *Prumnopitys taxifolia*. In contrast, *Prumnopitys ferruginea* and *Dacrycarpus dacrydioides* remain at similar levels as in LB 1.
- Other Trees increase to 15% of the pollen sum in LB 2 before declining to near zero at the top of the zone. *Syzygium maire* and *Metrosideros* briefly record values of 7-8% of the pollen sum until they decline to near zero.
- Shrubs rise sharply to 90% of the pollen sum by the top of the zone, with *Halocarpus* and Asteraceae making up 60% and 20% of the pollen sum, respectively. *Coprosma* peaks at 40% of the pollen sum mid-zone, before declining to 5% of the sum by 60,000 yrs BP.
- Herbs fluctuate between 10 and 15% of the pollen sum.
- Wetland Herbs & Aquatics are largely absent from zone LB 2, with only *Gleichenia* consistently present at low levels.
- Tree Ferns, Ferns & Fern Allies decline sharply, driven by a strong fall in *Cyathea smithii* to near zero by the top of zone LB 2, and to a lesser extent, a fall in monoete spores, also to near zero.

### **Interpretation**

This zone represents the end of the stadial complex that occurred between the Moerangi and Otamangakau interstadials, and is likely to equate to  $\delta^{18}\text{O}$  stage 4 (75,000 – 60,000 cal yrs BP). Between 80,000 and 60,000 yrs BP temperatures generally declined at Lizzie Bell, demonstrated by the strong decrease in *Dacrydium cupressinum* abundance, along with increased abundance of cold-tolerant shrub taxa *Halocarpus* and Asteraceae, and Poaceae.

Both pollen transfer functions showed decreases in estimated mean annual temperature across pollen zone LB 2, with the W-MAT estimate falling around 2°C to 7°C, and the PLS-C2 estimate falling even more dramatically, to around 5.5°C at the top of the zone. Low levels of drought-intolerant taxa *Dacrydium cupressinum* and *Cyathea smithii*, and a decline in monoete spores indicate that aridity increased at this time.

### **Zone LB 3. < 60,000 > 55,000 cal yrs BP ( $\delta^{18}\text{O}$ stage 3)**

- *Nothofagus* & Tree Conifers decline to very low levels throughout zone LB 3, before recovering to 10% of the pollen sum by the top of the zone.
- Other Trees are virtually absent from the zone; *Plagianthus* and *Nestegis* appear for the first time but at very low levels.
- Shrubs vary between 90% and 60% of the pollen sum; *Halocarpus* decreases from 60% to 20% of the pollen sum, whereas Asteraceae peaks at 40% of the pollen sum before decreasing to 12% of the sum. *Leptospermum*-type taxa and *Leucopogon* are all absent from zone LB 3.

- Herbs reach their peak in zone LB 3, reaching around 30% of the pollen sum.
- Wetland Herbs & Aquatics show a strong rise in relative abundance, driven almost entirely by *Gleichenia*.
- Tree Ferns, Ferns & Fern Allies are virtually absent in zone LB 3.

### **Interpretation**

The lack of tall tree taxa and the high levels of cold tolerant shrubs *Halocarpus* and Asteraceae, as well as high levels of Poaceae and an absence of tree fern and fern spores, implies that the climate was cold and dry; both transfer functions suggest that this period was the coldest period for the entire lignite sequence, with mean annual temperatures between 5.5°C (PLS-C2 estimate) and 7°C (W-MAT estimate) for the entire zone. The low shrub species richness at this time suggests that disturbance was likely to have been low.

### **Zone LB 4. < 60,000 > 55,000 cal yrs BP ( $\delta^{18}\text{O}$ stage 3)**

- *Nothofagus* & Tree Conifers make a dramatic recovery, reaching 85% of the pollen sum. Warm-loving *Dacrydium cupressinum* rises to comprise 60% of the pollen sum, whilst *Prumnopitys ferruginea*, *Prumnopitys taxifolia* and *Dacrycarpus dacrydioides* all increase to nearly 10% of the pollen sum each. In contrast, cold-tolerant *Nothofagus menziesii* and *Nothofagus* subg. *Fuscospora* are virtually absent from the zone.
- Shrubs decline to around 2% of the pollen sum; *Halocarpus*, *Dracophyllum* and Asteraceae fall most dramatically, to almost zero values.
- Herbs steadily decline across zone LB 4, to around 5% of the pollen sum;
- Wetland Herbs & Aquatics decline to very low levels, with the *Gleichenia* contributing the most to the fall.
- Tree Ferns, Ferns & Fern Allies increase dramatically in abundance in zone LB 4, driven by warmth-loving *Cyathea smithii* in particular, and more modest increases in *Dicksonia squarrosa*, monolet spores, and *Phymatosorus*.

### **Interpretation**

The large increase in conifer abundance, in particular *Dacrydium cupressinum*, low values for *Nothofagus* and a fall in abundance of cold-tolerant shrub taxa *Halocarpus* and Asteraceae, and Poaceae all point to a strong recovery in temperatures at this time. Both pollen transfer functions support this inference, with mean annual temperatures increasing between 1.5°C (W-MAT estimate) and 4°C (PLS-C2 estimate) to give an estimated mean annual temperature of between 8.5°C and 10°C, respectively; the W-MAT estimate is likely to be the better estimate given the high representation of critical, modern analogue taxa in this pollen zone. High levels of drought-intolerant taxa *Dacrydium cupressinum* and *Cyathea smithii* indicate a strong return to wet conditions; the high abundance of *Cyathea smithii* is further evidence of increased temperatures at this time.

### **Zone LB 5. < 60,000 > 55,000 cal yrs BP ( $\delta^{18}\text{O}$ stage 3)**

- *Nothofagus* & Tree Conifers decrease to around 45% of the pollen sum; the decline is mostly attributable to falls in *Dacrydium cupressinum* to 15% of the pollen sum, and *Dacrycarpus dacrydioides*

to near zero. In contrast, the more cold-tolerant gymnosperm *Prumnopitys taxifolia* increases to 15% of the pollen sum, and *Podocarpus* increases slightly.

- Shrubs increase to 45% of the pollen sum, driven by a rise in *Halocarpus* to 30% of the sum, and smaller rises in *Dracophyllum*, *Coprosma* and *Myrsine* to around 5% of the sum each.
- Herbs increase to around 10% of the pollen sum.
- Wetland Herbs & Aquatics increase, driven mostly by *Gleichenia* and to a lesser extent, *Astelia*.
- Tree Ferns, Ferns & Fern Allies decrease in abundance, with *Cyathea smithii* falling to 5% of the pollen sum, and *Dicksonia squarrosa* falling to near zero.

### **Interpretation**

The decline in *Dacrydium cupressinum* is most likely a consequence of both decreased precipitation and cooling of the climate, given that other warmth-loving conifers either remain fairly static (*Podocarpus*) or increase in abundance (*Prumnopitys taxifolia*) whilst cold tolerant taxa *Nothofagus* show no change. Although cold-tolerant *Halocarpus* increases, Asteraceae abundance remains unchanged, and Poaceae declines. The pollen transfer functions support a cooling inference at this time, with mean annual temperature decreasing between 1°C and 2°C to reach 7°C at the top of the pollen zone. The decline in *Cyathea smithii* and *Dicksonia squarrosa* indicate dry conditions, as does the reduction in wetland and aquatic taxa. A c. 40 cm thick deposit of coarse andesitic tephra at this time (Figure 31 c) is also likely to have retarded the growth of the tall tree conifers, in particular *Dacrydium cupressinum* and *Dacrycarpus dacrydioides*.

### **Zone LB 6. c. 55,000 cal yrs BP ( $\delta^{18}\text{O}$ stage 3)**

- *Nothofagus* & Tree Conifers recover to around 70% of the pollen sum. *Dacrydium cupressinum* peaks at 35% of the pollen sum, before falling to 15% at the top of the zone. The other tall tree conifers all increase in abundance; *Prumnopitys taxifolia*, *Podocarpus* and *Dacrycarpus dacrydioides* increase to >25%, 10% and 5% of the pollen sum, respectively.
- Shrubs fall to 20% of the pollen sum; *Halocarpus* is still the dominant taxon.
- Tree Ferns, Ferns & Fern Allies remain at low levels; only *Cyathea smithii* exceeds 5% of the pollen sum.

### **Interpretation**

By around 55,000 yrs BP temperatures improved slightly over earlier times; the slight decline in *Dacrydium cupressinum* is again driven partly by drier conditions, as indicated by the low levels of tree ferns and fern spores. In any event, the *Dacrydium* decline is offset by the rise in other warmth loving conifers, and also the decline in cold tolerant *Halocarpus* and Poaceae. Pollen transfer function data supports the idea of a slight warming at this time, with mean annual temperature increasing between 0.5°C (W-MAT estimate) and 1°C (PLS-C2 estimate) to reach between 7.5°C to 8°C by c. 55,000 yrs BP. Pollen zone LB 6 was truncated by the Otakeho debris avalanche followed by coarse channel fill debris-flow deposits and hyperconcentrated-flow deposits that engulfed vegetation at Lizzie Bell. Around 8.2 m of these deposits would have rapidly accumulated before organic material began to accumulate again.

## 8.2. Results of Quartz Analysis of Eltham Swamp

The results of the Eltham Swamp quartz dust grain-size analysis are shown in Figure 48 (concentration of quartz dust,  $\text{g}^{-1} \text{cm}^{-3}$  by size class), Figure 49 (concentration of quartz,  $\text{g}^{-1} \text{cm}^{-3}$  by size class, plus Eltham and Vostok quartz influx  $\text{g}^{-1} \text{cm}^{-2} \text{ka}$ ), Figure 51 (distribution of quartz by size range for individual samples), Figure 52a (distribution of quartz by size range, all samples combined), and Figure 52b (cumulative grain size distribution, all samples combined). Results from other studies used for illustrative purposes include Figure 47 (aeolian mass accumulation rate for marine core E26.1); Figure 50 (dust accumulation rate; and selected pollen curves from marine core P69); Figure 53 (modern Australian dust samples); Figure 54 (quartz grain size and influx at Waitui and Onaero); Figure 55 (dust concentration (dust volume  $10^{-9} \text{g/g}$  ice, and dust influx ( $\text{mg m}^{-2} \text{yr}^{-1}$ ) for Vostok); and Figure 56 (dust particle size distribution for marine cores E39.75 and E26.1).

In general, there is a much greater concentration of quartz per gram of sediment in the Eltham Core A prior to 15,955 cal yr BP than in the Late Glacial- early Holocene, and no quartz was detected in the period 14,860 to 13,909 cal yrs BP (Figure 48); this pattern is also reflected in the influx rate (Figure 49). This compares with Stewart & Neall's (1984) finding (Figure 50) that both aerosolic quartz and biogenic sediments from the marine core P69 accumulated more rapidly during glacial times, with peak accumulation rates since the Kawakawa / Oruanui ash was deposited occurring between 16,200 and 17,900 cal yrs BP, and between 17,900 and 21,900 cal yrs BP (Okareka eruption). Collectively, these proxies all indicate weakening of the zonal wind system.

Eltham quartz grains were mostly confined to  $< 200 \mu\text{m}$  in size, with around 90% of all grains by volume  $< 63 \mu\text{m}$ . The grain size distribution graph (Figure 52a) shows that Eltham had a bimodal grain size distribution, with a primary mode at  $10\text{-}20 \mu\text{m}$  (58.7%) and the secondary mode at  $40\text{-}60 \mu\text{m}$  (23.0%); Figure 52a shows that  $< 5\%$  of grains were  $< 10 \mu\text{m}$ . In contrast, grain sizes at Onaero and Waitui in northern Taranaki (Alloway *et al.* 1992a) were generally smaller with a unimodal distribution; grains were largely confined to  $< 125 \mu\text{m}$  with most grains  $< 63 \mu\text{m}$ . The primary mode at the time of maximum quartz deposition was  $20\text{-}30 \mu\text{m}$ , comprising 40-45% of the quartz dust influx during  $\delta^{18}\text{O}$  stage 2 at Onaero and Waitui, and 30% of the quartz dust influx during  $\delta^{18}\text{O}$  stage 4 at Onaero. Grains  $< 10 \mu\text{m}$  made up 35% of the quartz dust influx at Onaero and Waitui during  $\delta^{18}\text{O}$  stage 2, and 25% of the influx during  $\delta^{18}\text{O}$  stage 4 at Onaero (Figure 54).

The distinct, bimodal grain size distributions seen in Figures 51 and 52a are a consequence of two different deposition mechanisms; coarse grains represent sedimentation, particle agglomeration through impaction, and to a much lesser extent, downward turbulent diffusion (Harrison *et al* 2001) before fallout under gravity (dry deposition) according to Stokes Law; this is shown as a peak at around  $50 \mu\text{m}$  in Figure 52a. In contrast, the finer quartz grain fraction peak represents scavenging by rainfall (wet deposition) by way of incorporation in clouds as cloud condensation nuclei (in-cloud scavenging) or incorporation in rain drops (below-cloud scavenging) (Harrison *et al* 2001), and is shown as a peak at around  $15 \mu\text{m}$  in Figure 52a.

Dust deposited by wet deposition not only has a bimodal size distribution, but the modal sizes are typically smaller than the unimodal, dry fallout dust curves, as seen in Australian-derived dust in Brisbane (Figure 53, Hesse & McTainsh 1999). Although only 10-20% of aerosolic dust is removed by dry deposition, dry deposition is more important for larger grain sizes, and  $\geq 50\%$  of dust proximal to dust storms may be removed by dry deposition (Harrison *et al* 2001). The relative importance of wet and dry deposition is dependent on local meteorological conditions and therefore wet and dry deposition rates can vary substantially in time and space (Harrison *et al* 2001).

As a consequence of these properties, coarse dust fractions typically show an increase in size sorting with distance during dry fallout, therefore dust curves in these circumstances are unimodal and skewed towards the smaller size grains on the size continuum (Hesse & McTainsh 1999). These characteristics are seen in the dust particle-size distribution curves for marine cores E39.75 and E26.1 (Figure 56); the coarse dust component of these mid-and east Tasman cores are both fine-skewed, suggesting gravity fallout. Furthermore, the coarse component has a higher modal value in core E39.75 ( $25\text{-}30 \mu\text{m}$ ) that is more proximal to the Australian source

than core E26.1 with a mode of 19-23  $\mu\text{m}$ . The modal values for Core E26.1 are similar to those obtained by Alloway *et al.* (1992) for  $\delta^{18}\text{O}$  stage 2 at Onaero and Waitui, described above, as well as the Eltham dust profile, although data for marine cores E39.75 and E26.1 is for total dust, not just aerosolic quartz.

There were four main phases of grain size influx at Eltham between *c.* 9,800 and 36,200: (i) from about 9,900 to 12,500 cal yrs BP the modal grain sizes were 10-20  $\mu\text{m}$  and 20-63  $\mu\text{m}$ , both in very low concentrations, and the influx rate was very low, *c.*  $0.1\text{g}^{-1}\text{cm}^{-2}\text{ka}$ ; (ii) 12,500 to 15,100 cal yrs BP there was  $\approx 0$  dust influx; (iii) from 15,100 to 19,400 cal yrs BP, the influx rate trended upwards, reaching a peak of *c.*  $1.0\text{g}^{-1}\text{cm}^{-2}\text{ka}$  at 15,955 cal yrs BP. Modal grain sizes were 20-63  $\mu\text{m}$  and  $> 63\text{ }\mu\text{m}$  at this time; and (iv) between 19,400 and 36,000 cal yrs BP the influx rate fluctuated greatly, ranging between 0 and  $3.3\text{g}^{-1}\text{cm}^{-2}\text{ka}$  (Figure 49), whilst modal grain sizes were 10-20  $\mu\text{m}$  and 20-63  $\mu\text{m}$  (Figure 51).

Four major quartz influx peaks occur at Eltham around 35,675 cal yrs BP, 31,358 cal yrs BP, 21,303 cal yrs BP and 15,955 cal yrs BP, with smaller peaks at 28,364 cal yrs BP and 15,955 cal yrs BP (Figure 49). This compares with three QAR (quartz accumulation rate) peaks at Waitui and only two peaks at Onaero (Alloway *et al.* 1992) between the time the Rotoehu ash was deposited (55,000 years BP) and around the  $\delta\text{O}^{18}$  isotope Stage 1 and 2 transition *c.* 11,000 years BP (Alloway *et al.* 1992; Figure 54). In addition to the generally low quartz accumulation periods after 15,955 cal yrs BP at Eltham, low concentrations of quartz and low influx rates also occurred at 19,394 cal yrs BP, 24,190 cal yrs BP and 32,101 cal yrs BP.

In contrast to the influx signal at Eltham, marine core E26.1 in the eastern Tasman Sea showed dust influxes of  $\geq 0.1\text{g}^{-1}\text{cm}^{-2}\text{ka}$  between 75,000 and 35,000 yrs BP; between 35,000 and 25,000 yrs BP influx climbed to a peak of  $0.7\text{g}^{-1}\text{cm}^{-2}\text{ka}$ , before falling to  $> 0.2\text{g}^{-1}\text{cm}^{-2}\text{ka}$  between 25,000 and 10,000 yrs BP (Figure 56). At Eltham, influx varied between 0 and  $1.75\text{g}^{-1}\text{cm}^{-2}\text{ka}$  between 24,190 and 35,100 cal yrs BP, and peaks 10,000 years earlier than at E26.1, reaching a maximum of  $3.35\text{g}^{-1}\text{cm}^{-2}\text{ka}$  at 36,675 cal yrs BP. Potential reasons for this apparent discrepancy are that Hesse's (1994) record is for all dust, not just quartz dust; since the E26.1 record covers a long time span (350,000 years), it is presented at a coarse level of detail which may obscure fine-scale influx oscillations; and the objections described *supra* for core P69 with respect to fluvial and hemipelagic sediment inputs confounding aerosolic dust proxy records are presumably equally true for E26.1. Further, whereas Eltham is a terrestrial site, E26.1 is distal to terrestrial dust sources.

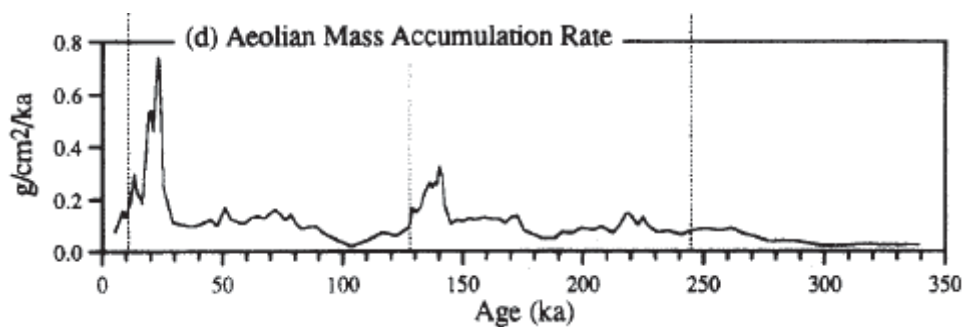


**Figure 47. Aeolian Mass Accumulation Rate for Marine Core E26.1.** Source: Hesse (1994)

At 35,675 cal yrs BP high concentrations of quartz grains in the 10-20  $\mu\text{m}$  range at Eltham coincide with a small QAR peak at Onaero (but not Waitui) ascribed by Alloway *et al.* (1992) to late  $\delta\text{O}^{18}$  Stage 3 (Figure 54). At Vostok, this peak occurs at 35,964 years BP with intermediate amounts ( $241 \times 10^{-9}\text{cm}^3/\text{g}$ ) of quartz accumulating (Jouzel *et al.* 1993) (Figure 55). These relatively low values at Waitui and Vostok and near zero values at Onaero, contrast with both high quartz influx and high quartz concentration at Eltham, where they are the highest, and second highest values recorded in the core, respectively.

At 31,358 cal yrs BP, the high quartz influx rate of *c.*  $1.8\text{g}^{-1}\text{cm}^{-2}\text{ka}$  and high concentrations of quartz grains in the 20-63  $\mu\text{m}$  range at Eltham most likely correlate to small QAR peaks at both Waitui and Onaero ascribed by

Alloway *et al.* (1992) to the end of  $\delta\text{O}^{18}$  isotope Stage 3. At Vostok, this peak occurs at 30,032 years BP ( $283 \times 10^{-9} \text{ cm}^3/\text{g}$ ) (Figure 55).

The 28,364 cal yrs BP sample expresses very high concentrations of 10-20 and 20-63  $\mu\text{m}$  quartz grains. This correlates to a peak at Vostok of  $313 \times 10^{-9} \text{ cm}^3/\text{g}$  (Figure 55), but a short, sharp decline at core P69 (Figure 50) and also a sharp decline at Onaero at the end of  $\delta\text{O}^{18}$  isotope Stage 2 (Figure 54).

The 24,190 cal yrs BP period of low quartz accumulation at Eltham contrasts with a peak in quartz deposits at Onaero and Waitui (Figure 54), coincident with Kawakawa / Oruanui ash deposits a thousand years earlier at  $25,360 \pm 160$  cal yrs BP (Vandergoes *et al.* 2013). At core P69, Kawakawa ash deposits coincide with a static, although relatively high, quartz accumulation rate, prior to the first of the 20-63  $\mu\text{m}$  quartz peaks that coincide with ash deposited by the Okareka eruption, at 22,500 cal yrs BP (Stewart & Neall 1984, Figure 50). Samples to either side of this 'anomalous sample,' (21,303 and 28,364 cal yrs BP), have much higher quartz concentrations; this relationship is also seen at Vostok: the decline in dust influx at Vostok coeval to 24,190 cal yrs BP (that, is, between 23,976 and 24,710 cal yrs BP) was not as dramatic as at Eltham: dust volumes fell to around  $200 \times 10^{-9} \text{ cm}^3/\text{g}$ , from values that were closer to  $600 \times 10^{-9} \text{ cm}^3/\text{g}$  only 1,500 years earlier (Jouzel *et al.* 1993) (Figure 55).

At 21,303 cal yrs BP a high quartz dust influx rate of *c.*  $1.0 \text{ g}^{-1}\text{cm}^{-2} \text{ ka}$  and very high concentrations of grains in the 10-20  $\mu\text{m}$  and 20-63  $\mu\text{m}$  ranges at Eltham are  $\approx$  coeval with the first of the 20-63  $\mu\text{m}$  range peaks at core P69, associated with the Okareka Ash (21,900 cal yrs BP; Figure 50). Although dust concentration was declining at Vostok at this time, values were still high at  $485 \times 10^{-9} \text{ cm}^3/\text{g}$  (Figure 55).

The period around 19,394 cal yrs BP at Eltham marks the boundary between high and low quartz accumulation rates (Figure 49), with an abrupt decrease in quartz dust deposits also seen in offshore cores (Carter *et al.* 2000). Quartz concentration before this time correlates to the largest QAR peaks at Waitui and Onaero (Alloway *et al.* 1992), which occur mid-  $\delta\text{O}^{18}$  isotope Stage 2 (Figure 54); Eltham peak quartz influx correlates to core P69's (Stewart & Neall 1984) 2-5  $\mu\text{m}$  (aerosolic dust) peak sedimentation rate between 19,310 and  $17,900 \pm 200$  cal yrs BP (Rerewhakaaitu tephra), and the last of the 20-63  $\mu\text{m}$  range (loess) peaks (Figure 50). Stewart & Neall (1984) highlight the fact that this time of maximum quartz accumulation occurs after the LGM.

A brief period of increasing quartz influx at 15,955 cal yr BP at Eltham (Figure 49) correlates most closely to a small increase in aerosolic dust at core P69 (Figure 50), and the 15,759 yrs BP peak at Vostok (Figure 55); this short-lived pulse is less obvious at either Waitui or Onaero (Figure 54).

Eden & Hammond (2003) state that between the end of the LGM and the beginning of the Holocene a 5,000 year period of rising sea levels and reforestation reduced dust sources (by flooding the current continental shelf) and reducing erodibility of mineral fines. This implied dust hiatus is seen at Eltham from 14,916 to 9,863 cal yrs BP in general, and 14,478 to 13,466 cal yrs BP in particular (Figure 48 and Figure 49).

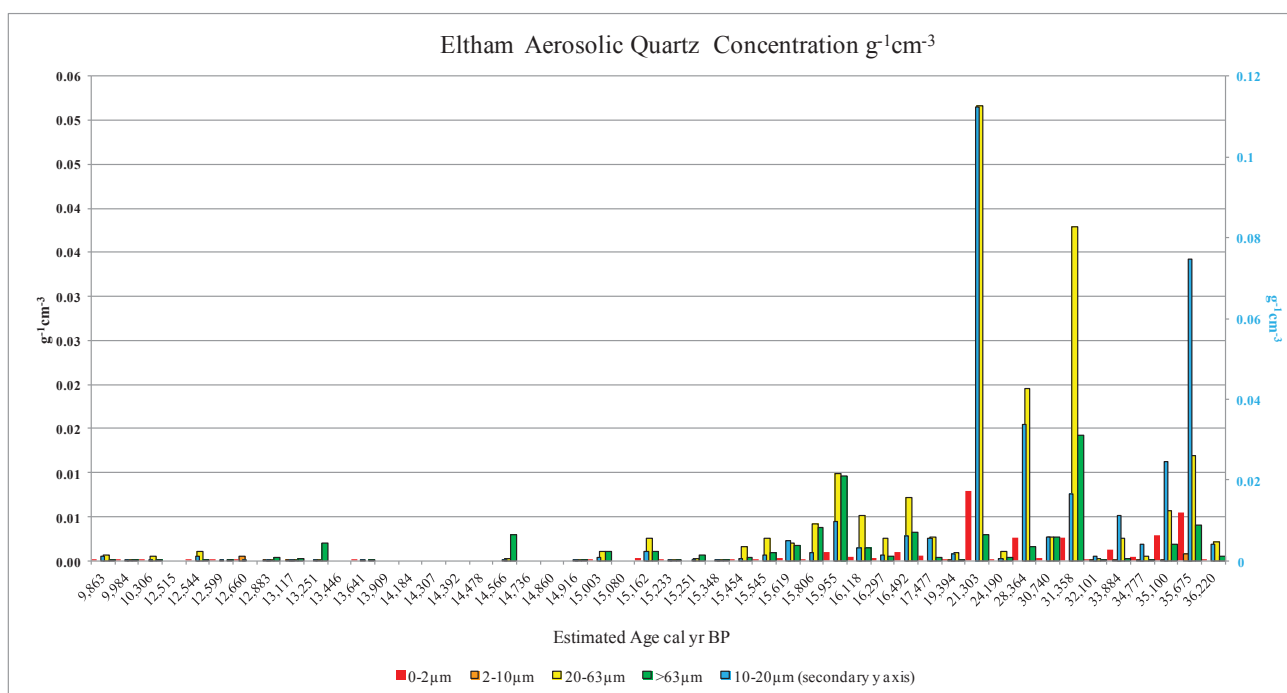
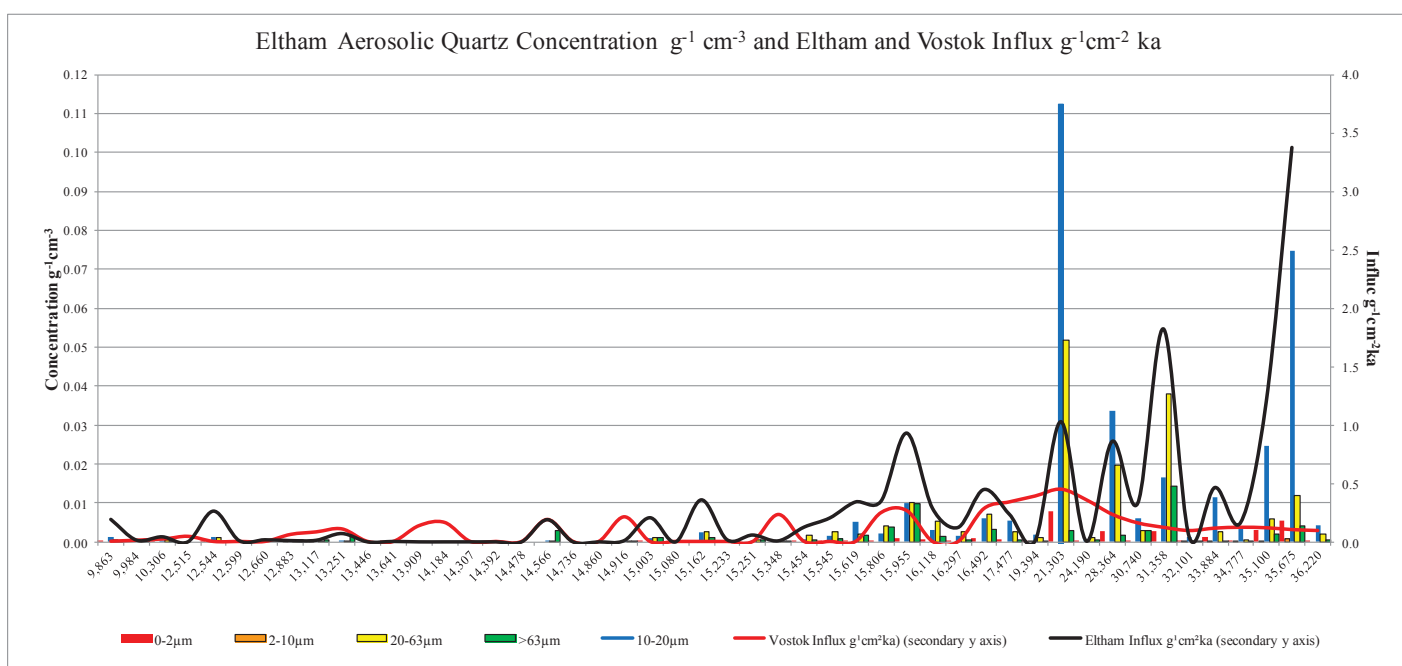
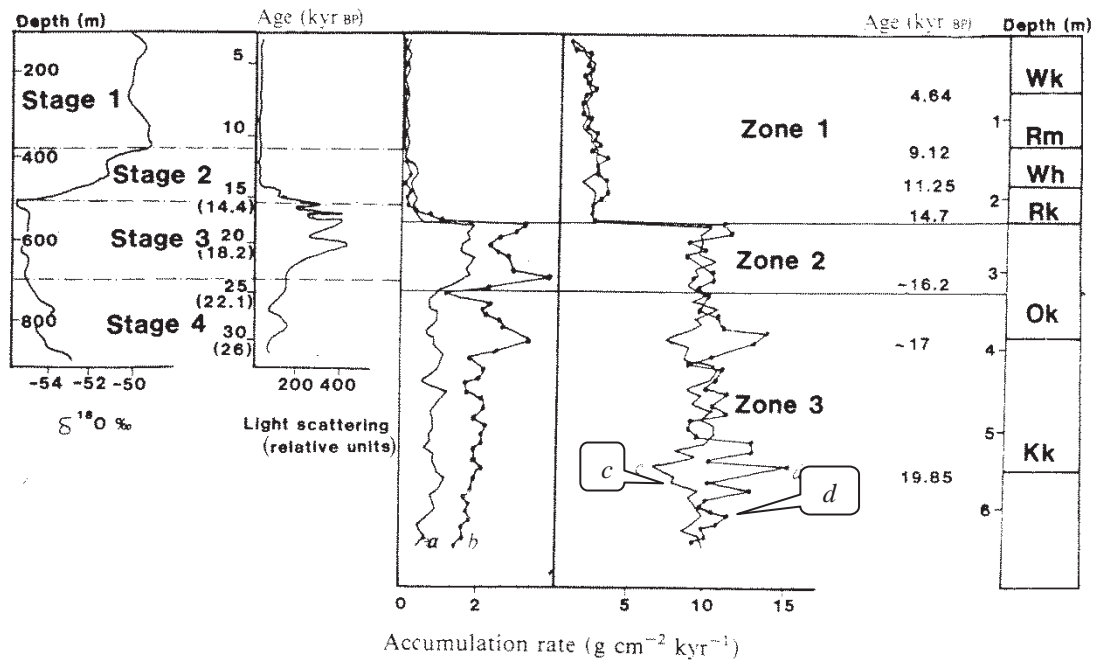


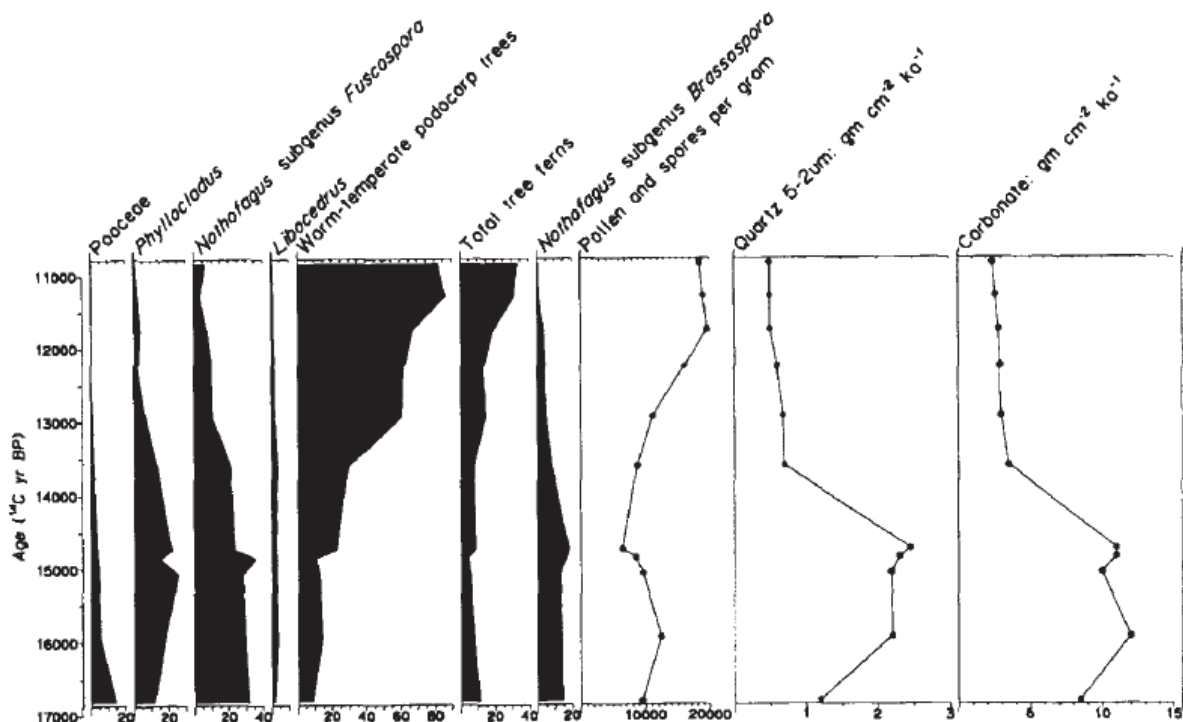
Figure 48. Concentration of quartz  $\text{g}^{-1}\text{cm}^{-3}$  of sediment by size class, Eltham Swamp. No quartz was detected at 12,515; 13,446; 13,909; 14,184; 14,307; 14,392; 14,478; 14,736; 14,860; and 15,080 cal yr BP.



**Figure 49. Eltham Quartz Concentration  $\text{g}^{-1} \text{cm}^{-3}$  and Eltham and Vostok Influx  $\text{g}^{-1} \text{cm}^2 \text{ka}$  for.** No quartz was detected at 12,515; 13,446; 13,909; 14,184; 14,307; 14,392; 14,478; 14,736; 14,860; and 15,080 cal yr BP. Note that 10-20  $\mu\text{m}$  grains are now plotted on the primary y axis.

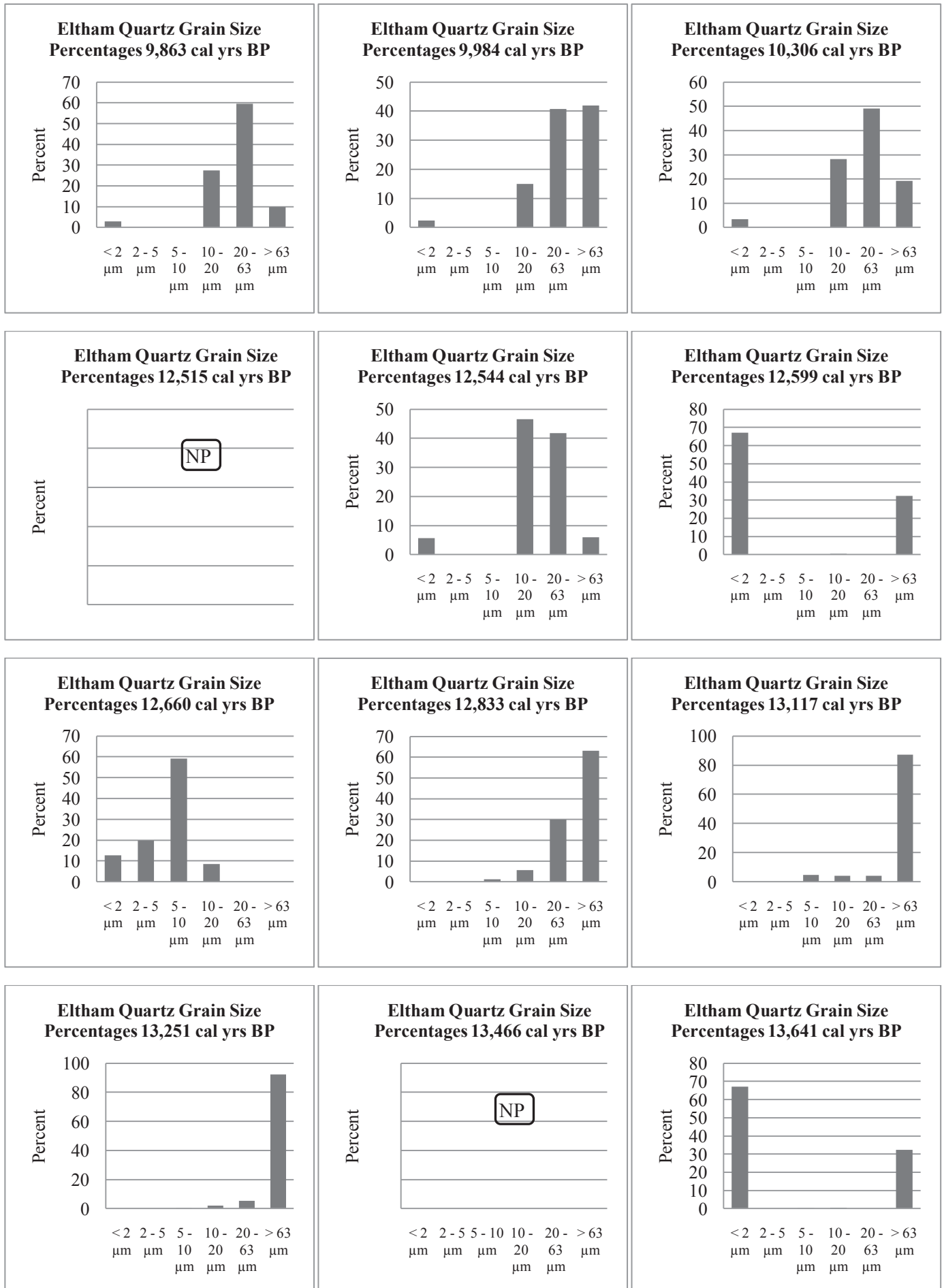


**Figure 50 (a). Dust Accumulation Rates from Marine Core P69.**  $\delta^{18}\text{O}$  and microparticle (from light scattering in relative units) are from Dome C ice core *a* = quartz dust 2-5 $\mu\text{m}$ ; *b* = quartz dust 20-63  $\mu\text{m}$ ; *c* = biogenic silica; *d* = carbonate. Zone 1 = post glacial sedimentation; Zone 2 = period of accelerated erosion at the end of the last glaciation; Zone 3 = sedimentation during last glaciation itself. Wk = Whakatane Ash; Rm = Rotoma Ash; Wh = Waiohau Ash; Rk = Rerewhakaaitu Ash; Ok = Okareka Ash; Kk = Kawakawa Oruanui Ash. *Source:* Stewart & Neall (1984)

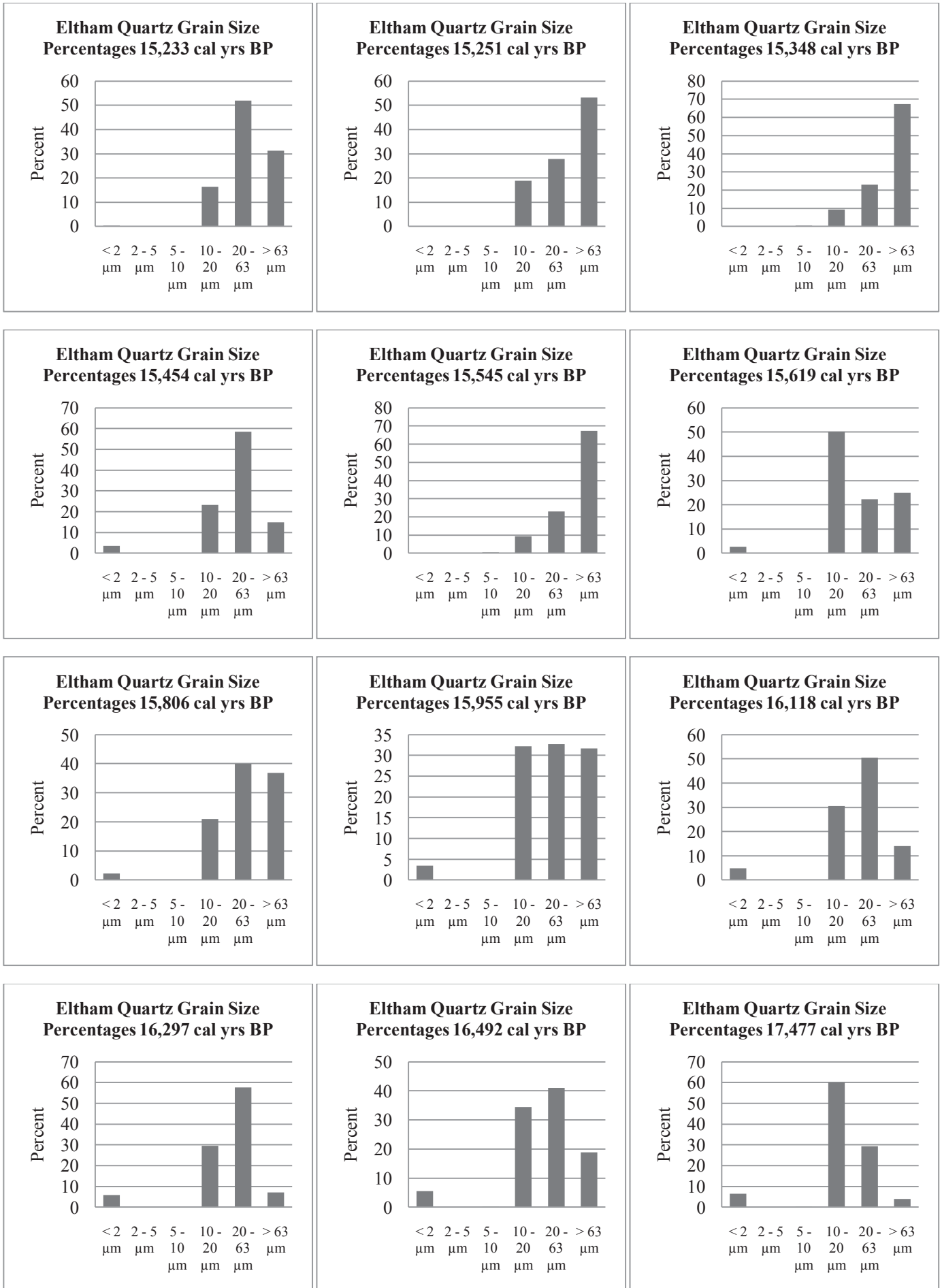


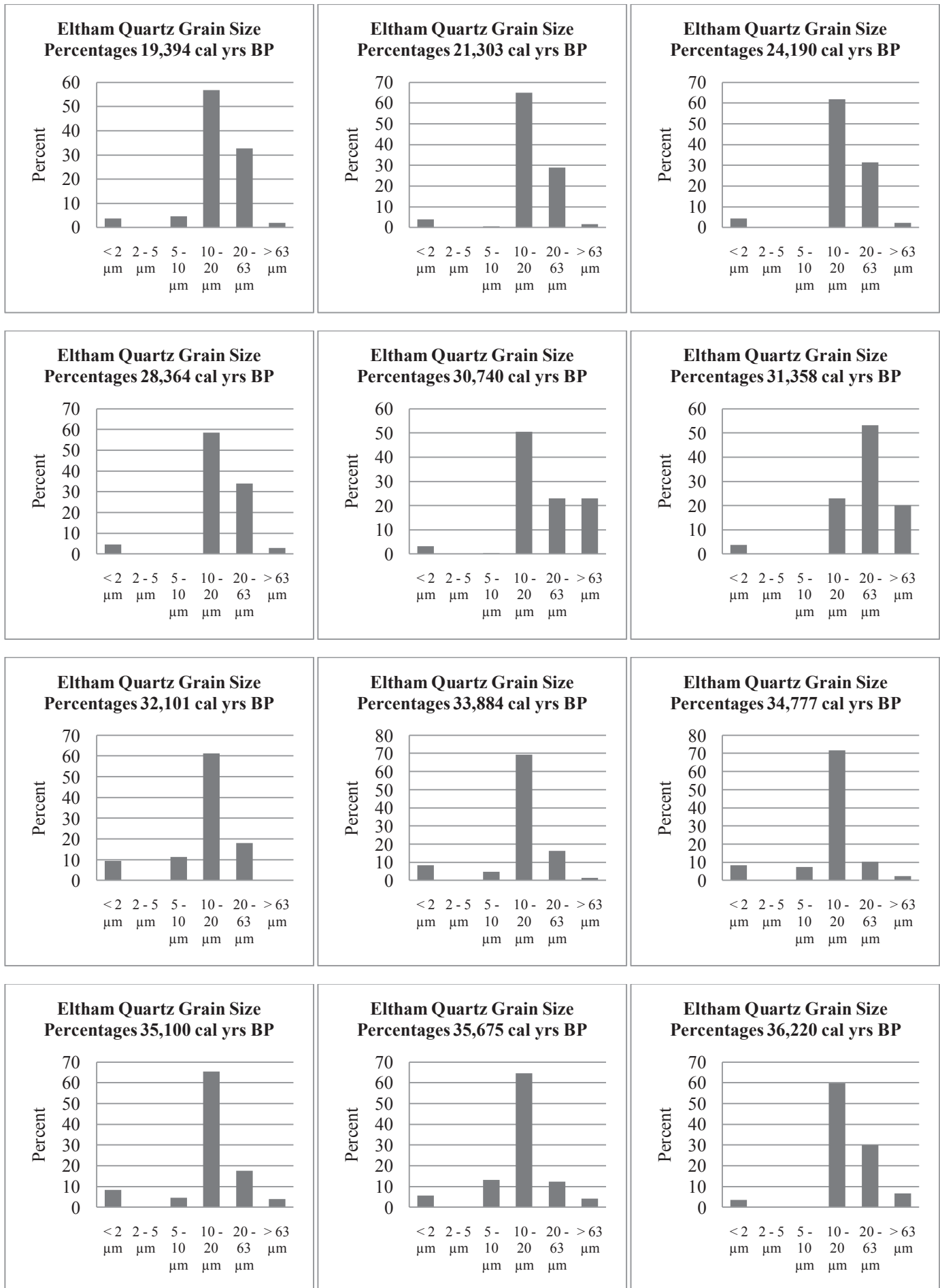
**Figure 50 (b). Dust Accumulation Rates and Selected Fossil Pollen Curves from Marine Core P69.** Diagram plots relative pollen percentages of cold-loving taxa (Poaceae, *Phyllocladus*, *Nothofagus* subg. *Fuscospora* and *Libocedrus*) and warm-loving podocarps against influxes of 2-5  $\mu\text{m}$  quartz and biogenic carbonate (from Stewart & Neall 1984) is shown. *Source:* McGlone (2001).

Figure 51. Eltham Quartz Grain Size Distributions for Individual Samples. NP = no quartz dust present









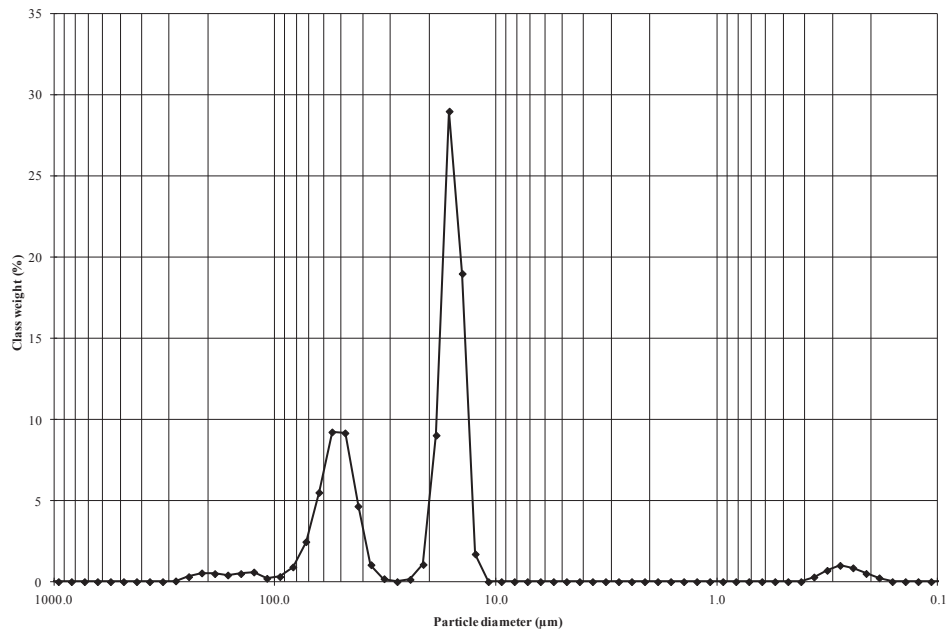


Figure 52(a). Eltham Quartz Grain Size Distribution for all Samples Combined

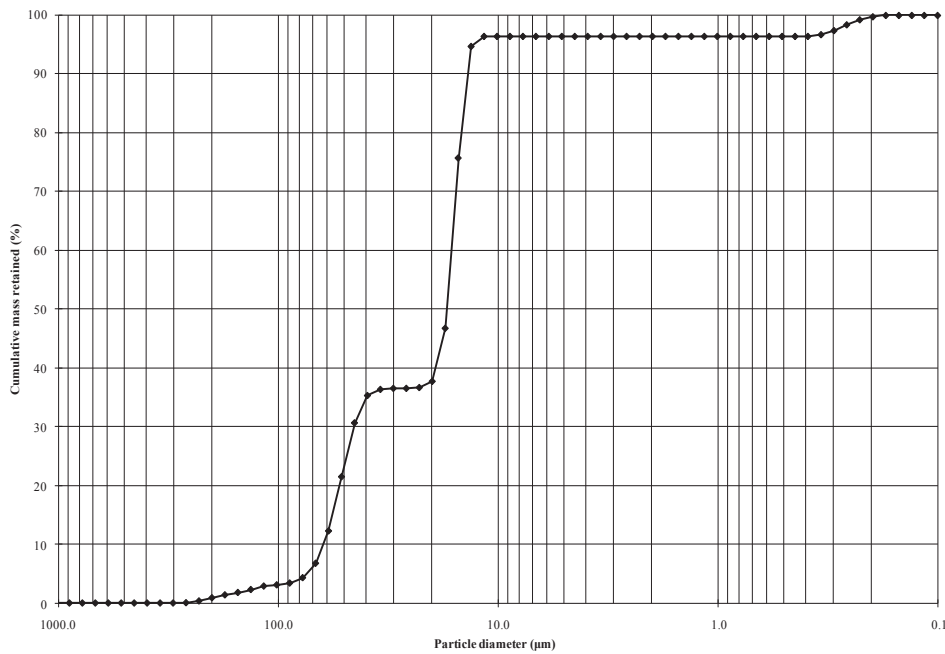


Figure 52 (b). Eltham Cumulative Quartz Grain Size Distribution

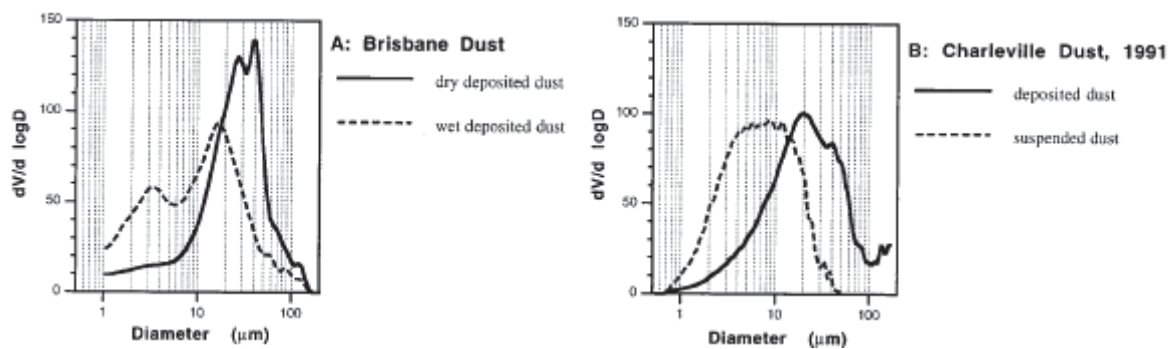


Figure 53. Modern Australian Dust Samples (A) deposited by wet deposition (dashed line) and dry deposition at Brisbane, 1993-1994; and (B) suspended (dashed line) and deposited (solid line) at Charleville, 1991. Source: Hesse & McTainsh (1999)

A High Resolution Record of Late Quaternary Climatic and Environmental Change in Taranaki, New Zealand

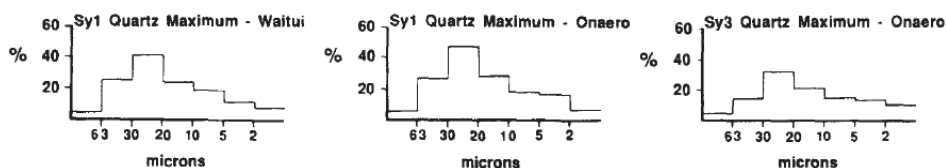


Figure 54 (a). Quartz Grain Size Distribution at Waitui and Onaero, North Taranaki. Source: Alloway *et al.* (1992).

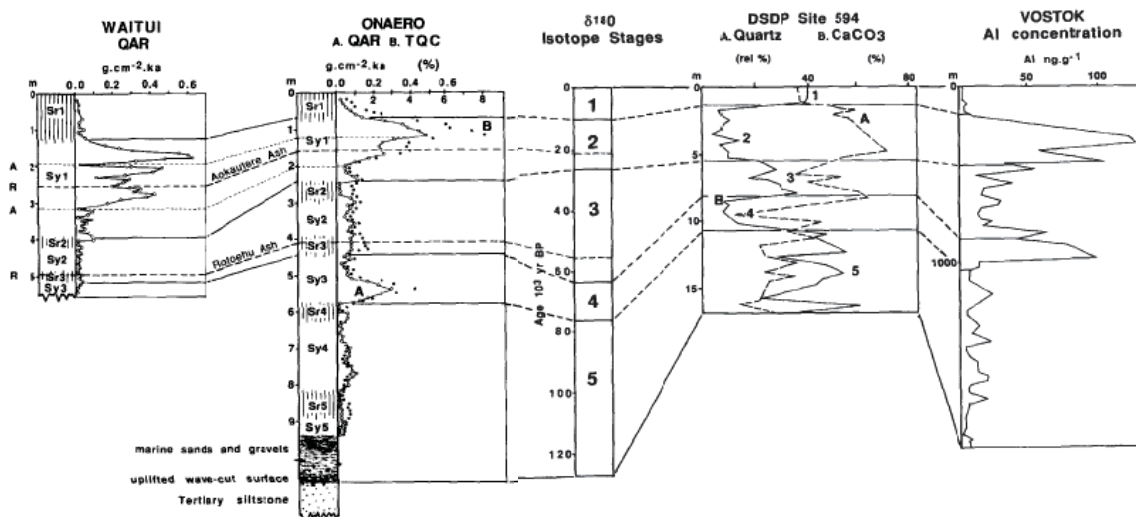


Figure 54 (b). Quartz Influx at Waitui and Onaero, North Taranaki. Column 1: Quartz Accumulation Rate (QAR)  $\text{g cm}^{-2} \text{ ka}$  at Waitui. Column 2: QAR and Total Quartz Content (TQC) % at Onaero. Column 3:  $\delta^{18}\text{O}$  Stage. Column 4: Quartz % and  $\text{CaCO}_3$  % at DSDP Site 594. Column 5: Aluminium concentration  $\text{ng g}^{-1}$  vs depth (m) from Vostok ice core. Source: Alloway *et al.* (1992)

A High Resolution Record of Late Quaternary Climatic and Environmental Change in Taranaki, New Zealand

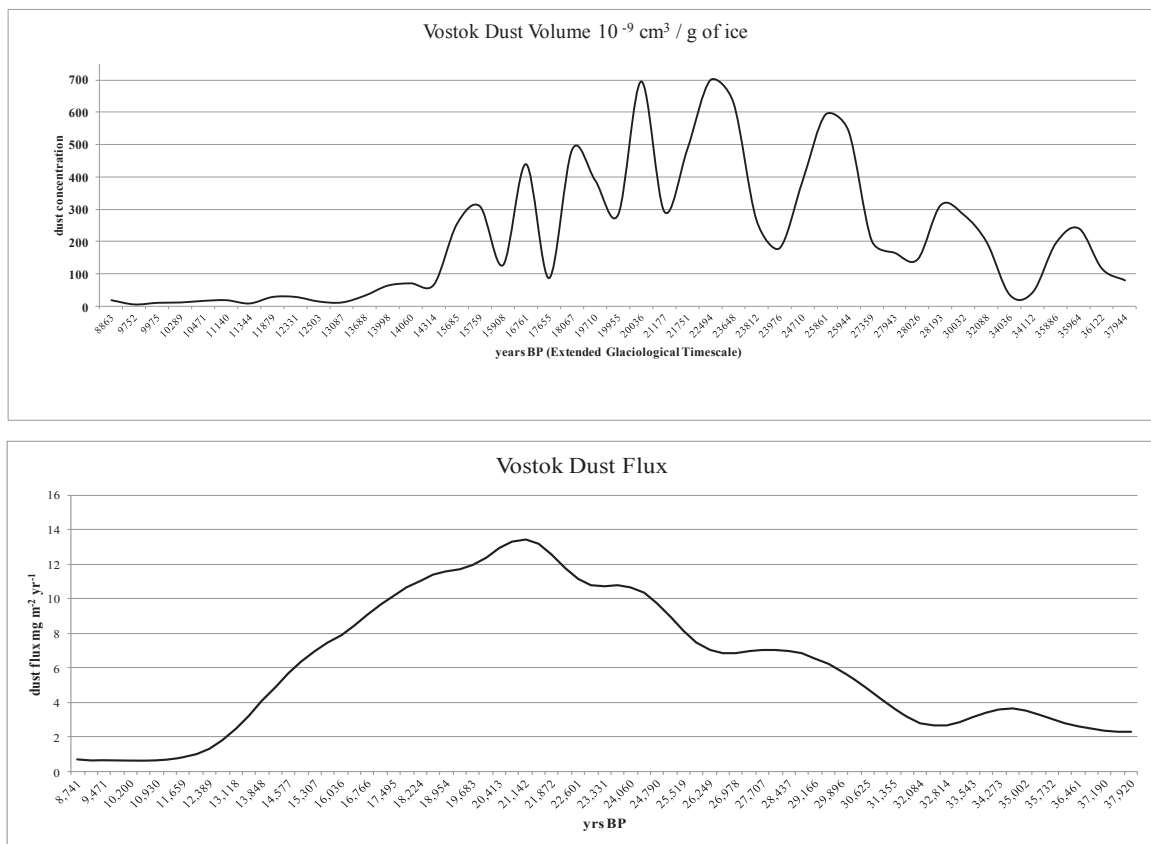
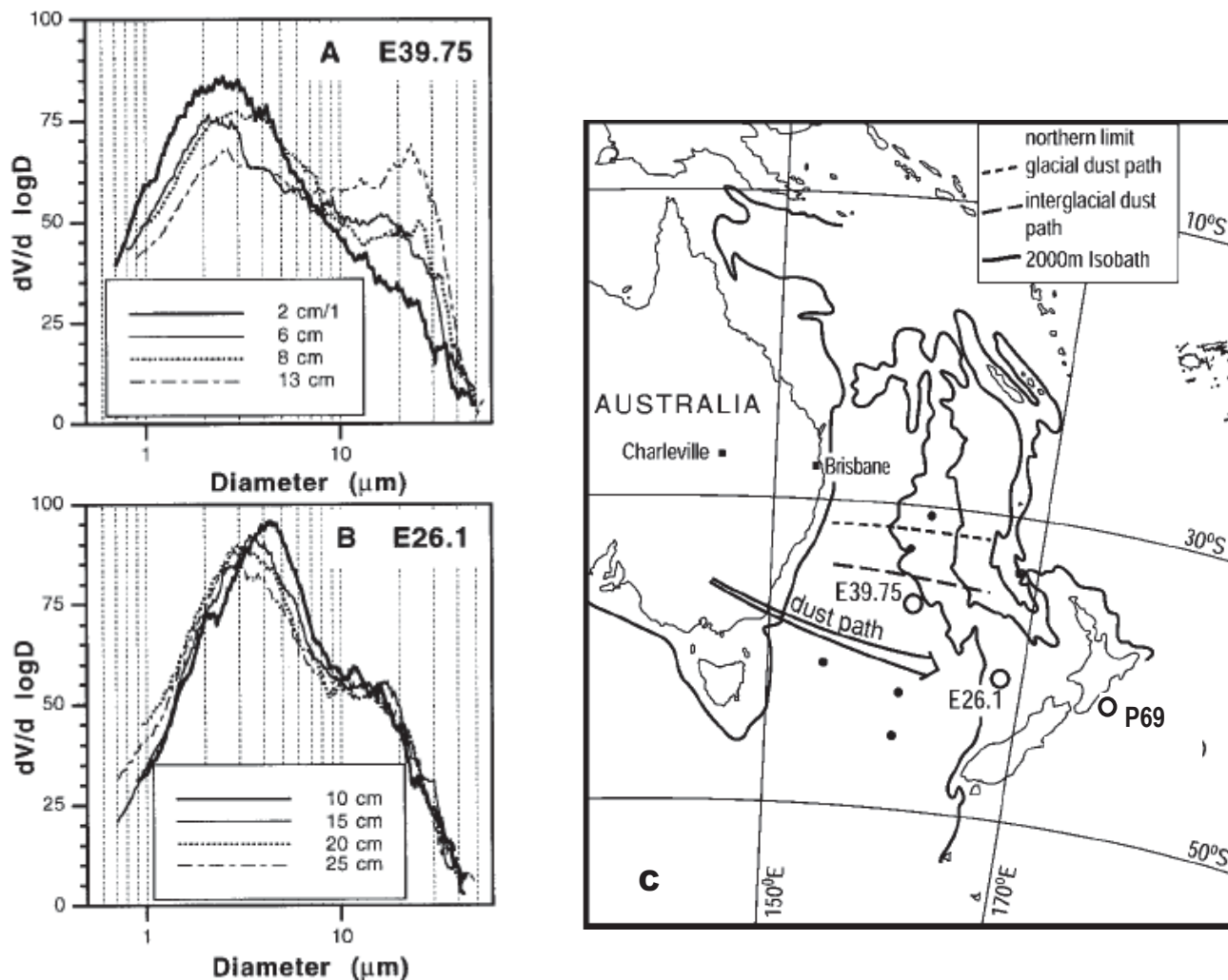


Figure 55. Vostok Dust Concentration and Influx. Source: Jouzel *et al.* (1987)



**Figure 56. Dust Particle Size Distributions from (A) Marine Cores E39.75 and (B) E26.1 and (C) Location Map of E39.75 and E26.1.** Particle size distributions are 7-point moving averages; for (A) depth ranges from 2 cm (7,600 yrs) to 13 cm (19,600 yrs) and for (B) ranges from 10 cm depth (10,000 yrs) to 25 cm (16,500 yrs). Particle size distribution curves are shown by volume density,  $dV/d \log D$  where  $D$  is diameter in  $\mu\text{m}$ . (C) shows the inferred northern limit of glacial and interglacial dust paths (broken lines), also the main core (large arrow) of the dust track from SE Australia to the Tasman Sea; solid circles show locations of previous cores; location of core P69 (Stewart & Neall 1984; McGlone 2001) is also shown. *Source:* Hesse & McTainsh (1999).

### 8.3. Results of Charcoal Analysis of Eltham Swamp

Figure 57 shows that small charcoal grains ( $< 20 \mu\text{m}$ ) generally occur throughout the core, with the exception of a hiatus in charcoal concentration for much of the LGWP between 15,000 and 13,500 cal yrs BP. Peaks in the  $< 20 \mu\text{m}$  charcoal concentration occur during (i) Moerangi Interstadial at 36,500 – 31,000 cal yrs BP, and *c.* 29,000 cal yrs BP; (ii) middle part of the LGIT, *c.* 17,500 cal yrs BP and *c.* 15,000 cal yrs BP; and (iii) the mid- EHW time, *c.* 11,000 cal yrs BP. Peak levels of small-size charcoal grains occur during the mid-LGIT interval around 15,000 cal yrs BP where they reach 5,700 grains  $\text{g}^{-1}$ .

Medium (20-50  $\mu\text{m}$ ) grains are less evenly distributed through the core than small grains, in particular they are less frequent during the Moerangi Interstadial between 36,500 and 33,000 cal yrs BP, and are largely absent throughout the entire LGWP between 15,000 and 13,000 cal yrs BP and the entire EHW interval between 11,250 and 10,000 cal yrs BP. Peak concentration of medium-size charcoal grains also occur during the mid- to late-LGIT interval around 15,500 cal yrs BP where they reach 2,800 grains  $\text{g}^{-1}$ .

Large ( $> 50 \mu\text{m}$ ) charcoal grains were generally restricted to the (i) Moerangi Interstadial at *c.* 40,000 cal yrs BP and 37,500 – 36,500 cal yrs BP; (ii) late LGIT, *c.* 15,500 – 15,000 cal yrs BP; and (iii) the LGR interval, approximately 13,500 - 12,500 cal yrs BP. Peak concentration of large-size charcoal grains also occur during the LGR interval, around 12,750 cal yrs BP where they reach 2,400 grains  $\text{g}^{-1}$ .

The  $< 20 \mu\text{m}$  and 20-50  $\mu\text{m}$  charcoal concentrations in particular appear to match the aerosolic quartz dust concentration: periods of high,  $< 20 \mu\text{m}$  and 20-50  $\mu\text{m}$  charcoal grain influx compare with periods of high or intermediate aerosolic quartz dust concentration for the period 36,500- 31,000 cal yrs BP; 29,000 cal yrs BP and 16,500-15,000 cal yrs BP at Eltham Swamp: strong winds at 35,675 cal yrs BP, 31,358 cal yrs BP and at 21,303 cal yrs BP in particular are indicated by a sharp rise in the quartz dust flux for all dust size particles, but in particular loess-sized grains<sup>34</sup>; intermediate-strength winds occurred between 24,190 and 30,740 cal yrs BP and 15,619 and 17,477 cal yrs BP, as indicated by concentrations  $> 0.015 \text{ g}^{-1}\text{cm}^{-3}$  for quartz dust in the 10-20  $\mu\text{m}$  to  $> 63 \mu\text{m}$  size range and/or influxes  $> 0.4 \text{ g}^{-1}\text{cm}^{-2} \text{ ka}$ ; Conversely, periods of no charcoal in both grain sizes at 15,000-13,500 cal yrs BP, and 11,250-10,000 cal yrs BP for 20-50  $\mu\text{m}$  charcoal grain, equates to periods of very low or nil dust concentration and low influx. An exception to this is the charcoal peak at 11,000 cal yrs BP for  $< 20 \mu\text{m}$  charcoal grains, when there was little or no detectable aerosolic quartz dust at Eltham.

In contrast to  $< 20 \mu\text{m}$  and 20-50  $\mu\text{m}$  charcoal grains whose peaks coincide with high dust flux the  $> 50 \mu\text{m}$  charcoal grain peaks at 15,500-15,000 and 13,500-12,500 cal yrs BP equate to periods of medium-low dust concentration, although the 40,000 cal yr and 37,500-36,500 cal yr peaks fall outside the time range of the aerosolic dust analysis.

---

<sup>34</sup> For 21,303 cal yrs BP concentration of 10-20  $\mu\text{m}$  quartz was  $0.11 \text{ g}^{-1}\text{cm}^{-3}$ , and concentration of 20-63  $\mu\text{m}$  quartz was  $0.05 \text{ g}^{-1}\text{cm}^{-3}$ ; total quartz dust influx was  $1.0 \text{ g}^{-1}\text{cm}^{-2}\text{ka}$ . For 35,675 cal yrs concentration was  $0.06 \text{ g}^{-1}\text{cm}^{-3}$  and  $0.01 \text{ g}^{-1}\text{cm}^{-3}$  respectively; influx was  $3.3 \text{ g}^{-1}\text{cm}^{-2}\text{ka}$ . Concentration of  $> 63 \mu\text{m}$  was  $0.005 \text{ g}^{-1}\text{cm}^{-3}$  for both ages.

LPG Ratio Charcoal Content ( $\log_{10}$  grains  $g^{-1}$ ) W-MAT & PLS-C2 Temperature ( C)

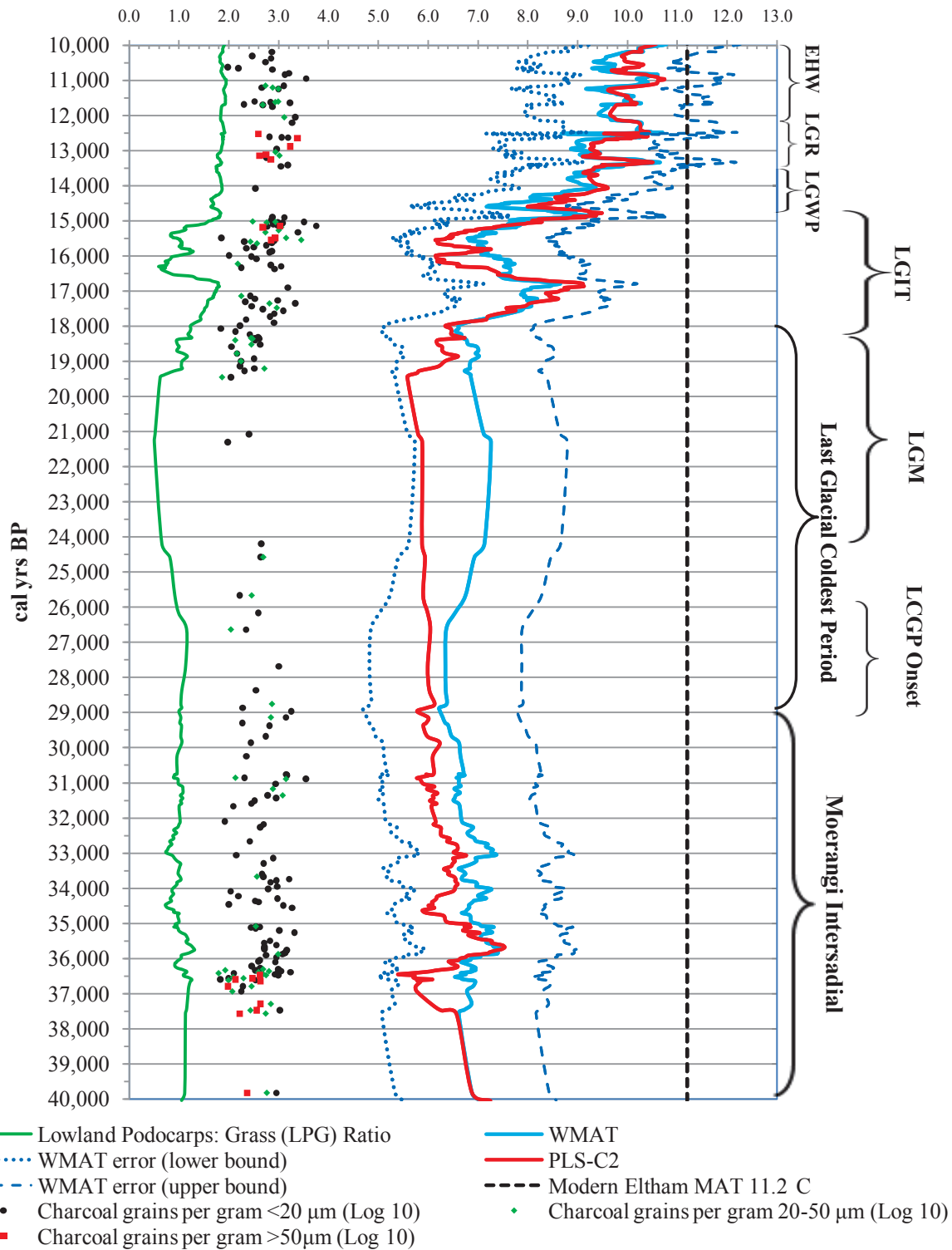


**Figure 57. Eltham Swamp LPG Ratio, Charcoal Concentrations, Temperature Reconstruction and Correlation to NZ Climate Events.** Charcoal numbers are given as  $\log_{10}$  numbers so that they would fit on the same abscissa as the other data.

## 9. Discussion

This chapter integrates results from previous research and the results from the current study. First, pollen transfer functions are discussed (section 9.1), since these drive many of temperature inferences given in section 9.2, Climate Phases and Chronocorrelation. The results of aerosolic quartz analysis and inferences about paleowind patterns are discussed in section 9.3, followed by discussion on charcoal and fire regimes (section 9.4). Finally, the relationship between climate and biodiversity change are discussed in section 9.5.

### 9.1. Pollen Transfer Functions

The Eltham pollen dataset was run through the Wilmshurst *et al.* (2007) transfer function using both WMAT and PLS-C2 models; the resultant temperature curves are shown in Figure 58. The models track each other quite closely; although the WMAT-estimated temperature tends to be 0.6°C to 1.0°C higher than the PLS-C2 temperature from around the time of the mid-Moerangi Interstadial (*c.* 37,500 cal yrs BP) until mid-LGIT (*c.* 18,000 cal yrs BP), highlighting a weakness of WMAT to estimate temperatures when there are no modern or few analogues, as occurred during glacial times. Nevertheless, the PLS-C2 curve remains within the error bounds for WMAT at all times; after 18,000 cal yrs BP the curves converge, with WMAT tending to estimate lower temperatures than PLS-C2, although the difference between the two curves is generally much smaller than before.

Newnham *et al.* (2012) assessed the extent to which the LGM pollen assemblages matched the pre-deforestation dataset to determine how suitable LGM fossil pollen data was for temperature reconstruction; that is, how reliable the modern analogue technique is under differing pollen assemblage scenarios. The measures used were (i) a critical taxa index – the number of taxa that are significantly correlated to mean annual temperature as defined by Wilmshurst *et al.* (2007) (Table 10). According to Newnham *et al.* (2012) this index shows the overlap in floral composition and *diversity* (my emphasis) between fossil pollen and modern analogue pollen; and (ii) the modern analogue index measures the total pollen percentages for critical taxa in the LGM pollen assemblage, thus quantifies the extent to which the LGM pollen spectra can be paired with the critical, pre-deforestation pollen assemblage. Newnham *et al.* (2012) showed that the critical taxa index decreased with latitude, suggesting that temperature reconstruction based on the pre-deforestation dataset is more reliable for northern sites than for southern sites.

Critical taxa and modern analogue indices were calculated to determine whether there is a difference in temperature reconstruction reliability between the various climatic periods at Eltham; these indices are shown in Figures 39 and 41. The critical taxa index (i) increases from around 10 to 15 between pollen zones ES 1 and mid-ES 4 (*c.* 40,000 to 30,000 cal yrs BP); (ii) trends downwards from 15 to < 10 between mid-pollen zone ES 4 and ES 6 (*c.* 30,000 to 19,400 cal yrs BP); (iii) increases to a peak of 20 in pollen zone 7 (*c.* 17,500 cal yrs BP); (iv) trends downwards from 15 to 10 between mid-pollen zone 7 and mid-pollen zone 10 (*c.* 17,500 to 12,000 cal yrs BP); and (v) averages around 12-13 for the top of pollen zone 10 and pollen zone 11 (*c.* 12,000 to 10,000 cal yrs BP). Changes in the modern analogue index shadow the critical taxa index except for (i) pollen zones ES 5 and ES 6 where the index trends upwards from 80% to 95%, (ii) the index falls to 70% in pollen zone ES 7; and (iii) pollen zones ES 9 and ES 10 where the index trends upwards from 60% to >80%.

This implies that based on the critical taxa index only, we can be generally more confident of modern analogue technique-derived temperature estimates in the mid-Moerangi Interstadial and mid-LGIT climate periods, but less confidence in temperature estimates for the late-Moerangi Interstadial to LGCP climate periods, late-LGIT to LGWP climate periods, and least confidence in estimates for the LGR and EHW climate periods, where there are fewer of Wilmshurst *et al.*'s (2007) critical taxa to compute a mean annual temperature. However, some confidence can be restored in modern analogue technique-derived temperature estimates for the LGCP, LGWP and LGR climate periods based on the modern analogue index, where the index is trending upwards, and > 80% of the enumerated taxa are critical taxa. This leaves the late-Moerangi Interstadial, late-LGIT and Holocene

climate periods where both the critical taxa and modern analogue indices are trending downwards, and comprise either < 10 critical taxa or have pollen sums comprised of < 80% critical taxa, respectively; on balance, we should interpret modern analogue technique-derived temperature estimates for these climate periods with caution.

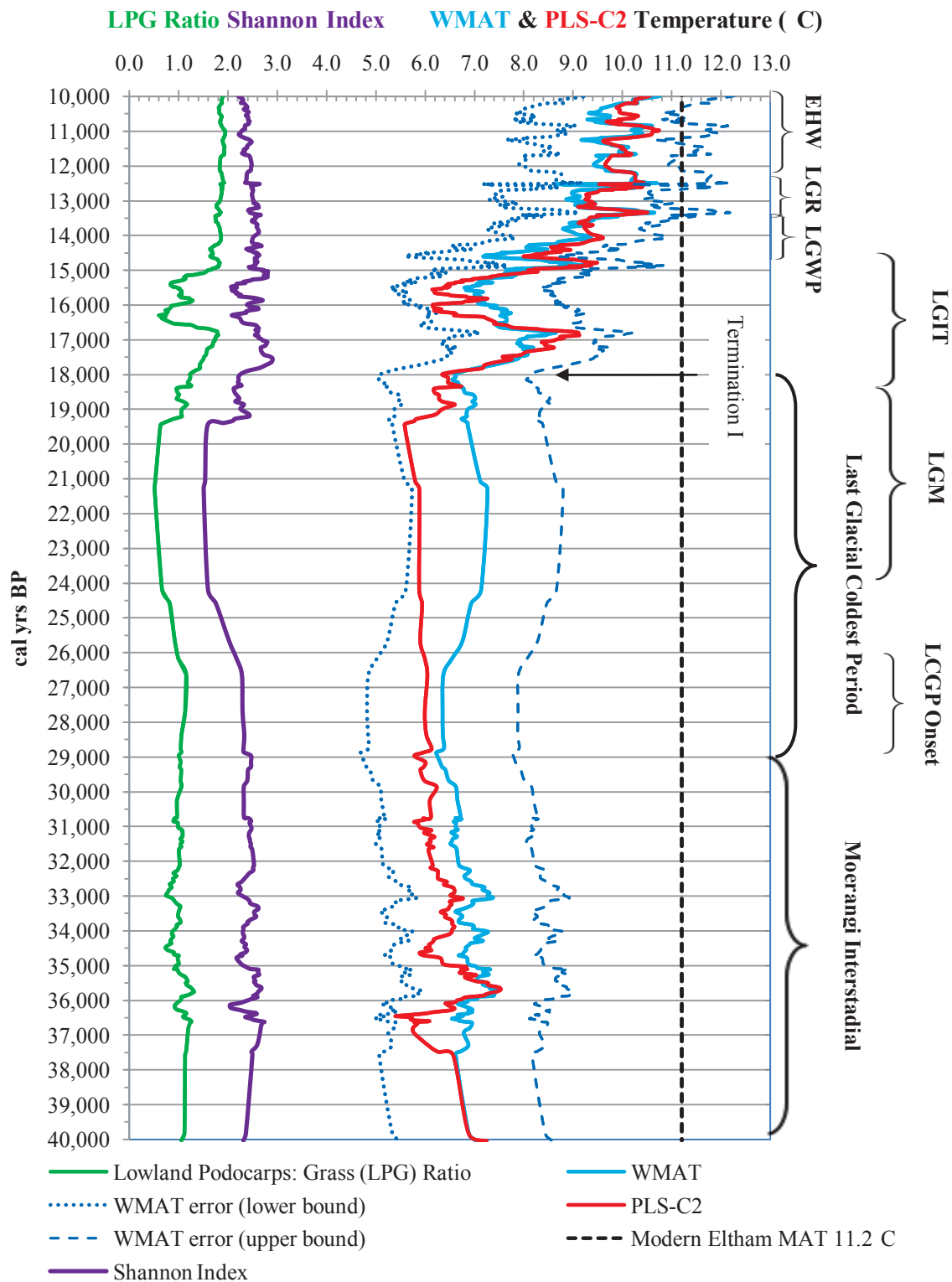


**Figure 58. Eltham Swamp LPG Ratio, Shannon Index, Inferred Temperature and Correlation to NZ Climate Events.**

## 9.2. Climatic Phases and Chronocorrelation

The purpose of this section is to synthesise the coastal Taranaki pollen results and inferred climate change from the individual sites described in section 8.1 into a composite chronological framework for Taranaki for the period 80,000 to 30,000 yrs BP, and compare these results to vegetation and climate histories from other, coeval areas in New Zealand (section 9.2.1). In addition, Eltham Swamp fossil pollen, aerosolic quartz dust and biodiversity data, along with inferred climate data, are compared to other, coeval areas in New Zealand and the NZ-INTIMATE climate event stratigraphy for the period 30,000 to 10,000 cal yrs BP. Combining paleovegetation records and paleoclimate data from all six sites gives a vegetation and climate history for Taranaki spanning 70,000 years, from 80,000 to 10,000 yrs BP (Table 9, and section 9.2.2).

### 9.2.1. Regional Taranaki Climate 80,000 – 30,000 yrs BP

#### $\delta^{18}\text{O}$ stage 5a

Warm temperatures inferred from fossil pollen assemblages at a number of western North Island sites are indicative of the warm Kaihuhu Interglacial – Otamangakau Interstadial (after McGlone 1985) or  $\delta^{18}\text{O}$  stage 5a. Warm conditions were also implied by  $\delta^{18}\text{O}$  –derived sea surface temperatures from core SO136-G3, extracted off the West Coast, South Island; SSTs at the  $\delta^{18}\text{O}$  stage 5b/ stage 5a boundary were equal to present, although SSTs trended downwards across  $\delta^{18}\text{O}$  stage 5a to end 3°C to 4°C cooler than present (Barrows *et al.* 2007).

The Lizzie Bell fossil pollen assemblage (current study) was dominated by warmth-loving taxa including *Dacrydium cupressinum*, *Prumnopitys taxifolia* and *Cyathea smithii*, and low levels of cold-tolerant shrub taxa and Poaceae. The inferred equable climate is supported by the pollen transfer function estimates that indicate that mean annual temperatures were between 9°C (W-MAT estimate) and 10°C (PLS-C2 estimate). Further, abundant *Cyathea smithii* and monolete spores indicate that moist conditions prevailed c. 80,000 yrs BP.

Other western North Island sites experienced similar, warm and wet conditions during  $\delta^{18}\text{O}$  stage 5a; at Airedale Reef, near Waitara (Newnham & Alloway 2004) the fossil pollen assemblage was dominated by *Dacrydium cupressinum*, *Prumnopitys*, *Dacrycarpus* and *Podocarpus*, with *Dacrydium* becoming the dominant taxa at the at this time. McGlone (1985) reported high relative frequencies of *Podocarpus* and *Dacrydium cupressinum* and lower values of *Nothofagus* subg. *Fuscospora* and Poaceae pollen at Otamangakau canal; and fossil pollen from Manaia Lignites at Inaha (McGlone *et al.* 1984) also indicated warmer conditions than the preceding cool climate episode due to the dominance of *Prumnopitys ferruginea* and *Dacrycarpus dacrydioides*; although conditions were still cooler than present, as indicated by the scarcity of other interglacial taxa.

The warmer interstadial climate that persisted 80,000 years ago appears to have been widespread across New Zealand, since conditions at distal locations including Lake Omapere in Northland (Newnham *et al.* 2004) and Okarito, West Coast South Island (Vandergoes *et al.* 2005; Shulmeister *et al.* 2001) were similar to those at Lizzie Bell. Lake Omapere forests comprised of very thermophilous taxa *Agathis australis* (correlation to mean annual temperature = 0.59; Wilmshurst *et al.* 2007); *Phyllocladus trichomanoides* and *Ascarina lucida*, and also cold-tolerant taxa such as *Nothofagus* subg. *Fuscospora* indicate a mixed podocarp-beech-*Agathis australis* forest predominated, implying a mild-warm climate. The Okarito pollen assemblage during  $\delta^{18}\text{O}$  stage 5a was dominated by *Dacrydium cupressinum*, with moderate levels of cold-tolerant *Halocarpus* and *Coprosma*, low levels of Poaceae and *Cyathea smithii*, and very low levels of *Nothofagus* subg. *Fuscospora* (Table 11). This pollen assemblage indicates a mild climate, warmer than  $\delta^{18}\text{O}$  stage 5b but not as warm as modern day conditions; and in contrast to Lizzie Bell, drier than present.

A High Resolution Record of Late Quaternary Climatic and Environmental Change in Taranaki, New Zealand

**Table 11. Comparison Between Inferred Climate at Taranaki and Other New Zealand Sites 10,000 - 80,000 cal yr BP**

kyr BP	Climate Phase	$\delta^{18}O$ Stage	Eltham (present study)	Stent Road (present study)	Okawe Stream (present study)	Opunake Beach (present study)	Lizzie Bell (present study)	Kaupokonui Beach (present study)	Otamangakau Canal (Turney <i>et al</i> 2003)	Kohuora (Newnham <i>et al.</i> 2007)	Okarito (Vandergoes <i>et al</i> 2005; Newnham <i>et al.</i> 2008)	Lake Poukawa Shulmeister <i>et al</i> 2001)	Inaha Tce McGlone <i>et al</i> 1984)
10	EHW	1	<i>Dacrydium</i> continues domination; cold-climate taxa decline						<i>P.Taxifolia</i> recovers, tree ferns at maximum, warmer, wetter	Rise in <i>Metrosideros</i> warm and wet	Rise in <i>Dacrydium</i> warmer and wetter	Increase in <i>P. taxifolia</i> , other podocarps, and <i>Cyathea</i> warmer, wetter	
11													
12	LGR												
13	LGWP	2	<i>Dacrydium Podocarpus P. taxifolia</i> , rise, grass falls. Wet, warm, light winds						Cooler, drier	Switch from <i>Prumnopitys</i> to <i>Dacrydium</i> warm, wetter, humid			
14													
15	LGIT	2						Decline in grasses rise in <i>P.taxifolia</i> & tree ferns wetter, warmer					
16													
17	LGM	2	Cool										
18													
19	LGM	2	Very cold, dry	<i>Phyllocladus, Halocarpus</i> rise. Poaceae high. Cold; dry						<i>Nothofagus</i> replaced with <i>Prumnopitys Podocarpus &amp; Dacrydium</i> warm, wetter	Rise in small trees & shrubs Termination I at 18 kyr BP		
20													
21	LGM	2		Poaceae, <i>Myrsine</i> dominate, <i>Nothofagus</i> & conifers scarce Cool, dry; disturbed						<i>Nothofagus</i> and grassland return; cooling	Decline in <i>Nothofagus</i> , Increase in podocarps Milder conditions Mid-LGCP warming complex	<i>Dacrydium</i> low; Asteraceae, Poaceae decrease; <i>N. fusca</i> at high levels. Cool, mild conditions	
22													
23	LGM	2											
24													
25	LSCP Onset	3	<i>Nothofagus</i> & podocarps fall, grasses rise. Cooler, dry but infrequent drought		<i>Nothofagus</i> & conifers at low levels; Asteraceae, <i>Halocarpus</i> , <i>Coprosma</i> <i>Leptospermum</i> still dominate; Cold, dry, not as windy as before								
26													
27	LSCP Onset	3											
28													
29	Moerangi Interstadial	3	<i>Nothofagus</i> subg. <i>Fuscospora</i> rise, <i>Dacrydium</i> stable, tree ferns fall Slightly cooler, dry							Mixed <i>Nothofagus</i> – thermophilous taxa; Moist interstadial			
30													
31	Moerangi Interstadial	3											<i>Dracophyllum, Myrsine Coprosma</i> shrubland – grassland Cool, dry
32													
33	Moerangi Interstadial	3											
34													

A High Resolution Record of Late Quaternary Climatic and Environmental Change in Taranaki, New Zealand

**Table 11. Comparison Between Inferred Climate at Taranaki and Other New Zealand Sites 10,000 - 80,000 cal yr BP**

kyr BP	Climate Phase	$\delta^{18}O$ Stage	Eltham (present study)	Stent Road (present study)	Okawe Stream (present study)	Opunake Beach (present study)	Lizzie Bell (present study)	Kaupokonui Beach (present study)	Otamangakau Canal (Turney <i>et al</i> 2003)	Kohuora (Newnham <i>et al.</i> 2007)	Okarito (Vandergoes <i>et al</i> 2005; Newnham <i>et al.</i> 2008)	Lake Poukawa Shulmeister <i>et al</i> 2001)	Inaha Tce McGlone <i>et al</i> 1984)
35	Stadial Complex	4	Slightly warmer, but still cool, dry  <i>Nothofagus</i> & herbs dominate Cool, dry, windy		<i>Leptospermum</i> dominate; Cold, dry, windy.	<i>P. taxifolia</i> & <i>P. ferruginea</i> dominate; <i>Dacrydium</i> , <i>Dacrycarpus</i> , <i>Podocarpus</i> plentiful. Warm, wet		rise > <i>P. taxifolia</i> ; <i>Pittosporum</i> , <i>Pseudopanax</i> , <i>Halocarpus</i> Asteraceae rise, slight cooling			Very low counts of podocarp-hardwood taxa, high counts of <i>Halocarpus</i> and <i>Phyllocladus</i> further cooling from previously	Nothofagus Asteraceae, <i>Coprosma</i> , <i>Myrsine</i> high; Cool, wet windy	<i>Nothofagus</i> , <i>P. ferruginea</i> , <i>Dacrydium</i> warming, wet
36													
37													
38													
39													
40													
42													
44													
46													
47													
48	Otamangakau Interstadial	5a					Grasses rise, few trees & ferns; cold, dry	<i>P. taxifolia</i> rise, fall in cold tolerant shrubs. Warming, wetter			Mixed podocarp forest warmer, wetter		
50													
55													
60													
65													
70													
75													
80													
85													

The warmer interstadial temperatures were responsible for eustatic sea level rises that, along with tectonic uplift, formed the Hauriri marine terrace that is situated around 5 km west of Waverley; the estimated age for the strandline (the intersection between the wave cut platform and the base of the cliff) is 80,000 years (Pillans 1990).

#### $\delta^{18}\text{O}$ stage 4

By c. 60,000 yrs BP a sharp fall in the relative proportion of thermophilous *Dacrydium cupressinum*, and increased abundance of cold-tolerant *Halocarpus*, Asteraceae, and Poaceae indicate that temperatures declined at Lizzie Bell. Both pollen transfer functions showed decreases in estimated mean annual temperature from  $\delta^{18}\text{O}$  stage 5a, with the W-MAT estimate falling around 2°C to give a mean annual temperature of 7°C. Sea surface temperatures from the West Coast, South Island at the  $\delta^{18}\text{O}$  stage 5a/ stage 4 boundary were c. 4°C cooler than present (Barrows *et al.* 2007). Precipitation likely decreased during  $\delta^{18}\text{O}$  stage 4, as indicated by low levels of drought-intolerant taxa *Dacrydium cupressinum*, *Cyathea smithii*, and monolete spores, whilst low shrub diversity implies that disturbance was likely to have been low.

The general pattern of cooling and increase in aridity inferred for Lizzie Bell during  $\delta^{18}\text{O}$  stage 4 was matched elsewhere in New Zealand. At Inaha the *Nothofagus* and Tree Conifers group decreased to around 10% of the pollen sum, with the warmth-loving podocarp *Dacrycarpus dacrydioides* in particular falling to < 5% of the sum, from as high as 45% in  $\delta^{18}\text{O}$  stage 5a (McGlone *et al.* 1984).

At Otamangakau Canal, McGlone (1985) noted large increases in the relative abundance of *Nothofagus* subg. *Fuscospora* and Poaceae, and to a lesser extent *Phyllocladus*, and corresponding decreases in *Podocarpus*, *Dacrydium cupressinum* and *Ascarina*, as indicative of cooling, although he suggested that this stadial was unlikely to be as cold as the LGM. At Lake Omapere (Newnham *et al.* 2004) thermophilous taxa including *Dacrydium cupressinum*, *Prumnopitys* and *Podocarpus* decreased in relative abundance, in favour of *Nothofagus* subg. *Fuscospora* pollen, and *Agathis australis* was absent from the record.

The climate at Lake Omapere was clearly cooler, and possibly drier than before, given the decline in *Dacrydium cupressinum* and also tree fern spores; Newnham *et al.* (2004) suggest that this sequence represents the MIS 4 - MIS 3 boundary. At Okarito,  $\delta^{18}\text{O}$  stage 4 was characterised by an almost complete absence of podocarp-hardwood forest, with the exception of the mildly-cold tolerant *Weinmannia racemosa*; whilst cold-tolerant *Phyllocladus* and Poaceae increased over  $\delta^{18}\text{O}$  stage 5a, with *Phyllocladus* becoming the dominant taxon (Vandergoes *et al.* 2005). Collectively, these changes in the pollen assemblage imply cooling for the period 71,000 to 60,000 yrs BP.

#### $\delta^{18}\text{O}$ stage 3 (i) 60,000- 50,000 yrs BP

After 60,000 yrs BP the climate warmed and became wetter at Lizzie Bell, as indicated by increasing conifer abundance, in particular *Dacrydium cupressinum*, high abundance of *Cyathea smithii*, and a decline in cold-tolerant *Nothofagus*, *Halocarpus* and Asteraceae, and Poaceae. Global warming at this time was also indicated by relatively high eustatic sea level rises, as indicated by the cutting of the Rakaupiko marine terrace strandline west of Waverley (Pillans 1983, 1990). The Rakaupiko terrace lies around 2m above the present-day HWM; Pillans (1983) estimated that this implied a paleo-sea level of -28m, given an uplift rate of 0.44mm/yr. These conditions persisted for < 5,000 years before temperatures decreased again at Lizzie Bell and also at Kaupokonui Beach. West Coast, South Island sea surface temperatures at the start of  $\delta^{18}\text{O}$  stage 3 were around 1.5°C cooler than present (Barrows *et al.* 2007).

At Lizzie Bell, *Dacrydium cupressinum* abundance fell in response to decreased precipitation and cooling; although cold-tolerant *Halocarpus* relative abundance increased over  $\delta^{18}\text{O}$  stage 4, cold tolerant *Nothofagus* and Asteraceae showed no change, and Poaceae declined. At Kaupokonui Beach, in contrast, *Nothofagus menziesii* was the dominant tall tree taxon, and cold-tolerant shrubs Asteraceae and *Halocarpus* were highly abundant.

A decline in *Cyathea smithii* and *Dicksonia squarrosa* and a reduction in wetland and aquatic taxa at both Lizzie Bell and Kaupokonui Beach indicate dry conditions occurred at this time. The Lizzie Bell pollen transfer functions indicate that mean annual temperature decreased between 1°C and 2°C to reach 7°C at the top of the pollen zone; this is the same as the Kaupokonui Beach estimates of 6°C (PLS-C2) to 7°C (W-MAT).

The cooling at this time likely corresponds to the second of the grass pollen peaks identified between  $\delta^{18}\text{O}$  stages 4-2 (that is, the first grass peak of  $\delta^{18}\text{O}$  stage 3) identified at Okarito by Vandergoes *et al.* (2005). At Inaha, *Nothofagus* and tree conifers fell to very low levels, with *Prumnopitys ferruginea* making up <1% of the pollen sum, whereas it had made up 5-10% of the sum during  $\delta^{18}\text{O}$  stage 4. Cold tolerant taxa including Poaceae, *Coprosma* and Asteraceae dominated the pollen assemblage, whilst tree ferns were at very low abundance; this assemblage is indicative of cool and dry conditions (McGlone *et al.* 1984).

By around 55,000 yrs BP temperatures improved slightly over earlier times at Lizzie Bell; a rise in warmth loving conifers (apart from *Dacrydium cupressinum*), and a decline in cold tolerant *Halocarpus* and Poaceae indicate a slight warming at this time, with mean annual temperature increasing between 0.5°C (W-MAT estimate) and 1°C (PLS-C2 estimate) to reach between 7.5°C and 8°C by *c.* 55,000 yrs BP. At the same time, the decline in *Dacrydium cupressinum* and the low levels of tree ferns and fern spores indicate drier conditions at Lizzie Bell. At Kaupokonui Beach between 55,000 and 47,600  $\pm$  1,300 cal yrs BP the climate warmed slightly, given a decline in cold tolerant shrubs, and a rise in *Myrsine* which is more competitive in a warmer climate; this inference is supported by the W-MAT pollen transfer function, with mean annual temperature increasing between 0.5 and 1°C over the previous pollen zone to reach 8°C. In contrast to Lizzie Bell, a small rise in ferns at Kaupokonui Beach indicates a slightly wetter environment than before, and the increase in wetland taxa may represent expansion in the wetland area.

At Lake Poukawa (Shulmeister *et al.* 2001) a mixed podocarp-beech forest developed at this time; *Podocarpus/Prumnopitys* comprised up to 20% of the pollen sum, *Nothofagus* subg. *Fuscospora* up to 30%, and *Dacrydium cupressinum*, *Dacrycarpus dacrydioides* and *Nothofagus menziesii* around 5% of the pollen sum each. Grass pollen abundance was very low, whilst *Cyathea* spore abundance was high; overall, a warm, wet climate persisted. A similar pollen assemblage and climate occurred at Lake Omapere (Newnham *et al.* 2004); high relative abundance of *Dacrydium cupressinum*, *Prumnopitys ferruginea*, *Metrosideros*, *Agathis australis* and *Cyathea smithii*, and low abundance of grasses all indicate a warm climate with well distributed rainfall.

### $\delta^{18}\text{O}$ stage 3 (ii) 50,000 – 40,000 yrs BP

The decline in Poaceae and cold-tolerant shrubs *Phyllocladus*, *Halocarpus* and Asteraceae, as well as the sharp rise in tall tree conifers, all point to climate amelioration around 47,600  $\pm$  1,300 cal yrs BP at Kaupokonui Beach. Conditions were still relatively cool, given the abundance of *Prumnopitys taxifolia* is several times greater than the more competitive, warmth-loving *Dacrydium cupressinum* (that is, up to 40% of the pollen sum, vs. 5%); decreases in *Nothofagus menziesii* and *Nothofagus* subg. *Fuscospora* abundance relative to conifers also support the premise of slight warming. The pollen transfer functions imply that that mean annual temperatures increased slightly, with both PLS-C2 and W-MAT estimates fluctuating between 7°C and 8°C across the pollen zone. Further, the increase in abundance of drought-intolerant tall tree taxa and tree ferns and *Phymatosorus* indicate that the climate was almost certainly wetter than previously.

Between 47,600  $\pm$  1,300 and 33,860  $\pm$  330 cal yrs BP the *Nothofagus* & Tree Conifers group at Kaupokonui Beach continued to increase in abundance. All taxa in this group increased in relative abundance, with *Prumnopitys taxifolia* still the most important species, followed by *Prumnopitys ferruginea*. Some slight cooling is evident over this time interval, given (i) *Prumnopitys ferruginea* increased in relative abundance at a faster rate than *Prumnopitys taxifolia*, (ii) *Nothofagus menziesii* and *Nothofagus* subg. *Fuscospora* increased slightly in abundance; (iii) *Libocedrus* appears in the record, albeit at trace levels, and (iv) cold tolerant shrubs and Poaceae all increased in abundance. Both pollen transfer function estimates imply a slight cooling of

between 0.5°C and 1°C, with a mean annual temperature of 7°C over this interval. Despite being cooler, precipitation remained high as indicated by consistently high tree fern abundance.

### $\delta^{18}\text{O}$ stage 3 (iii) 40,000 – 30,000 yrs BP

At Eltham Swamp the dominance of *Nothofagus menziesii* relative to other tall tree taxa between 40,000 and 37,500 cal yrs BP, high Poaceae abundance and low conifer percentages indicate a cooler climate than present. The pollen assemblage at Inaha *c.* 38,320 ± 1,310 also suggests a cooler climate than present; the pollen rain was dominated by the cold-tolerant shrub taxa *Halocarpus*, *Coprosma*, and Asteraceae, with the most common tall tree taxa comprised of *Nothofagus* subg. *Fuscospora*, *Libocedrus*, and *Nothofagus menziesii*, as well as Poaceae, all present at low levels (McGlone *et al.* 1984).

The source of *Nothofagus* pollen throughout the Eltham and Coastal Taranaki cores is puzzling since today it is not found on Mount Egmont, nor is it found west of Eltham (Wardle 1984). The nearest sources of contemporary beech pollen are to the east of Eltham (Ravine 1996); this suggests that either the climate was cold enough to support *Nothofagus*, or winds from the easterly quarter have brought the *Nothofagus* pollen to Eltham. The wind rose diagram for Normanby (Figure 59) suggests that sites to the NE (Retaruke area, Whangamomona- Tangarakau area) are more likely sources than to the south-east, in particular for *Nothofagus menziesii* which is not known for its long distance dispersal (Moar 1970; Wardle 1967; 1980). A South Island source such as North-west Nelson, Buller or the Richmond Ranges to the south and south-west (Wardle 1984) cannot be discounted for *Nothofagus* subg. *Fuscospora* which is known for its long distance dispersal (Moar 1970; Moar & Myers, 1978).

The period 37,500 - 35,500 cal yrs BP at Eltham Swamp was slightly warmer and drier than the previous period, indicated by the reduction in *Nothofagus menziesii* and Poaceae pollen, a slight increase in warmth-loving shrubs, combined with a decline in spore relative abundance in the Tree Ferns and Ferns and Fern Allies groups. Pollen transfer data (W-MAT) suggests temperatures increased between 0.5 and 1.5°C from the previous zone to around 8°C; in comparison the modern-day mean annual temperature is 11.2°C thus although conditions were warmer than previously, conditions were still cool compared to the modern MAT.

The climate at Okawe Stream *c.* 37,000 - 33,670 ± 550 cal yrs BP was also cool and dry, as indicated by low abundance of warmth-loving, drought intolerant conifers such as *Dacrydium cupressinum* and the tree fern *Cyathea smithii*, and high abundance of cold-tolerant taxa Asteraceae and Poaceae, and to a lesser extent *Halocarpus* and *Dracophyllum*. The high abundance of *r*-selected shrubs, in particular *Leptospermum* –type taxon, and the presence of *Libocedrus*, are responses to high volcanic disturbance in the form of a hyperconcentrated-flow deposit at this time. Both of the pollen transfer functions imply that mean annual temperatures throughout the period *c.* 37,000 - 33,670 ± 550 cal yrs BP were very stable, with W-MAT around 7.5°C, and PLS-C2 around 7°C for this interval.

At Eltham Swamp the decrease in relative frequency for the *Nothofagus* and Tree Conifers group and the increase in Poaceae pollen suggest the period 35,000 – 33,250 cal yrs BP was cooler than the previous period; these changes in taxa abundance drive the slight decline in inferred temperature from both PLS-C2 and WMAT transfer functions (*c.* 1°C each). Since abundance for both the Tree Ferns and Ferns and Fern Allies groups remains largely unchanged from the previous period, fairly dry conditions are likely to have persisted. Fossil beetle assemblages from south Taranaki between 34,410 and 33,480 cal yrs BP support a cooling inference; maximum likelihood climate estimate envelopes suggest that winter temperatures were between 1°C and 5°C cooler than present, with summer temperatures close to modern-day summer temperatures (Marra *et al.* 2009).

Between 34,370 ± 370 cal yrs BP and 33,350 ± 460 cal yrs BP at Opunake Beach a slight cooling also occurred, indicated by declining abundance of the more thermophilous taxa *Podocarpus*, *Dacrycarpus dacrydioides* and *Dacrydium cupressinum*; whilst more cold-tolerant *Prumnopitys ferruginea*, *Prumnopitys taxifolia*, *Halocarpus*

and Asteraceae increased in abundance. At this time ( $33,670 \pm 550$  and *c.* 31,000 yrs BP) the pollen assemblage at Okawe Stream also indicated cooling, as indicated by low levels of *Nothofagus menziesii* and *Nothofagus* subg. *Fuscospora*, and the virtual absence of other tall tree taxa, and the rise in Asteraceae and Poaceae. Conditions were likely to have been as dry as they were previously, given the persistence of low values of tree ferns and ferns, and the high abundance of *Leptospermum* suggests that disturbance remained high.

The inferred cooling between *c.* 37,000 at Okawe Stream through to 34,370 cal yrs BP at Opunake Beach may coincide with the second of the grass pollen peaks found at Okarito in the latter part of  $\delta^{18}\text{O}$  stage 3 (Vandergoes *et al.* 2005). This cool interval at Okarito was followed by a period of reduced Poaceae, *Halocarpus* and *Phyllocladus* abundance, and increased abundance of cold-intolerant *Myrsine* that indicated warming, just prior to the end of  $\delta^{18}\text{O}$  stage 3.

After *c.*  $33,350 \pm 460$  cal yrs BP the decrease in *Prumnopitys ferruginea* and *Prumnopitys taxifolia* and persistent low levels of *Nothofagus*, along with a slight increase in *Dacrydium cupressinum* and *Coprosma*, indicates slight warming over the previous zone at Opunake Beach. Pollen transfer functions show very slight ( $< 0.5^\circ\text{C}$ ) warming at this time, although again, the climate was likely to have remained cool, and disturbance was high. The rise in tree fern and fern spores points to a wetter climate. Both pollen transfer functions show a gradual upward trend in temperature, reaching  $8^\circ\text{C}$  sometime before 25,510 cal yr BP. The pollen assemblage at Opunake Beach at this time was similar to that at Otamangakau canal, and Inaha (McGlone 1985), that is, a shrubland-grassland adapted to cool, disturbed conditions.

Temperatures at Okawe Stream are likely to have remained low or slightly improved between *c.* 31,000 – *c.* 27,000 cal yrs BP, based on the observation that cold-tolerant *Dracophyllum* and *Coprosma* strongly increased their relative abundance, whilst taxa that are even more cold tolerant such as *Halocarpus*, Asteraceae and Poaceae either remained unchanged or declined in abundance. The environment was likely to have been as dry as it was previously since tree ferns and fern abundance remains low; *Leptospermum*-type taxon relative abundance decreased sharply, suggesting that disturbance was less frequent and/or less severe than previously. The pollen assemblage at Otamangakau canal and at Inaha was essentially a *Dracophyllum*, *Myrsine*, *Coprosma* shrubland-grassland at this time (McGlone 1985) and thus similar to Okawe Stream. McGlone (1985) discounted the presence of *Nothofagus* pollen, suggesting that it was derived from the Taranaki uplands to the east.

In contrast to slight warming at Opunake Beach and Okawe Stream, Eltham Swamp underwent a period of cooling between 33,250 and 28,000 cal yrs BP, given the upward trend in the *Nothofagus* taxa, and maintenance of grasses at high levels. However cooling was likely to be moderate, given that *Dacrydium cupressinum* declined only slightly, or remained at similar levels to the previous zone, and highly cold-tolerant taxa like *Phyllocladus* or *Halocarpus* did not increase dramatically in relative abundance. Pollen transfer data suggests a fall of perhaps  $0.5^\circ\text{C}$ , although caution should be used since such small changes fall within the error bounds of the transfer function. Tree Ferns and Ferns and Fern Allies relative abundance is depressed, suggesting that rainfall declined and relatively dry conditions persisted. Cool and dry conditions at this time were also implied by the pollen assemblage at Kohuora crater, which was also dominated by cold climate taxa and low numbers of tree fern and monolete fern spores (Newnham *et al.* 2007); furthermore, by the end of  $\delta^{18}\text{O}$  stage 3 sea surface temperatures were *c.*  $5.5^\circ\text{C}$  cooler than present (Barrows *et al.* 2007).

### 9.2.2. Eltham and NZ-INTIMATE CES

Figure 58 shows (i) estimated temperature and inferred climate events at Eltham, along with (ii) the ratio of the logarithm of podocarp pollen abundance to the logarithm of Poaceae pollen abundance (Lowland podocarps: grass or LPG ratio, Alloway *et al.* 2007; Lowe *et al.* 2008), and (iii) the Shannon index of diversity. The data in Figure 58 suggests that based on the W-MAT and PLS-C2 transfer functions, mean annual temperatures were depressed between 4.4°C and 5.7°C at the coldest part of the LGM (21,000 – 19,250 cal yrs BP) relative to the present mean annual temperature of 11.2°C, were around 4.2°C cooler than the present mean annual temperature during the climate reversal between 16,600 and 15,000 cal yrs BP based on the W-MAT transfer functions, and were around 2°C cooler during the Late Glacial Reversal (13,500 – 12,500 cal yrs BP) based on the W-MAT transfer functions. Table 12 compares the timing of Eltham climate events against NZ-INTIMATE-defined climate events.

The **Last Glacial Coldest Period** (LGCP) at Eltham occurred between 29,000 and 18,000 cal yrs BP which coincides well with the LGCP-onset estimates of Alloway *et al.* (2007) and Lowe *et al.* (2008). However, as described in the results for pollen zone ES 5b, this conclusion is based on both a small number of pollen samples (where enumerated dryland pollen taxa > 200) and also pollen counts that are very low (enumerated dryland pollen taxa < 30) and are insufficient to generate pollen transfer function derived temperature estimates, so should be used with caution.

At a finer level, Newnham *et al.* (2007) note that within the warming phase of the LGCP there are two periods of warmer, more variable temperatures at Okarito (27,000 - 24,500 cal yrs BP, and 23,000 - 21,000 cal yr BP) interspersed with a cooling phase (25,000 – 23,000 cal yrs BP). The earlier of the two warmer periods, referred to as the **mid-eLGM Interstadial** by Newnham *et al.* (2012b) may be evident at Eltham; the W-MAT-derived temperature shows that warming occurs between 27,000 and 24,000 cal yrs BP, although the PLS-C2 curve shows no change. The pollen assemblage for pollen zone ES 5b suggests that the period 24,500 to 21,000 cal yrs BP at Eltham was cool and probably dry; Figure 39 implies that the vegetation assemblage progressed from a Poaceae-dominated to Poaceae-*Nothofagus* dominated assemblage, through to a mixed podocarp assemblage. Again, it must be emphasised that these conclusions are based on low numbers of observations so should be used with care.

Vandergoes *et al.* (2005) suggest that one reason for **LGM** onset occurring earlier in the Southern Hemisphere than in the Northern Hemisphere may be regional insolation asymmetries: strong Southern Hemisphere cooling between 35,000 and 30,000 years ago occurred when the precession of the equinoxes meant that perihelion coincided with Southern Hemisphere winters, so that insolation was at a minimum for the 22,000 year, precessional cycle. According to Vandergoes *et al.* (2005) the resultant colder air and water masses were dispersed across the Southern Ocean by the northward displacement of pack ice, circumpolar current system and westerly winds; this in turn lead to cooling at the New Zealand landmass. LGM conditions were maintained in both hemispheres by a subsequent decline in Northern Hemisphere insolation, with the Northern Hemisphere LGM occurring around 25,000 to 24,000 yrs BP. A January perihelion leads to milder seasons in the Northern Hemisphere; since most of Earth's land mass is located north of the equator; cooler summers allow snow and ice to persist to the next winter, so that large ice sheets can accumulate over thousands of years.

This hemispheric asymmetry is further driven by three major factors that influence the thermal characteristics of the ocean surface: (i) evaporated water from subtropical Atlantic is transferred to the Pacific Ocean over the Panama Isthmus; (ii) the North Atlantic ocean transports this warm and saline subtropical water to the north, forming deep convection that drives the global thermohaline circulation (THC); and (iii) the Southern Ocean circumcurrent system causes extreme cooling of the surface water, so that dense, deep-ocean water forms around Antarctica. Interactions of these three factors result in an unstable oceanic circulation system prone to rebounds (Seidov *et al.* 2001). The bi-polar seesaw effect (Broecker, 1998, 2001; Stocker, 1998), "...an

oscillating meridional overturning regime powered by North Atlantic Deep Water (NADW) in the north, and Antarctic Bottom Water (AABW) in the south,” (Seidov *et al.* 2001) may explain these rebounds; the bipolar seesaw model thus predicts asynchrony between southern hemisphere and northern hemisphere high latitudes as a consequence of the net changes in ocean heat flux, although other mechanisms may be involved for this antiphased relationship at low latitudes (Newnham *et al.* 2012).

The **Last Glacial Maximum (*sensu stricto*)** temperature depression of 5.7°C between 24,000 and 18,000 cal yrs BP inferred for Eltham fits well with pre-existing estimates for LGM temperature depressions of 4 to 5°C at Lake Pukaki (Sandiford *et al.* 2003), 4.5 to 5.3°C at Lake Rotomanuka (Newnham *et al.* 1999), 5.2 to 6.7°C at Lake Maratoto (Wilmshurst *et al.* 2007), 6.5 to 7.8°C at Lake Poukawa (Shulmeister *et al.* 2001), all based on fossil pollen assemblages and 4.3°C and 6.5°C for the southern North Island based on MAT and PLS estimates derived from the New Zealand LGM pollen database (Newnham *et al.* 2012), and 6.35°C based on glaciological models and moraine data from the South Island (Putnam *et al.* 2013) and 5.5°C based on West Coast, South Island sea surface temperature estimates (Barrows *et al.* 2007).

Although LGM pollen assemblages at lowland sites are generally similar to contemporary subalpine sites, it does not necessarily follow that climatic factors can be extrapolated between these two circumstances: McGlone (1988) notes that if the subalpine plant communities found on the Taranaki lowlands during the LGM experienced similar temperatures to contemporary subalpine habitats, this implies a drop in temperature of around 8°C, which would eliminate most woody taxa in both islands. Since this did not occur, environmental factors in addition to mean annual temperature depression must have contributed to a decline in tall tree taxa in the LGM pollen record.

Such factors are likely to include increased frequency of harsh frosts, cold air drainage off Mount Egmont and the Pouakai Ranges; cold air masses migrating across the country and intensifying radiation frost severity (Wardle 1986); increased intensity and frequency of westerly winds, leading to increased evapotranspiration, stunted growth forms and increased damage to trees; and competition from *S*-adapted and *R*-adapted taxa such as Poaceae. McGlone (1988) suggests that for western areas, droughts are less likely to have increased during the LGM than in the east, so presumably the incidence of fire is of less significance than in the east also; charcoal data for the LGM is inconclusive because of the small numbers of samples available from Eltham Swamp for that time. This assumption is supported by low levels (< 400 grains g<sup>-1</sup>) of < 20 µm and 20-50 µm charcoal grains, and no grains > 50 µm in the well sampled, youngest part of the LGM at Eltham (19,400 to 18,000 cal yrs BP) (Figure 57).

The **Last Glacial-Interglacial Transition (LGIT)** extended from 20,000 to 10,000 cal yrs BP, with warming commencing around 18,000 in New Zealand, coinciding with increases in atmospheric CO<sub>2</sub> and methane (Monnin *et al.* 2001; Newnham *et al.* 2012). LGIT warming began at Eltham around 18,000 cal yr BP, somewhere between estimates based on speleothem data from Northwest Nelson (18,200 yrs BP) (Williams *et al.* 2004, 2005) and pollen-based estimates from Otamangakau Bog (17,900 yrs BP) (McGlone & Topping 1977; Alloway *et al.* 2007). Newnham *et al.* (2012) note that temperatures over the period 17,000 to 15,000 cal yrs BP (coincident with the Northern Hemisphere Heinrich event H1) are highly variable in New Zealand, however strong fluctuations noted in the speleothem δ<sup>18</sup>O records are not so apparent in pollen records, with temperatures at Eltham fluctuating 1.5°C to 2.5°C over this time.

The onset of LGIT warming in the current study is around 1,000 years earlier than pollen transfer function-based estimates using McGlone & Neall’s (1994) data, that suggest warming began around 17,000 cal yrs BP (Wilmshurst *et al.* 2007). This timing difference may be due in part to McGlone & Neall’s (1994) age estimate not being chronologically constrained as well as the current study, with their oldest radiocarbon date from the lowermost peat being 14,740 ± 420 cal yrs BP, and the estimated age of the remainder of the core extrapolated from an implied peat accumulation rate of 0.6 mm per year. In contrast, age estimates in the current study use

**Table 12. Comparison between Eltham, and NZ-INTIMATE, Climate Events**

ky BP	Auckland Maars (Sandiford <i>et al.</i> 2001, 2003; Shane & Hoverd 2002); Alloway <i>et al.</i> 2007	Otamangakau Bog (McGlone & Topping 1977; Turney <i>et al.</i> 2003)	Kaipō Bog (Hajdas <i>et al.</i> 2006; Newnham <i>et al.</i> 2012)	NW Nelson (Williams <i>et al.</i> 2004, 2005a,b)	Boundary Stream Tarn (Vandergoes <i>et al.</i> 2008)	Okarito (Vandergoes & Fitzsimons 2003; Vandergoes <i>et al.</i> 2005)	Eltham (present study)
10	EHW 11.0-10.0	11.6 – 10.2					
11			11.5-11.0	11.6-10.6			12.5-10.0
12	LGR 14.1 – 11.0				12.9 – 11.5		
13			13.8-12.6	13.5 – 11.6		13.5-11.0	13.5 – 12.5 ?
14		14.7-13.0		LGWP 14.8-13.5		15.0 – 13.5	14.6-13.5 ?
15		LGIT 17.9-14.7					Warming 15.0.-14.6
16				18.2-14.8		18.3- 14.4	Cooling? 16.6-15.0
17							18.0.-14.6 Warming
18	Termination I						
19							
20						21- 18.3	
21							
22							24.0- 18.0
23	Mid – LGCP warming						
24				29.5-18.2		27.0 – 21.0	
25							27.0 – 24
26							
27	LGCP 27.8-26.7					28.0 – 27.0	29.0-27
28							
29							
30							

*EHW = Early Holocene Warming; LGR = Late Glacial Reversal; LGCP = Last Glacial Coldest Period; LGIT = Last Glacial-Interglacial Transition; LGWP = Last Glacial Warm Period*

many more radiocarbon dates and well dated tephras than McGlone & Neall (1994) used, and interpolates age estimates between younger and older radiocarbon dates, rather than extrapolating from a younger date. As a consequence, the age model used in the current study is likely to be more reliable than that of McGlone & Neall (1994).

A further indication that McGlone & Neall's (1994) Eltham age model is possibly at fault is suggested by the fact that tall tree taxa did not reappear in their pollen record until  $14,740 \pm 420$  cal yrs BP. McGlone & Neall (1994) highlight the lag in reforestation at Eltham compared with neighbouring North Island areas: revegetation initially occurred in the Waikato lowlands (Lake Okoroire, Lake Rotokauri, and Lake Rotomanuka) around 17,650 cal years BP (Newnham *et al.* 1999), and sometime before 15,700 cal years BP at Tongariro (McGlone

& Topping 1977), and in the southern Ruahine Ranges (Lees 1986). McGlone & Neall (1994) suggest a lag at Eltham is unexpected since Tongariro, for example, would be expected to have a more continental climate than western Taranaki because it is (i) further inland, (ii) around 300m higher in altitude, and (iii) between 1 and 2°C cooler (assuming a lapse rate of 0.65°C per 100m), than both the Eltham (McGlone & Neall 1994) or Inglewood sites (Alloway *et al.* 1992). McGlone & Neall (1994) note that CLIMAP sea-surface temperature estimates around 18,000 BP were 2-4°C cooler in the west than at the same latitude in the east. The delay in Taranaki reforestation relative to the rest of the North Island might be explained if this temperature difference, and associated decreased precipitation continued into the late glacial. Their explanation is given weight by the presence of *Nothofagus menziesii* and *Libocedrus* which today are only common at altitudes > 600m in the central North Island, and > 875 - 900m on Mount Egmont, respectively (Wardle 1967; McGlone & Neall 1994). However, the lag in reforestation in McGlone & Neall's (1994) fossil pollen record is not seen in the current study.

In contrast to the cooler, drier conditions inferred for the apparent climate reversal at Eltham 16,600 – 15,000 cal yrs BP in the current study, McGlone & Neall (1994) found an almost complete lack of *Nothofagus* and tree conifers before 14,740 ± 420 cal yrs BP at Eltham, with only *Nothofagus* subg. *Fuscospora* recording values greater than 1% of the pollen sum, and Poaceae making up > 80% of the sum, indicating very cold temperatures. This apparent discrepancy can be reconciled to some extent if one assumes (i) that the warming onset occurred earlier than 14,740 cal yrs BP (due to the age model used), and (ii) the pollen assemblage in McGlone & Neall's (1994) study was already dominated by cold-climate taxa, so that any climate deterioration would not be obvious and therefore one would not see a climate reversal. The first part of this theory is supported by pollen transfer functions prepared by Wilmshurst *et al.* (2007) using McGlone & Neall's (1994) data, that show warming began around 17,000 cal yrs BP, suggesting that the age model used by McGlone & Neall (1994) has been modified. However, if McGlone & Neall's (1994) pollen spectra at 14,740 cal yrs BP equates to pollen spectra at 17,000 cal yrs BP (Wilmshurst *et al.* 2007) or 18,000 cal yrs BP (current study), the virtual absence of tall tree taxa in McGlone & Neall's (1994) record, and presence of abundant pollen in the current study remains problematic.

Cooler, drier conditions for 16,600 – 15,000 cal yrs BP were matched to a very moderate extent at Durham Road in Taranaki (Alloway *et al.* 1992; Turney *et al.* 2003) for the period 15,890 ± 440 to 14,960 ± 580, with declines in *Nothofagus* subg. *Fuscospora*, *Nothofagus menziesii* and *Libocedrus* to close to zero values, and very low values of *Dacrydium cupressinum* throughout the interval. In contrast, *Prumnopitys taxifolia* increased at Durham Road, fluctuating between 30 and 45%, consistent with warming, not cooling. At Otamangakau Bog (McGlone & Topping 1977; Turney *et al.* 2003), decreases in *Prumnopitys taxifolia* and *Dacrydium cupressinum* matched the decreases at Eltham, but in contrast to Eltham, grasses were at very low levels (< 2%), so any cooling at Otamangakau Bog was likely to be less intense than at Eltham.

At other, approximately coeval sites, there is mixed evidence for a climate reversal at this time; Newnham *et al.* (2007) found that at Kohuora Bog near Auckland, warm-loving conifers *Dacrydium cupressinum*, *Podocarpus* and *Prumnopitys* all increased in relative abundance, whilst *Nothofagus* subg. *Fuscospora*, *Nothofagus menziesii*, *Halocarpus* and Poaceae all decreased; no other climate reversal is evident in the Kohuora record, so it is unlikely that the disparity between Eltham and Kohuora is simply due to latitudinal differences in the timing of a cooling event. Approximately coeval temperature decreases of a similar magnitude to Eltham Swamp occurred at two South Island sites; from *c.* 17,000 to 16,000 cal yrs BP temperatures at Cass fell between 1.75°C (PLS estimate) and 0.75°C (W-MAT estimate)<sup>35</sup>, and at Clarks Junction both PLS- and WMAT-based temperature estimates showed decreases of around 0.75°C and 1°C, respectively, although Clarks Junction remained relatively cold until 12,000 cal yrs BP (Newnham *et al.* 2012).

---

<sup>35</sup> This highlights the tendency for WMAT-estimates to predict mean annual temperatures >1°C warmer than PLS estimates for sites where there were low percentages of tree pollen in the Late Glacial pollen assemblage, and also a lack of modern, analogous sites (Wilmshurst *et al.* 2007).

During investigation into the possible cause of the apparent climate cooling between 16,600 and 15,000 cal yrs BP, evidence arose that the pollen change may be the result of stratigraphic reworking during core recovery. Figure 36 shows that Core A(6) has an unusual, mottled appearance between 1,055 and 1,030 cm, with an abrupt change in lithology occurring at 1,055 cm when grey-brown pumiceous ash gives way to very dark peat. Sediments in the upper part of Core A (6) equating to the period of most intense warming (pollen zone ES 9a) change abruptly, and may represent some sedimentary reworking or admixing. The warm period seems to be confined to the organic rich sediments in the top of Core 6, whereas the lower part of Core 5 sees an abrupt return to cooler conditions (pollen zone ES 9b). In contrast, Figure 36 demonstrates that Core B (3) – B (5) shows a gradational change from peat down to inorganic sediment.

Furthermore, the bulk peat sample NZA 37495 obtained from these sediments in the top of Core A (6) gave an anomalously young  $^{14}\text{C}$  date of  $14,950 \pm 180$  cal yrs BP; as discussed in section 7.4.1 this age is younger than the organic silt sample NZA 37514 ( $16,100 \pm 310$  cal yrs BP) that lies 28cm higher in the core, suggesting that some younger material may have translocated downwards, possibly during core extraction.

On the other hand, several lines of evidence indicate that there is not necessarily a great deal of contamination. (i) First, statistical tests on pollen data provide at best very weak support for contamination. Assuming that any contamination at the top of pollen zone ES 7b with warm-climate taxa originated from at least pollen zone ES 9a, where warm-climate pollen taxa increases, or contamination of pollen zone ES 7a with cold-climate taxa originated from at least pollen zone ES 8, appropriate null hypotheses are that the differences in pollen assemblages between the respective pairs of pollen zones is zero, and the alternative hypothesis that the difference between the two zones  $\neq 0$ . Wilcoxon's signed rank test was applied to the pollen data for both pairs of zones; this test is appropriate for comparing observations containing two nominal variables (pollen zone and taxa) and a single measurement variable (pollen percentage) where the differences between the pairs are not assumed to be normally distributed (McDonald 2009).

Table 15 in Appendix 11.3 shows that for the first pairing of pollen zone ES 7a and zone ES 8 (19,437 -18,074 vs. 16,578-15,018 cal yrs BP), Poaceae, *Podocarpus*, *Prumnopitys ferruginea*, *Plagianthus* and Asteraceae in particular demonstrate large differences between the zones. Overall, the pollen assemblages in the two zones show only a moderately significant difference from zero ( $W = 95.5$ ,  $P = 0.49$ ). Consequently, one cannot reject the null hypothesis, since there is a 49% probability that the median pollen proportions in each zone are the same: there is only a 51% probability that the median difference is significantly different from 0, so a scenario of significant contamination is neither supported nor rejected.

For the second pairing of the top of pollen zone ES 7b and ES 9a (17,029-16,649 vs. 15,003-14,621 cal yrs BP), Poaceae, *Podocarpus*, *Dacrydium cupressinum* and *Coprosma* demonstrate large differences between the zones; overall, these two zones are more dissimilar than ES 7a and ES 8 ( $W = 99$ ,  $P = 0.37$ ), but again, one cannot reject the null hypothesis, and accept the alternate hypothesis; there is a 37% probability that the median pollen proportions in each zone are the same, and again a situation of significant contamination is neither supported nor rejected. Potential weaknesses of this approach are that there is no way of being certain as to which zone any contaminating material has originated from; furthermore, any contaminating material, may have been agitated and admixed with pollen from other levels as it was translocated downwards. This could easily make the respective assemblages statistically different from zones higher in the core, confounding this type of analysis.

(ii) Using the above logic, one might also assume that the charcoal profiles would be similar between the pairs if contamination was significant. Figure 41 shows that pollen zone ES 8 (16,578 - 15,018 cal yrs BP) has very high levels (c. 10,000 grains  $\text{g}^{-1}$ ) of  $< 20 \mu\text{m}$  and 20-50  $\mu\text{m}$  charcoal fragments, and up to 1,000 grains  $\text{g}^{-1}$  of grains  $> 50 \mu\text{m}$ . In contrast, charcoal grains in the bottom of pollen zone ES 7 (19,437 - 18,014 cal yrs BP) are an order of magnitude less for  $< 20 \mu\text{m}$  and 20-50  $\mu\text{m}$  grains, and no grains  $> 50 \mu\text{m}$  were observed. Pollen zone

ES 7b (17,029-16,649 cal yrs BP) has up to 1,000 grains  $\text{g}^{-1}$   $< 20 \mu\text{m}$  fragments, up to 500 grains  $\text{g}^{-1}$  of 20-50  $\mu\text{m}$  grains. In contrast, virtually no charcoal was observed in pollen zone ES 9a (15,000 - 14,600 cal yrs BP); together, these results suggest that the charcoal profiles for both pairings are very different; again, there is no support for significant sedimentary reworking.

(iii) A third indication that contamination is unlikely to be significant in pollen zone ES 7 is provided by the aerosolic quartz dust profiles for the respective pollen zones (Figure 48). Because the number of quartz samples is much smaller than the pollen samples, it was necessary to compare larger groupings than the pollen groupings examined in (i) above. Pollen zone ES 7 9 (that is, pollen zones ES 7a + ES 7b) has intermediate levels of dust, with dust volumes in the 20-63 $\mu\text{m}$  fraction approximately  $0.075 \text{ g}^{-1}\text{cm}^{-3}$  at 16,492 cal yr BP. Pollen zone ES 9a has very low levels of aerosolic quartz dust; levels of  $> 63 \mu\text{m}$  dust at 14,566 cal yrs BP are approximately the same as in pollen zone ES 7 but the remaining dust size fractions in pollen zone ES 9a record  $< 0.1 \text{ g}^{-1}\text{cm}^{-3}$ . Although both zones only have a small number of quartz samples (four for pollen zone ES 9a and three for pollen zone ES 7) and therefore caution is necessary when interpreting this data, if the sediments in pollen zone ES 7 were essentially translocated sediments from pollen zone ES 9a, one might expect the dust profiles to be more similar. Again, this approach potentially suffers from the same weakness as described for the Wilcoxon pollen analysis described above; that is, quartz could be derived from other, higher levels as it was translocated downwards.

In summary, the apparent climate reversal at Eltham Swamp in the current study is at best weakly supported by data from other sites, although the apparent intensity of the cooling is less marked at the other sites. On balance, evidence for the intense cooling episode at Eltham equivocal; given that it appears to be spatially restricted to the current study, one cannot conclude with certainty that it signals a full climate reversal, so subdividing the NZ-INTIMATE-defined LGIT climate event or introduction of a local cooling subdivision or 'member' (Barrell *et al.* 2013) is not recommended; however, if the cooling event is real, the apparent strong regional variability could prove useful for reconstructing regional climate regimes for this time frame.

The weakly-signalled **Late Glacial Warm Period** (LGWP) at Eltham (14,600 – 13,500 cal yrs BP) is broadly coeval with NZ-INTIMATE delineations (Lowe *et al.* 2008), when mean annual temperatures at Eltham came within  $0.6^\circ\text{C}$  of modern-day mean annual temperatures. It must be emphasised that the signal is weak, and is only discerned by reference to the PLS-C2 pollen transfer function curve that increased  $3.3^\circ\text{C}$ , and the WMAT curve that increased  $3.0^\circ\text{C}$  over this time, rather than an obvious signal in the individual pollen taxon curves. Consequently, identification of the LGWP is tentative only.

The **Late Glacial Reversal** (LGR) at Eltham (13,500 – 12,500 cal yrs BP) falls neatly within the LGR range of times in Table 12 including the Auckland maars (14,100 cal yrs BP) (Sandiford *et al.* 2001, Shane & Hoverd 2002) or Kaipo Bog (13,600 – 12,600 cal yrs BP) (Hajdas *et al.* 2006; Newnham *et al.* 2012). Whether the perceived cooling at Eltham at that time really does represent the LGR, given that the cooling signal is relatively weak, is unclear. The approximately  $1.25^\circ\text{C}$  decrease in mean annual temperature at Eltham at this time is intermediate between the decrease at Okarito to the south ( $2^\circ\text{C}$ ), West Coast South Island sea surface temperatures ( $0.5^\circ\text{C}$ ; Barrows *et al.* 2007) and Pukaki ( $0.5^\circ\text{C}$ ) to the north, and is approximately the same as the decrease at Kaipo Bog ( $0.5^\circ\text{C}$  to  $1^\circ\text{C}$ ). The onset of the apparent cooling at Eltham Swamp might be expected in terms of its latitude situation; Newnham *et al.* (2012) highlight the difference in LGR onset with latitude, noting that the timing of the cooling at Okarito in the south most closely aligns with the Antarctic Cold Reversal. In contrast, LGR onset at the lowland Pukaki site in the north is more closely coeval with the Younger Dryas chron, and cooling at the upland Kaipo Bog site in the North Island overlaps both the Antarctic Cold Reversal and Younger Dryas chrons, as does the cooling at Eltham Swamp.

Russell *et al.* (2006) suggested that LGR cooling was caused by a steepening of the thermal gradient between the Antarctic and the equator, in response to Southern Ocean cooling associated with the Antarctic Cold Reversal, and warming of equatorial waters. Whittaker *et al.* (2011) gave an alternative explanation, suggesting

that westerly winds intensified due to regional cooling, causing the northward shift of the sub-Antarctic and subtropical fronts (Figure 5); under either scenario, stronger westerlies ('roaring forties,' 'furious fifties') consequently migrated northward. There is little support for intensified westerlies at this time at Eltham Swamp; although there is an increase in aerosolic quartz influx after 13,251 cal yrs BP, following a hiatus in dust deposits (Figure 48), the increased influx is very small. This suggests that the intensified westerly winds were still not as strong as they were prior to 15,100 cal yrs BP, and/or the northward migration of the more vigorous westerlies did not extend as far north as Taranaki.

Tables 10 and 11 show that the comparison between inferred climate at Eltham and coastal Taranaki sites and other New Zealand sites between 10,000 and 80,000 cal yrs BP is good, although it should be noted that the chronological resolution of some records is quite coarse and therefore does not fit neatly within the bounds of the age divisions of the table.

### 9.3. Aerosolic Quartz

#### 9.3.1. Aerosolic Quartz at Eltham

The quartz-grain distribution at Eltham indicates both a tropospheric provenance, with the most grains prior to 16,000 cal yrs BP being  $< 10\mu\text{m}$ , and loess-sized grains after this time, with the bulk of grains  $> 20\mu\text{m}$ , reflecting the relative proximity of the dust source, and average wind velocities required to transport the grains, to the Eltham site. Taranaki sites where volcanic loess has been observed include near Hawera (Stewart *et al.* 1977) and Onaero River (Alloway *et al.* 1988). The stratigraphic log for Eltham (Figure 24), tephra reworking appears to have occurred at Eltham between 1,160 and 1,140 cm and 1,083 and 1,063 cm (*c.* 19,452 – 18,777 cal yrs BP and *c.* 25,300 – 22,000 cal yr BP) in particular: no bedding is evident in this part of Core A, and mean grain sizes and the total mass of quartz are much larger than at younger ages.

The period of tephra reworking at Eltham overlaps a period of sand-dune remobilisation in Horowhenua; Duller (1996) found evidence that the Koputaroa parabolic dune fields to the south of Foxton were re-mobilised in response to intensified westerlies beginning around 2,000 years before the Kawakawa / Oruanui ash deposits, through to about 10,000 yrs BP. Infrared stimulated luminescence dating indicated that the dunes were originally emplaced about 40,000 to 50,000 yrs BP during an interstadial, and had become unstable  $\leq 27,000$  yrs BP.

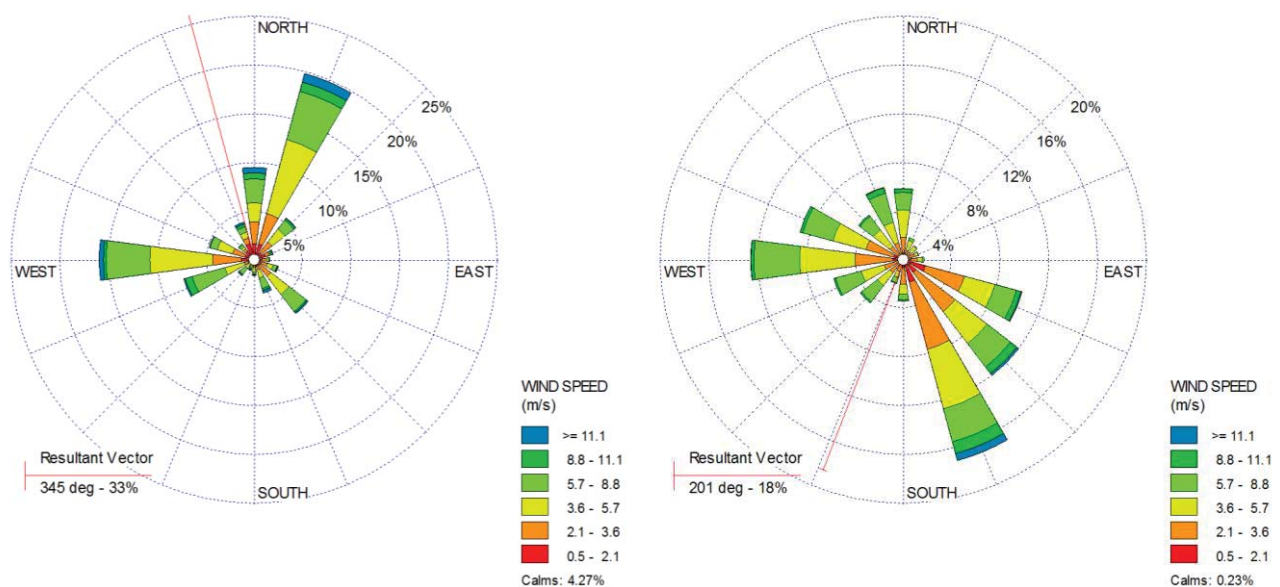
Several authors hypothesise that the LGM in New Zealand was characterised by stronger westerlies than present, leading to a moister climate on the west coast of the South Island, and a drier, more continental-type climate on the east of the main divide due to enhanced orographic rainfall in the west and Foehn winds and rain shadow effects in the east (Moar 1980, McGlone 1988). However, this view is equivocal; for example, Hesse & McTainsh (1999) found no evidence for increased wind strength in Australia during the LGM after examining dusts deposited in the Tasman Sea. A recent synthesis of New Zealand LGM terrestrial and marine data (Lorrey *et al.* 2012) with Kidson's (2000) Regional Climate Regime Classification has been interpreted as providing evidence for (i) predominantly anticyclonic/zonal circulation during the winter, with an increase in the influence of blocking anticyclones over the South Island, and N and E winds predominating; and (ii) zonal and trough circulation during the summer, with an increase in S and W winds. This would lead to lower than present mean annual temperatures, mean summer temperatures and mean annual rainfalls (Lorrey *et al.* 2012).

Hesse & McTainsh (1999) note that because there was no change in the coarse-sized population modal size over time at marine cores E39.75 and E26.1 (discussed in section 8.2), and because the fine-sized population is independent of the coarse population, fine grain size dust influx is not a satisfactory proxy for wind intensity. Oxygen isotope analyses of fine quartz dust in the New Zealand region show a remarkable similarity with the other Southern Hemisphere data, which is suggestive of global tropospheric dust circulation (which for the Southern Hemisphere has to be largely of Australian origin), rather than any local origin (such as the New Zealand continental shelf) (Vince Neall, *pers com.* 2014). Nevertheless, some researchers (eg Paul Hesse *pers.*

comm. 2013) remain unconvinced that the quartz dust record from Core P69 (Stewart & Neall 1984) is a record of aeolian quartz given its geographical position, and the likely high influx of fluvial and hemipelagic sediments. Furthermore, dust input may change not only in response to changing wind patterns, but also due to reduced production, as aggradation slowed and uplands and aggradational surfaces were revegetated. Therefore an alternative view is that changes in quartz dust influx are a consequence of changes in the size of New Zealand's continental shelf in response to sea-level changes, so that it is difficult to draw conclusions about the strength of zonal winds based on flux alone.

Other explanations for an increased dust flux during the LGM are also feasible; given the effectiveness of even sparse vegetation cover in suppressing dust entrainment (Wolfe & Nickling 1996; Wyatt & Nickling 1996; discussed below), reduced vegetation cover on the fans of aggrading rivers (Shulmeister *et al.* 2004) could also contribute to an enhanced dust source. Large areas of New Zealand's current continental shelf were exposed in response to LGM sea level lowering, in particular Golden Bay and Tasman Bay, the Manawatu coast, Wanganui Basin and South Taranaki Bight to the south of Taranaki; (Alloway *et al.* 1992; Eden & Hammond 2003); at the same time, large west coast North Island rivers (Manawatu, Rangitikei and Wanganui) would have had larger floodplains extending across the large continental shelf. These floodplains may have been important sources for dust deflation by westerly winds, whether or not they were more intense.

One possible explanation for different quartz deposition patterns between Eltham and Waitui, and Eltham and Onaero described in section 8.2 is that the northern Taranaki sites had different wind regimes and therefore deflated different source areas than Eltham during  $\delta^{18}\text{O}$  stage 2. The windrose diagram for Waitara (the closest weather station for Onaero and Waitui) shows a predominantly SSE wind 16% of the time, as well as SE (12%), ESE (10%) and W (12%) winds, with a resultant vector of SSE 18% of the time. In contrast, the windrose diagram for Normanby (the closest weather station to Eltham) shows that SSE-ESE winds occur only 5% of the time, and the predominant winds are NE and W (20% and 16% each respectively), with a resultant vector of NNW  $\frac{1}{3}$  of the time (Figure 59).



Normanby EDR (20.05.96–08.03.04)

Waitara (24.12.1980 – 31.03.1984)

Figure 59. Windrose Diagrams for Normanby (proxy for Eltham) and Waitara (proxy for Onaero and Waitui). EDR = Electronic Data Recording station.

Assuming that the predominant direction of regional and local winds were the same throughout  $\delta^{18}\text{O}$  stage 2 as they are today, predominant, northerly quarter winds at Normanby would have travelled across a smaller, exposed continental shelf than winds from the southern quarter at Onaero and Waitui, *ceteris paribus*; in addition, given that contemporary westerly quarter winds are both stronger and more frequent at Waitara than

Eltham, we might expect that this pattern also occurred during hypothesised periods of enhanced westerlies during the LGM (Stewart & Neall 1984).

However, Shulmeister *et al.* (2004) suggest that because the original source of quartz dust in New Zealand, Torlesse greywacke, is so widespread (covering  $\frac{1}{3}$  of the country in primary or modified form), we cannot be certain that the source of medium to coarse, quartz dust grains at Onaero and Waitui (and by extension, Eltham) is not Neogene mudstones or older quartzo-feldspathic units from the exposed continental shelf to the southwest, and that northern, southern and eastern sources are all possible. This caveat has some support from the windrose for Normanby that shows winds are far more frequent and intense from the northern quarter than the western quarter; however W, SSE and SE winds are more common and stronger than northerly winds at Waitara.

Furthermore, assumptions regarding geological provenance must be used cautiously: it is conceivable that streams entering the relict Eltham Swamp may have sequestered secondary deposits of quartzo-feldspathic sediments derived from mudstone-rich clasts that formed part of the Maitahi formation, a debris avalanche resulting from a collapse of Pouakai Volcano between *c.* 240,000 and 210,000 years BP (Gaylord & Neall 2012) to the north and east. In addition, several debris avalanches originating from Mount Egmont with run-outs extending into, or proximal to, the Eltham Swamp catchment are known to have entrained ripped-up fragments of Tertiary mudstones and/or sand stones (Zernack *et al.* 2011). These potential sources of medium to coarse quartzo-feldspathic sediments include the Waingongoro Formation ( $\leq 5$  m thick, emplaced *c.* 75,000 years BP); Waihi Formation ( $\leq 4$  m thick, emplaced *c.* 70,000 years BP); and the Ngaere Formation ( $\leq 5$  m thick, emplaced *c.* 27,000 – 28,000 years BP) (Zernack *et al.* 2011), although the contributions are likely to be very small.

In the absence of geochemical fingerprinting to determine provenance (Marx *et al.* 2009), the available data can help narrow down or eliminate potential sources for the Eltham dust. Dust accumulation generally decreases with distance from its source, and loess becomes finer with distance; this pattern is seen on the south bank of the Rakaia River in Canterbury (Eden & Hammond 2003) as the NW winds in particular deposit post-glacial loess from the river floodplain.

After  $17,600 \pm 200$  cal yrs BP the circumpolar, westerly wind system decreased in intensity and migrated southwards, so that quartz deposition abruptly declined; both dust concentration and dust flux at Vostok continued their downward trend, and  $\delta^{18}\text{O}$  isotope analysis conducted by Jouzel *et al.* (1993) of the ice cores indicated warming. Stewart & Neall (1984) also recorded a sharp decline in the accumulation of marine biological material (discussed above); collectively, these proxies all indicate weakening of the zonal wind system. Influx of medium and coarse silt fractions at Eltham would have declined not only because of changing wind patterns, but also due to reduced production, as aggradation slowed and uplands and aggradational surfaces were revegetated; by this time, degradation was well underway in East Coast rivers, and also the Rangitikei River (Alan Palmer 2013, *pers. comm.*).

### 9.3.2. Aerosolic Dust Entrainment Distances and Wind Intensity Definitions

The purpose of this section is to quantify the relationship between wind velocity, turbulence, and maximum theoretical distances that dust can be entrained. This enables hypotheses to be formed about paleowind strength and potential dust sources and therefore wind direction, and assists in understanding local versus long distance dust transport at Eltham during the late Quaternary.

The maximum distance  $L$  that a dust particle can travel is inversely proportional to the fourth power of the diameter of the particle (Pye 1987):

$$L = \bar{U}t = \frac{\bar{U}2\varepsilon}{K^2D^4} \quad (15)$$

where  $\bar{U}$  = mean wind velocity;  $t$  = time a particle can remain in suspension,  $\varepsilon$  = the coefficient of turbulent exchange (degree of vertical air mixing),  $K = \rho_p g / 18\mu^{36} = 8.07 \times 10^5 \text{ cm}^{-1}\text{s}^{-1}$ , and  $D$  = diameter in cm.

Thus minimum wind speeds required to transport the larger grains at Eltham can be determined, as well as the furthest theoretical distance large grains could have travelled. Assuming the major sources of Australian dust reaching New Zealand are the lower Lake Eyre Basin, including the Simpson Desert, and/or the Murray – Darling Basin (McTainsh 1989; Hesse & McTainsh 2003), a distance from Eltham of approximately 3,700 and 2,500 km respectively<sup>37</sup>, then Table 13 shows that for 63  $\mu\text{m}$  dust deflated from an Australia source to reach New Zealand would require wind speeds of 125  $\text{ms}^{-1}$  or 450 kph, a highly unlikely scenario, since winds of this velocity have never been recorded<sup>38</sup>, as well as maximum values of  $\varepsilon$ .

Whereas a 3  $\mu\text{m}$  grain could be easily borne across the Tasman Sea by winds of 15 $\text{ms}^{-1}$  (54 kph) under strong vertical mixing ( $\varepsilon = 10^5$ , the coefficient of turbulent exchange associated with moderate wind storms), a quartz grain 63  $\mu\text{m}$  in diameter carried by 15 $\text{ms}^{-1}$  winds and with vertical air mixing of  $\varepsilon = 10^5$  would travel only 3km before precipitating out of the air; and grains 45  $\mu\text{m}$  in diameter entrained by winds of 30  $\text{ms}^{-1}$  (108 kph) and maximum coefficient of turbulent exchange values (that is,  $10^7$ ), would fail to reach New Zealand.

Baldi & Salinger (2008) note that the 99<sup>th</sup> percentile wind gusts at New Plymouth Airport were a maximum of 96 kph for the period 1972-2006; Table 13 shows that 96 kph winds can theoretically entrain a range of different quartz grain sizes for > 2,500 km, for example 2.39  $\mu\text{m}$  ( $\varepsilon = 10^2 \text{ cm}^2 \text{ s}^{-1}$ ) to 23.9  $\mu\text{m}$  ( $\varepsilon = 10^6 \text{ cm}^2 \text{ s}^{-1}$ ). This highlights an important complicating variable in the quartz influx: wind intensity relationship – the degree of vertical air mixing regulates the maximum size of dust grain that can be entrained for a given wind speed.

A wind of 96 kph wind equates to a storm, scale 10 on the Beaufort scale, so could be expected to represent strong winds in the current schema, however a 2.39  $\mu\text{m}$  grain could be borne further by a weaker wind but with stronger vertical mixing conditions: a 48 kph wind with  $\varepsilon = 10^3 \text{ cm}^2 \text{ s}^{-1}$  could be carried over 12,500 km, so the presence of a 2.39  $\mu\text{m}$  grain alone is not necessarily a very useful paleoindicator. Fortunately, a typical windstorm typically has a coefficient of turbulence of  $10^4$  to  $10^5 \text{ cm}^2 \text{ s}^{-1}$  (Pye 1987) therefore a narrower, and more appropriate range of maximum grain sizes for a 96 kph wind is 7.56  $\mu\text{m}$  - 13.45  $\mu\text{m}$ . Taking the mean of these two grain sizes  $\approx 10 \mu\text{m}$ ; this is the boundary between intermediate and strong winds for the purposes of this study. In addition, the volume of dust at different fractions indicates relative wind intensity; the period of

<sup>36</sup> Where  $\rho_p$  is particle density (2.65 for quartz),  $g$  = acceleration due to gravity (980  $\text{cm s}^{-1}$ ) and  $\mu$  is the dynamic viscosity of air, 0.0001787 poise at sea level, at 10°C.

<sup>37</sup> Distance of Simpson Desert National Park, and average distance of Wagga Wagga and Griffith to Eltham, respectively.

<sup>38</sup> According to the Commission for Climatology, World Meteorological Organisation, the strongest gust recorded was 408 kph at Barrow Island (Australia!) during Cyclone Giselle on April 10, 1996.

**Table 13. Maximum Quartz Grain Entrainment Distances for Selected Wind Velocities, Turbulence and Grain Sizes.**

Mean wind velocity (ms <sup>-1</sup> ) <i>U</i>	Mean wind velocity (kph) <i>U'</i>	Beaufort Scale	Beaufort Description	Coefficient of Turbulent Exchange $\epsilon$	Grain Diameter (cm) <i>D</i>	Grain Diameter (µm) <i>D'</i>	Distance (km) <i>L</i>
15	54	7	strong	10 <sup>3</sup>	0.00030	3	5,682
30	108	11	storm	10 <sup>3</sup>	0.00050	5	1,473
15	54	7	strong	10 <sup>5</sup>	0.00100	10	4,602
15	54	7	strong	10 <sup>5</sup>	0.00120	12	2,219
15	54	7	strong	10 <sup>5</sup>	0.00120	20	2,219
15	54	7	strong	10 <sup>5</sup>	0.00120	20	2,219
15	54	7	strong	10 <sup>5</sup>	0.00630	63	3
15	54	7	strong	10 <sup>4</sup>	0.00630	63	0.3
30	108	11	storm	10 <sup>7</sup>	0.00450	45	2,245
125	450	12	hurricane	10 <sup>7</sup>	0.00630	63	2,453

**Maximum Quartz Grain Sizes for Beaufort Wind Scale Velocities, Likely Coefficient of Turbulent Exchange Values and ≈ 2,500 km Trans-Tasman Entrainment Distances**

1.67	6	1	light	10 <sup>2</sup>	0.000120	1.20	2,551
3.33	12	2	light	10 <sup>2</sup>	0.000142	1.42	2,513
5.28	19	3	moderate	10 <sup>2</sup>	0.000159	1.59	2,532
8.33	30	4	moderate	10 <sup>2</sup>	0.000178	1.78	2,544
8.33	30	4	moderate	10 <sup>3</sup>	0.000318	3.18	2,499
8.33	30	4	moderate	10 <sup>4</sup>	0.000565	5.65	2,508
11.12	40	5	fresh	10 <sup>2</sup>	0.000192	1.92	2,511
11.12	40	5	fresh	10 <sup>3</sup>	0.000342	3.42	2,512
11.12	40	5	fresh	10 <sup>4</sup>	0.000608	6.08	2,515
14.15	51	6	strong	10 <sup>2</sup>	0.000204	2.04	2,507
14.15	51	6	strong	10 <sup>3</sup>	0.000363	3.63	2,507
14.15	51	6	strong	10 <sup>4</sup>	0.000645	6.45	2,507
17.22	62	7	strong	10 <sup>2</sup>	0.000214	2.14	2,519
17.22	62	7	strong	10 <sup>3</sup>	0.000381	3.81	2,519
17.22	62	7	strong	10 <sup>4</sup>	0.000678	6.78	2,519
17.22	62	7	strong	10 <sup>5</sup>	0.001205	12.05	2,505
20.85	75	8	gale	10 <sup>3</sup>	0.000400	4.00	2,499
20.85	75	8	gale	10 <sup>4</sup>	0.000710	7.10	2,517
20.85	75	8	gale	10 <sup>5</sup>	0.001264	12.64	2,506
24.15	87	9	gale	10 <sup>3</sup>	0.000415	4.15	2,498
24.15	87	9	gale	10 <sup>4</sup>	0.000738	7.38	2,498
24.15	87	9	gale	10 <sup>5</sup>	0.001312	13.12	2,500
26.65	96	10	storm	10 <sup>2</sup>	0.000239	2.39	2,506
26.65	96	10	storm	10 <sup>3</sup>	0.000425	4.25	2,506
26.65	96	10	storm	10 <sup>4</sup>	0.000756	7.56	2,503
26.65	96	10	storm	10 <sup>5</sup>	0.001345	13.45	2,499
26.65	96	10	storm	10 <sup>6</sup>	0.002390	23.90	2,506
28.60	103	10	storm	10 <sup>4</sup>	0.000770	7.70	2,496
28.60	103	10	storm	10 <sup>5</sup>	0.001368	13.68	2,506
28.60	103	10	storm	10 <sup>6</sup>	0.002432	24.32	2,508
32.50	117	11	storm	10 <sup>4</sup>	0.000794	7.94	2,509
32.50	117	11	storm	10 <sup>5</sup>	0.001413	14.13	2,501
32.50	117	11	storm	10 <sup>6</sup>	0.002513	25.13	2,500
32.80	118	12	hurricane	10 <sup>4</sup>	0.000795	7.95	2,519
32.80	118	12	hurricane	10 <sup>5</sup>	0.001410	14.10	2,546
32.80	118	12	hurricane	10 <sup>6</sup>	0.001410	25.17	2,507
32.80	118	12	hurricane	10 <sup>7</sup>	0.001410	44.75	2,509

time between 19,394 and 15,160 cal yrs BP is identified as a time of intermediate winds, with the concentration of 20-63  $\mu\text{m}$  and  $> 63 \mu\text{m}$  quartz grains each lying between 0.002 and 0.010  $\text{g cm}^{-3}$ , falling midway between concentrations in periods of weak winds ( $\sim 0 \text{ g cm}^{-3}$ ) and strong winds (0.005 – 0.05  $\text{g cm}^{-3}$  for 20-63  $\mu\text{m}$  grains; 0.005-0.015  $\text{g cm}^{-3}$  for  $> 63 \mu\text{m}$  grains, respectively, and also high levels of 10-20  $\mu\text{m}$  grains (0.02-0.11  $\text{g cm}^{-3}$ ) (Figure 48).

The temporal dimension of weak-intermediate-strong wind categorisation is difficult to define. Since the aerosolic quartz dust samples are distilled from 1 cm slices of core, they relate to a period of time in the order of decades, rather than a point estimate representing an instantaneous deposit. Further, rather than stating that the wind intensity refers to say, estimated maximum mean wind speed for the time period under consideration, or  $n$  days where wind exceeds a certain wind speed (either of which is feasible), a more conservative explanation for the different dust fluxes over time is that at least one wind event exceeding a threshold wind speed-coefficient of turbulence combination, along with a minimum transit time, occurred in the time period under consideration.

Thus, it is entirely possible that a spike in the dust deposit graph is due to a single storm event; as mentioned in section 3.3.2 modern-day wind gusts  $> 145$  kph have return periods of 50 years at New Plymouth, and gusts  $\sim 110$  kph have return periods of only five years. Gusts of 103 kph would be capable of transporting Australian dust 13.68  $\mu\text{m}$  ( $\epsilon = 10^5 \text{ cm}^2 \text{ s}^{-1}$ ) to 24.32  $\mu\text{m}$  ( $\epsilon = 10^6 \text{ cm}^2 \text{ s}^{-1}$ ) to Taranaki, provided that the wind velocity does not fall below that speed for the  $\sim 24$  hours required to cross the Tasman (Table 13).

Quartz grains  $< 20 \mu\text{m}$  are assumed to be derived from local sources and also Australia or farther west, whereas grains  $> 63 \mu\text{m}$  are assumed to be locally-derived loess and transported only short distances in suspension. Table 13 shows that a 63  $\mu\text{m}$  particle could theoretically be carried only 3 km by 54 kph winds (strong winds under the Beaufort scale) when the coefficient of turbulence was  $10^5 \text{ cm}^2 \text{ s}^{-1}$ , and only 300 m when  $\epsilon = 10^4 \text{ cm}^2 \text{ s}^{-1}$  for a wind of the same speed, hence the most important transport mode for grains this size is by saltation. Grains between 20 and 63  $\mu\text{m}$  are a mixture of larger aerosolic quartz grains and locally derived loess.

The foregoing discussion suggests that (i) climatic conditions led to greater dust entrainment at 35,675 cal yrs BP, 31,358 cal yrs BP and at 21,303 cal yrs BP in particular, as indicated by a sharp rise in the quartz dust flux for all dust size particles, but especially loess-sized grains. Climatic conditions leading to greater dust entrainment likely included (a) cooler temperatures, leading to lower eustatic sea levels; this in turn would lead to enlarged dust source areas, including larger coastal plains to the west and south-west of Eltham, and river terraces that extended further to the west; (b) cool and dry conditions that lead to a reduced vegetation cover, allowing the rate of water and wind erosion to increase; (c) reduced rainfall, that could cause depletion in the sediment supply from higher elevations to river terraces or playa; and (d) strong winds. Figure 55 shows that dust influx at 31,358 cal yrs BP  $> 21,303$  cal yrs BP which in turn was much higher than at 35,675 cal yrs BP<sup>39</sup>. (ii) Intermediate dust influxes occurred between 24,190 and 30,740 cal yrs BP and 15,619 and 17,477 cal yrs BP, as indicated by concentrations  $> 0.015 \text{ g}^{-1}\text{cm}^{-3}$  for quartz dust in the 10-20  $\mu\text{m}$  to  $> 63 \mu\text{m}$  size range and/or influxes  $> 0.4 \text{ g}^{-1}\text{cm}^{-2} \text{ ka}$ . (iii) Low quartz dust influxes dominated at Eltham for the period 15,348 to 12,544 cal yrs BP, indicating that climatic conditions favoured low dust production and/or reduced dust entrainment (Figure 55). Warmer temperatures lead to an eustatic sea level rise, so that coastal plain dust source areas were smaller, and vegetation cover increased in response to temperature amelioration and increased rainfall, so that wind velocity at ground level was reduced. In addition, weaker winds likely predominated, indicated by the reduced, total quartz dust flux, in particular the larger fraction that is precipitated out of the air by gravity.

---

<sup>39</sup> For 21,303 cal yrs BP concentration of 10-20  $\mu\text{m}$  quartz was  $0.11 \text{ g}^{-1}\text{cm}^{-3}$ , and concentration of 20-63  $\mu\text{m}$  quartz was  $0.05 \text{ g}^{-1}\text{cm}^{-3}$ ; total quartz dust influx was  $1.0 \text{ g}^{-1}\text{cm}^{-2}\text{ka}$ . For 35,675 cal yrs concentration was  $0.06 \text{ g}^{-1}\text{cm}^{-3}$  and  $0.01 \text{ g}^{-1}\text{cm}^{-3}$  respectively; influx was  $3.3 \text{ g}^{-1}\text{cm}^{-2}\text{ka}$ . Concentration of  $> 63 \mu\text{m}$  was  $0.005 \text{ g}^{-1}\text{cm}^{-3}$  for both ages.

These conclusions should be used with caution, however. The Eltham aerosolic quartz dust record likely represents, at least in part, changing emissivity in proximal sources such as the coastal plains to the west of Eltham, and distal, Australian sources. As described in section 6.6, the changes to emissivity are driven by changes in aridity and the nature of the vegetation cover. Replacement of large tree, *C*-selected taxa with shrubby, *S*-selected taxa as conditions become more arid and windier might be expected to provide a negative feedback on dust emissivity; that is, as conditions become more arid, the relative proportion of flexible, wind-adapted plants would increase, which would reduce shear stress and the amount of dust entrained, and act as nursery plants for *C*-selected taxa as conditions ameliorated.

In addition, experimental observations may confound theoretical models based on Stoke's Law; therefore these conclusions must be used with caution. Prospero *et al.* (1970) found that the size distribution of dust particles originating from storms in the Sahara and Sahel regions in west Africa in June 1967 that were deposited over 5,000 km west in Barbados five days later was strongly skewed towards larger particles, with 25% >10  $\mu\text{m}$  and 4% > 20  $\mu\text{m}$ . Since a quartz particle > 20  $\mu\text{m}$  has a Stoke's settling velocity of 1.91 m minute<sup>-1</sup> (2.75 km day<sup>-1</sup>), dust would need to be lifted to > 14 km in height for any grains of this size to remain suspended long enough to reach the Caribbean within five days.

Since 14 km is close to the level of the tropical tropopause (Prospero *et al.* 1970), some other mechanism(s) must be responsible; possible mechanisms include (i) higher wind velocities by cold fronts at source could entrain a higher proportion of large grains than usual, and reduce the transit time across the Atlantic sufficiently to reduce settling losses (Prospero *et al.* 1970); (ii) vertical mixing depths may have been greater than usual, for example strong daytime heating of the land surface could lead to the formation of a deep thermally mixed layer (Harrison *et al.* 2001); or (iii) the lower atmosphere along the dust trajectory path may have been agitated more vigorously than usual (that is, the coefficient of turbulent exchange,  $\epsilon$ , is very high).

There is good evidence to suggest that for winds out of west Africa, mechanism (ii) occurs: formations of deep thermally mixed layers result in the dust load being lifted to the 'Saharan Air Layer' which can reach 5-7 km in height near the African source. Further west dust concentrations are greatest between 1.5 and 3.7 km in altitude, where they are incorporated in to the African easterly jet (Harrison *et al.* 2001) and the NE trade winds (Muhs *et al.* 2007) and transported to the Caribbean (Prospero *et al.* 1970); and the Central Amazon Basin (Swap *et al.* 1992). In contrast to the dust-laden winds out of west Africa, dust transported long distances eastward from central Asia tends to be elevated to higher altitudes by mechanism (i); that is, by sequences of cold fronts passing from the east (Harrison *et al.* 2001).

Importantly, Hesse & McTainsh (1999) note that unlike dust transported by the Saharan Air Layer, dust entrained by winds in south eastern Australia are lofted through the full height of the troposphere in westerly winds. Since the tropopause over Australia occurs at around 16 km in the summer months and ranges between 12 and 16 km in the winter months (Sturman & Tapper 1996), large dust grains entrained throughout the height of the troposphere could be carried eastward towards New Zealand before they settle out by dry deposition, in particular if higher coefficients of turbulent exchange ( $\epsilon$ ) occur. Thus although  $\delta\text{O}^{18}$  evidence suggests that the coarser the silt, the more it approximates a local, greywacke origin (Vince Neall, *pers com.* 2014), the appearance of large dust grains in the dust record may be at odds with the modelled, maximum grain sizes / maximum theoretical distances that dust can be entrained; therefore caution should be used in applying these theoretical estimates.

## 9.4. Charcoal and Fire Regimes

This section discusses the use of charcoal fragments in the Eltham Swamp core to determine the proximity and intensity of local and regional fires, the relationships between charcoal and wind, and the impact of fire on biodiversity and the pollen assemblage.

The discussion in section 5.3.4 suggests that based on charcoal fragments  $> 50 \mu\text{m}$ , local or regional fires were most frequent during (i) the Moerangi Interstadial at *c.* 40,000 cal yrs BP and 37,500 – 36,500 cal yrs BP; (ii) late LGIT, *c.* 15,500 – 15,000 cal yrs BP; and (iii) LGR, approximately 13,500 - 12,500 cal yrs BP. Peak fire intensity may have occurred around 12,750 cal yrs BP where levels of large-size charcoal grains reached a maximum. In contrast, the presence of charcoal fragments  $< 50 \mu\text{m}$  is less informative; some or even all of the charcoal could be derived from Australia or distal regions in New Zealand (Butler 2008), although it is unlikely that fragments  $< 20 \mu\text{m}$  came from local sources, given Clark's (1988) skip distance between the place of the fire and place of charcoal deposit; furthermore, the weak, but positive correlation between  $< 20 \mu\text{m}$  charcoal and aerosolic dust ( $r = 0.22$ ), and 20-50  $\mu\text{m}$  charcoal and 20-63  $\mu\text{m}$  aerosolic dust ( $r = 0.21$ ) (Table 13) hint at a common, Australian source, in contrast to the  $> 50 \mu\text{m}$  charcoal and  $> 63 \mu\text{m}$  aerosolic dust that are assumed to be local in origin and are not correlated ( $r = -0.09$ ).

Figure 64 shows that at least one period of no charcoal coincides with a period of no aerosolic quartz dust influx (14,307 – 14,860 cal yrs BP) in the Eltham record; this implies either (i) five centuries of increased aridity/lower rainfall and few fires in Australia occurred, so that finer mineral fractions were deflated but dust sources were not replenished. Higher aridity might lead to a decline in the production of plant biomass and therefore fuel, and consequently less charcoal available to entrain and transport to New Zealand; or (ii) four centuries of decreased aridity/higher rainfall and few fires in Australia occurred, so that mineral dusts were more resistant to deflation due to vegetation cover (section 9.3) and there was less charcoal available to entrain and transport to New Zealand; or (iii) a 400-year period of few, weak westerly winds predominated so that neither quartz dust nor charcoal were transported across the Tasman Sea. The first possibility seems unlikely, because an increase in precipitation might be expected to drive an increase in fluvial sediment re-supply to the major source areas (McTainsh 1989), and therefore a sharp increase in aerosolic quartz signature at Eltham after this hiatus; however, Figure 48 indicates that this did not happen.

The second possibility also seems unlikely, because Eucalypt forests would presumably accumulate a great deal of biomass in the absence of fire (assuming that the lack of fire would not suppress their life cycles) so that a sharp increase in  $< 20 \mu\text{m}$  charcoal fragments would occur when fires resumed. However, Figure 57 indicates that this did not happen either, therefore reduced westerly wind intensity and/or frequency remains the most likely explanation for the reduction in both aerosolic quartz and charcoal concentration.

It is likely significant that biodiversity appears to be largely unaffected by fluctuations in charcoal concentration, with the exception of a decline in diversity at the 15,500 cal yrs,  $> 50 \mu\text{m}$  peak when the Shannon index declines slightly. This suggests that even intense fires had little effect on the pollen assemblage at Eltham Swamp, possibly indicating that the burnt area was relatively small compared with the pollen catchment area, such that the pollen narrative was relatively unchanged. This conclusion is supported by the lack of correlation between both the Shannon Index and  $> 50 \mu\text{m}$  charcoal fragments ( $r = 0.05$ ), and total charcoal ( $r = 0.06$ ) (Table 14).

These conclusions must be tempered with the fact that factors relating to the production of charcoal, transportation and deposition can complicate paleofire reconstruction. It is not clear how changes in charcoal influx relate to the areal extent of the fire or its intensity (Marlon *et al.* 2013). Climatic and meteorological conditions and vegetation characteristics interact with each other with respect to fire; eg. warm temperatures promote both accumulation of biomass and conditions dry enough to allow fuel to combust, therefore fire occurs most in environments that are intermediate between very arid and very wet regions; vegetation change by way of post-fire succession is another example of vegetation and climate interactions affecting fire.

**Table 14. Correlations for Aerosolic Quartz Dust, Charcoal, MAT Estimates, C-, S-, and R-selected Taxa and Shannon Index for Eltham Swamp**

	Dust 0 -20 µm	Dust 20-63 µm	Dust >63 µm	Dust Total	Charcoal <20 µm	Charcoal 20-50 µm	Charcoal >50 µm	Charcoal Total	PLS-C2	WMAT	C-selected	S-selected	R-selected
Dust 20-63µm	0.81**												
Dust > 63 µm	0.30*	0.63**											
Dust Total	0.97**	0.92**	0.49*										
Charcoal <20 µm	0.22	0.24	0.21	0.24									
Charcoal 20-50 µm	-0.02	0.21	0.29*	0.07	0.13								
Charcoal >50 µm	-0.12	-0.14	-0.09	-0.14	-0.36*	-0.10							
Charcoal Total	0.24	0.23	0.07	0.19	-0.09	0.14	-0.10						
PLS-C2	-0.09	-0.13	-0.18	-0.12	0.17	0.03	-0.16	-0.17					
WMAT	0.07	0.00	0.04	0.04	0.11	0.03	-0.27	-0.09	0.82**				
C-selected	-0.32*	-0.35*	-0.24	-0.35*	-0.45*	-0.24	0.43*	0.05	0.09	0.05			
S-selected	0.13	0.28	0.36*	0.20	0.16	0.27	-0.27	0.24	0.08	0.03	-0.72**		
R-selected	0.34*	0.26	0.03	0.32*	0.24	0.10	-0.37*	-0.29*	-0.20	-0.09	-0.79**	0.14	
Shannon Index	0.06	0.07	0.09	0.07	-0.14	-0.11	0.05	0.06	-0.80**	-0.82**	-0.04	-0.11	0.15

PLS-C2 = Partial Least Squares pollen transfer function; W-MAT = Weighted Modern Analogue Temperature pollen transfer function  
 \* =  $p < 0.05$  (statistically significant at 95% confidence interval); \*\*  $p < 0.01$  (statistically highly significant at 99% confidence interval)

## 9.5. Climate Change and Biodiversity Changes

The following section examines the relationship between climate and biodiversity change recorded in the pollen diagram at Eltham Swamp. We use the following indices: taxa richness, Shannon index of diversity and Menhinick's index for species richness, and Berger-Parker index for species dominance, to assess diversity and climate change over past 40,000 years, and also changes in  $r$ - $K$  and  $C$ - $S$ - $R$  ratios to test the Intermediate Disturbance Hypothesis.

The Shannon Index curve (Figure 58) generally follows the PLS-C2-derived transfer function temperature curve, and to a lesser extent, the MAT-derived curve, from 40,000 cal yrs BP to the late LGIT-early LGWP at 15,000 cal yrs BP. After 15,000 cal yrs BP the diversity curve begins to trend downwards at a steady rate, when mean annual temperatures are  $\geq 9^\circ\text{C}$ . The correlations between the Shannon Index and Partial Least Squares-derived and Modern Analogue Technique-derived MAT are  $r = 0.81$  and  $r = 0.82$ , respectively (Table 14); in other words, temperature explains 66-67% of the variance in diversity, and climatic factors other than temperature (for example, wind or precipitation), sampling error and transfer function model errors account for the remaining one-third of the variance in diversity.

### *Intermediate Disturbance Hypothesis*

Townsend *et al.* (1997) suggest that the Intermediate Disturbance Hypothesis has received few vigorous tests, despite its importance. The authors suggest an appropriate test would have (i) a measure of disturbance relevant to the organism under consideration; and (ii) a number of comparable communities that differ in disturbance regimes, in order to falsify the hypothesis, with the goal of determining whether taxa richness peaks at intermediate levels of disturbance. The Eltham aerosolic quartz record meets both criteria: short-lived but intense, discrete pulses of dust accumulation would serve as 'disturbances,' and each time period could be considered a 'comparable community.'

The relationship between wind strength (as indicated by dust concentration and influx) and diversity supports the Intermediate Disturbance Hypothesis; taxa diversity is greater at intermediate levels of dust deposition than at low (zero) or high deposition rates, as suggested by the 'hump-shaped' curves in Figure 60. For each quartz dust sample, the number of taxa present in the fossil pollen assemblage was plotted against the mass of quartz dust present, by size fraction. The width of the intermediate zones (that is, inferred range of wind intensities and/or size of the dust sources) and range of diversity varies for the different size fractions. For example, maximum taxa richness (maximum number of taxa) for the 5-10  $\mu\text{m}$  size fraction is 27 taxa, occurring when the quartz concentration was around  $\log_{10} -4.78 = 1.68 \times 10^{-5} \text{ g cm}^3$ . In contrast, maximum taxa richness for the  $> 63 \mu\text{m}$  size fraction is 33 taxa, occurring when the quartz concentration was two orders of magnitude higher, at  $\log_{10} -2.97 = 1.08 \times 10^{-3} \text{ g cm}^3$ . With respect to influx, diversity was highest under intermediate dust fluxes levels (quartz dust influx of  $c. 0.25 - 0.5 \text{ g}^{-1}\text{cm}^{-2} \text{ ka}$ ) that occurred between 30,746 and 28,364 cal yrs BP; 17,477 to 16,118 cal yrs BP; and 15,619 to 14,916 cal yrs BP. Diversity was low under conditions of low dust fluxes (quartz dust influx of  $c. 0 - 0.25 \text{ g}^{-1}\text{cm}^{-2} \text{ ka}$ ) that characterised the periods 34,777 to 32,101 cal yrs BP, and 14,916 to 9,863 cal yrs BP; and also high dust fluxes (quartz dust influx of  $c. 0.5 - 3.3 \text{ g}^{-1}\text{cm}^{-2} \text{ ka}$ ) that occurred between 36,220 to 35,100 cal yrs BP, 32,101 to 30,746 cal yrs BP, 28,364 to 17,477 cal yrs BP and 16,118 to 15,806 cal yrs BP.

This suggests that the relative difference in disturbance between low and high wind strengths, and intermediate wind strengths, was greater for large ( $> 63 \mu\text{m}$  size fraction), locally derived quartz grains, than for smaller (5-10  $\mu\text{m}$  size fraction) grains of potentially more cosmopolitan origin. In other words, winds strong enough to mobilise large local grains had more impact on the forest assemblage and diversity (both positive and negative) than winds that entrained small grains from both local and more distal sources.

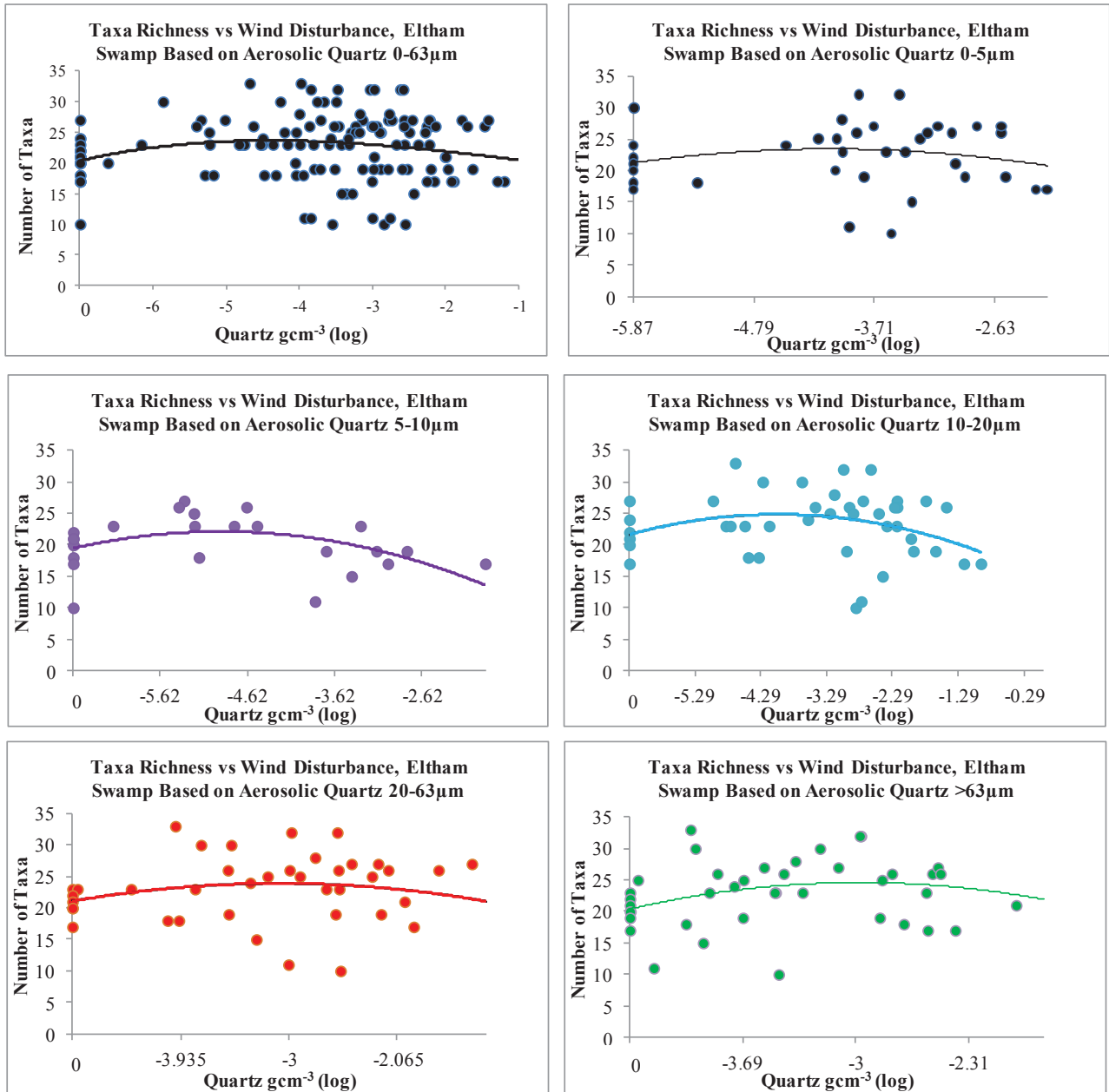


Figure 60. Taxa Richness vs Wind Disturbance, Eltham Swamp

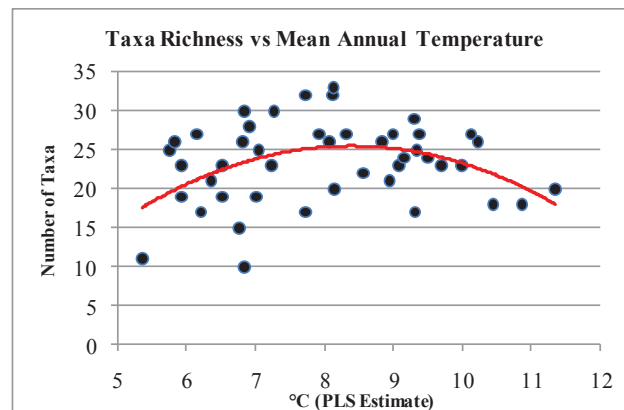


Figure 61. Taxa Richness vs Mean Annual Temperature, Eltham Swamp

Caveats to add to this conclusion is the fact that winds strong enough to entrain large grains could obviously also entrain small particles; in other words, whereas grains  $> 63 \mu\text{m}$  are of exclusively local origin (Table 13), grains say  $\leq 3 \mu\text{m}$  at Eltham could have been derived from any source  $\leq 5,682 \text{ km}$  (likely mostly west) of Eltham. Eustatic sea level changes would have flooded the previously exposed, Late Glacial Maximum shelf that extended from the south of the Taranaki peninsula across Tasman Bay and Golden Bay through to northwest Nelson; this would have progressively reduced potential dust sources to the south and south west of Eltham over time.

Second, other environmental variables that also influence vegetation distribution might be expected to be correlated with wind, such as temperature (Hiura 1995), precipitation and evapotranspiration potential (Currie & Paquin 1987). The inverse relationship between dust flux and temperature, and also dust flux and *C*-selected taxa may simply reflect the expansion of forest in response to temperature rise rather than decreases in wind intensity. Increased forest cover might be expected to reduce soil erosion and fine sediment entrainment, and provide stronger barriers to aeolian transport and deposition, however the vegetation best able to provide a negative feedback of this kind are *S*-selected taxa. Stress tolerant taxa are both better adapted to tolerate windy conditions due to their physiological adaptations, and provide a higher drag coefficient  $C_S$  because of some of these physiological adaptations (flexible, bendy stems and trunks, latticed twigs, etc; described in section 6.6) than more rigid, thick trunked *C*-selected taxa.

Stress selected taxa make up a bigger proportion of total taxa than *C*-selected taxa before *c.* 15,000 cal yrs BP, in particular at times of greatest quartz dust influx: 36,220- 35,100 cal yrs BP and 28,364 – 17,477 cal yrs BP (Figures 63 and 64); overall, this suggests that the relationships between diversity and wind, and predominant plant strategies and wind, are not simple. Furthermore, the relationship between mean annual temperature and taxa richness is also described by the intermediate disturbance-type parabola, suggesting that it is difficult to decouple the effects of wind on vegetation and diversity from other environmental variables that affect the plant assemblage (Figure 61). As a consequence of these methodological limitations, one cannot be certain that changes to late glacial floral diversity, for example, are not a consequence of a temporal overlap between LGM vegetation that was being replaced by Holocene vegetation, independently of any change to quartz dust influx.

### ***Impacts of Strong Winds on the Eltham Pollen Assemblage***

Given the forgoing discussion on *r-K* and *C-S-R* theory (sections 5.4.1 and 5.4.2) one might predict an increase in the proportion of small trees, shrubs and herbs relative to tall trees during periods of high winds, manifested by increases in the relative pollen concentration of these taxa during periods of high dust accumulation, and conversely, a greater proportion of *C*-selected taxa during periods of low wind intensity. In addition, the Intermediate Disturbance Hypothesis (section 5.5.2) would predict that diversity will vary as a function of winds of different intensity.

Very intense winds may damage or destroy vegetation cover, and lead to a reduction of both the bulk volume of soil, and the water holding capacity of soils (Munson *et al.* 2011). Since soil moisture is a major grain-binding agent, soil desiccation reduces the entrainment velocity threshold of the sediments (McGowan *et al.* 1996), allowing more dust to be eroded from the Taranaki soils. Strong, desiccating and dust entraining winds would create positive feedbacks: since trees are less able to grow in such circumstances, the reduction in vegetation cover leads to an increase in sediment erodibility.

As a consequence, the composition of Eltham's forest assemblage is predicted to change: a decline in the relative proportion of *C*-selected taxa (tall forest angiosperms) and conifers such as *Dacrydium cupressinum* and *Dacrycarpus dacrydioides* would occur, accompanied by an initial increase in *R*-selected, small pioneering trees, shrubs and herbs such as *Leptospermum scoparium*, *Kunzea ericoides* and *Aristotelia serrata*. The succession proceeds in favour of *S*-selected taxon such as *Libocedrus* which may undergo coppicing

following wind damage; *Prumnopitys taxifolia* which produces new roots when silt is deposited against the trunk; and *Weinmannia* and *Podocarpus totara* which can produce roots from wind thrown trunks (McSweeney 1982), and podocarps in general, which are tolerant of stressful conditions. As discussed in section 5.5.2, the Intermediate Disturbance Hypothesis predicts that diversity declines as *C*-selected taxa are replaced by fewer, hardy *S*-selected and *R*-selected taxa.

More intense winds from the west may also change the pollen assemblage because the potential pollen source area was more restricted to the west. The area to the west of Eltham would have been dominated by lowland forest – coastal taxa rather than by lowland forest - lower montane forest taxa in the east, thus one might predict that there would be less montane taxa such as *Nothofagus* in the pollen record.

As predicted under IDH, diversity declined during periods of high dust flux at (quartz dust influx of *c.* 0.5 – 3.3 g<sup>-1</sup>cm<sup>-2</sup> ka) that occurred between 36,220 to 35,100 cal yrs BP, 32,101 to 30,746 cal yrs BP, 28,364 to 17,477 cal yrs BP and 16,118 to 15,806 cal yrs BP, as shown by low values for both the Shannon index of diversity and Menhinick's index for species richness (Figure 63), and conversely, the peaks in the Berger-Parker index for species dominance (Figure 63). The decrease in diversity is driven by a decline in *C*-selected angiosperms, in particular *Hoheria*, *Plagianthus*, *Dodonaea*, *Nestegis*, Asteraceae and *Coprosma*; this is reflected in Table 14 where the correlation coefficients for *C*-selected taxa and aerosolic quartz dust influx for all fractions, and *C*-selected taxa and smaller charcoal fragments (<50 µm) is moderately negative.

The modest increases in the number of *R*-selected taxa (due to the introduction of *Chenopodium*, *Epilobium*, *Peperomia* and *Taraxacum*-type taxon, and pioneering trees and shrubs such as *Aristotelia serrata* and *Leptospermum*-type taxon), and *S*-selected taxa (*Libocedrus*, *Prumnopitys ferruginea* and *Prumnopitys taxifolia*) were insufficient to offset the decline in competitor taxa, so diversity declined. The prediction that there might be less *Nothofagus* in the pollen assemblage due to stronger westerlies is partly supported; although there is a small decline in the relative proportion of *N. menziesii*, the relative proportion of *Nothofagus* subg. *Fuscospora* pollen is largely unchanged from earlier periods. Correlations for *R*- and *S*-selected taxa and aerosolic quartz dust influx for all fractions are weak-moderately positive; correlations for *S*-selected taxa in particular increase with inferred wind intensity (that is,  $r = 0.13$  for dust < 20 µm,  $r = 0.28$  for 20-63 µm dust, and  $r = 0.36$  for dust > 63 µm, although only the latter is statistically significant ( $p < 0.05$ ; Table 14).

Support for the prediction that pollen influx would increase following strong winds was equivocal. Some *C*-selected taxa that are adapted to take advantage of high nutrient levels (for example, after periods of strong winds), and are cold tolerant, increased in absolute numbers, despite remaining at similar, or declining, relative proportions of the forest assemblage.

*Nothofagus menziesii*, *Nothofagus* subg. *Fuscospora*, *Hoheria* and *Plagianthus* all increased in absolute abundance (Figure 39); conversely *C*-selected taxa that are cold-avoidant such as *Elaeocarpus*, *Griselinia*, and *Pittosporum* all declined slightly in absolute abundance. This suggests that (i) climatic variables (temperature, wind, precipitation) were more important drivers of Late Quaternary vegetation change than edaphic changes at Eltham; or (ii) the mineral nutrient status of soils around Eltham was not a limiting factor for *C*-selected taxa at this time; or (iii) the nutrient load in windborne dust was insufficient to cause a significant change to soil fertility or the floral assemblage.

### ***Impacts of Intermediate Winds on the Eltham Pollen Assemblage***

Under IDH, an increase in diversity of plant taxa is predicted to occur following intermediate disturbance: gap creation and creation of new niches on the trunks of wind-thrown trees would lead to an increase in relative proportion of *R*-selected taxa (shrubs and herbs) and *S*-selected tall tree taxa. At the same time, since dust influx may still be important in terms of nutrient inputs even under low mass accumulation rates (Reynolds *et al.* 2001; Hesse & McTainsh 2003), the number of *C*-selected taxa that are adapted to take advantage of high nutrient levels in deposits of fresh alluvium or loess after periods of strong winds could remain fairly stable, even if *C*-selected taxa as a group decrease as a proportion of the forest assemblage.

As predicted, diversity of plant taxa increases when intermediate dust fluxes (quartz dust influx of *c.* 0.25 – 0.5 g<sup>-1</sup>cm<sup>-2</sup> ka) occurred between 30,746 and 28,364 cal yrs BP, 17,477 to 16,118 cal yrs BP and 15,619 to 14,916 cal yrs BP, with increases in the relative proportion of *R*-selected taxa (shrubs and herbs) and *S*-selected tall tree taxa occurring in response to gap creation, deposits of fresh alluvium or loess and creation of new niches by wind thrown trees, and conversely a decline in *C*-selected taxa. An exception to this trend occurs at 35,100 cal yrs BP when both *C*- and *S*-selected taxa are at low proportions, ruderal taxa dominate the assemblage, and diversity dips sharply. Diversity is highest at 16,492 cal yrs BP as shown by the Shannon diversity index and Menhinick's species richness index maxima, and Berger-Parker dominance index minima, respectively.

### ***Impacts of Weak Winds on the Eltham Pollen Assemblage***

A decline in diversity during periods of low disturbance is predicted under the Intermediate Disturbance Hypothesis. Assuming that soil nutrients were not depleted, since weaker winds or a reduction in westerly winds at Eltham (as indicated by low quartz accumulation) would be associated with reduced aerosolic nutrient deposits, the proportion of *C*-selected taxa such as angiosperms would increase; conversely, there would be reduced colonisation opportunities (gap formation) for *S*-selected taxa such as *Prumnopitys ferruginea*, *P. taxifolia*, *Podocarpus totara* and *Dacrydium cupressinum*, and *R*-selected plants.

If nutrients were depleted, the situation is more complicated: a lack of disturbance events which generate gaps in the canopy would mean that at first glance stress tolerant, *S*-selected taxa would not be favoured, and nutrient depletion alone would bring about a decline in species richness. Although Richardson *et al.* (2004) found a decline in diversity as levels of P decreased in soils at Franz Josef, conifers increased in richness, as a consequence of the extremely dense mycorrhizal infection of their roots (Dickie & Holdaway 2011) and therefore their superior ability to sequester P on poor soils. Thus we might expect overall diversity to decline, with the number of *C*- and *R*-selected taxa declining, and the proportion, if not the number, of *S*-selected taxa increasing.

The predicted decline in floral diversity during periods of low dust influx (quartz dust influx of *c.* 0 - 0.25 g<sup>-1</sup>cm<sup>-2</sup> ka) is evident: the Shannon diversity index trends downward from around 34,777 to 32,101 cal yrs BP, and 14,916 to 9,863 cal yrs BP (Figure 64). *C*-selected gymnosperms consistently outnumber *S*-selected taxa from around 15,003 cal yrs BP onwards, whereas *R*-selected taxa track the decline in *S*-selected taxa for the same time period. Despite reduced aerosolic inputs, it would appear that nutrients are not depleted, since *C*-selected taxa are trending upwards, and conversely *S*-selected taxa are trending downwards. The overall observed pattern is reduced colonisation opportunities (gap formation) for *S*- and *R*-selected taxa, and increasing dominance of conifers that are adapted to more benign conditions, especially *Dacrydium cupressinum*.

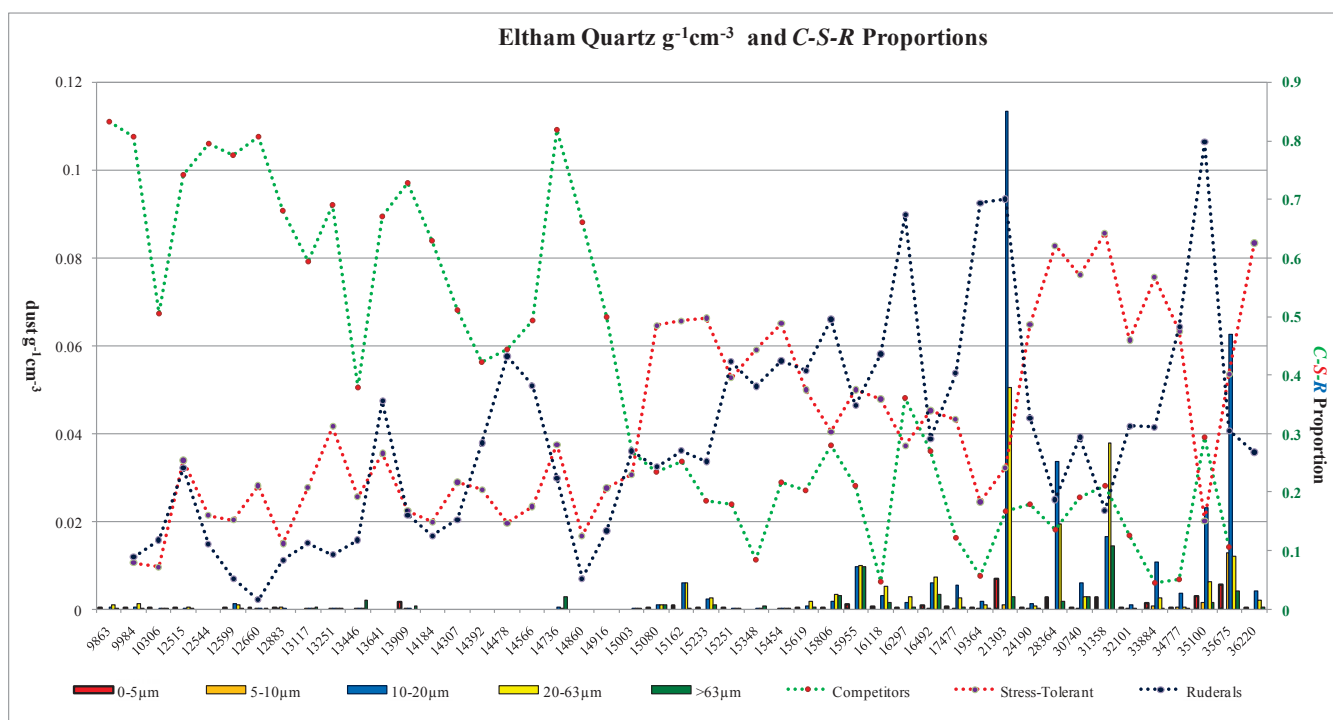


Figure 62. Weight of Quartz per  $\text{cm}^3$  of Sediment by Size Class, and Proportion of Taxa that are Competitive, Stress-tolerating or Ruderal, *sensu* Grime (1977).

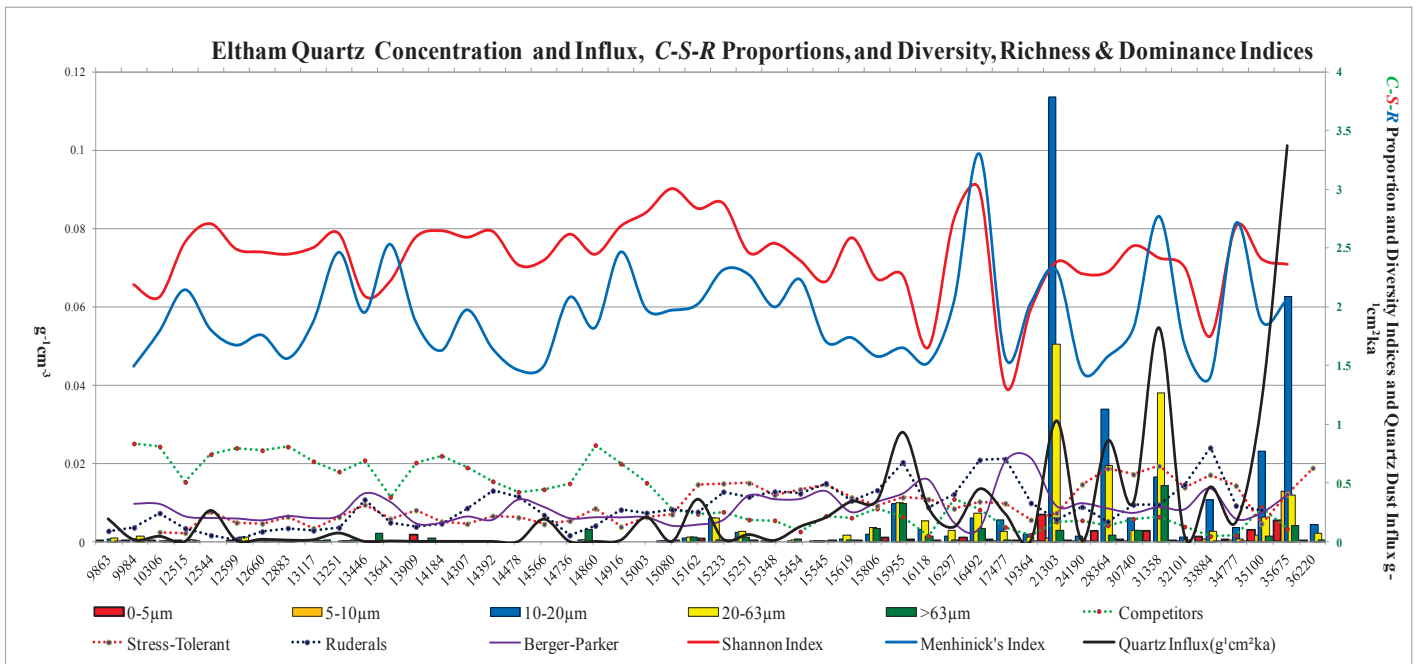


Figure 63. Quartz Concentration by Size Class, Quartz Influx, Proportion of Taxa that are Competitive, Stress-tolerating or Ruderal, *sensu* Grime (1977), and Diversity, Richness and Dominance Indices.

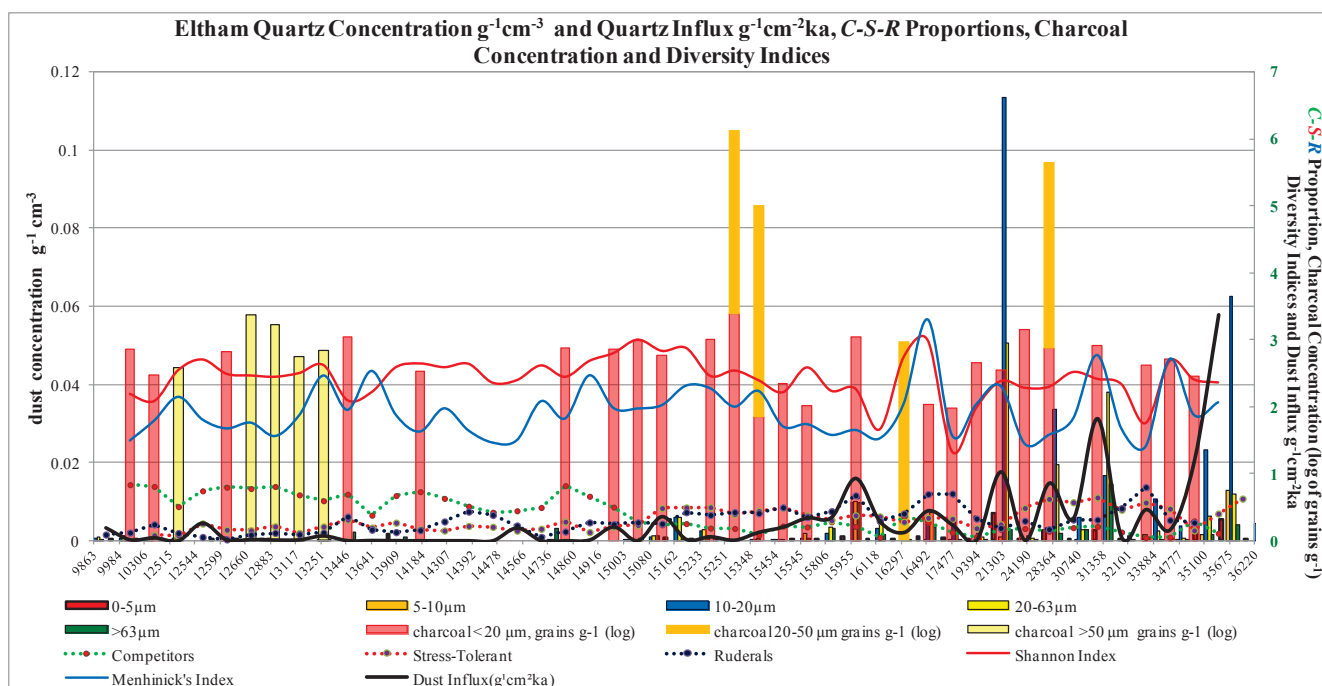


Figure 64. Eltham Quartz Concentration and Influx, Proportion of Taxa that are C-, S- or R-Strategists, and Charcoal Concentrations. Note that charcoal bars are stacked, that is  $\log_{10}$  of concentration of  $< 20 \mu\text{m}$  charcoal grains at 15,348 cal yrs BP is 3.39 (=2,455 grains  $\text{g}^{-1}$ ) and 20-50 $\mu\text{m}$  charcoal 2.74 (= 550 grains  $\text{g}^{-1}$ ).

## 10. Conclusions and Future Work

### 10.1. Conclusions

#### *Pollen Climate*

Long, high resolution fossil pollen analyses are relatively scarce in New Zealand; therefore the paleoenvironmental and paleoclimatic histories from the coastal Taranaki and Eltham sites presented here contribute to the growing number of New Zealand fossil pollen narratives by providing a detailed history of vegetation and climate change for the period 85,000 - 9,000 cal yrs BP.

The Eltham pollen record indicates that cold-climate taxa such as *Nothofagus menziesii*, *Nothofagus* subg. *Fuscospora*, *Hoheria*, *Plagianthus*, *Phyllocladus* and Poaceae dominated the pollen-vegetation assemblage 40,000 years ago. In addition to being cold, low numbers of fern and tree fern spores imply that conditions were drier than present. Pollen transfer functions derived from fossil pollen data enabled temperature reconstructions at Eltham and the coastal Taranaki sites. In general the inferred temperatures fluctuated in line with other New Zealand sites (Tables 10 and 11), and the inferred climate events are broadly synchronous with other sites in New Zealand; exceptions include the apparent cooling period between 16,600 and 15,000 at Eltham Swamp that is either not seen, or only weakly seen, at other sites.

The Eltham pollen record in particular distinguishes millennial-scale climate events identified by the NZ INTIMATE group over the past 30,000 years. In summary:

- The Last Glacial Coldest Period (LGCP) at Eltham (29,000 – 18,000 cal yrs BP) began around 1,200 years earlier than at Auckland and preceded Okarito by around 1,000 years. The PLS-C2 transfer function suggests that mean annual temperatures at the LGCP/ LGM at Eltham were 5.6°C cooler than present; as discussed above, this conclusion is based on sparse pollen data and should be used with caution.
- Termination I marked the boundary between the LGM and the Last Glacial-Interglacial Transition (LGIT); this event appears to have been synchronous between Eltham, Kaipo Bog (Hajdas *et al.* 2006; Newnham *et al.* 2012) and Okarito (Vandergoes *et al.* 2005), occurring *c.* 18,000 cal yrs BP at all sites.
- By around 18,000 cal yrs BP the cold-tolerant taxa began to be replaced by warm-loving podocarps including *Prumnopitys ferruginea*, *Prumnopitys taxifolia*, *Podocarpus*, and *Dacrydium cupressinum*, as well as *Ascarina lucida* and *Metrosideros*; and tree ferns and ferns increased in abundance as conditions became wetter than previously. Mean annual temperature increased from around 6.8°C to 9°C in 1,500 years.
- The LGIT *sensu* Alloway *et al.* (2003)<sup>40</sup> appears to have lasted around 3,400 years at Eltham, beginning around 18,000 cal yrs BP and concluding around 14,600 cal yrs BP which agrees well with NZ-INTIMATE Climate Event estimates of 18,200 to 14,800 cal yrs BP (Lowe *et al.* 2008), and speleothem data from Northwest Nelson (Williams *et al.* 2004, 2005).
- Against the general warming trend from 18,000 cal yrs BP, an apparent stark climate reversal occurred between 16,600 and 15,000 cal yrs BP at Eltham. Mean annual temperatures fell to around 7.9°C, around 1°C cooler than the warmest part of the Late Glacial, and around 3.3°C cooler than present. This cooling period is not recognised in the NZ-INTIMATE Climate Event Stratigraphy, and may be an artefact due to admixing of during core extraction.

---

<sup>40</sup> The LGIT can equally be defined as the interval between Termination I and the Holocene, i.e. 18,000 to 10,000 years BP

- The Late Glacial Warm Period (LGWP) at Eltham (14,500 – 13,500 cal yrs BP) was broadly synchronous with NZ-INTIMATE estimates (Lowe *et al.* 2008) and Northwest Nelson (14,800 – 13,500 cal yrs BP; Williams *et al.* 2004, 2005). Mean annual temperatures at Eltham came within 0.6°C of modern-day mean annual temperatures.
- The timing of the Late Glacial Reversal (LGR) at Eltham shows good agreement with NZ-INTIMATE estimates (Alloway *et al.* 2007; Lowe *et al.* 2008), that is, from around 13,500 to 12,500 cal yrs BP. The LGR at Eltham began and concluded at approximately the same time as Kaipo Bog (Hajdas *et al.* 2006; Newnham *et al.* 2012). In contrast, the LGR onset at Eltham preceded onset at the Auckland maars by 600 years and concluded 1,500 years earlier than at Auckland (Sandiford *et al.* 2001; Shane & Hoverd 2002). The mean annual temperature at Eltham during the LGR was approximately 2°C cooler than the present day MAT of 11.2°C.
- The Early Holocene Warming (EHW) event commenced at Eltham around 11,500 cal yrs BP, the same time as at Kaipo Bog (Hajdas *et al.* 2006; Newnham *et al.* 2012), Otamangakau Bog (Turney *et al.* 2003; Alloway *et al.* 2007) and largely synchronous with the Auckland maars (Sandiford *et al.* 2001) and Okarito (Vandergoes *et al.* 2005).
- By around 10,000 cal yrs BP, many cold-tolerant taxa such as *Nothofagus menziesii*, *Nothofagus* subg. *Fuscospora*, *Phyllocladus* and *Halocarpus* were virtually absent from the pollen record, and the warmth-loving and drought intolerant *Dacrydium cupressinum* dominated the pollen assemblage. Tree ferns and ferns were very abundant, suggesting that conditions were much wetter than previously.

The pollen records from the coastal Taranaki sites span  $\delta^{18}\text{O}$  Stage 5a (Otamangakau Interstadial, *c.* 80,000 yrs BP) through to  $\delta^{18}\text{O}$  Stage 2 (Last Glacial-Interglacial Transition, *c.* 18,500 cal yrs BP), and encompass the stadial complex between the Moerangi and Otamangakau Interstadials ( $\delta^{18}\text{O}$  Stage 4, *c.* 70,000 – 60,000 yrs BP). The resolution of these records is not as fine as the Eltham record, however they are mostly contiguous and they show good agreement in general with other Late Quaternary paleoenvironmental records. These records contribute to the small number of pollen-based paleoenvironmental and paleoclimatic narratives for New Zealand extending from the Otamangakau Stadial to the LGM time periods. In summary:

- Around 80,000 cal yrs BP, between the Otamangakau Interstadial and the ‘Stadial Complex’ (*sensu* McGlone 1985), conditions at Lizzie Bell were warmer and wetter than the preceding interstadial; at Lake Omapere, Northland, conditions were also warm and wet at this time (Newnham *et al.* 2004).
- Temperature reconstructions for Lizzie Bell at this time emphasise the difference in the relative ability of WMAT and PLS-C2 transfer functions to reliably reconstruct mean annual temperatures depending on how many modern analogues are available: the PLS-C2 estimates are 1.5 to 2°C higher than WMAT estimates for this period.
- $\delta^{18}\text{O}$  Stage 4 and the early part of  $\delta^{18}\text{O}$  Stage 3, encompassing the Stadial Complex climate phase, were cool with relatively low precipitation in Coastal Taranaki, and likely to have been windy since conditions were windy at Inaha Terrace (McGlone *et al.* 1984) and Wellington (Lewis & Mildenhall 1985). Pollen transfer functions suggest that the mean annual temperature at Lizzie Bell was between 8 and 9°C, whereas another coastal site, Stent Road, had a mean annual temperature of *c.* 7°C during the LGM; thus although  $\delta^{18}\text{O}$  Stage 4 was cool at Taranaki, it was not as cold as the LGM; Ryan *et al.* (2012) drew a similar conclusion for a marine core taken off the West Coast, South Island based on low Poaceae abundance.

- By 55,000- 50,000 yrs BP conditions at Lizzie Bell were warmer and drier than previously; in contrast the pollen assemblage at Lake Poukawa in Hawke's Bay (McGlone & Moar 1977) did not indicate a water deficit, and although Otamangakau Canal in the central North Island was drier, it was cooler (McGlone & Topping 1977). This likely reflects differences in regional wind patterns, altitude and/or rain shadow patterns.
- During the Moerangi Interstadial, both the Eltham and Coastal Taranaki pollen records show that cold-climate taxa such as *Nothofagus menziesii*, *Nothofagus* subg. *Fuscospora*, *Hoheria*, *Plagianthus*, *Phyllocladus* and Poaceae dominated the pollen assemblage. In addition to being cold, low numbers of fern and tree fern spores imply that conditions were drier than present.
- Temperatures during the Moerangi Interstadial never exceeded 7.2°C (4°C cooler than modern MAT) at Eltham; at Opunake Beach generally cool interstadial conditions are punctuated by a warm period at 32,000 cal yrs BP; a similar event occurred at Kohuora crater, Auckland (Newnham *et al.* 2007).

### *Aerosolic Quartz and Wind Climate*

The technique used in the current study to extract quartz from peats can be considered successful, insofar as relatively pure samples of quartz could be isolated in sufficient mass to be able to measure them, and relate the data to the age model and the coeval pollen influx. The method of quartz extraction from peat is the first to be applied in New Zealand and provides a novel new tool for developing paleowind proxies from peat deposits.

In general, Eltham quartz dust had a bimodal distribution with a primary mode in the 10-20 µm range (aerosolic quartz dust), and a secondary mode at 40-60 µm (loess); most grains deposited at Eltham prior to 15,955 cal yrs BP were < 10 µm and of tropospheric provenance, whereas most grains after 15,955 cal yrs BP were > 10µm and were loessal in origin.

The paleowind reconstructions from Eltham can be summarised as follows: strong winds dominated between 36,220 and 21,303 cal yrs BP; intermediate winds occurred between 21,300 and 15,825 cal yrs BP, and winds of light intensity dominated between 15,825 and 9,863 cal yrs BP.

Major dust peaks at 31,358 cal yrs BP; 21,303 cal yrs BP and 15,955 cal yrs BP all correlated well with the Vostok ice core (Jouzel *et al.* 1993) as well as marine core P69 (Stewart & Neall 1984) and/or Onaero and Waitui in northern Taranaki (Alloway *et al.* 1992). Similarly, dust minima after about 15,955 cal yrs BP at Eltham, Vostok, marine core P69, Onaero, and Waitui suggests that the quartz dust signature at Eltham is consistent with both global and regional estimates of dust influx.

With respect to influx, diversity was highest under intermediate dust fluxes (quartz dust influx of *c.* 0.25 – 0.5 g<sup>-1</sup>cm<sup>-2</sup>ka) that occurred between 30,746 and 28,364 cal yrs BP, 17,477 to 16,118 cal yrs BP and 15,619 to 14,916 cal yrs BP. Diversity was low under conditions of low dust influx (quartz dust influx of *c.* 0- 0.25 g<sup>-1</sup>cm<sup>-2</sup> ka) that characterised the periods 34,777 to 32,101 cal yrs BP, and 14,916 to 9,863 cal yrs BP; and also high dust influx (quartz dust influx of *c.* 0.5 – 3.3 g<sup>-1</sup>cm<sup>-2</sup>ka) that occurred between 36,220 to 35,100 cal yrs BP, 32,101 to 30,746 cal yrs BP, 28,364 to 17,477 cal yrs BP and 16,118 to 15,806 cal yrs BP.

As discussed above, these interpretations must be used cautiously. One cannot eliminate Neogene mudstones or older quartzo-feldspathic units from the exposed continental shelf to the southwest, as a potential source of Eltham quartz; furthermore, streams entering the Eltham Swamp catchment may have entrained secondary deposits of quartzo-feldspathic sediments from mudstone-rich clasts forming part of the Maitahi formation (Gaylord & Neall 2012) to the north and east. The Eltham aerosolic quartz dust record may reflect changing emissivity in proximal sources such as the coastal plains to the west of Eltham, and distal, Australian sources. Dust influx may have declined due to reduced production, as aggradation slowed and uplands and aggradational surfaces were revegetated during the Holocene.

### ***Vegetation Disturbance***

Combining fossil pollen data and aerosolic quartz dust results is a new technique to investigate the relationship between wind intensity and plant assemblages. The Eltham fossil pollen and aerosolic quartz data was analysed to determine how the relative proportions of competitive, stress tolerant and ruderal taxa respond to winds of differing intensities over time, as well as quantifying the impact of wind of different intensities on plant diversity over the period 36,220 to 9,863 cal yrs BP. In summary:

- *C*-selected taxa increased in relative abundance, and *S*-selected and *R*-selected taxa decreased over the last 15,000 years at Eltham, reflecting both temperature and wind intensity amelioration. The relationship between storm events and floral disturbance is difficult to distinguish from typical wind conditions. Neither fire nor volcanic eruption appeared to have any major impact on the floral assemblage at Eltham; in contrast, the impact of debris avalanches and lahars at the coastal Taranaki sites was striking. This may suggest that the pollen assemblage at Eltham is highly reflective of local vegetation rather than signalling regional floral characteristics.
- Biodiversity reached a maximum under conditions of medium wind intensity: biodiversity was lowest when wind disturbance was highest during the LGM and when wind disturbance was lowest during the Holocene when forests were stabilising and achieving a climax; conversely biodiversity was highest when winds were of intermediate strength during the LGIT.
- These results provide moderate support for the Intermediate Disturbance Hypothesis. A literature search found this hypothesis appears to have received relatively little attention in the New Zealand literature even for extant taxa; further, a search of the international literature found no reports of testing the IDH against fossil pollen data.

Quartz dust influx is a measure of changing climatic conditions; it is likely that these collective climatic variables influenced the vegetation. When vegetation biodiversity indices are compared with the quartz dust flux, they provide a quantifiable method for revealing any relationships between vegetation change, and the climate changes represented by the quartz flux record. Due to methodological limitations, these inferences should also be used with caution. As discussed above, other environmental variables that also influence vegetation distribution might be expected to be correlated with wind, such as temperature, precipitation and evapotranspiration potential. An intermediate disturbance-type parabola also describes the relationship between mean annual temperature and taxa richness, thus it is difficult to decouple the effects of wind on vegetation and diversity from other environmental variables that affect the plant assemblage. In other words, the negative correlation between dust influx and temperature, and also dust flux and *C*-selected taxa may simply reflect the expansion of Holocene forest cover in response to temperature amelioration rather than decreases in wind intensity. As discussed above, biodiversity indices were designed to describe populations where identification to species level is possible, however in palynology ‘taxa’ may relate to different taxonomic levels that are not strictly comparable. This makes it difficult to make inferences about floral diversity change with confidence.

## 10.2. Future Work

Several potential areas of new research involving loess, dust and quartz dust are apparent as a result of the current study. Despite the most likely source of the Late Glacial loess-sized dust fraction being the exposed current continental shelf off the North Island's west coast, with the fine silt-sized quartz dust fraction most likely of Australian origin, this has not yet been conclusively demonstrated (Alloway *et al.* 2007). A potentially fruitful area of research would be to undertake a thorough Taranaki dust provenance investigation. Dust provenance studies could involve using common mineralogical techniques such as oxygen isotope analysis (Lyon *et al.* 2009; Menicucci *et al.* 2013), major minerals analysis (An *et al.* 2012), trace element analysis (Petherick *et al.* 2009), or recently developed techniques such as particle-by-particle analysis using integrated Scanning Electron Microscope/ Energy-Dispersive X-ray Spectroscopy (SEM-EDS) in tandem with QEMSCAN® technology (Butcher *et al.* 2011; Haberlah *et al.* 2011).

Quartz data in the current study is all derived from Eltham Swamp; therefore it would be enlightening to extract quartz dust from coastal Taranaki sites to determine how wind patterns more distal from Mount Egmont compare to Eltham. In addition, performing aerosolic quartz analysis at a finer resolution than presented here could prove informative, in particular for the Late Glacial period where the analysis in the current study is at a relatively coarse level.

The quartz extraction technique used in this study destroyed non-quartz components, therefore it would be useful to conduct quartz analysis using an extraction technique that preserves phytoliths (for example, Wallace 1987) to establish the extent of vegetation that is poorly represented by the fossil pollen assemblage, for example *Beilschmiedia tawa*, and to allow construction of transfer functions for phytoliths (Prebble *et al.* 2002).

Other plant macrofossils that might be isolated from the Eltham peats and coastal lignites could prove useful as paleovegetation and paleoclimate indicators. Several samples at Eltham contained low numbers of stomatal guard cells that could potentially be used to estimate Quaternary CO<sub>2</sub> levels if they are from taxa that show a direct relationship to CO<sub>2</sub> (Beerling *et al.* 1995; Wagner *et al.* 1999, Steinhorsdottir *et al.* 2013), and other samples contained seeds which have been used to reconstruct late Quaternary vegetation in Central Otago (Wood & Walker 2008). Since much of this material is deliberately destroyed in the pollen or quartz extraction process, an appropriate sampling regime would need to be developed where multiple proxies are being extracted from the same sample.

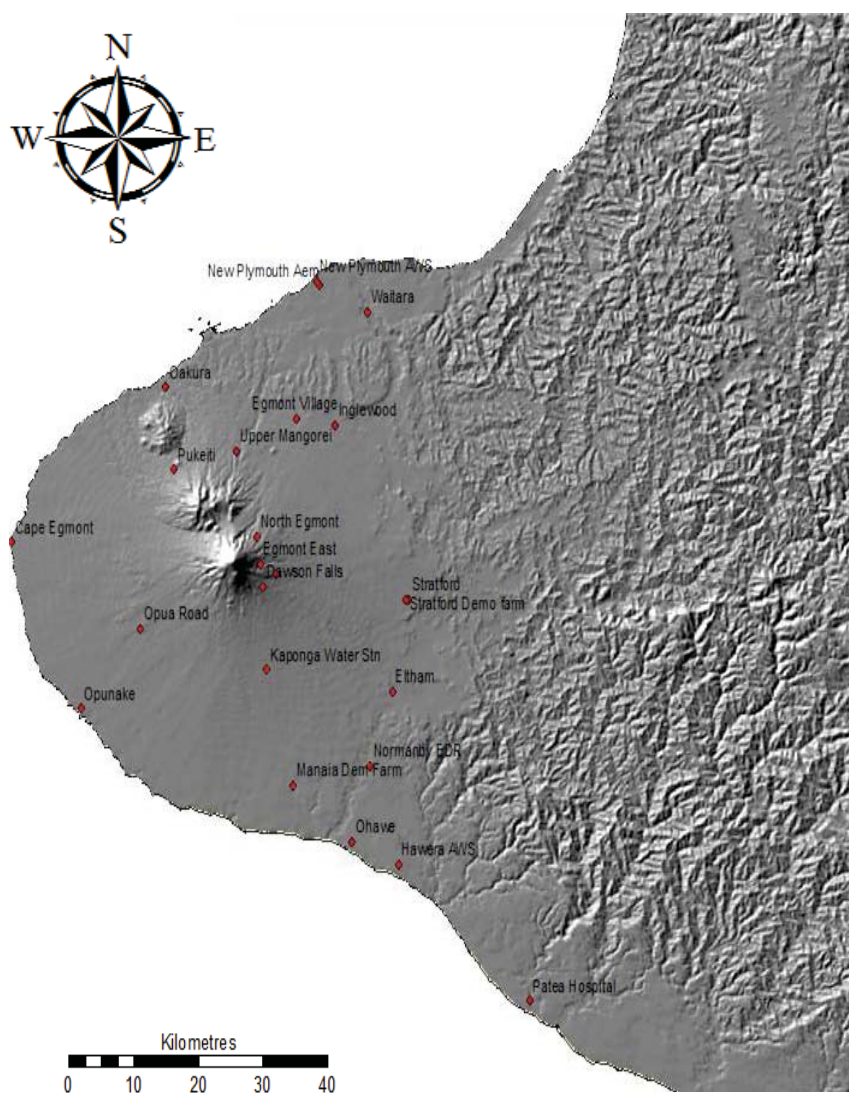
Logs protruding from lignite layers at Opunake Beach and Okaweu Stream, as well as exposed stumps from drowned forests at other Taranaki sites such as Waverley Beach, Waitotara River and Wai-iti Beach could also prove to be useful paleovegetation and paleoenvironment indicators. The advantage of using multiple proxies is that they can support or refute each other, so that more confident determinations can be made, and provide greater insights into variables that co-vary with or lag each other.

Chironomids have been recognised as potentially the best method for quantifying past temperature changes and have been successfully used in the central South Island (Vandergoes *et al.* 2008), but have not yet been applied in paleoclimate reconstructions from North Island sites. Future research might involve using an existing chironomid-transfer function (Dieffenbacher-Krall *et al.* 2007), augmented with new chironomid data from southern North Island lakes sites, for example Lake Rotokare, to develop quantitative Holocene and Lateglacial paleotemperature estimates from nearby lake deposits.

## **11. Appendices**

- 11.1. Taranaki Weather Stations
- 11.2. Palynological and Aerosolic Dust Sites Referred to in Text
- 11.3.  $^{14}\text{C}$  Calibration Curves for Eltham
- 11.4. Wilcoxon Signed Rank Test for Eltham Core A (6)
- 11.5. Aerosolic Quartz Extraction Methodology Rationale

## 11.1 Taranaki Weather Stations



## 11.2 Palynological and Aerosolic Dust Investigation Sites Mentioned in Text

1. Lake Omapere (Newnham *et al.* 2004)
2. Onepoto Crater (Hägg & Augustinus 2003)
3. Lake Pupuke (Shane & Hoverd 2002)
4. Kohuora Crater (Newnham *et al.* 2007)
5. Pukaki Crater (Newnham *et al.* 2007)
6. Kopouahi Bog (Hodder *et al.* 1991)
7. Lake Rotokauri (Newnham *et al.* 1999)
8. Lake Rotomanuka (Newnham *et al.* 1999)
9. Lake Okoroire (Newnham *et al.* 1999)
10. Lake Ngarotoiti (Lowe 1988)
11. Lake Rotopiko (Lowe 1988)
12. Lake Ngaroto (Lowe 1988)
13. Kaipo Bog (Newnham & Lowe 2000)
14. Waitara Buried Forest (referred to in this study)
15. Onearo (Alloway *et al.* 1992)
16. Otamangakau (McGlone & Topping 1977)
17. Retaruke (Ravine 1966)
18. Waitui (Alloway *et al.* 1992)
19. Inglewood (Alloway, McGlone *et al.* 1992)
20. Durham Road (Alloway, McGlone *et al.* 1992)
21. Ahukawakawa Swamp (McGlone 1982)
22. Waiweranui Steam (McGlone & Neall 1994)
23. Warea River (McGlone & Neall 1994)
24. Whangamomona (Ravine 1966)
25. Potaema Bog (McGlone *et al.* 1988)
26. Lake Rotokauri (referred to in this study)
27. Irirangi (referred to in this study; not used)
28. Manaia (McGlone *et al.* 1984)
29. Inaha Terrace, Hawera (McGlone *et al.* 1984)
30. Ararata Road, Hawera (Bussell 1988b)
31. Lake Waiiau Swamp (Bussel 1988b)
32. Lake Poukawa (Shulmeister *et al.* 2001)
33. Waverly Beach (Bussel 1988b)
34. Core P69 (McGlone 2001)
35. Koputaroa Dunes (Duller 1996)
36. Waimahoe (Lewis & Mildenhall 1985)
37. Wellington (Lewis & Mildenhall 1985)





1. Nettlebed Cave (Hellstrom *et al.* 1998)
2. Exhaleair Cave (Hellstrom *et al.* 1998)
3. Nelson (referred to in this study)
4. Taramakau Glacier (Suggate & Almond 2005)
5. Waipera (Moar & Mildenhall 1988)
6. Cass (Newnham *et al.* 2011)
7. Okarito (Vandergoes & Fitzsimons 2003)
8. Lake Mapourika (Suggate & Almond 2005)
9. Franz Josef Glacier (Denton & Hendy 1994)
10. Motukarara (Moar & Mildenhall 1988)
11. Upper Ruined Hut Bog (Marx *et al.* 2009)
12. Nokomai Mire Complex (Dickenson *et al.* 2002)
13. Clarks Junction (Newnham *et al.* 2011)

**Appendix 11.3 Table 15. Wilcoxon Signed-Rank Test for Potentially Admixed Section of Eltham Core A**

	Median pollen % 19,437 to 18,074 cal yr BP	Median pollen % 16,578 to 15,018 cal yr BP	absolute value of difference	rank	rank if positive	rank if negative	Median pollen % 15,003 to 14,621 cal yr BP	Median pollen % 17,029 to 16,649 cal yr BP	absolute value of difference	rank	rank if positive	rank if negative
	<b>7a</b>	<b>8</b>					<b>9a</b>	<b>7b (top)</b>				
Poaceae	48.6	40.6	8	21		21	13.9	19.7	5.8	22		22
<i>Plagianthus</i>	7.1	1.5	5.6	20		20	1.8	1.2	0.6	12	12	
<i>Podocarpus</i>	2.6	5.4	2.8	19	19		21.3	15.7	5.6	21	21	
Asteraceae	2.8	4.7	1.9	18	18	20	0.4	1.0	0.6	11		11
<i>Prumnopitys ferruginea</i>	2.3	0.8	1.5	17		17	6.1	6.2	0.1	2		2
<i>Epilobium</i>	1.5	0	1.5	16		16	-	-	-	-	-	-
<i>Nothofagus</i> subg. <i>Fuscospora</i>	1.9	3.1	1.2	15	15		0.5	0.8	0.3	5		5
<i>Nothofagus menziesii</i>	4.1	3	1.1	14		14	1.8	1.8	-	-	-	-
<i>Phyllocladus</i>	6.7	7.5	0.8	13	13		3.4	2.7	0.7	13	13	
Apiaceae	0.8	0	0.8	12		12	-	-	-	-	-	-
<i>Coprosma</i>	7.8	7.0	0.8	11		11	4.1	6.2	2.1	19		19
<i>Pseudowintera</i>	0	0.7	0.7	10	10		0	0.4	0.4	3	3	
<i>Elaeocarpus</i>	0	0.6	0.6	9	9		0.7	0	0.7	14	14	
<i>Ascarina lucida</i>	0.6	0	0.6	8		8	0	0.4	0.4	8.5		8.5
<i>Myrsine</i>	0.7	1.3	0.6	7	7		0.8	0.8	-	-	-	-
<i>Prumnopitys taxifolia</i>	1.9	1.4	0.5	5.5		5.5	12.2	12.5	0.3	6		6
<i>Nestegis</i>	1.6	1.1	0.5	5.5		5.5	1.1	1.2	0.1	1		1
<i>Macropiper excelsum</i>	0.4	0	0.4	3.5		3.5	-	-	-	-	-	-
<i>Pseudopanax</i>	0	0.4	0.4	3.5	3.5		0	0.4	0.4	8.5		8.5
<i>Dacrydium cupressinum</i>	3.2	2.8	0.4	2		2	11.6	15.5	3.9	20		20
<i>Pittosporum</i>	0	0.3	0.3	1	1		1.3	0.5	0.8	16	16	
<i>Libocedrus</i>	-	-	-	-	-	-	0	1.2	1.2	18		18
<i>Aristotelia</i>	-	-	-	-	-	-	0.8	0	0.8	16	16	
<i>Collospermum</i>	-	-	-	-	-	-	0	0.8	0.8	16		16
<i>Dracophyllum</i>	-	-	-	-	-	-	0	0.4	0.4	8.5		8.5
<i>Chenopodium</i>	-	-	-	-	-	-	0	0.4	0.4	8.5		8.5
<i>Leptospermum</i> -type	-	-	-	-	-	-	0.5	0.3	0.2	4	4	
<i>Dacrycarpus dacrydioides</i>	-	-	-	-	-	-	4.6	4.6	-	-	-	-
			<b>W: 96</b>						<b>W: 99</b>			
			<b>n: 21</b>						<b>n: 22</b>			
			<b>P-value: 0.49</b>						<b>P-value: 0.37</b>			

## 11.4. Aerosolic Quartz Extraction Methodology Rationale

### Introduction

The purpose of this section is to examine in more detail the rationale underpinning aerosolic quartz extraction experimental design, specifically the reasons for using  $\text{H}_2\text{SiF}_6$  and the Horiba Partica LA-950 particle size analyser to extract and analyse aerosolic quartz. In addition, discussion of Stokes' Law is of relevance when interpreting the behaviour of aerosolic quartz in the atmosphere, as well as pollen rain.

### Hydrofluorosilicic Acid ( $\text{H}_2\text{SiF}_6$ ) Treatment

$\text{H}_2\text{SiF}_6$  dissolves minerals that have aluminium in tetrahedral sites in the reaction



Quartz, pyrophyllite, talc and cristobalite are resistant to attack by  $\text{H}_2\text{SiF}_6$  because they lack aluminium in tetrahedral coordination (Dauphin 1980), making  $\text{H}_2\text{SiF}_6$  a suitable agent for purifying quartz from aerosolic dust. However, since  $\text{H}_2\text{SiF}_6$  decomposes into free hydrofluoric acid (HF) which attacks quartz (Chapman *et al.* 1969) and this would modify the original grain-size distributions, special treatment is required: the  $\text{H}_2\text{SiF}_6$  was stored in cool conditions (4°C) with excess quartz when not in use, and used at <18°C. Preserving the original size range was enhanced by processing samples in narrow size ranges, by sieving to <63  $\mu\text{m}$  and > 63  $\mu\text{m}$ .

To investigate the propensity of  $\text{H}_2\text{SiF}_6$  to confound quartz extraction, Chapman *et al.* (1969) investigated  $\text{H}_2\text{SiF}_6$  decomposition at temperatures higher than room temperature, yielding HF that would attack quartz. Quartz and albite samples in the size range of 20-2  $\mu\text{m}$  were reacted with 30%  $\text{H}_2\text{SiF}_6$  for 72 hours at temperatures of 4, 18, 23 and 35°C. Although albite was readily attacked at temperatures as low as 4°C, and losses were as high as 36%, > 92% of quartz was recovered, even at temperatures as high as 35°C:

**Table 16. Percentage Recovery of Quartz and Albite after  $\text{H}_2\text{SiF}_6$  Treatment at Various Temperatures**

Temperature (°C)	Quartz recovery (%)	Albite recovery (%)
4	99.0	63.3
18	99.4	48.0
23	97.4	37.7
35	92.6	23.5

Source: Chapman *et al.* (1969)

In addition, Chapman *et al.* (1969) tested whether the loss of quartz from various treatments in their procedure was due to mechanical loss, by calculating percentage recovery of various size fractions after ten cycles of washing in water, centrifugation and decantation. With untreated ground quartz, mechanical loss increased with increasing size, and little loss occurred with samples pre-treated with HF except for particles 20-10  $\mu\text{m}$ . In both cases, recovery was > 97% for 20-2  $\mu\text{m}$  and 2-0.2  $\mu\text{m}$ .

To test the effect of time and particle size, Chapman *et al.* (1969) performed 1 $\times$ , 2 $\times$  or 3 $\times$ , 72 hour  $\text{H}_2\text{SiF}_6$  treatment cycles. Two treatments removed virtually all albite in the 5-2  $\mu\text{m}$  and 10-5  $\mu\text{m}$  range, with little additional albite removed after the third treatment; for larger grain size fractions there was a significant improvement in albite removal with each subsequent treatment. In contrast, percentage recovery of quartz was > 90% for all fractions even after three treatments, with the exception of the 2-0.2  $\mu\text{m}$  size fraction which fell to

81% and 73% recovered after two and three treatments respectively. Chapman *et al.* (1969) ascribed this loss to dissolution of quartz by  $\text{H}_2\text{SiF}_6$  rather than mechanical loss (given that mechanical loss in Table 17 is so low), therefore they proposed using a correction factor of 1.1 for each  $\text{H}_2\text{SiF}_6$  treatment.

**Table 17. Percentage Recovery of Untreated and 1N HF-Pre-Treated Quartz after Ten Washing-Centrifugation-Decantation Cycles**

Size fraction	Percentage Recovery	
	Untreated	Treated with HF
50-20 $\mu\text{m}$	89.3	98.6
20-10 $\mu\text{m}$	94.5	95.7
10-2 $\mu\text{m}$	97.3	97.1
2-0.2 $\mu\text{m}$	98.3	98.8

Source: Chapman *et al.* (1969)

## Hydrofluorosilicic Acid ( $\text{H}_2\text{SiF}_6$ ) Handling

The  $\text{H}_2\text{SiF}_6$  was stored with 63-100  $\mu\text{m}$  quartz sand to remove any free HF (Sridhar *et al.* 1975); neutralising the sample prior to  $\text{H}_2\text{SiF}_6$  treatment and keeping it cool (ideally  $<18^\circ\text{C}$ ) is also needed to prevent  $\text{H}_2\text{SiF}_6$  decomposing into free hydrofluoric acid which attacks quartz, and silicon tetrafluoride:  $\text{H}_2\text{SiF}_6 \leftrightarrow 2 \text{HF} + \text{SiF}_4$  (Chapman *et al.* 1969). Further, a low pH reduces quartz recovery because strong acids such as HCl enhance the ability of any free HF molecules to dissolve silica by (i) increasing the relative amount of HF through a shift in the equilibrium of the following equation:



and (ii) adsorbing as the hydronium ion on the solid silica surface where it behaves as a catalyst (Gaines 2004).

Neutralisation of solutions of hexafluorosilicic acid with alkali metal bases produces the corresponding alkali metal fluorosilicate salts:



thus boric acid ( $\text{H}_3\text{BO}_3$ ) works by forcing the free F<sup>-</sup> anions into complex salts. This process reduces the virulence of HF, particularly its ability to sequester ionic calcium from blood serum which can lead to cardiac arrest (Nuansa Kimia Sejati Chemical Company 2011), and bone damage (Continental Chemical USA). Gaines (2004) suggests that although [concentrated] boric acid is typically used to neutralise HF (typically at rates of 1g boric acid per 1 mL of 49% HF), the resultant monofluoroboric acid also dissolves glass, and instead recommends addition of an organic amine such as triethanolamine to neutralise HF. In contrast, the US Environmental Protection Agency (2011) suggests that dilute solutions of boric acid *are* appropriate to avoid problems with HF; and some researchers rely on repeated washing with distilled water to neutralise the  $\text{H}_2\text{SiF}_6$  (Dauphin 1980). Given the propensity for monofluoroboric acid to dissolve glass, 50ml polypropylene falcon tubes were used for all  $\text{H}_2\text{SiF}_6$  treatments; furthermore, the formation of monofluoroboric acid reduces the tendency for insoluble fluoride precipitates to form such as  $\text{CaF}_2$ , which is why it was originally added (Gaines 2004), therefore I felt justified in using  $\text{H}_3\text{BO}_3$  as a neutraliser.

## Grain Size Analysis

Earlier studies of New Zealand aerosolic dust (Stewart *et al.* 1984; Stewart *et al.* 1986, Wallace 1987; Alloway 1989) separated sediments into various size fractions using beaker sedimentation ('sieve and pipette' analysis) and/or centrifugation by applying Stokes' Law or its derivatives (Jackson 1956; Alloway *et al.* 1992).<sup>41</sup> Stokes' Law states that a small, smooth sphere falling in a viscous fluid does so under the influence of gravity, ultimately acquiring a constant velocity, according to the formula

$$V = \frac{2ga^2(s_p - s_l)}{9\eta} \quad (19)$$

where  $a$  is the radius of the sphere (dust grain, pollen grain etc),  $s_p$  and  $s_l$  the density or specific gravity of the sphere and the medium (water) respectively,  $g$  is the acceleration of gravity and  $\eta$  is the coefficient of viscosity.  $V$  will be in cm per second if  $g$  is in cm per sec<sup>2</sup>,  $a$  in cm,  $d_1$  and  $d_2$  in g per cm<sup>3</sup> and  $\eta$  in dyne-sec per cm<sup>2</sup> or poises<sup>42</sup>.

By combining Stoke's equation with differential specific gravity  $\Delta s = s_p - s_l$  (that is, specific gravity of the particles relative to the liquid), Jackson (1956) gives a working form of Stoke's Law as

$$V = \frac{g(s_p - s_l)D^2}{18\eta} = k_1 D_2 \quad (20)$$

Since  $v = h/t$ , where  $h$  is the depth of fall in cm, and  $t$  is time in seconds, time required for sedimentation is given by

$$t = \frac{18\eta h}{g(s_p - s_l)D^2} = \frac{k^2}{D^2} \quad (21)$$

It is a simple matter to utilise these formulae in a spreadsheet (Table 18) to derive theoretical times to separate different grain-size fractions. Utilising a spreadsheet in this way rather than reading off a nomograph (eg Jackson 1956) has the added advantage of allowing one to quickly calculate times for any size beakers when using gravity sedimentation, or manipulating speed and time for centrifuges where there are integer constraints in the centrifuge settings. Table 18 shows the difference in times for sedimentation versus centrifugation; for example 7.8 hours to separate out 2  $\mu\text{m}$  grains in a 10 cm test-tube by gravity or 40 seconds at 5,000 rpm in the centrifuge, thus highlighting a major advantage of centrifugation over gravity separation.

<sup>41</sup> For example, Alloway *et al.* (1992a) sieved into 63- 30  $\mu\text{m}$  and < 30  $\mu\text{m}$  and used differential settling to derive 2, 5, 10, 20, 30 and 63  $\mu\text{m}$  fractions.

<sup>42</sup>  $g = 980.665 \text{ cms}^{-2}$ ,  $\eta = 0.0112$  poises (at 16°C);  $d_2 = 1.12$  (at 16°C).

**Table 18. Times to Separate Different Grain-Size Fractions by Sedimentation and Centrifugation<sup>43</sup>**

Sedimentation			Centrifugation					
Time to settle by sedimentn. (sec) per cm	Time to settle (sec) by sedimentn per tube (10cm length)	Time to settle (hr) by sedimentn per tube (10cm length)	Time to settle (sec) by centrifugation per cm	Time to settle (sec) by centrifugation per tube (10cm length)	Revs per second	Revs per minute	settling velocity (depth fall cm / seconds) (Stokes Law)	grain diam. (µm)
$t_s$					$N$	$RPM$	$v$	$D^*$
$=t^*h$	$=18*\eta^*h/g*\Delta s^*D^2$	$=t^*60$	$= (tc^*log_{10}(R/S)) / (3.8I^*N^2*D^2*tc)$	$=t/R$	$=RPM/60$	(user defined)		
4	45	0.0	16.1	160.7	1.7	100	0.00002259798	50
9	86	0.0	7.8	77.5	3.3	200	0.00001172675	36
28	279	0.1	4.0	40.2	8.3	500	0.00000361568	20
112	1,117	0.3	4.0	40.2	16.7	1000	0.00000090392	10
447	4,470	1.2	1.8	17.9	50.0	3000	0.00000022598	5
2,793	27,935	7.8	4.0	40.2	83.3	5000	0.00000003616	2
11,174	55,869	15.5	9.1	45.7	83.3	5000	0.00000000904	1
178,781	893,907	248.3	50.7	253.3	141.7	8500	0.00000000056	0.25

In addition to being time consuming, techniques such as settling and sieve and pipette methods are relatively imprecise due to both laboratory technique and operator error (Syvitski *et al.* 1991; Beuselinck *et al.* 1998), with reported errors in existing studies (when errors are reported at all) sometimes exceeding 40% (Sperraza *et al.* 2004). A major shortcoming of grain-size analysis is that size-frequency curves are generally derived from a small number of observations; Oser (1972) suggests this is mainly a consequence of the intensive labour required.

A further disadvantage of settling and sieve and pipette methods is that a large amount of material (at least 10 g) is typically needed for standard methods for grain-size analysis based on sedimentation rates for fine grain-size fractions and sieving for coarse fractions (Gee & Bauder 1986). Given that small volumes of aerosolic dust were extracted from the mostly peat samples (occasionally < 0.1g), coupled with a desire to obtain the highest resolution output as practicable to allow meaningful inferences from the data and comparisons with high resolution pollen data, it became apparent that the classic techniques were not appropriate for fast and accurate analysis of a large number of small samples (Beuselinck *et al.* 1998).

One potential weakness of laser diffraction over differential sedimentation techniques is that laser diffraction does not take into account particles smaller than the lower detection limit when calculating size distribution, whereas sedimentation analysis does; for example, the Horiba does not take into account particles < 30 nm in its calculations. Comparison between outputs from laser diffraction, which expresses size distribution in volume units, and sedimentation based analysis, which expresses size distribution in weight units (Loizeau *et al.* 1994), is made possible simply by expressing the outputs of both as percentages.

Accordingly, laser diffraction was used to determine grain-size characteristics of the wind-blown sediments. Laser grain-size analysis is based upon diffraction of light by the particles in the sample; particles of a given

<sup>43</sup> Gravitational constant,  $g$  980.665  $\text{cm s}^{-2}$ ; specific gravity, water (from table),  $sI = 0.998$ ; temp °C,  $T = 20.0$ ; specific gravity, particle,  $sp = 2.65$ ; differential specific gravity ( $sp-sI$ ),  $\Delta s = 1.652$ ; viscosity in poise (from table),  $\eta = 0.01005$ ; depth of fall (cm),  $h = 10$ .

size diffract the light through a given angle and at different intensities such that the angle of diffraction increases, and scattered light intensity decreases with a decrease in particle size (Loizeau *et al.* 1994; Horiba Inc 2011). When a beam of monochromatic light passes through the suspended sediments, the diffracted light is focused onto a detector that perceives the angular distribution of scattered light intensity, whilst undiffracted light is focused onto the detector by a lens situated between the sediment sample and the detector. Together, particles passing through the beam create a stable diffraction pattern (Singer *et al.* 1988).

Laser particle-size analysers typically calculate grain-size distribution from the light intensity arriving at the detectors using one of two diffraction theories; (i) Fraunhofer theory estimates particle size from extinction efficiency, that is, light scattering and absorption, with the assumption that light extinction efficiency remains constant irrespective of grain size. In other words, light only undergoes diffraction, and no refraction (Beuselinck *et al.* 1998) according to the formula

$$I(\theta) = 1/\theta^2 \int_0^\infty R^2 n(R) J_1^2(\theta kR) dR \quad (22)$$

where  $\theta$  is the scattering angle,  $R$  is the radius of the particle,  $J$  is the Bessel function of the first kind (Loizeau *et al.* 1994)<sup>44</sup>,  $(n)R$  is the grain size distribution function,  $k = 2\pi/\lambda$ , where  $\lambda$  is the wavelength of the incident light, and. A weakness of Fraunhofer theory is that grain-size measurements tend to underestimate particle sizes when  $d \approx \lambda$ , that is, when particle diameter approaches the wavelength of the light (Sperazza *et al.* 2004). (ii) Mie theory allows light extinction efficiency to vary with grain-particle size, and therefore is less susceptible to under-estimates of grain size as  $d$  approaches  $\lambda$ .

The trade-off for greater accuracy using Mie-theory is that the indices for the refraction and absorption of both the particles being analysed and the suspension medium are required (Sperazza *et al.* 2004). For the aerosolic quartz work described here, simplifying assumptions are that the suspension fluid is pure, deionised water held at a constant 20°C, and that the previous chemical treatments have rendered the samples into pure quartz. Therefore, a single refractive index can be taken from the literature for each component, in contrast to having to derive a new refractive index for each sample of mixed-mineral sediment.

The Horiba Partica LA-950 particle-size analyser used in this study employs a 650 nm red-laser diode, a 405 nm blue-light emitting diode (LED) and Mie scattering; the manufacturers claim the LA-950 can accurately measure 30 nm diameter particles with an accuracy of "...± 0.6% of standard tolerance on these [National Institute of Standard and Technology] traceable polystyrene latex standards: 100 nm, 500 nm, 1.020 µm, 12.01 µm, 102 µm & 1004 µm grain size distribution," (Horiba Inc 2011).

The accuracy of particle analysers depends upon sample pre-treatment and operation of the analyser; in addition, Sperazza *et al.* (2004) note that the statistical output of laser particle-size analysers are typically associated with some uncertainties, such as skewing in non-Gaussian grain-size distributions. For example, a positively skewed grain-size distribution – a distribution with a large percentage of fine grain sizes – has more uncertainty associated with the ninetieth percentile than the tenth percentile. To combat precision and accuracy issues, at least two sub-samples were analysed from each sample, with two analysis runs on each sub-sample conducted, giving at least four readings for each sample. The precision of the measurements can be assessed by comparing median sizes of the sub-samples taken from a single sample (Dauphin 1980).

The high surface to volume ratios of clay-size particles increases the attractive forces between particles, so that they tend to agglomerate or flocculate (Sperazza *et al.* 2004). To prevent agglomeration from occurring in the

<sup>44</sup> Bessel functions of the first kind,  $J_\alpha(x)$ , are solutions of Bessel's first order differential equations

$$x^2 \frac{d^2 y}{dx^2} + x \frac{dy}{dx} + (x^2 - \alpha^2) y = 0 \quad (23)$$

that are finite at the origin ( $x = 0$ ) for integer  $\alpha$ , and diverge as  $x$  approaches zero for negative non-integer  $\alpha$ .

Eltham samples<sup>45</sup>, ultrasound was used at low-medium intensity for up to 60 seconds per run, noting that excess sonication has been known to break grains (skewing grain-size distribution curves towards smaller size fractions) and flocculate grains (skewing grain-size distribution curves in the opposite direction, that is towards greater size fractions). In addition, suspension circulation speeds were adjusted to prevent flocculation. Collectively, these options appeared to adequately disperse the aliquot, without the need to add chemical dispersants such as sodium hexametaphosphate (Sperazza *et al.* 2004; Horiba Inc. 2011). Aliquots of around 0.1 g were introduced in a dry state to the analyser, as recommended by Horiba Inc. (2011).

The ‘density’ of the sample added for analysis is measured by the degree of obscuration of the light source; Sperazza *et al.* (2004) defined optimal obscuration as “...when a sufficient number of suspended particles are present to significantly diffract the laser beam but the suspension is not so dense to render the suspension impenetrable by the laser light.” Horiba Inc (2011) recommend adding a volume of sediment sufficient to achieve 85% light transmission (that is, 15% obscuration) for both the laser beam (larger particles) and LED (smaller particles) to achieve optimal obscuration; this value was found to provide stable results for a comparable, Mie-scattering laser analyser.

The pipette and sieve method and laser grain-size analysis yield slightly different results because they define size differently, and therefore measure different properties of the same particle. The pipette method defines grain size as equivalent to the diameter of a sphere settling out of the same solute at the same speed as the unknown mineral grain, whereas the sieve component of pipette and sieve analysis defines grain size as the dimension of one side of a perfect square hole that the grain can only just pass through. Laser grain size analysis perceives the grain as a two dimensional object and defines grain size as equivalent to a sphere that yields the same diffraction signature as the unknown grain (Konert & Vandenberghe 1997).

Furthermore, both techniques are prone to error due to a potential limitation when applying Stoke’s law to sediment grain-size analysis: Stoke’s Law assumes that the mineral grains are smooth spheres, rather than rough textured or plate-like discs characteristic of many clays or non-spherical sediments (Beuselinck *et al.* 1998; Konert & Vandenberghe 1997).

Konert & Vandenberghe (1997) tested predicted values from Stoke’s laws particles against laser-particle analysers and sieve and pipette methods. In general, laser-particle analysis gave slightly coarser estimates of > 63 µm particles than did sieve and pipette methods, due to the non-spherical nature of sands. Particles with so-called ‘Stokes diameters’ of around 2 µm had actual lengths of around 10 µm and thicknesses of around 0.4 µm; since these grains have different fall velocities to ideal, spherical grains. Konert & Vandenberghe (1997) demonstrated the differences in theoretical settling times for spherical particles and plate-like clays in either a broadside-settling or edgewise-settling orientation, using the following set of modified Stokes’s law equations:

Equation (19) is modified to give the settling velocity for a disc falling broadside,  $V_{db}$ .

$$V_{db} = \frac{0.238 g (s_p - s_1) a^{\frac{1}{3}} r_e^2}{\eta h} \quad (24)$$

and changing the constant in (24) gives the settling velocity for a disc falling edgewise,  $V_{de}$ :

$$V_{de} = \frac{0.357 g (s_p - s_1) a^{\frac{1}{3}} r_e^2}{\eta h} \quad (25)$$

where  $r_e$  is the radius of the volume equivalent sphere: the radius of a disc  $a$  and  $r_e$  are related by

$$a = r_e \left( \frac{4a}{3h} \right)^{1/3} \quad (26)$$

<sup>45</sup> I noticed this effect in some early runs of the Eltham aerosolic quartz (for example, size fractions of 3,000 µm were reported in material that had been dry sieved to < 63 µm), indicating that sediment aggregation was occurring.

Substituting (26) into (25) gives

$$V_d = \frac{0.1965 g (s_p - s_1)}{\eta} ha \quad (27)$$

Equating  $V$  and  $V_d$  gives

$$\frac{2}{9} r^2 = 0.1965 ha \quad (28)$$

For a disc settling broadside, putting the thickness ratio  $R$  (defined as  $h/a = R$ ) into (28) gives

$$\frac{r}{a} = 0.94 \sqrt{R} \quad (29)$$

and for a disc settling edgewise, putting the thickness ratio  $R$  into (29) gives

$$\frac{r}{a} = 1.15 \sqrt{R} \quad (30)$$

Thus a disc-shaped particle 10  $\mu\text{m}$  across (radius 5  $\mu\text{m}$ ) with a thickness of 0.36  $\mu\text{m}$  yields a thickness ratio  $R$  of  $h/a = 0.36/5 = 0.072$ , and an  $r/a$  ratio of  $0.94 \sqrt{0.072} = 0.252$ . Using the same ratios, we can calculate that a spherical grain with a radius of 1  $\mu\text{m}$  is equivalent to a disc-shaped grain with radius 3.95  $\mu\text{m}$  with thickness  $h$  of 0.29  $\mu\text{m}$ <sup>46</sup>, and for the same discoid grain falling edgewise a spherical grain with a radius of 1  $\mu\text{m}$  is equivalent to a disc-shaped grain with radius 3.25  $\mu\text{m}$  with thickness  $h$  of 0.23  $\mu\text{m}$ . For Eltham, the effect is minimised to some degree by removing clays from the sediments.

## X-Ray Diffraction

The efficacy of  $\text{H}_2\text{SiF}_6$  treatment to remove feldspars was assessed by repeated XRD measurements. The series of XRD<sup>47</sup> patterns for samples 5/150-151 and 5/155-156 show a decrease in feldspar with each successive  $\text{H}_2\text{SiF}_6$  treatment, with multiple feldspar peaks occurring prior to  $\text{H}_2\text{SiF}_6$  treatment and little to no feldspar peaks after six days'  $\text{H}_2\text{SiF}_6$  treatment (Figure 65). Accordingly, all samples were given six days of  $\text{H}_2\text{SiF}_6$  treatment.

<sup>46</sup> Equivalent radius is  $1 \div 0.252 = 3.95$  and equivalent thickness is  $0.073 \div 0.252 = 0.289$ .

<sup>47</sup> All XRD samples were processed by Associate Professor Bob Stewart at speed = 2°/minute, time/step = 0.05°, wavelength = 1.78897Å (Co).

A High Resolution Record of Late Quaternary Climatic and Environmental Change in Taranaki, New Zealand

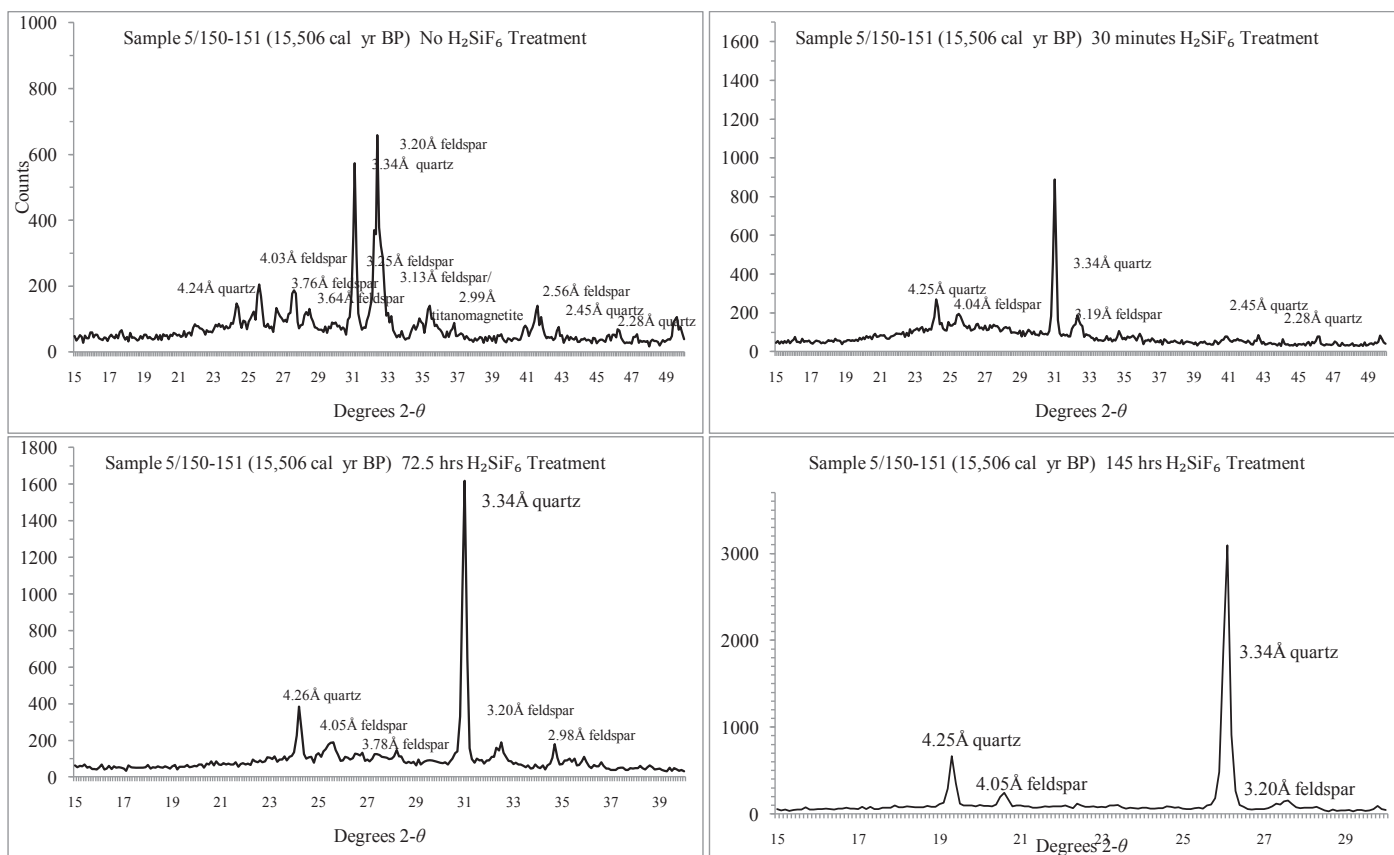


Figure 65 (a). XRD Plots for Selected Eltham Quartz Dust Samples (15,506 cal yr BP)

A High Resolution Record of Late Quaternary Climatic and Environmental Change in Taranaki, New Zealand

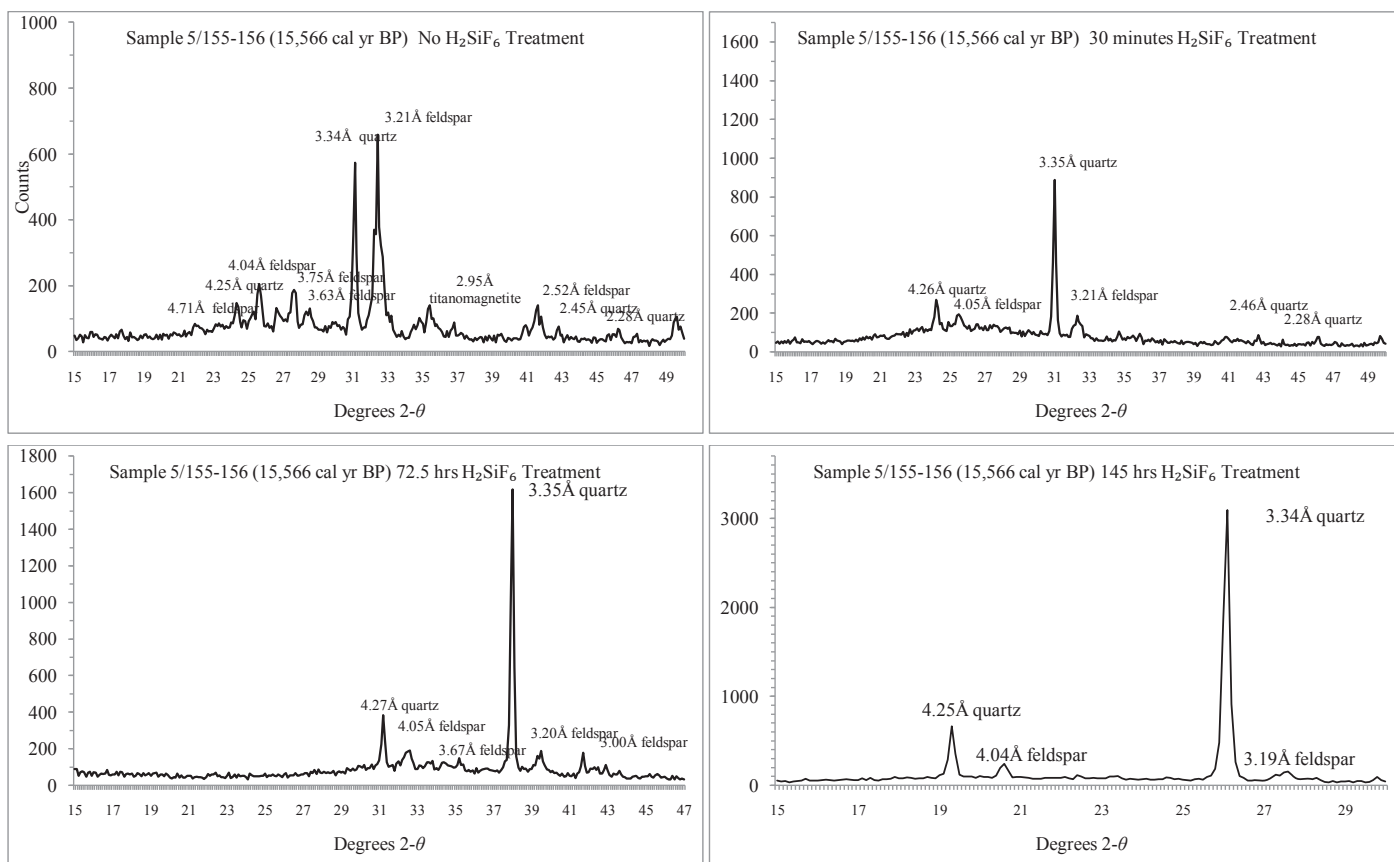


Figure 65 (b). XRD Plots for Selected Eltham Quartz Dust Samples (15,566 cal yr BP)

## 12. References

- Aguilera, N; & Jackson, M. (1953) Iron Oxide Removal from Soils and Clays. *Soil Science Society of America Journal* 17 (4) 359-364
- Abbott, M; Seltzer, G; Kelts, K; & Southon, J. (1997) Holocene Paleohydrology of the Tropical Andes from Lake Records. *Quaternary Research* 47 70-80
- Allan, H. (1982) *Flora of New Zealand Vol 1 Indigenous Tracheophyta* (2<sup>nd</sup> ed) Wellington: Government Printer
- Alloway, B. (1989) *The Late Quaternary Cover Bed Stratigraphy and Tephrochronology of North-eastern and Central Taranaki, New Zealand*. A Thesis Presented in Partial Fulfilment of the Requirements for the Degree of Doctor of Philosophy in Soil Science at Massey University. Palmerston North, New Zealand: Massey University
- Alloway, B. (2005) Are the Andisols in Taranaki telling us something about Paleowind & -Precipitation Conditions Over the Last 30,000 Years? In B. Alloway & J. Shulmeister (Eds) Proceedings of the 2005 NZ-INTIMATE Meeting, GNS-Rafter Laboratory, Wellington July 4-5 2005. *Institute of Geological & Nuclear Sciences Report 2005/18*. Lower Hutt, New Zealand: Institute of Geological & Nuclear Sciences
- Alloway B; Lowe, D; Barrell, D; Newnham, R; Almond, P; Augustinus, P; Bertler, N; Carter, L; Litchfield, N; McGlone, M; Shulmeister, J; Vandergoes, M; Williams, P; & NZ-INTIMATE members (2007) Towards a Climate Event Stratigraphy for New Zealand over the past 30,000 years (NZ-INTIMATE project). *Journal of Quaternary Science* 22: 9-35
- Alloway, B; McComb, P; Neall, V; Vucetich, C; Gibb, J; Sherburn, S; & Stirling, M. (2005) Stratigraphy, Age and Correlation of Voluminous Debris-Avalanche Events from an Ancestral Egmont Volcano: Implications for Coastal Plain Construction and Regional Hazard Assessment. *Journal of the Royal Society of New Zealand* 35 229-267
- Alloway, B; McGlone, M; Neall, V; & Vucetich, C. (1992) The Role of Egmont-sourced Tephra in Evaluating the Paleoclimatic Correspondence between the Bio- and Soil-Stratigraphic Records of central Taranaki, New Zealand. *Quaternary International* 13-14 187-194
- Alloway, B; Neall, V; & Vucetich, C. (1988) Localised Volcanic Loess Deposits in North Taranaki, North Island, New Zealand. In D. Eden & R. Furkert (Eds) *Loess: Its Distribution, Geology and Soils. Proceedings of an International Symposium on Loess 14-21 February 1987*. Rotterdam, the Netherlands: A.A. Balkema
- Alloway, B; Neall, V; & Vucetich, C. (1995) Late Quaternary (post 28,000 year B.P) Tephrostratigraphy of Northeast and Central Taranaki, New Zealand. *Journal of the Royal Society of New Zealand* 25 (4) 385-458
- Alloway, B; Stewart, R; Neall, V; & Vucetich, C. (1992a) Climate of the Last Glaciation in New Zealand, based on Aerosolic Quartz Influx in an Andesitic Terrain. *Quaternary Research* 38 170-179
- Alloway, B; Stewart, R; Neall, V; & Vucetich, C. (1992b) Particle Size Analyses of Late Quaternary Allophane-Dominated Andesitic Deposits from New Zealand. *Quaternary International* 13/14 167-174
- An, F; Ma, H; Wei, H; & Lai, Z. (2012) Distinguishing Aeolian Signature from Lacustrine Sediments of the Qaidam Basin in Northeastern Qinghai-Tibetan Plateau and its Palaeoclimatic Implications. *Aeolian Research* 4 17-30

- Anderson, A. (2009) Media, Politics and Climate Change: Towards a New Research Agenda *Sociology Compass* 3/2 166–182
- Anderson, B; & Mackintosh, A. (2006) Temperature Change is the Major Driver of Late-Glacial and Holocene Glacier Fluctuations in New Zealand. *Geology* 34 121-124
- Anderson, K; & Ditlevsen, P. (1998) Glacial/Interglacial Variations of Meridional Transport and Washout of Dust: A One-Dimensional Model. *Journal of Geophysical Research* 103 D8 8955-8962
- Argue, C. (1986) Pollen Morphology of *Amphianthus*, *Artanema*, *Curanga*, *Glossostigma*, and *Peplidium* (Scrophulariaceae-Gratiolales). *American Journal of Botany* 73 (11) 1570-1576
- Arimoto, R. (2001) Eolian Dust and Climate: Relationships to Sources, Tropospheric Chemistry, Transport and Deposition. *Earth Science Reviews* 54 29-42
- Asselin, H; & Payette, S. (2005) Detecting Local-Scale Fire Episodes on Pollen Slides. *Review of Palaeobotany & Palynology* 137 31-40
- Augustinus, P; D'Costa, D; Deng, Y; Hagg, J; & Shane, P. (2011) A Multi-Proxy Record of Changing Environments from ca. 30 000 to 9000 cal. A BP: Onepoto Maar Palaeolake, Auckland, New Zealand. *Journal of Quaternary Science* 26 (4) 389-401
- Ayotte, P; Hébert, M; & Marchand, P. (2005) Why is Hydrofluoric Acid a Weak Acid? *Journal of Chemical Physics* 123 (18) 184501 1 – 184501 8
- Baldi, M; & Salinger, M. (2008) *Climate Trends, Hazards and Extremes – Taranaki Synthesis Report. NIWA Client Report: 2008-080*. National Institute of Water & Atmospheric Research Ltd: Wellington
- Ban, K. (2009) It's now or never in bid to curb climate change, Ban warns. *UN News Service* 14 December 2009 <http://www.un.org/apps/news/story.asp?NewsID=33241&Cr=climate+change&Cr1=> accessed 24.02.11
- Banks, N; Wallace, C; Outred, H; Flenley, J; & Rowland, R. (2003a) A Comparative Pollen Analysis of Peat with Neighbouring Palaeosols at three sites in the Tongariro Volcanic Centre, New Zealand. *Abstracts, Geosciences 2003 Conference, Dunedin New Zealand*. Wellington, New Zealand: Geoscience Society of New Zealand.
- Banks, N; Wallace, C; Outred, H; Flenley, J; & Rowland, R. (2003b) Is the Taupo Ignimbrite an Effective Barrier to the Downward Translocation of Palynomorphs? *New Zealand Natural Sciences* 28 1-7
- Bannister, P; & Lord, J. (2006) Comparative Winter Frost Resistance of Plant Species from Southern Africa, Australia, New Zealand and South America Grown in a Common Environment (Dunedin, New Zealand). *New Zealand Journal of Botany* 44 109-119
- Barnosky, A. (2001) Distinguishing the Effects of the Red Queen and Court Jester on Miocene Mammal Evolution in the Northern Rocky Mountains. *Journal of Vertebrate Paleontology* 21 (1) 172-185
- Barrell, D; Almond, P; Vandergoes, M; Lowe, D; Newnham, R; & INTIMATE Members (2013) A Composite Pollen-based Stratotype for Inter-Regional Evaluation of Climatic Events in New Zealand over the Past 30,000 years (NZ-INTIMATE Project). *Quaternary Science Reviews* 74 4-20
- Barrows, T; Juggins, S; De Dekker, P; Calvo, E; & Pelejaró, C. (2007) Long-Term Sea Surface Temperature and Climate Change in the Australian-New Zealand Region. *Paleoceanography* 22 1-17

- Barrows, T; Lehman, S; Fifield, L; & De Dekker, P. (2007) Absence of Cooling in New Zealand and the Adjacent Ocean During the Younger Dryas Chronozone. *Science* 318 86-89
- Barrows, T; Stone, J; Fifield, L; & Cresswell, R. (2002) The Timing of the Last Glacial Maximum in Australia. *Quaternary Science Reviews* 21 159-173
- Baylis, G. (1980) Mycorrhiza and the Spread of Beech. *New Zealand Journal of Ecology* 3 151-153
- Beu, A. (1999) Fossil Records of the Cold-Water Scallop *Zygochlamys delicatula* (Mollusca: Bivalvia) off Northernmost New Zealand: How Cold was the Last Glacial Maximum? *New Zealand Journal of Geology & Geophysics* 42 543-550
- Beerling, D; Birks, H; & Woodward, F. (1995) Rapid Late-Glacial Atmospheric CO<sub>2</sub> Changes Reconstructed from the Stomatal Density Record of Fossil Leaves. *Journal of Quaternary Science* 10 379-384
- Bellingham, P; & Richardson, S. (2006) Tree Seedling Growth and Survival over 6 years across Different Microsites in a Temperate Rain Forest. *Canadian Journal of Forest Research* 36 910-918
- Benton, M. (2009) The Red Queen and the Court Jester: Species Diversity and the Role of Biotic and Abiotic Factors through Time. *Science* 323 728-732
- Berger, W; & Parker, F. (1970) Diversity of Planktonic Foraminifera in Deep-Sea Sediments. *Science* 168 1345-1347
- Bergin D; & Steward, G. (2004) *Kauri. Ecology, Establishment, Growth, and Management. New Zealand Indigenous Tree Bulletin 2*. Rotorua, New Zealand: New Zealand Forest Research Institute
- Beuselinck, L; Govers, G; Poesen, J; & Degraer, G. (1998) Grain-Size Analysis by Laser Diffractometry: Comparison with the Sieve-Pipette Method. *Catena* 32 193-208
- Beveridge, A. (1973) Regeneration of Podocarps in Central North Island Forests. *New Zealand Journal of Forestry* 18 23-35
- Birks, H; & Line, J. (1992) The Use of Rarefaction Analysis for Estimating Palynological Richness from Quaternary Pollen-Analytical Data. *The Holocene* 2 (1) 1-10
- Biswas, S; & Mallik, A. (2010) Disturbance Effects on Species Diversity and Functional Diversity in Riparian and Upland Plant Communities. *Ecology* 91 (1) 28-35
- Bjorck, S; Walker, M; Cwynar, L; Johnsen, S; Knudsen, K-L; Lowe, J; Wohlfarth, B; & INTIMATE Members (1998) An Event Stratigraphy for the Last Termination in the North Atlantic Region based on the Greenland Icecore Record: A Proposal by the INTIMATE Group. *Journal of Quaternary Science* 13 283-292
- Blaauw, M. (2010) Methods and Code for 'Classical' Age-Modelling of Radiocarbon Sequences. *Quaternary Geochronology* doi:10.1016/j.quageo.201001.002
- Blaauw, M. (2013) Out of Tune: the Dangers of Aligning Proxy Archives. *Quaternary Science Reviews* 36 38-49
- Blaauw, M; & Christen, J. (2011) Flexible Paleoclimate Age-Depth Models Using an Autoregressive Gamma Process. *Bayesian Analysis* 6 (3) 457-474
- Blodgett, D; Suruda, A; & Crouch, B. (2001) Fatal Unintentional Occupational Poisonings by Hydrofluoric Acid in the U.S. *American Journal of Industrial Medicine* 40 215-220

- Blott, S; & Pye, K. (2001) GRADISTAT: A Grain Size Distribution and Statistics Package for the Analysis of Unconsolidated Sediments. *Earth Surface Processes & Landforms* 26 1237-1248
- Blunier, T; Schwander, J; Stauffer, B; Stocker, T; Dällenbach, A; Indermühle, A; & Tschumi, J. (1997) Timing of the Antarctic Cold Reversal and the Atmospheric CO<sub>2</sub> Increase with respect to the Younger Dryas Event. *Geophysical Research Letters* 24 (21) 2683-2686
- Blunier, T; Chappellaz, J; Schwander, J; Dällenbach, A; Stauffer, B; Stocker, T; Raynaud, D; Jouzel, J; Clausen, H; Hammer, C; & Johnsen, S. (1998) Asynchrony of Antarctic and Greenland Climate Change during the Last Glacial Period. *Nature* 384 739-742
- Bradley, R. (1999) *Palaeoclimatology: Reconstructing Climates of the Quaternary*. (2nd ed). Vol 68 San Diego: International Geophysics Series Academic Press
- Brewer, A; & Williamson, M. (1994) A New Relationship for Rarefaction. *Biodiversity & Conservation* 3 373-379
- Broecker, W. (1998) Paleocean Circulation during the Last Deglaciation: A Bipolar Seesaw? *Paleoceanography* 13: 119-121.
- Broecker, W. (2001) The Big Climate Amplifier Ocean Circulation-Sea Ice-Storminess-Dustiness-Albedo. In D. Seidov, B. Haupt & M. Maslin (Eds) *Geophysical Monograph 126* Washington, D.C: American Geophysical Union
- Bronk Ramsey, C. (2008) Deposition Models for Chronological Records. *Quaternary Science Reviews* 27 (1-2) 42-60
- Bronk Ramsey, C. (2009) Dealing with Outliers and Offsets in Radiocarbon Dating. *Radiocarbon* 51 (3) 1023-1045
- Bronk Ramsey, C. (2009) Bayesian Analysis of Radiocarbon dates. *Radiocarbon* 51 (3) 337-360
- Bryant, J; Chapin, F; & Klein, D. (1983) Carbon / Nutrient Balance of Boreal Plants in Relation to Vertebrate Herbivory. *Oikos* 40 (3) 357-368
- Buckland, S; Magurran, A; Green, R; & Fewster, R. (2005) Monitoring Change in Biodiversity through Composite Indices. *Philosophical Transactions of the Royal Society B* 360 243-254
- Buckland, S; Studeny, A; Magurran, A; & Newson, S. (2011) Biodiversity Monitoring: The Relevance of Detectability. In A. Magurran & B. McGill (Eds) *Biological Diversity: Frontiers in Measurement and Assessment*. New York, NY: Oxford University Press
- Burckle, L; Shackleton, N; & Bromble, S. (1981) Late Quaternary Stratigraphy for the Equatorial Pacific Based upon the Diatom *Coscinodiscus nodulifer*. *Micropaleontology* 27 (4) 352-355
- Burgess, S; Salinger, M; Gray, W; & Mullan, A. (2006) *Climate Hazards and Extremes –New Plymouth District; Cyclones of Topical Origin*. NIWA Client Report WLG2006-27. Wellington, New Zealand: National Institute of Water & Atmospheric Research
- Burgess S; Salinger, M; Turner, R; & Reid, S (2007) *Climate Hazards and Extremes –Taranaki Region: High Winds and Tornadoes*. NIWA Client Report WLG2007-48 for New Plymouth District Council. Wellington, New Zealand: National Institute of Water & Atmospheric Research

- Burrows, C. (1965) Some Discontinuous Distributions of Plants within New Zealand and their Ecological Significance. Part II: Disjunctions between Otago-Southland and Nelson-Marlborough and Related Distribution Patterns. *Tuatara* 12 9-29
- Bussell, M. (1988a) Modern Pollen Rain, Central-Western North Island, New Zealand. *New Zealand Journal of Botany* 26 297-315
- Bussell, M. (1988b) Mid and Late Holocene Pollen Diagrams and Polynesian Deforestation, Wanganui District, New Zealand. *New Zealand Journal of Botany* 26 431-451
- Bussell, M. (1993) A late Pleistocene Vegetational and Climatic History of part Oxygen Isotope Stage 5, Ararata, South Taranaki, New Zealand. *Journal of the Royal Society of New Zealand* 23 (2) 129-145
- Butcher, A; Haberlah, D; Strong, C; Love, B; & McTainsh, G. (2011) *EM-EDS Based Particle-by-Particle Characterisation of a Large Australian Dust Storm*. INQUA XVIII Presentation, Stade de Suisse Ball Saal, Bern, Switzerland 25.07.12
- Butler, K. (2008) Interpreting Charcoal in New Zealand's Paleoenvironment – What do those Charcoal Fragments Really Tell Us? *Quaternary International* 184 122-128
- Caçador, I; Netro, J; Duarte, B; Barroso, D; Pinto, M; & Marques, J. (2013) Development of an Angiosperm Quality Assessment Index (AQUA-Index) for Ecological Quality Evaluation of Portuguese Water Bodies – a Multi-Metric Approach. *Ecological Indicators* 25 141-148
- Calvo, E; & Pelejero, C. (2004) Dust-Induced Changes in Phytoplankton Composition in the Tasman Sea during the last four Glacial Cycles. *Paleoceanography* 19 PA2020 1-10
- Campbell, C. (1998) Late Holocene Lake Sedimentology and Climate Change in Southern Alberta, Canada. *Quaternary Research* 49 96–101
- Campbell, E; Heine, J; & Pullar, W. (1973) Identification of Plant Fragments and Pollen from Peat Deposits in the Rangitaiki Plains and Maketu Basins. *New Zealand Journal of Botany* 11 317-330
- Cameron, R. (1963) A Study of the Rooting Habits of Rimu and Tawa in Pumice Soils. *New Zealand Journal of Forestry* 8 771–785.
- Carter, L; & Manighetti, B. (2005) Ocean Changes off New Zealand during Antarctic Cold Reversal- Younger Dryas Time. In B. Alloway & J. Shulmeister (Eds) *Proceedings of the 2005 NZ-INTIMATE Meeting, GNS-Rafter Laboratory, Lower Hutt, 4-5 July*. Institute of Geological and Nuclear Sciences Science Report SR 2005/18. Lower Hutt, New Zealand: Institute of Geological and Nuclear Sciences Science
- Carter, L; Manighetti, B; Elliot, M; Trustrum, N; & Gomez, B. (2002) Source, Sea Level and Circulation Effects on the Sediment Flux to the Deep Ocean over the past 15 ka off eastern New Zealand. *Global & Planetary Change* 33 339-355
- Carter, L; Neil, H; & McCave, I. (2000) Glacial to Interglacial Changes in Non-Carbonate and Carbonate Accumulation in the SW Pacific Ocean, New Zealand. *Palaeogeography, Palaeoecology, Palaeoclimatology* 162 333-356
- Catford, J; Daehler, C; Murphy, H; Sheppard, A; Hardesty, B; Westcott, D; Rejmánek, M; Bellingham, P; Pergl, J; Horovitz, C; & Hulme, P. (2012) The Intermediate Disturbance Hypothesis and Plant Invasions: Implications for Species Richness and Management. *Perspectives in Plant Biology, Evolution & Systematics* 14 231-241

- Chadwick, L; Derry, O; Vitousek, P; Huebert, B; & Hedin, L. (1999) Changing Sources of Nutrients During Four Million Years of Ecosystem Development. *Nature* 397 491-497
- Chapin, F; Schulze, E-D; & Mooney, H. (1990) The Ecology and Economics of Storage in Plants. *Annual Review of Ecology & Systematics* 21 423-447
- Chapman, S; Syers, J; & Jackson, M. (1969) Quantitative Determine of Quartz in Soils, Sediments and Rocks by Pyrosulfate Fusion and Hydrofluosilicic Acid. *Soil Science* 107 (5) 348-355
- Chaves, M; Pereira, J; Maroco, J; Rodrigues, M; Ricardo, C; Osório, M; Carvalho, I; Faria, T; & Pinheiro, C. (2002) How Plants Cope with Water Stress in the Field: Photosynthesis and Growth. *Annals of Botany* 89 907-916
- Čiamporová, M; Dekánková, K; & Ovečk, M. (1998) Root Morphology and Anatomy of Fast- and Slow-Growing Grass Species. In H. Lambers, H. Poorter & M. van Vuren (Eds) *Inherent Variation in Plant Growth. Physiological Mechanisms and Ecological Consequences*. Leiden, the Netherlands: Backhuys Publishers
- Clapperton, C. (1993) Glacier Readvances in the Andes at 12,500 –10,000 yr BP: Implications for Mechanism of Late-glacial Climatic Change. *Journal of Quaternary Science* 8 (3) 197-215
- Clark, J. (1988) Particle Motion and the Theory of Charcoal Analysis: Source Area, Transport, Deposition and Sampling. *Quaternary Research* 30 67-80
- Clarkson, B. (1985) The Vegetation of the Kaitake Range, Egmont National Park. *New Zealand Journal of Botany* 23 15-31
- Clarkson, B. (1990) A Review of Vegetation Development following Recent (<450 years) Volcanic Disturbance in North Island, New Zealand. *New Zealand Journal of Ecology* 14 59-71
- Clarkson, B; Schipper, L; & Lehmann, A. (2004) Vegetation and Peat Characteristics in the Development of Lowland Restiad Bogs, North Island, New Zealand. *Wetlands* 24 133-151
- Clarkson, D. (1985) Factors Affecting Mineral Nutrient Acquisition by Plants. *Annual Review of Plant Physiology* 36 77-115
- Clements, F. (1928) *Plant Succession and Indicators: A Definitive Edition of Plant Succession and Plant Indicators*. New York: W.H. Wilson
- CLIMAP (1981) Seasonal Reconstruction of the Earth's Surface at the Last Glacial Maximum. *Geological Society of America Map & Chart Series C36*
- Cockayne, L. (1897) On the Freezing of New Zealand Alpine Plants: Notes of an Experiment Conducted in the Freezing Chamber, Lyttelton. *Transactions and Proceedings of the New Zealand Institute* 30 435-442
- Cockayne, L. (1912) Observations Concerning Evolution Derived from Ecological Studies in New Zealand. *Transactions of the New Zealand Institute* 44 1-50
- Coley, P. (1983) Herbivory and Defensive Characteristics of Tree Species in a Lowland Tropical Forest. *Ecological Monographs* 53 (2) 209-234
- Coley, P; Bryant, J; & Chapin, F. (1985) Resource Availability and Plant Antiherbivore Defence. *Science* 230 (4728) 895-899

- Collins, S. (1992) Fire Frequency and Community Heterogeneity in Tallgrass Prairie Vegetation. *Ecology* 73 2001-2006
- Collins, S; & Glenn, S. (1997) Intermediate Disturbance and its Relationship to Within- and Between-Patch Dynamics. *New Zealand Journal of Ecology* 21 (1) 103-110
- Collins, S; Glenn, S; & Gibson, D. (1995) Experimental Analysis of Intermediate Disturbance and Initial Floristic Composition: Decoupling Cause and Effect. *Ecology* 76 486-492
- Colombaroli, D; Beckman, M; van der Knaap, W; Curdy, P; & Tinner, W. Changes in Biodiversity and Vegetation Composition in the central Swiss Alps during the Transition from Pristine Forest to First Farming. *Diversity & Distributions* 19 157-170
- Connell, R; & Slayter, R. (1977) Mechanisms of Succession in Natural Communities and their Roll in Community Stability and Organization. *The American Naturalist* 111 1119-1144
- Continental Chemical USA (2011) *Boric Acid B(OH)<sub>3</sub>* <http://www.continentalchemicalusa.com/bulk-chemicals/boric-acid.html> last accessed 04.10.11
- Cook, J; Mark, A; & Shore, B. (1980) Responses of *Leptospermum scoparium* and *L. ericoides* (Myrtaceae) to Waterlogging. *New Zealand Journal of Botany* 18 233-246
- Coomes, D; & Bellingham, P. (2011) Temperate and Tropical Podocarps: How Ecologically Alike are they? *Smithsonian Contributions to Botany* 95 119-140
- Coomes, D; Allen, R; Bentley, W; Burrows, L; Canham, C; Fagan, L; Forsyth, D; Gaxiola-Alcantar, A; Parfitt, R; Ruscoe, W; Wardle, D; Wilson, D; & Wright, E. (2005) The Hare, the Tortoise and the Crocodile: The Ecology of Angiosperm Dominance, Conifer Persistence and Fern Filtering. *Journal of Ecology* 93 918-935
- Cope, M; & Chaloner, W. (1980) Fossil Charcoal as Evidence of Past Atmospheric Composition. *Nature* 238 647-649
- Cowling, S. (1999) Simulated Effects of Low Atmospheric CO<sub>2</sub> on Structure and Composition of North American Vegetation at the Last Glacial Maximum. *Global Ecology & Biogeography* 8 81-93
- Cranwell, L. (1953) New Zealand Pollen Studies: The Monocotyledons. *Bulletin of the Auckland Institute and Museum* 3. Cambridge, MA: Harvard University Press
- Cranwell, L; & von Post, L. (1936) Post-Pleistocene Pollen Diagrams from the Southern Hemisphere. *Geografiska Annaler* 18 308-347
- Crozier, M; & Pillans, B. (1991) Geomorphic Events and Landform Response in South-Eastern Taranaki, New Zealand. *Catena* 18 471-487
- Cullen, L; Duncan, R; Wells, A; & Stewart, G. (2003) Floodplain and Regional Scale Variation in Earthquake Effects on Forests, Westland New Zealand. *Journal of the Royal Society of New Zealand* 33 (4) 693-701
- Currie, D; Mittelbach, G; Cornell, H; Field, R; Guégan, J-F; Hawkins, B; Kaufman, D; Kerr, J; Oberdorff, T; O'Brien, E; & Turner, J. (2004) Predictions and Tests of Climate-Based Hypotheses of Broad-Scale Variation in Taxonomic Richness. *Ecology Letters* 7 1121-1134
- Currie, D; & Paquin, V. (1987) Large-Scale Biogeographical Patterns of Species Richness in Trees. *Nature* 329 326-327

- Dansgaard, W; Johnsen, S; Clausen H; Dahl-Jensen, D; Gundestrup, N; Hammer, C; Hvidberg, C; Steffensen, J; Sveinbjörnsdottir, A; Jouzel, J; & Bond, G. (1993) Evidence for General Instability of Past Climate from a 250-Kyr Ice-Core Record. *Nature* 364 218 - 220
- Dauphin, J. (1980) Size Distribution of Chemically Extracted Quartz used to Characterize Fine-Grained Sediments. *Journal of Sedimentary Petrology* 50 (1) 205-214
- Death, R; & Barquín, J. (2012) Geographic Location Alters the Diversity-Disturbance Response. *Freshwater Science* 31 (2) 636-646
- Deb, P; & Sundriyal, R. (2011) Vegetation Dynamics of an Old-Growth Lowland Tropical Rainforests in North-east India: Species Composition and Stand Heterogeneity. *International Journal of Biodiversity & Conservation* 3 (9) 405-430
- de Langre, E. (2008) Effects of Wind on Plants. *Annual Review of Fluid Mechanics* 40 141-168
- de Vleeschouwer, F; Chambers, F; & Swindles, G. (2011) Coring and Sub-Sampling peatlands for Palaeoenvironmental Research. *Mires & Peats* 7 Article 1 1-10 <http://www.mires-and-peat.net> last accessed 31.07.12
- Delmonte, B; Basile-Doelsch, I; Petit, J; Maggi, V; Revel-Rolland, M; Michard, A; Jagoutz, E; & Grousset, F. (2004) Comparing the EPICA and Vostok Dust Records during the last 220,000 years: Stratigraphical Correlation and Provenance in Glacial Periods. *Earth Science Reviews* 66 63-87
- Delmonte, B; Petit, J; Anderson, K; Basile-Doelsch, I; Maggi, V; & Lipenkov, V. (2004) Dust Size Evidence for Opposite Regional Atmospheric Circulation Changes over East Antarctica during the Last Climatic Transition. *Climate Dynamics* 23 427-438
- Delmonte, B; Petit, J; Basile-Doelsch, I; Jagoutz, E; & Maggi, V. (2007) Late Quaternary Interglacials in East Antarctica from Ice-Core Dust Records. In F. Sirocko, M. Claussen, M. Goñi, & T. Litt (Eds) *The Climate of Past Interglacials*. Amsterdam, the Netherlands: Elsevier
- Denton, G; & Hendy, C. (1994) Younger Dryas Age Advance of Franz Josef Glacier in the Southern Alps of New Zealand. *Science* 264 1434-1437
- Denton, G; Lowell, T; Heusser, C; Schlüchter, C; Andersen, B; Heusser, L; Moreno, P; & Marchant, D. (1999) Geomorphology, Stratigraphy and Radiocarbon Chronology of Lanquihue Drift in the area of the southern Lake District, Seno Reloncaví, and Isla de Chiloé, Chile. *Geografiska Annaler A* 81 167-229
- Dickie, I; & Holdaway, R. (2010) Podocarp Roots, Mycorrhizas, and Nodules. *Smithsonian Contributions to Botany* 95 175-187
- Dickinson, K; Chagué-Goff, C; Mark, A; & Cullen, L. (2002) Ecological Processes and Trophic Status of Two Low-Alpine Patterned Mires, south-central South Island, New Zealand. *Austral Ecology* 27 369-384
- Dieffenbacher-Krall, A; Vandergoes, M; & Denton, G. (2007) An Inference Model for Mean Summer Air Temperatures in the Southern Alps, New Zealand, using Subfossil Chironomids. *Quaternary Science Reviews* 26 2487-2504
- Dobhal, P; Kohli, R; & Batish, D. (2011) Impacts of *Lantana camara* L. Invasion on Riparian Vegetation of Nayar Region in Garhwal Himalayas (Uttarkhand, India). *Journal of Ecology & the Natural Environment* 3 (1) 11-22

- Domack, E; Leventer, A; Dunbar, R; Taylor, F; Brachfeld, S; Sjunneskog, C; & ODP Leg 178 Scientific Party (2001) Chronology of the Palmer Deep Site, Antarctic Peninsula: A Holocene Palaeoenvironmental Reference for the Circum-Antarctic. *The Holocene* 11 (1) 1-9
- Druce, A. (1964) The Vegetation. In A. Scanlon (Ed) *Egmont National Park Handbook*. New Plymouth, New Zealand: Egmont National Park Board
- Druce, A. (1986, unpublished) Indigenous Higher Plants (Psilopsids, Lycopods, Quillwort Ferns, Gymnosperms, Flowering Plants) of Mount Egmont/ Mount Taranaki, Sea-Level to the Summit (8260 ft/ 2518m).
- Druitt, D; Enright, N; & Ogden, J. (1990) Altitudinal Zonation in the Mountain Forests of Mt Hauhungatahi, North Island, New Zealand. *Journal of Biogeography* 17 (2) 205-220
- Duller, G. (1996) The Age of the Koputaroa Dunes, Southwest North Island, New Zealand. *Palaeogeography, Palaeoclimatology, Palaeoecology* 121 105-114
- Eden, D; Froggatt, P; Page, M; & Trustrum, N. (1993) A Multiple-source Holocene Tephra Sequence from Lake Tutira, Hawke's Bay, New Zealand. *New Zealand Journal of Geology & Geophysics* 36 233-242
- Eden, D; & Hammond, A. (2003) Dust Accumulation in the New Zealand Region Since the Last Glacial Maximum. *Quaternary Science Reviews* 22 2037-2053
- Edwards, G; & Walker, D. (1983) *C<sub>3</sub>, C<sub>4</sub>: Mechanisms, and Cellular and Environmental Regulation of Photosynthesis*. London, United Kingdom: Blackwell Scientific Publications
- Efford, J; Clarkson, B; & Bylsma, R. (2012) Effect of the AD 1655 Burrell Lapilli Eruption on Treeline Vegetation, Egmont Volcano. In A. Pittari & R. Hansen (Eds) *Abstracts, Geosciences 2012 Conference, Hamilton New Zealand*. Wellington, New Zealand: Geoscience Society of New Zealand Miscellaneous Publication 134A.
- EPICA Community Members (2004) Eight Glacial Cycles from an Antarctic Ice Core. *Nature* 429 623-628
- EPICA Community Members (2006) One-to-one Coupling of Glacial Climate Variability in Greenland and Antarctica. *Nature* 444 195-198
- Erwin, D. (2009) Climate as a Driver of Evolutionary Change. *Current Biology* 19 R575-R583
- Fægri, K; Kaland, P; & Krzywinski, K. (1989) *Textbook of Pollen Analysis* 4<sup>th</sup> ed. : Caldwell, NJ: Blackburn Press
- Fairbanks, R; Chiu, T-C; Cao, L; Mortlock, R; & Kaplan, A. (2006) Rigorous Quality Control Criteria for Screening Coral Samples and Radiocarbon Calibration Data based on <sup>14</sup>C, <sup>230</sup>Th/<sup>234</sup>U/<sup>238</sup>U and <sup>231</sup>Pa/<sup>235</sup>U Dated Corals – A Reply to the Comment by Yusuke Yokoyama and Tezer M. Esat on “Extending the Radiocarbon Calibration beyond 26,000 years Before Present using Fossil Corals,” *Quaternary Science Reviews* 25 3084-3087
- Falkowski, P; Barber, R; & Smetacek, V. (1998) Biogeochemical Controls and Feedbacks on Ocean Primary Production. *Science* 281 200-206
- Finegan, B. (1984) Forest Succession. *Nature* 312 109-114
- Fisher, R; Corbet, A; & Williams, C. (1943) The Relation between the Number of Species and the Number of Individuals in a Random Sample of an Animal Population. *Journal of Animal Ecology* 12 42-58

- Flenley, J. (2003) Some Prospects for Lake Sediment Analysis in the 21<sup>st</sup> Century. *Quaternary International* 105 77-80
- Flenley, J; & Butler, K. (2001) Evidence for Continued Disturbance of an Upland Rainforest in Sumatra for the last 7,000 years of an 11,000 year Record. *Palaeogeography, Palaeoclimatology, Palaeoecology* 171 289-305
- Fox, J. (2013) The Intermediate Disturbance Hypothesis should be Abandoned. *Trends in Ecology & Evolution* 28 (2) 86-92
- Franks, A; Neall, V; & Pollock, J. (1991) *Soils of Part of Eltham County, North Island, New Zealand*. DSIR Land Resources Scientific Report No. 14. Lower Hutt, New Zealand: DSIR Land Resources
- Gabrielli, P; Wegner, A; Petit, J; Delmonte, B; De Dekker, P; Gaspari, V; Fisher, H; Ruth, U; Kriews, M; Boutron, C; Cescon, P; & Barbante, C. (2010) A Major Glacial-Interglacial change in Aeolian Dust Composition as Inferred from Rare Earth Elements in Antarctic Ice. *Quaternary Science Review* 29 265-273
- Gaines, P. (2004) *Compatibility and Precision Issues*. <http://www.esslab.com/iv/tech/iv-icp-operations/part06.html> last accessed 17.08.11
- Gaxiola, A; Burrows, L; & Coomes, D. (2008) Tree Fern Trunks Facilitate Seedling Regeneration in a Productive Lowland Temperate Rain Forest. *Oecologia* 155 325-335
- Gaylord, D; & Neall, V. (2012) Subedifice Collapse of an Andesitic Stratovolcano: The Maitahi Formation, Taranaki Peninsula, New Zealand. *Geological Society of America Bulletin* 124 181-199
- Goslar, T; der Knapp, W; Kamenik, C; & Van Leeuwin, J. (2009) Free-Shape <sup>14</sup>C Age-Depth Modelling of an Intensively Dated Modern Peat Profile. *Journal of Quaternary Science* 24 (5) 481-499
- Gotelli, N; & Colwell, R. (2011) Estimating Species Richness. In A. Magurran & B. McGill (Eds) *Biological Diversity: Frontiers in Measurement and Assessment*. New York, NY: Oxford University Press
- Goudie, A. (1983) Dust Storms in Space and Time. *Progress in Physical Geography* 7 502-530
- Gould, B. (2008) From Sea to Summit: An Overview of Trees and Plants on Mt. Taranaki, Taranaki, North Island, New Zealand. *Australasian Parks and Leisure* 11 (3) 7-10
- Grant, D. (1967) Factors Affecting the Establishment of Manuka (*Leptospermum scoparium*). *Proceedings of the Twentieth New Zealand Weed and Pest Control Conference* 129-134
- Grant-Taylor, T. (1964) Volcanic History of Western Taranaki. *New Zealand Journal of Geology & Geophysics* 7 78-86
- Grant-Taylor, T. (1978) Deposits of Cold Climates in the North Island. In R. Suggate (Ed) *The Geology of New Zealand Volume II*. Wellington, New Zealand: New Zealand Geological Survey pp592-598
- Green, & Lowe, D. (1985) Stratigraphy and Development of c. 17,000 year old Lake Maratoto, North Island, New Zealand, with some Inferences about Postglacial Climate Change. *New Zealand Journal of Geology & Geophysics* 28 675-699
- Greenwood R; & Atkinson, I. (1977) Evolution of Divaricating Plants in New Zealand in Relation to Moa-Browsing. *Proceedings of the New Zealand Ecological Society* 24 21-33

- Gregory, J. (1930) Australian Origin of Red Rain in New Zealand. *Nature* 125 410-411
- Grime, J. (1977) Evidence for the Existence of Three Primary Strategies in Plants and its Relevance to Ecological and Evolutionary Theory. *The American Naturalist* 111 (982) 1169-1194
- Grime, J. (1979) *Plant Strategies and Vegetation Processes*. Chichester, NY: John Wiley & Sons
- Grime, J. (1988a) The C-S-R Model of Primary Plant Strategies – Origins, Implications and Tests. In L. Gottlieb & K. Jain (Eds) *Plant Evolutionary Biology*. London, United Kingdom: Chapman & Hall
- Grime, J. (1988b) A Comment on Loehle's Critique of the Triangular Model of Primary Plant Strategies. *Ecology* 69 (5) 1618-1620
- Grimm, E. (1987) CONISS: A FORTRAN 77 Program for Stratigraphically Constrained Cluster Analysis by the Method of Incremental Sum of Squares. *Computers & Geosciences* 13 (1) 13-35
- Grimm, E. (2011) *TILIA version 1.7.16* Springfield, IL: Illinois State Museum Research and Collections Centre
- Grönlund, E; & Asikainen, E. (1992) Local Agricultural History of Saario Village (Tohmajärvi, North Karelia) since 1607 AD – a Paleaeoecological Approach. In E. Grönlund (Ed) *The First Meeting of Finnish Palaeobotanists: State of the Art in Finland – May 2-4, 1990*. University of Joensuu, *Publications of the Karelian Institute* 106 61-74.
- Haase, P. (1986) A Study of a *Libocedrus bidwillii* Population at Pegleg Flat, Arthurs Pass, New Zealand. *New Zealand Journal of Ecology* 9 153-156
- Haberlah, D; Strong, C; Pirrie, D; Rollinson, G; Gottlieb, P; Botha, P; & Butcher, A. (2011) Automated Petrography Applications in Quaternary Science. *Quaternary Australasia* 28 (2) 3-12
- Hägg, J; & Augustinus, P. (2003) *Scientific Data Report from the Onepoto Crater Drilling (NZ-Maar) Project: December 2000/July 2001*. Department of Geography Working Paper 18. Auckland, New Zealand: University of Auckland
- Hajdas, I; Lowe, D; Newnham, R; & Bonani, G. (2006) Timing of the Late-Glacial Climate Reversal in the Southern Hemisphere Using High Resolution Radiocarbon Chronology for Kaipo Bog, New Zealand. *Quaternary Research* 65 340-345
- Haldorsen, S. (1981) Grain Size Distribution of Subglacial Till and its Relation to Glacial Crushing and Abrasion. *Boreas* 10 91-105
- Hammer, Ø ; Harper, D; & Ryan, P. (2001) PAST: Paleontological Statistics Software Package for Education and Data Analysis. *Palaeontologia Electronica* 4 (1) 9 pp [http://palaeo-electronica.org/2001\\_1/past/past.pdf](http://palaeo-electronica.org/2001_1/past/past.pdf) last accessed 25.07.12
- Hammer, O; & Harper, D. (2006) *Paleontological Data Analysis*. Malden, MA: Blackwell Publishing
- Harrison, S; Kohfield, K; Roelandt, C; & Claquin, T. (2001) The Role of Dust in Climate Changes Today, at the Last Glacial Maximum and in the Future. *Earth Science Reviews* 54 43-80
- Haslett, S. (2002) *Quaternary Environmental Micropalaeontology*. London, United Kingdom Arnold
- Heck, K; Belle, G; & Simberloff, D. (1975) Explicit Calculation of the Rarefaction Diversity Measurement and the Determination of Sufficient Sample Size. *Ecology* 56 1459-1461

- Hellstrom, J; McCulloch, M; & Stone, J. (1998) A Detailed 31,000 year Record of Climate and Vegetation Change, from the Isotope Geochemistry of two New Zealand Speleothems. *Quaternary Research* 50 167-178
- Henderson, J; Jackson, M; Syers, J; Clayton, R; & Rex, R. (1971) Cristobalite Authigenic Origin in Relation to Montmorillonite and Quartz Origin in Betonites. *Clays & Clay Minerals* 19 229-238
- Hendy, C; & Wilson, A. (1968) Paleoclimate Data from Speleothems. *Nature* 219 48-51
- Hesse, P. (1994) The Record of Continental Dust from Australia in Tasman Sea Sediments. *Quaternary Science Reviews* 13 (3) 257-272
- Hesse, P; & McTainsh, G. (1999) Last Glacial Maximum to Early Holocene Wind Strength in the Mid-Latitudes of the Southern Hemisphere from Aeolian Dust in the Tasman Sea. *Quaternary Research* 52 343-349
- Hesse, P; & McTainsh, G. (2003) Australian Dust deposits: Modern Processes and the Quaternary Record. *Quaternary Science Reviews* 22 (18-19) 2007-2035
- Heusser, C; & Rabassa, J. (1987) Cold Climate Episode of Younger Dryas Age in Tierra del Fuego. *Nature* 328 609-611
- Hewitt, A. (1992) New Zealand Soil Classification. DSIR Land Resources Scientific Report No. 19. Lower Hutt, New Zealand: DSIR Land Resources
- Higuera, P; Peters, M; Brubaker, L; & Gavin, D. (2007) Understanding the Origin and Analysis of Sediment-Charcoal Records with a Simulation Model. *Quaternary Science Reviews* 26 1790-1809
- Hiura, T. (1995) Gap Formation and Species Diversity in Japanese Beech Forests: A Test of the Intermediate Disturbance Hypothesis. *Oecologia* 104 (3) 265-271
- Hodder, A; De Lange, P; & Lowe, D. (1991) Dissolution and Depletion of Ferromagnesian Minerals from Holocene Tephra Layers in an Acid Bog, New Zealand, and Implications for Tephra Correlation. *Journal of Quaternary Science* 6 (3) 195-208
- Hogg, A; Bronk-Ramsey, C; Turney, C; & Palmer, J. (2009) Bayesian Evaluation of the Southern Hemisphere Radiocarbon Offset During the Holocene. *Radiocarbon* 51 (4) 1165-1176
- Horiba Scientific Inc. (2011) <http://www.horiba.com/scientific/products/particle-characterization/particle-size-analysis/details/la-950-108/> last accessed 22.10.11
- Horrocks, M; & Ogden, J. (1998a) Fine Resolution Palynology of Erua Swamp, Tongariro, New Zealand, since the Taupo Tephra Eruption of c 1718 B.P. *New Zealand Journal of Botany* 36 285-293
- Horrocks, M; & Ogden, J. (1998b) Fine Resolution Palynology of Gibsons' Swamp, Central North Island, New Zealand, since c. 13 000 B.P. *New Zealand Journal of Botany* 36 273-283
- Hsiao, T; & Acevedo, E. (1974) Plant Responses to Water Deficits, Water-Use Efficiency, and Drought Resistance. *Agricultural Meteorology* 14 59-84
- Hughes, A; Byrnes, J; Kimbro, D; & Stachowicz, J. (2007) Reciprocal Relationships and Potential Feedbacks between Biodiversity and Disturbance. *Ecology Letters* 10 849-864

- Ivy-Ochs, S; Schlüchter, C; Kubrik, P; & Denton, G. (1999) Moraine Exposure Dates Imply Synchronous Younger Dryas Glacier Advances in the European Alps and Southern Alps of New Zealand. *Geografiska Annaler* 81A 313-323
- Imbrie, J; & Imbrie, K. (1979) *Ice Ages: Solving the Mystery*. Short Hills, NJ: Enslow Publishers
- Jackson, M. (1956) *Soil Chemical Analysis – Advanced Course*. Madison, WI: University of Wisconsin
- Jackson, M; Levelt, T; Syers, J; Rex, R; Clayton, R; Sherman, G; & Uehara, G. (1971) Geomorphological Relationships of Tropospheric Derived Quartz in the Soils of the Hawaiian Islands. *Soil Society of America Proceedings* 35 515-525
- Jane, G. (1986) Wind Damage as an Ecological Process in Mountain Beech Forests of Canterbury, New Zealand. *New Zealand Journal of Ecology* 9 25-39
- Jouzel, J; Barkov, N; Barnola, J; Bender, M; Chappelaz, J; Genthon, C; Kotlyakov, V; Lipenkov, V; Lorius, C; Petit, J; Raynaud, D; Raisbeck, G; Ritz, C; Sowers, T; Stievenard, M; Yiou, F; & Yiou, P. (1993) Extending the Vostok Ice-Core Record of Paleoclimate to the Penultimate Glacial Period. *Nature* 364 407-412.
- Jouzel, J; Lorius, C; Petit, J; Genthon, C; Barkov, N; Kotlyakov, V; & Petrov, V. (1987) Vostok Ice Core: A Continuous Isotope Temperature Record Over the Last Climatic Cycle (160,000 years). *Nature* 329 (6138) 403-408
- Jouzel, J; Vaikmae, R; Petit, J; Martin, M; Duclos, Y; Stievenard, M; Lorius, C; Toots, M; Mélières, M; Burkle, L; Barkov, N; & Kotlyakov, V. (1995) The Two-Step Shape and Timing of the Last Deglaciation in Antarctica. *Climate Dynamics* 11 151-161
- Kautsky, L. (1988) Life Strategies of Aquatic Soft Bottom Macrophytes. *Oikos* 53 (1) 126-135
- Kidson, J. (2000) An Analysis of New Zealand Synoptic Types and Their Use in Defining Weather Regimes. *International Journal of Climatology* 20 299-316
- Kidston, J; Renwick, J; & McGregor, J. (2009) Hemispheric-Scale Seasonality of the Southern Annular Mode and Impacts on the Climate of New Zealand. *Journal of Climate* 22 (18) 4759-4770
- Knight, A; McTainsh, G; & Simpson, R. (1995) Sediment Loads in an Australian Dust Storm: Implications for Present and Past Dust Processes. *Catena* 24 195-213
- Kohfield, K; & Harrison, S. (2001) DIRTMAP: The Geological Record of Dust. *Earth Science Reviews* 54 81-114
- Konert, M; & Vandenberghe, J. (1997) Comparison of Laser Grain-Size Analysis with Pipette and Sieve Analysis: A Solution for the Underestimation of the Clay Fraction. *Sedimentology* 44 523-535
- Köstner, B; Schulze, E-D; Kelliher, F; Hollinger, D; Beyers, J; Hunt, J; McSeveny, T; Meserth, R; & Weir, P. (1992) Transpiration and Canopy Conductance in a Pristine Broad-leaved Forest of *Nothofagus*: An Analysis of Xylem Sap Flow and Eddy Correlation Measurements. *Oecologia* 91 350-359
- Kumar, A; Marcot, B; & Saxena, A. (2006) Tree Species Diversity and Distribution Patterns in Tropical Forests of Garo Hills. *Current Science* 91 (10) 1370-1381
- Lageard, J. (1997) *Radiocarbon Dating and its Application*. Manchester, United Kingdom: Manchester Metropolitan University

- Lambers, H; & Poorter, H. (1992) Inherent Variation in Growth Rate Between Higher Plants: A Search for Physiological Cause and Ecological Consequence. *Advances in Ecological Research* 23 187-260
- Lancashire, A; Flenley, J; & Harper, M. (2002) Late Glacial Beech Forest: An 18,000 – 5,000 BP Pollen Record from Auckland, New Zealand. *Global & Planetary Change* 33 315-327
- Large, M; & Braggins, J. (1991) Spore Atlas of New Zealand Ferns and Fern Allies. Supplement to *New Zealand Journal of Botany* 29 1-168
- Lawton, R. (1982) Wind Stress and Elfin Stature in a Montane Rain Forest Tree: An Adaptive Explanation. *American Journal of Botany* 69 (8) 1224-1230
- Leathwick, J; & Mitchell, N. (1992) Forest Pattern, Climate and Volcanism in central North Island, New Zealand. *Journal of Vegetation Science* 3 603-616
- Lecointre, J; Neall, V; & Palmer, A. (1998) Quaternary Lahar Stratigraphy of the Western Ruapehu Ring Plain, New Zealand. *New Zealand Journal of Geology & Geophysics* 41 225-245
- Lees, C. (1986) Late Quaternary Palynology of the Southern Ruahine Range North Island, New Zealand. *New Zealand Journal of Botany* 24 315-329
- Lees, C. (1987) *Late Holocene Changes in the Vegetation of Western Taranaki Investigated by Soil Palynology*. A Thesis Presented in Partial Fulfilment of the Requirements for the Degree of Doctor of Philosophy. Palmerston North, New Zealand: Massey University
- Lees, C; & Neall, V. (1993) Vegetation Response to Volcanic Eruptions on Egmont Volcano, New Zealand during the last 1500 years. *Journal of the Royal Society of New Zealand* 23 (2) 91-127
- Lees, C; Neall, V; & Palmer, A. (1998) Forest Persistence at Coastal Waikato, 24 000 years BP to Present. *Journal of the Royal Society of New Zealand* 28 (1) 55-81
- Le Roux, G; Pourcelot, L; Masson, O; Duffa, C; Vray, F; & Renaud, P. (2008) Aerosol Deposition and Origin in French Mountains Estimated with Soil Inventories of <sup>210</sup>Pb and Artificial Radionuclides. *Atmospheric Environment* 42 1517–1524
- Lewis, K; & Mildenhall, D. (1985) The Late Quaternary Seismic, Sedimentary and Palynological Stratigraphy beneath Evans Bay, Wellington Harbour. *New Zealand Journal of Geology & Geophysics* 28 129-152
- Lignum, J; Jarvis, I; & Pearce, M. (2008) A Critical Assessment of Standard Processing Methods for the Preparation of Palynological Samples. *Review of Palaeobotany & Palynology* 149 133-149
- Lindbladh, M; & Bradshaw, R. (1998) The Development and Demise of a Medieval Forest-Meadow System at Linnaeus' Birthplace in Southern Sweden: Implications for Conservation and Forest History. *Vegetation History & Archaeobotany* 4 153-160
- Lintott, W; & Burrows, C. (1973) A Pollen Diagram and Macrofossils from Kettlehole Bog Cass, South Island, New Zealand. *New Zealand Journal of Botany* 11 269-282
- Loizeau, J-L; Arbouille, D; Santiago, S; & Vernet, J-P. (1994) Evaluation of a Wide Range Laser Diffraction Grain Size Analyser for use with Sediments. *Sedimentology* 41 353-361
- Lorrey, A; Vandergoes, M; Almond, P; Renwick, J; Stephens, T; Bostock, H; Mackintosh, A; Newnham, R; Williams, P; Ackerley, D; Neil, H; & Fowler, A. (2012) Palaeocirculation across New Zealand during the Last Glacial Maximum at ~21 ka. *Quaternary Science Reviews* 36 189-213

- Lotter, A, Birks, H, Hofmann, W; & Marchetto, A. (1997) Modern Diatom, Cladocera, Chironomid, and Chrysophyte Cyst Assemblages as Quantitative Indicators for the Reconstruction of Past Environmental Conditions in the Alps. I. Climate. *Journal of Paleolimnology* 18 395-420.
- Lowe, D. (1988) Late Quaternary Volcanism in New Zealand: Towards an Integrated Record Using Distal Airfall Tephra in Lakes and Bogs. *Journal of Quaternary Science* 3 (2) 111-120
- Lowe, D; Blaauw, M; Hogg, A; & Newnham, R. (2013) Ages of 24 Widespread Tephra Erupted since 30,000 years ago in New Zealand, with Re-evaluation of the Timing and Palaeoclimatic Implications of the Lateglacial Cool Episode Recorded at Kaipo Bog. *Quaternary Science Reviews* 74 170-194
- Lowe, D; Shane, P; Alloway, B; & Newnham, R. (2008) Fingerprints and Age Models for Widespread New Zealand Tephra Marker Beds Erupted since 30,000 Years Ago: A Framework for NZ-INTIMATE. *Quaternary Science Reviews* 27: 95 -126
- Lyon, I; Burley, S; McKeever, P; Saxton, J; & Macaulay, C. (2009) Oxygen Isotope Analysis of Authigenic Quartz in Sandstones: A Comparison of Ion Microprobe and Conventional Analytical Techniques. In R. Worden & S. Morad (Eds) *Quartz Cementation in Sandstones* Oxford: Blackwell Publishing Ltd.
- MacArthur, R. (1972) *Geographical Ecology: Patterns in the Distribution of Species*. New York, NY: Harper Row
- MacArthur, R; & Wilson, E. (1967) *The Theory of Island Biogeography*. Princeton, NJ: Princeton University Press
- Macken, A; Staff, R; & Reed, E. (2013) Bayesian Age-Depth Modelling of Late Quaternary Deposits from Wet and Blanche Caves, Naracoorte, South Australia: A Framework for Comparative Faunal Analyses. *Quaternary Geochronology* 17 26-43
- Mackey, R; & Currie, D. (2001) The Diversity-Disturbance Relationship: Is it Generally Strong and Peaked? *Ecology* 82 (12) 3479-3492
- Mackie, D; & Hunter, K. (2007) Australian Dust: From Uplift to Uptake. *Chemistry in New Zealand* October 82-83
- MacPhail, M. (1980) Fossil and Modern *Beilschmiedia* (Lauraceae) Pollen in New Zealand. *New Zealand Journal of Botany* 18 453-457
- MacPhail, M; & McQueen, D. (1983) The Value of New Zealand Pollen and Spores as Indicators of Cenozoic Vegetation and Climates. *Tuatara* 26 37-59
- Mahowald, N; & Luo, C. (2003) A Less Dusty Future? *Geophysical Research Letters* 30 (17) 1-4
- Marlon, J; Bartlein, P; Daniu, A-L; Harrison, S; Maezumi, S; Power, M; Tinner, W; & Vanni re, B. (2013) Global Biomass Burning: A Synthesis and Review of Holocene Paleofire Records and their Controls. *Quaternary Science Reviews* 65 5-25
- Marra, M; Crozier, M; & Goff, J. (2009) Palaeoenvironment and Biogeography of a Late MIS 3 Fossil Beetle Fauna from South Taranaki, New Zealand. *Journal of Quaternary Science* 24 (1) 97-107
- Marra, M; Smith, E; Shulmeister, J; & Leschen, R. (2004) Late Quaternary Climate Change in the Awatere Valley, South Island, New Zealand using a Sine Model with a Maximum Likelihood Envelope on Fossil Beetle Data. *Quaternary Science Reviews* 23 1637-1650
- Marshall, P. (1903) Dust Storms in New Zealand. *Nature* 68 223

- Marshall, P; & Kidson, E. (1929) The Dust-Storm of October 1928. *New Zealand Journal of Science & Technology* 10 291-299
- Martin, T; & Ogden, J. (2002) The Seed Ecology of *Ascarina lucida*: A Rare New Zealand Tree Adapted to Disturbance. *New Zealand Journal of Botany* 40 397-404
- Marx, S; McGowan, H; & Kamber, B. (2009) Long-range Dust Transport from Eastern Australia: A Proxy for Holocene Aridity and ENSO-type Climate Variability. *Earth & Planetary Science Letters* 282 167–177
- McCave, I; Bryant, R; Cook, H; & Coughanowr, C. (1986) Evaluation of a Laser-Diffraction-Size Analyser for Use with Natural Sediments. *Journal of Sedimentary Petrology* 56 561–564.
- McCraw, J. (1975) Quaternary Airfall Deposits of New Zealand. In R. Suggate & M.Creswell (Eds) *Quaternary Studies: Selected Papers from the IX INQUA Congress Christchurch, New Zealand*. Wellington: New Zealand: Royal Society of New Zealand
- McDonald, J. (2009) *Handbook of Biological Statistics* (2<sup>nd</sup> ed). Baltimore, MD: Sparky House Publishing
- McGlone, M. (1982) Modern Pollen Rain, Egmont National Park, New Zealand. *New Zealand Journal of Botany* 20 253-262
- McGlone, M. (1985) Biostratigraphy of the Last Interglacial-Glacial Cycle, southern North Island, New Zealand. *Victoria University of Wellington Geology Department Publication* 31 17-31. Wellington, New Zealand: Victoria University of Wellington
- McGlone, M. (1988) New Zealand. In B. Huntley & T. Webb III (eds) *Vegetation History*. Dordrecht, the Netherlands: Kluwer: Academic Publishing
- McGlone, M. (2001) A Late Quaternary Pollen Record from Marine Core P69, Southeastern North Island, New Zealand. *New Zealand Journal of Geology & Geophysics* 44 69-77
- McGlone, M; & Basher, L. (1995) The Deforestation of the Upper Awatere Catchment, Inland Kaikoura Range, Marlborough, South Island, New Zealand. *New Zealand Journal of Ecology* 19 (1) 53-66
- McGlone, M; & Moar, N. (1977) The *Ascarina* Decline and Post-Glacial Climatic Change in New Zealand. *New Zealand Journal of Botany* 15 485-489
- McGlone, M; & Neall, V. (1994) The Late Pleistocene and Holocene Vegetation History of Taranaki, North Island, New Zealand. *New Zealand Journal of Botany* 32 251-269
- McGlone, M; Neall, V; & Clarkson, B. (1988) The Effect of Recent Volcanic Events and Climatic Changes on the Vegetation of Mt Egmont (Mt Taranaki), New Zealand. *New Zealand Journal of Botany* 26 123-144
- McGlone, M; Neall, V; & Pillans, B. (1984) Inaha Terrace Deposits: A Late Quaternary Terrestrial Record in South Taranaki, New Zealand. *New Zealand Journal of Geology & Geophysics* 27 35-49
- McGlone, M; & Topping, W. (1973) Late Otiran / Early Aranuiian Vegetation in the Tongariro Area, Central North Island, New Zealand. *New Zealand Journal of Botany* 11 283-290
- McGlone, M; & Topping, W. (1977) Aranuiian (Post-Glacial) Pollen Diagrams from the Tongariro Region, North Island, New Zealand. *New Zealand Journal of Botany* 15 749-760
- McGlone, M; & Topping, W. (1983) Late Quaternary Vegetation, Tongariro region, Central North Island, New Zealand. *New Zealand Journal of Botany* 21 53-76

- McGlone, M; & Webb, C. (1981) Selective Forces Influencing the Evolution of Divaricating Plants. *New Zealand Journal of Ecology* 4 20-28
- McGlone, M; & Wilmshurst, J. (1999) A Holocene Record of Climate, Vegetation Change and Peat Bog Development, East Otago, South Island, New Zealand. *Journal of Quaternary Science* 14 (3) 239-254
- McGowan, H; Sturman, A; & Owens, I. (1996) Aeolian Dust Transport and deposition by Foehn Winds in an Alpine Environment, Lake Tekapo, New Zealand. *Geomorphology* 15 135-146
- McKellar, M. (1973) Dispersal of *Nothofagus* Pollen in Eastern Otago, South Island, New Zealand. *New Zealand Journal of Botany* 11 749-760
- McLea, W. (1990) Palynology of Pohehe Swamp, northwest Wairarapa, New Zealand: A Study of Climatic and Vegetation Changes during the last 41,000 Years. *Journal of the Royal Society of New Zealand* 20 (2) 205-220
- McSweeney, G (1982) Matai/Totara Flood Plain Forests in South Westland. *New Zealand Journal of Ecology* 5 121-128
- McTainsh, G. (1989) Quaternary Aeolian Dust Processes and Sediments in the Australian Region. *Quaternary Science Reviews* 8 (3) 235-253
- McTainsh, G; Lynch, A; & Hales, R. (1997) Particle-Size Analysis of Aeolian Dusts, Soils and Sediments in Very Small Quantities using a Coulter Multisizer. *Earth Surface Processes & Landforms* 22 1207-1216
- Menhinick, E . (1964) A Comparison of Some Species-Individuals Diversity Indices Applied to Samples of Field Insects. *Ecology* 45 (4) 859-861
- Menicucci, A; Matthews, J; & Spero, H. (2013) Oxygen Isotope Analyses of Biogenic Opal and Quartz using a Novel Microfluorination Technique. *Rapid Communication Mass Spectrometry* 27 (16) 1873-1881
- Middleton, N. (1984) Dust Storms in Australia: Frequency, Distribution and Seasonality. *Search* 15 46-47
- Mildenhall, D. (1973) Problem of Interpretation of two Pollen Diagrams from an Otiran (uppermost Pleistocene) section near Waikanae. In M. Te Punga & D. Mildenhall (Eds) *IX INQUA Congress Guidebook for Excursion A13 Western North Island* 134-135
- Mildenhall, D. (1976) Exotic Pollen Rain on the Chatham Islands During the Late Pleistocene. *New Zealand Journal of Geology & Geophysics* 19 (3) 327-333
- Mildenhall, D. (1994) Palynostratigraphy and Paleoenvironments of Wellington, New Zealand, During the Last 80 ka, based on Palynology of Drillholes. *New Zealand Journal of Geology & Geophysics* 37 421-436
- Milne, J. (1973) *Upper Quaternary Geology of the Rangitikei Drainage Basin*. Unpublished PhD Thesis, Victoria University of Wellington.
- Milne, J. (1973) Maps and Sections of River Terraces in the Rangitikei Basin, North Island, New Zealand. 4 Sheets. *New Zealand Soil Survey Report 4*. Wellington, New Zealand: Department of Scientific & Industrial Research
- Mix, A; Bard E; & Schneider, R. (2001) Environmental Processes of the Ice Age: Land, Oceans, Glaciers (EPILOG). *Quaternary Science Reviews* 20 (4) 627-657

- Moar, N. (1970) Recent Pollen Spectra from three Localities in the South Island, New Zealand. *New Zealand Journal of Botany* 11 291-304
- Moar, N. (1980) Late Otiran and Early Aranuian Grassland in Central South Island, New Zealand. *New Zealand Journal of Ecology* 3 4-12
- Moar, N. (1993) *Pollen Grains of New Zealand Dicotyledonous Plants*. Lincoln, New Zealand: Manaaki Whenua Press
- Moar, N; & Mildenhall, D. (1988) Pollen Assemblages from Late Quaternary Deposits in Canterbury. Appendix to Brown, L; & Wilson, D. Stratigraphy of the Late Quaternary Deposits of the Northern Canterbury Plains, New Zealand. *New Zealand Journal of Geology & Geophysics* 31 305-335
- Moar, N; & Myers, J. (1978) A Note on Pollen Dispersal in Canterbury, New Zealand. *New Zealand Journal of Botany* 16 413-415
- Moar, N; & Wilmshurst, J. (2003) A Key to the Pollen of New Zealand Cyperaceae. *New Zealand Journal of Botany* 41 325-334
- Moberg, A; Sonechkin, D; Holmgren, K; Dansko, N; & Karlén, W. (2005) Highly Variable Northern Hemisphere Temperatures Reconstructed from Low- and High-Resolution Proxy Data. *Nature* 433 613-617
- Mokma, D; Syers, J; & Jackson, M. (1972) Aeolian Additions to Soils and Sediments in the South Pacific Area. *Journal of Soil Science* 23 (2) 147-162
- Mokma, D; Jackson, M; Syers, J; & Stevens, P. (1973) Mineralogy of a Chronosequence of Soils from Greywacke and Mica Schist Alluvium, Westland New Zealand. *New Zealand Journal of Science* 16 769-797
- Molino, J-F; & Sabatier, D. (2001) Tree Diversity in Forests: A Validation of the Intermediate Disturbance Hypothesis. *Science* 294 1702-1704
- Monnin, E; Indermuhle, A; Dallenbach, A; Fluckiger, J; Stauffer, B; Stocker, T; Raynaud, D; & Barnola, J. (2001) Atmospheric CO<sub>2</sub> Concentrations over the Last Glacial Termination. *Science* 291 112-115
- Monk, C. (1966) An Ecological Significance of Evergreenness. *Ecology* 47 (3) 504-505
- Mooney, H. (1972) The Carbon Balance of Plants. *Annual Review of Ecology & Systematics* 3 315-346
- Mooney, H; & Gulmon, S. (1982) Constraints on Leaf Structure and Function in Reference to Herbivory. *BioScience* 32 (30) 198-201
- Moreno, P; Francois, J; Moy, C; & Villa-Martínez, R. (2010) Covariability of the Southern Westerlies and Atmospheric CO<sub>2</sub> during the Holocene. *Geology* 38 (8) 727-730
- Muhs, D; Budahn, J; Prospero, J; & Carey, S. (2007), Geochemical Evidence for African Dust Inputs to Soils of Western Atlantic Islands: Barbados, the Bahamas, and Florida. *Journal of Geophysical Research* 112 F02009, doi:10.1029/2005JF000445
- Muller, R; & MacDonald, G. (2001) *Ice Ages and Astronomical Causes: Data, Spectral Analysis and Mechanisms*. Chichester, United Kingdom: Praxis Publishing

- Munson, S; Belnap, J; Schelz, C; Moran, M; & Carolin, T. (2011) On the Brink of Change: Plant Responses to Climate on the Colorado Plateau. *Ecosphere* 26 (1) Article 68 1-15
- Neall, V. (1975) Climate-Controlled Tephra Redeposition on Pouakai Ring Plain, Taranaki, New Zealand. *New Zealand Journal of Geology & Geophysics* 18 (2) 317-326
- Neall, V. (1977) Genesis and Weathering of Andisols in Taranaki, New Zealand. *Soil Science* 123 (6) 400-408
- Neall, V. (1979) *Sheets P19, P20 and P21. New Plymouth, Egmont and Manaia*, 1<sup>st</sup> ed. Geological Map of New Zealand 1:50,000. Wellington, New Zealand: Department of Scientific & Industrial Research
- Nelson, C; Hendy, C; & Cuthbertson, A. (1994) Oxygen Isotope Evidence for Climatic Contrasts between Tasman Sea and Southwest Pacific Ocean during the Late Quaternary. In G. van der Lingen, K. Swanson & R. Muir (Eds) *Evolution of the Tasman Sea*. Rotterdam, the Netherlands: A.A. Balkema
- Newnham, R. (1992) A 30,000 year Pollen, Vegetation and Climate Record from Otakairangi (Hikurangi), Northland, New Zealand. *Journal of Biogeography* 19 541-554
- Newnham, R; & Alloway, B. (2004) A Terrestrial Record of Last Interglacial Climate Preserved by Voluminous Debris Avalanche Inundation in Taranaki, New Zealand. *Journal of Quaternary Science* 19 (3) 299-314
- Newnham, R; de Lange, P; & Lowe, D. (1995) Holocene Vegetation, Climate and Ontogenesis of a Raised-Bog Complex, Northern New Zealand from Pollen, Plant Macrofossils and Tephrochronological Investigations. *The Holocene* 5 267-282
- Newnham, R; Eden, D; Lowe, D; & Hendy, C. (2003) Rerewhakaaitu Tephra, a Land–Sea Marker for the Last Termination in New Zealand, with Implications for Global Climate Change. *Quaternary Science Reviews* 22 (2-4) 289-308.
- Newnham, R; & Lowe, D. (2000) Fine-Resolution Pollen Record of Late Glacial Climate Reversal from New Zealand. *Geology* 28 (8) 759-762
- Newnham, R; Lowe, D; Giles, T; & Alloway, B. (2007) Vegetation and Climate of Auckland, New Zealand, since ca. 32 000 cal. yr ago: Support for an Extended LGM. *Journal of Quaternary Science* 22 (5) 517-534
- Newnham, R; Lowe, D; & Green, J. (1989) Palynology, Vegetation, and Climate of Waikato Lowlands, North Island, New Zealand, since c. 18,000 years ago. *Journal of the Royal Society of New Zealand* 19 127-150
- Newnham, R; Lowe, D; Green, J; Turner, G; Harper, M; McGlone, M; Stout, S; Horie, S; & Froggatt, P. (2004) A Discontinuous ca. 80 ka Record of Late Quaternary Environmental Change from Lake Omapere, Northland, New Zealand. *Palaeogeography, Palaeoclimatology, Palaeoecology* 207 165-198
- Newnham, R; Lowe, D; & Matthews, B. (1998) A Late Holocene and Prehistoric Record of Environmental Change from Lake Waikaremoana, New Zealand. *The Holocene* 8 (4) 443-454
- Newnham, R; Lowe, D; & Williams, P. (1999) Quaternary Environmental Change in New Zealand: A Review. *Progress in Physical Geography* 23 (4) 567-610

- Newnham, R; Vandergoes, M; Sikes, E; Carter, L; Wilmshurst, J; Lowe, D; McGlone, M; & Sandiford, A. (2012a) Does the Bipolar Seesaw Extend to the Terrestrial Southern Mid-Latitudes? *Quaternary Science Reviews* 36 214-222
- Newnham, R; McGlone, M; Moar, N; Wilmshurst, J; & Vandergoes, M. (2012b) The Vegetation Cover of New Zealand at the Last Glacial Maximum. *Quaternary Science Reviews* <http://dx.doi.org/10.1016/j.quascirev.2012.08.022>
- Nichols, J. (1956) The Historical Ecology of the Indigenous Forest of the Taranaki Upland. *New Zealand Journal of Forestry* 7 17-34
- Norton, D; McGlone, M; & Wigley, T. (1986) Quantitative Analysis of Modern Pollen-Climate Relationships in New Zealand. *New Zealand Journal of Botany* 24 331-342
- Nuansa Kimia Sejati Chemical Company (2011) *Boric Acid*. <http://www.nuansakimia.com/boric-acid-h3bo3.html> last accessed 04.10.11
- O'Brien, E. (1993) Climatic Gradients in Woody Plant Species Richness – Towards an Explanation Based on an Analysis of Southern Africa's Woody Flora. *Journal of Biogeography* 20 181-198
- Odgaard, B. (1999) Fossil Pollen as a Record of Past Biodiversity. *Journal of Biogeography* 26 (1) 7-17
- Ogden, J. (1985) An Introduction to Plant Demography with Special Reference to New Zealand Trees. *New Zealand Journal of Botany* 23 751-772
- Oser, R. (1972) Sedimentary Components of Northwest Pacific Pelagic Sediments. *Journal of Sedimentary Petrology* 42 (2) 461-467
- Parnell, A; Buck, C; & Doan, T. (2011) A Review of Statistical Chronology Models for High-Resolution, Proxy-Based Holocene Palaeoenvironmental Reconstruction. *Quaternary Science Reviews* 30 2948-2960
- Patterson III, W; Edwards, K; & Maguire, D. (1987) Microscopic Charcoal as a Fossil Indicator of Fire. *Quaternary Science Reviews* 6 3-23
- Peet, R. (1974) The Measurement of Species Diversity. *Annual Review of Ecology & Systematics* 5 285-307
- Petherick, L; McGowan, H; & Kamber, B. (2009) Reconstructing Transport Pathways for Late Quaternary Dust from Eastern Australia using the Composition of Trace Elements of Long Traveled Dusts. *Geomorphology* 105 67-79
- Petit, J; Jouzel, J; Raynaud, D; Barkov, N; Barnola, J-M; Basile, I; Bender, M; Chappellaz, J; Davis, M; Delaygue, G; Delmotte, M; Kotlyakov, V; Legrand, M; Lipenkov, V; Lorius, C; Pépin, L; Ritz, C; Saltzman, E; & Stievenard, M. (1999) Climate and Atmospheric History of the past 420,000 years from the Vostok Ice Core, Antarctica. *Nature* 399 429-436
- Pianka, E. (1970) On *r*- and *K*-Selection. *American Naturalist* 104 (940) 592-597
- Pickett, S; Collins, S; & Armesto, J. (1987) Models, Mechanisms and Pathways of Succession. *The Botanical Review* 53 334-371
- Pillans, B. (1983) Upper Quaternary Marine Terrace Chronology and Deformation, South Taranaki, New Zealand. *Geology* 11 292-297

- Pillans, B. (1990) *Late Quaternary Marine Terraces, South Taranaki- Wanganui (NZMS 260 sheet Q22 and part sheets Q20, Q21, R21, & R22) 1: 100 000 New Zealand Geological Survey Miscellaneous Series Map 18 (1 sheet) and notes*. Wellington, New Zealand: Department of Scientific & Industrial Research
- Pillans, B; McGlone, M; Palmer, A; Mildenhall, D; Alloway, B; & Berger, G. (1993) The Last Glacial Maximum in central and southern North Island, New Zealand: A Palaeoenvironmental Reconstruction using Kawakawa Tephra Formation as a Chronostratigraphic Marker. *Palaeogeography, Palaeoclimatology, Palaeoecology* 101 283-304
- Pocknall, D. (1978) Relative Pollen Representation in Relation to Vegetation Composition, Westland, New Zealand. *New Zealand Journal of Botany* 16 379-386
- Pocknall, D. (1981a) Pollen Morphology of the New Zealand Species of *Dacrydium* Solander, *Podocarpus* L'Heritier, and *Dacrycarpus* Endlicher (Podocarpaceae). *New Zealand Journal of Botany* 19 259-266
- Pocknall, D. (1981b) Pollen Morphology of *Phyllocladus* L.C. et A. Rich. *New Zealand Journal of Botany* 19 67-95
- Pocknall, D. (1982) Modern Pollen Spectra from Mountain Localities, South Island, New Zealand. *New Zealand Journal of Botany* 20 361-371
- Porter, S. (1975) Equilibrium-line Altitudes of late Quaternary Glaciers in the Southern Alps, New Zealand. *Quaternary Research* 5 27-47
- Prebble, M; Schallenberg, M; Carter, J; & Shulmeister, J. (2002) An Analysis of Phytolith Assemblages for the Quantitative Reconstruction of late Quaternary Environments of the Lower Taieri Plain, Otago, South Island, New Zealand. I. Modern Assemblages and Transfer Functions. *Journal of Paleolimnology* 27: 393-413
- Price, R; Stewart, R; Woodhead, J; & Smith, I. (1999) Petrogenesis of High-K Arc Magmas: Evidence from Egmont Volcano, North Island, New Zealand. *Journal of Petrology* 40 (1) 167-197
- Procter, J. (2009) *Towards Improving Volcanic Mass Flow Hazard Assessment at New Zealand Stratovolcanoes*. A Thesis Presented in Partial Fulfilment of the Requirements for the Degree of Doctor of Philosophy. Palmerston North, New Zealand: Massey University
- Prospero, J; Bonatti, M; Schubert, C & Carlson, T (1970) Dust in the Caribbean Atmosphere Traced to an African Dust Storm. *Earth & Planetary Science Letters* 9 287-293.
- Pye, K. (1987) *Aeolian Dust and Dust Deposits*. London, United Kingdom: Academic Press
- Pyne, S. (1991) *Burning Bush—a Fire History of Australia*. New York: Henry Holt and Company
- Quinn, C; Brown, E; Heslewood, M; & Crayne, D. (2005) Generic Concepts in Styphelieae (Ericaceae): the *Cyathodes* Group. *Australian Systemic Botany* 18 439-454
- Rafter Radiocarbon Laboratory (2001) [www.gns.cri.nz/atom/rafter](http://www.gns.cri.nz/atom/rafter) last accessed 24.08.12
- Ravine, D. (1996) *Matemateaonga Ecological District: Survey for the Protected Natural Areas Programme*. Department of Conservation: Wanganui
- Rea, D. (1994) The Paleoclimatic Record Provided by Eolian Deposition in the Deep Sea: The Geologic History of Wind. *Reviews of Geophysics* 32 (2) 159-195

- Rea, D; Leinen, M; & Janecek, T. (1985) Geologic Approach to the Long-Term History of Atmospheric Circulation. *Science* 227 (4688) 721-725
- Reid, M. (2005) Diatom-based Models for Reconstructing Past Water Quality and Productivity in New Zealand Lakes. *Journal of Paleolimnology* 33 13-38
- Reimer, P; Baillie, M; Bard, E; Bayliss, A; Beck, J; Blackwell, P; Bronk Ramsey, C; Buck, C; Burr, G; Edwards, R; Friedrich, M; Grootes, P; Guilderson, T; Hajdas, I; Heaton, T; Hogg, A; Hughen, K; Kaiser, K; Kromer, B; McCormac, F; Manning, S; Reamer, R; Richards, D; Southon, J; Talamo, S; Turney, C; van der Plicht, J; & Weyhenmeyer, C. (2009) IntCal09 and Marine09 Radiocarbon Age Calibration Curves, 0-50,000 years cal. BP. *Radiocarbon* 51 1111-1150
- Revel-Rolland, M; de Deckker, P; Delmonte, B; Hesse, P; Magee, J; Basile-Doelsch, I; Grousset, F; & Bosch, D. (2006) Eastern Australia: A Possible Source of Dust in East Antarctica Interglacial Ice. *Earth and Planetary Science Letters* 249 (1) 1-13
- Rex, R; Syers, J; Jackson, M; & Clayton, R. (1969) Eolian Origin of Quartz in Soils of Hawaiian Islands and in Pacific Pelagic Sediments. *Science* 163 277-279
- Reynolds, R; Belnap, J; Reheis, M; Lamothe, P; & Luiszer, F. (2001) Aeolian Inputs in Colorado Plateau Soils: Nutrient Inputs and Recent Change in Source. *Proceedings of the National Academy of Science* 98 (13) 7123-7127
- Richardson, S; Peltzer, D; Allen, R; McGlone, M; & Parfitt, R. (2004) Rapid Development of Phosphorus Limitation in Temperate Rainforest along the Franz Josef Soil Chronosequence. *Oecologia* 139 267-276
- Rodbell, D; & Seltzer, G. (2000) Rapid Ice Margin Fluctuations During the Younger Dryas in the Tropical Andes. *Quaternary Research* 54 328-338
- Roden, J. (2003) Modelling the Light Interception and Carbon Gain of Individual Fluttering Aspen (*Populus tremuloides* Michx) Leaves. *Trees: Structure & Function* 17 117-126
- Rojas, M; Moreno, P; Kageyama, M; Crucifix, M; Hewitt, C; Abe-Ouchi, A; Ohgaito, R; Brady, E; & Hope, P. The Southern Westerlies during the Last Glacial Maximum in PMIP2 Simulations. *Climate Dynamics* 32 525-548
- Russell, J; Dixon, K; Gnanadeskian, A; Stouffer, R; & Toggweiler, J. (2006) Southern Ocean Westerlies in a Warming World: Propping Open the Door to the Deep Ocean. *Journal of Climate* 19 (24) 6382-6390
- Ryan, A. (1984) *Flying Weather. Manual of New Zealand Aviation Climatology.* Wellington, New Zealand: New Zealand Meteorological Service
- Ryan, M; Dunbar, G; Vandergoes, M; Neil, H; Hannah, M; Newnham, R; Bostock, H; & Alloway, B. (2012) Vegetation and Climate in Southern Hemisphere Mid-Latitudes since 210 ka: New Insights from Marine and Terrestrial Pollen Records from New Zealand. *Quaternary Science Reviews* 48 80-98
- Sakai, A; & Wardle, P. (1978) Freezing Resistance of New Zealand Trees and Shrubs. *New Zealand Journal of Ecology* 1 51-61
- Salinger, J; Burgess, S; Turner, R; & Moore, S. (2007) Climate hazards and extremes –Taranaki Region: Tornado update. NIWA Client Report WLG2007-78 for New Plymouth District Council, November 2007. Wellington, New Zealand: National Institute of Water & Atmospheric Research

- Salinger, M; & Porteous, A. (2006) New Zealand climate: Patterns of drought. Resource Management Under Stormy Skies, Christchurch, 20-23 November 2006
- Salinger, M; Renwick, J; & Mullan, A. (2001) Interdecadal Pacific Oscillation and South Pacific Climate. *International Journal of Climatology* 21 1705-1721
- Salisbury, F; & Ross, C. (1992) *Plant Physiology* (4<sup>th</sup> ed) Belmont, California: Wadsworth Publishing Company
- Sandiford, A; Alloway, B; & Shane, P. (2001) A 28,000-6,000 cal yr Record of Local and Distal Volcanism Preserved in a Paleolake, Auckland, New Zealand. *New Zealand Journal of Geology & Geophysics* 44 323-336
- Sandiford, A; Newnham, R; Alloway, B; & Ogden, J. (2003) A 28 000 – 7 600 cal yr BP Pollen Record of Vegetation and Climate Change from Pukaki Crater, northern New Zealand. *Palaeoecography, Palaoclimatology, Palaeoecology* 201 235-247
- Schramm, C; & Leinen, M. (1987) Eolian Transport to Hole 595A from the Late Cretaceous through the Cenozoic. *Deep Sea Drilling Project Reports Volume 91*
- Schulze, E-D; & Chapin, F. (1987) Plant Specialisation to Environments of Different Resource Availability. In E-D. Schulze & H. Zwölfer (Eds) *Potentials and Limitations of Ecosystem Analysis. Ecological Studies Volume 61* Springer-Verlag: Berlin
- Seidov, D; Haupt, B; Barron, E; & Maslin, M. (2001) Ocean Bi-Polar Seesaw and Climate: Southern versus Northern Meltwater Impacts. In D. Seidov, B. Haupt, & M. Maslin (Eds) *The Oceans and Rapid Climate Change: Past, Present, and Future*. Washington, DC: AGU
- Shane, P; & Hoverd, J. (2002) Distal Record of Multi-Sourced Tephra in Onepoto Basin, Auckland, New Zealand: Implications for Volcanic Chronology, Frequency and Hazards. *Bulletin of Volcanology* 64 441-454
- Shea, K; Roxburgh, S; & Rauschert, E. (2004) Moving from Pattern to Process: Coexistence Mechanisms under Intermediate Disturbance Regimes. *Ecology Letters* 7 491-508
- Sheil, D; & Burslem, D. (2003) Disturbing Hypotheses in Tropical Forests. *Trends in Ecology & Evolution* 18 (1) 18-26
- Shotyk, W. (1996) Peat Bog Archives of Atmospheric Metal Deposition: Geochemical Assessment of Peat Profiles, Natural Variation in Metal Concentrations, and Metal Enrichment Factors. *Environmental Reviews* 4 149-183
- Shotyk, W; Weiss, D; Kramers, J; Frei, R; Cheburkin, A; Gloor, M; & Reese, S. (2001) Geochemistry of the Peat Bog at Etang de la Gruere, Jura Mountains, Switzerland, and its record of Pb and Lithogenic Trace Elements (Sc, Ti, Y, Zr, Hf, and REE) since 12,370 <sup>14</sup>C yr BP. *Geochimica Cosmochimica Acta* 65 2337-2360
- Shulmeister, J; Goodwin, I; Renwick, J; Harle, K; Armand, L; McGlone, M; Cook, E; Dodson, J; Hesse, P; Mayewski, P; & Curran, M. (2004) The Southern Hemisphere Westerlies in the Australasian Sector over the Last Glacial Cycle: A Synthesis. *Quaternary International* 118-119 23-53

- Shulmeister, J; McLea, W; Singer, C; McKay, R; & Hosie, C. (2003) Late Quaternary Pollen records from the lower Cobb Valley and Adjacent Areas, North-West Nelson, New Zealand. *New Zealand Journal of Botany* 41 503-533
- Shulmeister, J; Shane, P; Lian, O; Okuda, M; Carter, J; Harper, M; Dickinson, W; Augustinus, P; & Heijnis, H. (2001) A Long Late-Quaternary Record from Lake Poukawa, Hawke's Bay, New Zealand. *Palaeogeography, Palaeoclimatology, Palaeoecology* 176 81-107
- Silvertown, J. (1982) *Introduction to Plant Population Biology*. London, United Kingdom: Longman
- Singer, C; Shulmeister, J; & McLea, B. (1998) Evidence Against a Significant Younger Dryas Cooling Event in New Zealand. *Science* 281 812-814
- Singer, J; Anderson, J; Ledbetter, M; McCave, I; Jones, K; & Wright, R. (1988) An Assessment of Analytical Techniques for the Size Analysis of Fine Grained Sediments. *Journal of Sedimentary Petrology* 58 (3) 534-543
- Smale, M. (1984) White Pine Bush - An Alluvial Kahikatea (*Dacrycarpus dacrydioides*) Forest Remnant, eastern Bay of Plenty, New Zealand. *New Zealand Journal of Botany* 22 201-206
- Smale, M. (2008) *Deer Impacts on Tawa (Beilschmiedia tawa) Regeneration*. DoC Research & Development Series 300. Wellington, New Zealand: Department of Conservation
- Small, E. (1972) Photosynthetic Rates in Relation to Nitrogen Recycling as an Adaptation to Nutrient Deficiency in Peat Bog Plants. *Canadian Journal of Botany* 50 2227-2233
- Smith, B; Mark, A; & Wilson, J. (1995) A Functional Analysis of New Zealand Alpine Vegetation: Variation in Canopy Roughness and Functional Diversity in response to an experimental Wind Barrier. *Functional Ecology* 9 904-912
- Smith, G; & Fritz, W. (1989) Volcanic Influences on Terrestrial Sedimentation. *Geology* 17 375-376
- Smith, V; & Ennos, A. (2003) The Effects of Air Flow and Stem Flexure on the Mechanical and Hydraulic Properties of the Stems of Sunflowers *Helianthus annuus* L. *Journal of Experimental Botany* 54 (383) 845-849
- Sousa, W. (1979) Disturbance in Marine Intertidal Boulder Fields: The Nonequilibrium Maintenance of Species Diversity. *Ecology* 60 (6) 1225-1239
- Sperazza, M; Moore, J; & Hendrix, M. (2004) High-Resolution Particle Size Analysis of Naturally Occurring Very Fine-Grained Sediment Through Laser Diffraction. *Journal of Sedimentary Research* 74 736-743
- Sridhar K; Jackson, M; & Clayton, R. (1975) *Soil Society of America Proceedings* 39 1209-1213
- Steinmann, P; & Shotyk, W. (1997a) Chemical Composition, pH, and Redox State of Sulphur and Iron in Complete Vertical Pore Water Profiles from two Sphagnum Peat Bogs, Jura Mountains Switzerland. *Geochimica Cosmochimica Acta* 61 1146-1163
- Steinmann, P; & Shotyk, W. (1997b) Geochemistry, Mineralogy, and Geochemical Mass Balance on Major Elements in two Peat Bog Profiles, Jura Mountains Switzerland. *Chemical Geology* 138 25-53

- Steinhorsdottir, M; Wohlfarth, B; Kylander, M; Blaauw, M; & Reimer, P. (2013) Stomatal Proxy Records of CO<sub>2</sub> Concentrations from the Last Termination Suggests an Important Role for CO<sub>2</sub> at Climate Change Transitions. *Quaternary Science Reviews* 68 43-58
- Stephens, J; Molan, P; & Clarkson, B. (2005) A Review of *Leptospermum scoparium* (Myrtaceae) in New Zealand. *New Zealand Journal of Botany* 43 431-449
- Stewart, R; & Neall, V. (1984) Chronology of Palaeoclimatic Change at the end of the Last Glaciation. *Nature* 311 47-48
- Stewart, R; Neall, V; Pollock, A; & Syers, J. (1977) Parent Material Stratigraphy of an Egmont Loam Profile, Taranaki, New Zealand. *Australian Journal of Soil Research* 177-90
- Stewart, R; Neall, V; & Syers J. (1984) Occurrence and Source of Quartz in Six Basaltic Soils from Northland, New Zealand. *Australian Journal of Soil Research* 22 365-377
- Stewart, R; Neall, V; & Syers J. (1986) Origin of Quartz in Selected Soils and Sediments, North Island, New Zealand. *New Zealand Journal of Geology & Geophysics* 29 147-152
- Stewart, R; Zernack, A; Procter, J; & Alloway, B. (2006) *Field Trip 5 Guide: Taranaki*. GSNS-NZGS Joint Conference, Massey University 4-7 December 2006.
- Stirling, G; & Wilsey, B. (2001) Empirical Relationships between Species Richness, Evenness, and Proportional Diversity. *The American Naturalist* 138 (3) 286-299
- Stocker, T. (1998) The Seesaw Effect. *Science* 282 61-62
- Stockmarr, J. (1971) Tablets with Spores used in Absolute Pollen Analysis. *Pollen et Spores* 13 (4) 615-621
- Stuiver, M., & Reimer, P. (1993) Extended <sup>14</sup>C Database and Revised CALIB Radiocarbon Calibration Program. *Radiocarbon* 35 215-230
- Sturman, A; & Tapper, N. (2005) *The Weather and Climate of Australia and New Zealand* (2<sup>nd</sup> ed) Melbourne, Australia: Oxford University Press:
- Stumm, W; & Morgan, J. (1981) *Aquatic Chemistry: An Introduction Emphasising Chemical Equilibria in Natural Waters*. (2<sup>nd</sup> ed) New York, NY: John Wiley & Sons
- Suggate, R; & Almond, P. (2005) The Last Glacial Maximum (LGM) in Western South Island, New Zealand: Implications for the Global LGM and MIS 2. *Quaternary Science Reviews* 24 (16-17) 1923-1940
- Sutherland, R; Kim, K; Zondervan, A; & McSaveny, M. (2007) Orbital Forcing of Mid-Latitude Southern Hemisphere Glaciations since 100 ka inferred from Cosmogenic Nuclide Ages of Moraine Boulders from the Cascade Plateau, Southwest New Zealand. *Geological Society of America Bulletin* 119 443-451
- Svensson, R; Lindgarth, M; Siccha, M; Lenz, M; Molis, M; Wahl, M; & Pavia, H. (2007) Maximum Species Richness at Intermediate Frequencies of Disturbance: Consistency among Levels of Productivity. *Ecology* 88 (4) 830-838
- Swap, R; Garstang, M; Greco, S; Talbot, R; & Källberg, P. (1992) Saharan Dust in the Amazon Basin. *Tellus* 44B 133-149
- Swindale, L; & Jackson, M. (1960) A Mineralogical Study of Soil Formation in Four Rhyolite-Derived Soils from New Zealand. *New Zealand Journal of Geology & Geophysics* 3 141-183

- Syers, J; Jackson, M; Berkheiser, V; Clayton, R; & Rex, R. (1969) Eolian Sediment Influence on Pedogenesis During the Quaternary. *Soil Science* 107 (6) 421-427
- Syvitski, J; Leblanc, K; & Asprey, K. (1991) Interlaboratory, Interinstrument Calibration Experiment. In: J. Syvitski (Ed) *Principles, Methods and Application of Particle Size Analysis*. Cambridge, United Kingdom: Cambridge University Press
- Tapper, N., Hurry, L., 1993. *Australia's Weather Patterns: An Introductory Guide*. : Mount Waverley, Australia: Dellasta Pty Ltd.
- Tausch, R; Wigand, P; & Burkhardt, J. (1993) Viewpoint: Plant Community Thresholds, Multiple Steady States, and Multiple Successional Pathways: Legacy of the Quaternary? *Journal of Range Management* 46 (5) 439-447
- Tegen, I; Harrison, S; Kohfield, K; & Prentice, I. (2002) Impact of Vegetation and Preferential Source Areas on Global Dust Aerosol: Results from a Model Study. *Journal of Geophysical Research* 170 (D21) 4576-4603
- Telewski, F. (2012) Is Windswept Tree Growth Negative Thigmotropism? *Plant Science* 184 20-28
- Telford, R; Heegaard, E; & Birks, H. (2004) All Age-Depth Models are Wrong: But How Badly? *Quaternary Science Reviews* 23 1-5
- Thiede, J. (1979) Wind Regime over the Late Quaternary Southwest Pacific Ocean. *Geology* 7 (5) 259-263
- Thompson, C. (1981) *The Climate and Weather of the Taranaki Region*. New Zealand Meteorological Service Miscellaneous Publication 115 (9). Wellington, New Zealand: New Zealand Meteorological Service
- Thorndycraft, V; Benito, G; Sánchez-Moya, Y; & Sopeña, A. (2011) Bayesian Age Modelling Applied to Palaeoflood Geochronologies and the Investigation of Holocene Flood Magnitude and Frequency. *The Holocene* 22 13-22
- Timmins, S. (1983) Mt Tarawera 1. Vegetation Types and Successions. *New Zealand Journal of Ecology* 6 99-105
- Tinkler, R. (2005) *New Zealand Fossil Pollen Maps: An Integrative Methodology to reconstruct the Palaeoenvironment since the Last Glacial Maximum*. Massey University School of People, Environment & Planning Occasional Paper 2005/1. Palmerston North, New Zealand: Massey University
- Tinner, W; Hu, F-S; Beer, R; Kaltenrieder, P; Scheurer, B; & Krähenbühl, U. (2006) Postglacial Vegetational and Fire History: Pollen, Plant Macrofossil and Charcoal Records from two Alaskan Lakes. *Vegetational History & Archaeobotany* 15 279-293
- Tipper, J. (1979) Rarefaction and Rarefication: The Use and Abuse of a Method in Paleoecology. *Paleobiology* 5 (4) 423-434
- Townsend, C; Scarsbrook, M; & Dolédi, S. (1997) The Intermediate Disturbance Hypothesis, Refugia and Biodiversity in Streams. *Limnology & Oceanography* 42 (5) 938-949
- Tsoar, H; & Pye, K. (1987) Dust Transport and the Question of Loess Formation. *Sedimentology* 34 139-153
- Tukey, H. (1970) The Leaching of Substances from Plants. *Annual Review of Plant Physiology* 21 305-324

- Turner, M. (2008) Eruption Cycles and Magmatic Processes at a Reawakening Volcano, Mt Taranaki, New Zealand. A Thesis Presented in Partial Fulfilment of the Requirements for the Degree of Doctor of Philosophy in Earth Science at Massey University. Palmerston North, New Zealand: Massey University
- Turner, M; Cronin, S; Bebbington, S; Smith, I; & Stewart, R. (2011) Integrating Records of Explosive and Effusive Activity from Proximal and Distal Sequences: Mt. Taranaki, New Zealand. *Quaternary International* 246 364-373
- Turney, C; McGlone, M; & Wilmshurst, J. (2003) Asynchronous Climate Change between New Zealand and the North Atlantic during the Last Deglaciation. *Geology* 31 (3) 223-226
- Turney, C; Roberts, R; de Jonge, N; Prior, C; Wilmshurst J; McGlone, M; & Cooper, J. (2007) Redating the Advance of the New Zealand Franz Josef Glacier during the Last Termination: Evidence for Asynchronous Climate Change. *Quaternary Science Reviews* 26 3037-3042
- Ui, T; Kawachi, S; & Neall, V. (1986) Fragmentation of Debris Avalanche Material During Flowage – Evidence from the Pungarehu Formation, Mount Egmont, New Zealand. *Journal of Volcanology & Geothermal Research* 27 255-264
- Ulrich, S; Stewart, G; Duncan, R; & Almond, P. (2005) Tree Regeneration in a New Zealand Rain Forest Influenced by Disturbance and Drainage Interactions. *Journal of Vegetation Science* 16 423-432
- US Environmental Protection Agency (2011) *Method 3052 Microwave Assisted Acid Digestion of Siliceous and Organically Based Matrices*. <http://www.epa.gov/wastes/hazard/testmethods/sw846/pdfs/3052.pdf> last accessed 04.10.11
- van de Vijver, B. and Beyens, L. 1999. Moss Diatom Communities from Ile de la Possession (Crozet, Subantarctica) and their Relationship with Moisture. *Polar Biology* 22 219-231.
- van Gardingen, P; & Grace, J. (1991) Plants and Wind. *Advances in Botanical Research* 18 189-253
- van Valen, L. (1973) A New Evolutionary Law. *Evolutionary Theory* 1 1-30
- Vandergoes, M; Dieffenbacher-Krall, A; Newnham, R; Denton, G; & Blaauw, M. (2008) Cooling and Changing Seasonality in the Southern Alps, New Zealand during the Antarctic Cold Reversal. *Quaternary Science Reviews* 27 (5/6) 589-601
- Vandergoes, M; & Fitzsimons, S. (2003) The Last Glacial-Interglacial Transition (LGIT) in south Westland, New Zealand: Paleocological Insight into mid-Latitude Southern Hemisphere Climate Change. *Quaternary Science Reviews* 22 1461-1476
- Vandergoes, M; Hogg, A; Lowe, D; Newnham, R; Denton, G; Southon, J; Barrell, D; Wilson, C; McGlone, M; Allan, A; Almond, P; Petchey, F; Dabell, K; Dieffenbacher-Krall, A; & Blaauw, M. (2013) A Revised Age for the Kawakawa/Oruanui Tephra, a Key Marker for the Last Glacial Maximum in New Zealand. *Quaternary Science Reviews* <http://dx.doi.org/10.1016/j.quascirev.2012.11006>
- Vandergoes, M; Newnham, R; Preusser, F; Hendy, C; Lowell, T; Fitzsimons, S; Hogg, A; Kasper, H; & Schlüchter, C. (2005) Regional Insolation Forcing of Late Quaternary Climate Change in the Southern Hemisphere. *Nature* 436 242-244
- Von Storch, H; Zorita, E; Jones, J; Dimitriev, Y; González-Rouco, F; & Tett, S. (2004) Reconstructing Past Climate from Noisy Data. *Science* 306 679-6827.
- Vucetich, C; Vella, P; & Warnes, P. (1996) Antepenultimate Glacial to Last Glacial Deposits in Southern Wairarapa, New Zealand. *Journal of the Royal Society of New Zealand* 26 (4) 469-482

- Wadsworth, R. (1959) An Optimum Wind Speed for Plant Growth. *Annals of Botany* 23 (89) 195-199
- Wagner, F; Bohncke, S; Dilcher, D; Kürschner, W; van Geel, B; & Visscher, H. (1999) Century-Scale Shifts in Early Holocene Atmospheric CO<sub>2</sub> Concentration. *Science* 284 1971-1973
- Waikato Radiocarbon Dating Laboratory (2012) *Radiocarbon Dating*  
<http://c14.arch.ox.ac.uk/embed.php?File=webinfo.html> last accessed 24.08.12
- Walanus, A. (2008) Drawing the Optimal Depth-Age Curve on the Basis of Calibrated Radiocarbon Dates. *Geochronometria* 31 1-5
- Wallace, R. (1987) *The Mineralogy of the Tokomaru Silt Loam and the Occurrence of Cristobalite and Tridymite in Selected North Island Soils*. A Thesis Presented in Partial Fulfilment of the Requirements for the Degree of Doctor of Philosophy in Soil Science at Massey University. Palmerston North, New Zealand: Massey University
- Wardle, J. (1984) *The New Zealand Beeches: Ecology, Utilisation and Management*. New Zealand Forest Service: Christchurch
- Wardle, P. (1963) Evolution and Distribution of the New Zealand Flora, as Affected by Quaternary Climates. *New Zealand Journal of Botany* 1 (1) 3-17
- Wardle, P. (1967) Biological Flora of New Zealand 2. *Nothofagus menziesii* (Hook. f.) Oerst. Fagaceae, Silver Beech. *New Zealand Journal of Botany* 5 276-302
- Wardle, P. (1977) Plant Communities of Westland National Park (New Zealand) and Neighbouring Lowland and Coastal Areas. *New Zealand Journal of Botany* 15 323-298
- Wardle, P. (1980) Primary Succession in Westland National Park and its Vicinity, New Zealand. *New Zealand Journal of Botany* 18 221-232
- Wardle, P. (1980b) Ecology and Distribution of Silver Beech (*Nothofagus menziesii*) in the Paringa District, South Westland, New Zealand. *New Zealand Journal of Ecology* 3 23-36
- Wardle, P. (1986) Frequency of Cloud Cover on New Zealand Mountains in Relation to Subalpine Vegetation. *New Zealand Journal of Botany* 24 553-565
- Wardle, D; Wisser, S; Allen, R; Doherty, J; Bonner, K; & Williamson, W. (2008) Aboveground and Belowground Effects of Single-tree Removals in New Zealand Rain Forest. *Ecology* 89 (5) 1232-1245
- Watanabe, O; Jouzel, J; Johnsen, S; Parrenin, F; Shoji, H; & Yoshida, N. (2003) Homogeneous Climate Variability across East Antarctica over the past three Glacial Cycles. *Nature* 422 509-512
- Weber, M; Kuhn, G; Sprenk, D; Rolf, C; Ohlwein, C; & Ricken, W. (2012) Dust Transport from Patagonia to Antarctica – A New Stratigraphic Approach from the Scotia Sea and its Implications. *Quaternary Science Reviews* 36 177-188
- Weiss, D; Shotyk, W; Cheburkin, A; Gloor, M; & Reese, S. (1997) Atmospheric Lead Deposition from 12,400 to ca. 2,000 yrs BP in a Peat Bog Profile, Jura Mountains, Switzerland. *Water Air Soil Pollution* 100 (3-4) 311-324
- Weiss, D; Shotyk, W; Rieley, J; Page, S; Gloor, M; Reese, S; & Martinez-Cortiza, A. (2002) The Geochemistry of Major and Selected Trace Elements in a Forested Peat Bog, Kalimantan, SE Asia,

and its Implications for Past Atmospheric Dust Deposition. *Geochimica et Cosmochimica Acta* 66 (13) 2307–2323

- Wellman, C; & Gray, J. (2000) The Microfossil Record of Early Land Plants. *Philosophical Transactions of the Royal Society of London Series B* 355 (1398) 717-732
- Wells, A; Yetton, M; Duncan, R; & Stewart, G. (1999) Prehistoric Dates of the Most Recent Alpine Fault Earthquakes, New Zealand. *Geology* 27 (11) 995-998
- Wells, A; Duncan, R; & Stewart, G. (2001) Forest Dynamics in Westland, New Zealand: The Importance of Large, Infrequent Earthquake-Induced Disturbance. *Journal of Ecology* 89 1006-1018.
- Weng, C; Hooghiemstra, H; & Duivenvoorden, J. (2006) Challenges in Estimating Past Plant Diversity from Fossil Pollen Data: Statistical Assessment, Problems and Possible Solutions. *Diversity & Distributions* 12 310-318
- Whittaker, R; & Goodman, D. (1979) Classifying Species According to their Demographic Strategy. I. Population Fluctuations and Environmental Heterogeneity. *American Naturalist* 113 185-200
- Whittaker, T; Hendy, C; & Hellstrom, J. (2011) Abrupt Millennial Scale Changes in Intensity of Southern Hemisphere Westerly Winds during Marine Isotope Stages 2-4. *Geology* 39 455-458
- Widmann, J; Duchez, J; Yang, J; Conny, J; & Mulholland, G. (2005) Measurement of the Optical Extinction Coefficient of Combustion-Generated Aerosol. *Aerosol Science* 36 283-289
- Will, G. (1974) Forestry. In N. Read (Ed) *Soil Groups of New Zealand Part 1. Yellow-Brown Pumice Soils*. Wellington, New Zealand: New Zealand Society of Soil Science
- Williams, P; King, D; Neil, H; & Zhao, J.-X. (2005b) Palaeoclimatic Events and Cycles Determined from Late Pleistocene to Holocene Speleothem  $^{18}\text{O}$  and  $^{13}\text{C}$  Records from Central New Zealand. In B. Alloway & J. Shulmeister (Eds) *Proceedings of the 2005 NZ-INTIMATE Meeting, GNS-Rafter Laboratory, Lower Hutt 4-5 July*. Institute of Geological and Nuclear Sciences Science Report SR2005/18. Lower Hutt, New Zealand: Institute of Geological & Nuclear Sciences
- Williams, P; King, D; Zhao, J.-X.; & Collerson, K. (2004) Speleothem Master Chronologies: Combined Holocene  $^{18}\text{O}$  and  $^{13}\text{C}$  Records from the North Island of New Zealand and their Palaeoenvironmental Interpretation. *The Holocene* 14 194-208
- Williams, P; King, D; Zhao, J.-X.; & Collerson, K. (2005a) Late Pleistocene to Holocene Composite Speleothem  $^{18}\text{O}$  and  $^{13}\text{C}$  Chronologies from South Island, New Zealand – did a Global Younger Dryas Really Exist? *Earth & Planetary Science Letters* 230 301-317
- Williams, P; Neil, H; & Zhao, J.-X. (2010) Age Frequency Distribution and Revised Stable Isotope Curves for New Zealand Speleothems: Palaeoclimatic Implications. *International Journal of Speleology*, 39 (2) 99-112
- Wilmshurst, J; & McGlone, M. (1996) Forest Disturbance in the Central North Island, New Zealand, following the 1850 Taupo Eruption. *The Holocene* 6 (4) 399-411
- Wilmshurst, J; McGlone, M; Leathwick, J; & Newnham, R. (2007) A Pre-Deforestation Pollen-Climate Calibration Model for New Zealand and Quantitative Temperature Reconstructions for the Past 18 000 years. *Journal of Quaternary Science* 22 (5) 535-547

- Wilmshurst, J; Wisler, S; & Charman, D. (2003) Reconstructing Holocene Water Tables in New Zealand using Testate Amoebae: Differential Preservation of Tests and Implications for the use of Transfer Functions. *The Holocene* 13: 61–72
- Wilson, J; Allen, R; & Hewitt, A. (1996) A Test of the Hump-back Theory of Species Richness in New Zealand Native Forest. *New Zealand Journal of Ecology* 20 (2) 173-177
- Windom, H. (1969) Atmospheric Dust Records in Permanent Snowfields: Implications to Marine Sedimentation. *Geology Society of America Bulletin* 80 761-782
- Wolfe, S; & Nickling, W. (1996) Shear Stress Partitioning in Sparsely Vegetated Desert Canopies. *Earth Surface Processes & Landforms* 21 607-619
- Wood, J; & Walker, S. (2008) Macrofossil Evidence for Pre-Settlement Vegetation of Central Otago's Basin Floors and Gorges. *New Zealand Journal of Botany* 45 239-255
- Woodward, C; & Shulmeister, J. (2006) New Zealand Chironomids as Proxies for Human-Induced and Natural Environmental Change: Transfer Functions for Temperature and Lake Production (chlorophyll *a*). *Journal of Paleolimnology* 36 407-429
- World Meteorological Organization (1990) *Report of the Meeting of Experts on Global Aerosol Data System (GADS) No. 73* Hampton, VA: World Meteorological Organization.
- Wyatt, V; & Nickling, W. (1996) Drag and Shear Stress Partitioning in Sparse Desert Creosote Communities. *Canadian Journal of Earth Science* 34 1486-1498
- Yokoyama, Y; Lambeck, K; de Deckker, P; Johnson, P; & Fifield, K. (2000) Timing of the Last Glacial Maximum from Observed Sea-Level Minima. *Nature* 406 713-716
- Yung, Y; Lee, T; Wang, C-H; & Shieh, Y-T. (1996) Dust: A Diagnostic of the Hydrologic Cycle during the Last Glacial Maximum. *Science* 271 962-963
- Zernack, A. (2008) *A Sedimentological and Geochemical Approach to Understanding Cycles of Stratovolcano Growth and Collapse at Mount Taranaki, New Zealand*. A Thesis Presented in Partial Fulfilment of the Requirements for the Degree of Doctor of Philosophy. Palmerston North, New Zealand: Massey University
- Zernack, A; Cronin, S; Neall, V; & Proctor, J. (2011) A Medial to Distal Volcaniclastic Record of an Andesite Stratovolcano: Detailed Stratigraphy of the Ring-Plain Succession of South-west Taranaki, New Zealand. *International Journal of Earth Sciences (Geologische Rundschau)* 100 1937-1966
- Zernack, A; Neall, V; & Tinkler, R. (2012) Using Physical Properties of the 30-25 ka Poto Tephra from Mt. Taranaki, New Zealand as a Tool for Correlation between Outcrop and Core Records. In A. Pittari & R. Hansen (Eds) *Abstracts, Geosciences 2012 Conference, Hamilton New Zealand*. Geoscience Society of New Zealand Miscellaneous Publication 134A. Wellington, New Zealand: Geoscience Society of New Zealand.
- Zernack, A; Proctor, J; & Cronin, S. (2009) Sedimentary Signatures of Cyclic Growth and Destruction of Stratovolcanoes: A Case Study from Mt. Taranaki, New Zealand. *Sedimentary Geology* 220 288-305
- Zhang, Y; & Carmichael, G. (1999) The Role of Mineral Aerosol in Tropospheric Chemistry in East Asia – A Case Study. *Journal of Applied Meteorology* 38 353-366